AD A122744

AFWAL-TR-82-2121
Volume I

STRUCTURAL ELEMENT AND REAL BLADE IMPACT TESTING

ROBERT S. BERTKE

UNIVERSITY OF DAYTON RESEARCH INSTITUTE
300 COLLEGE PARK AVENUE
DAYTON, OHIO 45469

JANUARY 1983

FINAL REPORT FOR PERIOD OCTOBER 1977 - JUNE 1980

APPROVED FOR PUBLIC RELEASE; DISTRIBUTION UNLIMITED.

DTIC
ELECTE
MAY 05 1983
S D
E

AERO PROPULSION LABORATORY
AIR FORCE WRIGHT AERONAUTICAL LABORATORIES
AIR FORCE SYSTEMS COMMAND
WRIGHT-PATTERSON AIR FORCE BASE, OHIO 45433

DTIC FILE COPY

83 05 05- 001

NOTICE

When Government drawings, specifications, or other data are used for any purpose other than in connection with a definitely related Government procurement operation, the United States Government thereby incurs no responsibility nor any obligation whatsoever; and the fact that the government may have formulated, furnished, or in any way supplied the said drawings, specifications, or other data, is not to be regarded by implication or otherwise as in any manner licensing the holder or any other person or corporation, or conveying any rights or permission to manufacture use, or sell any patented invention that may in any way be related thereto.

This report has been reviewed by the Office of Public Affairs (ASD/PA) and is releasable to the National Technical Information Service (NTIS). At NTIS, it will be available to the general public, including foreign nations.

This technical report has been reviewed and is approved for publication.

Sandra K. Drake

SANDRA K. DRAKE
Project Engineer
Engine Assessment Branch

Robert W. Baker

ROBERT W. BAKER, Maj, USAF
Chief, Engine Assessment Branch
Turbine Engine Division

FOR THE COMMANDER

H. I. Bush

H. I. BUSH
Director
Turbine Engine Division
Aero Propulsion Laboratory

"If your address has changed, if you wish to be removed from our mailing list, or if the addressee is no longer employed by your organization please notify AFWAL/POTA, *W-PAFB, OH 45433 to help us maintain a current mailing list".*

Copies of this report should not be returned unless return is required by security considerations, contractual obligations, or notice on a specific document.

Unclassified

SECURITY CLASSIFICATION OF THIS PAGE *(When Data Entered)*

REPORT DOCUMENTATION PAGE		READ INSTRUCTIONS BEFORE COMPLETING FORM
1. REPORT NUMBER AFWAL-TR-82-2121, Vol I	2. GOVT ACCESSION NO. AD-A127744	3. RECIPIENT'S CATALOG NUMBER
4. TITLE *(and Subtitle)* STRUCTURAL ELEMENT AND REAL BLADE IMPACT STUDY		5. TYPE OF REPORT & PERIOD COVERED Final Report for Period October 1977-June 1980
		6. PERFORMING ORG. REPORT NUMBER UDR-TR-82-03
7. AUTHOR(s) Robert S. Bertke		8. CONTRACT OR GRANT NUMBER(s) F33615-77-C-5221
9. PERFORMING ORGANIZATION NAME AND ADDRESS University of Dayton Research Institute 300 College Park Ave, Dayton OH 45469		10. PROGRAM ELEMENT, PROJECT, TASK AREA & WORK UNIT NUMBERS P.E. 62203F Project 3066 12 33
11. CONTROLLING OFFICE NAME AND ADDRESS Aero Propulsion Laboratory (AFWAL/POTA) AF Wright Aeronautical Laboratories (AFSC) Wright-Patterson Air Force Base, OH 45433		12. REPORT DATE January 1983 13. NUMBER OF PAGES 442
14. MONITORING AGENCY NAME & ADDRESS *(if different from Controlling Office)*		15. SECURITY CLASS. *(of this report)* Unclassified 15a. DECLASSIFICATION/DOWNGRADING SCHEDULE

16. DISTRIBUTION STATEMENT *(of this Report)*

Approved for public release; distribution unlimited.

17. DISTRIBUTION STATEMENT *(of the abstract entered in Block 20, if different from Report)*

18. SUPPLEMENTARY NOTES

19. KEY WORDS *(Continue on reverse side if necessary and identify by block number)*

Fan blades, Foreign Object Damage (FOD), Titanium, Stainless Steel, Boron/Aluminum Composite, Leading Edge Impact Damage, Strain, Strain Rate, Artificial Bird Impacts, Ice Impacts, Deflections

20. ABSTRACT *(Continue on reverse side if necessary and identify by block number)*

This report gives damage results of an experimental program concerned with performing nonrotating bench impact tests on test specimens rangine from simple cantilevered beams and plates to real fan blades. This study was carried out under Task VI "Structural Element Tests" which is part of the overall program "Foreign Object Impact Damage Criteria."

DD FORM 1 JAN 73 1473 EDITION OF 1 NOV 65 IS OBSOLETE

Unclassified

SECURITY CLASSIFICATION OF THIS PAGE *(When Data Entered)*

Three types of blade materials, geometries, and sizes were investigated using ice and substitute bird material as the impactors. The fan blades investigated were the J79 using 403 stainless steel material, the F101 blade using 8Al-1Mo-1V (8-1-1 titanium, and the APSI metal matrix blade material of boron/aluminum.

In the study, simple element specimens, such as beams and plates, were impact tested with progressive introduction of airfoil geometric parameters to validate experimentally the analytical predictions of Tasks V and VIII of the overall program. General Electric Company was to conduct the Tasks V and VIII phases of the program. The blade geometry parameters investigated included the aspect ratio, thickness to chord ratio, shape, camber, and twist. Impact tests were also conducted on actual fan blades to permit deriving correlation of the impact damage between the structural element specimens and full-scale blades.

Data collected from the impact tests included accurate impact conditions, dynamic displacement of specimens at discreet points, strain/time histories local to the impact site and at critical blade stress regions identified from the structural response models, pre-test and post-test material properties, and damage assessment.

Because of the enormous amount of data (especially strain and strain rate plots versus time), the Task VI work is described in two reports (Volumes I and II). This report (Volume I) describes in detail selected impacts where the strain data is expanded for the first several milliseconds. Deflection data, impact damage assessment, and maximum strain rate data are also given in this report (Volume I). The Volume II report gives all of the unexpanded strain and strain rate data.

PREFACE

The work reported herein was conducted by the Impact Physics Group of the Experimental and Applied Mechanics Division at the University of Dayton Research Institute (UDRI), Dayton, Ohio, under Purchase Order No. 200-4BA-14K-47844 for the General Electric Company, Aircraft Engine Group, Evendale, Ohio. The work is the result of a subcontract of F33615-77-C-5221.

The work described herein was conducted in the UDRI Impact Physics Facility, at the University of Dayton during the period of October 1977 to June 1980 and is part of Task VI of the overall program. The Principal Investigator was Mr. Robert S. Bertke of the University of Dayton Research Institute. Project supervision was provided by Dr. S. Bless and Mr. G. Roth of UDRI.

The General Electric Manager was Mr. J. McKenzie and the Principal Investigator for G.E. was Mr. A. Storace.

The author wishes to acknowledge the following persons of the University of Dayton Research Institute who provided direct support to this work. Mr. C. E. Acton and Mr. H. Williams conducted the majority of the experimental testing, Mr. R. Tocci conducted the photographic coverage, and Ms. G. Miller conducted the typing of this manuscript.

Accession For
NTIS GRA&I
DTIC TAB
Unannounced
Justification
By
Distribution/
Availability Codes
Dist | Avail and/or Special
A

DTIC COPY INSPECTED

TABLE OF CONTENTS

SECTION		PAGE
1	INTRODUCTION	1
2	EXPERIMENTAL PROGRAM	3
	2.1 STUDY OBJECTIVES AND APPROACH	3
	2.1.1 Test Conditions for Various Blade Types	16
	2.1.2 Specimen Materials and Geometries	18
	2.1.2.1 F101 Test Specimens	18
	2.1.2.2 J79 Test Specimens	22
	2.1.2.3 APSI Test Specimens	22
	2.1.3 Impactors	23
	2.2 EXPERIMENTAL SETUP AND PROCEDURES	23
	2.2.1 Large Bore Compressed Gas Gun Range	25
	2.2.2 Blade and Specimen Mounting Procedure	26
	2.2.3 Slice Size Determination	29
	2.2.4 Impact Velocity Measurements	29
	2.3 DATA COLLECTION	31
	2.3.1 Strain Measurements	31
	2.3.2 Target Deflection Measurements	32
	2.4 DAMAGE ASSESSMENT	33
	2.4.1 Mode and Extent or Damage Measurements	33
3	EXPERIMENTAL RESULTS	35
	3.1 SIMPLE ELEMENT TEST SPECIMENS	35
	3.1.1 Impact Results of Structural Element Tests	36
	3.1.1.1 Impact Results for Group 1 Specimens	59
	3.1.1.2 Impact Results for Group 2 Specimens	71
	3.1.1.3 Impact Results for Group 3 Specimens	84
	3.1.1.4 Impact Results for Group 4 Specimens	84
	3.1.1.5 Impact Results for Group 5 Specimens	99

TABLE OF CONTENTS (Continued)

SECTION			PAGE
	3.1.1.6	Impact Results for Group 6 Specimens	115
	3.1.1.7	Impact Results for Group 7 Specimens	124
	3.1.1.8	Impact Results for Group 8 Specimens	124
	3.1.1.9	Impact Results for Group 9 Specimens	134
	3.1.1.10	Impact Results for Group 10 Specimens	145
	3.1.1.11	Impact Results for Group 11 Specimens	160
	3.1.1.12	Impact Results for Group 12 Specimens	160
	3.1.1.13	Impact Results for Group 13 Specimens	167
	3.1.1.14	Impact Results for Group 14 Specimens	186
	3.1.1.15	Impact Results for Group 15 Specimens	186
	3.1.1.16	Impact Results for Group 16 Specimens	195
	3.1.1.17	Impact Results for Group 17 Specimens	211
	3.1.1.18	Impact Results for Group 18 Specimens	211
	3.1.1.19	Impact Results for Group 19 Specimens	220
3.2	IMPACT RESULTS ON ACTUAL BLADES		239
	3.2.1	Impact Results for Group 1B Blades	249
	3.2.2	Impact Results for Group 2B Blades	249
	3.2.3	Impact Results for Group 3B Blades	249
	3.2.4	Impact Results for Group 4B Blades	256
	3.2.5	Impact Results for Group 5B Blades	266
	3.2.6	Impact Results for Group 6B Blades	266
	3.2.7	Impact Results for Group 7B Blades	285
	3.2.8	Impact Results for Group 8B Blades	285
	3.2.9	Impact Results for Group 9B Blades	304

TABLE OF CONTENTS (Continued)

SECTION			PAGE
	3.2.10	Impact Results for Group 10B Blades	313
	3.2.11	Impact Results for Group 11B Blades	325
	3.2.12	Impact Results for Group 12B Blades	334
	3.2.13	Impact Results for Group 13B Blades	353
	3.2.14	Impact Results for Group 14B Blades	353
	3.2.15	Impact Results for Group 15B Blades	365
4	SUMMARY AND CONCLUSIONS		367
	REFERENCES		371
APPENDIX A - STRAIN GAGE LOCATIONS			373
APPENDIX B - TYPICAL DAMAGE FROM IMPACTS			389

LIST OF ILLUSTRATIONS

FIGURE		PAGE
1	Bird-Blade Interface Geometry	17
2	Method Used to Determine Twist for Each Group 19 Boron/Aluminum Specimen	24
3	Photograph Showing Preslicer Utilized	27
4	Photograph of Range Set-Up	28
5	Photograph of System Utilized to Restrain F101 Blade Tip	30
6	Moiré Fringe Displacement Data for Shot 4-0056 (Group 1 Specimen)	61
7	Sketch of Specimen Used in Shots for Displacement Data Utilizing the Moiré Fringe Apparatus	62
8	Strain of Shot 2-0131 for Gage #1	63
9	Strain of Shot 2-0131 for Gage #2	64
10	Strain of Shot 2-0131 for Gage #3	65
11	Strain of Shot 2-0131 for Gage #4	66
12	Strain of Shot 2-0131 for Gage #5	67
13	Strain of Shot 2-0131 for Gage #6	68
14	Sketch Showing Axis Orientation for All Tip Deflection Plots Using the High Speed Films	69
15	Tip Deflection Plot of Shot 2-0131	70
16	Tip Deflection Plot of Shot 2-0090	72
17	Tip Bow Plot of Shot 2-0090	73
18	Tip Deflection Plot of Shot 2-0091	74
19	Tip Deflection Plot of Shot 2-0093	75
20	Tip Deflection Plot of Shot 2-0094	76
21	Sequence of Frames of High Speed Film of Shot 2-0094	77

LIST OF ILLUSTRATIONS (Continued)

FIGURE		PAGE
22	Strain of Shot 2-0174 for Gage #1	78
23	Strain of Shot 2-0174 for Gage #2	79
24	Strain of Shot 2-0174 for Gage #3	80
25	Strain of Shot 2-0174 for Gage #4	81
26	Strain of Shot 2-0174 for Gage #5	82
27	Strain of Shot 2-0174 for Gage #6	83
28	Strain of Shot 2-0115 for Gage #1	85
29	Strain of Shot 2-0115 for Gage #2	86
30	Strain of Shot 2-0115 for Gage #3	87
31	Strain of Shot 2-0115 for Gage #4	88
32	Strain of Shot 2-0115 for Gage #5	89
33	Strain of Shot 2-0115 for Gage #6	90
34	Tip Reflection of "y" Direction for Shot 2-0115	91
35	Tip Reflection of "x" Direction for Shot 2-0115	92
36	Strain of Shot 2-0127 for Gage #1	93
37	Strain of Shot 2-0127 for Gage #2	94
38	Strain of Shot 2-0127 for Gage #3	95
39	Strain of Shot 2-0127 for Gage #4	96
40	Strain of Shot 2-0127 for Gage #5	97
41	Strain of Shot 2-0127 for Gage #6	98
42	Strain of Shot 2-0096 for Gage #1	100
43	Strain of Shot 2-0096 for Gage #2	101
44	Strain of Shot 2-0096 for Gage #3	102
45	Strain of Shot 2-0096 for Gage #4	103

LIST OF ILLUSTRATIONS (Continued)

FIGURE		PAGE
46	Strain of Shot 2-0096 for Gage #5	104
47	Strain of Shot 2-0096 for Gage #6	105
48	Tip Deflection for Shot 2-0096	106
49	Tip Deflection for Shot 2-0097	107
50	Tip Deflection for Shot 2-0098	108
51	Strain of Shot 2-0195 for Gage #1	109
52	Strain of Shot 2-0195 for Gage #2	110
53	Strain of Shot 2-0195 for Gage #3	111
54	Strain of Shot 2-0195 for Gage #4	112
55	Strain of Shot 2-0195 for Gage #5	113
56	Strain of Shot 2-0195 for Gage #6	114
57	Moiré Fringe Deflection Data for Shot 4-0054	116
58	Moiré Fringe Deflection Data for Shot 4-0055	117
59	Strain of Shot 2-0176 for Gage #1	118
60	Strain of Shot 2-0176 for Gage #2	119
61	Strain of Shot 2-0176 for Gage #3	120
62	Strain of Shot 2-0176 for Gage #4	121
63	Strain of Shot 2-0176 for Gage #5	122
64	Strain of Shot 2-0176 for Gage #6	123
65	Strain of Shot 2-0130 for Gage #1	125
66	Strain of Shot 2-0130 for Gage #2	126
67	Strain of Shot 2-0130 for Gage #3	127
68	Strain of Shot 2-0130 for Gage #4	128
69	Strain of Shot 2-0130 for Gage #5	129
70	Strain of Shot 2-0130 for Gage #6	130

LIST OF ILLUSTRATIONS (Continued)

FIGURE		PAGE
71	Tip Deflection in "y" Direction for Shot 2-0130	131
72	Tip Deflection in "x" Direction for Shot 2-0130	132
73	Tip Deflection Resultant Direction for Shot 2-0130	133
74	Strain of Shot 2-0167 for Gage #1	135
75	Strain of Shot 2-0167 for Gage #2	136
76	Strain of Shot 2-0167 for Gage #3	137
77	Strain of Shot 2-0167 for Gage #4	138
78	Strain of Shot 2-0167 for Gage #5	139
79	Strain of Shot 2-0167 for Gage #6	140
80	Tip Deflection in "y" Direction for Shot 2-0167	141
81	Tip Deflection in "x" Direction for Shot 2-0167	142
82	Tip Deflection Resultant for Shot 2-0167	143
83	Deflection Plot of "y" Versus "x" Direction of Various Times for Shot 2-0167	144
84	Strain of Shot 2-0190 for Gage #1	146
85	Strain of Shot 2-0190 for Gage #2	147
86	Strain of Shot 2-0190 for Gage #3	148
87	Strain of Shot 2-0190 for Gage #4	149
88	Strain of Shot 2-0190 for Gage #5	150
89	Strain of Shot 2-0190 for Gage #6	151
90	Tip Deflection in "y" Direction for Shot 2-0190	152
91	Tip Deflection in "x" Direction for Shot 2-0190	153
92	Strain of Shot 2-0177 for Gage #1	154
93	Strain of Shot 2-0177 for Gage #2	155

LIST OF ILLUSTRATIONS (Continued)

FIGURE		PAGE
94	Strain of Shot 2-0177 for Gage #3	156
95	Strain of Shot 2-0177 for Gage #4	157
96	Strain of Shot 2-0177 for Gage #5	158
97	Strain of Shot 2-0177 for Gage #6	159
98	Strain of Shot 2-0158 for Gage #1	161
99	Strain of Shot 2-0158 for Gage #2	162
100	Strain of Shot 2-0158 for Gage #3	163
101	Strain of Shot 2-0158 for Gage #4	164
102	Strain of Shot 2-0158 for Gage #5	165
103	Strain of Shot 2-0158 for Gage #6	166
104	Strain of Shot 2-0163 for Gage #1	168
105	Strain of Shot 2-0163 for Gage #2	169
106	Strain of Shot 2-0163 for Gage #3	170
107	Strain of Shot 2-0163 for Gage #4	171
108	Strain of Shot 2-0163 for Gage #5	172
109	Strain of Shot 2-0163 for Gage #6	173
110	Tip Deflection in "y" Direction for Shot 2-0163	174
111	Tip Deflection in "x" Direction for Shot 2-0163	175
112	Tip Deflection Resultant for Shot 2-0163	176
113	Strain of Shot 2-0161 for Gage #1	177
114	Strain of Shot 2-0161 for Gage #2	178
115	Strain of Shot 2-0161 for Gage #3	179
116	Strain of Shot 2-0161 for Gage #4	180
117	Strain of Shot 2-0161 for Gage #5	181

LIST OF ILLUSTRATIONS (Continued)

FIGURE		PAGE
118	Strain of Shot 2-0161 for Gage #6	182
119	Deflection of Tip in "y" Direction for Shot 2-0161	183
120	Deflection of Tip in "x" Direction for Shot 2-0161	184
121	Tip Deflection Resultant for Shot 2-0161	185
122	Strain of Shot 2-0135 for Gage #1	187
123	Strain of Shot 2-0135 for Gage #2	188
124	Strain of Shot 2-0135 for Gage #3	189
125	Strain of Shot 2-0135 for Gage #4	190
126	Strain of Shot 2-0135 for Gage #5	191
127	Strain of Shot 2-0135 for Gage #6	192
128	Deflection of Tip in "y" Direction for Shot 2-0135	193
129	Deflection of Tip in "x" Direction for Shot 2-0135	194
130	Strain of Shot 2-0149 for Gage #1	196
131	Strain of Shot 2-0149 for Gage #2	197
132	Strain of Shot 2-0149 for Gage #3	198
133	Strain of Shot 2-0149 for Gage #4	199
134	Strain of Shot 2-0149 for Gage #5	200
135	Strain of Shot 2-0149 for Gage #6	201
136	Strain of Shot 2-0142 for Gage #1	202
137	Strain of Shot 2-0142 for Gage #2	203
138	Strain of Shot 2-0142 for Gage #3	204
139	Strain of Shot 2-0142 for Gage #4	205
140	Strain of Shot 2-0142 for Gage #5	206

LIST OF ILLUSTRATIONS (Continued)

FIGURE		PAGE
141	Strain of Shot 2-0142 for Gage #6	207
142	Deflection of Tip in "y" Direction for Shot 2-0142	208
143	Deflection of Tip in "x" Direction for Shot 2-0142	209
144	Tip Deflection Resultant for Shot 2-0142	210
145	Strain of Shot 2-0212 for Gage #1	212
146	Strain of Shot 2-0212 for Gage #2	213
147	Strain of Shot 2-0212 for Gage #3	214
148	Strain of Shot 2-0212 for Gage #4	215
149	Strain of Shot 2-0212 for Gage #5	216
150	Strain of Shot 2-0212 for Gage #6	217
151	Tip Deflection in "y" Direction for Shot 2-0212	218
152	Tip Deflection in "y" Direction for Shot 2-0212	219
153	Strain of Shot 2-0144 for Gage #1	221
154	Strain of Shot 2-0144 for Gage #2	222
155	Strain of Shot 2-0144 for Gage #3	223
156	Strain of Shot 2-0144 for Gage #4	224
157	Strain of Shot 2-0144 for Gage #5	225
158	Strain of Shot 2-0144 for Gage #6	226
159	Tip Deflection in "y" Direction for Shot 2-0144	227
160	Tip Deflection in "x" Direction for Shot 2-0144	228
161	Tip Deflection Resultant for Shot 2-0144	229
162	Strain of Shot 2-0147 for Gage #1	230

LIST OF ILLUSTRATIONS (CONTINUED)

FIGURE		PAGE
163	Strain of Shot 2-0147 for Gage #2	231
164	Strain of Shot 2-0147 for Gage #3	232
165	Strain of Shot 2-0147 for Gage #4	233
166	Strain of Shot 2-0147 for Gage #5	234
167	Strain of Shot 2-0147 for Gage #6	235
168	Tip Deflection in "y" Direction for Shot 2-0147	236
169	Tip Deflection in "x" Direction for Shot 2-0147	237
170	Tip Deflection Resultant for Shot 2-0147	238
171	Strain of Shot 2-0018 for Gage #1	250
172	Strain of Shot 2-0018 for Gage #2	251
173	Strain of Shot 2-0018 for Gage #4	252
174	Strain of Shot 2-0018 for Gage #5	253
175	Strain of Shot 2-0018 for Gage #6	254
176	Strain of Shot 2-0018 for Gage #9	255
177	Strain of Shot 2-0019 for Gage #9	257
178	Strain Rate of Shot 2-0019 for Gage #9	258
179	Strain of Shot 2-0020 for Gage #1	259
180	Strain of Shot 2-0020 for Gage #4	260
181	Strain of Shot 2-0020 for Gage #5	261
182	Strain of Shot 2-0020 for Gage #6	262
183	Strain of Shot 2-0020 for Gage #7	263
184	Strain of Shot 2-0020 for Gage #9	264
185	Strain Rate of Shot 2-0020 for Gage #9	265
186	Strain of Shot 2-0201 for Gage #1	267
187	Strain of Shot 2-0201 for Gage #2	268

LIST OF ILLUSTRATIONS (Continued)

FIGURE		PAGE
188	Strain of Shot 2-0201 for Gage #3	269
189	Strain of Shot 2-0201 for Gage #4	270
190	Strain of Shot 2-0201 for Gage #5	271
191	Strain of Shot 2-0201 for Gage #6	272
192	Strain of Shot 2-0198 for Gage #1	273
193	Strain of Shot 2-0198 for Gage #2	174
194	Strain of Shot 2-0198 for Gage #3	275
195	Strain of Shot 2-0198 for Gage #4	276
196	Strain of Shot 2-0198 for Gage #5	277
197	Strain of Shot 2-0198 for Gage #6	278
198	Strain of Shot 2-0231 for Gage #1	279
199	Strain of Shot 2-0231 for Gage #2	280
200	Strain of Shot 2-0231 for Gage #3	281
201	Strain of Shot 2-0231 for Gage #4	282
202	Strain of Shot 2-0231 for Gage #5	283
203	Strain of Shot 2-0231 for Gage #6	284
204	Strain of Shot 2-0009 for Gage #1	286
205	Strain of Shot 2-0009 for Gage #4	287
206	Strain of Shot 2-0009 for Gage #5	288
207	Strain of Shot 2-0009 for Gage #6	289
208	Strain of Shot 2-0009 for Gage #7	290
209	Strain of Shot 2-0009 for Gage #8	291
210	Strain of Shot 2-0010 for Gage #1	292
211	Strain of Shot 2-0010 for Gage #4	293
212	Strain of Shot 2-0010 for Gage #5	294

LIST OF ILLUSTRATIONS (Continued)

FIGURE		PAGE
213	Strain of Shot 2-0010 for Gage #6	295
214	Strain of Shot 2-0010 for Gage #7	296
215	Strain of Shot 2-0010 for Gage #8	297
216	Strain of Shot 2-0021 for Gage #1	298
217	Strain of Shot 2-0021 for Gage #2	299
218	Strain of Shot 2-0021 for Gage #3	300
219	Strain of Shot 2-0021 for Gage #4	301
220	Strain of Shot 2-0021 for Gage #5	302
221	Strain of Shot 2-0021 for Gage #6	303
222	Strain of Shot 2-0014 for Gage #6	305
223	Strain Rate of Shot 2-0014 for Gage #6	306
224	Strain of Shot 2-0011 for Gage #1	307
225	Strain of Shot 2-0011 for Gage #4	308
226	Strain of Shot 2-0011 for Gage #5	309
227	Strain of Shot 2-0011 for Gage #6	310
228	Strain of Shot 2-0011 for Gage #7	311
229	Strain of Shot 2-0011 for Gage #8	312
230	Strain of Shot 2-0024 for Gage #1	314
231	Strain of Shot 2-0024 for Gage #2	315
232	Strain of Shot 2-0024 for Gage #3	316
233	Strain of Shot 2-0024 for Gage #4	317
234	Strain of Shot 2-0024 for Gage #5	318
235	Strain of Shot 2-0024 for Gage #6	319
236	Strain Rate of Shot 2-0024 for Gage #3	320

LIST OF ILLUSTRATIONS (Continued)

FIGURE		PAGE
237	Leading Edge Tip Deflection in "y" Direction for Shot 2-0024	321
238	Leading Edge Tip Deflection in "x" Direction for Shot 2-0024	322
239	Trailing Edge Tip Deflection in "y" Direction for Shot 2-0024	323
240	Trailing Edge Tip Deflection in "x" Direction for Shot 2-0024	324
241	Strain of Shot 2-0219 for Gage #1	326
242	Strain of Shot 2-0219 for Gage #2	327
243	Strain of Shot 2-0219 for Gage #3	328
244	Strain of Shot 2-0219 for Gage #4	329
245	Strain of Shot 2-0219 for Gage #5	330
246	Strain of Shot 2-0219 for Gage #6	331
247	Tip Deflection in "y" Direction for Shot 2-0219	332
248	Tip Deflection in "x" Direction for Shot 2-0219	333
249	Strain of Shot 2-0234 for Gage #1	335
250	Strain of Shot 2-0234 for Gage #2	336
251	Strain of Shot 2-0234 for Gage #3	337
252	Strain of Shot 2-0234 for Gage #4	338
253	Strain of Shot 2-0234 for Gage #5	339
254	Strain of Shot 2-0234 for Gage #6	340
255	Tip Deflection in "y" Direction for Shot 2-0234	341
256	Tip Deflection in "x" Direction for Shot 2-0234	342

LIST OF ILLUSTRATIONS (Continued)

FIGURE		PAGE
257	Strain of Shot 2-0023 for Gage #1	343
258	Strain of Shot 2-0023 for Gage #4	344
259	Strain of Shot 2-0023 for Gage #5	345
260	Strain of Shot 2-0023 for Gage #6	346
261	Strain of Shot 2-0023 for Gage #7	347
262	Strain of Shot 2-0023 for Gage #8	348
263	Leading Edge Tip Deflection in "y" Direction for Shot 2-0023	349
264	Leading Edge Tip Deflection in "x" Direction for Shot 2-0023	350
265	Trailing Edge Tip Deflection in "y" Direction for Shot 2-0023	351
266	Trailing Edge Tip Deflection in "x" Direction for Shot 2-0023	352
267	Strain of Shot 2-0022 for Gage #1	354
268	Strain of Shot 2-0022 for Gage #2	355
269	Strain of Shot 2-0022 for Gage #3	356
270	Strain of Shot 2-0022 for Gage #4	357
271	Strain of Shot 2-0022 for Gage #5	358
272	Strain of Shot 2-0022 for Gage #6	359
273	Strain Rate of Shot 2-0022 for Gage #6	360
274	Leading Edge Tip Deflection in "y" Direction for Shot 2-0022	361
275	Leading Edge Tip Deflection in "x" Direction for Shot 2-0022	362
276	Trailing Edge Tip Deflection in "y" Direction for Shot 2-0022	363
277	Trailing Edge Tip Deflection in "x" Direction for Shot 2-0022	364

LIST OF ILLUSTRATIONS (Continued)

FIGURE		PAGE
1A	Strain Gage Locations for Group 1B, 2B, 3B, and 4B Blades	373
2A	Strain Gage Locations for Group 6B, 7B, 8B, and 9B Blades	374
3A	Strain Gage Locations for Group 12B and 13B Blades	375
4A	Strain Gage Locations for Group 4B and 5B Blades	376
5A	Strain Gage Locations for Group 14B and 15B Blades	377
6A	Strain Gage Locations for Group 10B and 11B Blades	378
7A	Strain Gage Locations for Group 1, 2, and 6 Structural Element Test Specimens	379
8A	Strain Gage Locations for Group 3, 7, 8, and 9 Structural Element Test Specimens	380
9A	Strain Gage Locations for Group 4 Structural Element Test Specimens	381
10A	Strain Gage Locations for Group 5 Structural Element Test Specimens	382
11A	Strain Gage Locations for Group 10 Structural Element Test Specimens	383
12A	Strain Gage Locations for Group 11, 12, and 13 Structural Element Test Specimens	384
13A	Strain Gage Locations for Group 14 and 16 Structural Element Test Specimens	385
14A	Strain Gage Locations for Group 15 Structural Element Test Specimens	386
15A	Strain Gage Locations for Group 17 Structural Element Test Specimens	387
16A	Strain Gage Locations for Group 18 and 19 Structural Element Test Specimens	388

LIST OF ILLUSTRATIONS (Continued)

FIGURE		PAGE
1B	Damage for Group 1 Titanium Specimen Due to 85 g (3 ounce) Artificial Bird Impact (Shot 4-0056)	389
2B	Damage for Group 1 Titanium Specimen for 85 g (3 ounce) Artificial Bird Impact (Shot 4-0052)	390
3B	Specimen Due to 85 g (3 ounce) Artificial Bird Impact (Shot 2-0131)	391
4B	Damage for Group 2 Titanium Specimen for 5.08 cm Diameter Ice Ball Impact (Shot 2-0173)	392
5B	Damage for Group 2 Titanium Specimen for 5.08 cm Diameter Ice Ball Impact (Shot 2-0174)	393
6B	Damage for Group 3 Titanium Specimen for 85 g (3 ounce) Artificial Bird Impact (Shot 2-0127)	394
7b	Damage for Group 4 Titanium Specimen for 85 g (3 ounce) Artificial Bird Impact (Shot 2-0096)	394
8B	Damage for Group 4 Titanium Specimen for 85 g (3 ounce) Artificial Bird Impact (Shot 2-0097)	395
9B	Damage for Group 4 Titanium Specimen for 85 g (3 ounce) Artificial Bird Impact (Shot 2-0098)	395
10B	Damage for Group 6 Titanium Specimen for 85 g (3 ounce) Artificial Bird Impact (Shot 4-0053)	396
11B	Damage for Group 6 Titanium Specimen for 85 g (3 ounce) Artificial Bird Impact (Shot 4-0054)	397
12B	Damage for Group 6 Titanium Specimen for 85 g (3 ounce) Artificial Bird Impact (Shot 4-0055)	398
13B	Damage for Group 6 Titanium Specimen for 85 g (3 ounce) Artificial Bird Impact (Shot 2-0175)	399

LIST OF ILLUSTRATIONS (Continued)

FIGURE		PAGE
14B	Damage for Group 6 Titanium Specimen for 85 g (3 ounce) Artificial Bird Impact (Shot 2-0176).	399
15B	Damage for Group 7 Titanium Specimen Due to 85 g (3 ounce) Artificial Bird Impact (Shot 2-0128).	400
16B	Damage for Group 7 Titanium Specimen Due to 85 g (3 ounce) Artificial Bird Impact (Shot 2-0129).	401
17B	Damage for Group 7 Titanium Specimen Due to 85 g (3 ounce) Artificial Bird Impact (Shot 2-0130).	401
18B	Damage for Group 8 Titanium Specimen Due to 85 g (3 ounce) Artificial Bird Impact (Shot 2-0166).	402
19B	Damage for Group 8 Titanium Specimen Due to 85 g (3 ounce) Artificial Bird Impact (Shot 2-0167).	403
20B	Damage for Group 9 Titanium Specimen Due to 680 g (1.5 pound) Artificial Bird Impact (Shot 2-0180).	404
21B	Damage for Group 9 Titanium Specimen Due to 680 g (1.5 pound) Artificial Bird Impact (Shot 2-0192).	405
22B	Damage for Group 10 Titanium Specimen Due to 85 g (3 ounce) Artificial Bird Impact (Shot 2-0177).	406
23B	Damage for Group 10 Titanium Specimen Due to 85 g (3 ounce) Artificial Bird Impact (Shot 2-0179).	406
24B	Damage for Group 11 Stainless Steel Specimen Due to 680 g (1.5 pound) Artificial Bird Impact (Shot 2-0157).	407
25B	Damage for Group 11 Stainless Steel Specimen Due to 680 g (1.5 pound) Artificial Bird Impact (Shot 2-0158).	408

FIGURE		PAGE
26B	Damage for Group 12 Stainless Steel Specimen Due to 680 g (1.5 pound) Artificial Bird Impact (Shot 2-0159).	409
27B	Damage for Group 12 Stainless Steel Specimen Due to 680 g (1.5 pound) Artificial Bird Impact (Shot 2-0163).	410
28B	Damage for Group 13 Stainless Steel Specimen Due to 680 g (1.5 pound) Artificial Bird Impact (Shot 2-0161).	411
29B	Damage for Group 13 Stainless Steel Specimen Due to 680 g (1.5 pound) Artificial Bird Impact (Shot 2-0162).	412
30B	Damage for Group 14 Boron/Aluminum Composite Specimen Due to 85 g (3 ounce) Artificial Bird Impact (Shot 2-0139).	413
31B	Damage for Group 15 Boron/Aluminum Composite Specimen Due to 85 g (3 ounce) Artificial Bird Impact (Shot 2-0149).	414
32B	Damage for Group 15 Boron/Aluminum Composite Specimen Due to 85 g (3 ounce) Artificial Bird Impact (Shot 2-0150).	415
33B	Damage for Group 15 Boron/Aluminum Composite Specimen Due to 85 g (3 ounce) Artificial Bird Impact (Shot 2-0151).	416
34B	Damage for Group 16 Boron/Aluminum Composite Specimen Due to 85 g (3 ounce) Artificial Bird Impact (Shot 2-0138).	417
35B	Damage for Group 16 Boron/Aluminum Composite Specimen Due to 85 g (3 ounce) Artificial Bird Impact (Shot 2-0140).	418
36B	Damage for Group 16 Boron/Aluminum Composite Specimen Due to 85 g (3 ounce) Artificial Bird Impact (Shot 2-0141).	419
37B	Damage for Group 16 Boron/Aluminum Composite Specimen Due to 85 g (3 ounce) Artificial Bird Impact (Shot 2-0142).	420

LIST OF ILLUSTRATIONS (Continued)

FIGURE		PAGE
38B	Damage for Group 17 Boron/Aluminum Composite Specimen Due to 85 g (3 ounce) Artificial Bird Impact (Shot 2-0213).	421
39B	Damage for Group 18 Boron/Aluminum Composite Specimen Due to 85 g (3 ounce) Artificial Bird Impact (Shot 2-0144).	422
40B	Damage for Group 18 Boron/Aluminum Composite Specimen Due to 85 g (3 ounce) Artificial Bird Impact (Shot 2-0145).	423
41B	Damage for Group 19 Boron/Aluminum Composite Specimen Due to 85 g (3 ounce) Artificial Bird Impact (Shot 2-0146).	424
42B	Damage for Group 19 Boron/Aluminum Composite Specimen Due to 85 g (3 ounce) Artificial Bird Impact (Shot 2-0147).	425
43B	Damage for Group 1? Boron/Aluminum Composite Specimen Due to 85 g (3 ounce) Artificial Bird Impact (Shot 2-0148).	426
44B	Damage for Group 3B F101 Titanium Blade Due to 680 g (1.5 pound) Artificial Bird Impact (Shot 2-0019).	427
45B	Damage for Group 4B F101 Titanium Blade Due to 680 g (1.5 pound) Artificial Bird Impact (Shot 2-0020).	428
46B	Damage for Group 4B F101 Titanium Blade Due to 680 g (1.5 pound) Artificial Bird Impact (Shot 2-0201).	429
47B	Damage for Group 5B F101 Titanium Blade Due to Ice Cylinder (Slab Ice) Impact (Shot 2-0231).	430
48B	Damage for Group 7B J79 Stainless Steel Blade Due to 85 g (3 ounce) Artificial Bird Impact (Shot 2-0021).	431
49B	Damage for Group 8B J79 Stainless Steel Blade to 680 g (1.5 pound) Artificial Bird Impact (Shot 2-0015).	432

LIST OF ILLUSTRATIONS (Continued)

FIGURE		PAGE
50B	Damage for Group 9B J79 Stainless Steel Blade Due to 680 g (1.5 pound) Artificial Bird Impact (Shot 2-0024).	433
51B	Damage for Group 10B J79 Stainless Steel Blade Due to 5.08 cm (2.0 inch) Ice Ball Impact (Shot 2-0222).	434
52B	Damage for Group 10B J79 Stainless Steel Blade Due to 5.08 cm (2.0 inch) Ice Ball Impact (Shot 2-0226).	435
53B	Damage for Group 11B J79 Stainless Steel Blade Due to Ice Cylinder (Slab Ice) Impact (Shot 2-0235).	436
54B	Damage for Group 12B APSI Boron/Aluminum Composite Blade Due to 85 g (3 ounce) Artificial Bird Impact (Shot 2-0016).	437
55B	Damage for Group 12B APSI Boron/Aluminum Composite Blade Due to 85 g (3 ounce) Artificial Bird Impact (Shot 2-0023).	438
56B	Damage for Group 13B APSI Boron/Aluminum Composite Blade Due to 85 g (3 ounce) Artificial Bird Impact (Shot 2-0022).	439
57B	Damage for Group 14B APSI Boron/Aluminum Composite Blade Due to 5.08 cm (2.0 inch) Ice Ball Impact (Shot 2-0216).	440
58B	Damage for Group 14B APSI Boron/Aluminum Composite Blade Due to 5.08 cm (2.0 inch) Ice Ball Impact (Shot 2-0218).	441
59B	Damage for Group 15B APSI Boron/Aluminum Composite Blade Due to Ice Cylinder (Slab Ice) Impact (Shot 2-0233).	442

LIST OF TABLES

TABLE		PAGE
1	IMPACT PARAMETERS	5
2	BLADE PARAMETERS	5
3	BASELINE TEST CONDITIONS FOR TITANIUM SPECIMENS	8
4	IMPACT TESTS FOR STAINLESS STEEL SPECIMENS	8
5	TEST CONDITIONS FOR BORON/ALUMINUM COMPOSITE SPECIMENS	9
6	PARAMETRIC MATRIX DEFINING STRUCTURAL ELEMENTS AND IMPACTS CONDITIONS	10
7	SHAPE,SIZE, AND CONFIGURATION DETAILS OF STRUCTURAL ELEMENTS	11
8	MATRIX AND TEST CONDITIONS FOR ACTUAL BLADE IMPACTS	15
9	GENERAL EQUATIONS UTILIZED TO DETERMINE TEST CONDITIONS	19
10	TEST CONDITIONS FOR STARLING IMPACT	20
11	TEST CONDITIONS FOR LARGE BIRD (680 g) IMPACT	21
12	PREIMPACT TWIST MEASUREMENTS FOR GROUP 19 BORON/ALUMINUM STRUCTURAL ELEMENT SPECIMENS	25
13	RESULTS OF STATIC IMPACT TESTING	37
14	RESULTS OF STATIC IMPACT TESTING ON ACTUAL BLADES	240

UNIVERSITY OF DAYTON
RESEARCH INSTITUTE
DAYTON, OHIO 45469

SECTION 1
INTRODUCTION

Turbine blade damage resulting from the ingestion of foreign objects is a real threat to aircraft operation and an obstacle to the development of more efficient engines. Foreign objects range from large birds and ice to small hard particles such as sand. Impacts will almost always cause at least localized minor damage that may be corrected by maintenance procedures. Impact damage to blades may also be severe enough to cause catastrophic failure of an engine, resulting in immediate power loss, and jeopardizing the entire aircraft.

The threat is inevitably associated by the environment in which the engine is constrained to operate. Engine speed, blade material, blade geometry, point of impact, and type and size of the impactor all play important roles in determining the nature and severity of damage which might occur. The blade designers' task is to either design a blade which has a specified level of resistance to foreign object damage (FOD) or to evaluate a given blade and predict the extent of damage to be expected from a particular threat.

The FOD response of fan blades can be divided into two separate problem areas. One concerns the local blade damage and the second deals with the structural damage. Local damage occurs during the impact event and is confined to within several projectile diameters of the center of the impact site. Structural damage occurs at later times and at points which are, in general, well away from the impact site.

The overall design problem has two aspect The first aspect is a ballistic impact problem. In this instance, a

method must be developed to relate the mode and extent of damage to the threat and target parameters. The second aspect of the design problem is to relate the ballistic impact induced damage to the residual properties of the blade. It is the degradation of the mechanical properties of the blade that is ultimately the most serious consequence of an FOD event.

This report describes the results of an experimental program concerned with performing nonrotating bench impact tests on test specimens of simple cantilevered beams and plates to real blades. This study was carried out under Task VI "Structural Element Tests", which is part of the overall program "Foreign Object Impact Damage Criteria". The simple elements, such as beams and plates, were to be tested with progressive introduction of airfoil geometric parameters to validate experimentally the analytical predictions of Tasks V and VIII of the overall program. The purpose of Task V is to derive parametric relationships describing the changes in dynamic structural response of impacted simple elements such as plates and beams with the progressive introduction of blade airfoil geometric features. The purpose of Task VIII is to derive criteria for predicting foreign object impact damage tolerance.

Because of the enormous amount of data generated in this Task VI work, the reporting was divided into two separate volumes. This report (Volume I) describes the results of all the impact tests; however, the strain gage results are given only for selected impacts and only for the first 9 ms of the impact event. Volume II of the report contains all of the complete strain and strain rate data.

SECTION 2
EXPERIMENTAL PROGRAM

The experimental program involved conducting nonrotating bench impact tests on test specimens ranging from simple cantilevered beams and plates to real blades. The response of the test specimens to impacts of substitute birds or ice was determined in the testing. Three types of blade materials, geometries, and sizes were investigated using ice and substitute bird materials as the impactors. The impactors were gun launched to impact the leading edge of the test specimens in the majority of the testing.

2.1 STUDY OBJECTIVES AND APPROACH

The overall objective of this study was to experimentally determine the response (both local and structural) of the various blade materials investigated. The data collected from the impact tests included accurate impact conditions, dynamic displacement of the specimens at discreet points, strain/time histories local to the impact site and at critical blade stress regions identified from the structural response models, pretest and post-test material properties, and damage assessment. The simple elements were tested with progressive introduction of airfoil geometric parameters to validate experimentally the analytical predictions of Tasks V and VIII. Impact tests were also conducted on real blades to derive a correlation between structural element blades to derive a correlation between structural element specimens and full-scale blades.

The purpose of Task V was to derive parametric relationships describing the changes in dynamic structural response of impacted simple elements such as plates and beams with the progressive introduction of blade airfoil geometric features. The purpose of Task VI was to obtain empirical data showing how dynamic structural response of impacted simple elements

such as plates and beams is affected by the progressive introduction of blade airfoil geometric features. The purpose of Task VIII was to derive criteria for predicting blade foreign object impact damage tolerance. This criteria will be formulated by General Electric Company to make full use of the transient dynamic analysis and experimental results obtained from all the tasks of the overall program. It is anticipated that this criteria will be based on the combination of theory and regression analysis.

The three blade types investigated in the study were the J79 blade using 403 stainless steeel; the F101 blade using 8Al-1MO-1V (8-1-1) titanium; and the APSI metal matrix boron/aluminum blade. The geometries of the test specimens were similar to the geometries at the 50 percent span location of the three blade types investigated. For example, the material, leading edge thickness, trailing edge thickness, taper angle, specimen thickness, width, and span length of the test specimens were identical to that of the actual blades at the 50 percent span location.

A baseline series of tests was conducted on the titanium material, a supplementary series was conducted on the stainless steel material, and a more complete series was conducted on the advanced composite material. Titanium was chosen as the baseline material, as it is the most common current blade material. Stainless steel, being a metal, was ancitipated to behave basically similar to titanium and would not require such complete investigation. The composite material was expected to behave significantly different from the metals and a more thorough investigation would be required.

A list of the impact parameters used in the impact tests is presented in Table 1. Four impact masses corresponding to 85 g (3 ounce) birds, 680 g (1.5 pound) birds, 50.8 mm (2-inch) ice balls, and 750 g (1.65 pound) ice slabs were used in the testing. The impact velocity was varied from a low

TABLE 1. IMPACT PARAMETERS

Mass	85 g (3 ounce) bird	M_1	(4)
	680 g (1.5 pound) bird	M_2	
	50.8 mm (2.0-inch) ice ball	M_3	
	750 g (1.65 pound) slab ice	M_4	
Impact Velocity	No damage	V_1	(3)
	Threshold damage	V_2	
	Severe damage	V_3	
Location	70% span level		(2)
	30% span level		
Impact Angle	Center-normal		
	Leading edge - oblique		

TABLE 2. BLADE PARAMETERS

Basic Geometry/ Materials	J79 - 403 stainless steel	(3)
	F101-8-1-1 titanium	
	APSI - boron/aluminum composite	
Blade Geometry Parameters	Aspect Ratio (1/2 blade-like, blade-like)	(2)
	Thickness/Chord Ratio (1/2 blade-like, blade-like)	(3)
	Shape (constant thickness, airfoil, blade-like)	(3)
	Shrouds (none, blade-like)	(2)
	Camber (none, blade-like)	(2)
	Twist (none, blade-like)	(2)

velocity range to generate elastic deformation response of the target specimens (no damage), through a medium range to generate plastic deformation (threshold damage), and finally, to a high velocity range where plastic/tear deformations were produced (severe damage). Impact locations and angles on the target specimens were varied to validate the Task V analysis for both center (normal) and leading edge (oblique) impact effects. Two span locations of 70 to 30 percent levels were investigated in the testing.

A list of the blade parameters that are considered to be important to the blade structural response to impacts is presented in Table 2. As indicated earlier, the three blade types which were investigated included, the J79 blade using 403 stainless steel, the F101 blade using 8-1-1 titanium, and the APSI blade using boron/aluminum as the composite material. These three first stage blades selected for modeling and impact testing are representative of first stage airfoils from Air Force inventory (J79), production development (F101) and boron/aluminum blades, respectively. The only shrouded blade is the F101 blade which has a tip shroud.

The real blade geometry effects which are believed to effect impact response were independently introduced in the testing and analysis. These effects include aspect ratio, thickness to chord ratio, shape, shrouds, camber, and twist. As indicated earlier, the geometries of the test specimens were similar of the three blade types at the 50 percent span level.

If all of these impact and blade parameters of Tables 1 and 2 were investigated separately and independently, then a total of 13,824 test conditions would have to be considered. This is not a reasonable number of calculations or impact tests to conduct and the number was reduced in a logical manner. The study was conducted by progressively (in series) adding the blade geometry variables to reduce the number of independent specimen geometries for each material. Also, fewer impact

tests were conducted for parameters which were anticipated to show a high degree of correlation with analysis, while additional shots were conducted where the degree of correlation with analysis was expected to be low. The blade geometry variables were incorporated in the order shown in Table 2.

As indicated earlier, the titanium material was used as the baseline material. The test conditions of the impact tests conducted on the titanium material are summarized in Table 3. This baseline series of impact tests considered all impact conditions and the blade geometrical effects were introduced progressively (not independently) except camber and twist. It was established early in the study that camber and twist would be very expensive to incorporate on titanium; therefore, camber and twist would be investigated utilizing stainless steel and the composite specimens. The impact tests for all the materials were conducted at ambient temperature conditions.

The supplementary series of impact tests on 403 stainless steel specimens is summarized in Table 4. The basic behavior of stainless steel was assumed to be similar to that of the titanium material. Ice impactors were also considered not to be an important threat on the stainless steel specimens, therefore ice impacts were not considered. As indicated earlier, the camber and twist blade parameters were investigated using the stainless steel specimens. The camber and twist blade parameters were introduced progressively (not independently). In addition, flat specimens with a bladelike aspect ratio were also investigated in regards to their response to oblique bird impacts. Only 680 g (1.5 pound) substitute bird impacts were considered in the impact testing of the stainless steel specimens. All the impacts were conducted at the 70 percent span location with the impacts being oblique leading edge impacts.

The boron/aluminum composite material specimen series of impact tests is outlined in Table 5. The composite material was considered to behave quite differently from the metals; therefore,

TABLE 3. BASELINE TEST CONDITIONS FOR TITANIUM SPECIMENS

Impact Parameters	Mass (85 g and 680 g birds, 50.8 mm ice balls)	(3)
	Impact Velocity (no damage, threshold damage, severe damage)	(3)
	Location/Angle (70% span/ Center-normal; Edge-oblique)	(2)
	(30% span/Center-normal; Edge-oblique)	(2)
Blade Geometry Parameters	Aspect Ratio (1/2 blade-like, blade-like)	(2)
	Thickness/Chord Ratio (1/2 blade-like, blade-like)	(2)
	Shape (constant thickness, airfoil, blade-like)	(3)
	Shrouds (none, blade-like)	(2)

TABLE 4. IMPACT TESTS FOR STAINLESS STEEL SPECIMENS

Impact Parameters	Mass (680 g birds)	(1)
	Impact velocity (no damage, threshold damage, severe damage)	(3)
	Location Angle (70% span/ edge-oblique)	(1)
Blade Geometry Parameters	Aspect Ratio (blade-like)	(1)
	Shape (constant thickness)	
	Camber	(1)
	Twist	(1)

TABLE 5. TEST CONDITIONS FOR BORON/ALUMINUM COMPOSITE SPECIMENS

Impact Parameters	Mass (85 g bird)
	Impact Velocity (no damage, threshold damage, severe damage)
	Location Angle (70% span/edge-oblique)
Blade Geometry Parameters	Aspect Ratio (1/2 blade-like, blade-like)
	Thickness/Chord Ratio (1/2 blade-like, blade-like)
	Shape (constant thickness, blade-like
	Camber
	Twist

all the impact conditions were given consideration. The only projectile considered was the 85 g (3 ounce) substitute bird. All of the impacts were leading edge oblique impacts at the 70 percent span location on the specimens. The blade parameters investigated included the aspect ratio, thickness to chord ratio, shape, camber, and twist. Again, as for the titanium material, the blade geometrical effects were introduced progressively (not independently).

The test matrix for the impacts on the various material specimens is described in Table 6. Testing is organized into groups. For each group of tests, specimen size, impact location, impactor geometry, impactor type and size, and angle of incidence were fixed. The velocity was varied to obtain no damage, threshold damage, and severe damage on the specimens. The table describes the structural elements, element fixity and material, the loading and impactor, and the impact location and angle for each group. Details of the shape, size and configuration of the structural elements are provided in Table 7. The structural

TABLE 6. PARAMETRIC MATRIX DEFINING STRUCTURAL ELEMENTS AND IMPACTS CONDITIONS

Group Number	Structural Element and Comments	Impactor	Impact Location	Impact Incidence	Shroud Restraint	Specimen Material
1	Flat Plate with Blade-Type Aspect Ratio	85 g (3 ounce) Bird	Center Impact @ 70% Span	Normal	No	Ti 8-1-1
2	Same as Group 1	50.8 mm (2 inch) Ice Ball	Edge Impact @ 30% Span	Oblique	No	Ti 8-1-1
3	Same as Group 1	85 g (3 ounce) Bird	Edge Impact @ 70% Span	Oblique	No	Ti 8-1-1
4	Flat Plate with One-Half Blade-Type Aspect Ratio	85 g (3 ounce) Bird	Center Impact @ 70% Span	Normal	No	Ti 8-1-1
5	Same as Group 4	680 g (1.5 lb) Bird	Edge Impact @ 30% Span	Oblique	No	Ti 8-1-1
6	Flat Plate with Blade-Type Aspect Ratio and One-Half Blade-Type Thickness/Chord Ratio	85 g (3 ounce) Bird	Center Impact @ 70% Span	Normal	No	Ti 8-1-1
7	Plate with Blade-Type Aspect Ratio and Airfoil (Tapered Cross Section)	85 g (3 ounce) Bird	Edge Impact @ 70% Span	Oblique	No	Ti 8-1-1
8	Same as Group 7	680 g (1.5 lb) Bird	Edge Impact @ 70% Span	Oblique	No	Ti 8-1-1
9	Plate with Blade-Type Aspect Ratio and Bladelike Cross Section	680 g (1.5 lb) Bird	Edge Impact @ 70% Span	Oblique	No	Ti 8-1-1
10	Same as Group 9	85 g (3 ounce) Bird	Center Impact @ 70% Span	Normal	Yes	Ti 8-1-1
11	Flat Plate with Blade-Type Aspect Ratio	680 g (1.5 lb) Bird	Edge Impact @ 70% Span	Oblique	No	403 Stainless Steel
12	Cambered Flat Plate with Blade-Type Aspect Plate	680g (1.5 lb) Bird	Edge Impact @ 70% Span	Oblique	No	403 Stainless Steel
13	Cambered Twisted Flat Plate with Blade-Type Aspect Ratio	680 g (1.5 lb) Bird	Edge Impact @ 70% Span	Oblique	No	403 Stainless Steel
14	Cross Ply Flat Panel with Blade-Type Aspect Ratio	85 g (3 ounce) Bird	Edge Impact @ 70% Span	Oblique	No	Boron/ Aluminum
15	Cross Ply Flat Panel with One-Half Blade-Type Aspect Ratio	85 g (3 ounce) Bird	Edge Impact @ 70% Span	Oblique	No	Boron/ Aluminum
16	Cross Ply Flat Panel with Blade-Type Aspect Ratio and One-Half Blade-Type Thickness to Chord Ratio	85 g (3 ounce) Bird	Edge Impact @ 70% Span	Oblique	No	Boron/ Aluminum
17	Cross Ply Panel with Blade-Type Aspect Ratio and Bladelike Cross Section	85 g (3 ounce) Bird	Edge Impact @ 70% Span	Oblique	No	Boron/ Aluminum
18	Cross Ply Flat Panel with Blade-Type Aspect Ratio and Camber	85 g (3 ounce) Bird	Edge Impact @ 70% Span	Oblique	No	Boron/ Aluminum
19	Cross Ply Flat Panel with Blade-Type Aspect Ratio with Camber and Twist	85 g (3 ounce) Bird	Edge Impact @ 70% Span	Oblique	No	Boron/ Aluminum

TABLE 7. SHAPE, SIZE, AND CONFIGURATION DETAILS OF STRUCTURAL ELEMENTS

Groups	Specimen Span Length (mm)	Specimen Cross Section	Specimen Material
1-3 4-5	311.150 155.575	Specimen Cross Section #1 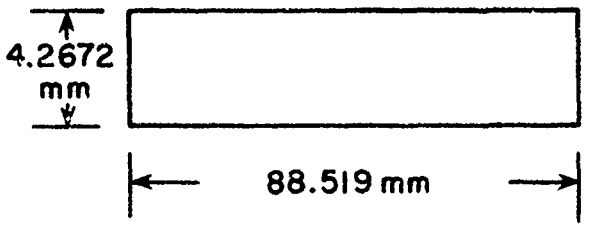	Ti 8-1-1
6	311.150	Specimen Cross Section #2 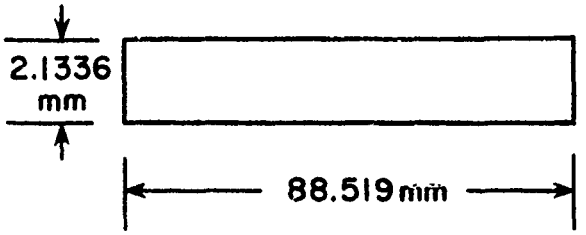	Ti 8-1-1
7-8	311.150	Specimen Cross Section #3 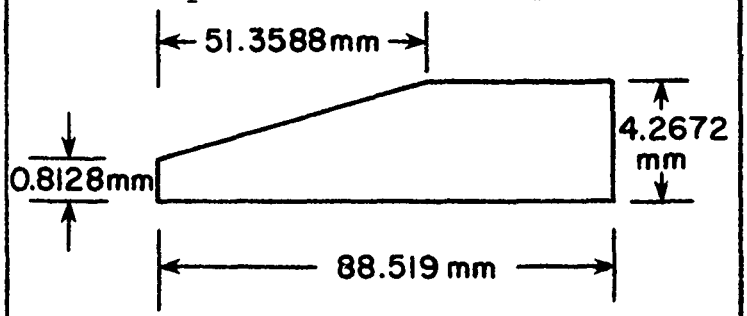	Ti 8-1-1
9-10	311.150	Specimen Cross Section #4 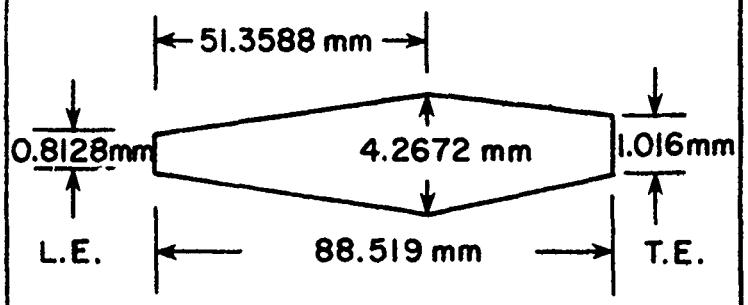	Ti 8-1-1

TABLE 7. SHAPE, SIZE, AND CONFIGURATION DETAILS OF STRUCTURAL ELEMENTS (Continued)

Groups	Specimen Span Length (mm)	Specimen Cross Section	Specimen Material
11	245.872	Specimen Cross Section #5 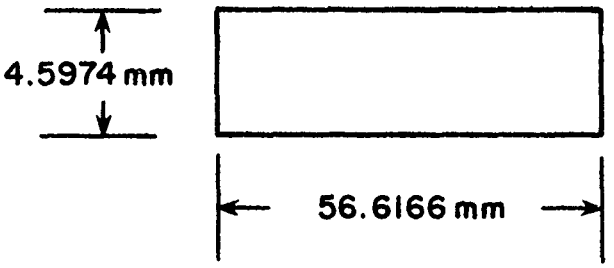 	403 Stainless Steel
12	245.872	Specimen Cross Section #6 Same as specimen Cross Section #5, but with Camber with Radius of Curvature of 27.7 cm.	403 Stainless Steel
13	245.872	Specimen Cross Section #7 Same as specimen Cross Section #6, but with twist of 49° through free span	403 Stainless Steel
14 15	154.940 77.470	Specimen Cross Section #8 Cross Ply Layup (0°/22°/0°/-22°) 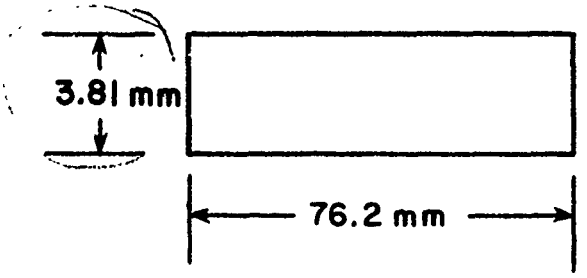 	B/Al
16	154.940	Specimen Cross Section #9 Cross Ply Layup (0°/22°/0°/-22°) 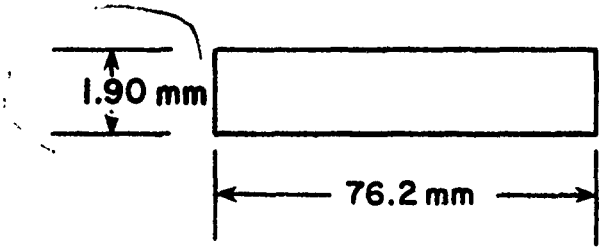 	B/Al

TABLE 7. SHAPE, SIZE, AND CONFIGURATION DETAILS OF STRUCTURAL ELEMENTS (Continued)

Groups	Specimen Span Length (mm)	Specimen Cross Section	Specimen Material
17	101.600	Specimen Cross Section #10 Cross Ply Layup (0°/22°/0°/-22°) with blade-like cross section 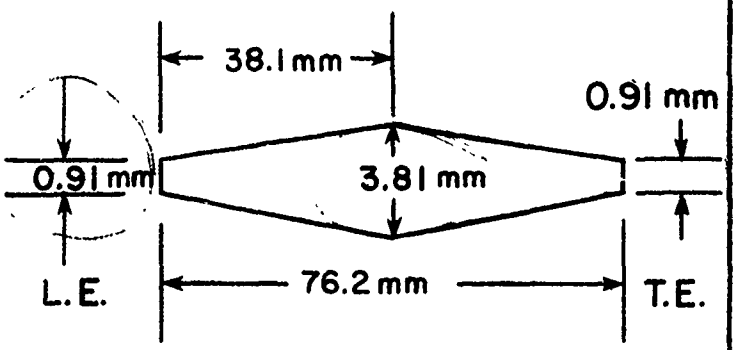 	B/Al
18	154.940	Specimen Cross Section #11 Constant Chord Airfoil Shape Cross Ply Layup (0°/22°/0°/-22°) with Camber of Radius of Curvature of 101.6 mm (4.0 inches). 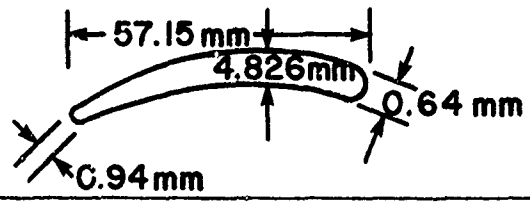 	B/Al
19	154.940	Specimen Cross Section #12 Same as Specimen Cross Section #11, but with twist of approximately 3.0°.	B/Al

elements are discussed in greater detail in a later section of this report.

Additional structural element impact tests are described in detail in this report for the loading model validation experiments of Task III of the overall program. In this work, normal impacts of 85 g (3 ounce) artificial birds were conducted on 8-1-1 titanium flat contilevered plates at the 70 percent span location at impact velocities which ensured elastic-plastic structural deformation of the specimens. The impacts were centered on the chord of the specimens such that the full 85 g (3 ounce) mass of the bird loaded the plates. A Moiré fringe device was used to accurately measure the deflection of the cantilevered plates for the various impacts. Two thicknesses of flat plates were evaluated. One specimen type was a flat plate with a blade-type aspect ratio and nominal thickness of the actual F101 blade at the 50 percent span level. The second type of specimen was a flat plate with a blade-type aspect ratio and one-half blade-type thickness to chord ratio of the actual blade at the 50 percent span location. The results of this testing is described in detail in the following section of this report.

In addition to impact testing of beam and plate-like test specimens, a number of impact tests were also conducted on full scale component blades. This impact testing of the actual blades was coordinated with the full scale blade testing of Task IV A where the impact tests were conducted to establish the strain rate limits for the material property tests of Task IV A. The results of the Task IV A impact tests of actual blades is described in the following section of this report. The test matrix for the Task IV A and Task VI work is outlined in Table 8. The Task IV A blade testing was to establish the strain rate limits of the blades; therefore, the impact velocities to be used in these impact tests corresponded to those which would be typical of an impact at 70 percent span and

TABLE 8. MATRIX AND TEST CONDITIONS FOR ACTUAL BLADE IMPACTS

Group Number	Blade Type and Comments	Purpose of Test	Impactor	Impact Location	Impact Incidence	Shroud Restraint	Specimen Material
1B	F101	Determine Strain Rates	85g (3 ounce) Bird	Edge Impact @ 30% Span	Oblique	Yes	Ti 8-1-1
2B	F101	Determine Strain Rates	85g (3 ounce) Bird	Edge Impact @ 70% Span	Oblique	Yes	Ti 8-1-1
3B	F101	Determine Strain Rates	680g (1.5 lb.) Bird	Edge Impact @ 30% Span	Oblique	Yes	Ti 8-1-1
4B	F101	Determine Strain Rates	680g (1.5 lb.) Bird	Edge Impact @ 70% Span	Oblique	Yes	Ti 8-1-1
5B	F101	Analysis	Slab Ice	Edge Impact @ 70% Span	Oblique	Yes	Ti 8-1-1
6B	J79	Determine Strain Rates	85g (3 ounce) Bird	Edge Impact @ 30% Span	Oblique	No	403 Stainless Steel
7B	J79	Determine Strain Rates	85g (3 ounce) Bird	Edge Impact @ 70% Span	Oblique	No	403 Stainless Steel
8B	J79	Determine Strain Rates	680g (1.5 lb.) Bird	Edge Impact @ 30% Span	Oblique	No	403 Stainless Steel
9B	J79	Determine Strain Rates and Analysis	680g (1.5 lb.) Bird	Edge Impact @ 70% Span	Oblique	No	403 Stainless Steel
10B	J79	Analysis	50.8 mm (2 inch) Ice Ball	Edge Impact @ 30% Span	Oblique	No	403 Stainless Steel
11B	J79	Analysis	Slab Ice	Edge Impact @ 30% Span	Oblique	No	403 Stainless Steel
12B	APSI	Determine Strain Rates	85g (3 ounce) Bird	Edge Impact @ 30% Span	Oblique	No	Boron/ Aluminum
13B	APSI	Determine Strain Rates and Analysis	85 g (3 ounce) Bird	Edge Impact @ 70% Span	Oblique	No	Boron/ Aluminum
14B	APSI	Analysis	50.8 mm (2 inch) Ice Ball	Edge Impact @ 30% Span	Oblique	No	Boron/ Aluminum
15B	APSI	Analysis	Slab Ice	Edge Impact @ 30% Span	Oblique	No	Boron/ Aluminum

30 percent span levels at full power settings of the engine during take-off for each of the blade types. Impacts at the 70 percent span level are representative of the highest velocity impacts experienced by a blade. Impacts at the 30 percent span level are typical of those in the highest stress regions of the blade where it is most vulnerable to the effects of impact degradation. In the case for the Task VI blade impacts, the impact velocity was varied to obtain no damage, threshold damage, and severe damage of the blade. The impact angles on the various test specimen and actual blade impacts were to correspond to the impact angles that would occur on the actual blades for a given span location. These impact angles, impact velocities, and bird mass values were determined from the blade geometry, the blade velocity for a given span location, and the aircraft speed. The following paragraphs describe an effort to calculate the projectile-blade relationships for an impact.

2.1.1 Test Conditions for Various Blade Types

The effort consisted of deriving bird slice relationships for the bird-blade interface geometry shown in Figure 1. The calculations are for obtaining the maximum bird slice that a row of blades would experience from a large bird impact. The calculations were performed for a starling impact (85 g) and a large bird impact (680 g) on the J79, F101, and APSI blades.

Three assumptions are made in the calculations. The first assumption is that the bird geometry is cylindrical with a length to diameter ratio equal to two. The second assumption is that the bird density is equal to 0.91 g/cm^3 (0.033 lb/in^3). (See References 1, 2, 3, and 4.) The last assumption is that the bird axial velocity is equal to the aircraft velocity. This velocity was assumed to be approximately 61 m/s (200 ft/s) for take-off and landing situations where FOD strikes are most likely to occur.

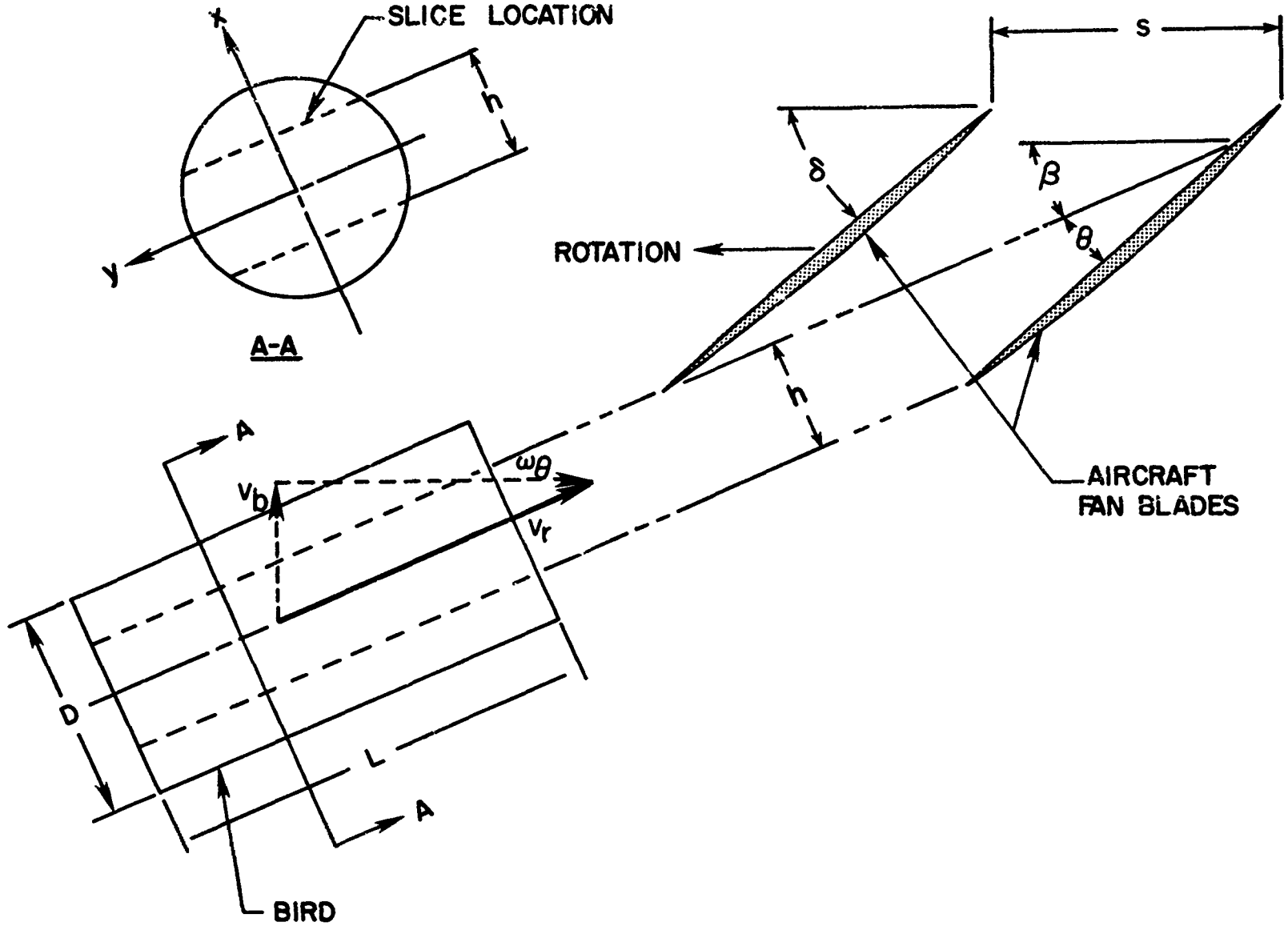

Figure 1. Bird-Blade Interface Geometry.

The input parameters from the blade required to make the calculations are: (1) the number of blades per stage (N); (2) the blade rotational speed (n); (3) the span radius where the impact is to occur (r_i); and (4) the blade orientation angle (δ).

The bird input parameters necessary are: (1) the axial velocity of the bird (V_b) which is assumed to be equal to the aircraft velocity and (2) the bird weight (W_b).

Table 9 gives the general equations utilized to determine the test conditions (impact velocity, impact angle, and bird slice weight) for an impact on a particular blade span location, and bird size.

Table 10 and 11 give the calculated test condition parameters for the three blade types. Table 10 gives the results for a starling (85 g) bird and Table 11 gives the calculations for a large bird (680 g). Both tables are for impacts at the 30 and 70 percent span locations with the engines at full power settings during takeoff for each of the blade types.

2.1.2 Specimen Materials and Geometries

As indicated earlier, the three blade types to be investigated were the F101 blade using 8-1-1 titanium, the J79 blade using 403 stainless steel, and the APSI blade using boron/aluminum material. These choices correspond to those which would be investigated analytically and experimentally in other tasks of the overall program. The geometries of the test specimens used in the study were similar to the geometries of the actual blades at the 50 percent span location. The material, leading edge and trailing edge thickness, overall thickness, taper angle, chord width, and span length values of the test specimens were identical to that of the various blade types.

2.1.2.1 F101 Test Specimens

The test specimens simulating the F101 blade were fabricated from 8-1-1 titanium material. The leading

TABLE 9. GENERAL EQUATIONS UTILIZED TO DETERMINE TEST CONDITIONS

Bird Geometry

Bird Diameter	$D = \sqrt[3]{2W_b/\pi\rho}$	(cm)
Bird Length	$L = 2D$	(cm)

Bird-Blade Interaction Parameters

Relative Velocity	$V_r = (W_\theta^2 + V_b^2)^{1/2}$	(m/s)
Bird Tangential Velocity @ r_i	$W_\theta = 2\pi n r_i/6000$	(m/s)
Bird-Blade Angle Relative to Tangent @ r_i	$\beta = \sin^{-1} V_b/V_r$	(°)
Blade Tangential Spacing @ r_i	$S = 2\pi r_i/N$	(cm)
Bird Slice Width	$h = S \sin \beta = \frac{2\pi r_i}{N} \frac{V_B}{V_r}$	(cm)
Bird-Blade Impingement Angle	$\theta = \delta - \beta$	(°)
Bird Slice Weight	$W_s = 2\rho L \int_{-\frac{h}{2}}^{\frac{h}{2}} 2\sqrt{(\frac{D}{2})^2 - x^2}\, dx$	

$$W_s = 2\rho\, D \left[h\sqrt{(\tfrac{D}{2})^2 - (\tfrac{h}{2})^2} + \frac{1}{2} D^2 \sin^{-1} (\tfrac{h}{D}) \right]$$

TABLE 10. TEST CONDITIONS FOR STARLING IMPACT

Parameter	J79		APSI		F101	
Rotor Speed, n (rpm)	7460		17500		7555	
N^{o} Blades, N (-)	21		28		50	
Tip Radius, R_t (cm)	37.21		27.94		56.34	
Root Radius, R_R (cm)	13.23		12.57		29.74	
Span Location (%)	30	70	30	70	30	70
Radius, r_i (cm)	20.42	30.02	17.18	23.33	37.72	48.36
Orientation Angle, δ (°)	72.0	51.0	49.8	27.0	52.5	33.5
Chord Length, C (cm)	5.66	5.66	7.37	7.77	8.38	9.40
Calculated Values						
Blade Tangential Velocity, W_θ (m/s)	159	234	315	428	298	383
Bird Axial Velocity, V_b (m/s)	61	61	61	61	61	61
Relative Velocity, V_r (m/s)	170	242	321	432	304	388
Bird Weight, W_b (g)	85.3	85.3	85.3	85.3	85.3	85.3
Bird Slice Width, h (cm)	2.18	2.26	0.74	0.74	0.94	0.94
Bird Slice Weight, W_s (g)	57.15	58.51	20.41	20.41	25.86	26.31
Bird-Blade Incidence Angle, θ(°)	51.1	36.4	38.8	18.9	41.0	24.0
Angle β (°)	20.9	14.6	11.0	8.1	11.5	9.1
Bird Diameter, D (cm)	3.89	3.89	3.89	3.89	3.89	3.89

TABLE 11. TEST CONDITIONS FOR LARGE BIRD (680 g) IMPACT

Parameter	J79		APSI		F101	
Rotor Speed, n (rpm)	7460		17500		7555	
N° Blades, N (-)	21		28		50	
Tip Radius, R_t (cm)	37.21		27.94		56.34	
Root Radius, R_R (cm)	13.23		12.57		29.74	
Span Location (%)	30	70	30	70	30	70
Radius, r_i (cm)	20.42	30.02	17.18	23.22	37.72	48.36
Orientation Angle, δ (°)	72.0	51.0	49.8	27.0	52.5	33.5
Chord Length, C (cm)	5.66	5.66	7.37	7.77	8.38	9.40
Calculated Values						
Blade Tangential Velocity, W_θ (m/s)	159	234	315	428	298	383
Bird Axial Velocity, V_b (m/s)	61	61	61	61	61	61
Relative Velocity, V_r (m/s)	170	242	321	432	304	388
Bird Weight, W_b (g)	680.4	680.0	680.4	680.4	680.4	680.4
Bird Slice Width, h (cm)	2.18	2.26	0.74	0.74	0.94	0.97
Bird Slice Weight, W_s (g)	240.41	249.48	81.65	81.65	104.33	104.33
Bird-Blade Incidence Angle, θ(°)	51.1	36.4	38.8	18.9	41.0	24.4
Angle β (°)	20.9	14.6	11.0	8.1	11.5	9.1
Bird Diameter, D (cm)	7.80	7.80	7.80	7.80	7.80	7.80

edge thickness for the plate specimens with a blade-type aspect ratio and an airfoil (tapered cross section) shape was 0.813 mm (0.032 inches). The trailing edge thickness was 1.016 mm (0.040 inches) and the maximum thickness was 4.267 mm (0.168 inches). The chord width was 88.519 mm (3.485 inches) and the span length was 311.150 mm (12.250 inches). All of the titanium specimens were shot peened to an intensity of 0.005 - 0.008 N using glass beads).50 - 0.84 mm (0.023 - 0.033 inch) diameter.

2.1.2.2 J79 Test Specimens

The test specimens simulating the J79 blade were fabricated of 403 stainless steel material. The maximum thickness of the blade-type aspect ratio specimens were 4.5974 mm (0.181 inches) and the chord width was 56.617 mm (2.229 inches). The span length for the specimens was 245.872 mm (9.680 inches). The camber for the J79 specimens had a radius of curvature of 276.900 mm (10.9 inches). The twist angle for the J79 specimens was 49 degrees from the root to the leading edge tip of the specimens.

2.1.2.3 APSI Test Specimens

Test specimens of boron/aluminum material simulating the APSI blade were fabricated by the General Electric Company. The leading edge thicness for the airfoil cross section specimens was 0.559 mm (0.022 inches) and the maximum thickness was 3.937 mm (0.155 inches). The specimens were symmetrical in shape. The chord width was 76.2 mm (3.0 inches) and the span length was 154.940 mm (6.1 inches). The cambered panels were fabricated using a J79 specimen die. The radius of curvature for the cambered specimens was about 101.6 mm (4.0 inches). The twist angle for the twisted panels was approximately 3.0 degrees from the root to the leading edge tip of the specimens. The specimens had a stainless steel wire mesh outer ply. The symmetrical layup used in the specimens was

0°/22°/0°/-22° with the number of plies being sufficient to obtain the desired thickness.

Measurements of the twist of the boron/aluminum specimens with camber and twist (Group 19 specimens of Tables 6 and 7) were determined before the impact for each specimen. Figure 2 shows how these twist measurements were conducted while Table 12 gives the measurements for each specimen.

2.1.3 Impactors

The substitute birds used in the study for real birds were 85 g (3 ounce) and 680 g (1.5 pound) sizes. The 85 g (3 ounce) bird was used to simulate a starling size bird while the 680 g (1.5 pound) bird was used to simulate a seagull sized bird. The artificial birds were cylindrical in shape with a length to diameter ratio of two. The artificial bird material was a mixture of microballoons and gelatin to obtain a porosity of 10 to 15 percent. The small bird had a diameter of 38.1 mm (1.5 inches) while the larger bird had a diameter of 76.2 mm (3.0 inches).

The mass of the 50.8 mm (2 inch) ice balls was approximately 65 grams. These ice balls were molded using demineralized water. The slab ice was molded to a shape of a cylinder having a diameter of 73.0 mm (2.875 inches) and a length of 203.2 mm (8.0 inches). The mass of the slab ice in the impacts varied from 687 to 867 grams depending on the final diameter and length values.

2.2 EXPERIMENTAL SETUP AND PROCEDURES

The impact tests were conducted on the large compressed gas gun range. The range configuration is capable of launching 25.4 to 76.2 mm (1.0 to 3.0 inch) diameter spheres or cylinders up to velocities of 350 m/s (1,150 ft/s) using air as the gas medium. Higher velocities can be obtained using helium as the

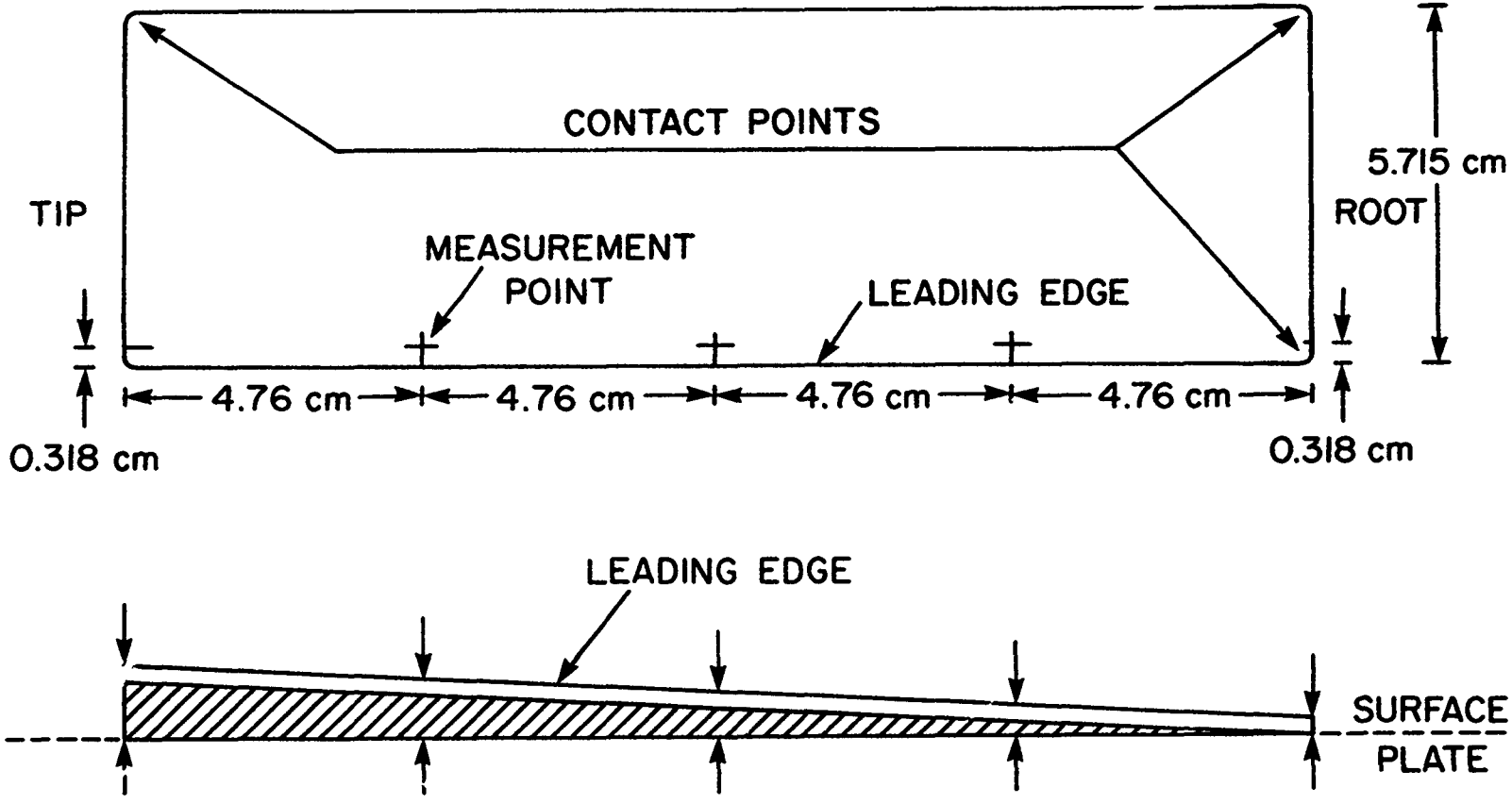

MEASUREMENT POINTS FOR CALCULATING TWIST OF COMPOSITE SPECIMENS. TASK VI CONSTANT CHORD AIRFOIL-TYPE 2 (TWISTED).

Figure 2. Method Used to Determine Twist for Each Group 19 Boron/Aluminum Specimen.

TABLE 12. PREIMPACT TWIST MEASUREMENTS FOR GROUP 19 BORON/ ALUMINUM STRUCTURAL ELEMENT SPECIMENS

Specimen No.	Root (mm)	#1 (mm)	#2 (mm)	#3 (mm)	Tip (mm)
VI AF-13	2.311	4.496	6.731	8.839	10.795
VI AF-14	2.261	4.064	6.147	8.052	9.728
VI AF-15	2.286	4.318	5.994	7.696	9.271
VI AF-16	2.413	4.242	6.248	8.230	9.906
VI AF-17	2.235	4.445	6.477	8.382	10.058
VI AF-18	2.413	4.318	6.147	7.747	9.348
VI AF-19	2.489	4.166	5.766	7.239	8.560
VI AF-20	2.311	3.962	5.207	6.858	8.484
VI AF-21	2.261	4.343	6.426	8.331	10.160
VI AF-22	2.388	4.369	6.223	7.798	9.423
VI AF-24	2.362	5.080	7.696	10.211	12.548
VI AF-25	2.438	4.826	7.137	9.474	11.430

gas medium in the gun. A brief description of the range setup is given below.

2.2.1 Large Bore Compressed Gas Gun Range

Early in the study, the range setup used for the artificial bird impacts was on an 89 mm (3.5 inch) diameter smooth-bore gas gun having a launch length of 6.1 m (20.0 feet) and a sabot stopper section having a length of 2.9 m (9.5 feet). The projectile was launched in a standard one-piece balsa wood sabot with a cylindrical pocket. The size of the pocket in the sabot depended on the bird size to be fired. After launch, the gas pressure was released through slots in the sabot stopper tube and the sabot was stopped in the stopper section. The projectile would free-flight to the target over a distance of about 1.8 m (6.0 feet). A preslicer was used in

conjunction with the launch system to slice a portion of the bird or ice projectile prior to impact such that only the center portion of the impactor diameter would actually load the target specimen since the majority of the impacts were leading edge hits. The preslicer shown in Figure 3 was not used for the normal chord center impacts on the flat plate or beam impacts. In the leading edge impacts, the specimens were positioned such that slicing would occur; thus, only the center portion of the projectile would load the target specimen as shown in Figure 1.

The normal center impacts on the cantilevered flat plates were conducted using a 51 mm (2.0 inch) diameter smooth bore gun having a length of 7.9 m (26.0 feet). This particular gun setup was utilized without a sabot stopper section or a preslicer. In this case, the impactors were again launched in a standard one-piece balsa wood sabot having a cylindrical pocket. No attempt was made to stop balsa wood sabots for this setup configuration; the balsa wood sabot was permitted to impact the target specimens along with the desired impactor. The mass of the balsa wood sabot was added to the impactor mass to give the total impact mass for these impacts.

The final setup configuration used in the study was a setup using an 89 mm (3.5 inch) diameter smooth-bore launch tube having a length of 6.1 m (20.0 feet). A stopper section together with a vent section having a length of 1.83 m (6.0 feet) was used with the launch system. Molded urethane plastic sabots were utilized with the launch system to launch the impactor. Figure 4 shows the setup of the launch system. A metal target box was utilized to confine the target specimens as shown in Figure 4.

2.2.2 Blade and Specimen Mounting Procedure

All of the testing was conducted using the cantilevered method of mounting. The specimens were cantilever mounted in a vise-like fixture which conformed to the base

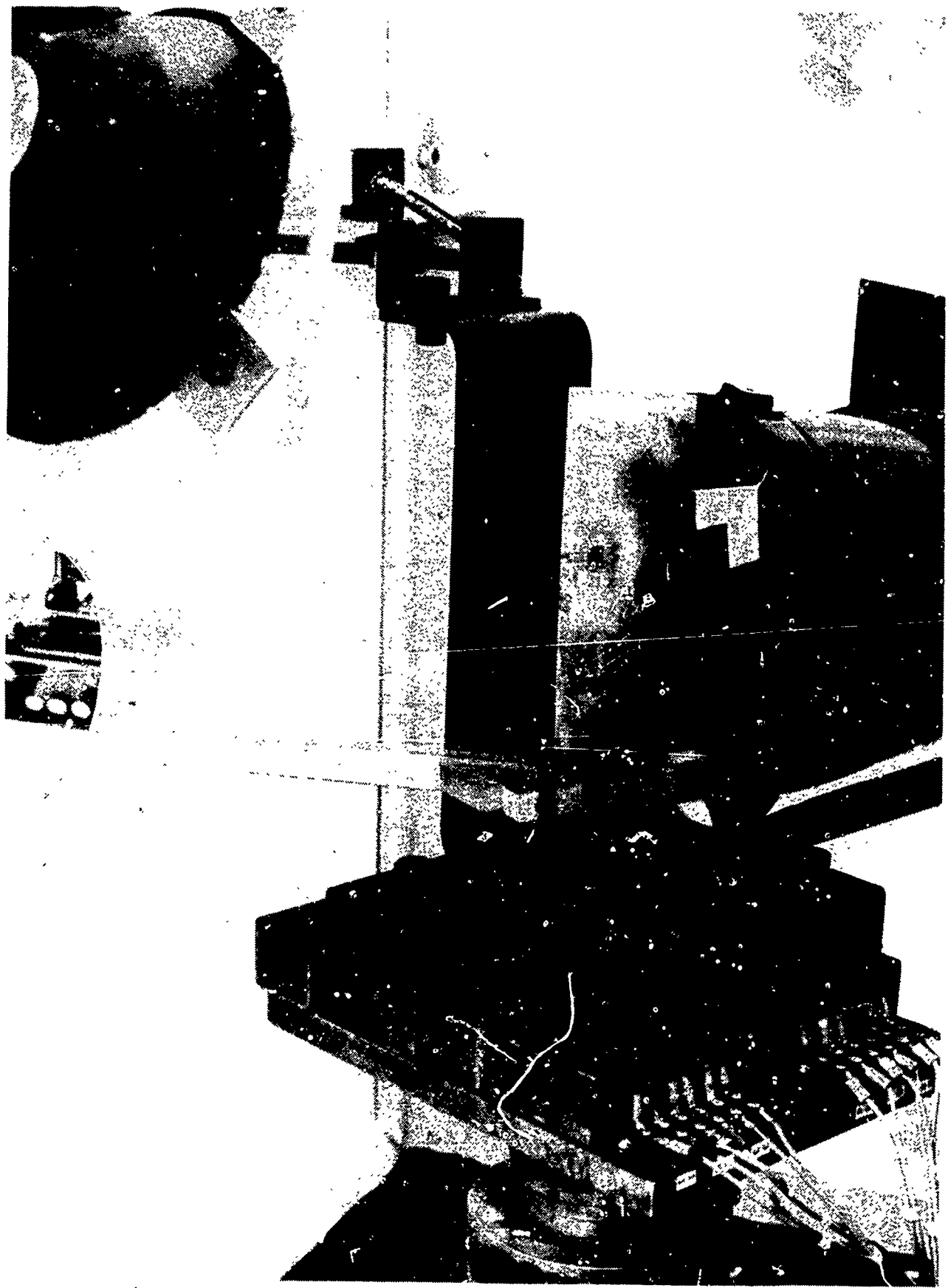

Figure 3. Photograph Showing Preslicer Utilized.

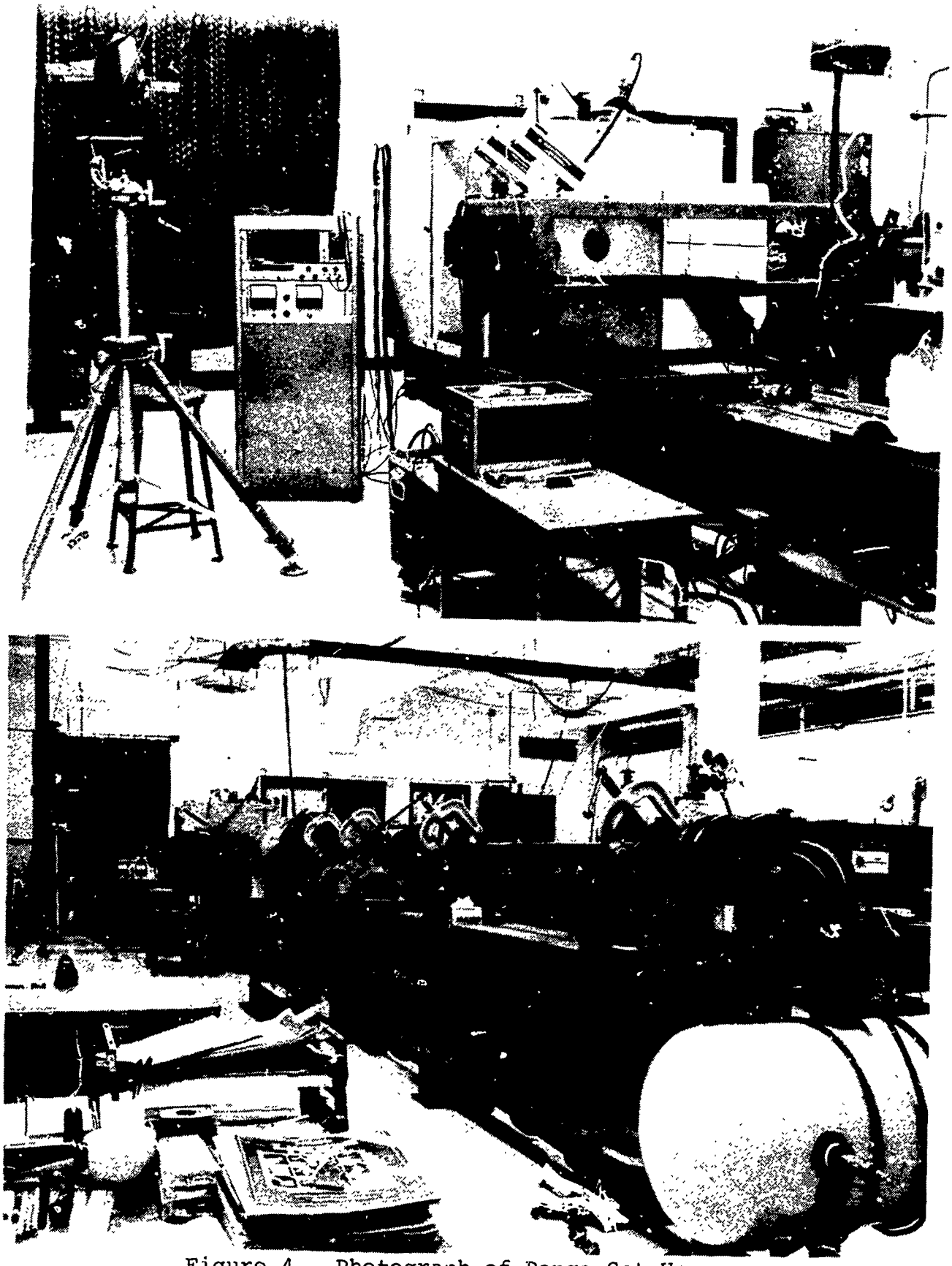

Figure 4. Photograph of Range Set-Up.

cross-sectional geometry of the specimens. Each blade type used a special fixture to cantilever the blades. All of the fixtures were either directly or indirectly attached to the range "H" beam to provide a rigid and sturdy mounting system. The use of these mounting fixtures also permitted proper alignment and orientation of the targets with respect to the projectile trajectory.

In the case of the F101 blades, the tip was also restrained to simulate the tip shrouds in the actual engine. Figure 5 shows the system utilized to restrain the tip of the F101 blades.

2.2.3 Slice Size Determination

The mass of the projectile which actually impacts the target was of great importance in the leading edge impacts. The most satisfactory technique for determining the impact mass involved recovering the presliced portion and the nondeflected portion (slice across leading edge of the target) of the impactor and accurately weighing them. The mass recovered was then subtracted from the initial mass of the impactor to provide a reliable and accurate value for the impact slice mass.

2.2.4 Impact Velocity Measurements

The projectile velocity for the large bore compressed gas gun was measured by utilizing a pair of HeNe laser/photomultiplier stations spaced a known distance apart. Each laser projects a beam that intersects the projectile trajectory normal to trajectory and illuminates one of the photomultiplier stations. When the projectile interrupts the first beam, the first photomultiplier station generates a voltage pulse to start a counter-timer and trigger a light source for a still camera. The counter-timer is stopped and the other light source is triggered when the projectile interrupts the second laser beam. The projectile impact velocity was then calculated from the recorded measured time and the distance traveled (as determined

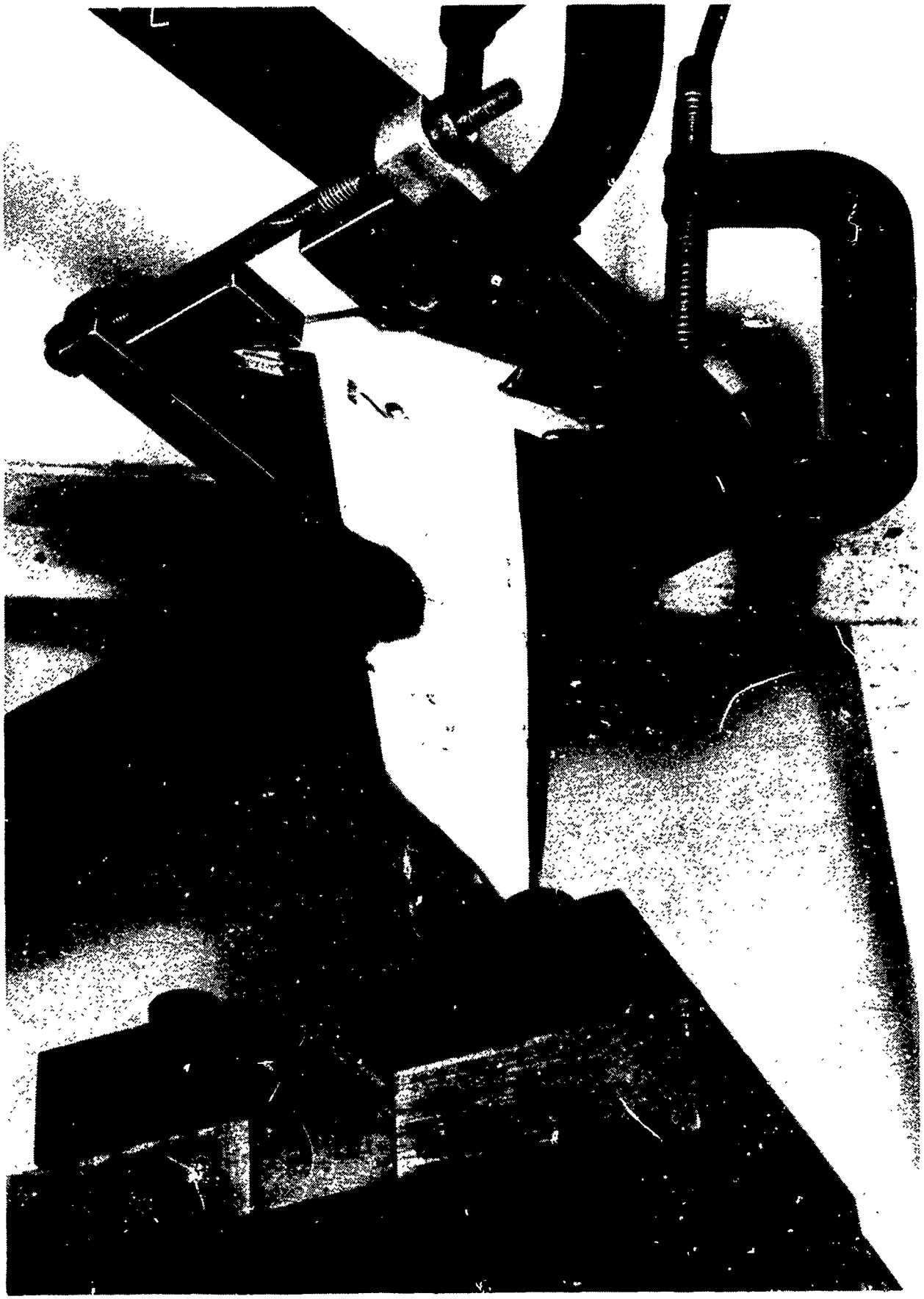

Figure 5. Photograph of System Utilized to Restrain F101 Blade Tip.

by reference to the two shadow pictures). This technique provided accurate velocity measurements and also information on the integrity of the impactor just prior to impact.

2.3 DATA COLLECTION

The data collected from the impact tests included accurate impact conditions, dynamic displacements of the specimens at discreet locations, strain/time histories local to the impact site and at critical blade stress regions identified from the structural response models, and damage assessment of the impacted targets. Each test was documented to record test conditions, test results, and damage results to permit an accurate interpretation of the results. These results could then be compared with the predictions from the analyses of Tasks V and VIII of the overall program.

Measurement techniques considered in this task were high-frequency response strain gaging, high speed photography and Moiré fringe displacement measurement. Particular emphasis was placed on the development of efficient methods to improve measurement accuracies. A number of tests were duplicated to also provide a measure of the statistical variation in the data.

2.3.1 Strain Measurements

The strain was detected utilizing high frequency strain gages mounted at critical locations on the target specimens and actual blades. Strain versus time and strain rate versus times curves were used to evaluate the results of the impacts. Gages were located at the root of the target specimens and blades and on the side of the targets opposite the impact site.

Digital data acquisition equipment was employed to record the data. The digital system has a "quick-look" capability which is very helpful in evaluating data soon after the test. The system has a 200 kHz bandwidth and a storage

capability of 2048 data points. The data was recorded on cassette tapes to provide a permanent record.

The significant local impact frequencies were estimated to extend to 20 kHz; therefore, low pass filters were used with the system to attenuate frequencies above 20 kHz. The sampling rate for the actual blade shots was 100 kHz while the sampling rate for the majority of the specimen impacts was 20 kHz.

The far field structural response was estimated to extend to about 4 kHz. Prior to impact testing on the majority of the actual blades, frequency checks were made to establish the natural frequencies of the blades. In this case, the sampling rate used was 20 kHz with 4 kHz low-pass filters to attenuate frequencies above 4 kHz. After the impact was conducted the blades were again frequency checked to establish the natural frequencies. Any difference between the pre-test and post-test frequency checks could be attributed tc blade damage due to the impact.

2.3.2 Target Deflection Measurements

Deflection of the test specimens and actual blades were recorded on selected impacts by utilizing either a high speed photographic or Moiré fringe technique. The high speed cameras used in the study were either the Hycam (16 mm framing camera) or the Dynafax 35 mm drum type framing. The maximum framing rate for the Hycam is about 7,000 frames per second while the framing rate for the Dynafax is about 20,000 frames per second.

The Moiré fringe technique was used to measure test specimen deflection on several normal impacts. This technique has been developed by the University of Dayton to measure the dynamic deflection of large panels subjected to impulsive loads. (See Reference 4.) It possesses unique features which are well matched to the measurement of out-of-plane displacements of a specimen surface. The system employed could view

about a 0.6 m (2.0 foot) squre area and resolve displacements of 0.25 mm (0.01 inch) to maximum displacements of about 10.2 cm (4.0 inches). The Moiré patterns or fringes caused by a deflected surface were monitored by a high speed framing camera. The framing rate of the camera was about 6,000 frames per second which was suitable for recording the dynamic response of the specimens due to an impact. The data of the displacements is presented in the form of deflection versus particular specimen location curves for various time periods.

2.4 DAMAGE ASSESSMENT

The damage assessment portion of the data collected in the study was given particular consideration. The mode of damage was determined and the extent of damage measured. It was anticipated that tests would be conducted on the impact damaged specimens and blades to determine the residual tensile strength and residual fatigue strength properties; however, the majority of the damage was demonstrated to be plastic deflections at the root area or actual breaking off at the root section for the blades and test specimens. Thus, very few of the specimens or blades displayed damage where the residual tensile strength or fatigue strength would be affected to any extent.

2.4.1 Mode and Extent of Damage Measurements

The foreign object damage (FOD) problem can be divided into two separate areas, both of which are associated with a damage threshold. One deals with local blade or specimen damage; the other is associated with large scale structural damage. It was the purpose of this study to investigate and evaluate the damage for both the local and structural damage areas.

Since the impactors in the study were either artificial birds or ice, the damage mode for the metal materials usually was in the form of plastic deformation at the root area without cracking or curlback or a large amount of local bending

at the impact site. In several cases, the specimens broke off at the root area. The local damage was characterized by measuring the maximum plastic deformation of the target leading edge (L.E.) and trailing edge (T.E.) whenever possible. Twist damage was also measured where specimens encountered twist damage. Plastic deformation at the root area was characterized by measuring the maximum deformation for the whole span length.

The damage for the APSI blade and test specimens was similar to that for the metal materials except that in several instances, material would be broken out at the impact site. This mass loss damage was characterized by length and width measurement of the affected area. If plastic deformation was experienced, the damage was characterized by measuring the maximum deformation identical to the technique used for the metal materials.

In all cases, photographs of the damaged blades and test specimens were taken to document the damage. These photographs are presented in Appendix B of this report.

SECTION 3
EXPERIMENTAL RESULTS

The experimental results of the impact tests are summarized in the following paragraphs. A total of about 200 shots were fired to obtain 133 good impact data shots in the study. The majority of testing (92 shots) was conducted on simple element test specimens and 41 data shots were conducted on full scale blades.

3.1 SIMPLE ELEMENT TEST SPECIMENS

As indicated earlier, the three blade types investigated in the study included the F101 blade using 8-1-1 titanium, the J79 blade using 403 stainless steel, and the APSI blade using boron/aluminum material. These choices correspond to those which were investigated analytically and experimentally in other tasks of the overall program. The geometries of the structural element test specimens were similar to the geometries of the actual blades at the 50 percent span location. The material, leading edge and trailing edge thickness, overall thickness, taper angle, chord width, and span length values of the test specimens were identical to that of the various blade types. These simple elements were tested with progressive introduction of airfoil geometric parameters to validate experimentally the analytical predictions of other tasks in the program and to derive a correlation between the structural element specimens and full scale blades.

The test matrix for the structural element tests was given earlier in Table 6 for various groups of specimens. This table described the structural elements, element fixity and material, the type of impactor and loading, and the impact location and angle. The shape, size, and configuration of the structural elements was given earlier in Table 7. This table gives the span length, specimen shape and cross-section, and material of each structural element specimen.

Results of the static impact test on the structural element specimens are given in Table 13. The table gives the test conditions, specimen geometry and material type for each impact, the figure of Appendix A which describes the strain gage locations, the impact mass loading the specimens, the span location and type of impact, and a description of the damage generated on each specimen. Appendix A presents Figures 1A through 16A which are sketches showing the strain gage locations for both specimen and real blade impacts.

As indicated earlier, 93 impacts were conducted on structural element test specimens. Five of the specimens in this testing were tested without strain gages to measure out-of-plane displacements of a specimen surface using the Moiré fringe apparatus. The remaining impact tests were conducted using specimens instrumented with six strain gages. High speed photography was also used in every test in which strain gages were installed on the specimens. In many cases, the tip deflection of the specimens was plotted versus time using the high speed films to make these measurements. Strain gage techniques are described in Section 2.3.1.

In all cases when damage was generated, photographs of the damaged structural element test specimens and real blades were taken to document the damage. Typical photographs of the damage generated in the ice and artificial bird impacts are presented in Appendix B.

The details of the shape, size, and configuration of the structural elements were given earlier in Table 7. The table gives 19 different groups of specimens which were investigated in the study.

3.1.1 Impact Results of Structural Element Tests

The testing involved conducting either center or leading-edge impacts on 19 different groups of structural element specimens. As indicated earlier, the impactors were

TABLE 13. RESULTS OF STATIC IMPACT TESTING

Group No.	Shot No.	Projectile Type	Projectile Mass (g)	Mass Impacting Target (g)	Target Material and Description	Span Location for Impact (%)	Impact Distance from Root (cm)	Strain Gauge Locations	Impact Angle (°)	Shroud Restraint	Impact Velocity (m/s)	Damage Description and Comments	High-Speed Camera Type	Camera Framing Rate (frames/sec)	Deformation Plot
1	4-0052	Micro-balloon gelatin bird (cylinder) (3.81 cm dia. x 7.62 cm long)	82.0	82.0	8-1-1 Ti flat plate with blade-type aspect ratio of F101 blade)	Center impact @ 70% span	22.5	No gauges	90.0	No	125.0	Plastic deformation of specimen at root; 1.35 cm deflection on left side and 1.51 cm deflection on right side measured at tip.	No film	--	No
1	4-0056	Micro-balloon gelatin bird (cylinder) (3.81 cm dia. x 7.62 cm long)	82.6	82.6	8-1-1 Ti flat plate with blade-type aspect ratio of F101 blade)	Center impact @ 70% span	22.2	No gauges	90.0	No	201.0	Plastic deformation of specimen at root; 7.62 cm deflection for both specimen sides measured at tip.	No film	--	No
1	2-0090	Micro-balloon gelatin bird (cylinder) (3.81 cm dia. x 7.62 cm long)	101.2	101.2	8-1-1 Ti flat plate with blade-type aspect ratio of F101 blade	Center impact @ 70% span	21.8	See Figure 7A	90.0	No	122.6	Plastic deformation of specimen at root; 1.98 cm deflection measured at tip.	Dynafax	20,800	Yes
1	2-0091	Micro-balloon gelatin bird (cylinder) (3.81 cm dia. x 7.62 cm long)	107.4	107.4	8-1-1 Ti flat plate with blade-type aspect ratio of F101 blade	Center impact @ 70% span	21.8	See Figure 7A	90.0	No	85.7	Plastic deformation of specimen at root; 0.71 cm deflection measured at tip.	Dynafax	20,752	Yes
1	2-0092	Micro-balloon gelatin bird (cylinder) (3.81 cm dia. x 7.62 cm long,	98.6	98.6	8-1-1 Ti flat plate with blade-type aspect ratio of F101 blade	Center impact @ 70% span	21.8	See Figure 7A	90.0	No	43.9	Plastic deformation of specimen at root; 0.15 cm deflection measured at tip.	No film	--	No
1	2-0093	Micro-ballon gelatin bird (cylinder) (3.81 cm dia. x 7.62 cm long)	99.2	99.2	8-1-1 Ti flat plate with blade-type aspect ratio of F101 Llade	Center impact @ 70% span	21.8	See Figure 7A	90.0	No	59.1	Plastic deformation of specimen through free span; 0.38 cm deflection measured at tip.	Hycam	Timing marks 1000/sec	Yes

TABLE 13. RESULTS OF STATIC IMPACT TESTING (CONTINUED)

Group No.	Shot No.	Projectile Type	Projectile Mass (g)	Mass Impacting Target (g)	Target Material and Description	Span Location for Impact (%)	Impact Distance from Root (cm)	Strain Gauge Locations	Impact Angle (°)	Shroud Restraint	Impact Velocity (m/s)	Damage Description and Comments	High-Speed Camera Type	Camera Framing Rate (frames/sec)	Deformation Plot
1	2-0094	Micro-balloon gelatin bird (cylinder) (3.81 cm dia. x 7.62 cm long)	100.5	100.5	8-1-1 Ti flat plate with blade-type aspect ratio of F101 blade	Center impact @ 70% span	21.8	See Figure 7	90.0	No	177.4	Plastic deformation of specimen at root; 6.50 cm deflection measured at tip.	Hycam	Timing marks 1,000/sec	Yes
1	2-0131	Micro-balloon gelatin bird (cylinder) (3.81 cm dia. x 7.62 cm long)	85.9	85.9	8-1-1 Ti flat plate with blade-type aspect ratio of F101 blade	Center impact @ 70% span	21.8	See Figure 7	90.0	No	189.6	Plastic deformation of specimen at root and impact site; 5.69 cm deflection measured at tip.	Hycam	Timing marks 1,000/sec	Yes
2	2-0168	5.08 cm dia. ice ball	64.7	64.7	8-1-1 Ti flat plate with blade-type aspect ratio of F101 blade	Center impact @ 30% span	9.3	See Figure 7	90.0	No	181.7	Plastic deformation of specimen at impact site; 0.32 cm bow measured at impact site. No strain gauge data.	No film	--	No
2	2-0169	5.08 cm dia. ice ball	63.5	63.5	8-1-1 Ti flat plate with blade-type aspect ratio of F101 blade	Center impact @ 30% span	9.3	See Figure 7	90.0	No	183.8	Plastic deformation of specimen at impact site; 0.32 cm bow measured at impact site.	Dynafax	20,544	No
2	2-0170	5.08 cm dia. ice ball	62.4	62.4	8-1-1 Ti flat plate with blade-type aspect ratio of F101 blade	Center impact @ 30% span	9.3	See Figure 7	90.0	No	130.0E	No strain gauge data or film. Velocity estimated. No visible damage on specimen.	No film	--	No

TABLE 13. RESULTS OF STATIC IMPACT TESTING (CONTINUED)

Group No.	Shot No.	Projectile Type	Projectile Mass (g)	Mass Impacting Target (g)	Target Material and Description	Span Location for Impact (%)	Impact Distance from Root (cm)	Strain Gauge Locations	Impact Angle (°)	Shroud Restraint	Impact Velocity (m/s)	Damage Description and Comments	High-Speed Camera Type	Camera Framing Rate (frames/sec)	Deformation Plot
2	2-0171	5.08 cm dia. ice ball	62.5	62.5	8-1-1 Ti flat plate with blade-type aspect ratio of F101 blade	Center impact @ 30% span	9.3	See Figure 7	90.0	No	116.5	No visible damage; projectile broke up upon launch.	Dynafax	20,464	No
2	2-0172	5.08 cm dia. ice ball	64.0	64.0	8-1-1 Ti flat plate with blade-type aspect ratio of F101 blade	Center impact @ 30% span	9.3	See Figure 7	90.0	No	125.3	No visible damage on specimen.	Dynafax	20,736	No
2	2-0173	5.08 cm dia. ice ball	61.7	61.7	8-1-1 Ti flat plate with blade-type aspect ratio of F101 blade	Center impact @ 30% span	9.3	See Figure 7	90.0	No	259.1	Specimen bowed 1.14 cm on right side and 1.40 cm on left side at impact site. Specimen twisted 0.46 cm. Impact hit off center to left side.	Dynafax	20,576	No
2	2-0174	5.08 cm dia. ice ball	65.9	65.9	8-1-1 Ti flat plate with blade-type aspect ratio of F101 blade	Center impact @ 30% span	9.3	See Figure 7	90.0	No	262.2	Specimen bowed 1.68 cm on right side and 1.60 cm on left side at impact site. Specimen twisted 0.16 cm.	Dynafax	20,720	No
3	2-0111	Micro-balloon gelatin bird (cylinder) (3.81 cm dia. x 7.62 cm long)	81.8	18.1	8-1-1 Ti flat plate with blade-type aspect ratio of F101 blade	Center impact @ 70% span	21.8	See Figure 8	36.4	No	86.6	No visible damage on specimen.	Dynafax	20,832	No
3	2-0112	Micro-balloon gelatin bird (cylinder) (3.81 cm dia. x 7.62 cm long)	80.0	23.3	8-1-1 Ti flat plate with blade-type aspect ratio of F101 blade	Center impact @ 70% span	21.8	See Figure 8	36.4	No	110.1	No visible damage on specimen.	Dynafax	20,864	No

TABLE 13. RESULTS OF STATIC IMPACT TESTING (CONTINUED)

Group No.	Shot No.	Projectile Type	Projectile Mass (g)	Mass Impacting Target (g)	Target Material and Description	Span Location for Impact (%)	Impact Distance from Root (cm)	Strain Gauge Locations	Impact Angle (°)	Shroud Restraint	Impact Velocity (m/s)	Damage Description and Comments	High-Speed Camera Type	Camera Framing Rate (frames/sec)	Deformation Plot
3	2-0113	Micro-balloon gelatin bird (cylinder) (3.81 cm dia. x 7.62 cm long)	64.6	54.9	8-1-1 Ti flat plate with blade-type aspect ratio of F101 blade	Center impact @ 70% span	21.8	See Figure 8	36.4	No	188.4	No visible damage on specimen. Specimen moved in mount due to impact.	Dynafax	20,816	No
3	2-0114	Micro-balloon gelatin bird (cylinder) (3.81 cm dia. x 7.62 cm long)	84.6	45.9	8-1-1 Ti flat plate with blade-type aspect ratio of F101 blade	Center impact @ 70% span	21.8	See Figure 8	36.4	No	191.2	No visible damage on specimen.	No film	--	No
3	2-0115	Micro-balloon gelatin bird (cylinder) (3.81 cm dia. x 7.62 cm long)	82.6	53.1	8-1-1 Ti flat plate with blade-type aspect ratio of F101 blade	Center impact @ 70% span	21.8	See Figure 8	36.4	No	302.1	Plastic deformation at root and impact site. Leading edge deflection at tip-1.83 cm. Trailing edge deflection at tip-1.59 cm. Specimen twist through span-0.24 cm.	Hycam	Timing marks 1,000/sec	Yes
3	2-0121	Micro-balloon gelatin bird (cylinder) (3.81 cm dia. x 7.62 cm long)	85.2	66.2	8-1-1 Ti flat plate with blade-type aspect ratio of F101 blade	Center impact @ 70% span	21.8	See Figure 8	36.4	No	445.7	No visible damage on specimen.	No film	--	No
3	2-0126	Micro-balloon gelatin bird (cylinder) (3.81 cm dia. x 7.62 cm long)	81.4	20.7	8-1-1 Ti flat plate with blade-type aspect ratio of F101 blade	Center impact @ 70% span	21.8	See Figure 8	24.4	No	441.2	No visible damage on specimen.	Hycam	Timing marks 1,000/sec	No
3	2-0127	Micro-balloon gelatin bird (cylinder) (3.81 cm dia. x 7.62 cm long)	83.0	22.8	8-1-1 Ti flat plate with blade-type aspect ratio of F101 blade	Center impact @ 70% span	21.8	See Figure 8	24.4	No	439.3	No visible damage specimen.	Hycam	Timing marks 1,000/sec	No

TABLE 13. RESULTS OF STATIC IMPACT TESTING (CONTINUED)

Group No.	Shot No.	Projectile Type	Projectile Mass (g)	Mass Impacting Target (g)	Target Material and Description	Span Location for Impact (%)	Impact Distance from Root (cm)	Strain Gauge Locations	Impact Angle (°)	Shroud Restraint	Impact Velocity (m/s)	Damage Description and Comments	High-Speed Camera Type	Camera Framing Rate (frames/sec)	Deformation Plot
4	2-0095	Micro-balloon gelatin bird (cylinder) (3.81 cm dia. x 7.62 cm long)	101.1	101.1	8-1-1 Ti flat plate with one-half blade-type aspect ratio of F101 blade	Center impact @ 70% span	10.9	See Figure 9	90.0	No	52.7	Plastic deformation of specimen at root; 0.71 cm deflection measured at tip. Specimen mount moved due to impact.	Hycam	Timing marks 1,000/sec	No
4	2-0096	Micro-balloon gelatin bird (cylinder) (3.81 cm dia. x 7.62 cm long)	98.6	98.6	8-1-1 Ti flat plate with one-half blade-type aspect ratio of F101 blade	Center impact @ 70% span	10.9	See Figure 9	90.0	No	99.4	Plastic deformation of specimen at root; 1.11 cm deflection measured at tip.	Hycam	Timing marks 1,000/sec	Yes
4	2-0097	Micro-balloon gelatin bird (cylinder) (3.81 cm dia. x 7.62 cm long)	95.9	95.9	8-1-1 Ti flat plate with one-half blade-type aspect ratio of F101 blade	Center impact @ 70% span	10.9	See Figure 9	90.0	No	90.2	Plastic deformation of specimen at root; 0.71 cm deflection measured at tip.	Hycam	Timing marks 1,000/sec	Yes
4	2-0098	Micro-balloon gelatin bird (cylinder) (3.81 cm dia. x 7.62 cm long)	96.4	96.4	8-1-1 Ti flat plate with one-half blade-type aspect ratio of F101 blade	Center impact @ 70% span	10.9	See Figure 9	90.0	No	150.6	Plastic deformation of specimen at root; 6.12 cm deflection measured at tip.	Hycam	Timing marks 1,000/sec	Yes
5	2-0193	Micro-balloon gelatin bird (cylinder) (7.62 cm dia. x 15.24 cm long)	670.3	79.3	8-1-1 Ti flat plate with one-half blade-type aspect ratio of F101 blade	Center impact @ 30% span	10.9	See Figure 10	41.0	No	190.9	No visible damage on specimen. No strain gauge data or film.	No film	--	No

TABLE 13. RESULTS OF STATIC IMPACT TESTING (CONTINUED)

Group No.	Shot No.	Projectile Type	Projectile Mass (g)	Mass Impacting Target (g)	Target Material and Description	Span Location for Impact (%)	Impact Distance from Root (cm)	Strain Gauge Locations	Impact Angle (°)	Shroud Restraint	Impact Velocity (m/s)	Damage Description and Comments	High-Speed Camera Type	Camera Framing Rate (frames/sec)	Deformation Plot
5	2-0194	Micro-balloon gelatin bird (cylinder) (7.62 cm dia. x 15.24 cm long)	668.1	154.5	8-1-1 Ti flat plate with one-half blade type aspect ratio of F101 blade	Center impact @ 30% span	10.9	See Figure 10	41.0	No	191.8	No visible damage on specimen.	Dynafax	20,320	No
5	2-0195	Micro-balloon gelatin bird (cylinder) (7.62 cm dia. x 15.24 cm long)	681.6	79.9	8-1-1 Ti flat plate with one-half blade type aspect ratio of F101 blade	Center impact @ 30% span	10.9	See Figure 10	41.0	No	232.3	No visible damage on specimen.	Dynafax	20,480	No
6	4-0053	Micro-balloon gelatin bird (cylinder) (3.81 cm dia. x 7.62 cm long)	83.1	83.1	8-1-1 Ti flat plate with blade-type aspect ratio and one-half blade-type thickness/ chord ratio of F101 blade	Center impact @ 70% span	23.6	No gauges	90.0	No	74.9	Plastic deformation of specimen at root; 3.02 cm deflection on left side and 3.18 cm deflection on right side measured at tip.	No film	--	No
6	4-0054	Micro-balloon gelatin bird (cylinder) (3.81 cm dia. x 7.62 cm long)	83.5	83.5	8-1-1 Ti flat plate with blade-type aspect ratio and one-half blade-type thickness/ chord ratio of F101 blade	Center impact @ 70% span	23.1	No gauges	90.0	No	126.1	Specimen broke off at root.	No film	--	No

TABLE 13. RESULTS OF STATIC IMPACT TESTING (CONTINUED)

Group No.	Shot No.	Projectile Type	Projectile Mass (g)	Mass Impacting Target (g)	Target Material and Description	Span Location for Impact (%)	Impact Distance from Root (cm)	Strain Gauge Locations	Impact Angle (°)	Shroud Restraint	Impact Velocity (m/s)	Damage Description and Comments	High-Speed Camera Type	Camera Framing Rate (frames/sec)	Deformation Plot
6	4-0055	Micro-balloon gelatin bird (cylinder) (3.81 cm dia. x 7.62 cm long)	82.6	82.6	8-1-1 Ti flat plate with blade-type aspect ratio and one-half blade-type thickness/ chord ratio of F101 blade	Center impact @ 70% span	22.5	No gauges	90.0	No	103.8	Plastic deformation of specimen at root; 10.95 cm deflection for both sides measured at tip.	No film	--	No
6	2-0175	Micro-balloon gelatin bird (cylinder) (3.81 cm dia. x 7.62 cm long)	85.2	85.2	8-1-1 Ti flat plate with blade-type aspect ratio and one-half blade-type thickness/ chord ratio of F101 blade	Center impact @ 70% span	21.8	See Figure 7	90.0	No	134.1E Velocity Estimated	Plastic deformation of specimen at root and impact site. Impact site deflection-0.81 cm. Tip deflection-15.24 cm on left side and 14.73 cm on right side. Specimen impacted 0.64 cm to left of center.	Dynafax	20,736	No
6	2-0176	Micro-balloon gelatin bird (cylinder) (3.81 cm dia. x 7.62 cm long)	85.3	85.3	8-1-1 Ti flat plate with blade-type aspect ratio and one-half blade-type thickness/ chord ratio of F101 blade	Center impact @ 70% span	21.8	See Figure 7	90.0	No	66.0	Plastic deformation of specimen at root. Tip deflection is 7.87 cm for both sides of specimen.	Dynafax	20,688	No

TABLE 13. RESULTS OF STATIC IMPACT TESTING (CONTINUED)

Group No.	Shot No.	Projectile Type	Projectile Mass (g)	Mass Impacting Target (g)	Target Material and Description	Span Location for Impact (%)	Impact Distance from Root (cm)	Strain Gauge Locations	Impact Angle (°)	Shroud Restraint	Impact Velocity (m/s)	Damage Description and Comments	High-Speed Camera Type	Camera Framing Rate (frames/sec)	Deformation Plot
7	2-0128	Micro-balloon gelatin bird (cylinder) (3.81 cm dia. x 7.62 cm long)	82.6	35.1	8-1-1 Ti plate with blade-type aspect ratio and airfoil shape (tapered cross section) of F101 blade	Edge impact @ 70% span	21.8	See Figure 8	24.4	No	323.2	Plastic deformation of specimen at leading edge at impact site. Impact site leading edge deflection-1.65 cm. Tip deflection is 1.14 cm for leading edge and 0.89 cm for trailing edge.	Hycam	Timing marks 1,000/sec	No
7	2-0129	Micro-balloon gelatin bird (cylinder) (3.81 cm dia. x 7.62 cm long)	84.2	13.7	8-1-1 Ti plate with blade-type aspect ratio and airfoil shape (tapered cross section) of F101 blade	Edge impact @ 70% span	21.8	See Figure 8	24.4	No	135.4	No visible damage on specimen.	Hycam	Timing marks 1,000/sec	No
7	2-0130	Micro-balloon gelatin bird (cylinder) (3.81 cm dia. x 7.62 cm long)	85.1	15.1	8-1-1 Ti plate with blade-type aspect ratio and airfoil shape (tapered cross section) of F101 blade	Edge impact @ 70% span	21.8	See Figure 8	24.4	No	211.0	Plastic deformation on specimen leading edge at impact site with 0.16 cm bow.	Hycam	Timing marks 1,000/sec	Yes

TABLE 13. RESULTS OF STATIC IMPACT TESTING (CONTINUED)

Group No.	Shot No.	Projectile Type	Projectile Mass	Mass Impacting Target (g)	Target Material and Description	Span Location for Impact (%)	Impact Distance from Root (cm)	Strain Gauge Locations	Impact Angle (°)	Shroud Restraint	Impact Velocity (m/s)	Damage Description and Comments	High-Speed Camera Type	Camera Framing Rate (frames/sec)	Deformation Plot
8	2-0164	Micro-balloon gelatin bird (cylinder) (7.62 cm dia. x 15.24 cm long)	683.2	188	8-1-1 Ti plate with blade-type aspect ratio and airfoil shape (tapered cross section of F101 blade	Edge impact @ 70% span	21.8	See Figure 8	24.4	No	59.1	Plastic deformation on specimen leading edge at impact site with 0.16 cm bow.	Hycam	Timing marks 1,000/sec	No
8	2-0165	Micro-balloon gelatin bird (cylinder) (7.62 cm dia. x 15.24 cm long)	679.4	24.1	8-1-1 Ti plate with blade-type aspect ratio and airfoil shape (tapered cross section of F101 blade	Edge impact @ 70% span	21.8	See Figure 8	24.4	No	112.2	No visible damage on specimen.	Hycam	Timing marks 1,000/sec	No
8	2-0166	Micro-balloon gelatin bird (cylinder) (7.62 cm dia. x 15.24 cm long)	699.2	120.1	8-1-1 Ti plate with blade-type aspect ratio and airfoil shape (tapered cross section of F101 blade	Edge impact @ 70% span	21.8	See Figure 8	24.4	No	189.0	Plastic deformation of specimen at root. Deflection of tip for leading edge is 15.72 cm and 14.45 cm for trailing edge. Specimen twist measured 1.27 cm.	Hycam	Timing marks 1,000/sec	No

TABLE 13. RESULTS OF STATIC IMPACT TESTING (CONTINUED)

Group No.	Shot No.	Projectile Type	Projectile Mass (g)	Mass Impacting Target (g)	Target Material and Description	Span Location for Impact (%)	Impact Distance from Root (cm)	Strain Gauge Locations	Impact Angle (°)	Shroud Restraint	Impact Velocity (m/s)	Damage Description and Comments	High-Speed Camera Type	Camera Framing Rate (frames/sec)	Deformation Plot
8	2-0167	Micro-balloon gelatin bird (cylinder) (7.62 cm dia. x 15.24 cm long)	618.6	119.5	8-1-1 Ti plate with blade-type aspect ratio and airfoil shape (tapered cross section) of F101 blade	Edge impact @ 70% span	21.8	See Figure 8	24.4	No	130.5	Plastic deformation of specimen at root. Deflection at tip for leading edge is 20.96 cm and 20.32 for trailing edge. Specimen twist measured 0.64 cm.	Hycam	Timing marks 1,000/sec	Yes
9	2-0180	Micro-balloon gelatin bird (cylinder) (7.62 cm dia. x 15.24 cm long)	681.0	329.2	8-1-1 Ti plate with blade-type aspect ratio and blade-like cross-section of F101 blade	Edge impact @ 70% span	21.8	See Figure 8	24.4	No	122.3	Specimen broke off at root.	Dynafax	20,704	No
9	2-0181	Micro-balloon gelatin bird (cylinder) (7.62 cm dia. x 15.24 cm long)	649.2	138.1	8-1-1 Ti plate with blade-type aspect ratio and blade-like cross-section of F101 blade	Edge impact @ 70% span	21.8	See Figure 8	24.4	No	61.9	No visible damage on specimen.	No film	--	No
9	2-0182	Micro-balloon gelatin bird (cylinder) (7.62 cm dia. x 15.24 cm long)	681.0	--	8-1-1 Ti plate with blade-type aspect ratio and blade-like cross-section of F101 blade	Edge impact @ 70% span	21.8	See Figure 8	24.4	No	100.0E	No strain gauge data or film. Impact velocity estimated and impact mass not determined.	No film	--	No

TABLE 13. RESULTS OF STATIC IMPACT TESTING (CONTINUED)

Group No.	Shot No.	Projectile Type	Projectile Mass (g)	Mass Impacting Target (g)	Target Material and Description	Span Location for Impact (%)	Impact Distance from Root (cm)	Strain Gauge Locations	Impact Angle (°)	Shroud Restraint	Impact Velocity (m/s)	Damage Description and Comments	High-Speed Camera Type	Camera Framing Rate (frames/sec)	Deformation Plot
9	2-0183	Micro-balloon gelatin bird (cylinder) (7.62 cm dia. x 15.24 cm long)	681.4	--	8-1-1 Ti plate with blade-type aspect ratio and blade-like cross-section of F101 blade	Edge impact @ 70% span	21.8	See Figure 8	24.4	No	89.6	Bird hit target tank upon entry. No visible damage on specimen. Impact mass unable to be determined.	Dynafax	20,592	No
9	2-0184	Micro-balloon gelatin bird (cylinder) (7.62 cm dia. x 15.24 cm long)	670.0	--	8-1-1 Ti plate with blade-type aspect ratio and blade-like cross-section of F101 blade	Edge impact @ 70% span	21.8	See Figure 8	24.4	No	100.3	No visible damage on specimen. Bird velocity to load specimen after being presliced too low to complete second slice by target specimen.	Dynafax	20,544	No
9	2-0185	Micro-balloon gelatin bird (cylinder) (7.62 cm dia. x 15.24 cm long)	680.0	--	8-1-1 Ti plate with blade-type aspect ratio and blade-like cross-section of F101 blade	Edge impact @ 70% span	21.8	See Figure 8	24.4	No	114.0	No visible damage on specimen. Bird hit target tank upon entry. Impact mass unable to be determined.	Dynafax	20,608	No
9	2-0186	Micro-balloon gelatin bird (cylinder) (7.62 cm dia. x 15.24 cm long)	590.0	--	8-1-1 Ti plate with blade-type aspect ratio and blade-like cross-section of F101 blade	Edge impact @ 70% span	21.8	See Figure 8	24.4	No	120.1	No visible damage on specimen. No film. Unable to determine impact mass.	No film	--	No

TABLE 13. RESULTS OF STATIC IMPACT TESTING (CONTINUED)

Group No.	Shot No.	Projectile Type	Projectile Mass (g)	Mass Impacting Target (g)	Target Material and Description	Span Location for Impact (%)	Impact Distance from Root (cm)	Strain Gauge Locations	Impact Angle (°)	Shroud Restraint	Impact Velocity (m/s)	Damage Description and Comments	High-Speed Camera Type	Camera Framing Rate (frames/sec)	Deformation Plot
9	2-0187	Micro-balloon gelatin bird (cylinder) (7.62 cm dia. x 15.24 cm long)	675.0	--	8-1-1 Ti plate with blade-type aspect ratio and blade-like cross-section of F101 blade	Edge impact @ 70% span	21.8	See Figure 8	24.4	No	151.2	No visible damage on specimen. No film. Unable to determine impact mass.	No film	--	No
9	2-0188	Micro-balloon gelatin bird (cylinder) (7.62 cm dia. x 15.24 cm long)	675.2	--	8-1-1 Ti plate with blade-type aspect ratio and blade-like cross-section of F101 blade	Edge impact @ 70% span	21.8	See Figure 8	24.4	No	183.0E	No visible damage on specimen. No film and velocity was estimated. Unable to determine impact mass.	Dynafax	20,816	No
9	2-0189	Micro-balloon gelatin bird (cylinder) (7.62 cm dia. x 15.24 cm long)	679.5	40.5	8-1-1 Ti plate with blade-type aspect ratio and blade-like cross-section of F1C1 blade	Edge impact @ 70% span	21.8	See Figure 8	24.4	No	144.6	No visible damage on specimen.	Dynafax	20,704	No
9	2-0190	Micro-balloon gelatin bird (cylinder) (7.62 cm dia. x 15.24 cm long)	681.6	101.1	8-1-1 Ti plate with blade-type aspect ratio and blade-like cross-section of F101 blade	Edge impact @ 70% span	21.8	See Figure 8	24.4	No	185.4	No visible damage on specimen.	Dynafax	20,224	Yes

TABLE 13. RESULTS OF STATIC IMPACT TESTING (CONTINUED)

Group No.	Shot No.	Projectile Type	Projectile Mass (g)	Mass Impacting Target (g)	Target Material and Description	Span Location for Impact (%)	Impact Distance from Root (cm)	Strain Gauge Locations	Impact Angle (°)	Shroud Restraint	Impact Velocity (m/s)	Damage Description and Comments	High-Speed Camera Type	Camera Framing Rate (frames/sec)	Deformation Plot
9	2-0191	Micro-balloon gelatin bird (cylinder) (7.62 cm dia. x 15.24 cm long)	679.9	--	8-1-1 Ti plate with blade-type aspect ratio and blade-like cross-section of F101 blade	Edge impact @ 70% span	21.8	See Figure 8	24.4	No	239.9	No visible damage on specimen. Bird hit target tank upon entry. No film.	No film	--	No
9	2-0192	Micro-balloon gelatin bird (cylinder) (7.62 cm dia. x 15.24 cm long)	686.2	77.3	8-1-1 Ti plate with blade-type aspect ratio and blade-like cross-section of F101 blade	Edge impact @ 70% span.	21.8	See Figure 8	24.4	No	203.7	Severe damage. Specimen bent and broke at root area.	Dynafax	20,352	No
10	2-0177	Micro-balloon gelatin bird (cylinder) (3.81 cm dia. x 7.62 cm long)	85.3	85.3	8-1-1 Ti plate with blade-type aspect ratio and blade-like cross-section of F101 blade	Center impact @ 70% span	21.8	See Figure 11	90.0	Yes	126.5	Plastic deformation of specimen at impact site. Bow of 0.89 cm on left side of specimen and 0.95 cm on right side.	Dynafax	21,024	No
10	2-0178	Micro-balloon gelatin bird (cylinder) (3.81 cm dia. x 7.62 cm long)	84.3	84.3	8-1-1 Ti plate with blade-type aspect ratio and blade-like cross-section of F101 blade	Center impact @ 70% span	21.8	See Figure 11	90.0	Yes	29.3	No visible damage on specimen. Velocity estimated.	Dynafax	20,736	No

TABLE 13. RESULTS OF STATIC IMPACT TESTING (CONTINUED)

Group No.	Shot No.	Projectile Type	Projectile Mass (g)	Mass Impacting Target (g)	Target Material and Description	Span Location for Impact (%)	Impact Distance from Root (cm)	Strain Gauge Locations	Impact Angle (°)	Shroud Restraint	Impact Velocity (m/s)	Damage Description and Comments	High-Speed Camera Type	Camera Framing Rate (frames/sec)	Deformation Plot
10	2-0179	Micro-balloon gelatin bird (cylinder) (3.81 cm dia. x 7.62 cm long)	85.3	85.3	8-1-1 Ti plate with blade-type aspect ratio and blade-like cross-section of F101 blade	Center impact @ 70% span	21.8	See Figure 11	90.0	Yes	203.4	Shroud restraint tore loose from mount. Tip deflection of 17.59 cm on left side of specimen and 17.72 cm on right side.	Dynafax	20,688	No
11	2-0157	Micro-balloon gelatin bird (cylinder) (7.62 cm dia. x 15.24 cm long)	682.3	265.7	403 Stainless steel flat plate with blade-type aspect ratio of J79 blade	Edge impact @ 70% span	17.2	See Figure 12	36.4	No	101.8	Specimen rocked back in mount. Plastic deformation of specimen at root by bending. Tip deflection of 17.24 cm of leading edge and 16.26 cm of trailing edge.	Hycam	Timing marks 1,000/sec	No
11	2-0158	Micro-balloon gelatin bird (cylinder) (7.62 cm dia. x 15.24 cm long)	652.8	253.8	403 Stainless steel flat plate with blade-type aspect ratio of J79 blade	Edge impact @ 70% span	17.2	See Figure 12	36.4	No	54.3	No local damage; however, specimen bent at root. Tip deflection of 7.14 cm.	Hycam	Timing marks 1,000/sec	No
12	2-0159	Micro-balloon gelatin bird (cylinder) (7.62 cm dia. x 15.24 cm long)	666.7	~300.0	403 Stainless steel cambered flat plate with blade-type aspect ratio of J79 blade	Edge impact @ 70% span	17.2	See Figure 12	36.4	No	47.9	No visible damage to specimen. Velocity low enough such that bird was not cut all the way through by specimen. Impact mass estimated.	Hycam	Timing marks 1,000/sec	No

TABLE 13. RESULTS OF STATIC IMPACT TESTING (CONTINUED)

Group No.	Shot No.	Projectile Type	Projectile Mass (g)	Mass Impacting Target (g)	Target Material and Description	Span Location for Impact (%)	Impact Distance from Root (cm)	Strain Gauge Locations	Impact Angle (°)	Shroud Restraint	Impact Velocity (m/s)	Damage Description and Comments	High-Speed Camera Type	Camera Framing Rate (frames/sec)	Deformation Plot
12	2-0163	Micro-balloon gelatin bird (cylinder) (7.62 cm dia. x 15.24 cm long)	712.7	172.3	403 Stainless steel cambered flat plate with blade-type aspect ratio of J 79 blade	Edge impact @ 70% span	17.2	See Figure 12	36.4	No	92.4	Plastic deformation of specimen by bending at root. Tip deflection of 9.84 cm.	Hycam	Timing marks 1,000/sec	Yes
13	2-0161	Micro-balloon gelatin bird (cylinder) (7.62 cm dia. x 15.24 cm long)	606.4	148.6	403 Stainless steel cambered twisted plate with blade-type aspect ratio of J79 blade	Edge impact @ 70% span	17.2	See Figure 12	36.4	No	63.7	Plastic deformation of specimen by bending at root. Tip deflection of 2.54 cm.	Hycam	Timing marks 1,000/sec	Yes
13	2-0162	Micro-balloon gelatin bird (cylinder) (7.62 cm dia. x 15.24 cm long)	692.0	192.3	403 Stainless steel cambered twisted plate with blade-type aspect ratio of J79 blade	Edge impact @ 70% span	17.2	See Figure 12	36.4	No	98.5	Plastic deformation of specimen by bending at root. Tip deflection of 17.78 cm.	Hycam	Timing marks	No
14	2-0132 specimen # VI 3B	Micro-balloon gelatin bird (cylinder) (3.81 cm dia. x 7.62 cm long)	85.0	8.4	Boron/Al cross ply flat panel with blade-type aspect ratio of APSI blade	Edge impact @ 70% span	10.8	See Figure 13	18.9	No	85.1	No visible damage to specimen.	Hycam	Timing marks 1,000/sec	No

TABLE 13. RESULTS OF STATIC IMPACT TESTING (CONTINUED)

Group No.	Shot No.	Projectile Type	Projectile Mass (g)	Mass Impacting Target (g)	Target Material and Description	Span Location for Impact (%)	Impact Distance from Root (cm)	Strain Gauge Locations	Impact Angle (°)	Shroud Restraint	Impact Velocity (m/s)	Damage Description and Comments	High-Speed Camera Type	Camera Framing Rate (frames/sec)	Deformation Plot
14	2-0133 specimen # VI 1B	Micro-balloon gelatin bird (cylinder) (3.81 cm dia. x 7.62 cm long)	85.6	12.9	Boron/Al cross ply flat panel with blade-type aspect ratio of APSI blade	Edge impact @ 70% span	10.8	See Figure 13	18.9	No	105.8	No visible damage to specimen.	Hycam	Timing marks 1,000/sec	No
14	2-0134 specimen # VI 1A	Micro-balloon gelatin bird (cylinder) (3.81 cm dia. x 7.62 cm long)	87.5	10.7	Boron/Al cross ply flat panel with blade-type aspect ratio of APSI blade	Edge impact @ 70% span	10.8	See Figure 13	18.9	No	161.9	Plastic deformation of specimen by bending at root. Tip deflection of 0.13 cm.	Hycam	Timing marks 1,000/sec	No
14	2-0135 specimen # VI 1B	Micro-balloon gelatin bird (cylinder) (3.81 cm dia. x 7.62 cm long)	84.5	16.5	Boron/Al cross ply flat panel with blade-type aspect ratio of APSI blade	Edge impact @ 70% span	10.8	See Figure 13	18.9	No	184.8	No visible damage on specimen.	Hycam	Timing marks 1,000/sec	Yes
14	2-0136 specimen # VI 1B	Micro-balloon gelatin bird (cylinder) (3.81 cm dia. x 7.62 cm long)	83.8	17.3	Boron/Al cross ply flat panel with blade-type aspect ratio of APSI blade	Edge impact @ 70% span	10.8	See Figure 13	18.9	No	243.9E	Plastic deformation of specimen by bending at root. Tip deflection of 0.23 cm. Specimen also spalled and broke opposite impact site on leading edge over an area of 5.84 x 1.65 cm velocity estimated.	Hycam	Timing marks 1,000/sec	No

TABLE 13. RESULTS OF STATIC IMPACT TESTING (CONTINUED)

Group No.	Shot No.	Projectile Type	Projectile Mass (g)	Mass Impacting Target (g)	Target Material and Description	Span Location for Impact (%)	Impact Distance from Root (cm)	Strain Gauge Locations	Impact Angle (°)	Shroud Restraint	Impact Velocity (m/s)	Damage Description and Comments	High-Speed Camera Type	Camera Framing Rate (frames/sec)	Deformation Plot
14	2-0137 specimen # VI 3B	Micro-balloon gelatin bird (cylinder) (3.81 cm dia. x 7.62 cm long)	83.0	15.9	Boron/Al cross ply flat panel with blade-type aspect ratio of APSI blade	Edge impact @ 70% span	10.8	See Figure 13	18.9	No	256.1	No visible damage on specimen.	Hycam	Timing marks 1,000/sec	No
14	2-0139 specimen # VI 3A	Micro-balloon gelatin bird (cylinder) (3.81 cm dia. x 7.62 cm long)	84.8	20.8	Boron/Al cross ply flat panel with blade-type aspect ratio of APSI blade	Edge impact @ 70% span	10.8	See Figure 13	18.9	No	312.8	Specimen broke at root. Tip deflection of 8.26 cm.	Hycam	Timing marks 1,000/sec	No
15	2-0149 specimen # VI 5A	Micro-balloon gelatin bird (cylinder) (3.81 cm dia. x 7.62 cm long)	85.3	~30.0	Boron/Al cross ply flat panel with one-half blade-type aspect ratio of APSI blade	Edge impact @ 70% span	5.4	See Figure 14	18.9	No	185.4	No visible damage on specimen. Impact mass was estimated because bird hit "C" clamp in back of specimen.	Hycam	Timing marks 1,000/sec	No
15	2-0150 specimen # VI 5B	Micro-balloon gelatin bird (cylinder) (3.81 cm dia. x 7.62 cm long)	83.6	23.8	Boron/Al cross ply flat panel with one-half blade-type aspect ratio of APSI blade	Edge impact @ 70% span	5.4	See Figure 14	15.9	No	306.4	Specimen broke off at root.	Hycam	Timing marks 1,000/sec	No

TABLE 13. RESULTS OF STATIC IMPACT TESTING (CONTINUED)

Group No.	Shot No.	Projectile Type	Projectile Mass (g)	Mass Impacting Target (g)	Target Material and Description	Span Location for Impact (%)	Impact Distance from Root (cm)	Strain Gauge Locations	Impact Angle (°)	Shroud Restraint	Impact Velocity (m/s)	Damage Description and Comments	High-Speed Camera Type	Camera Framing Rate (frames/sec)	Deformation Plot
15	2-0151 specimen # VI 5A	Micro-balloon gelatin bird (cylinder) (3.81 cm dia. x 7.62 cm long)	83.6	46.1	Boron/Al cross ply flat panel with one-half blade-type aspect ratio of APSI blade	Edge impact @ 70% span	5.4	See Figure 14	18.9	No	229.9	Specimen broke off at root.	Hycam	Timing marks 1,000/sec	No
16	2-0138 specimen # VI 7A	Micro-balloon gelatin bird (cylinder) (3.81 cm dia. x 7.62 cm long)	84.2	19.0	Boron/Al cross ply flat panel with blade-type aspect ratio and one-half blade-type thickness to chord ratio of APSI blade	Edge impact @ 70% span	10.8	See Figure 13	18.9	No	241.8	Specimen broke off at 70% span location at impact site.	Hycam	Timing marks 1,000/sec	No
16	2-0140 specimen # VI 7B	Micro-balloon gelatin bird (cylinder) (3.81 cm dia. x 7.62 cm long)	83.4	50.1	Boron/Al cross ply flat panel with blade-type aspect ratio and one-half blade-type thickness to chord ratio of APSI blade	Edge impact @ 70% span	10.8	See Figure 13	18.9	No	119.5	Specimen broke off at root. Also broke off at 70% span location at impact site approximately 12.7 cm long along leading edge and 5.72 cm long along trailing edge from tip.	Hycam	Timing marks 1,000/sec	No

TABLE 13. RESULTS OF STATIC IMPACT TESTING (CONTINUED)

Group No.	Shot No.	Projectile Type	Projectile Mass (g)	Mass Impacting Target (g)	Target Material and Description	Span Location for Impact (%)	Impact Distance from Root (cm)	Strain Gauge Locations	Impact Angle (°)	Shroud Restraint	Impact Velocity (m/s)	Damage Description and Comments	High-Speed Camera Type	Camera Framing Rate (frames/sec)	Deformation Plot
	2-0141 specimen # VI 8A	Micro-balloon gelatin bird (cylinder) (3.81 cm dia. x 7.62 cm long)	85.4	27.9	Boron/Al cross ply flat panel with blade-type aspect ratio and one-half blade-type thickness to chord ratio of ASPI blade	Edge impact @ 70% span	10.8	See Figure 13	18.9	No	96.0	Specimen broke at root of impact side giving 90° bend at break. Material holding specimen together on side opposite impact.	Hycam	Timing marks 1,000/sec	No
16	2-0142 specimen # VI 8B	Micro-balloon gelatin bird (cylinder) (3.81 cm dia. x 7.62 cm long)	86.1	5.5	Boron/Al cross ply flat panel with blade-type aspect ratio and one-half blade-type thickness to chord ratio of APSI blade	Edge impact @ 70% span	10.8	See Figure 13	18.9	No	71.3	General bending through free span with tip deflection of 0.40 cm.	Hycam	Timing marks 1,000/sec	Yes
17	2-0206	Micro-balloon gelatin bird (cylinder) (3.81 cm dia. x 7.62 cm long)	85.3	4.5	Boron/Al cross ply panel with blade-like cross-section	Edge impact @ 70% span	7.1	See Figure 15	18.9	No	79.0	No visible damage on specimen.	Dynafax	20,384	No
17	2-0207	Micro-balloon gelatin bird (cylinder) (3.81 cm dia. x 7.62 cm long)	84.7	6.2	Boron/Al cross ply panel with blade-like cross-section	Edge impact @ 70% span	7.1	See Figure 15	18.9	No	122.9	No visible damage on specimen. Bird tumbling during flight.	Dynafax	20,364	No

TABLE 13. RESULTS OF STATIC IMPACT TESTING (CONTINUED)

Group No.	Shot No.	Projectile Type	Projectile Mass (g)	Mass Impacting Target (g)	Target Material and Description	Span Location for Impact (%)	Impact Distance from Root (cm)	Strain Gauge Locations	Impact Angle (°)	Shroud Restraint	Impact Velocity (m/s)	Damage Description and Comments	High-Speed Camera Type	Camera Framing Rate (frames/sec)	Deformation Plot
17	2-0208	Micro-balloon gelatin bird (cylinder) (3.81 cm dia. x 7.62 cm long)	83.4	2.8	Boron/Al cross ply panel with blade-like cross-section	Edge impact @ 70% span	7.1	See Figure 15	18.9	No	137.6	No visible damage. Bird tumbling during flight.	Dynafax	20,384	No
17	2-0209	Micro-balloon gelatin bird (cylinder) (3.81 cm dia. x 7.62 cm long)	82.2	4.5	Boron/Al cross ply panel with blade-like cross-section	Edge impact @ 70% span	7.1	See Figure 15	18.9	No	122.9	No visible damage. Bird tumbling during flight.	Dynafax	20,240	No
17	2-0210	Micro-balloon gelatin bird (cylinder) (3.81 cm dia. x 7.62 cm long)	80.0	0.0	Boron/Al cross ply panel with blade-like cross-section	Edge impact @ 70% span	7.1	See Figure 15	18.9	No	121.0	No visible damage. Bird missed specimen.	No film	--	No
17	2-0211	Micro-balloon gelatin bird (cylinder) (3.81 cm dia. x 7.62 cm long)	82.0	5.3	Boron/Al cross ply panel with blade-like cross-section	Edge impact @ 70% span	7.1	See Figure 15	18.9	No	133.8	No visible damage on specimen.	Dynafax	20,368	No
17	2-0212	Micro-balloon gelatin bird (cylinder) (3.81 cm dia. x 7.62 cm long)	81.7	8.0	Boron/Al cross ply panel with blade-like cross-section	Edge impact @ 70% span	7.1	See Figure 15	18.9	No	194.2	No visible damage on specimen.	Dynafax	20,448	Yes

TABLE 13. RESULTS OF STATIC IMPACT TESTING (CONTINUED)

Group No.	Shot No.	Projectile Type	Projectile Mass (g)	Mass Impacting Target (g)	Target Material and Description	Span Location for Impact (%)	Impact Distance from Root (cm)	Strain Gauge Locations	Impact Angle (°)	Shroud Restraint	Impact Velocity (m/s)	Damage Description and Comments	High-Speed Camera Type	Camera Framing Rate (frames/sec)	Deformation Plot
17	2-0213	Micro-balloon gelatin bird (cylinder) (3.81 cm dia. x 7.62 cm long)	81.5	31.7	Boron/Al cross ply panel with blade-like cross-section	Edge impact @ 70% span	7.1	See Figure 15	18.9	No	247.3	Specimen broke into many smaller type pieces at impact site area.	Dynafax	20,224	No
18	2-0143 specimen # VI AF2	Micro-balloon gelatin bird (cylinder) (3.81 cm dia. x 7.62 cm. long)	85.9	3.1	Boron/Al cross ply constant chord airfoil panel with blade-type aspect ratio and camber	Edge impact @ 70% span	10.8	See Figure 16	18.9	No	138.7	No visible damage on specimen.	Hycam	Timing marks 1,000/sec	No
18	2-0144 specimen # VI AF1	Micro-balloon gelatin bird (cylinder) (3.81 cm dia. x 7.62 cm long)	82.8	6.7	Boron/Al cross ply constant chord airfoil panel with blade-type aspect ratio and camber	Edge impact @ 70% span	10.8	See Figure 16	18.9	No	202.7	No visible damage on specimen.	Hycam	Timing marks 1,000/sec	Yes
18	2-0145 specimen # VI AF3	Micro-balloon gelatin bird (cylinder) (3.81 cm dia. cm	87.3	35.6	Boron/Al cross ply constant chord airfoil panel with blade-type aspect ratio and camber	Edge impact @ 70% span	10.8	See Figure 16	18.9	No	319.8	Specimen broke off at root and also just below 70% span location.	Hycam	Timing marks 1,000/sec	No

TABLE 13. RESULTS OF STATIC IMPACT TESTING (CONCLUDED)

Group No.	Shot No.	Projectile Type	Projectile Mass (g)	Mass Impacting Target (g)	Target Material and Description	Span Location for Impact (%)	Impact Distance from Root (cm)	Strain Gauge Locations	Impact Angle (°)	Shroud Restraint	Impact Velocity (m/s)	Damage Description and Comments	High-Speed Camera Type	Camera Framing Rate (frames/sec)	Deformation Plot
19	2-0146 specimen # VI AF 25	Micro-balloon gelatin bird (cylinder) (3.81 cm dia. x 7.62 cm long)	85.6	47.0	Boron/Al cross ply constant chord airfoil panel with blade-type aspect ratio, camber, and twist	Edge impact @ 70% span	10.8	See Figure 16	[illegible]	No	208.8	Specimen broke off at root.	Hycam	Timing marks 1,000/sec	No
19	2-01 specimen # VI AF 24	Micro-balloon gelatin bird (cylinder) (3.81 cm dia. x 7.62 cm long)	85.7	11.2	Boron/Al cross ply constant [illegible]ord airfoil panel with blade-type aspect ratio, camber, and twist	Edge impact @ 70% span	10.8	See Figure 16	18.9	No	159.1	No visible damage on specimen.	Hycam	Timing marks 1,000/sec	Yes
19	2-0148 specimen # VI AF 22	Micro-balloon gelatin bird (cylinder) (3.81 cm dia. x 7.62 cm long)	85.9	33.1	Boron/Al cross ply constant chord airfoil panel with blade-type aspect ratio, camber, and twist	Edge impact @ 70% span	10.8	See Figure 16	18.9	No	185.7	Specimen broke off at root.	Hycam	Timing marks 1,000/sec	No

either artificial birds or ice projectiles which were fired on the cantilevered specimens. In several cases, the specimen tip was also restrained to simulate a tip shroud. The strain and strain rate data resulting from the impact are presented in the Volume II Report in the form of plots of strain and strain rate versus time. The test conditions for the starling-sized bird for either 30 or 70 percent span locations were presented in Table 10. Table 11 gave the test conditions for the large bird (680 g or 1.5 pound) impacts. The impact velocity was varied in the testing from a low velocity range to generate elastic deformation response (no visible damage), to a medium range to generate plastic deformation (threshold damage), and finally a high velocity range where plastic/tear deformations were produced (severe damage). Because of the huge amount of data generated in the testing, it is not practical to expand on every impact; therefore, the strain gage results of one impact of each group is described in detail in this report. The strain versus time curves are expanded to only about the first 9 ms of the impact event. All of the strain and strain rate plots versus time are contained in the Volume II report. Tension is characterized as a positive strain value while compression is a negative strain for all cases unless noted. Tip deflection versus time curves are developed for selected impacts and given for each group. In addition, the Moiré fringe technique to measure the dynamic deflection of specimens subjected to substitute bird impact was used in two groups (Group 1 and 6).

The following paragraphs describe the results of the impact tests on each group of specimens.

3.1.1.1 Impact Results for Group 1 Specimens

Impact testing on Group 1 titanium flat plate specimens with a blade type aspect ratio consisted of eight shots. Two of the impacts were conducted to obtain dynamic deflection data using the Moiré fringe apparatus and the remaining six impacts were on strain gage instrumented

specimens. The strain gage locations on this group of specimens are described in Figure 7A of Appendix A. In shots 2-0090 through 2-0094, the balsa wood sabot used to launch the artificial bird was permitted to impact the specimen along with the bird.

The dynamic displacement data for the normal impact at about the 70 percent span location is shown in Figure 6 for Shot 4-0056. Figure 7 shows in detail the specimen size, the impact location, and the span portion of the specimen of which displacement data was obtained. The data of Figure 6 was plotted at various times from 0.16 to 15.17 m sec. The shot was a normal impact of an 83 g (3 ounce size) artificial bird at 201 m/s velocity. Plastic bending of the specimen only occurred at the root. The tip was displaced 7.62 cm. Figure 1B of Appendix B shows the damage generated for Shot 4-0056 while Figure 2B gives the damage for Shot 4-0052.

Typical strain data for the Group 1 specimens is shown in Figures 8 through 13 (for Shot 2-0131). The strain gage locations on the specimen is given in Figure 7A of Appendix A. The 86 g bird normal impact at about the 70 percent location for Shot 2-0131 was at a velocity of 190 m/s. The damage generated of the specimen for this shot was plastic deflection at the root and impact site. The tip was displaced 5.69 cm. Figure 3B shows a photograph of the damage for this shot.

Dynamic displacement data was also obtained for the specimen tip for Shot 2-0131 using the high speed photograph film. Figure 14 shows a sketch of the axis orientation used in all of the dynamic tip displacement measurements using the high speed photography films. In this case, since it was a normal impact, the deflection should occur in the direction parallel to the bird trajectory (y-direction) and none should occur in the direction perpendicular to the bird trajectory (x-direction of Figure 14). Figure 15 gives the

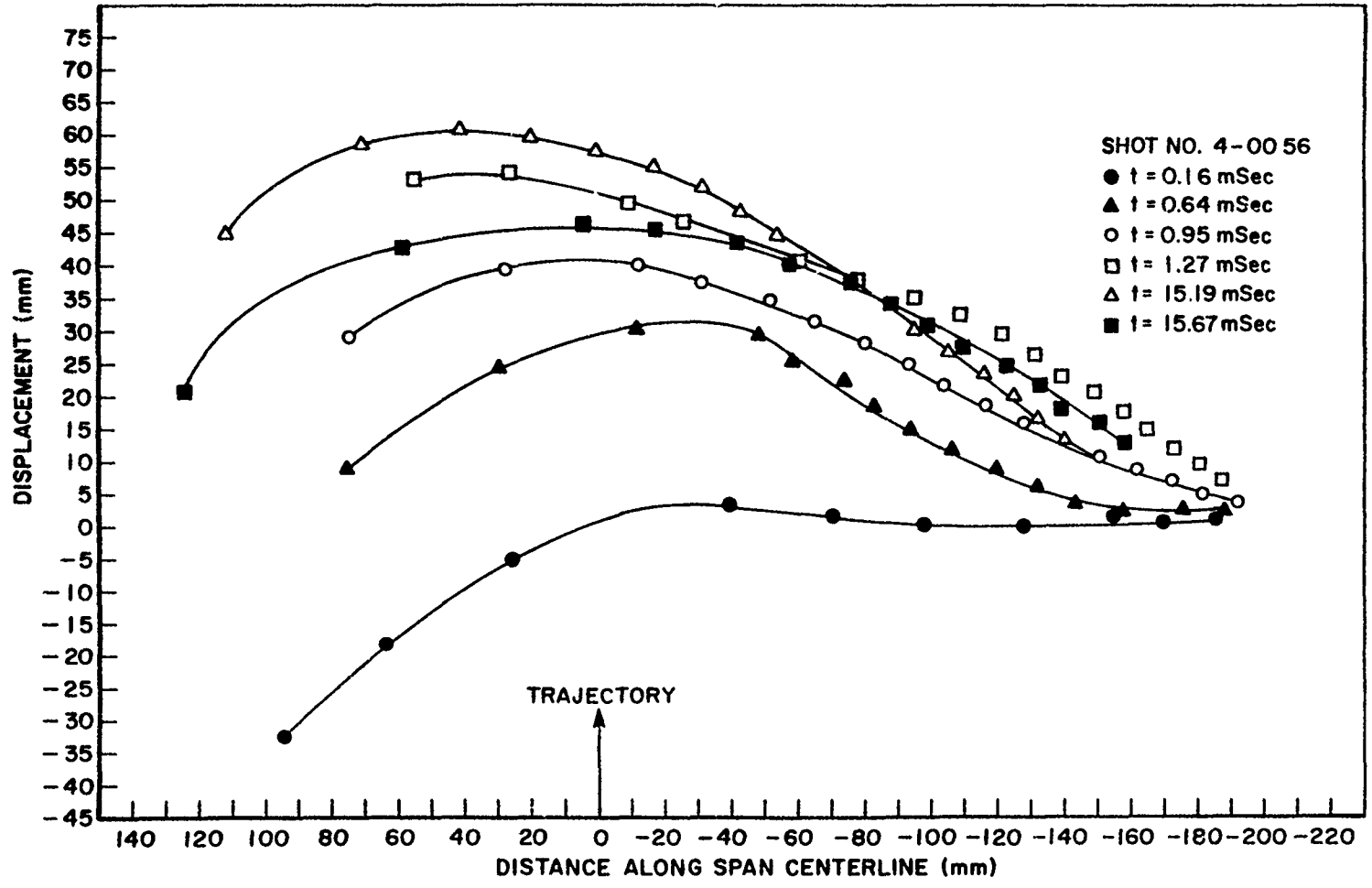

Figure 6. Moiré Fringe Displacement Data for Shot 4-0056 (Group 1 Specimen).

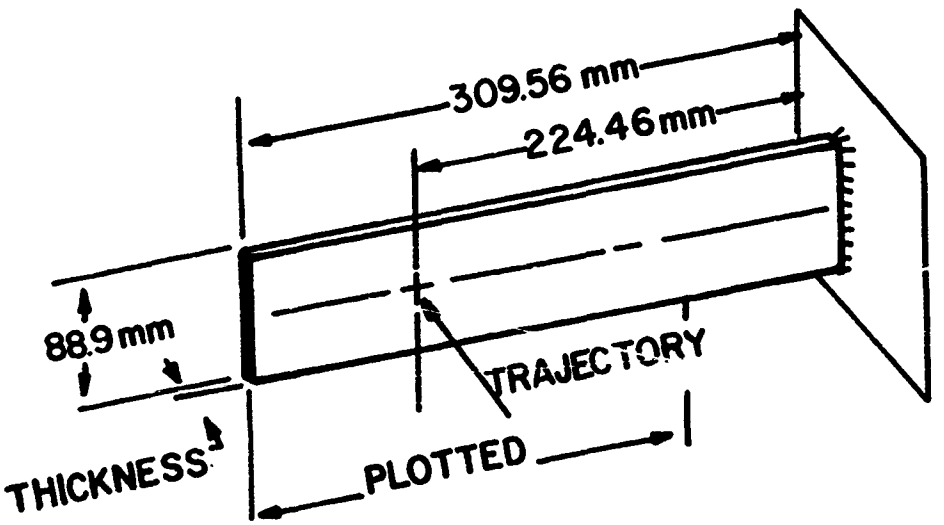

Figure 7. Sketch of Specimen Used in Shots for Displacement Data Utilizing the Moiré Fringe Apparatus.

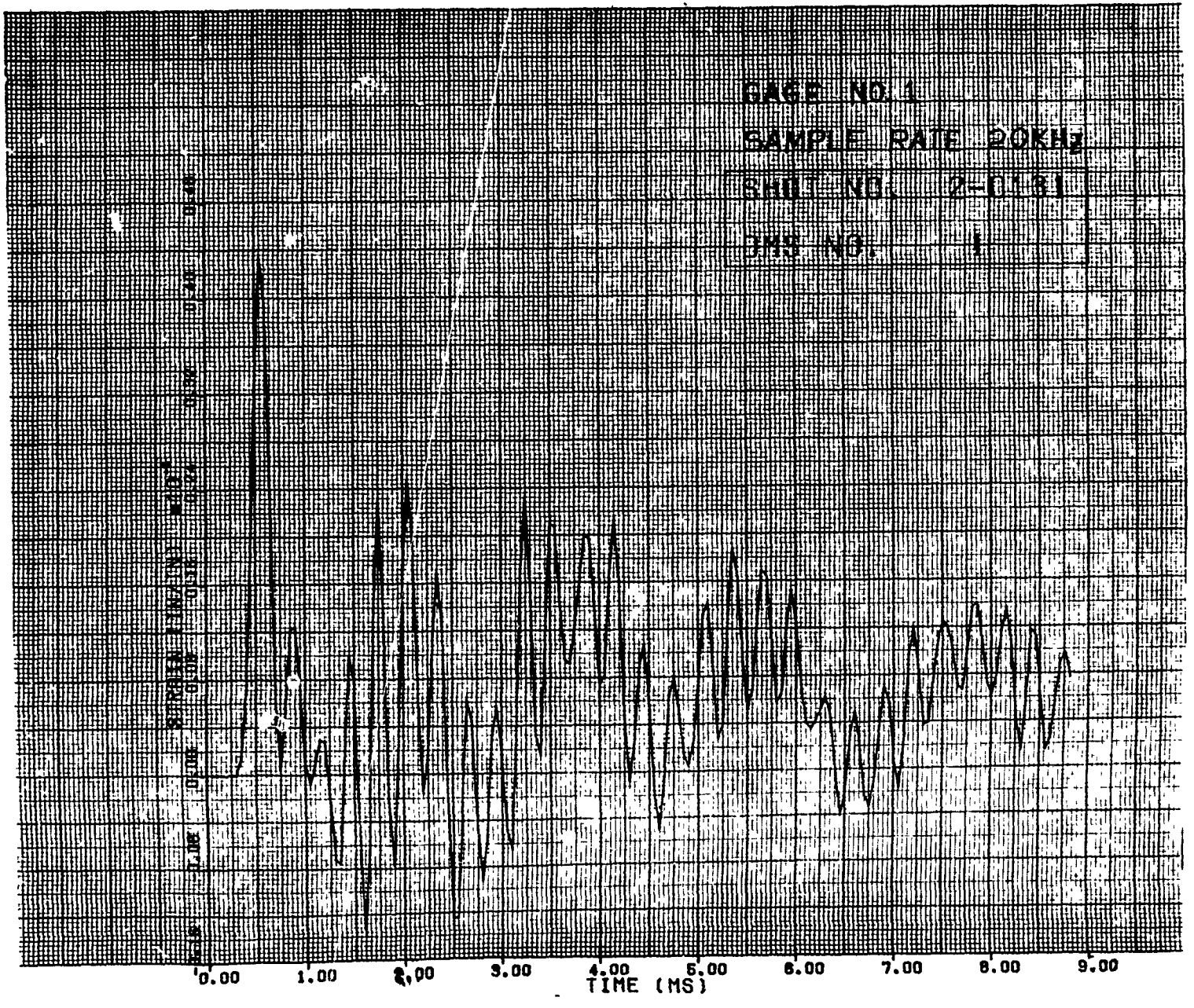
GAGE NO. 1
SAMPLE RATE 20KHz
SHOT NO. 2-0181
DMS NO. 1
0.00
1.00
2.00
3.00
4.00
5.00
6.00
7.00
8.00
9.00
TIME (MS)

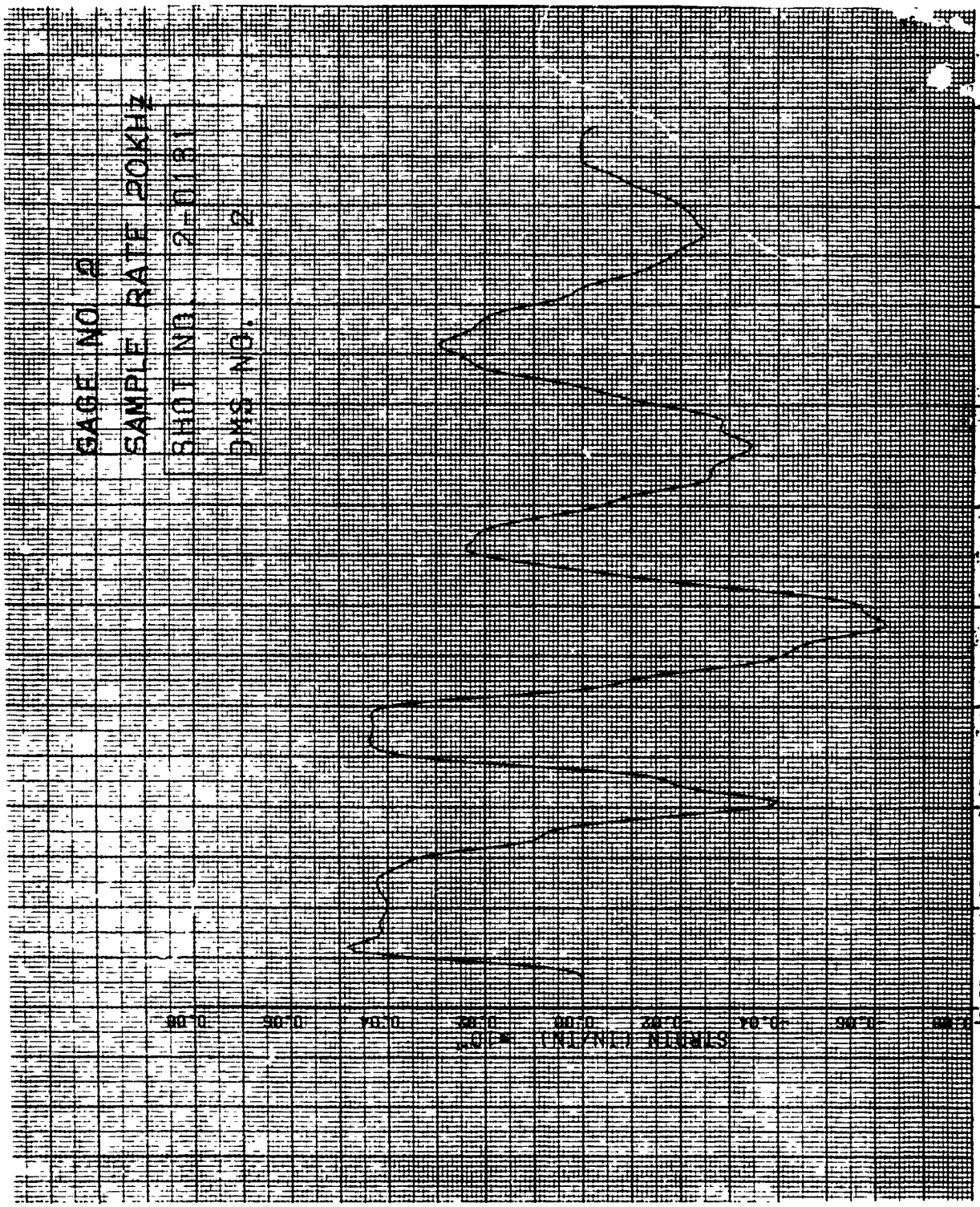

Figure 9. Strain of Shot 2-0131 for Gage #2.

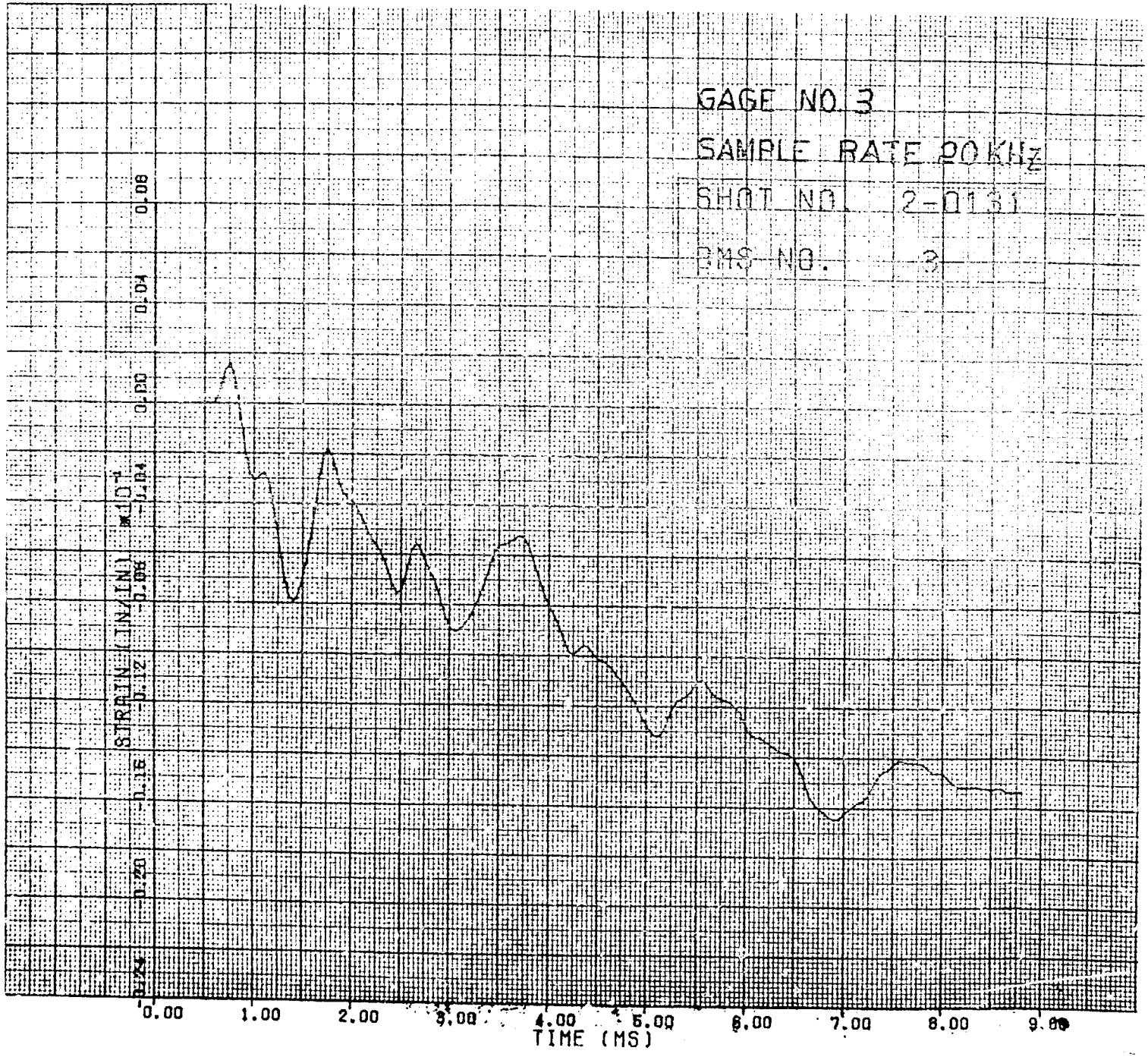

Figure 10. Strain of Shot 2-0131 for Gage #3.

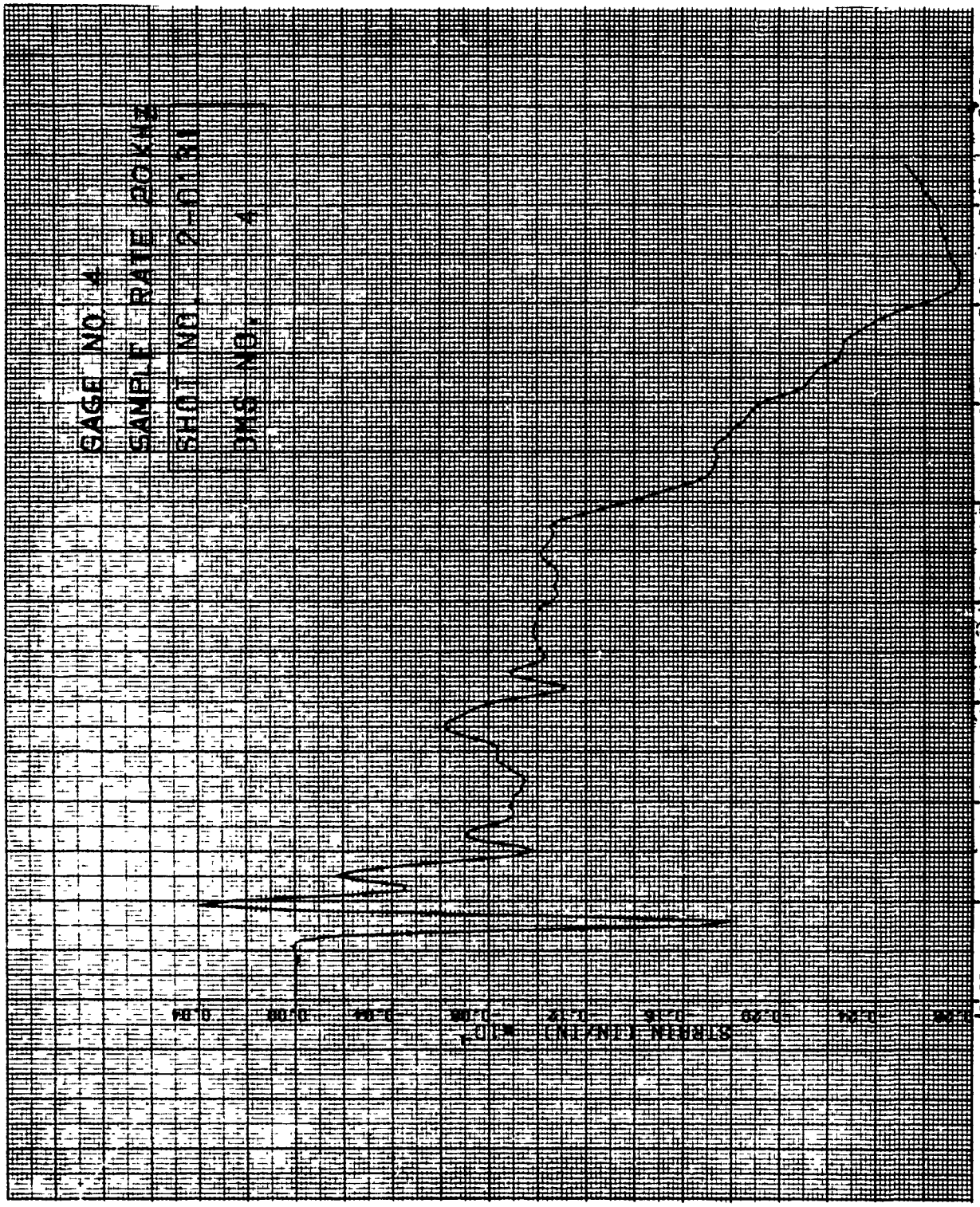

Figure 11. Strain of Shot 2-0131 for Gage #4.

GAGE No. 5
SAMPLE RATE 20KHZ
SHOT NO. 2-0-81
GMS NO. 5
STRAIN (IN/IN) *10⁻⁴
-0.01
-0.04
-0.09
-0.14
-0.19
-0.24
-0.29
-0.34
-0.39
0.00
1.00
2.00
3.00
4.00
5.00
6.00
7.00
8.00
TIME (MS)

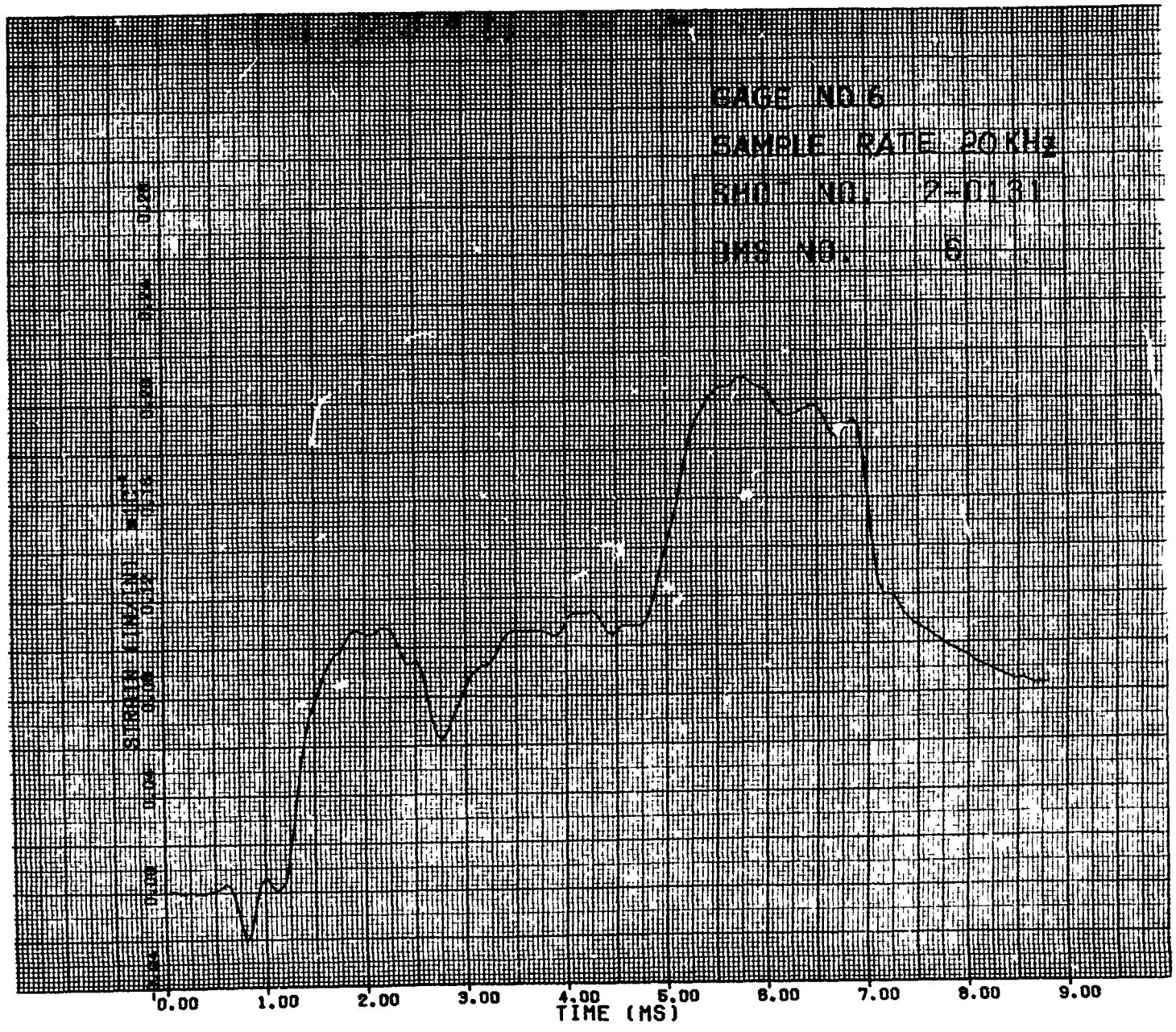

Figure 13. Strain of Shot 2-0131 for Gage #6.

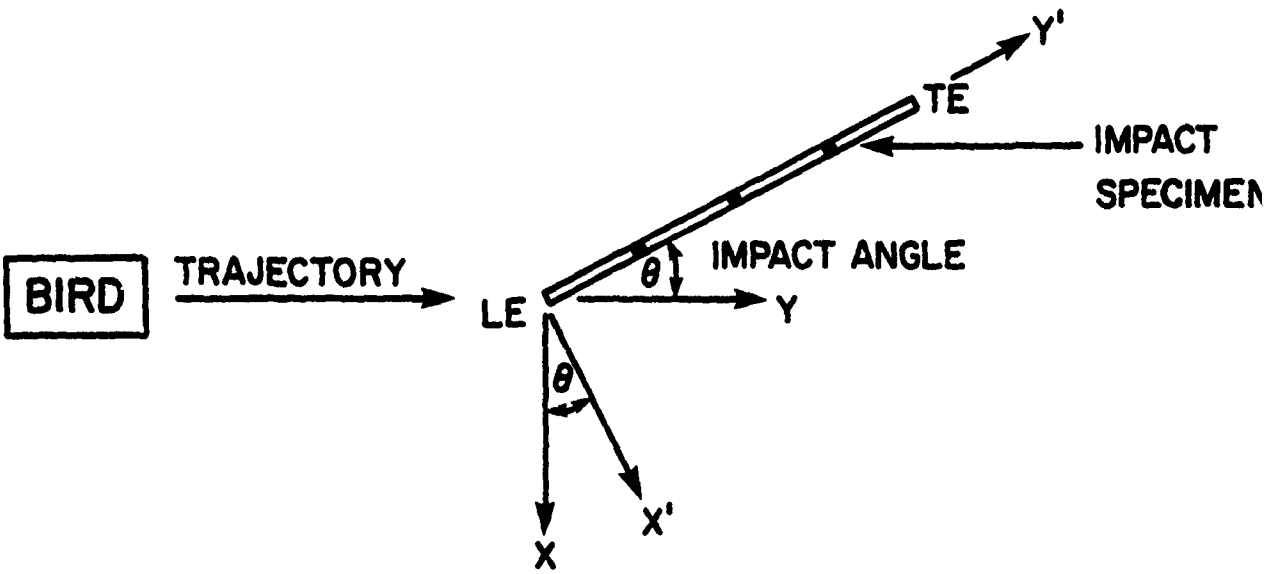

Figure 14. Sketch Showing Axis Orientation for All Tip Deflection Plots Using the High Speed Films.

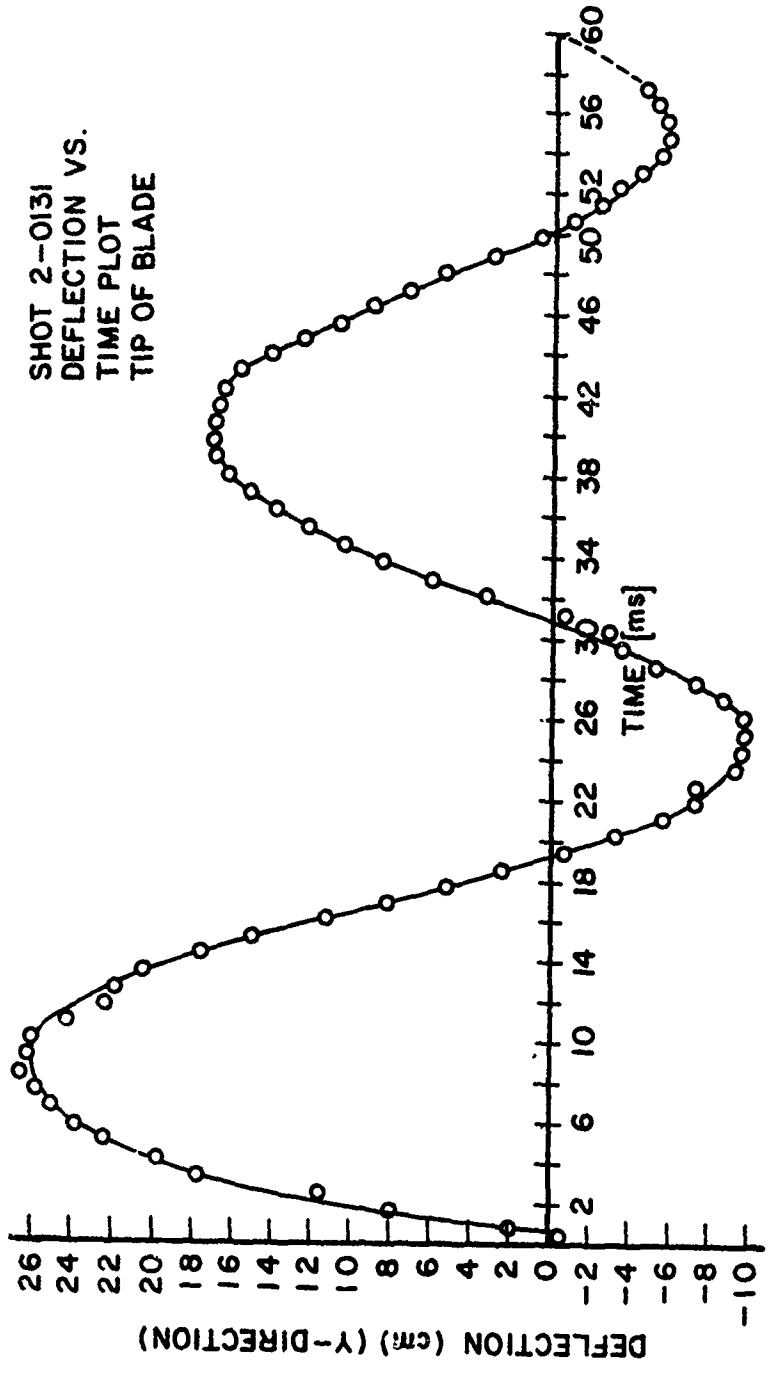

Figure 15. Tip Deflection Plot of Shot 2-0131.

dynamic tip deflection versus time plot during the impact event for Shot 2-0131.

Additional dynamic tip deflection plots are given in Figure 16 through 20 measured from the high speed photography films. Figure 16 gives the tip deflection plot for Shot 2-0090 while Figure 17 gives a plot of the bowing in the specimen tip versus time for Shot 2-0090. Figure 18 gives the tip deflection results for Shot 2-0091 while Figure 19 gives the results for Shot 2-0093. Figure 20 shows the tip deflection results for Shot 2-0094. Figure 21 gives a sequence of frames at different times of the high speed film for Shot 2-0094. Notice that the balsa wood sabot was permitted to impact the specimen as well as the substitute bird. As indicated earlier, the balsa wood sabot was used in Shots 2-0090 through 2-0094 for the impacts of the Group 1 specimens. The impact velocity for these balsa wood sabot shots ranged from 44 to 177 m/s.

3.1.1.2 Impact Results for Group 2 Specimens

Impact testing of Group 2 titanium flat plate with a blade type aspect ratio specimens consisted of seven shots as shown in Table 13. In this group, ice sphere (5.1 cm diameter) 63 g impacts were conducted at a span location of 30 percent. The center impacts were normal and the impact velocity ranged from 117 to 262 m/s.

The typical strain data for the Group 2 specimens (Shot 2-0174) are presented in Figures 22 through 27 for the various gage locations given in Figure 7A of Appendix A. The impact velocity for Shot 2-0174 was 262 m/s which generated plastic deflection damage at the impact site of about 1.65 cm (tip measurement).

Figures 4B and 5B of Appendix B show photographs of the damage for Shots 2-0173 and 2-0174, respectively.

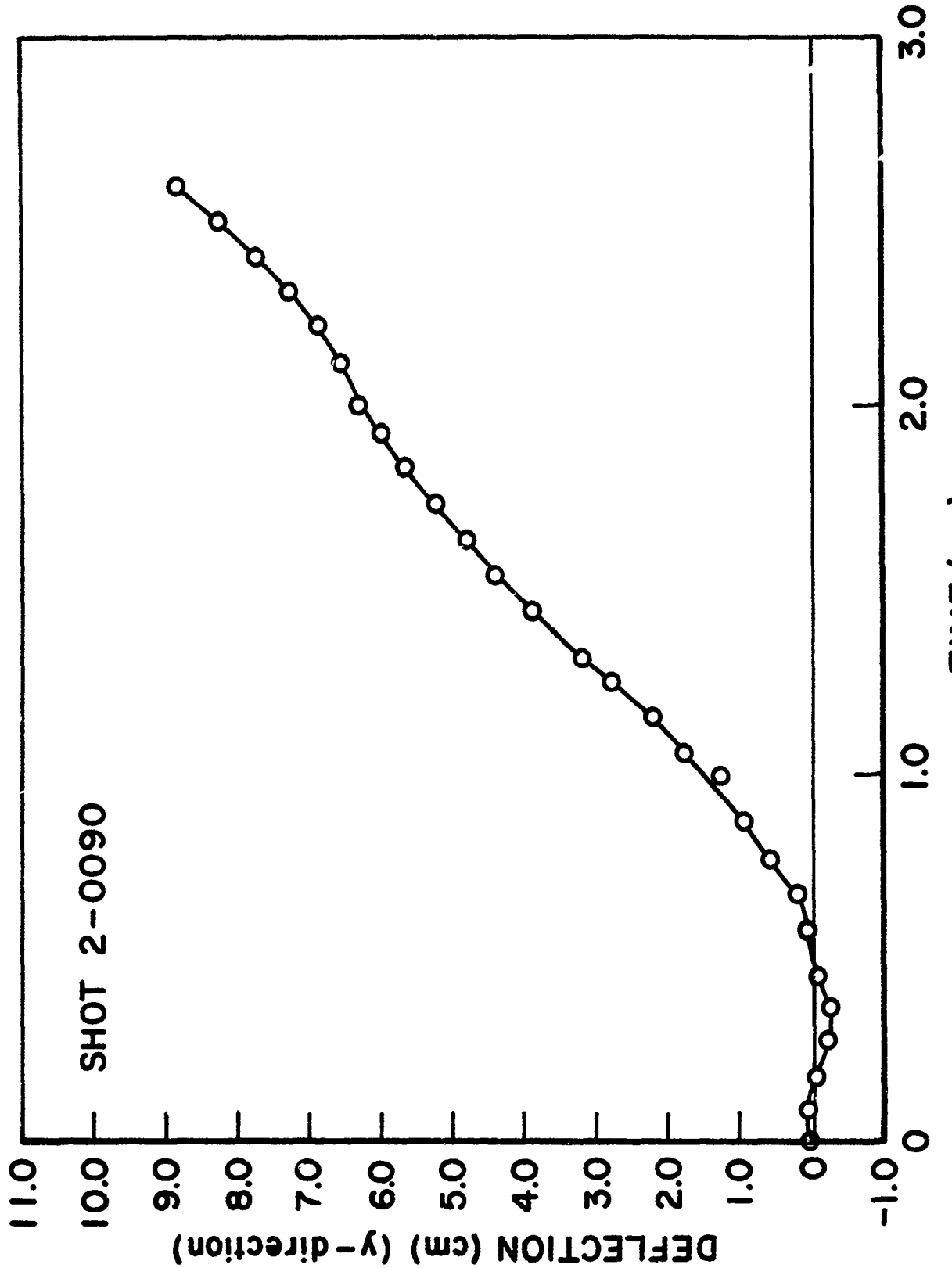

Figure 16. Tip Deflection Plot of Shot 2-0090.

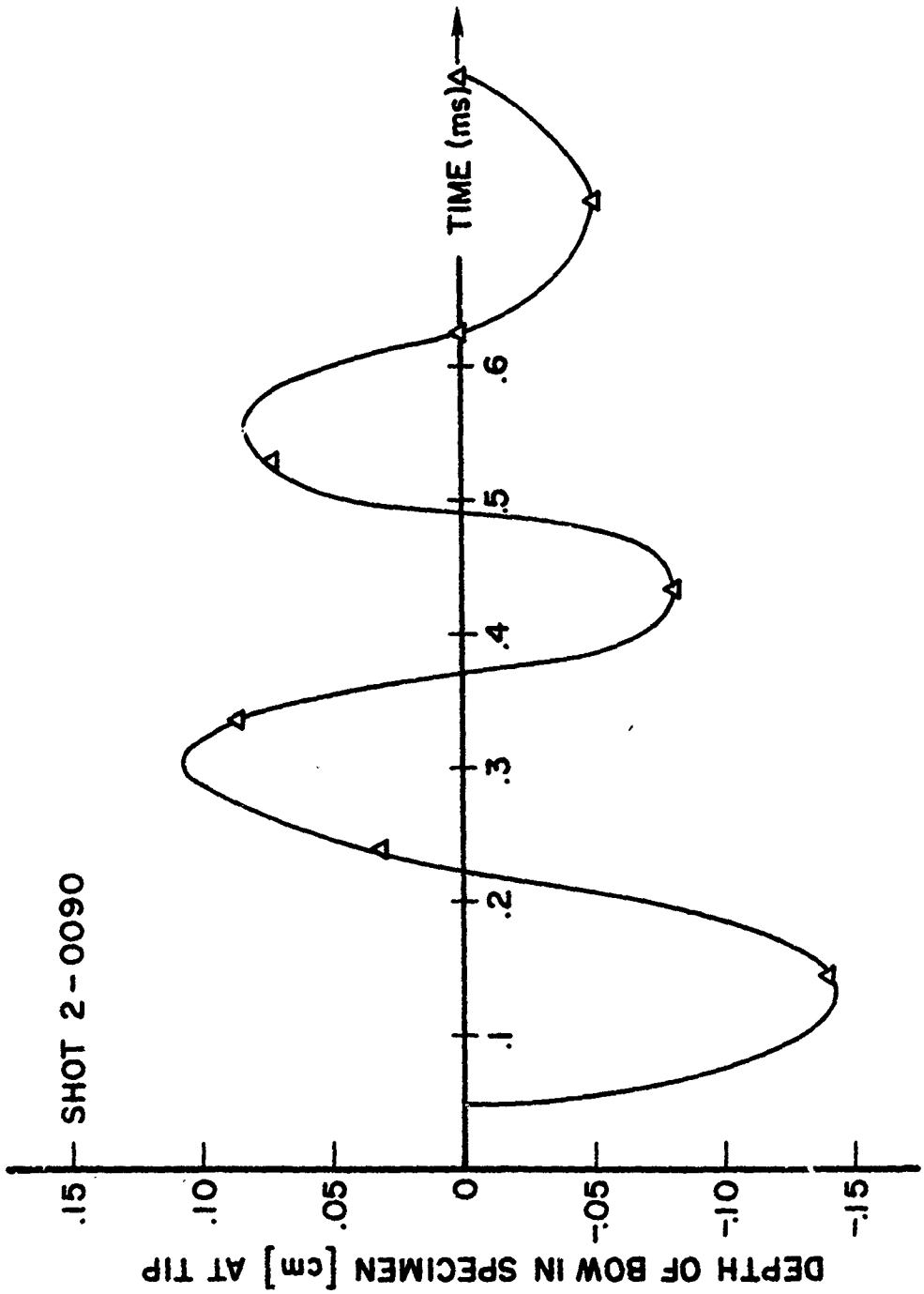

Figure 17. Tip Bow Plot of Shot 2-0090.

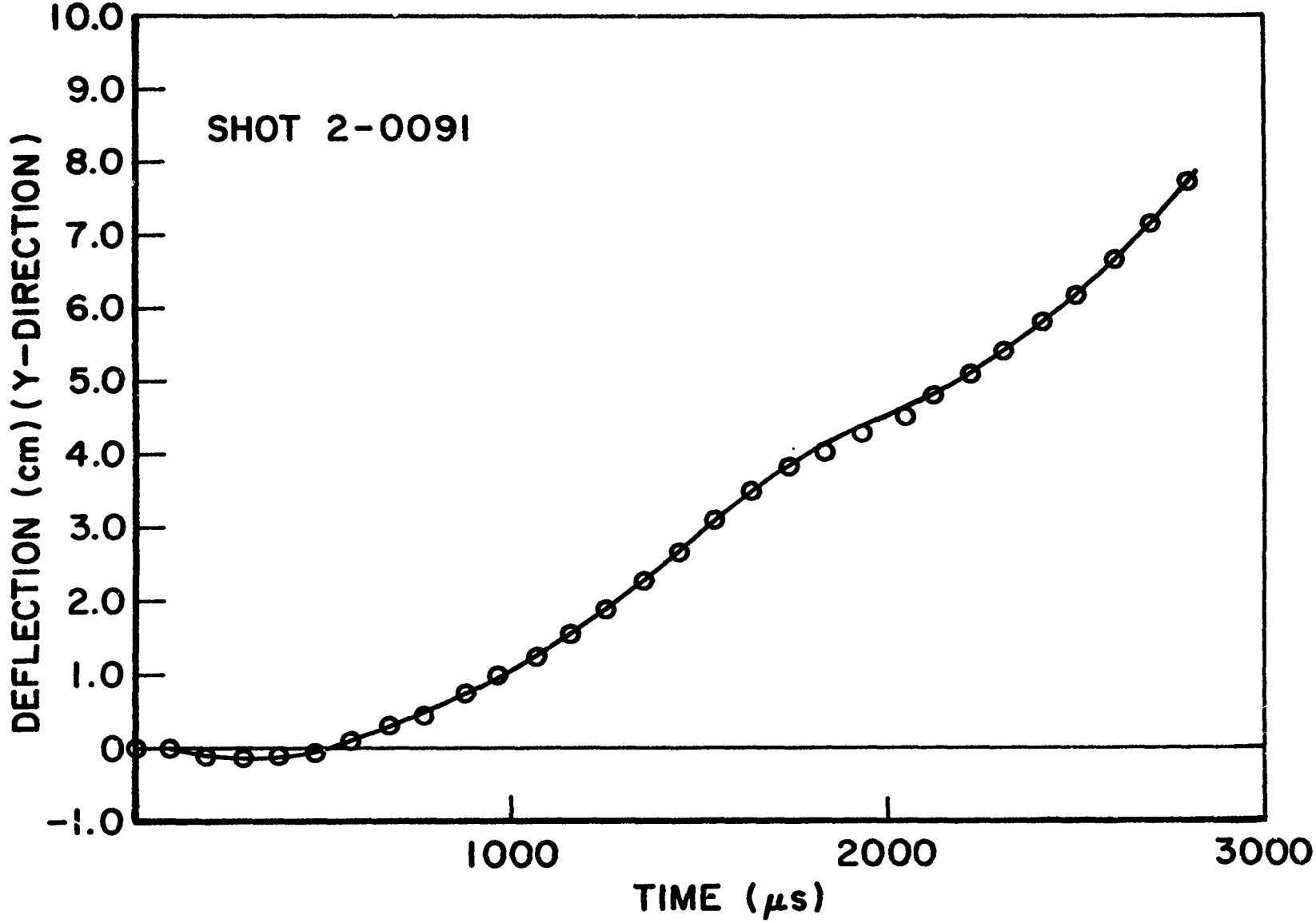

Figure 18. Tip Deflection Plot of Shot 2-0091.

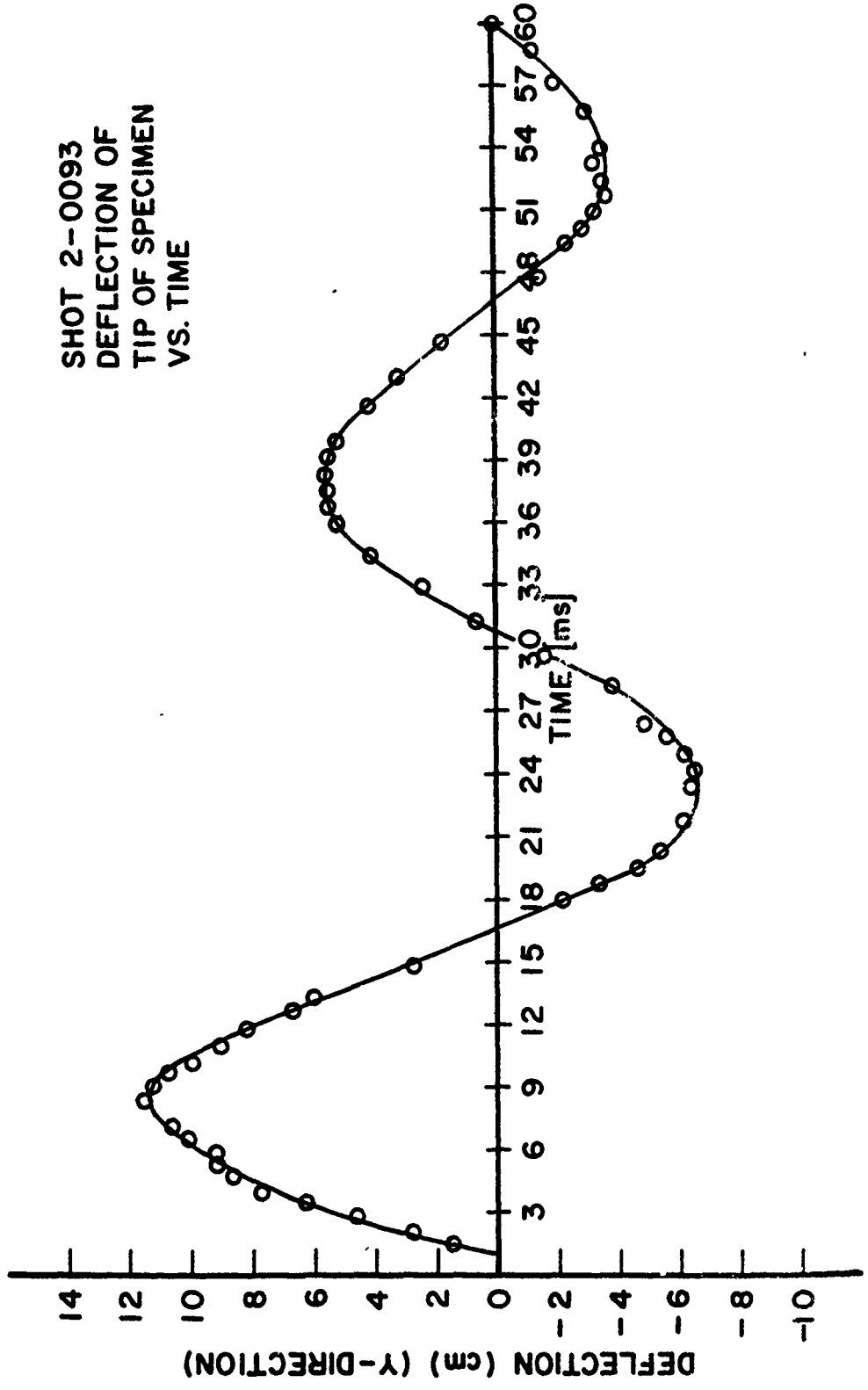

Figure 19. Tip Deflection Plot of Shot 2-0093.

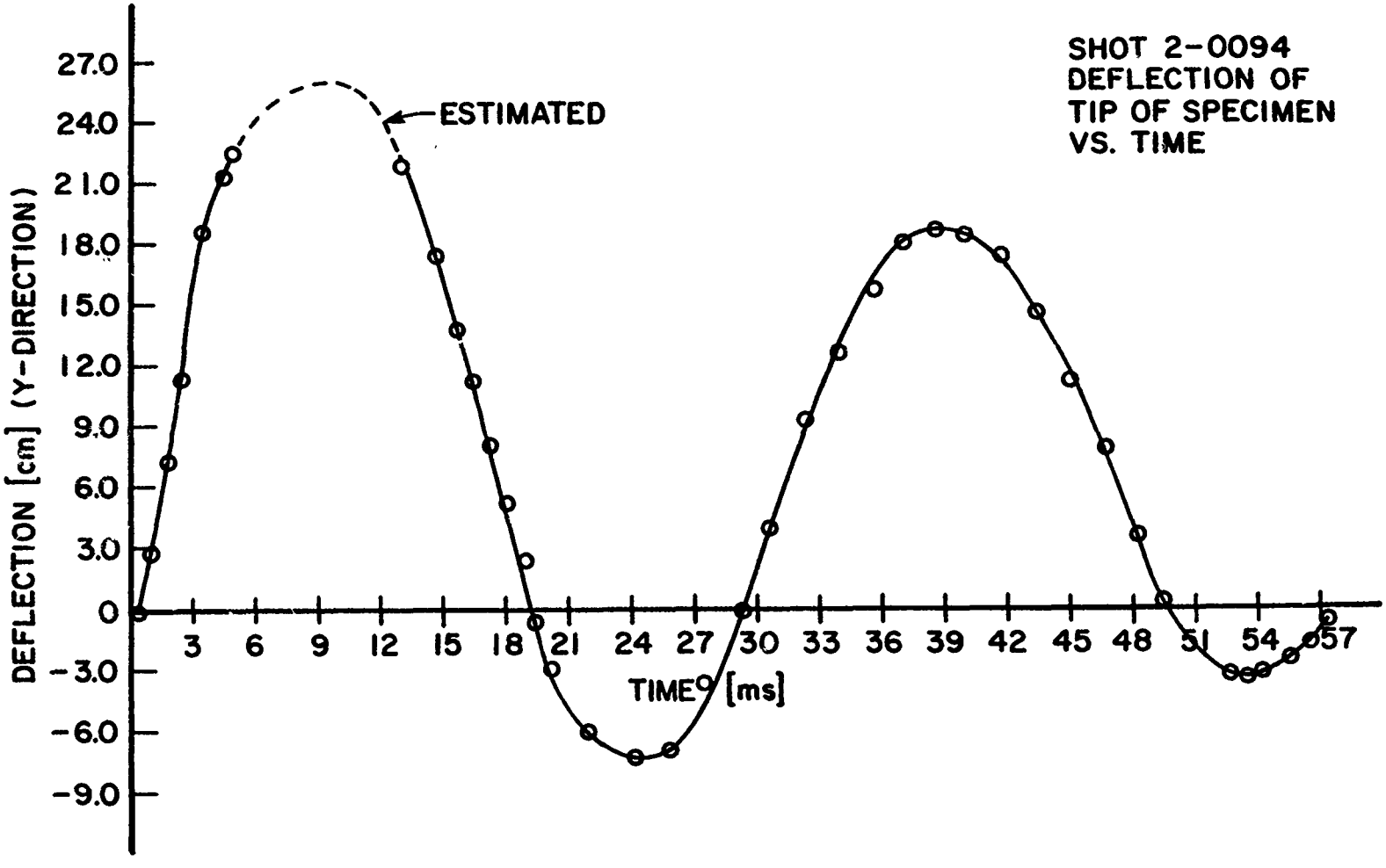

Figure 20. Tip Deflection Plot of Shot 2-0094.

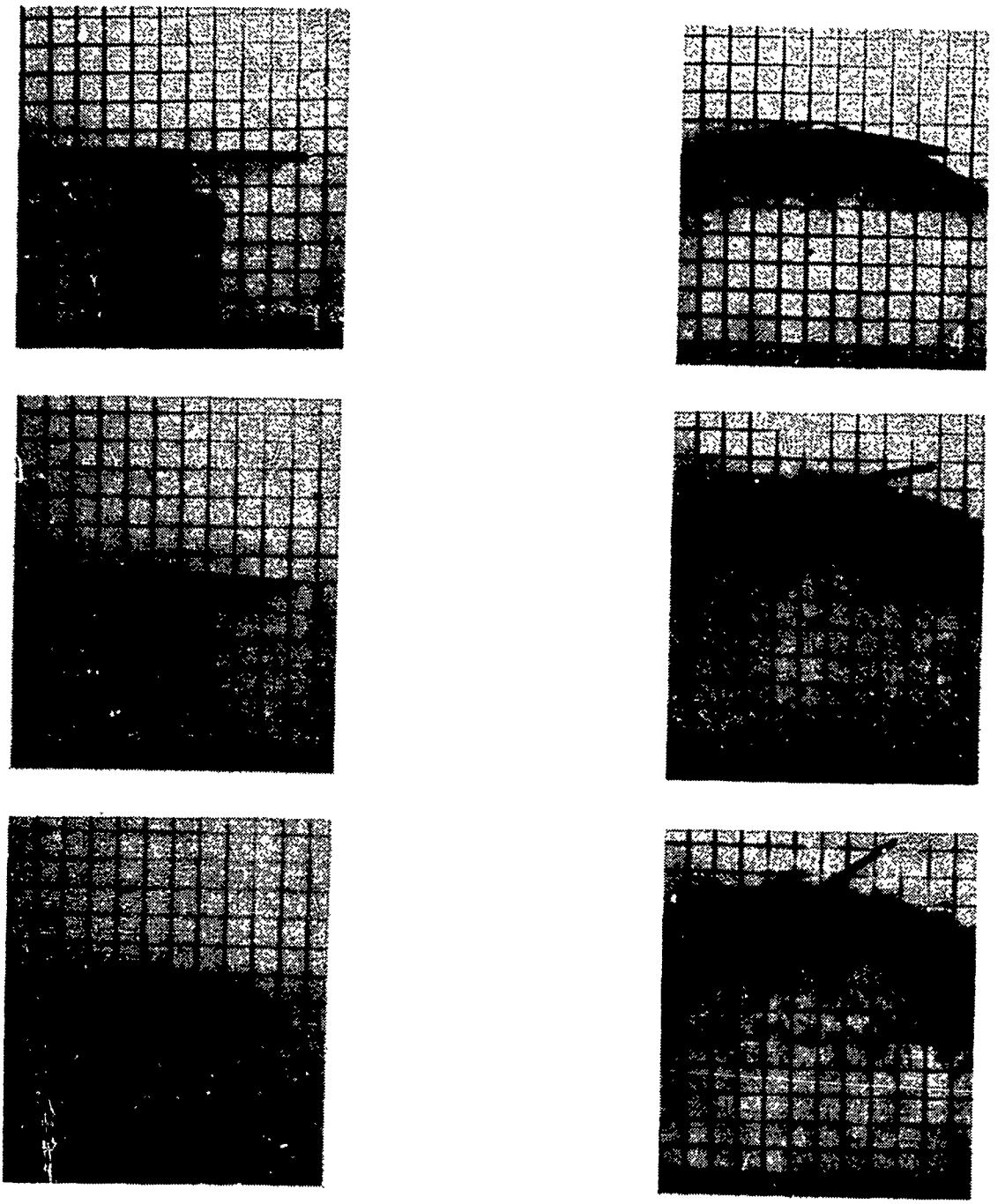

Figure 21. Sequence of Frames of High Speed Film of Shot 2-0094.

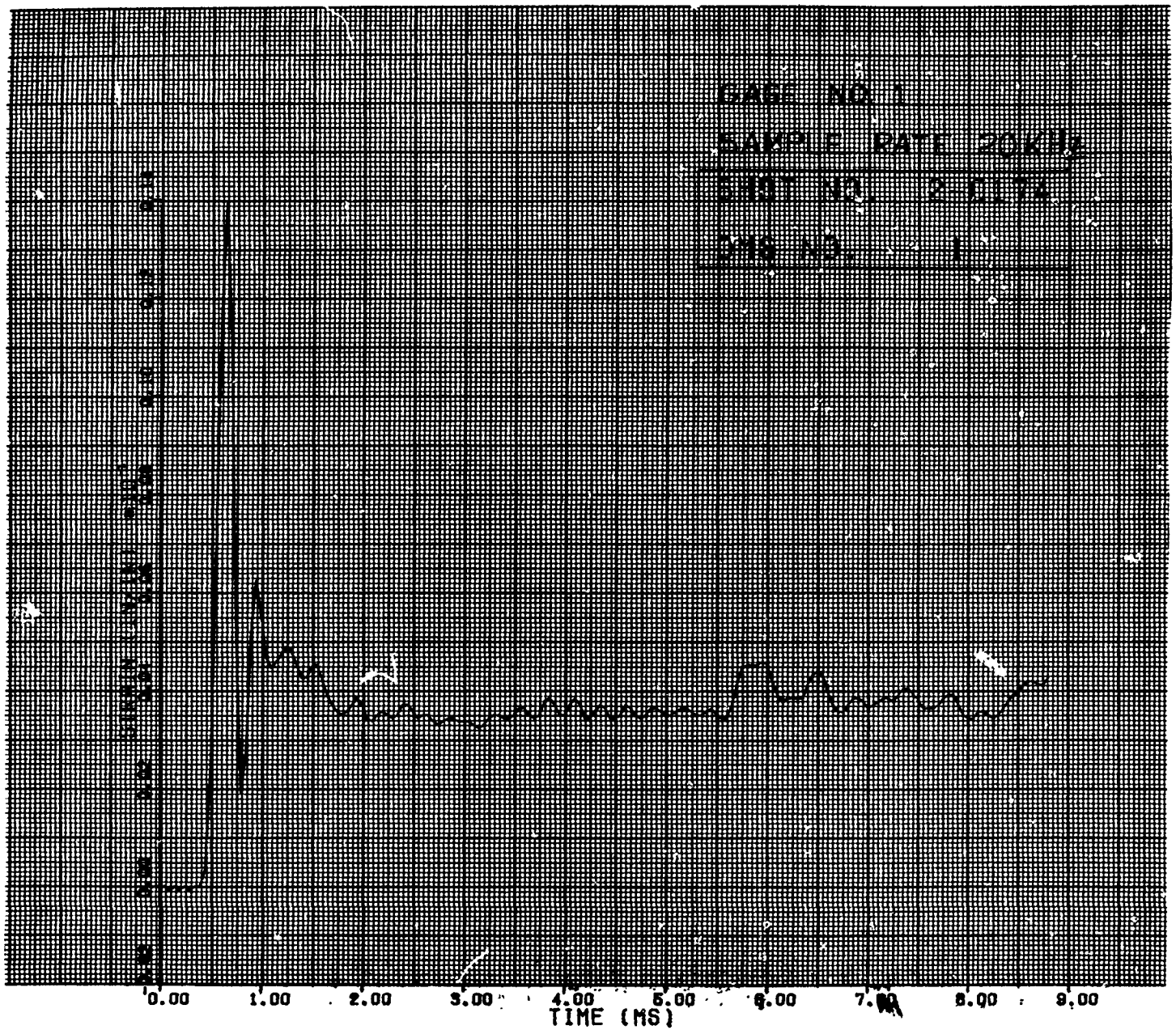

Figure 22. Strain of Shot 2-0174 for Gage #1.

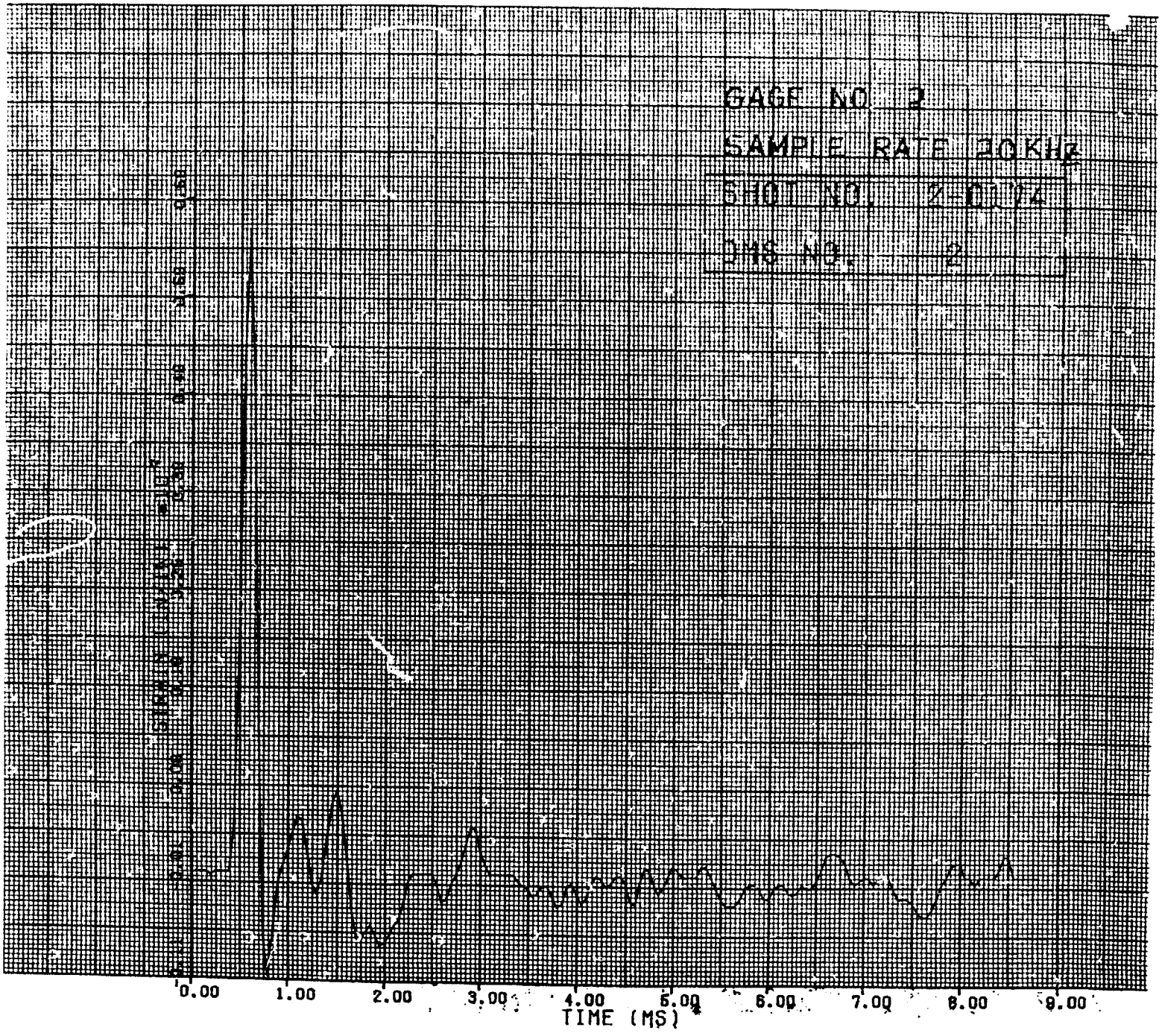

Figure 23. Strain of Shot 2-0174 for Gage #2.

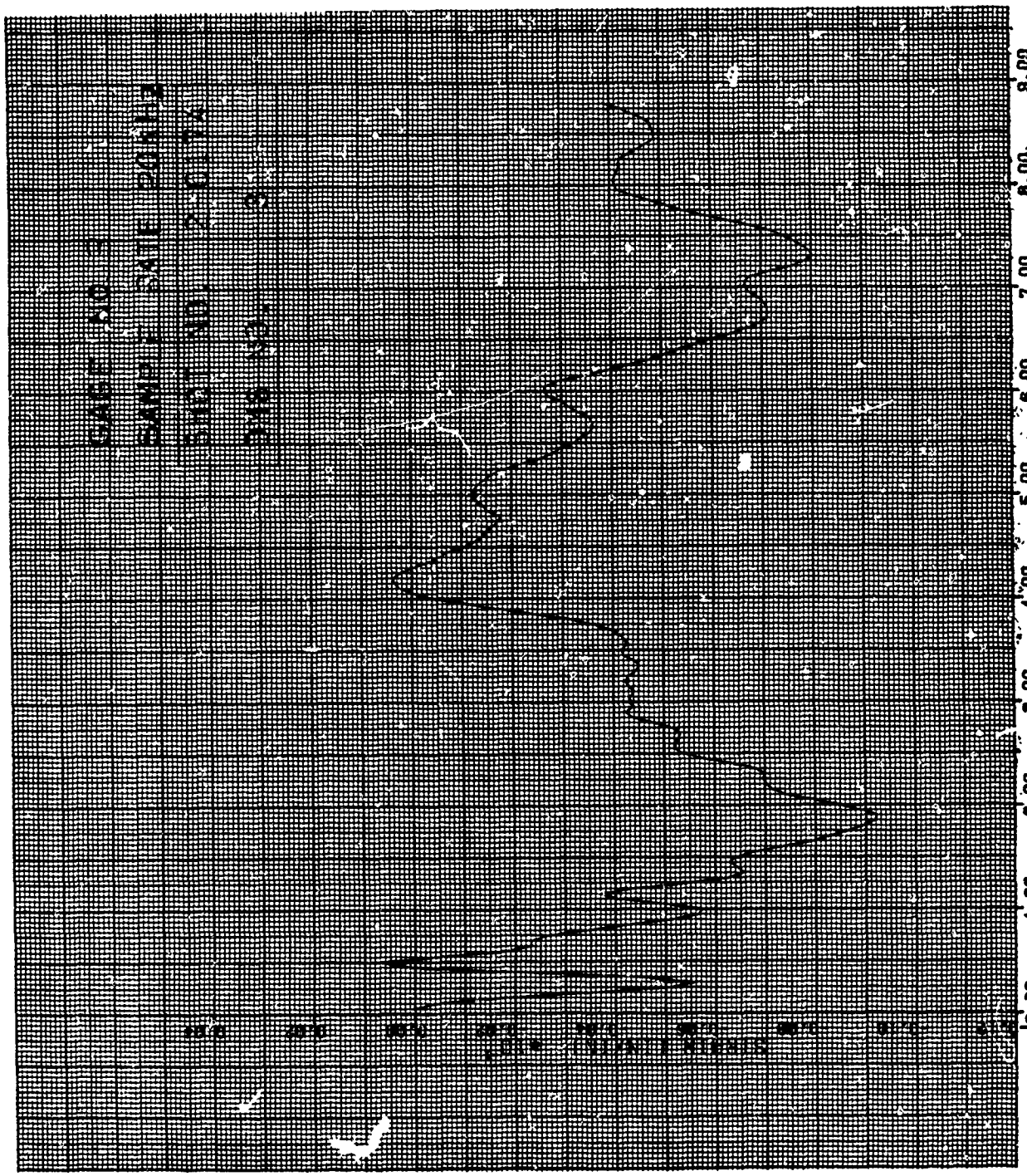

Figure 24. Strain of Snot 2-0174 for Gage #3.

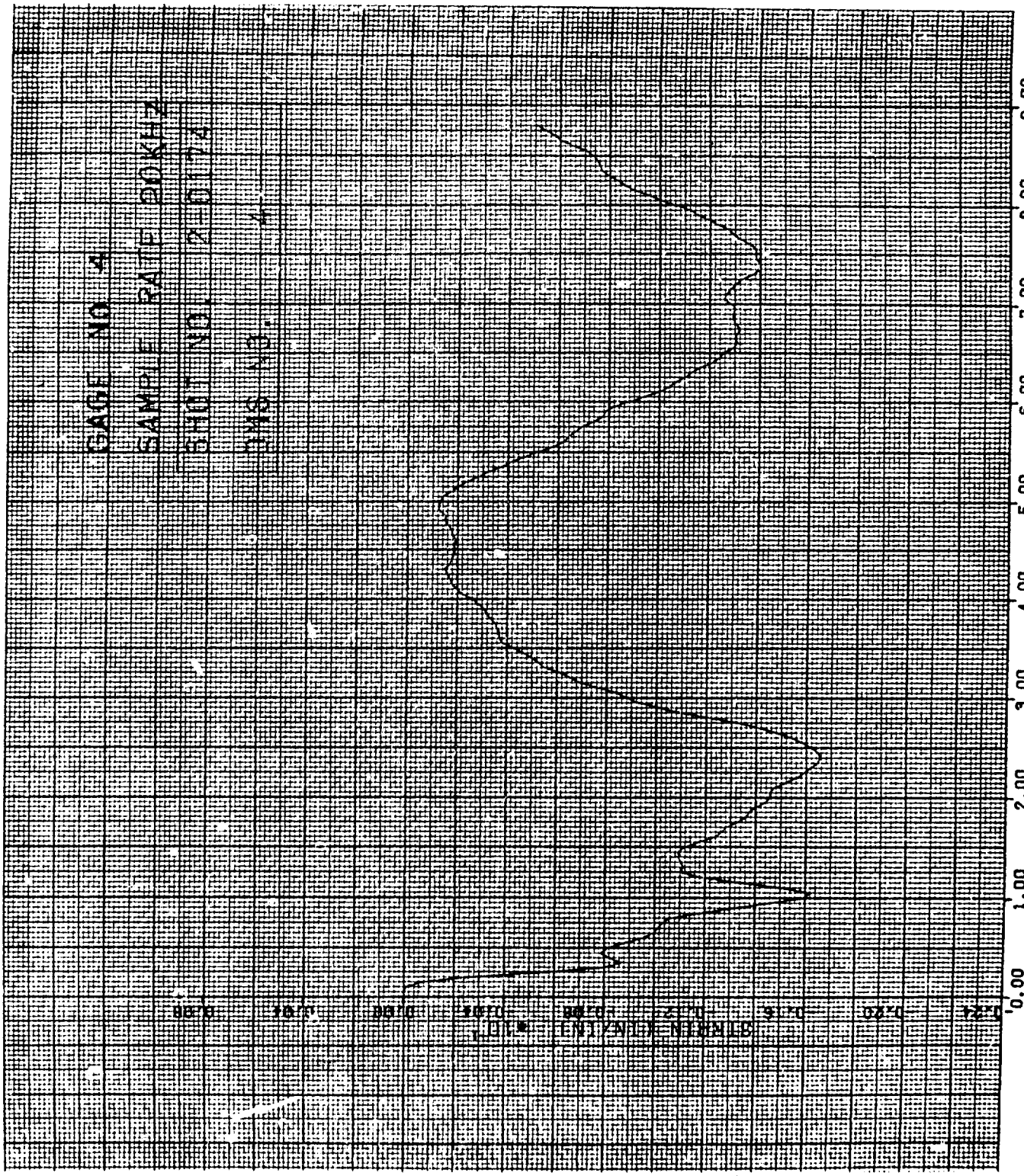

Figure 25. Strain of Shot 2-0174 for Gage #4.

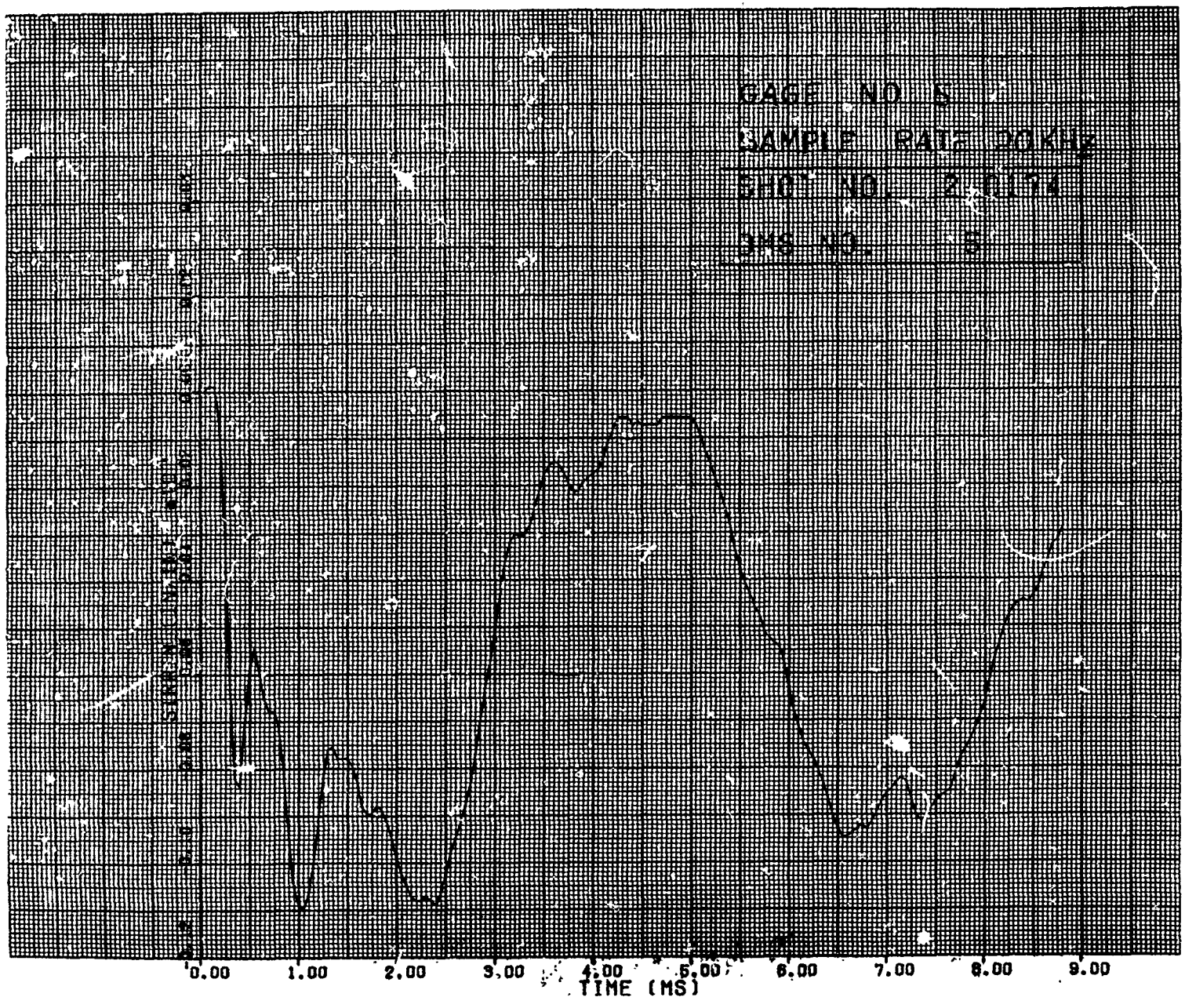

Figure 26. Strain of Shot 2-0174 for Gage #5.

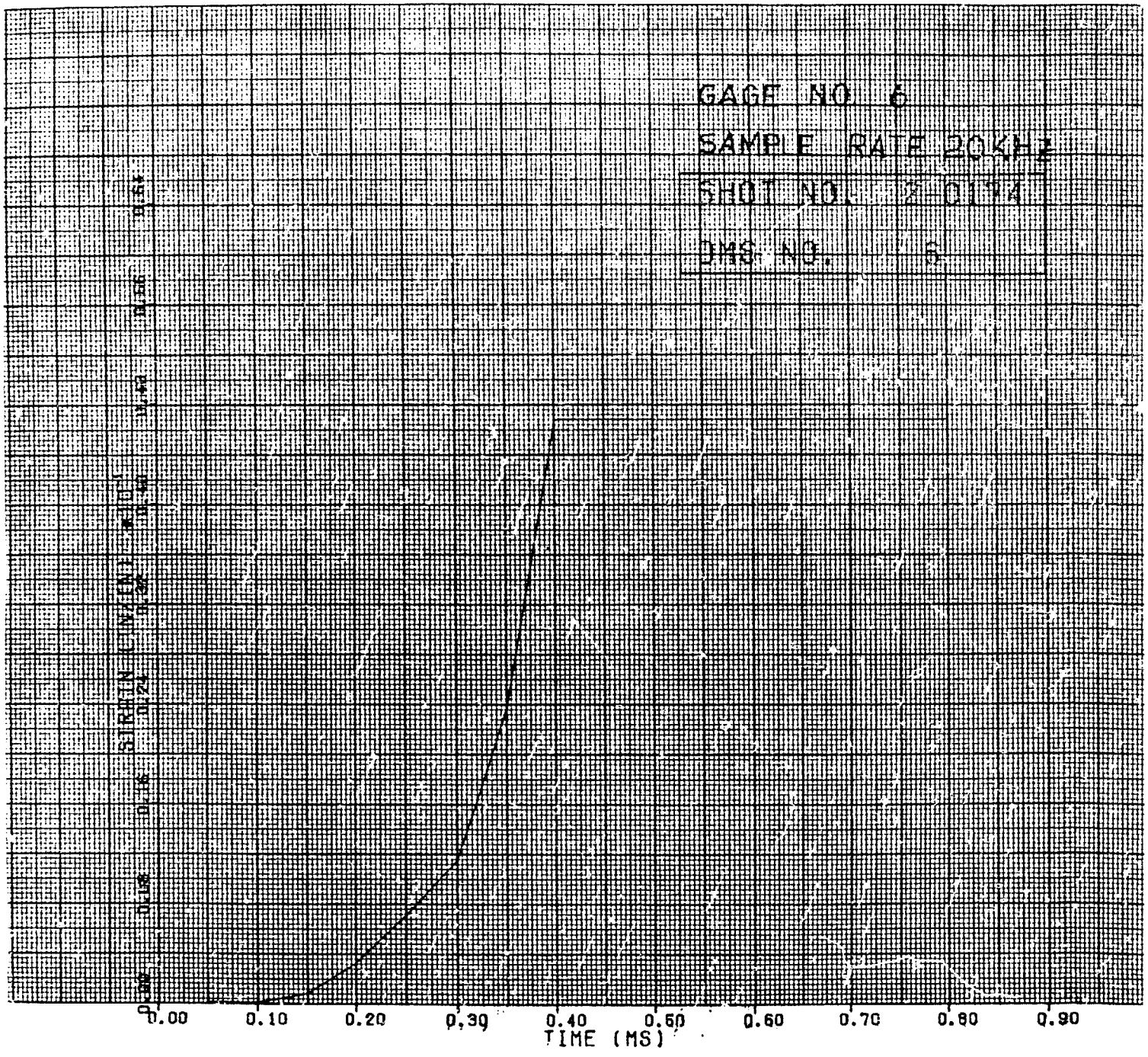

Figure 27. Strain of Shot 2-0174 for Gage #6.

3.1.1.3 Impact Results for Group 3 Specimens

The impact testing of the Group 3 titanium flat plate specimens with a blade-like aspect ratio consisted of eight shots using the small 85 g (3 ounce) substitute bird. The impacts were edge impacts at the 70 percent span level using an angle of incidence of either 37.4 or 24.4 degrees. Six of the impacts were conducted at 36.4 degree impact angle which is not the proper impact angle for this group. These six impacts were inadvertently conducted at the wrong angle. The remaining two shots were fired with the specimens positioned at the proper impact angle of 24.4 degrees. The impact velocity for the 36.4 degree shots ranged from 110 to 446 m/s. The impact velocity for both 24.4 degree impacts was at about 440 m/s.

For the 36.4 degree impact angle shots, the typical strain gage data for the Group 3 specimens (Shot 2-0115) are presented in Figures 28 through 33. Figure 8A of Appendix A gives the strain gage location for this group of specimens. The damage of the specimen for Shot 2-0115 was in the form of plastic deformation at the root and impact site. The deformation at the tip was determined to be 1.83 cm for the leading edge and 1.59 cm for the trailing edge. The specimen had a twist through the span of about 0.24 cm. Figures 34 and 35 give dynamic tip displacement results determined from the high speed photography films for the "y" and "x" directions, respectively.

For the 24.4 degree impacts, the typical strain gage data for Shot 2-0127 are presented in Figures 36 through 41. No visible damage resulted for an impact at about 439 m/s. Figure 6B shows a photograph of this specimen after impact.

3.1.1.4 Impact Results for Group 4 Specimens

Four Group 4 titanium flat plate specimens with a one-half blade type aspect ratio were tested using

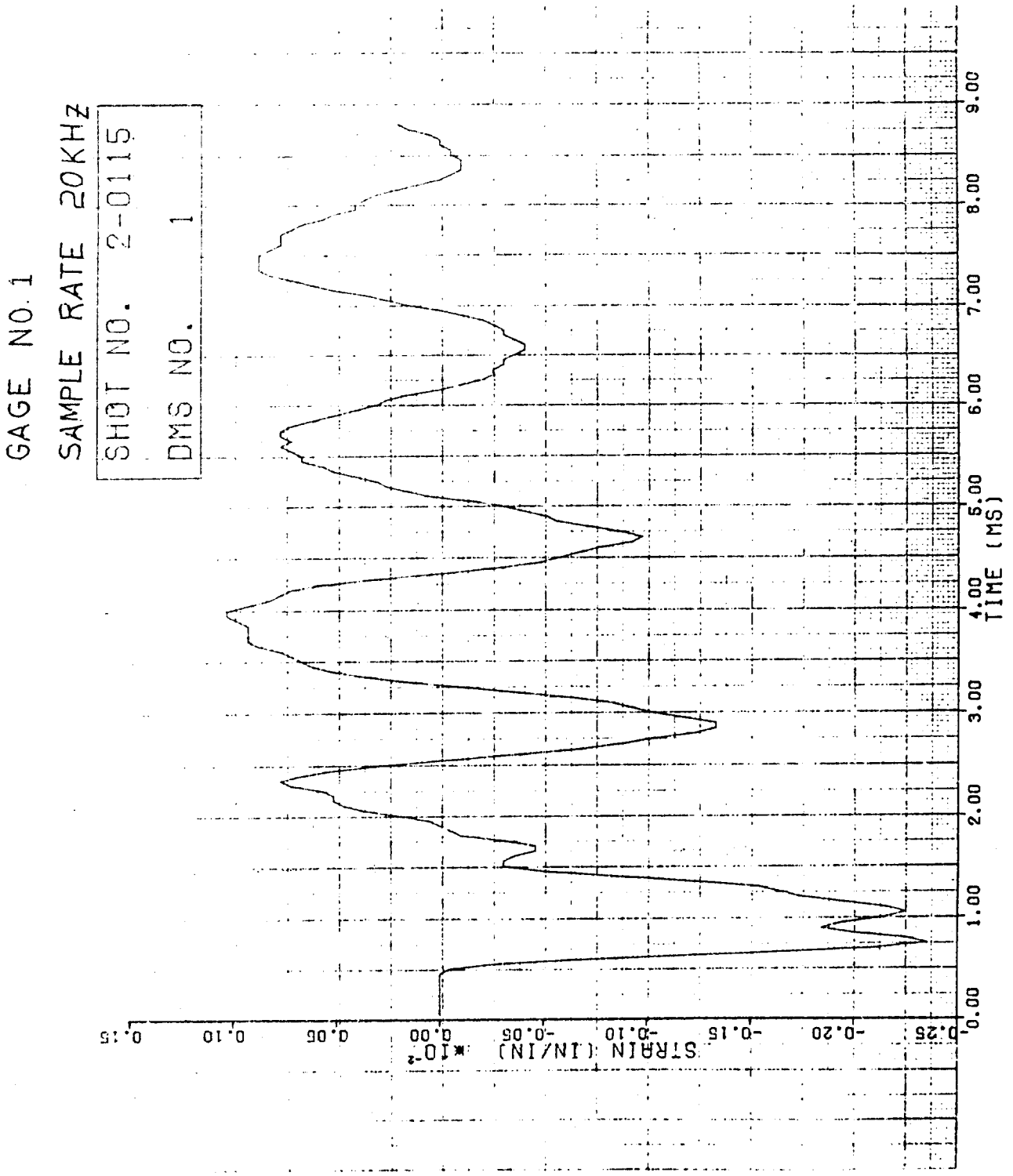

Figure 28. Strain of Shot 2-0115 for Gage #1.

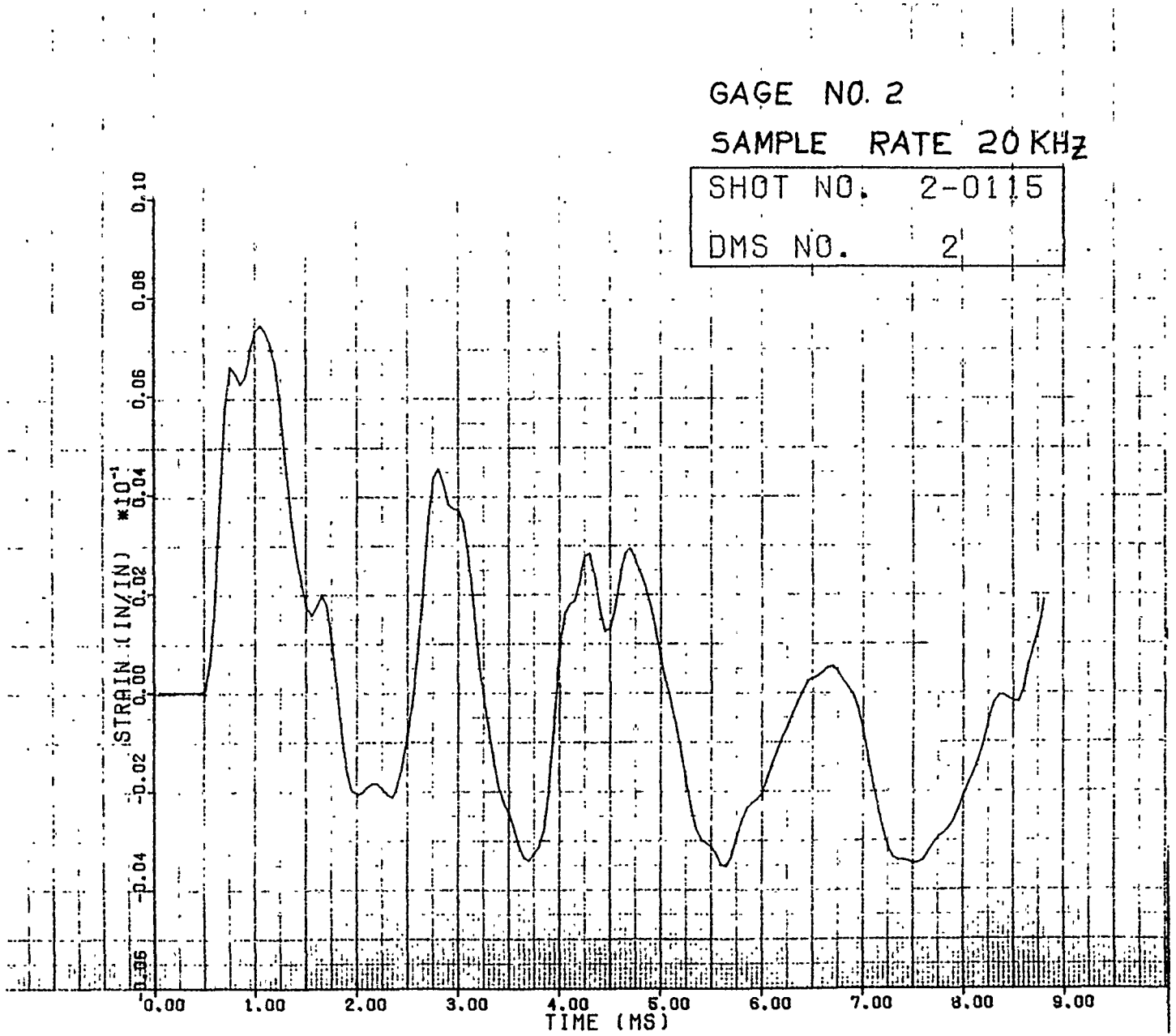

Figure 29. Strain of Shot 2-0115 for Gage #2.

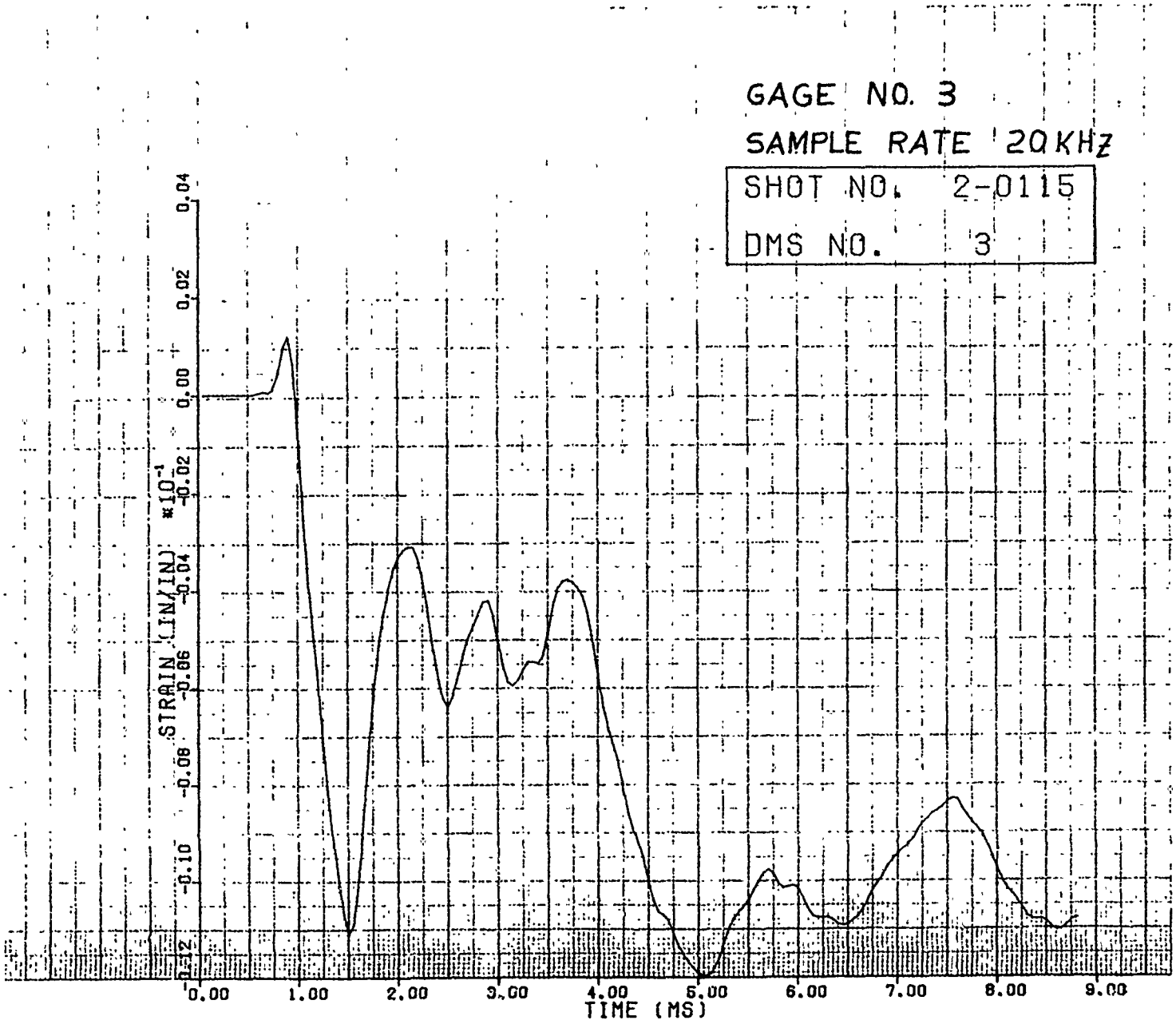
GAGE NO. 3
SAMPLE RATE 20KHz
SHOT NO. 2-0115
DMS NO. 3
STRAIN (IN/IN) *10^-1
0.04
0.02
0.00
-0.02
-0.04
-0.06
-0.08
-0.10
-0.12
0.00
1.00
2.00
3.00
4.00
5.00
6.00
7.00
8.00
9.00
TIME (MS)

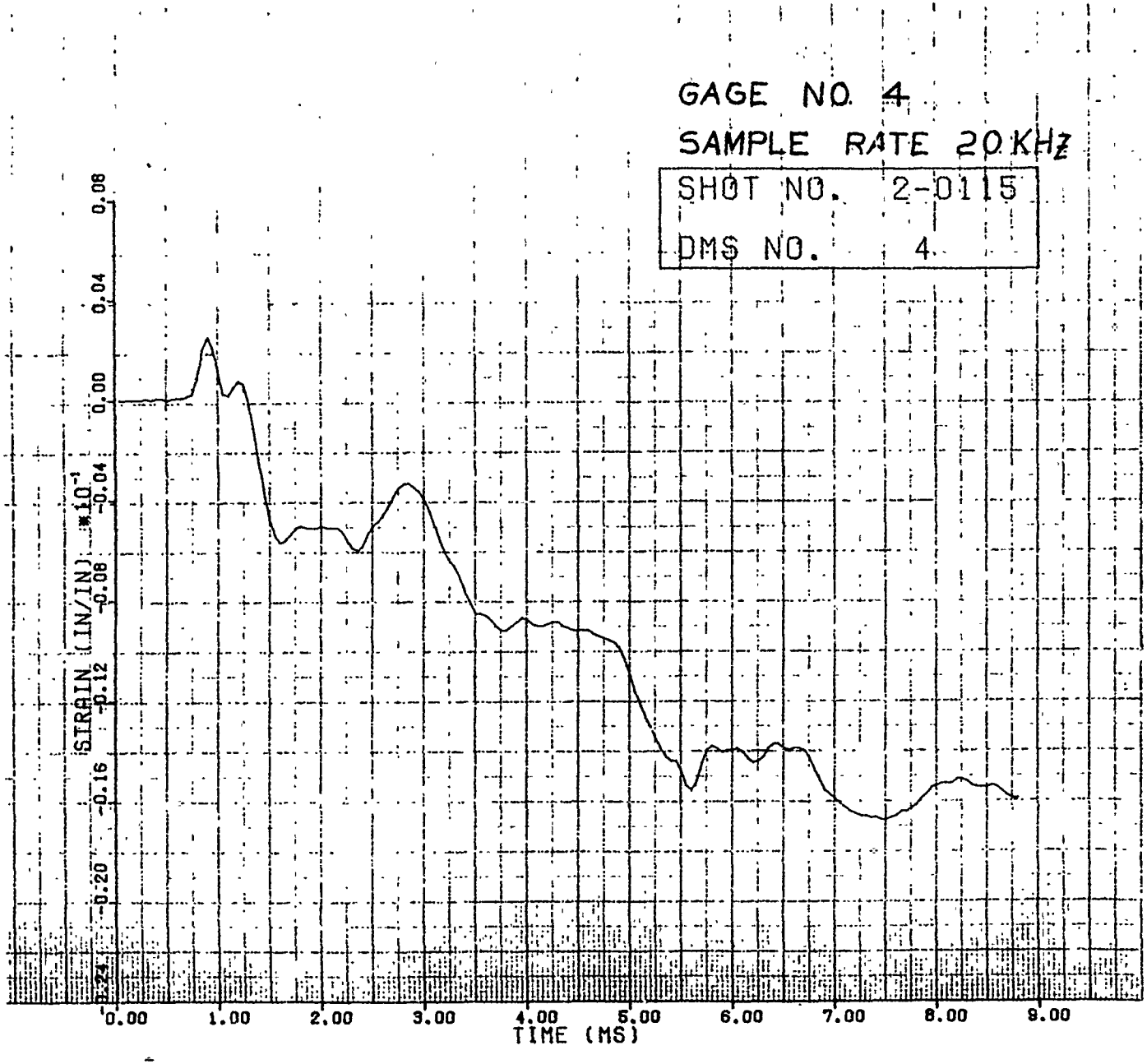

Figure 31. Strain of Shot 2-0115 for Gage #4.

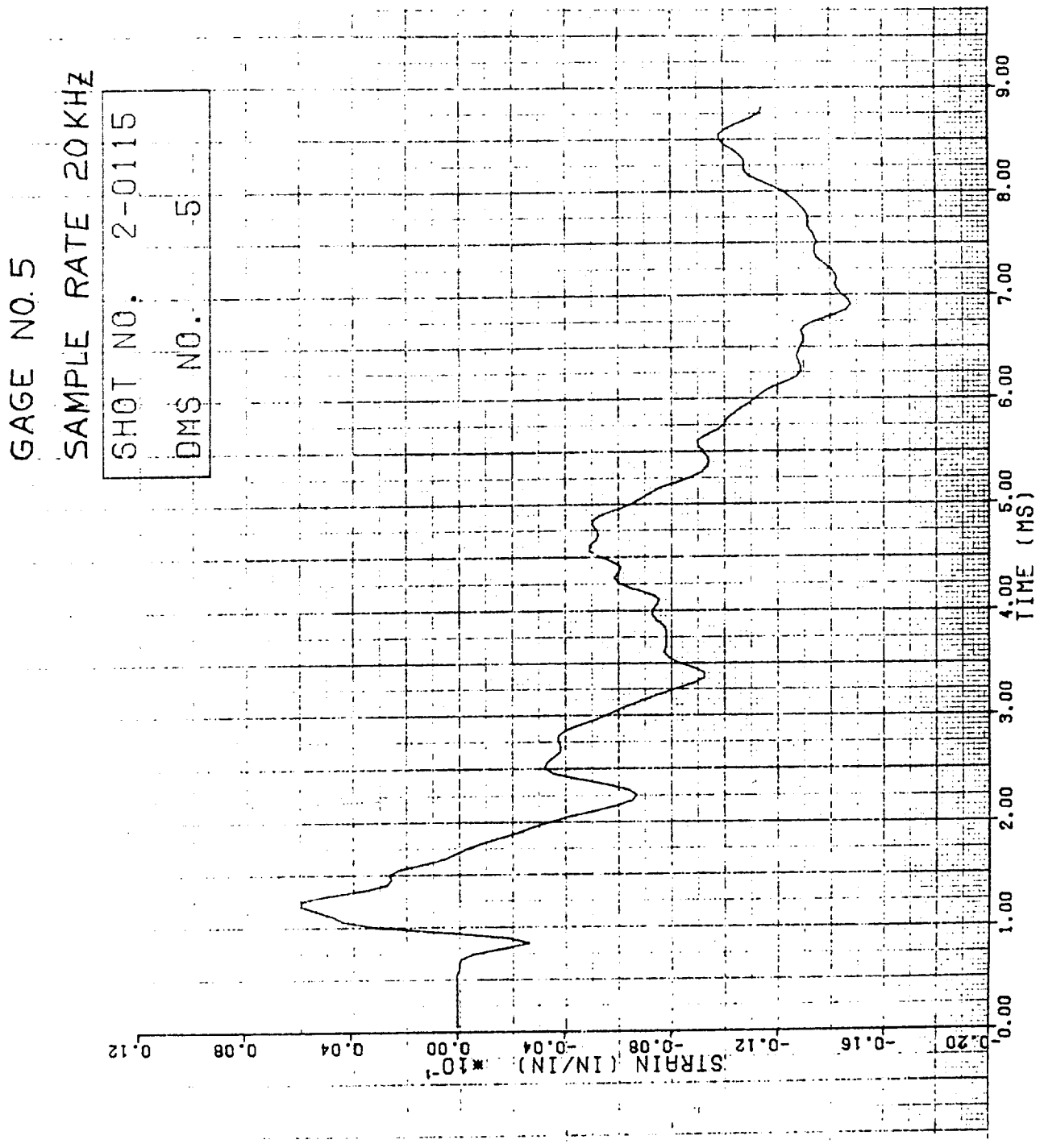

Figure 32. Strain of Shot 2-0115 for Gage #5.

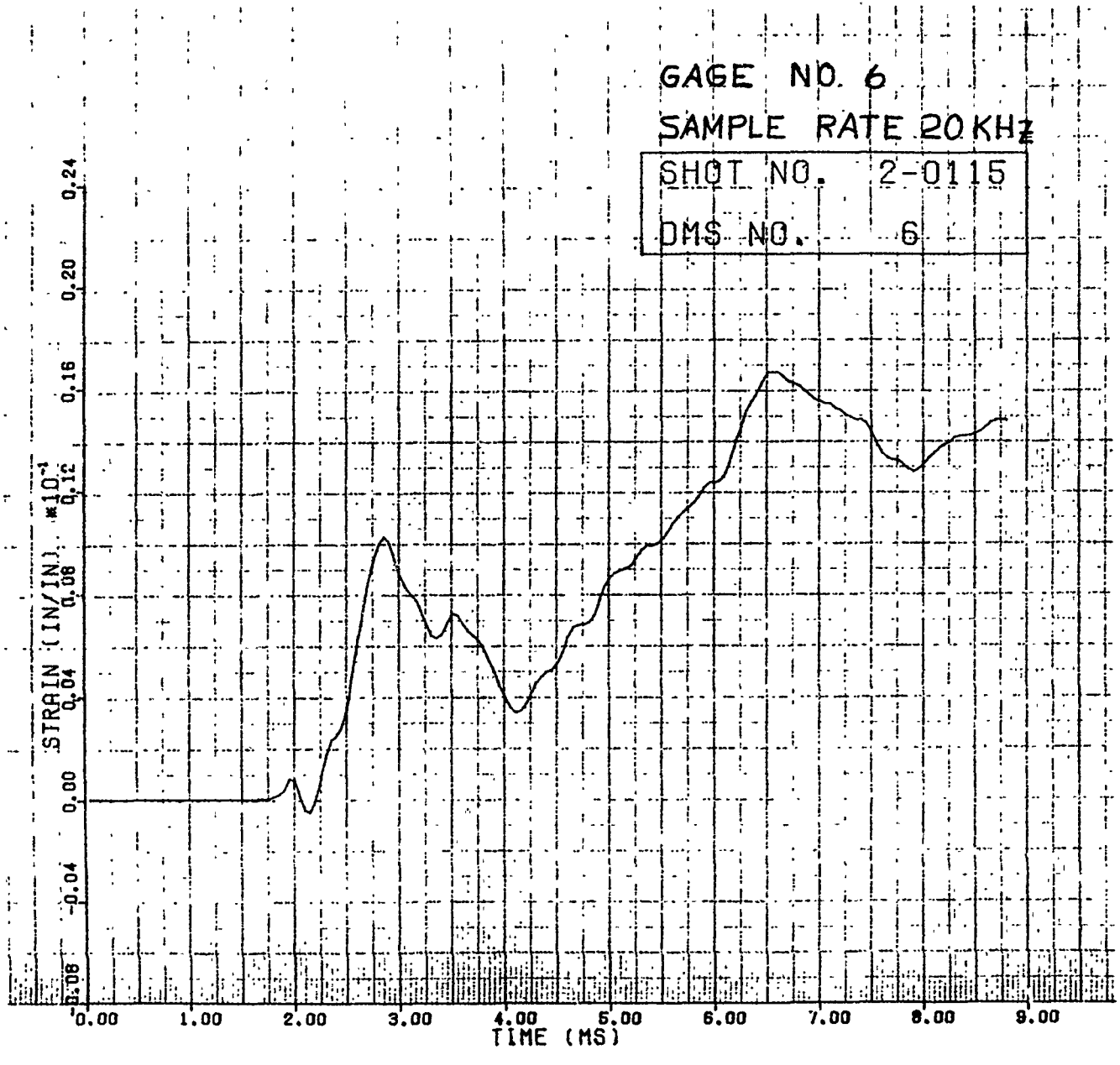

Figure 33. Strain of Shot 2-0115 for Gage #6.

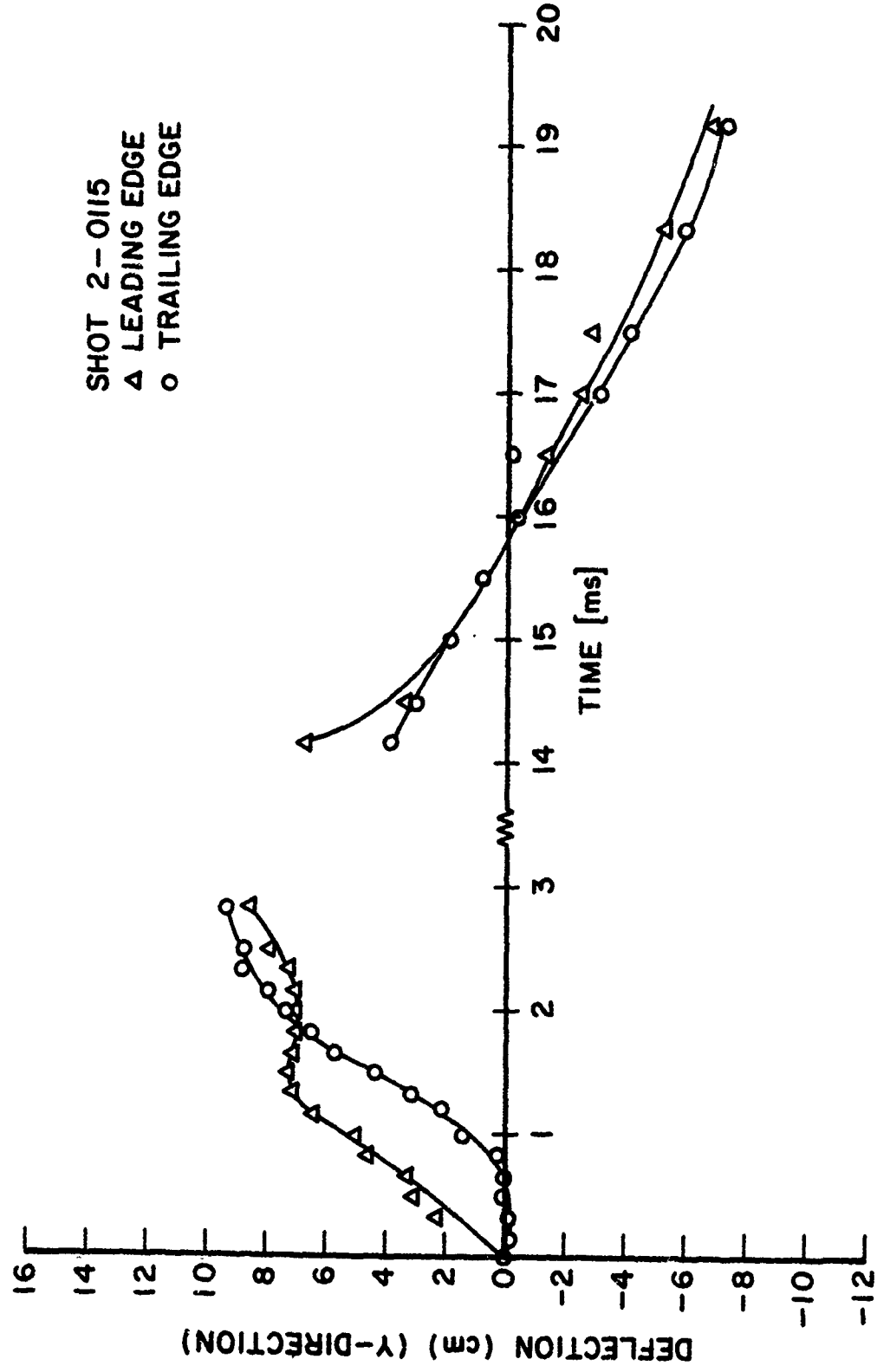

Figure 34. Tip Reflection on "y" Direction for Shot 2-0115.

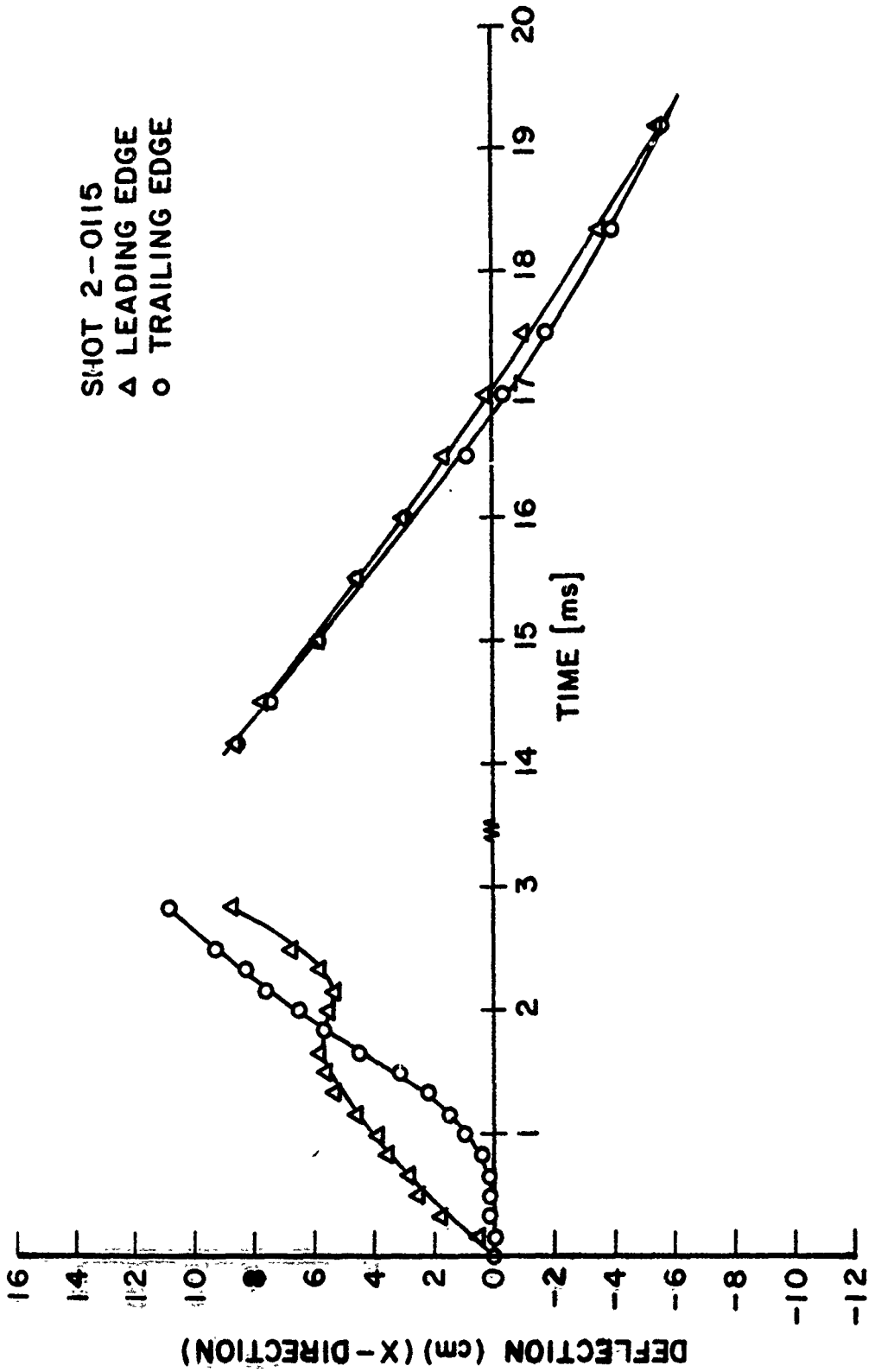

Figure 35. Tip Reflection on "x" Direction for Shot 2-0115.

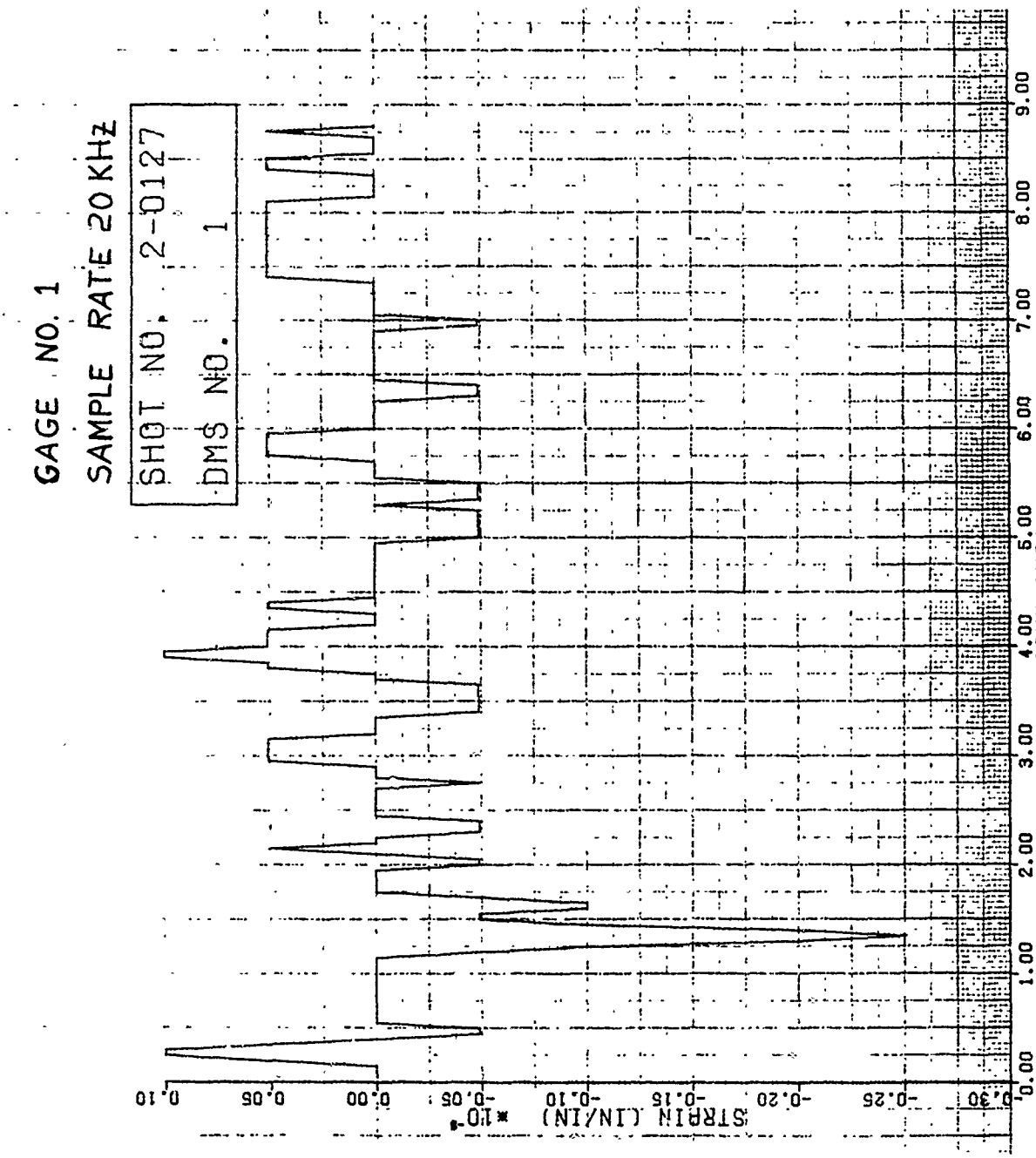

Figure 36. Strain of Shot 2-0127 for Gage #1.

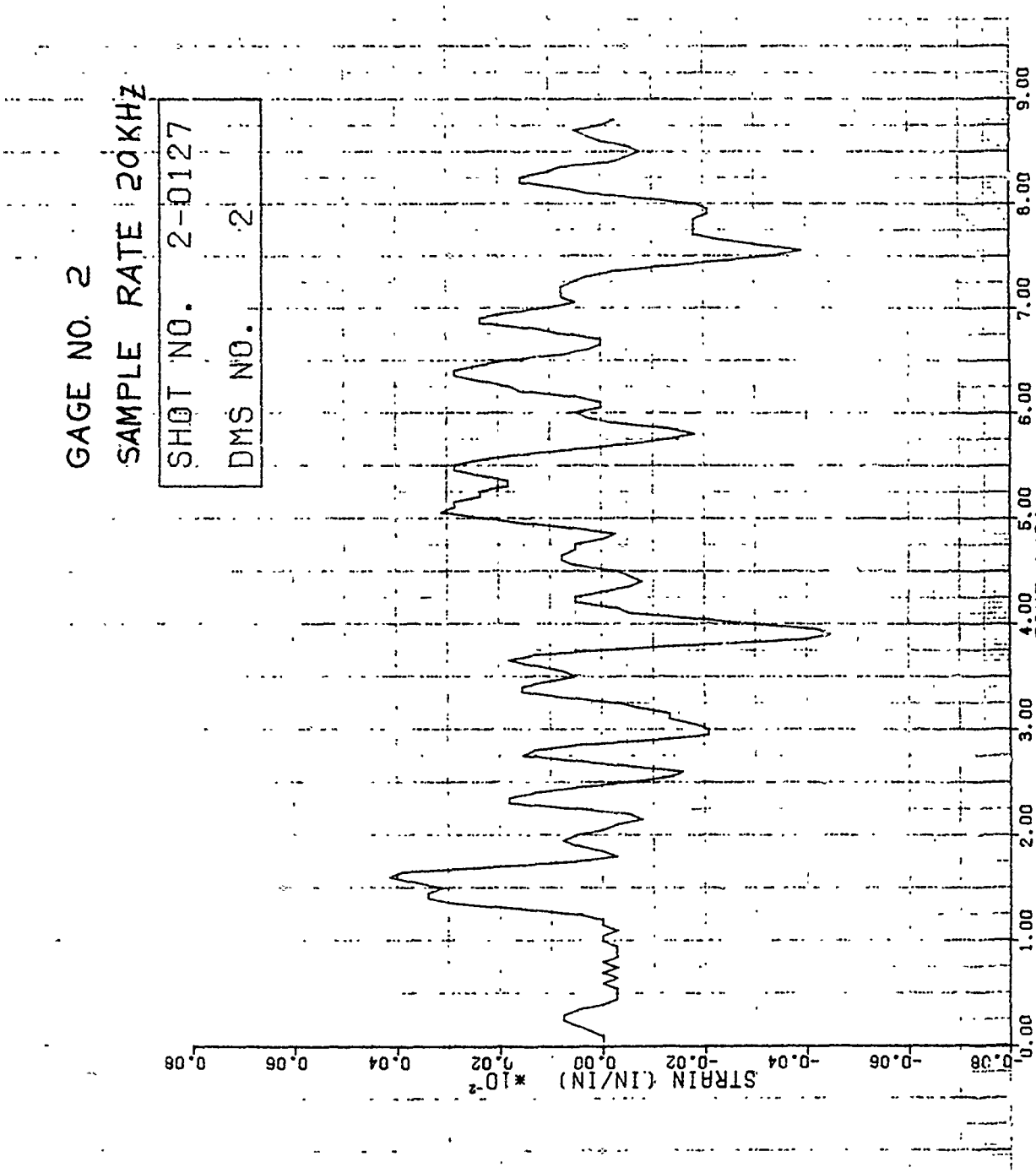

Figure 37. Strain of Shot 2-0127 for Gage #2.

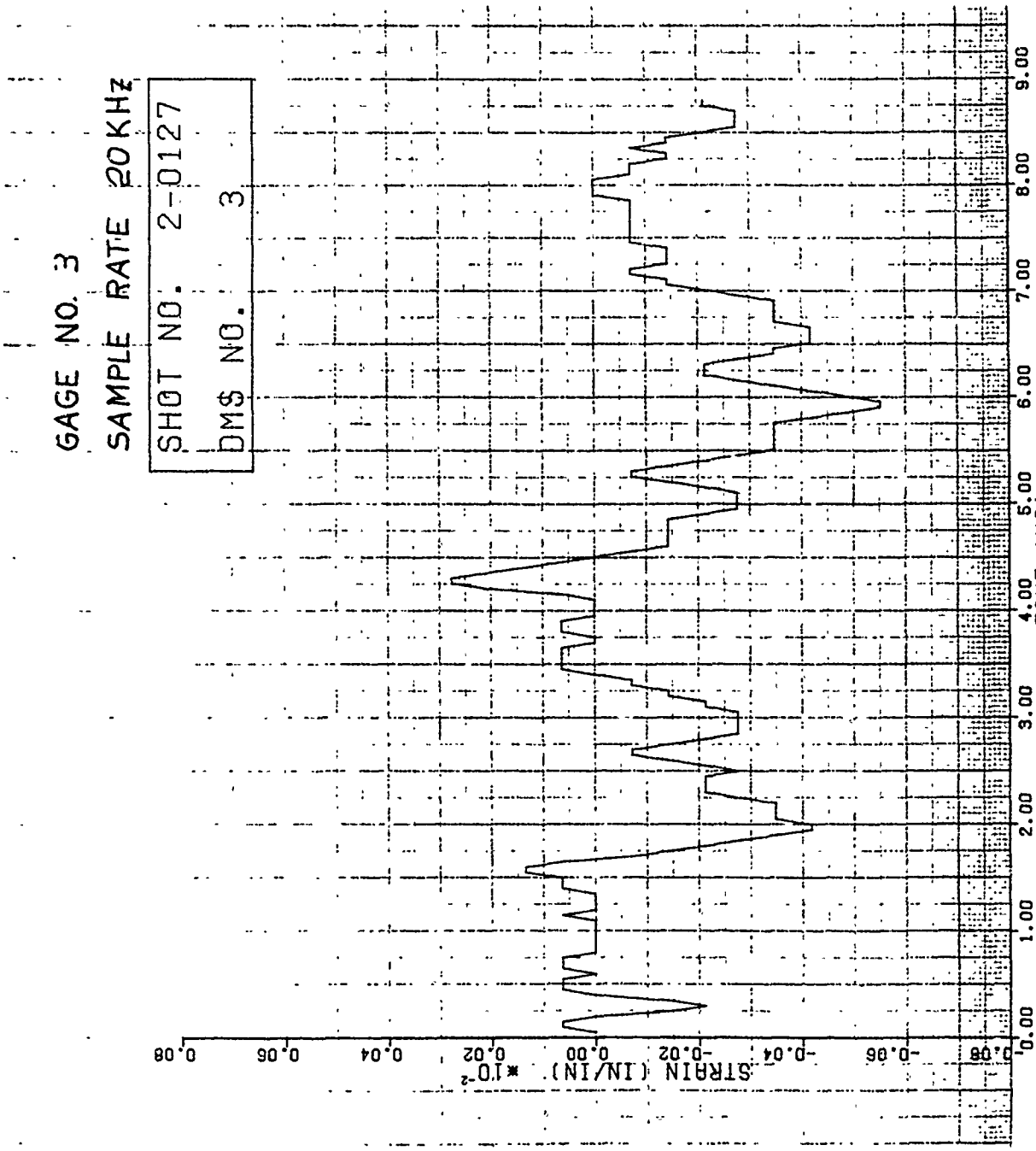

Figure 38. Strain of Shot 2-0127 for Gage #3.

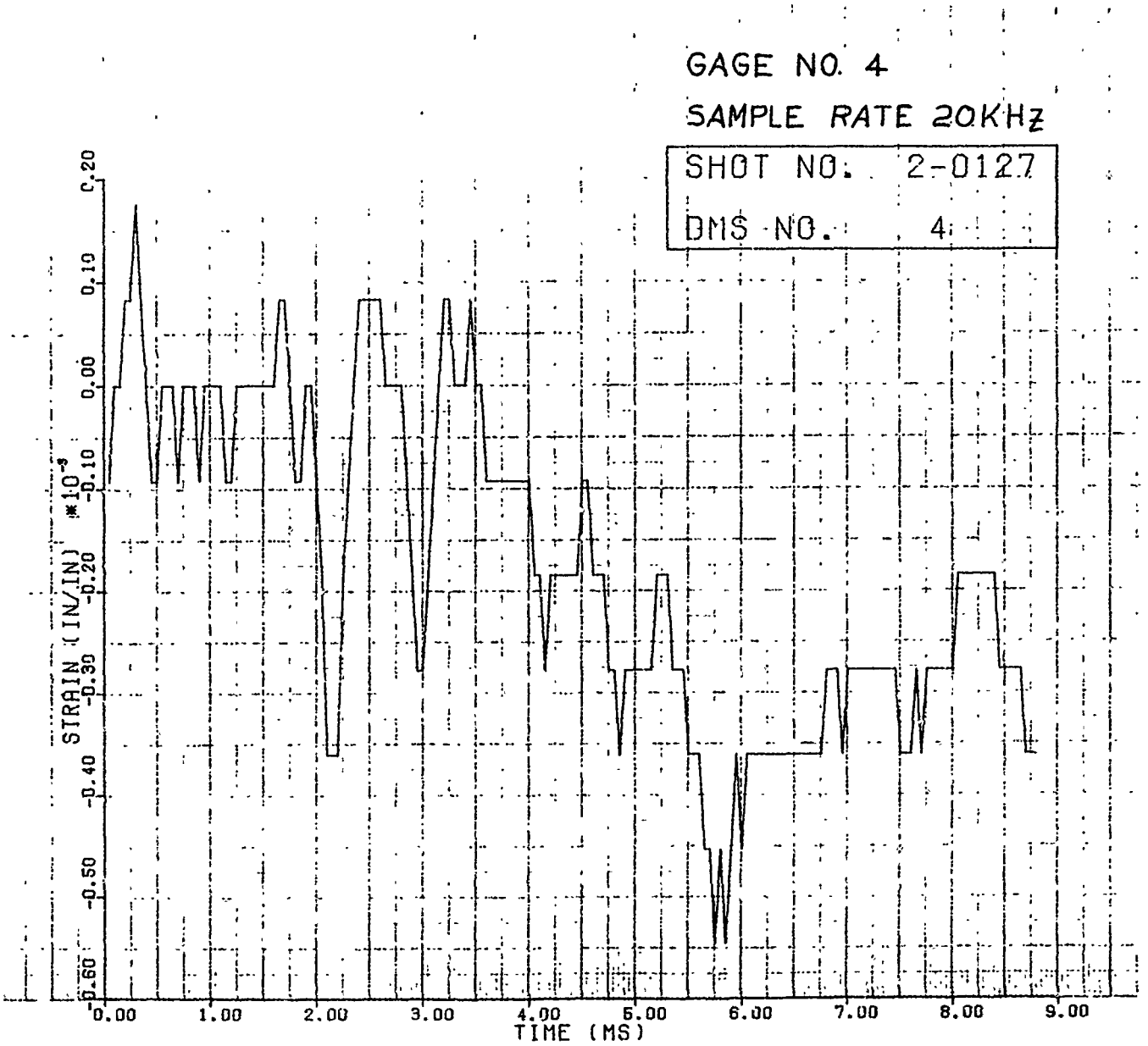

Figure 39. Strain of Shot 2-0127 for Gage #4.

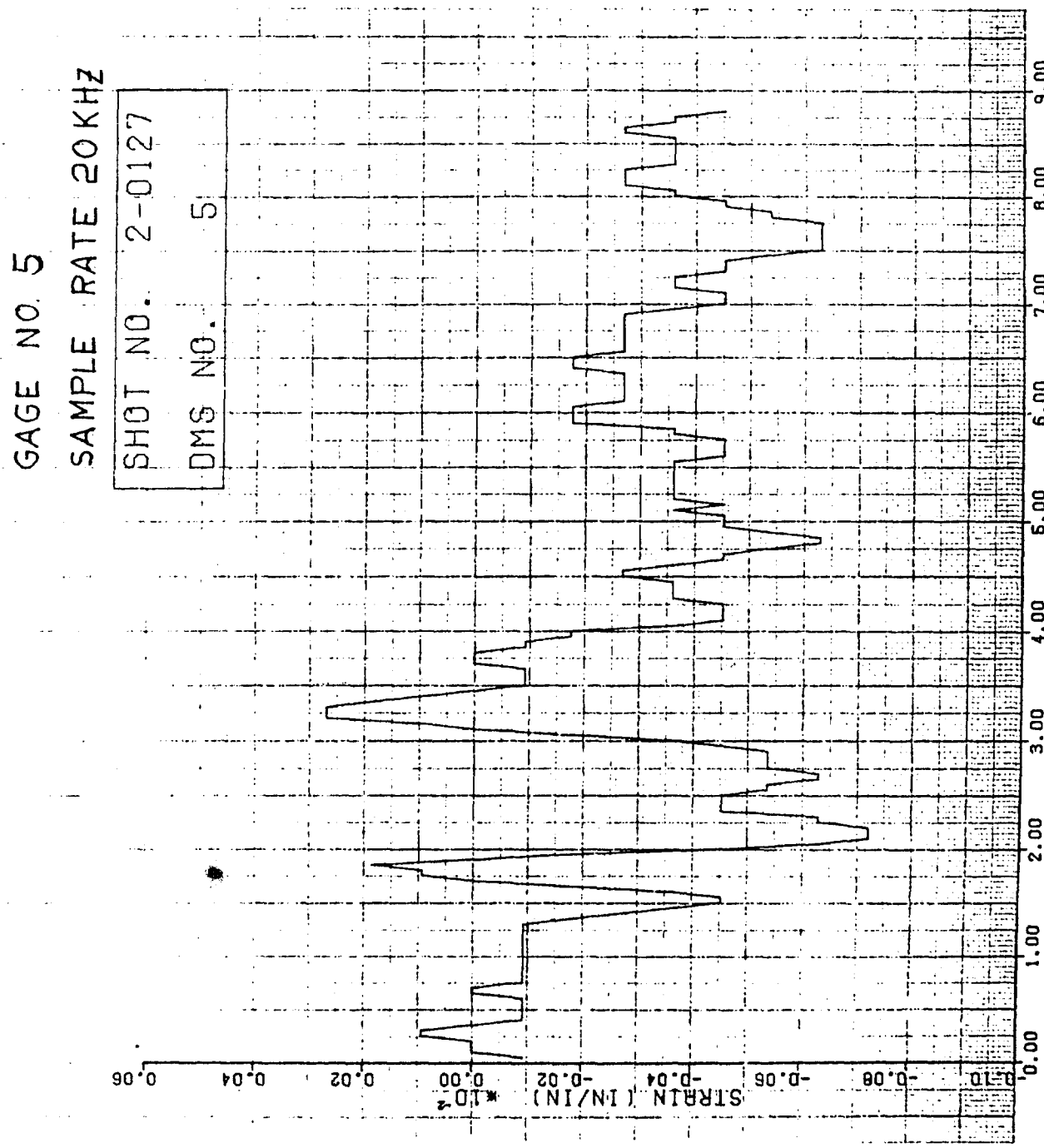

Figure 40. Strain of Shot 2-0127 for Gage #5.

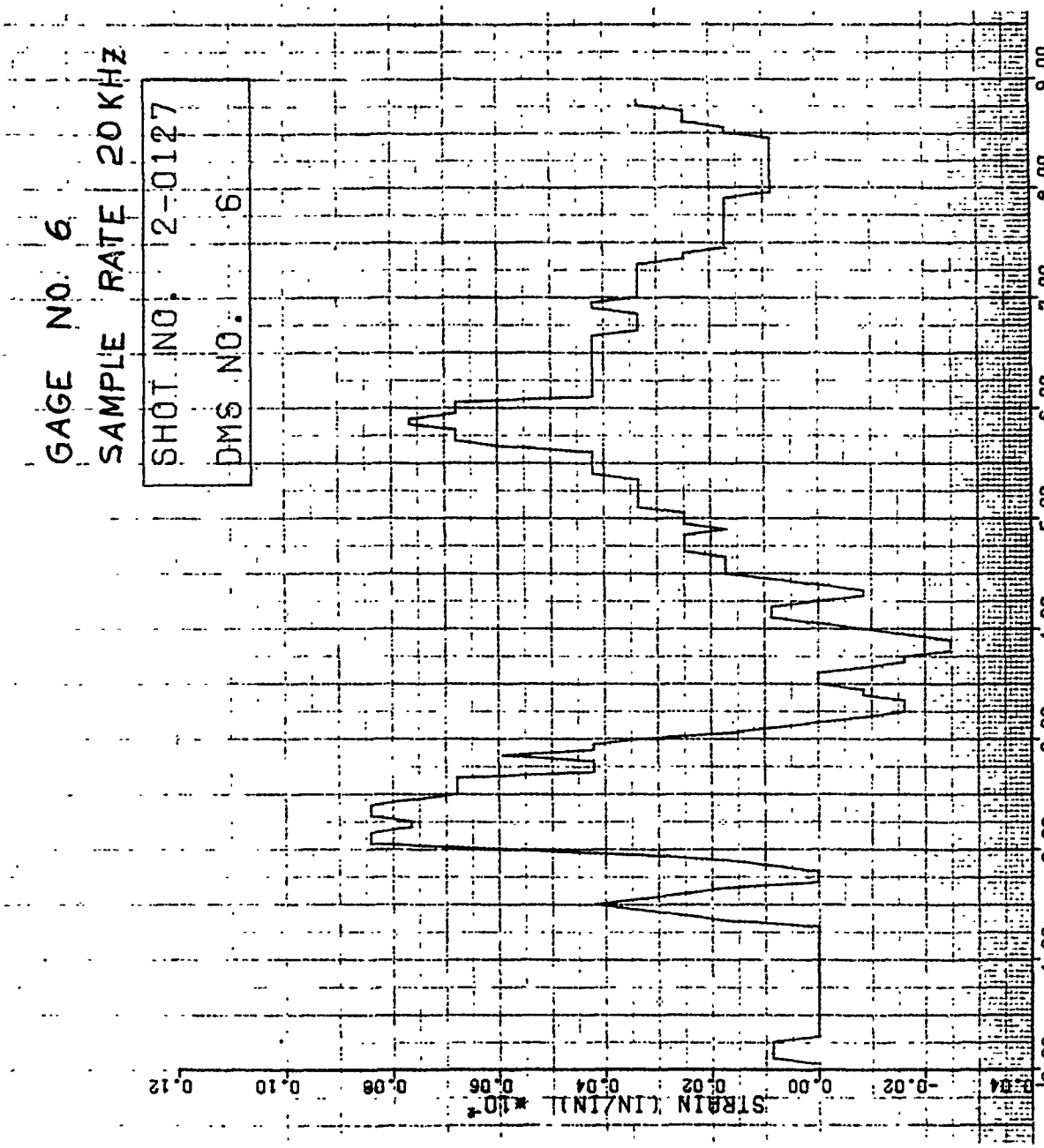

Figure 41. Strain of Shot 2-0127 for Gage #6.

balsa wood sabots with the small 85 g (3 ounce) substitute bird. The impacts were center impacts at the 70 percent span location normal to the specimen at velocities ranging from 53 to 151 m/s. Again, the balsa wood sabots were permitted to impact the specimens along with the artificial bird. Figure 9A of Appendix A gives the strain gage locations for this group of specimens.

Typical strain gage results are presented in Figures 42 through 47 for Shot 2-0096. The impact velocity for this impact was 99 m/s and the resulting damage was plastic deformation and bending of the specimen at its root. The measured plastic deflection was 1.11 cm (measured at tip).

Figures 48, 49, and 50 present the dynamic displacement plots in the"y" direction from the high speed films for Shots 2-0096, 2-0097, and 2-0098, respectively. The most severe damage was received in Shot 2-0098 where the tip deformation (plastic) was 6.12 cm at an impact velocity of 151 m/s.

Figures 7B through 9B show photographs of the damage generated for Shots, 2-0096, 2-0097, and 2-0098, respectively.

3.1.1.5 Impact Results for Group 5 Specimens

Three Group 5 titanium flat plate specimens with a one-half blade type aspect ratio were tested using the medium size 680 g (1.5 pound) substitute bird. The impacts were edge (slicing) impacts at the 30 percent span location at an impact angle of 41.0 degrees at velocities ranging from 191 to 232 m/s. In all cases, no visible damage was received from the impacts of the 680 g birds. Figure 10A of Appendix A gives the strain gage locations for this group of specimens.

Typical strain gage results are presented in Figures 51 through 56 for a bird impact mass of 80 g

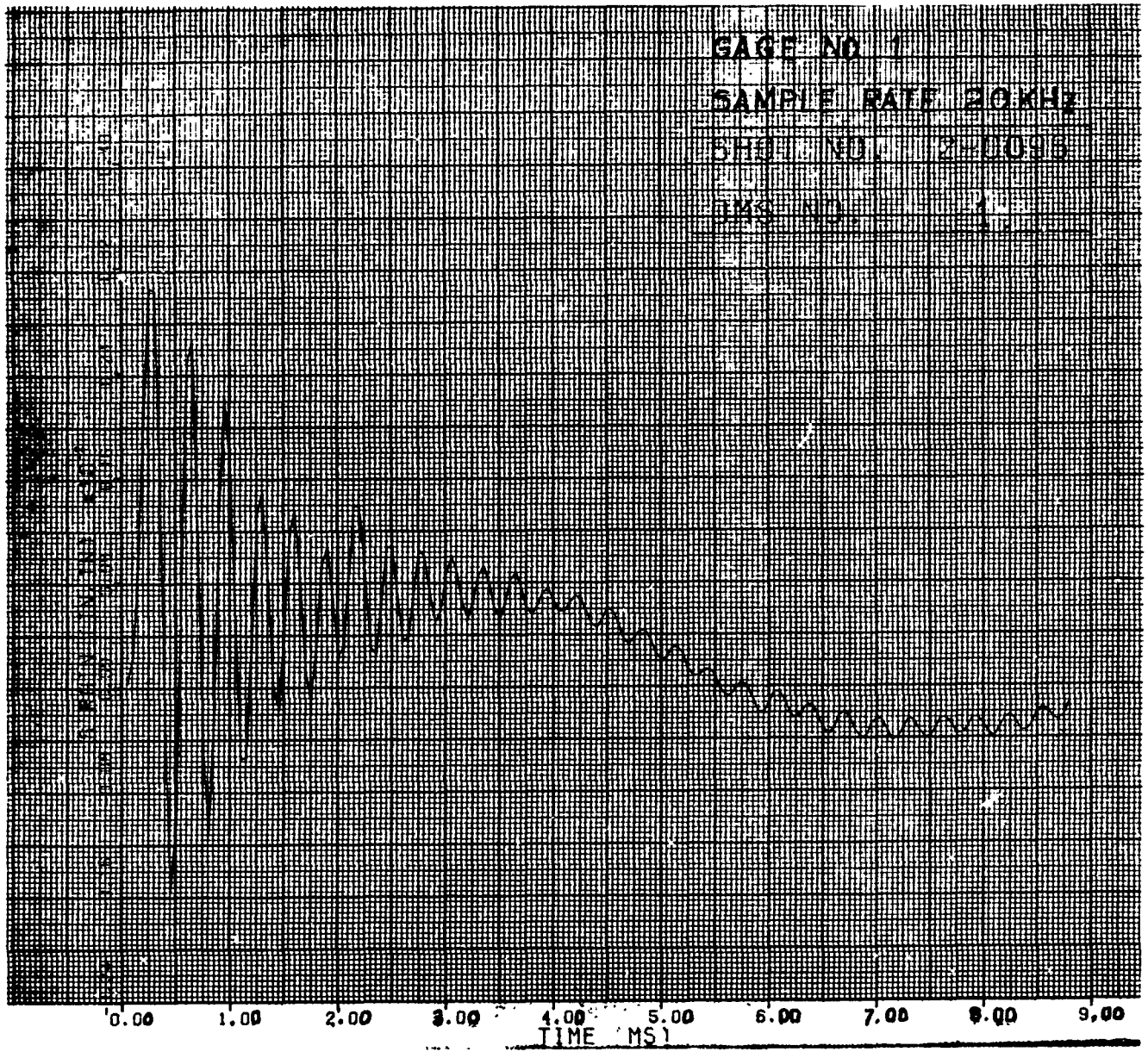

Figure 42. Strain of Shot 2-0096 for Gage #1.

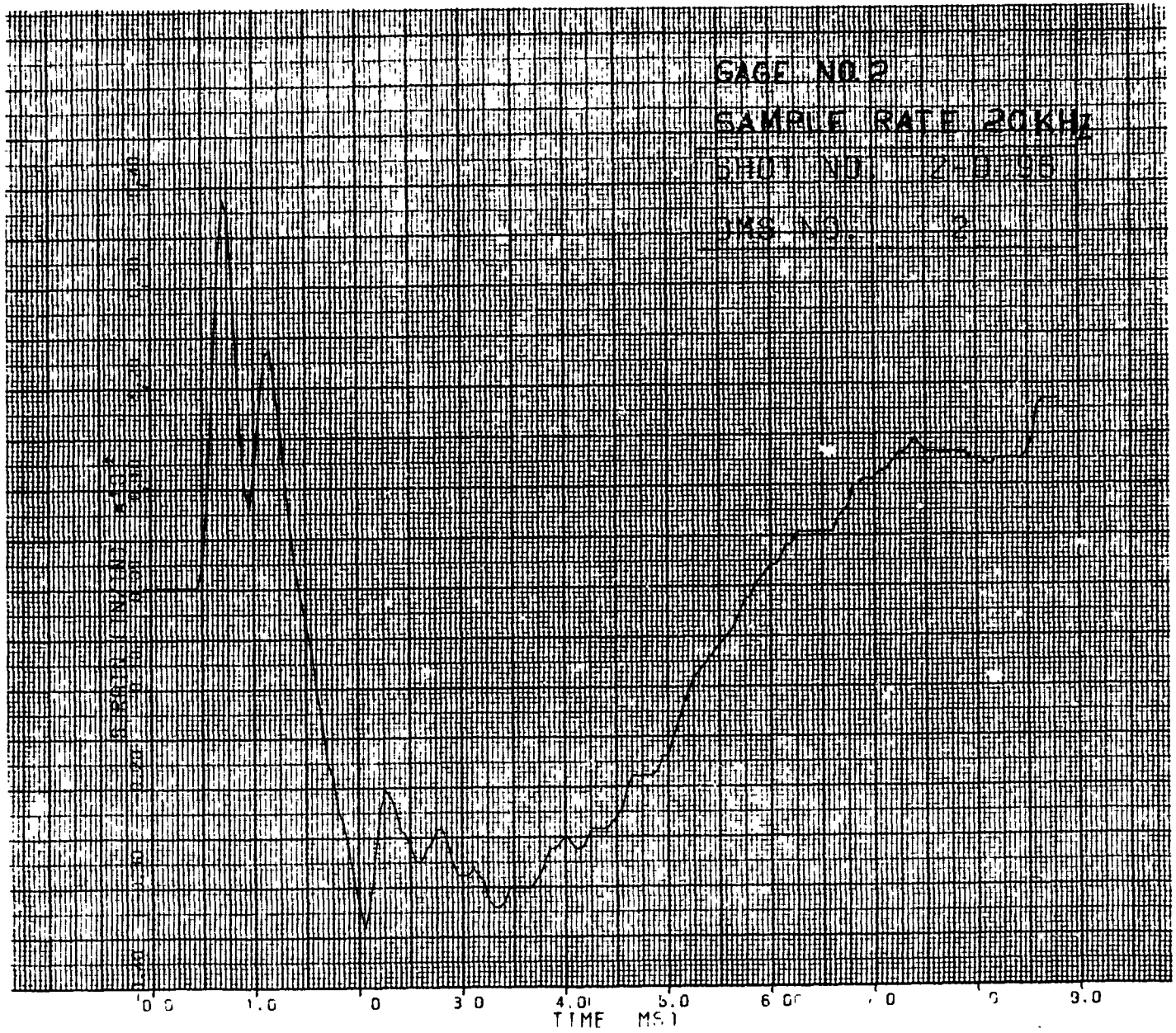

Figure 43. Strain of Shot 2-0096 for Gage #2.

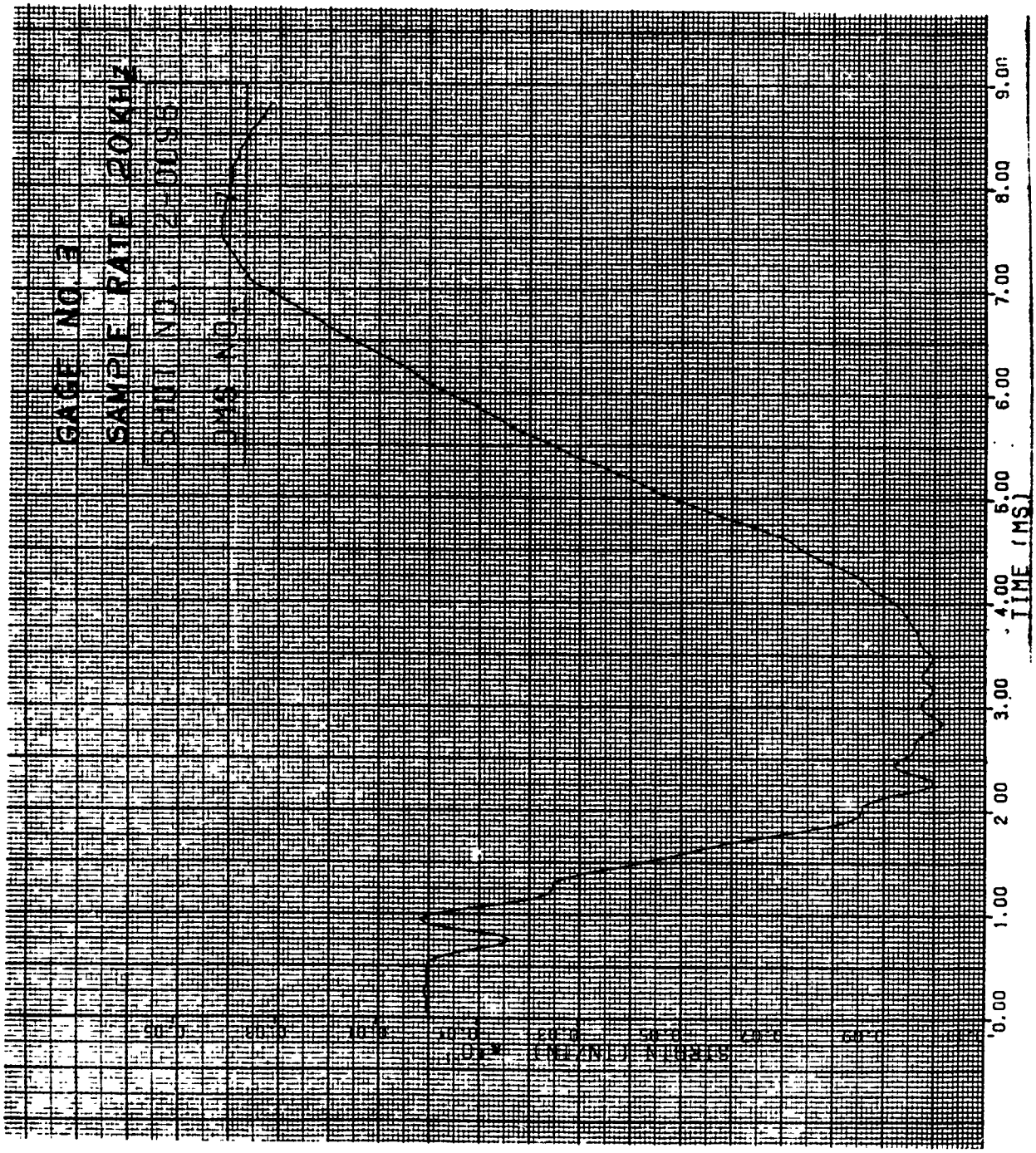

Figure 44. Strain of Shot 2-0096 for Gage #3.

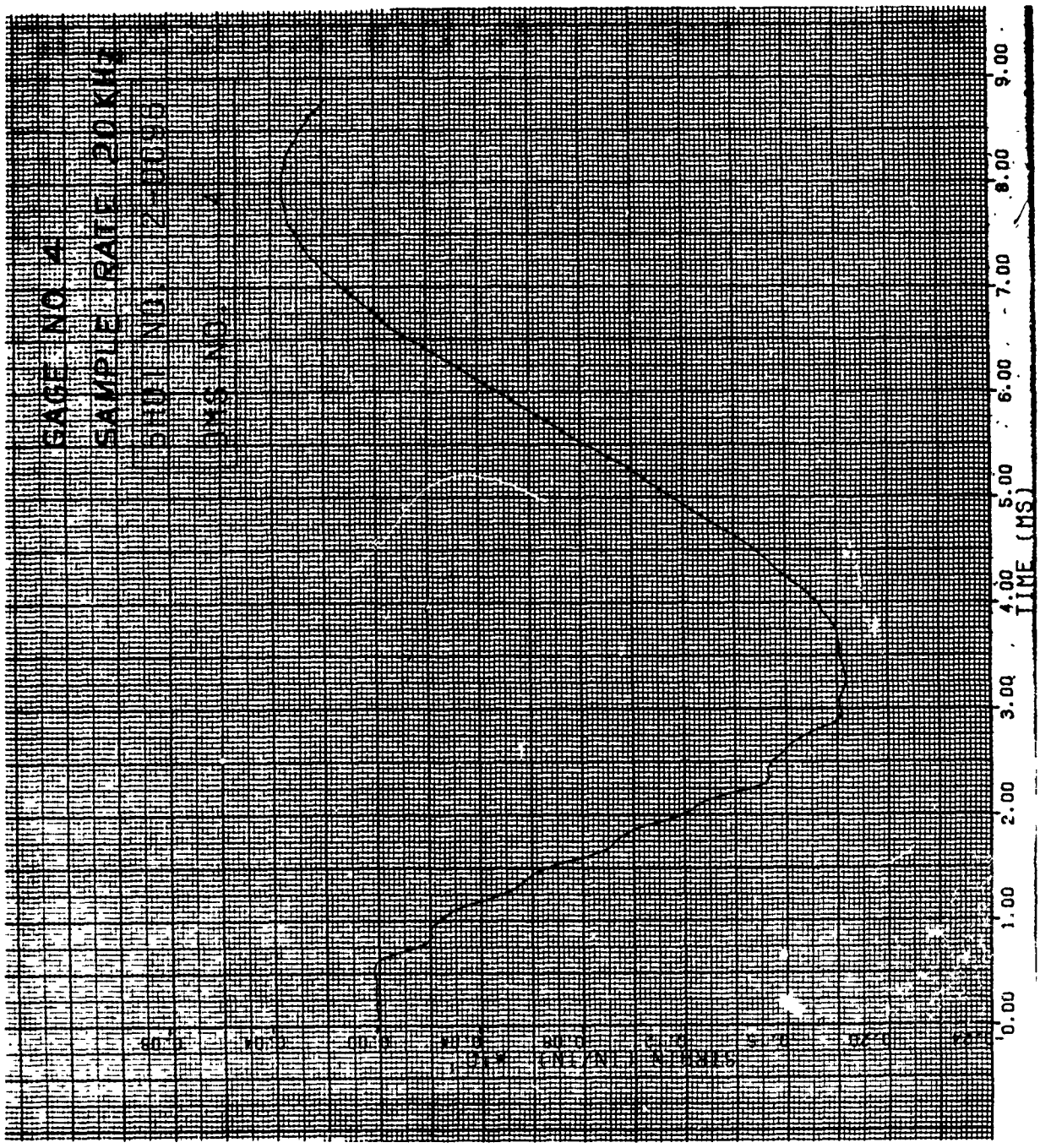

Figure 45. Strain of Shot 2-0096 for Gage #4.

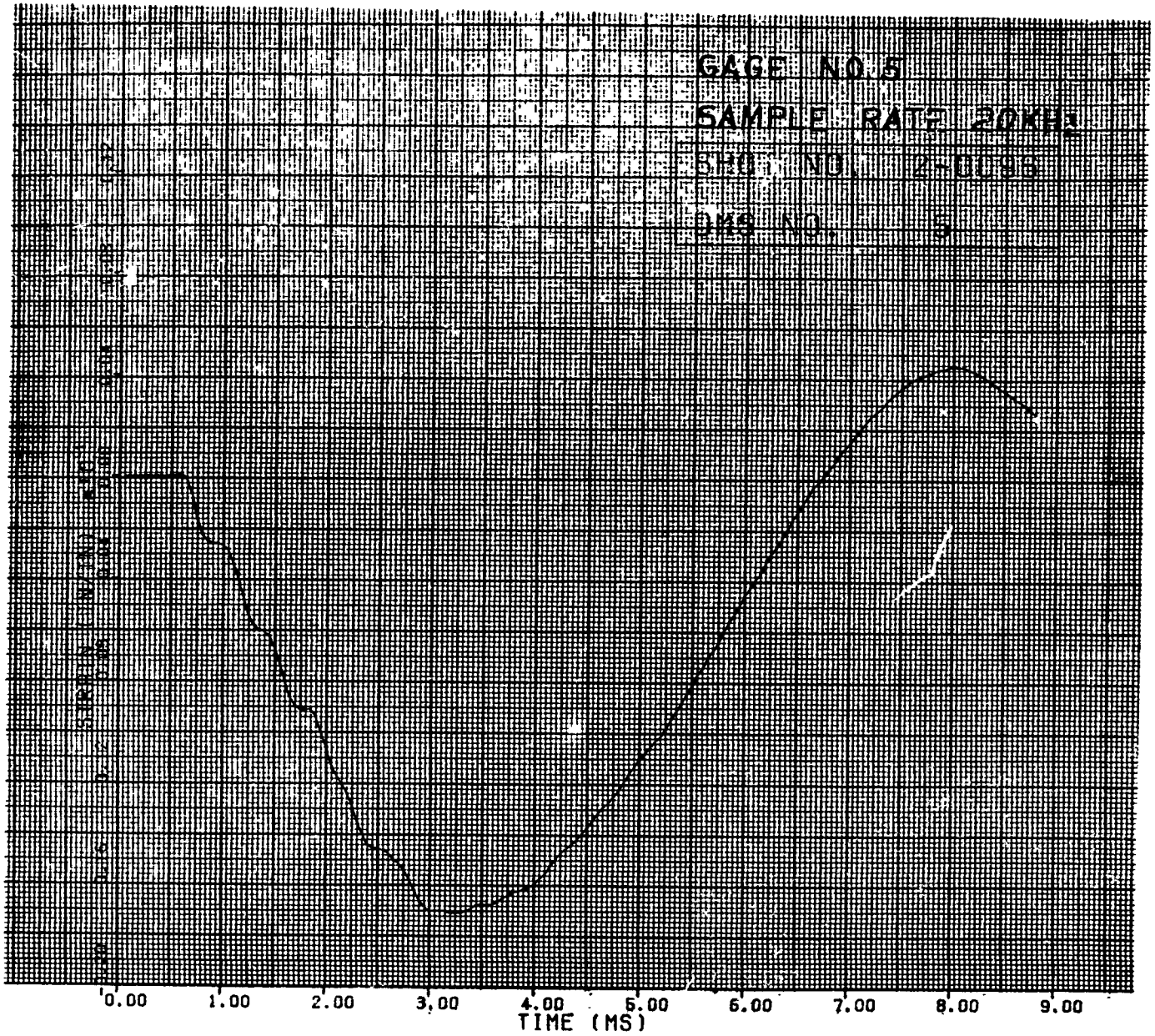

Figure 46. Strain of Shot 2-0096 for Gage #5.

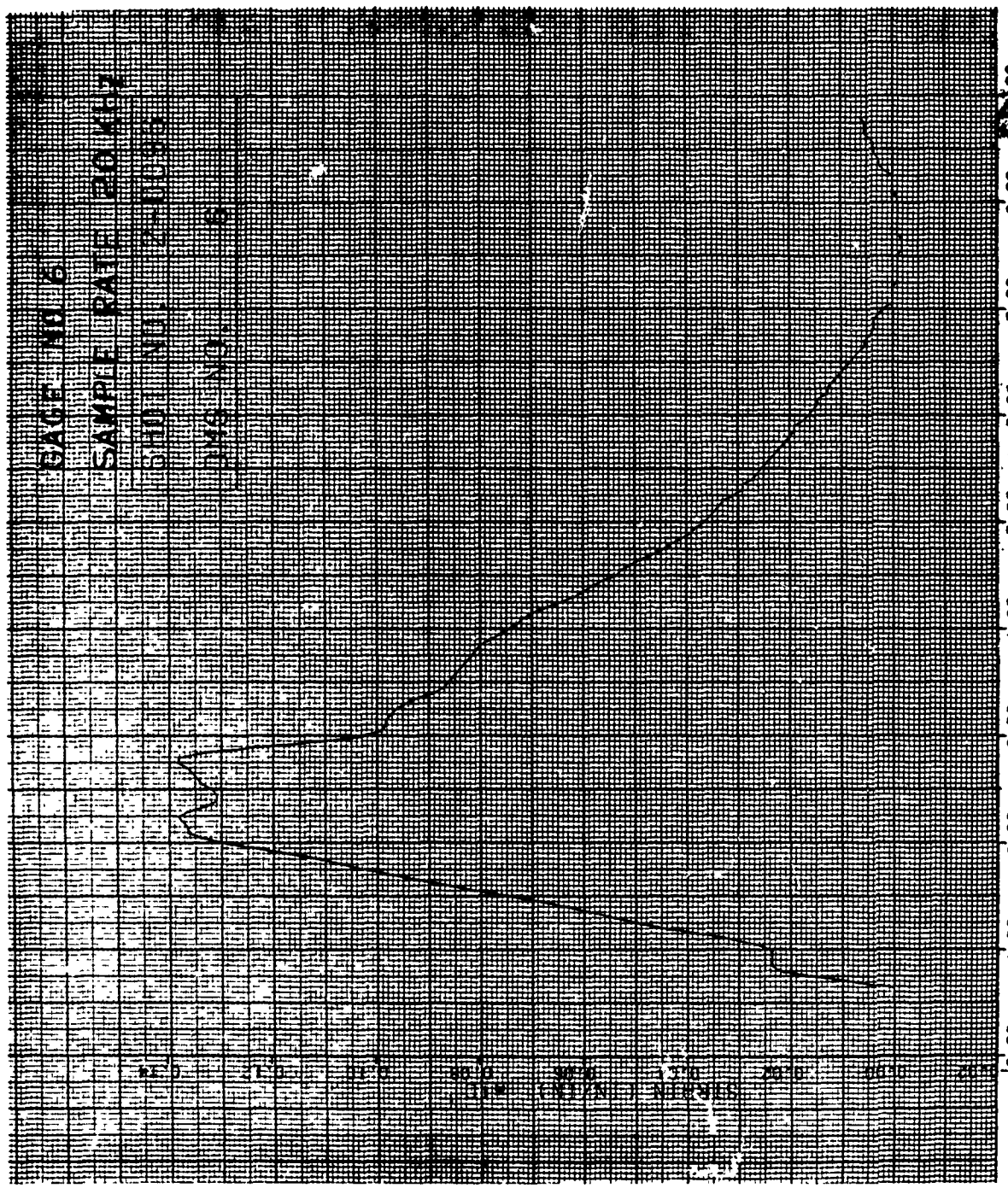

Figure 47. Strain of Shot 2-0096 for Gage #6.

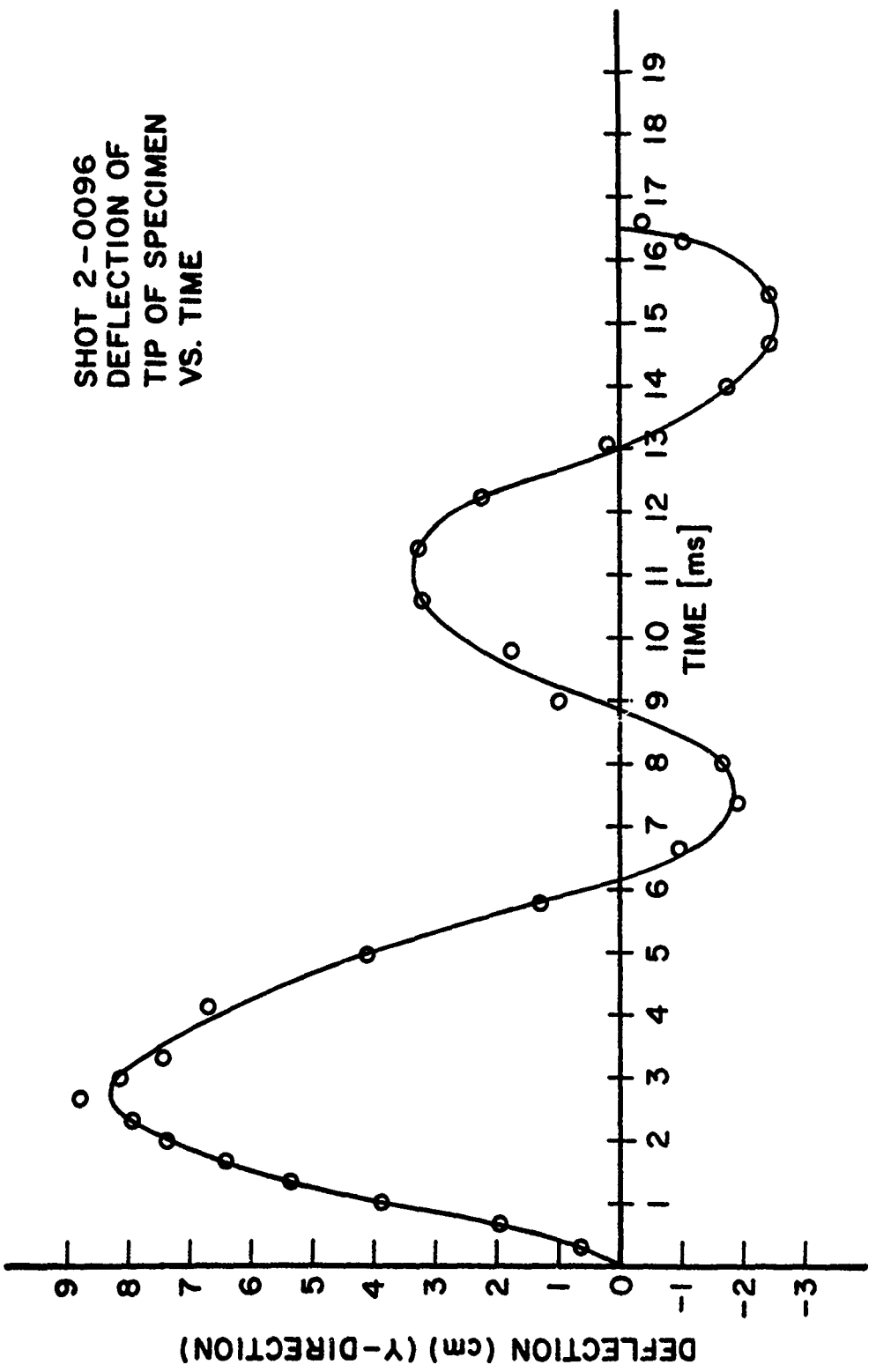

Figure 48. Tip Deflection for Shot 2-0096.

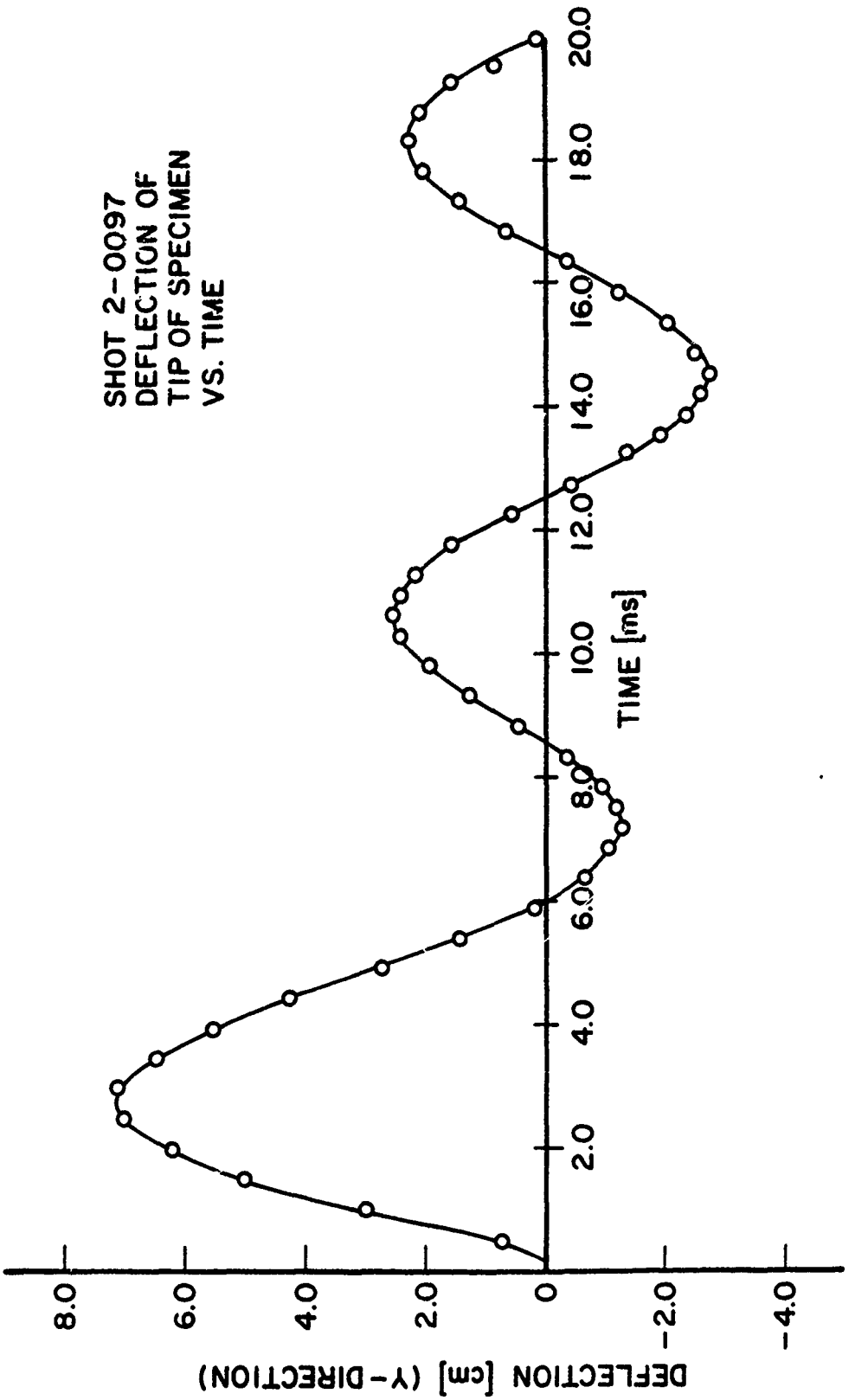

Figure 49. Tip Deflection for Shot 2-0097.

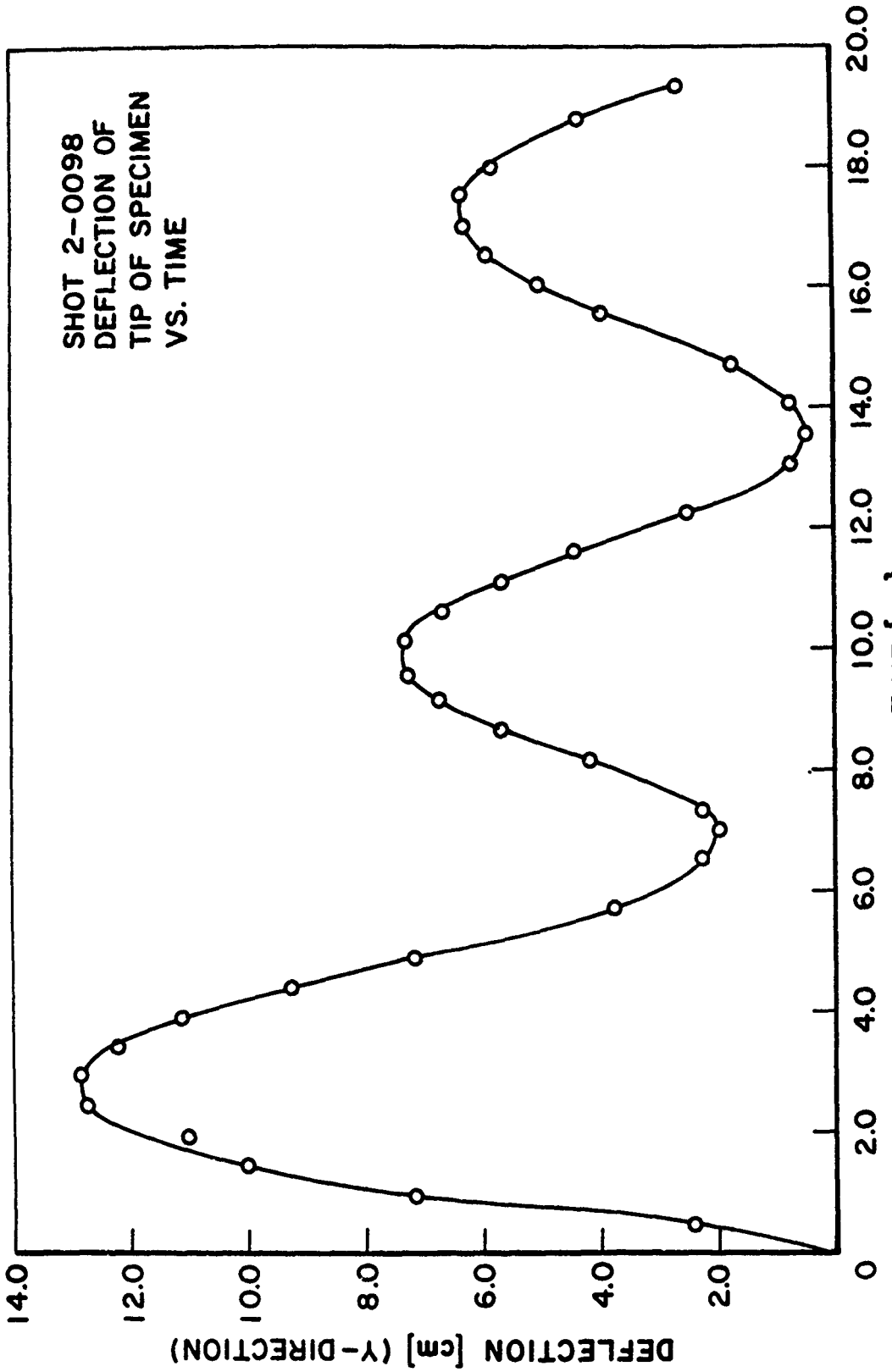

Figure 50. Tip Deflection for Shot 2-0098.

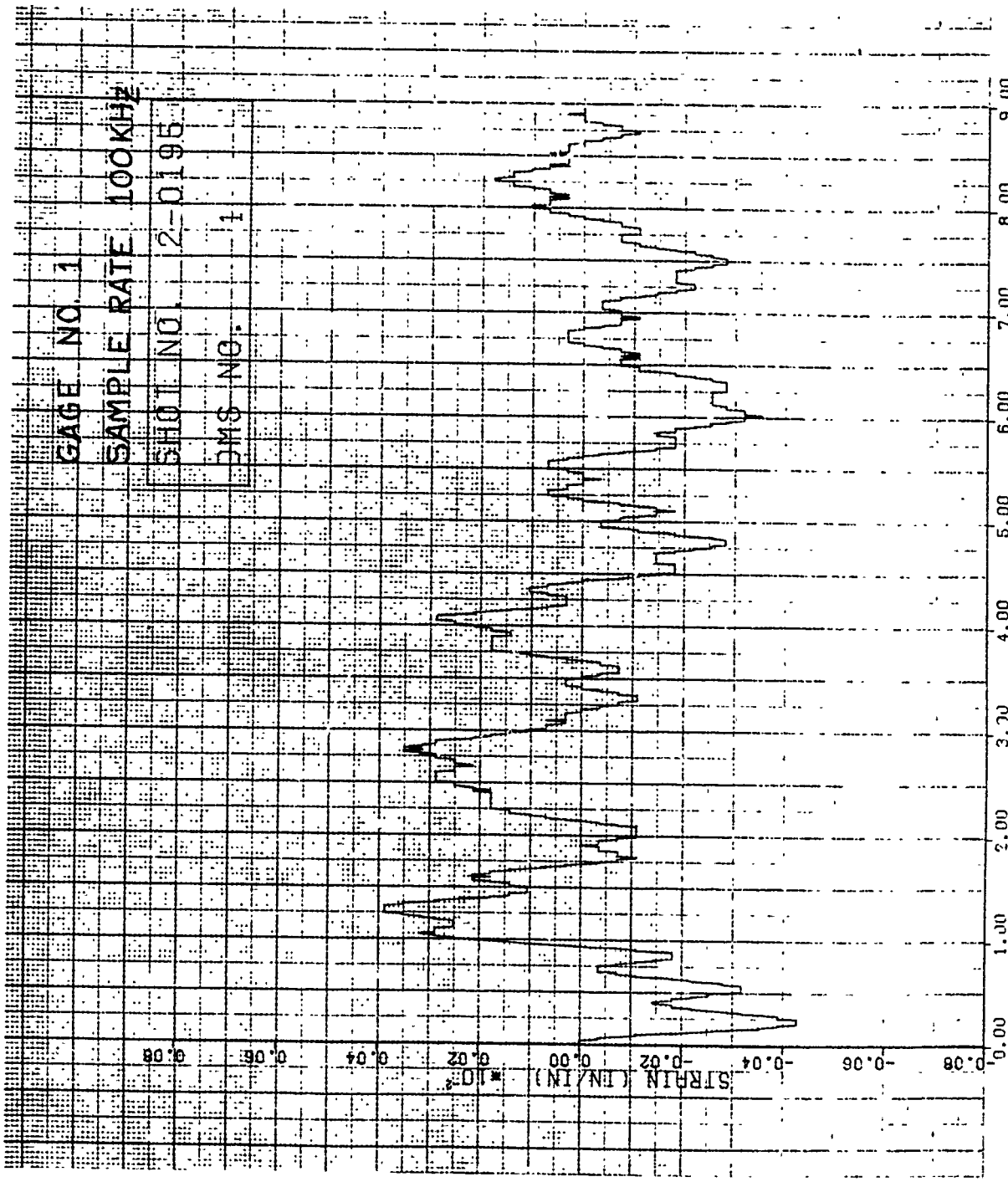

Figure 51. Strain of Shot 2-0195 for Gage #1.

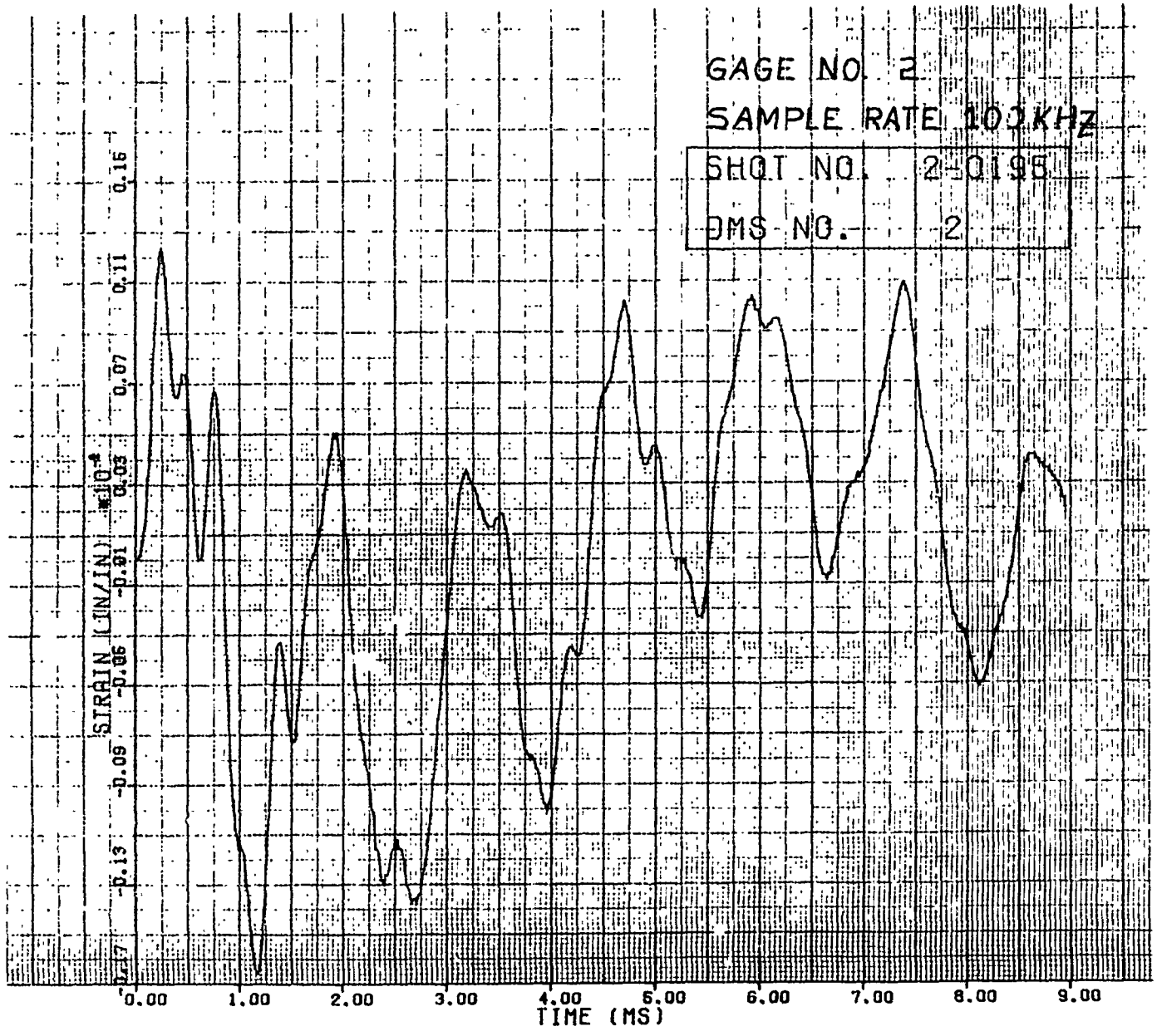

Figure 52. Strain of Shot 2-0195 for Gage #2.

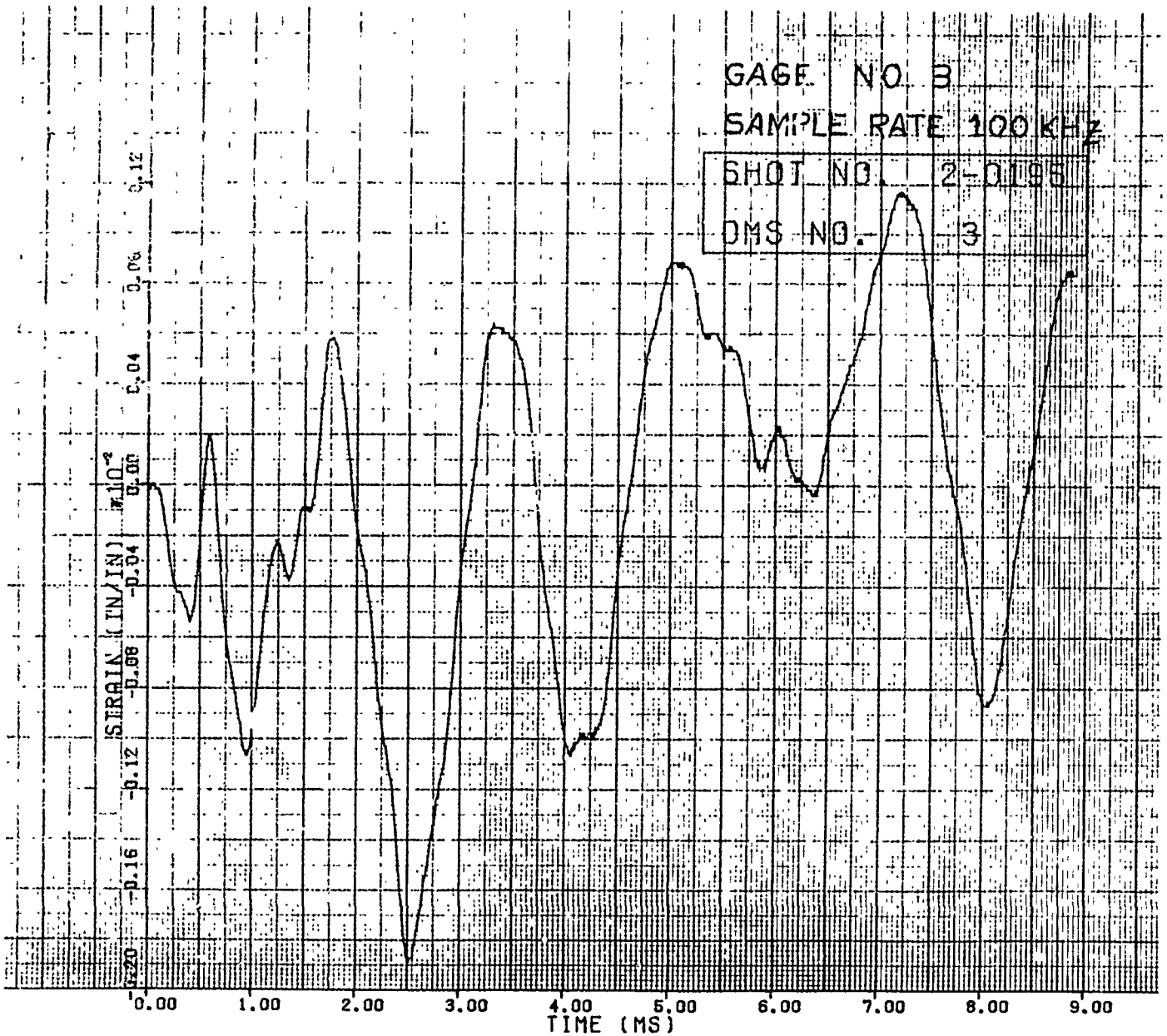

Figure 53. Strain of Shot 2-0195 for Gage #3.

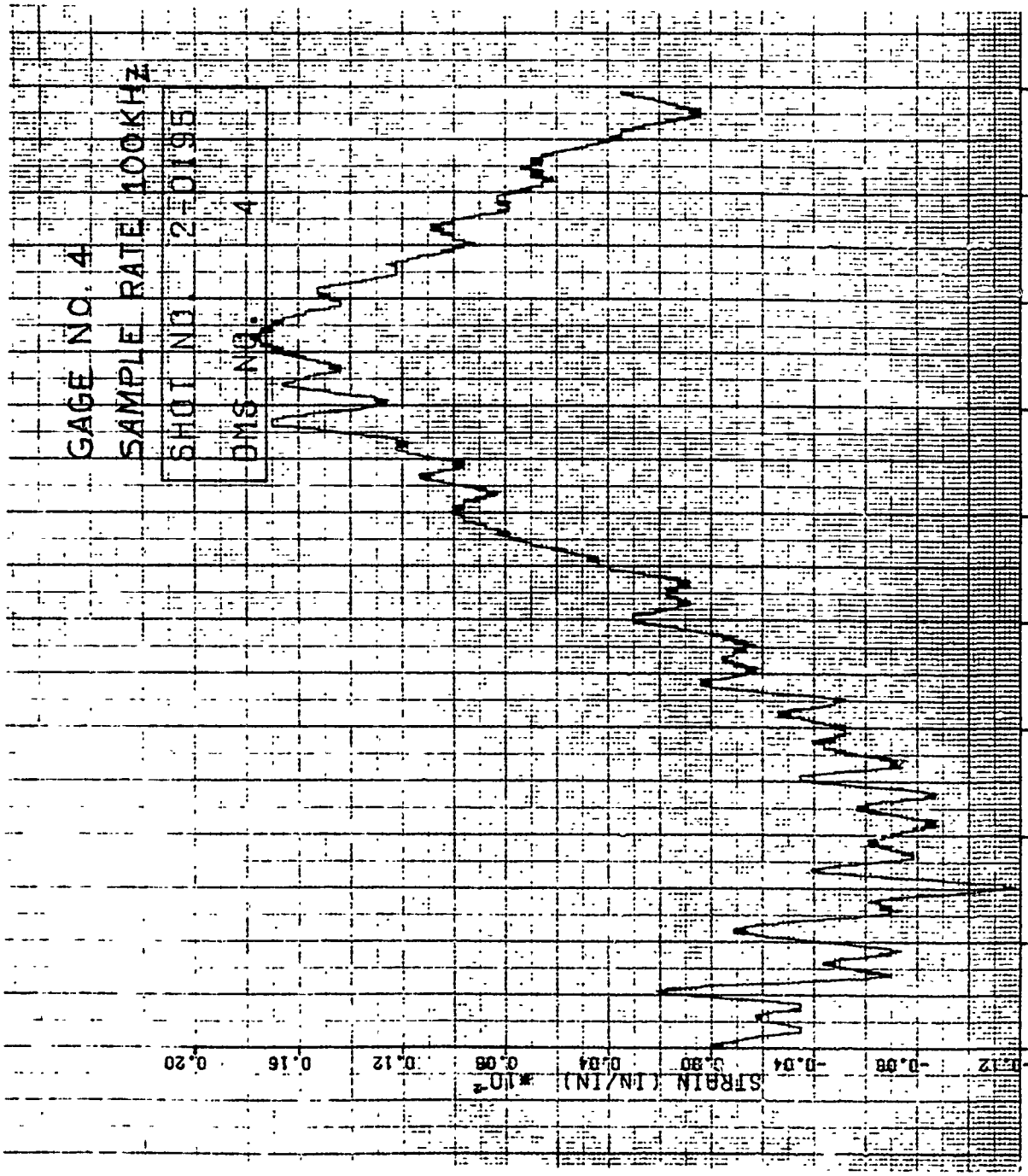

Figure 54. Strain of Shot 2-0195 for Gage #4.

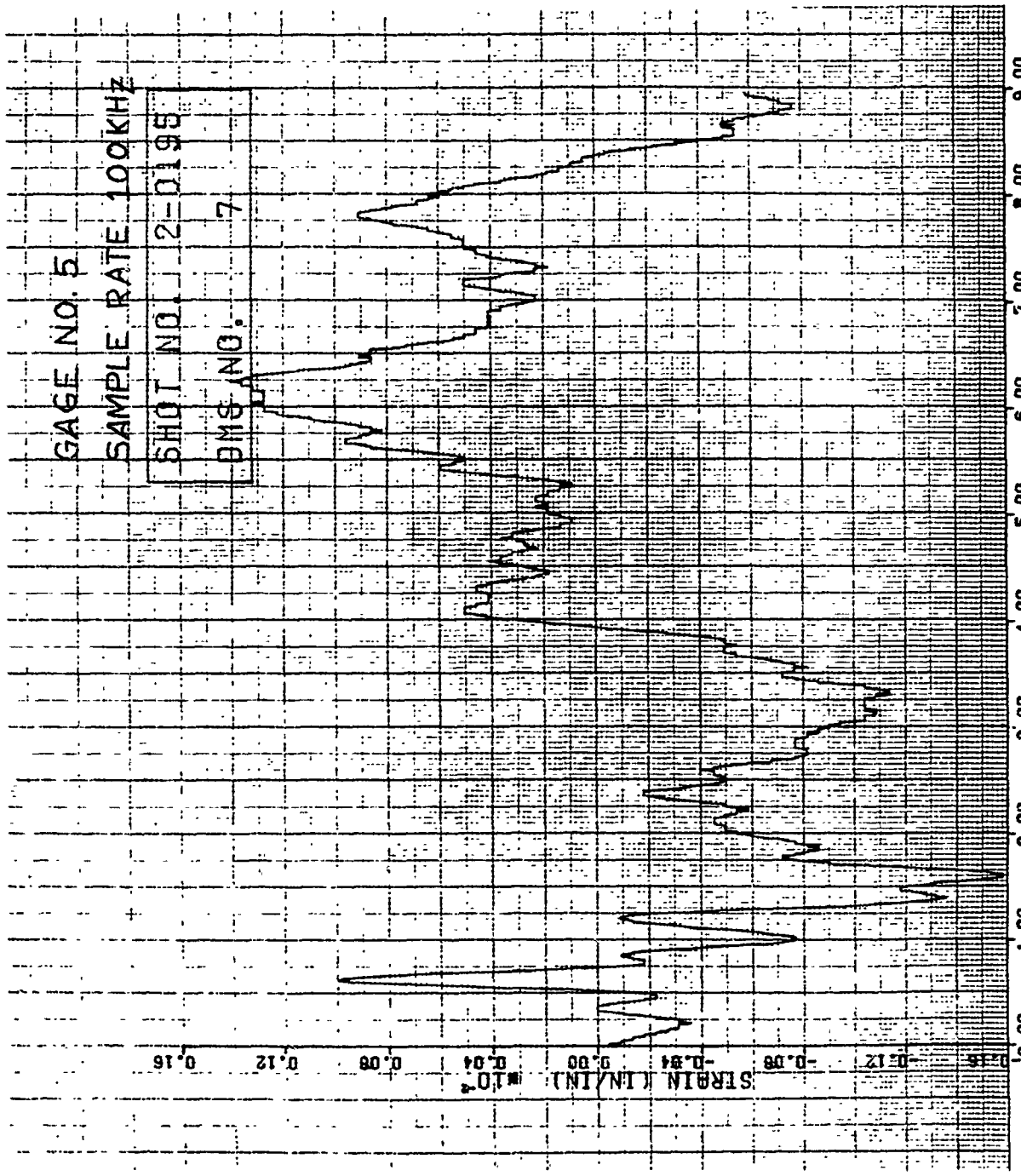

Figure 55. Strain of Shot 2-0195 for Gage #5.

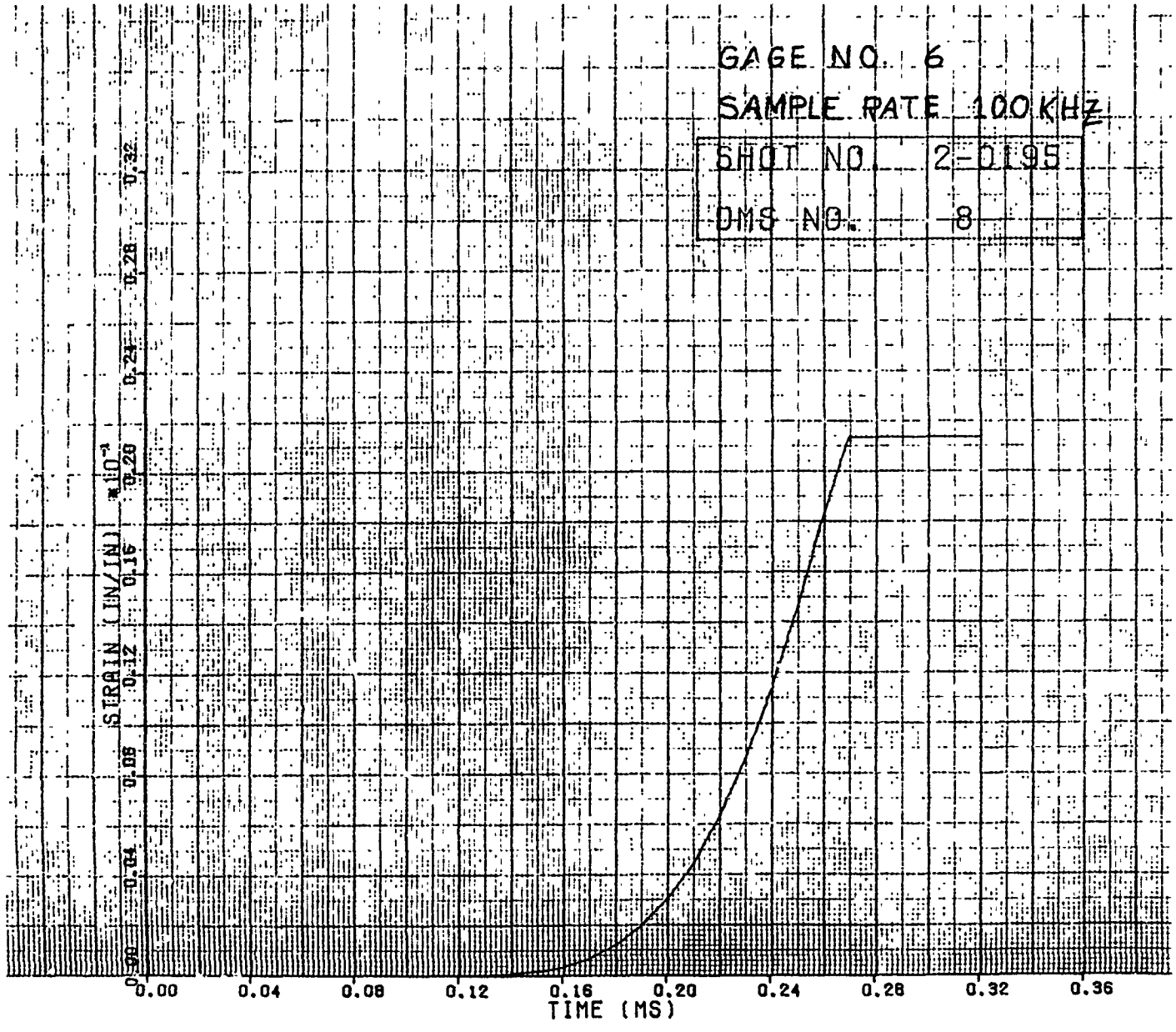

Figure 56. Strain of Shot 2-0195 for Gage #6.

at a velocity 232 m/s. As indicated earlier, no damage was generated on the specimen for this impact (Shot 2-0195).

3.1.1.6 Impact Results for Group 6 Specimens

Five Group 6 titanium flat plate specimens with a blade-like aspect ratio and a one-half blade-like thickness to chord ratio were impacted by the small 85 g (3 ounce) substitute bird. The impacts were center impacts at the 70 percent span location normal to the specimen at velocities ranging from 75 to 134 m/s. Three of the impacts were conducted using the Moiré fringe device to determine displacement at different span locations at various times. Two of the impacts were conducted using strain gages to monitor strain. Figure 7A of Appendix A gives the locations of the strain gages.

Figures 57 and 58 give dynamic displacement plots for Shots 4-0054 and 4-0055, respectively. The specimen for Shot 4-0054 broke off at its root at an impact velocity of 126 m/s which is noticeable in Figure 57. The time for Figure 57 plot varied from 0.16 ms to 2.18 ms after impact occurred.

The plastic deformation and bending of the specimen at its root of Shot 4-0055 was determined to be 10.95 cm (measurement taken at tip). The impact velocity for this impact was 104 m/s. The deflection during the impact event for Shot 4-0055 given in Figures 58 is plotted for times varying from 0.15 to 2.45 ms.

Typical strain gage results are presented in Figures 59 through 64 for the bird impact mass of about 85 g at a velocity of 66 m/s (Shot 2-0176). The plastic deformation of the specimen at its root was determined to be 7.87 cm (tip measurement).

Figures 10B through 12B give photographs of the damage caused in the same shot sequence, namely 4-0053,

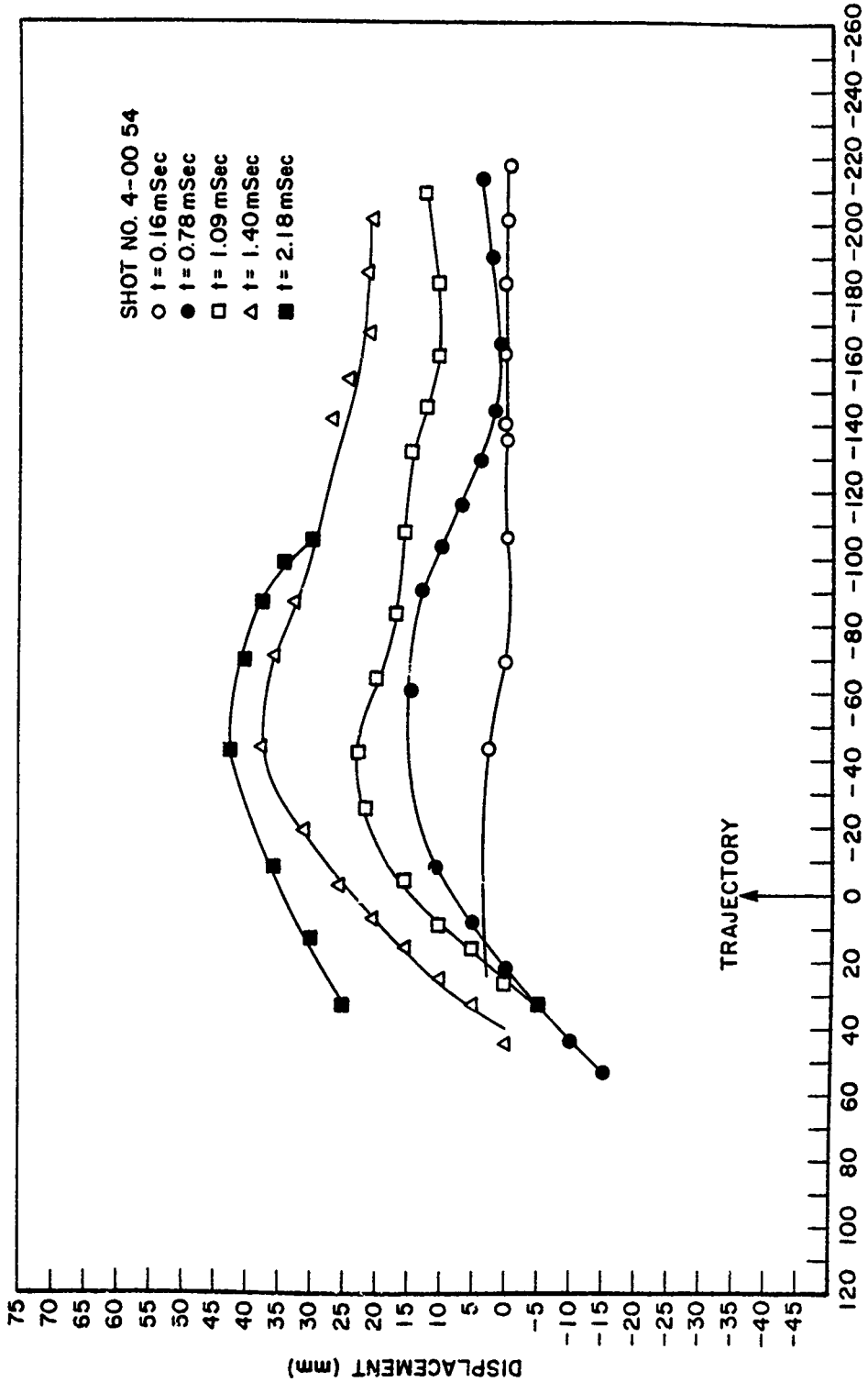

Figure 57. Moiré Fringe Deflection Data for Shot 4-0054.

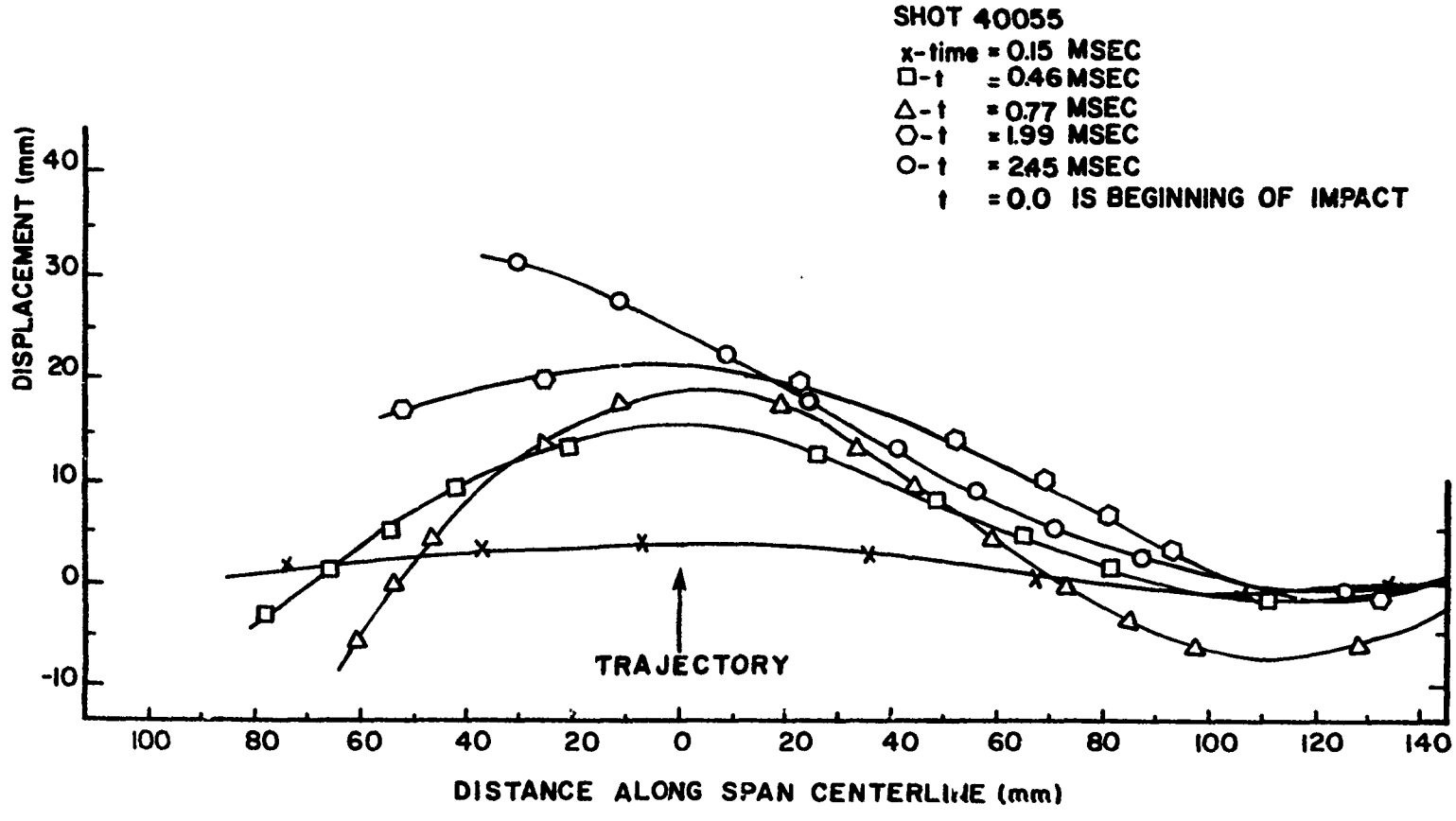

Figure 58. Moiré Fringe Deflection Data for Shot 4-0055.

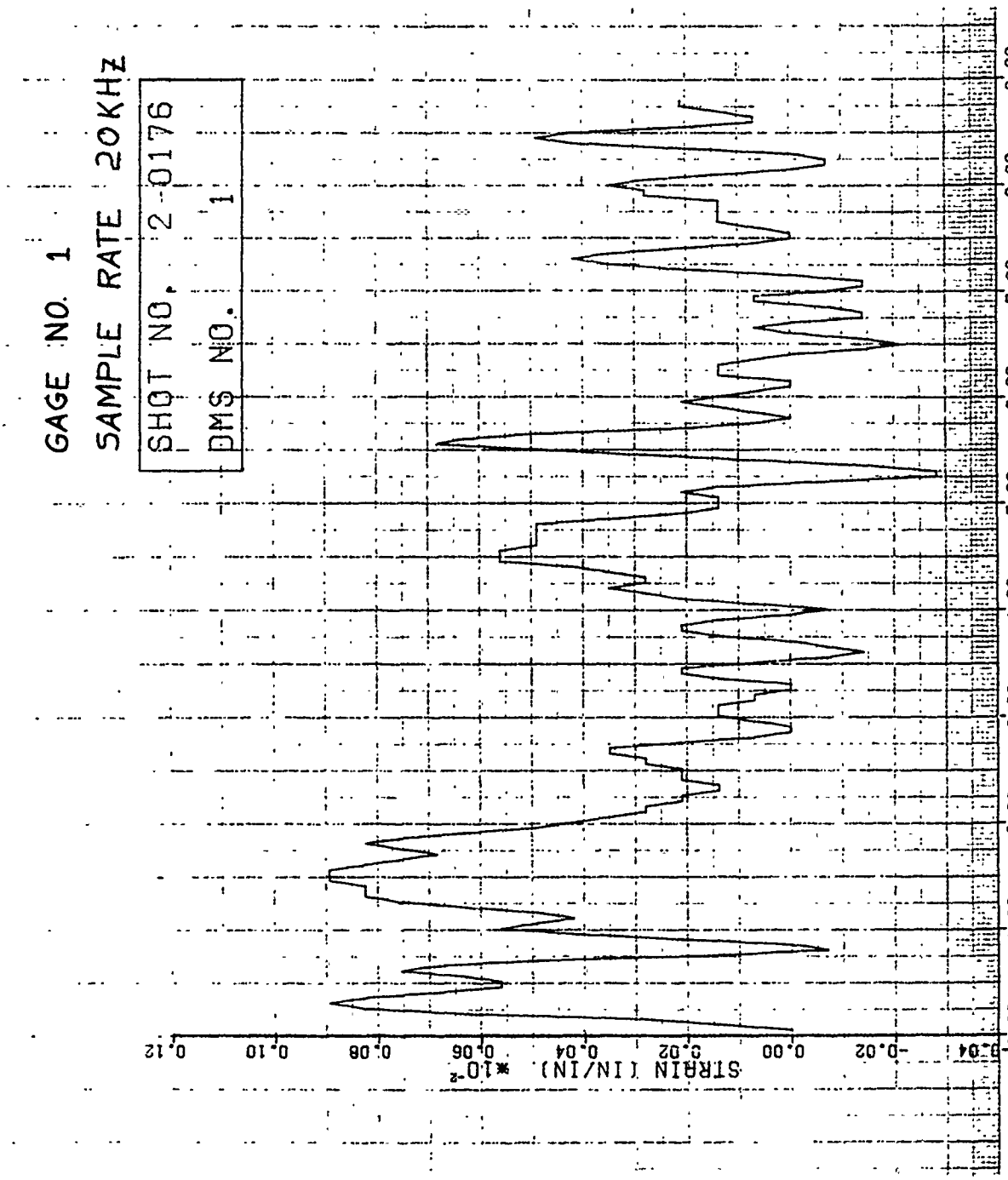

Figure 59. Strain of Shot 2-0176 for Gage #1.

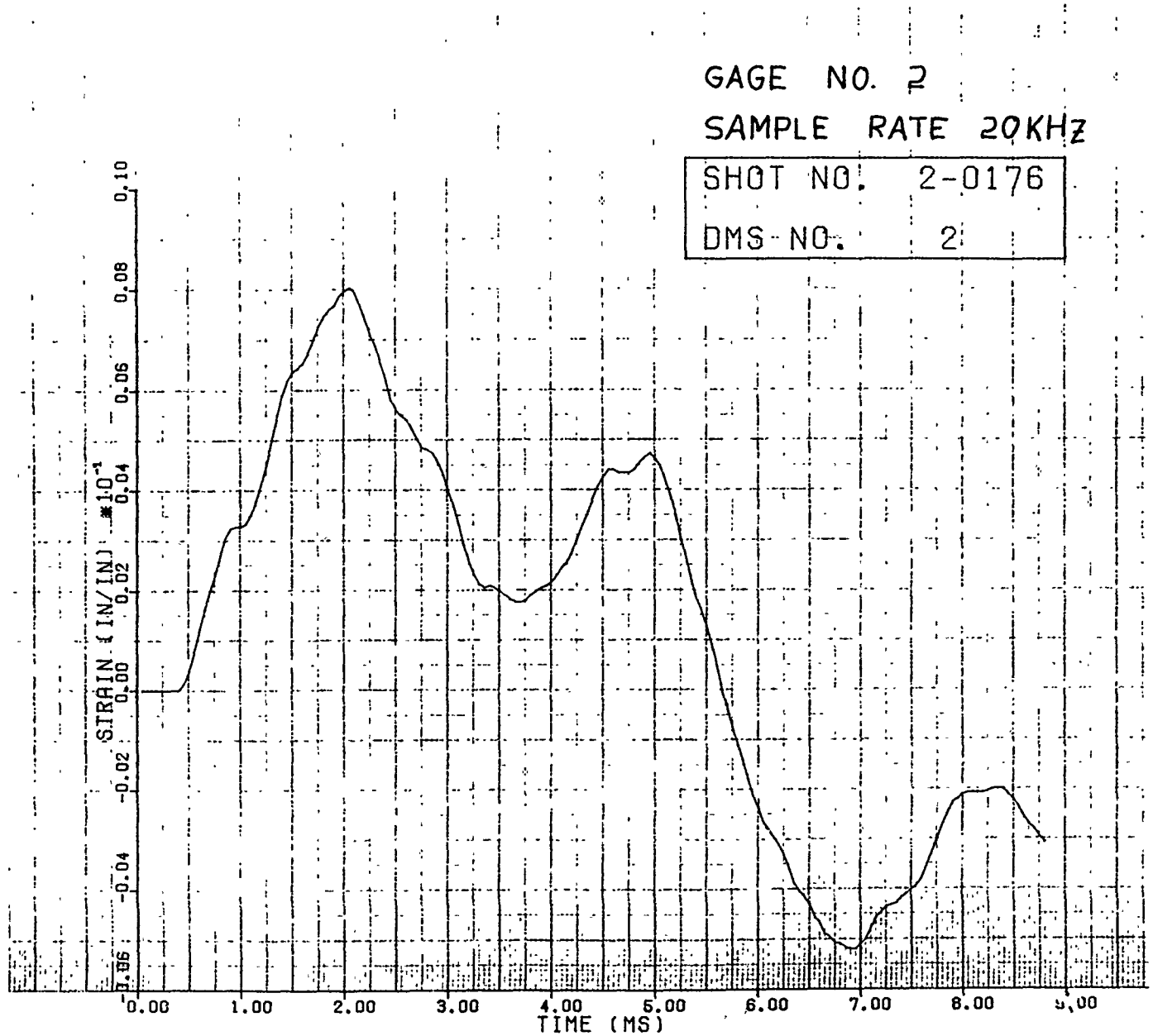

Figure 60. Strain of Shot 2-0176 for Gage #2.

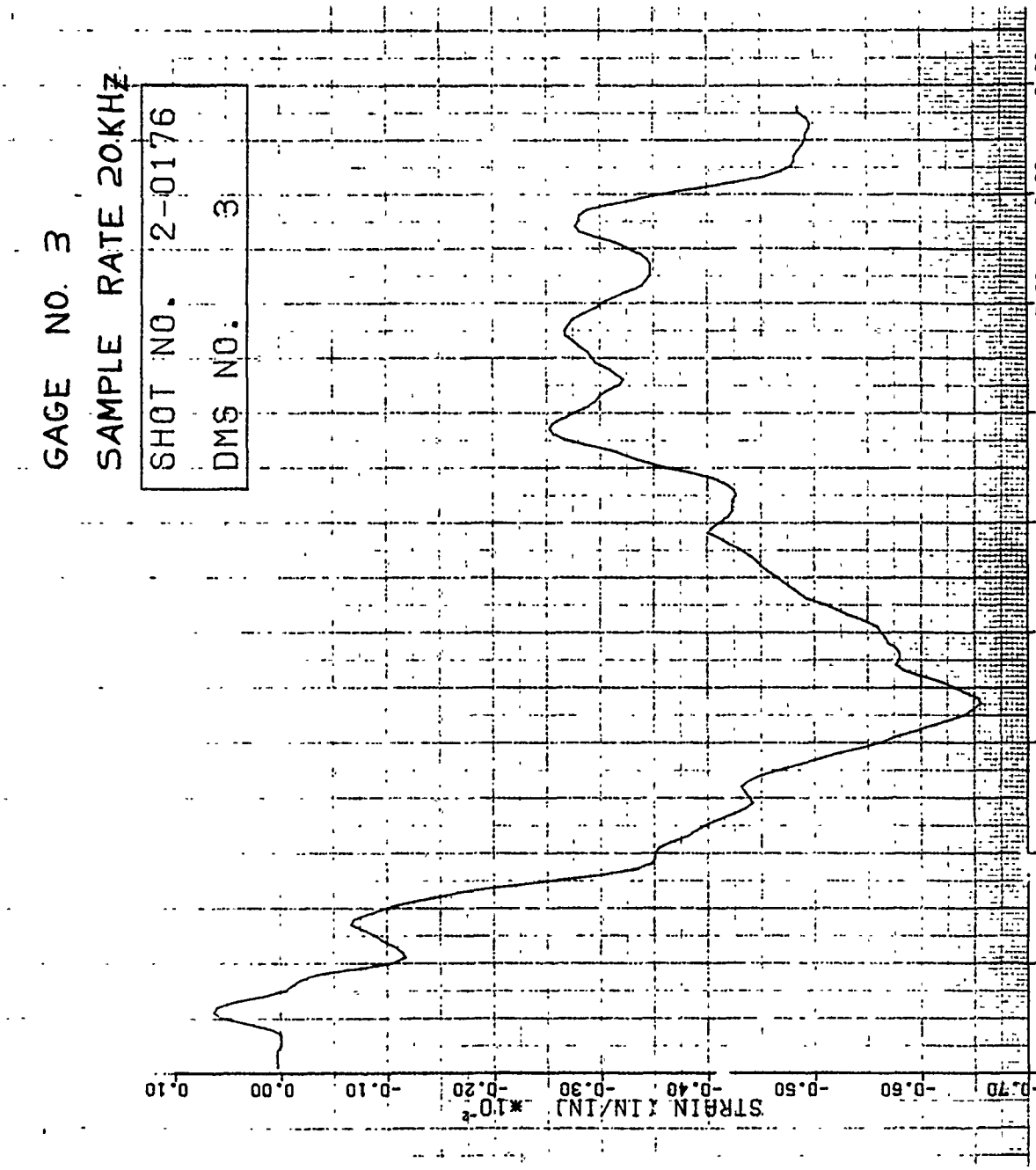

Figure 61. Strain of Shot 2-0176 for Gage #3.

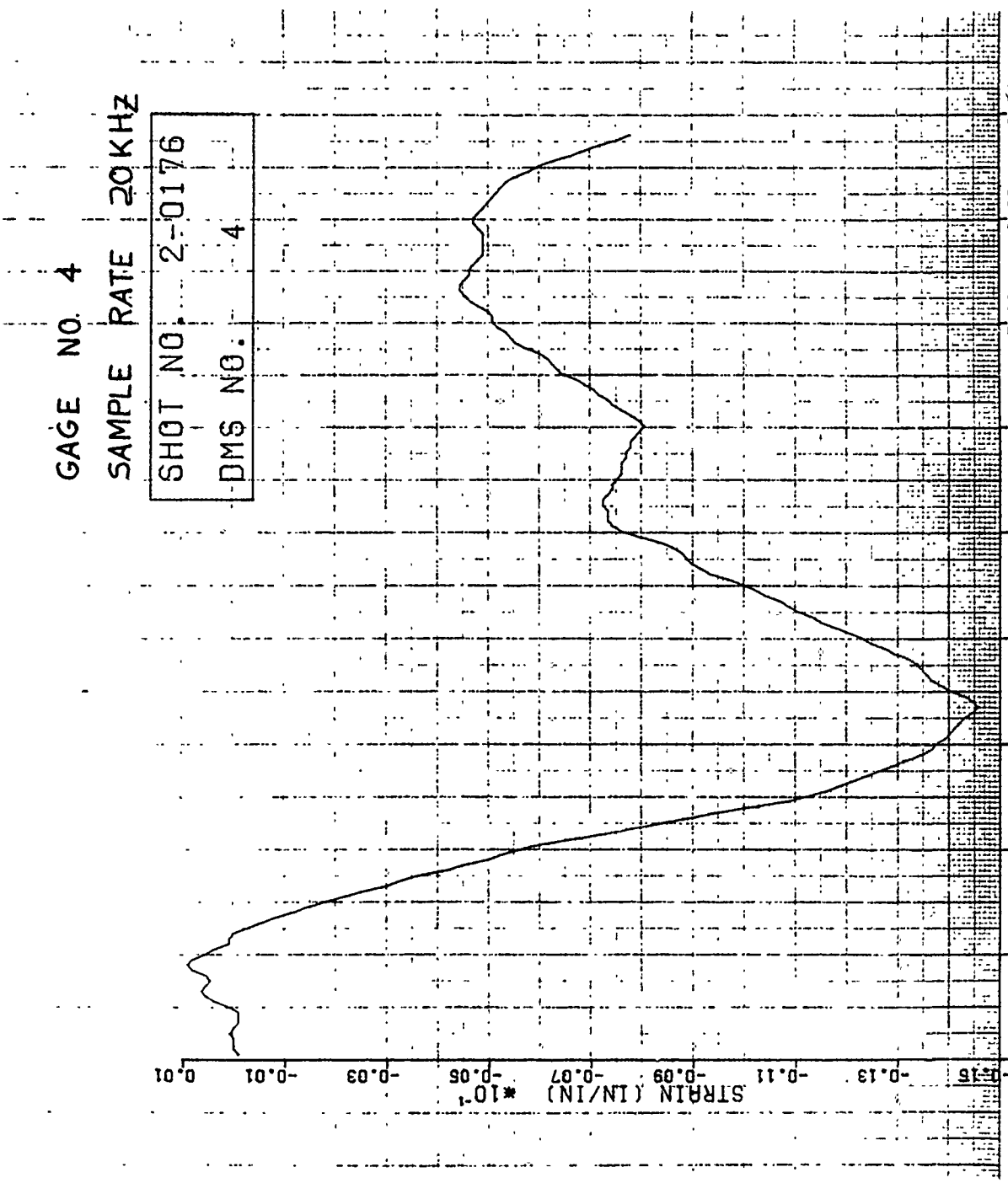

Figure 62. Strain of Shot 2-0176 for Gage #4.

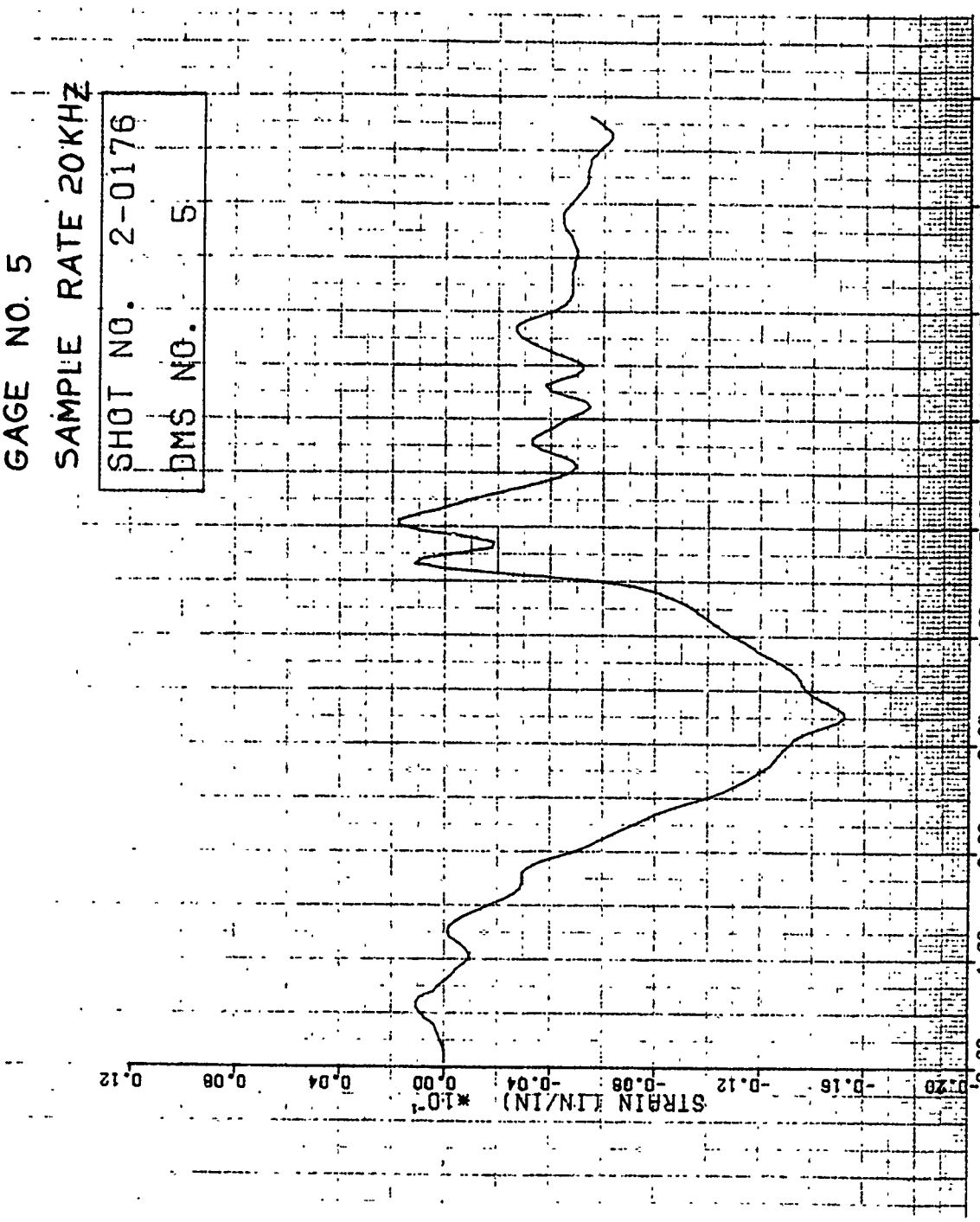

Figure 63. Strain of Shot 2-0176 for Gage #5.

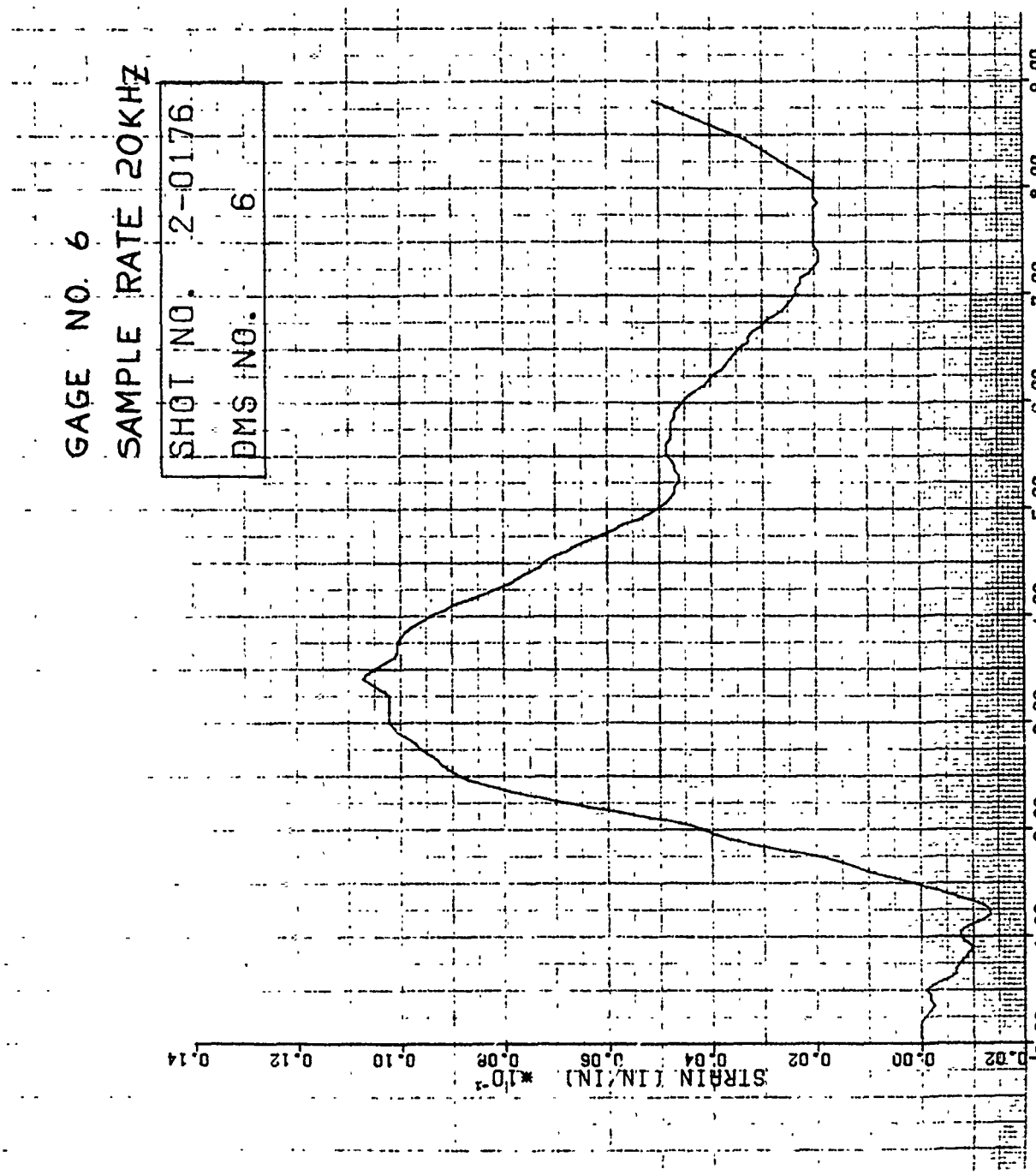

Figure 64. Strain of Shot 2-0176 for Gage #6.

4-0054, and 4-0055. Figures 13B and 14B present photographs of the damage for the strain data impacts of Shots 2-0175 and 2-0176, respectively.

3.1.1.7 Impact Results for Group 7 Specimens

Three Group 7 titanium plate specimens with a blade-type aspect ratio and airfoil shape (tapered cross section) were impacted by the small 85 g (3 ounce) artificial birds. The impacts were edge (slicing) impacts at the 70 percent span location at an impact angle of 24.4 degrees and at velocities ranging from 135 to 323 m/s. The damage received ranged from none for the 135 m/s impact to plastic deformation of the specimen at its leading edge at the impact site for the 323 m/s impact. In this case, the deformation at the leading edge was determined to be 1.65 cm. The tip deformation was 1.14 cm for the leading edge and 0.89 cm for the trailing edge.

Typical strain gage results are presented in Figures 65 through 70 for Shot 2-0130. Figure 8A of Appendix A gives the strain gage locations on the specimens. The impact velocity for this impact was 211 m/s and the impact mass was 15.1 g. Dynamic displacement versus time plots for the "y", "x", and resultant directions for Shot 2-0130 are given in Figures 71 through 73, respectively.

Figures 15B through 17B give photographs of the damage for the bird impacts of Shots 2-0128, 2-0129, and 2-0130, respectively.

3.1.1.8 Impact Results for Group 8 Specimens

Four Group 8 titanium specimens with the same geometry as for the Group 7 specimens were impacted by the medium 681 g (1.5 pound) artificial birds. The impacts were edge (slicing) impacts at the 70 percent span location at an impact angle of 24.4 degrees and at velocities ranging from 59 to 189 m/s. The impact mass ranged from a low of 24.1 g to a high of 188.5 g. Damage received on the specimens from the

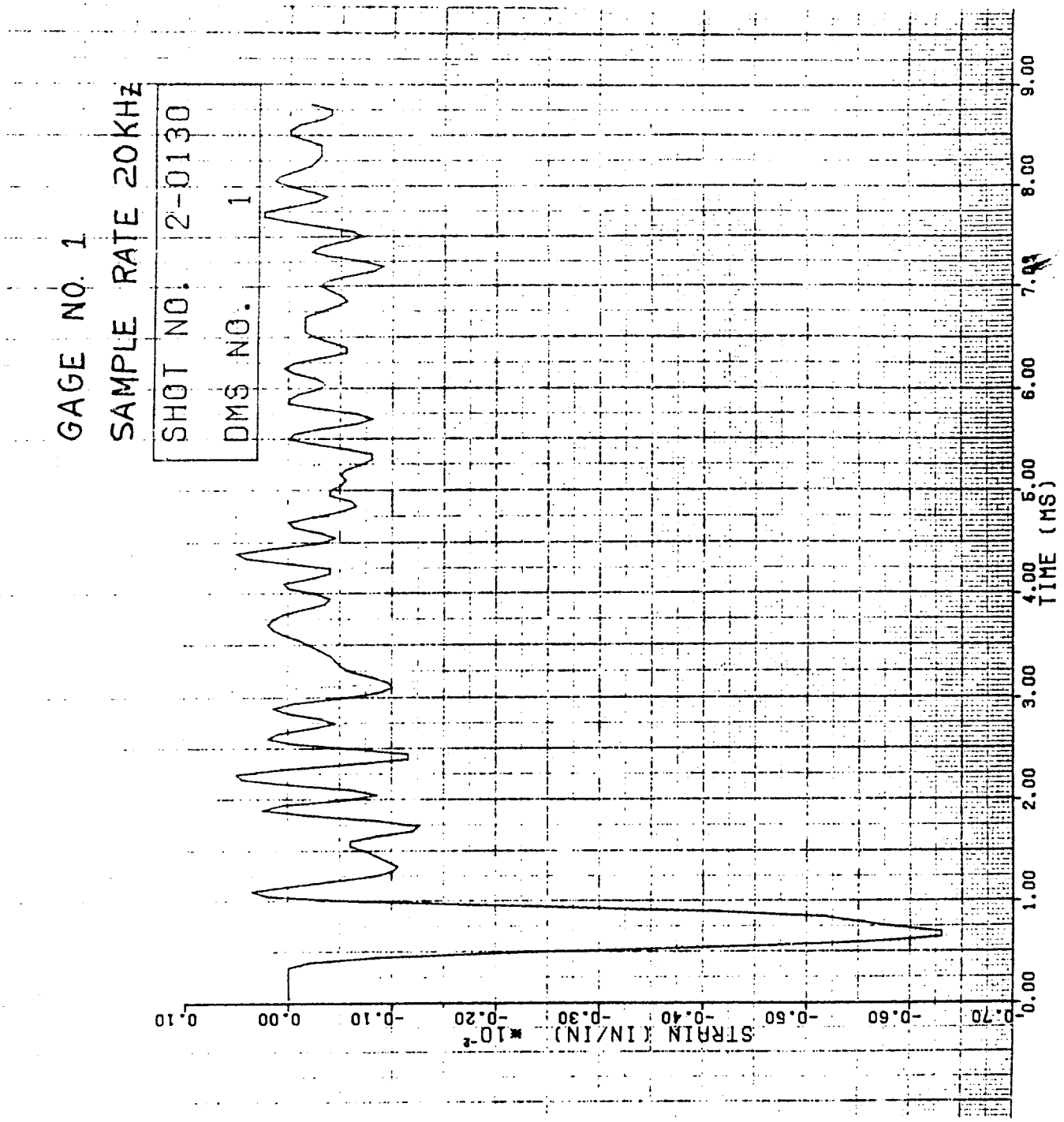

Figure 65. Strain of Shot 2-0130 for Gage #1.

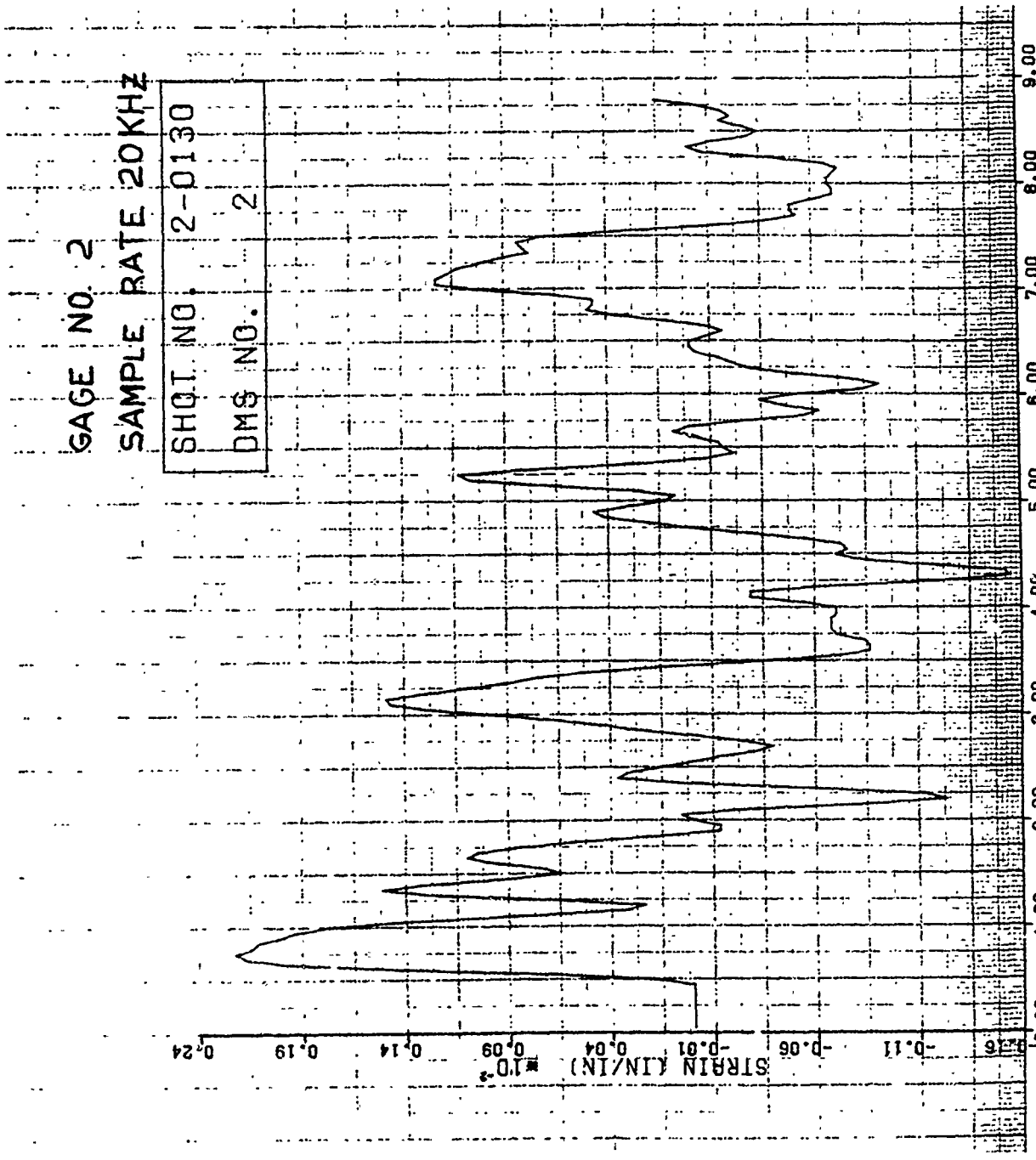

Figure 66. Strain of Shot 2-0130 for Gage #2.

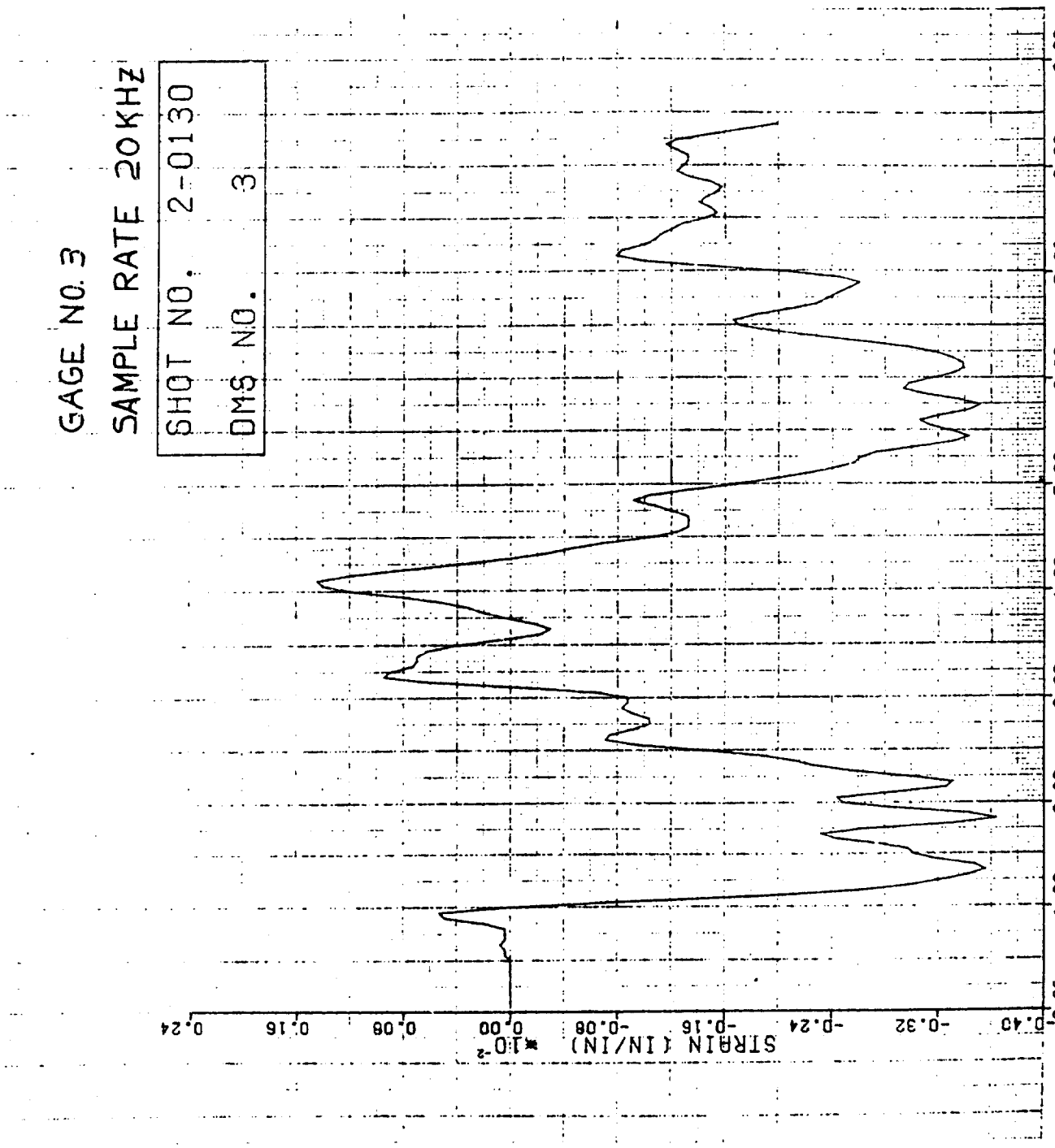

Figure 67. Strain of Shot 2-0130 for Gage #3.

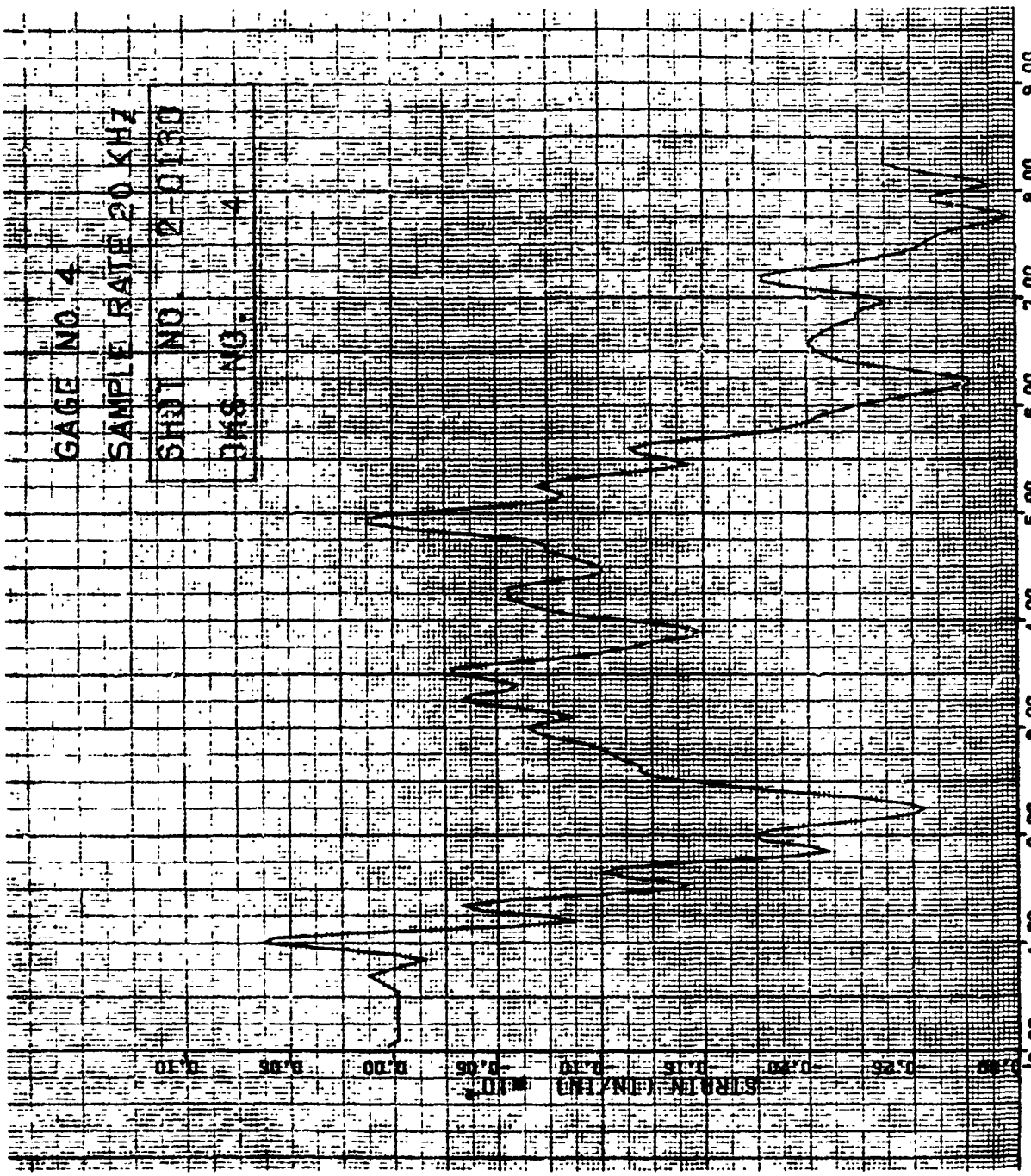

Figure 68. Strain of Shot 2-0130 for Gage #4.

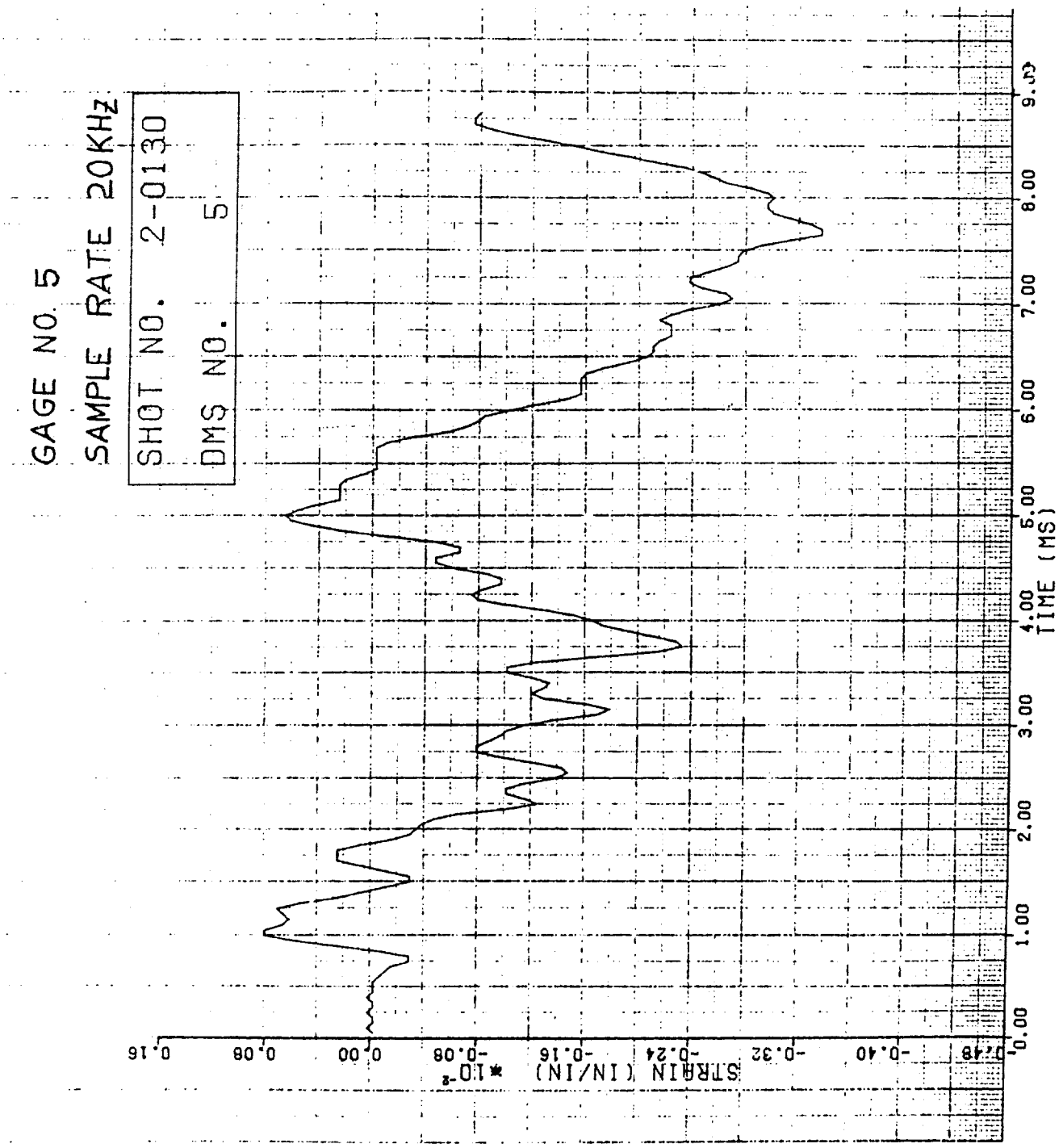

Figure 69. Strain of Shot 2-0130 for Gage #5.

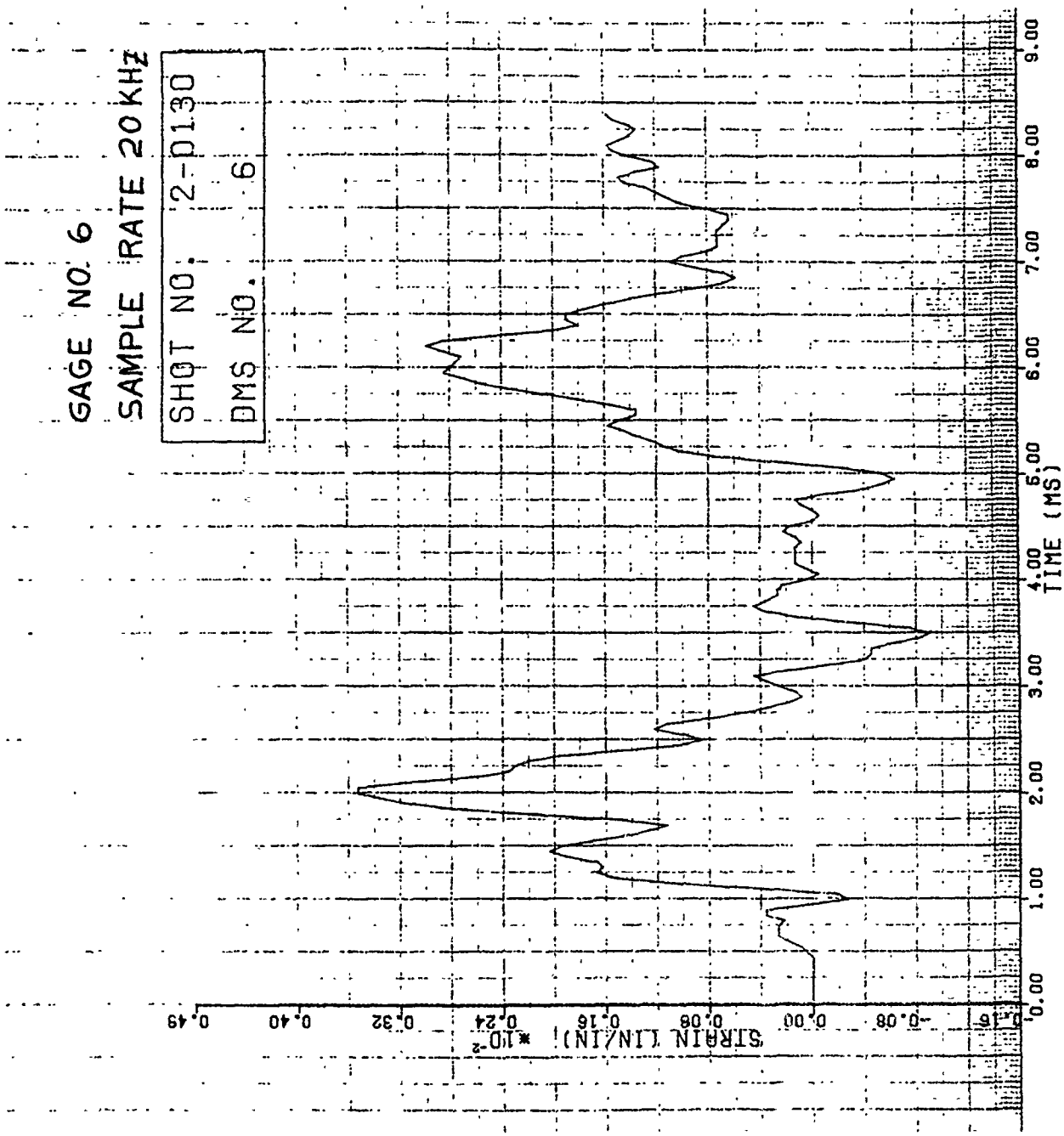

Figure 70. Strain of Shot 2-0130 for Gage #6.

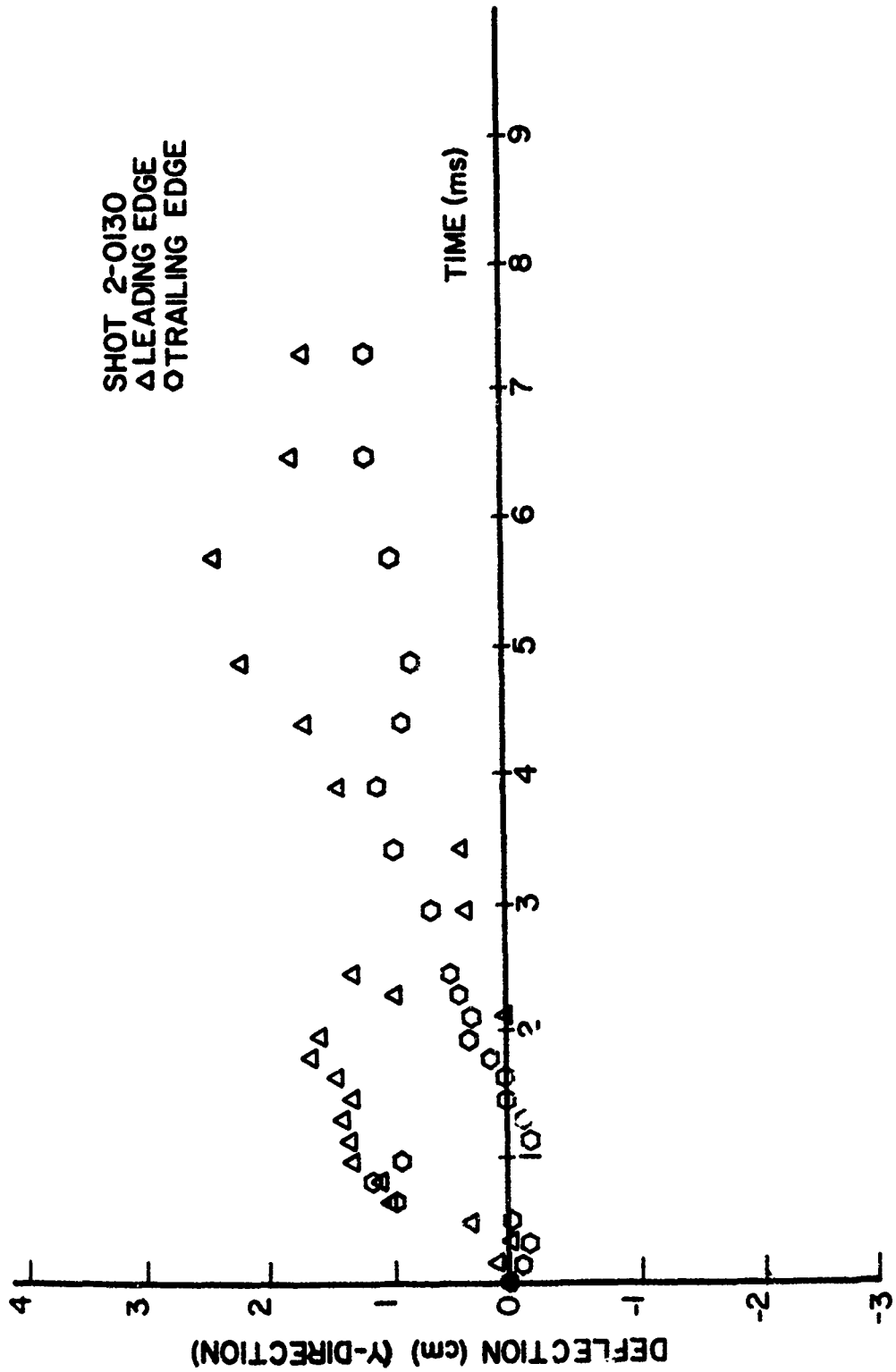

Figure 71. Tip Deflection in "y" Direction for Shot 2-0130.

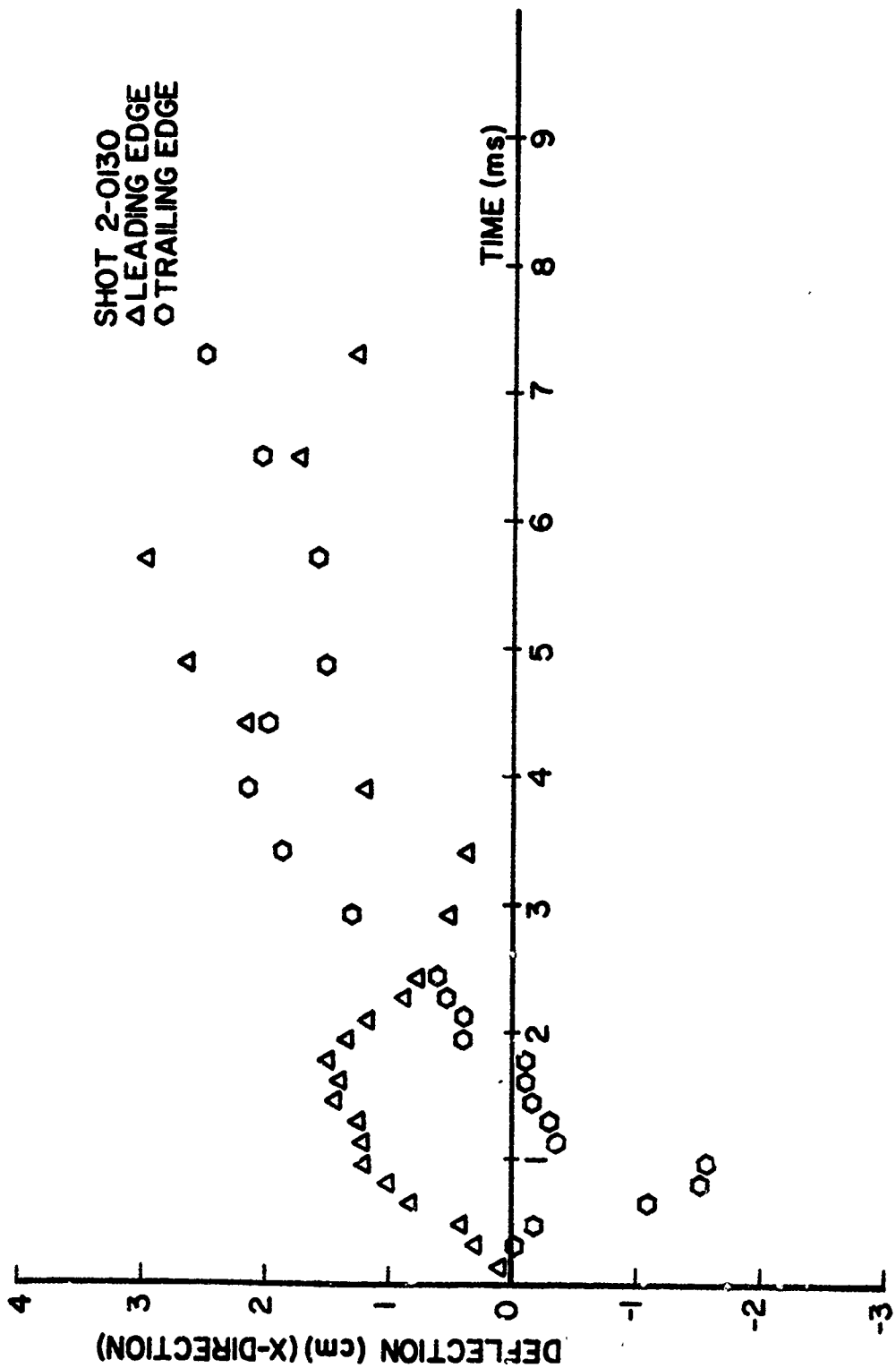

Figure 72. Tip Deflection in "x" Direction for Shot 2-0130.

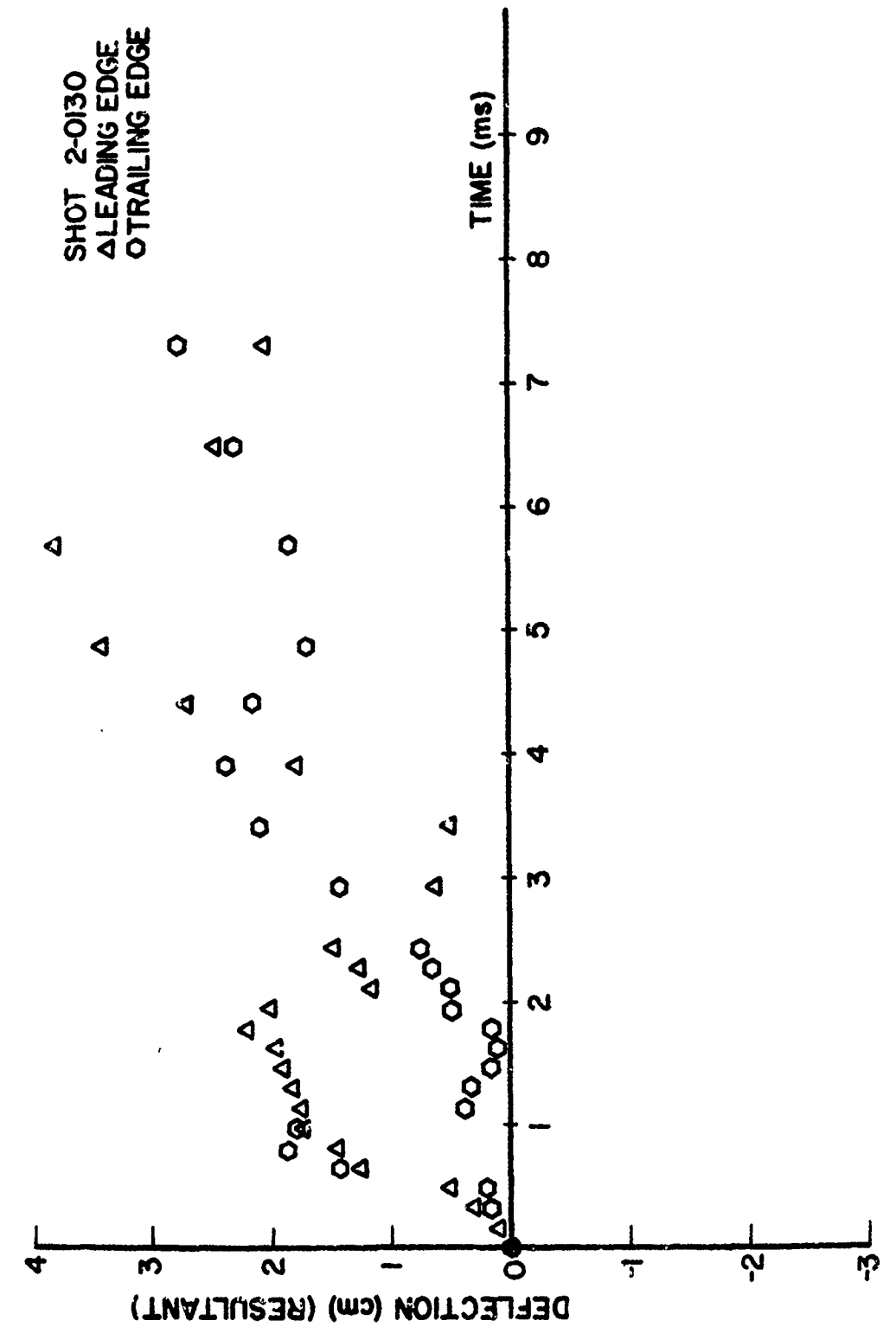

Figure 73. Tip Deflection Resultant Direction for Shot 2-0130.

bird impacts ranged from no visible damage for an impact of 112 m/s and impact mass of 24.1 g to very severe damage on specimens impacted at 189 and 131 m/s with impact mass values of 120.1 and 119.5 g, respectively. This severe damage was in the form of plastic deformation of the specimen at its root. The most severe damage was received for the 131 m/s impact (Shot 2-0167) with a plastic deflection of 20.96 cm for the leading edge and 20.32 cm for the trailing edge (measurements taken at tip). A specimen twist through the span was also measured to be 0.64 cm.

Typical strain gage results are presented in Figures 74 through 79 for Shot 2-0167. Figure 8A of Appendix A gives the strain gage locations on the specimens. The impact velocity of 131 m/s and bird mass of 119.5 g gave the most severe damage of these four impacts. Dynamic displacement versus time plots of the "y", "x", and resultant directions are given in Figures 80 through 82, respectively. As shown by the figures, displacement data is not available for a portion of the curves because the tip of the specimen moved out of view of the camera. Figure 83 presents a dynamic displacement plot of "y" direction versus the "x" direction for various times.

Figures 18B and 19B give photographs of the damage for the bird impacts of Shots 2-0166 and 2-0167, respectively.

3.1.1.9 Impact Results for Group 9 Specimens

Thirteen Group 9 titanium plate specimens with a blade-type aspect ratio and blade-like cross section were impacted by the medium 681 g (1.5 pound) substitute bird. The impacts were edge (slicing) impacts at the 70 percent span location at an impact angle of 24.4 degrees and at velocities ranging from 63 to 240 m/s. The impact mass ranged from a low of 40.5 g to a high of 329.2 g. In eight of the impacts, the impact mass was unable to be determined because either the bird hit the target box during entry or the impact velocity

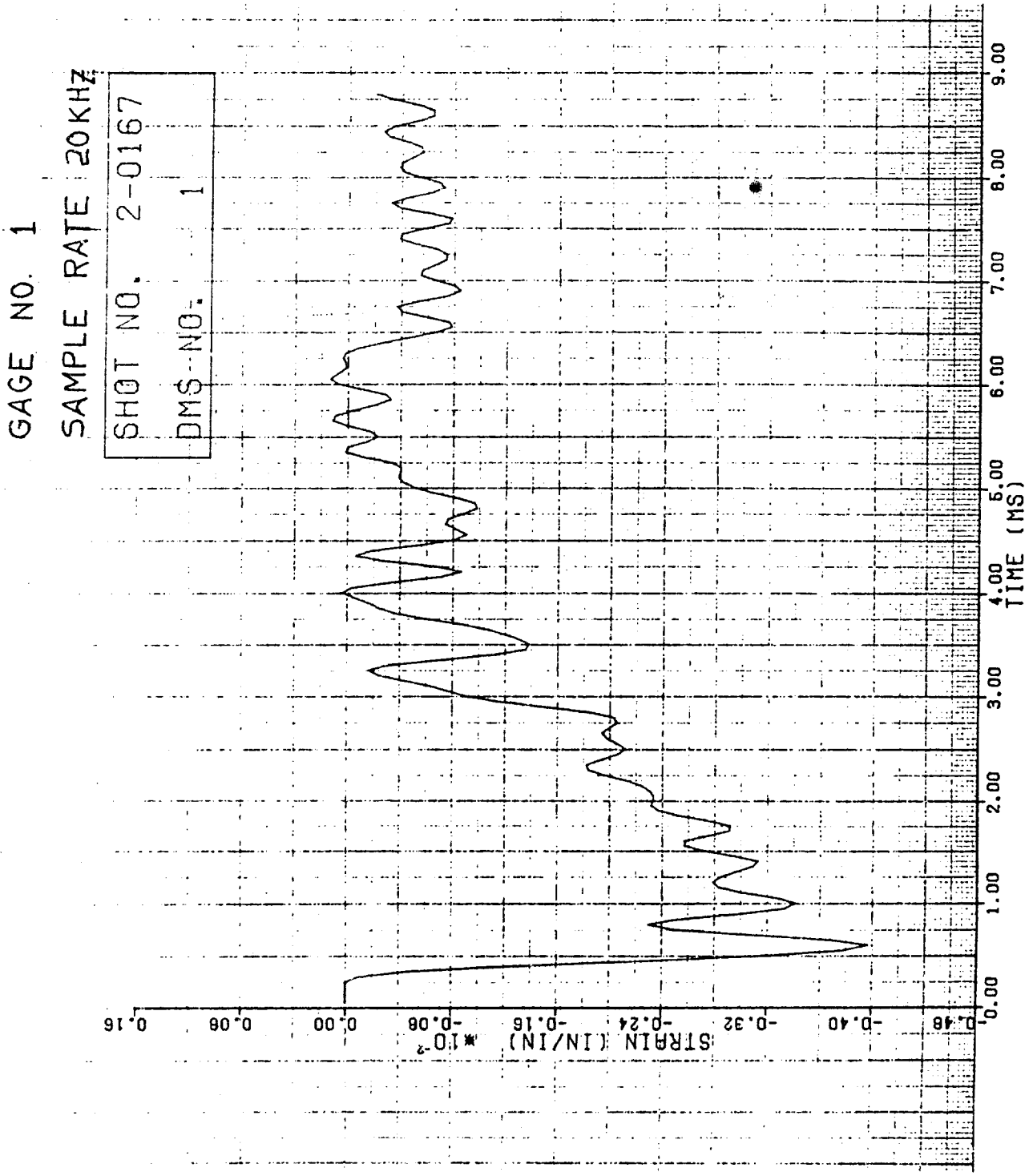

Figure 74. Strain of Shot 2-0167 for Gage #1.

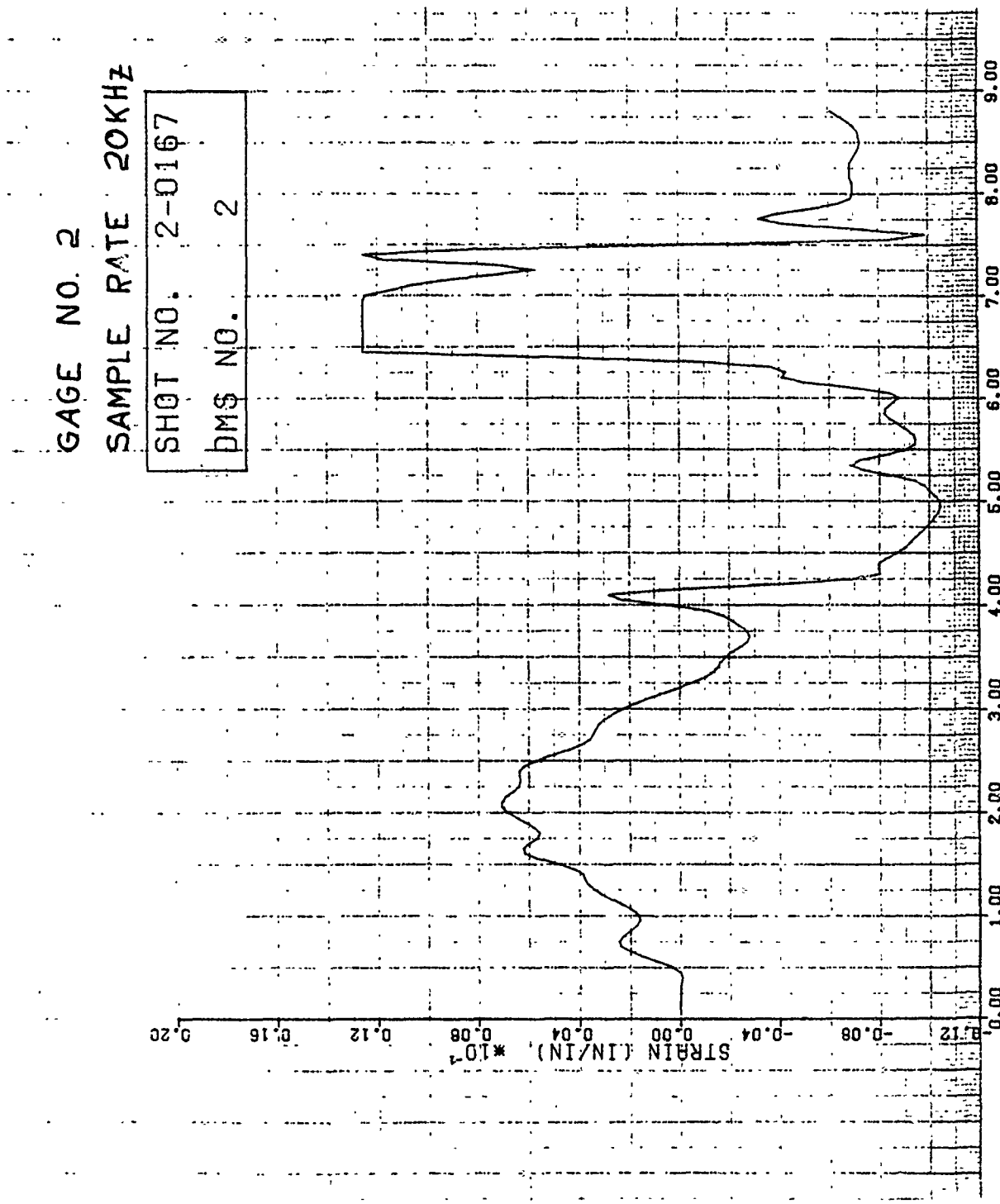

Figure 75. Strain of Shot 2-0167 for Gage #2.

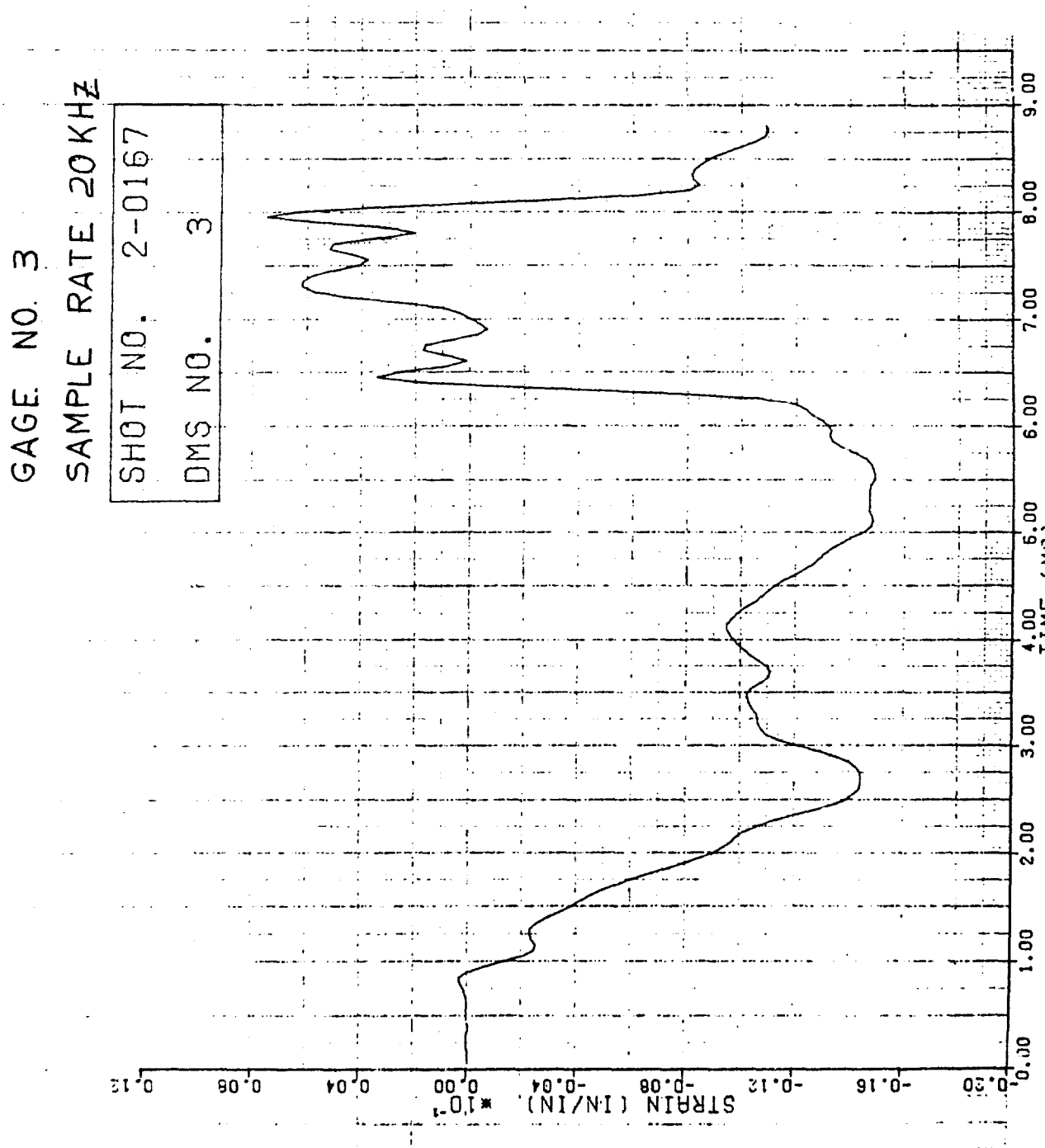

Figure 76. Strain of Shot 2-0167 for Gage #3.

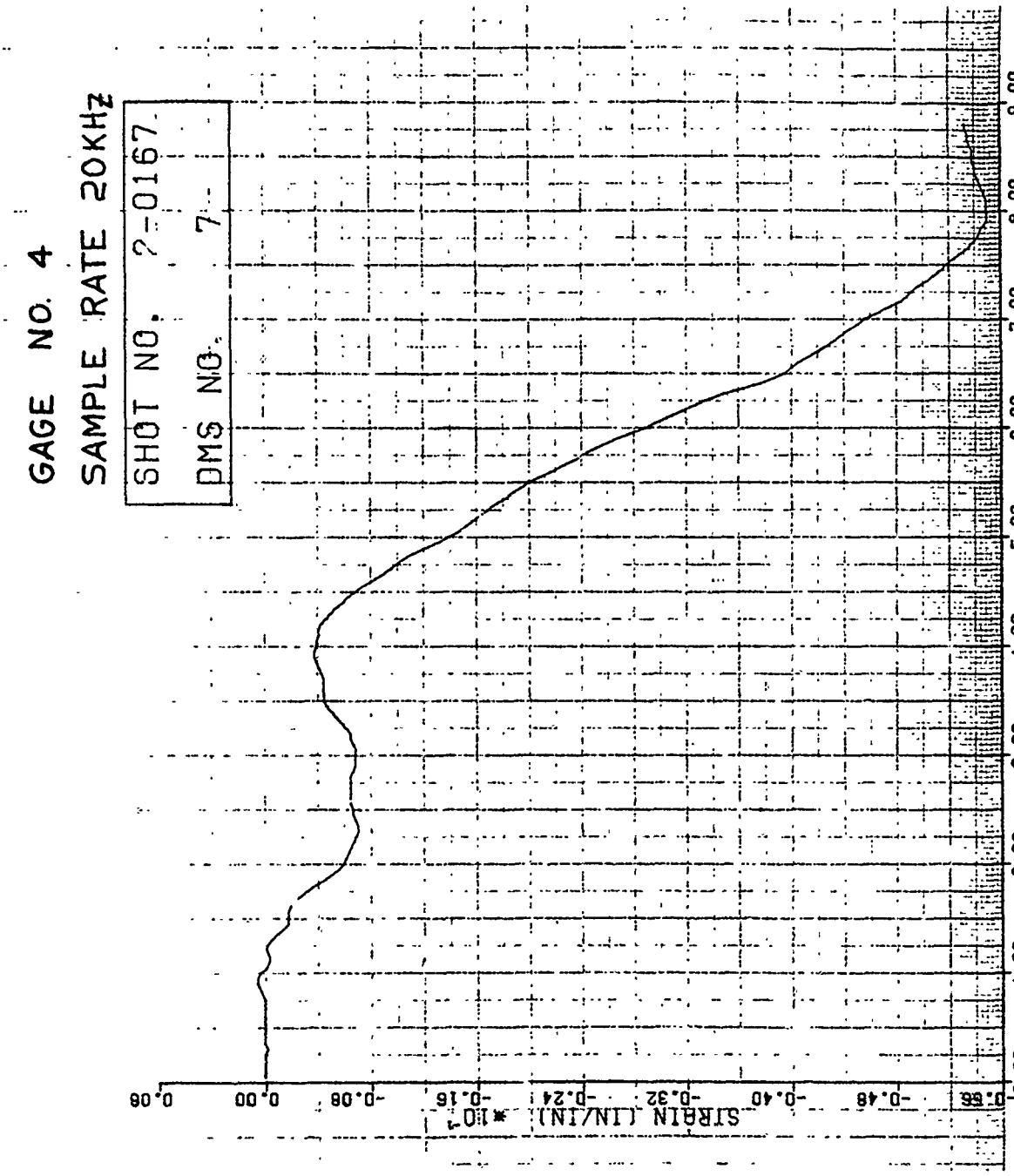

Figure 77. Strain of Shot 2-0167 for Gage #4.

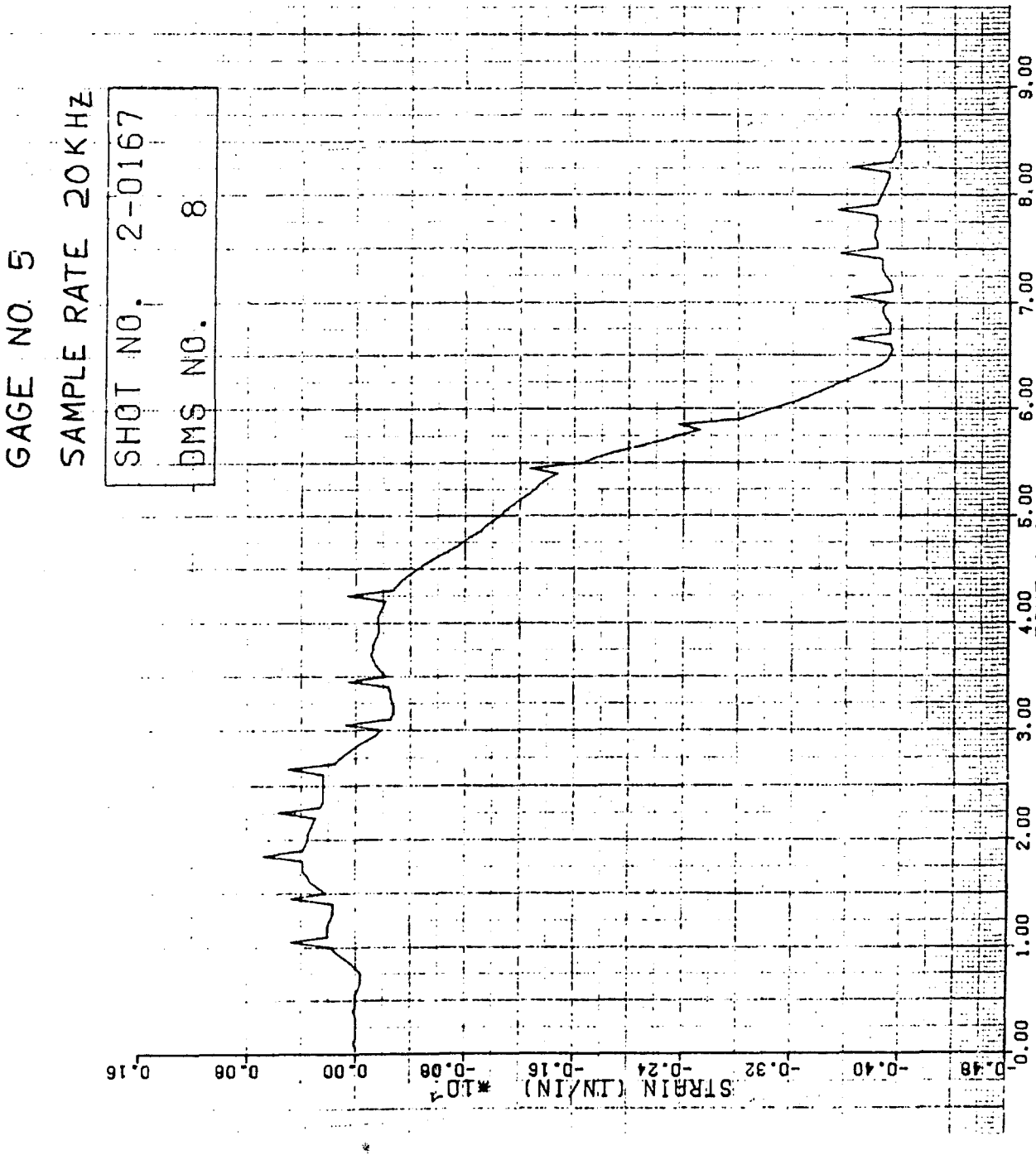

Figure 78. Strain of Shot 2-0167 for Gage #5.

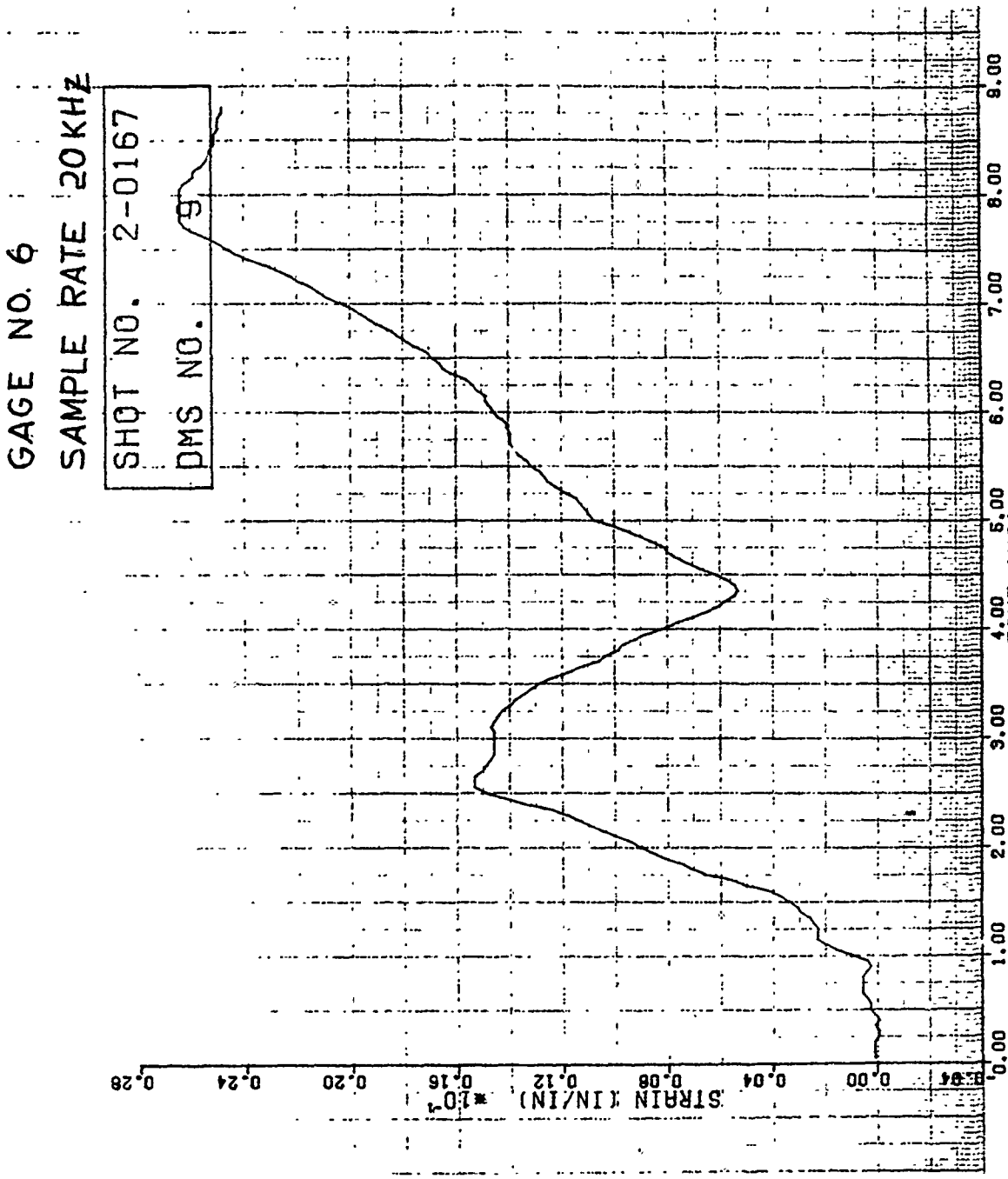

Figure 79. Strain of Shot 2-0167 for Gage #6.

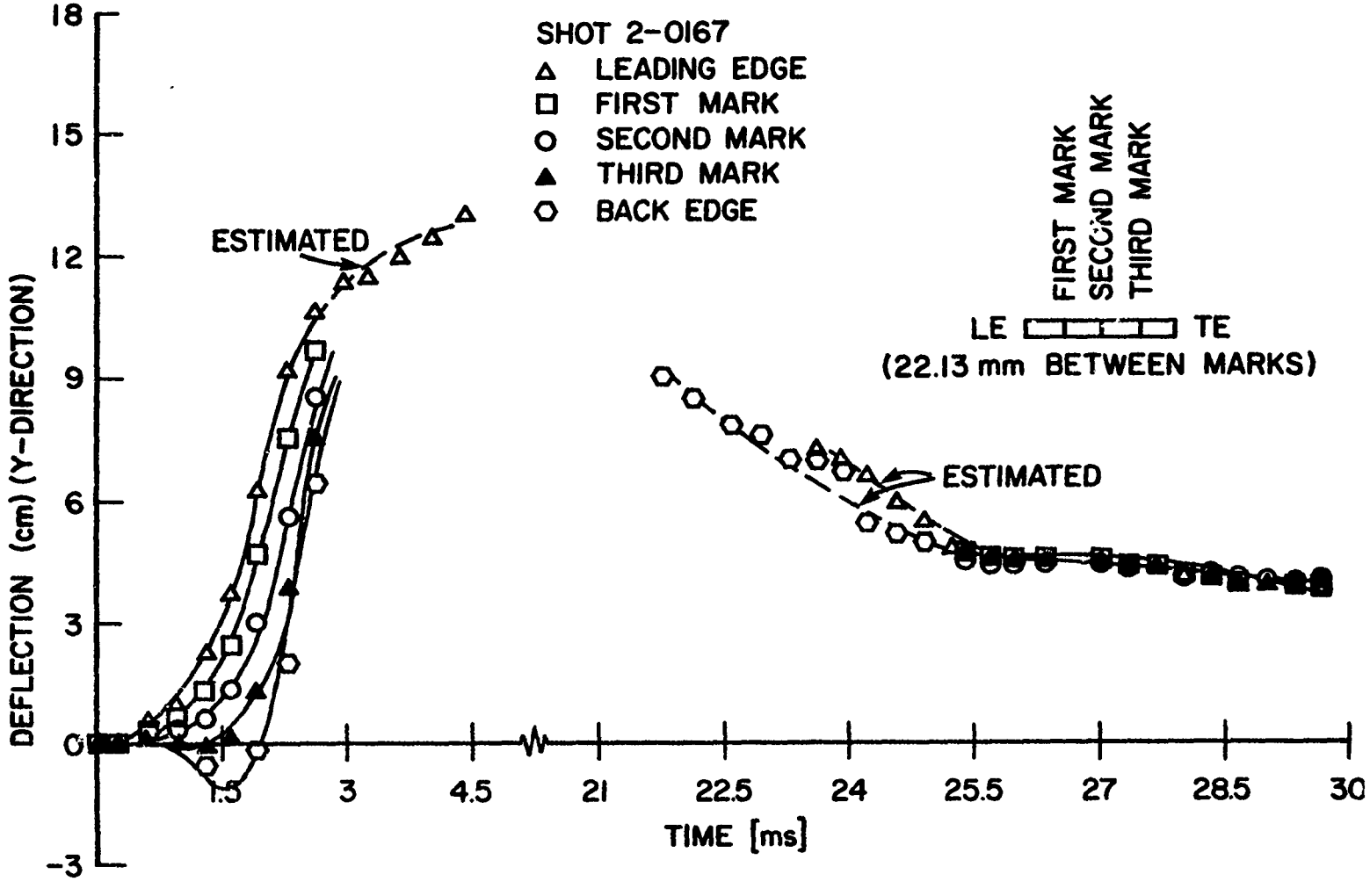

Figure 80. Tip Deflection in "y" Direction for Shot 2-0167.

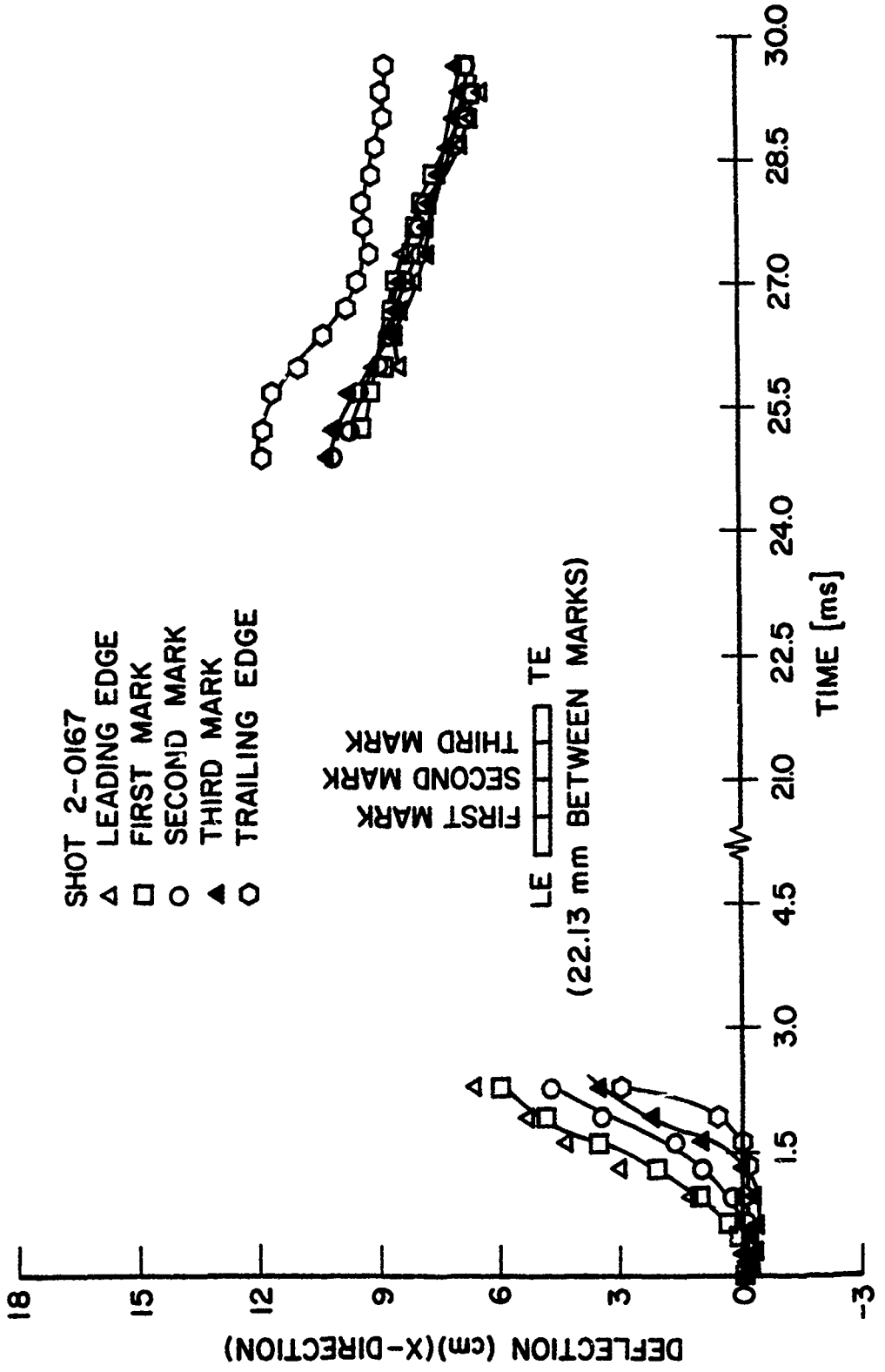

Figure 81. Tip Deflection in "x" Direction for Shot 2-0167.

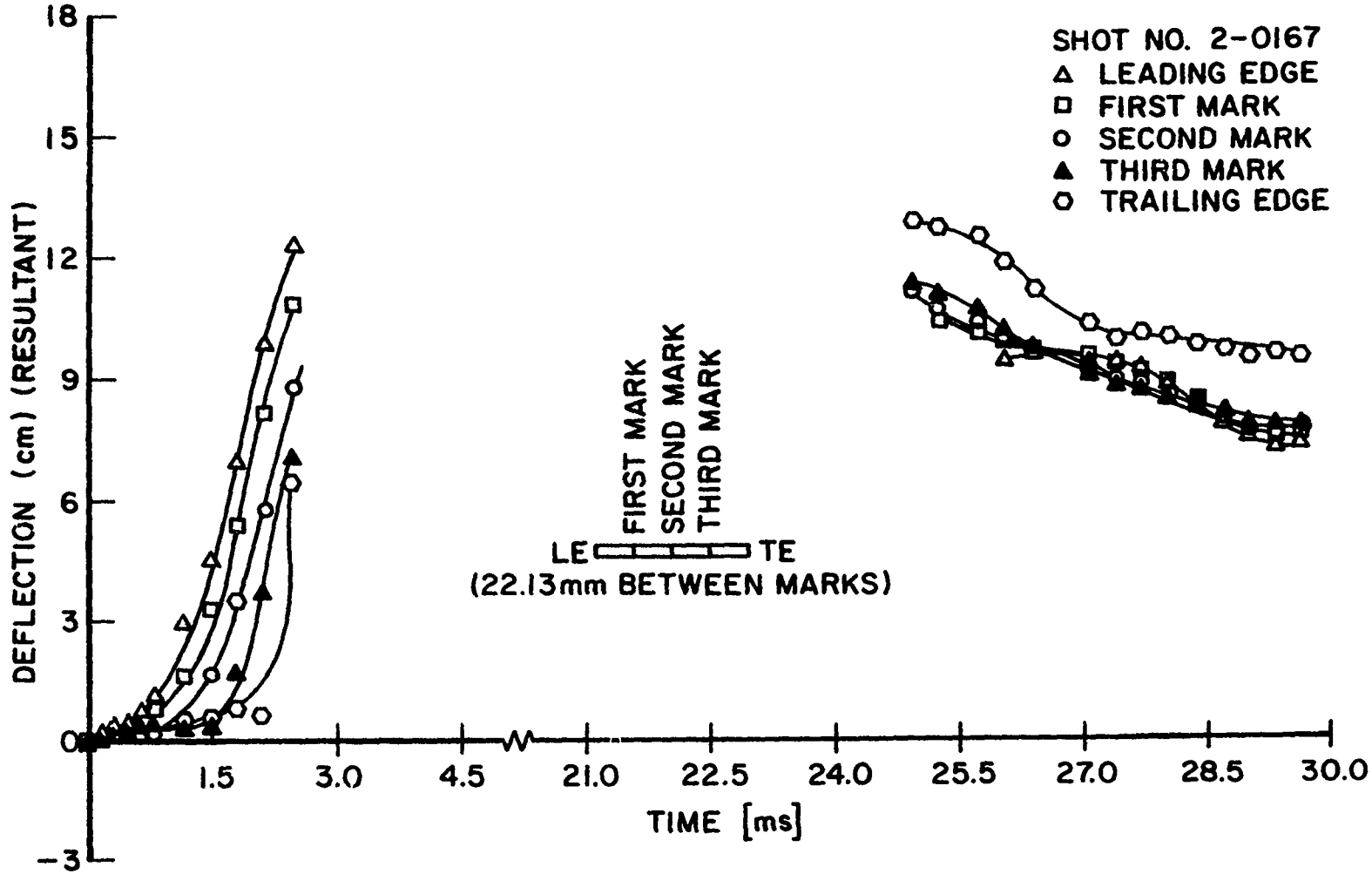

Figure 82. Tip Deflection Resultant for Shot 2-0167.

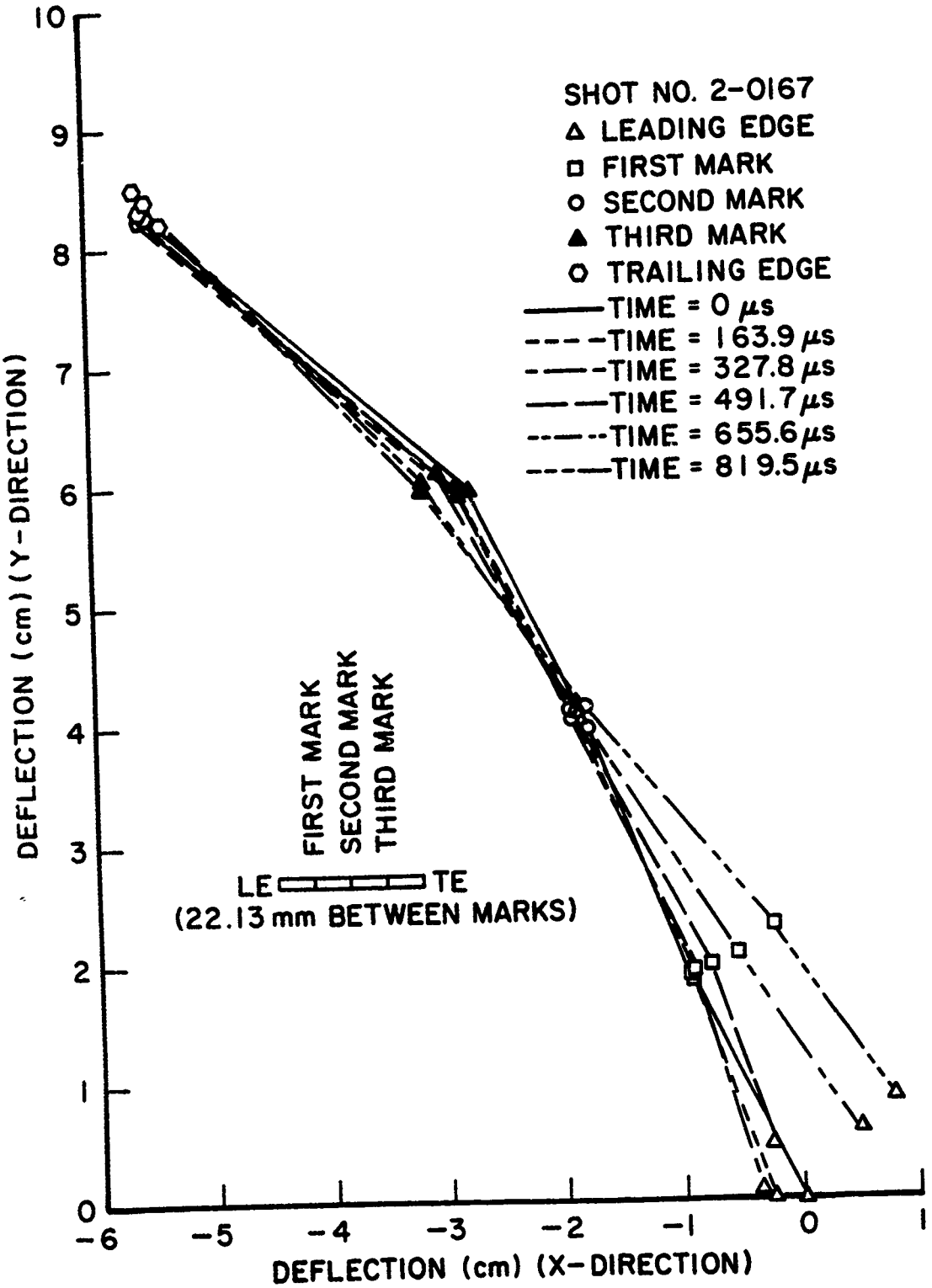

Figure 83. Deflection Plot of "y" Versus "x" Direction of Various Times for Shot 2-0167.

was too low to completely slice the bird upon impact with the specimen. Damage generated on the specimens ranged from no visible damage to the specimen breaking off at its root.

Typical strain gage results are presented in Figures 84 through 89 for Shot 2-0190. Figure 8A of Appendix A gives the strain gage locations for this group of specimens. The impact velocity of Shot 2-0190 was 185 m/s and the impact mass was 101.1 g. No visible damage on the specimen resulted from the impact. Dynamic displacement versus time plots of the "y" and "x" directions are presented in Figures 90 and 91, respectively. Figures 20B and 21B give photographs of the damage for the bird impacts of Shos 2-0180 and 2-0192, respectively.

3.1.1.10 Impact Results for Group 10 Specimens

The Group 10 titanium specimens with the same geometry as for the Group 9 specimens were impacted by the small 85 g (3 ounce) size artificial bird. The impacts were center impacts at the 70 percent span location at a normal impact angle and at velocities ranging from 29 to 203 m/s. In this group, the specimen tip was also restrained as well as the root. No visible damage resulted from the 29 m/s impact; however, the most severe damage occurred in the 203 m/s impact. In this case, the tip came loose from its mount and the tip plastic deflection was 17.59 cm on the trailing edge side and 17.72 cm on the leading edge side.

Typical strain results for this group of specimens are given in Figures 92 through 97 for Shot 2-0177. The impact velocity for this impact was 127 m/s. The damage was in the form of plastic deformation at the impact site with a bow of 0.89 cm on the trailing edge side and 0.95 cm on the leading edge side. No dynamic displacement data was calculated for this impact.

Figures 22B and 23B show the damage received from Shots 2-0177 and 2-0179, respectively.

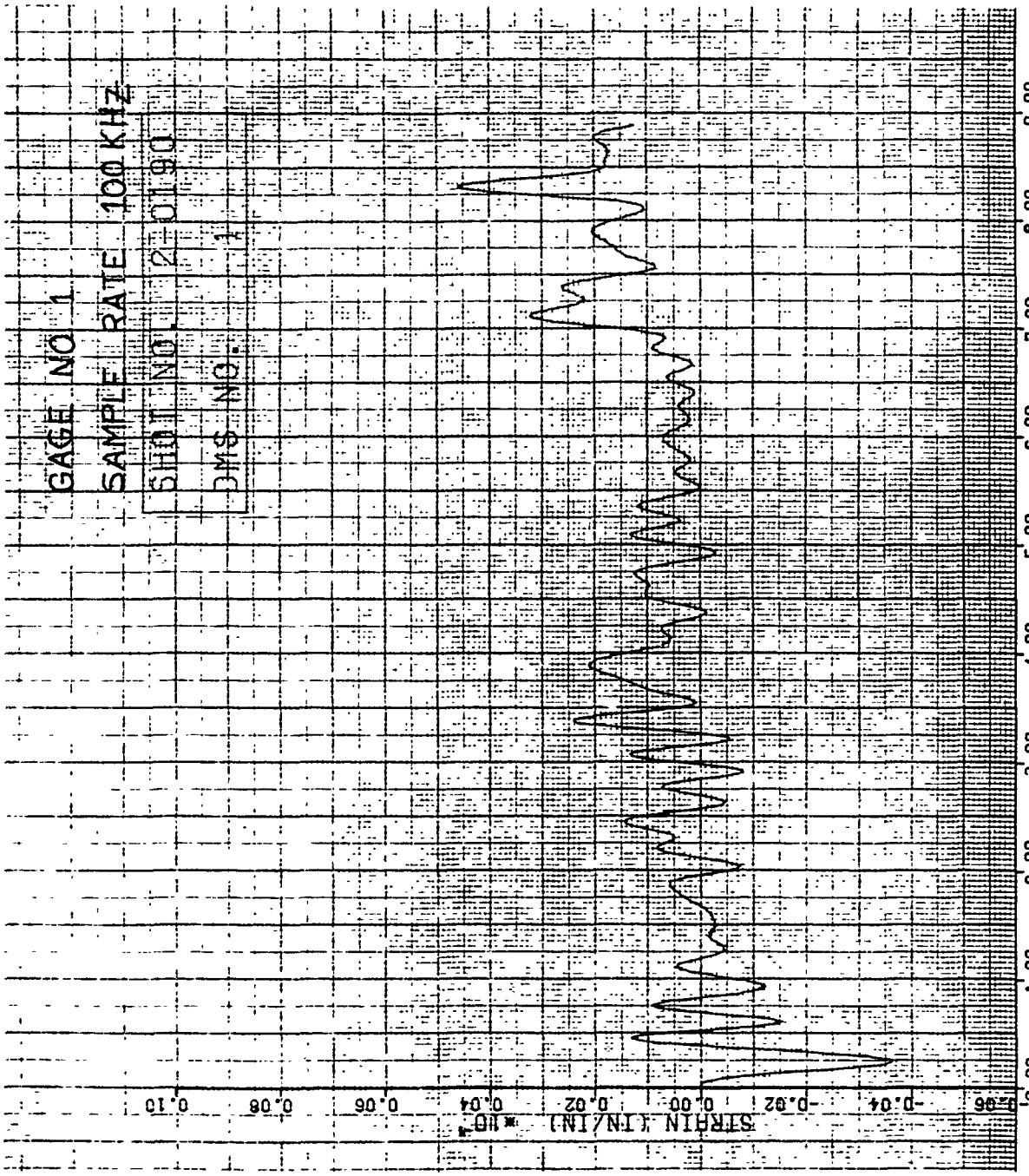

Figure 84. Strain of Shot 2-0190 for Gage #1.

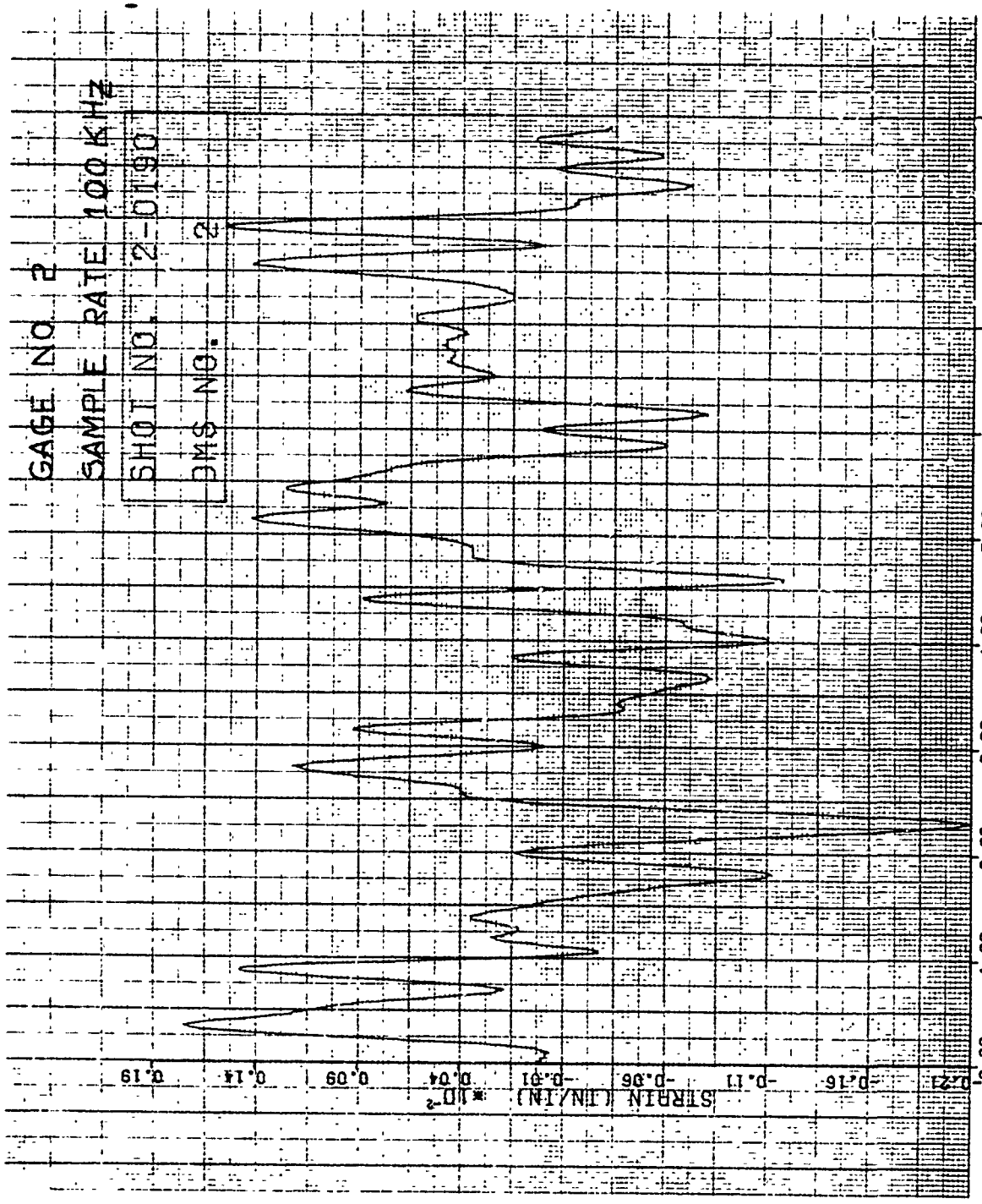

Figure 85. Strain of Shot 2-0190 for Gage #2.

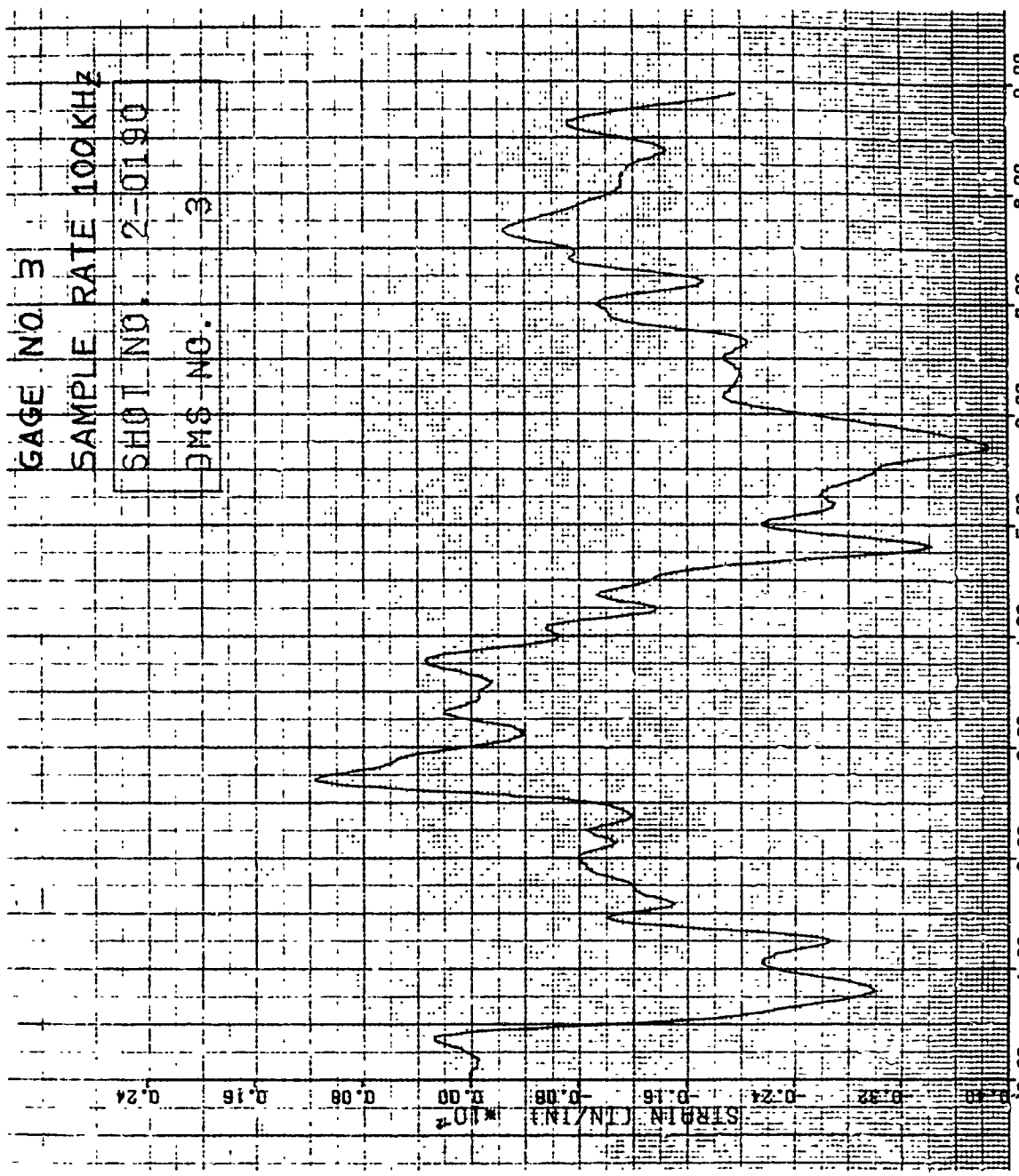

Figure 86. Strain of Shot 2-0190 for Gage #3.

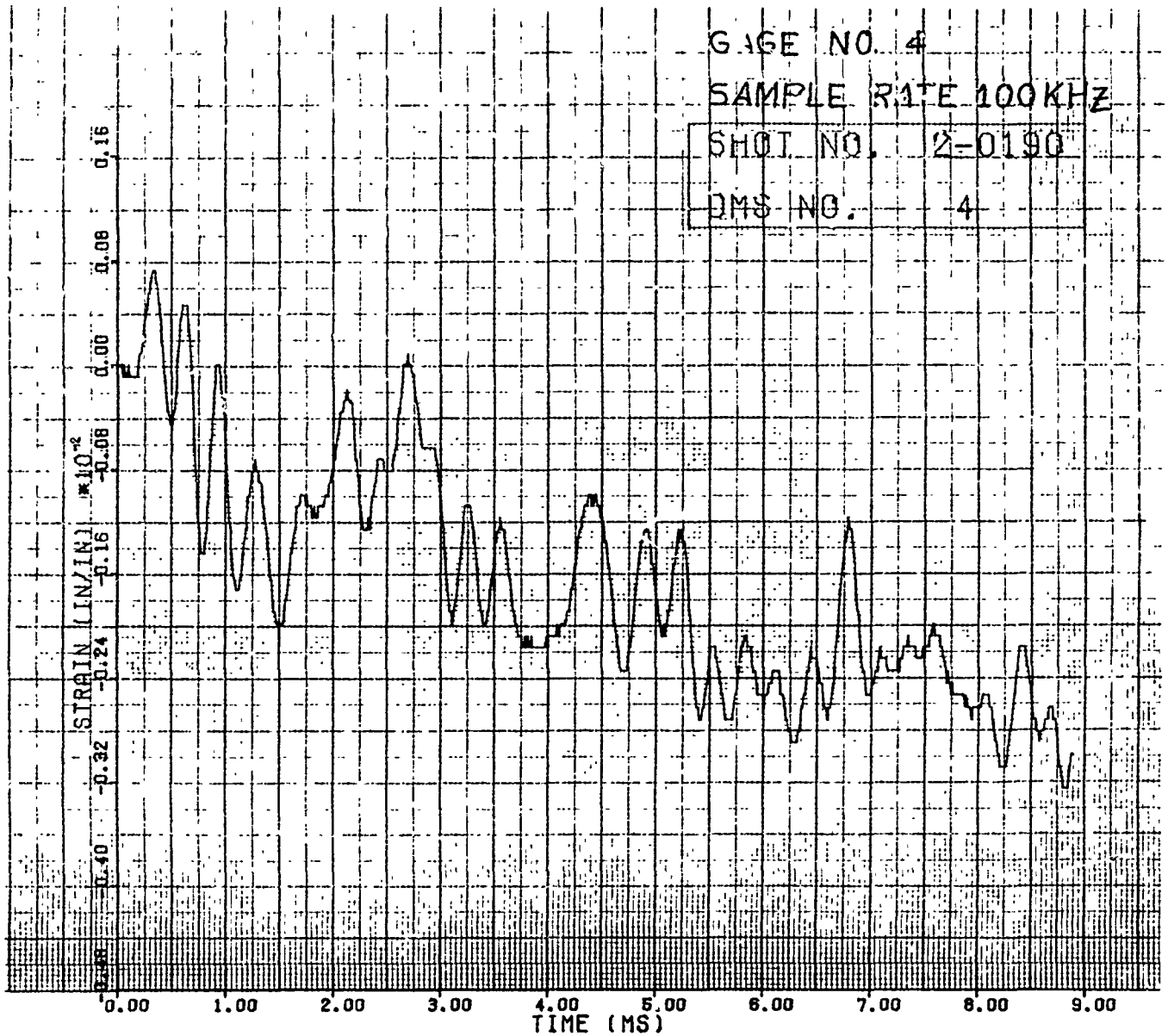

Figure 87. Strain of Shot 2-0190 for Gage #4.

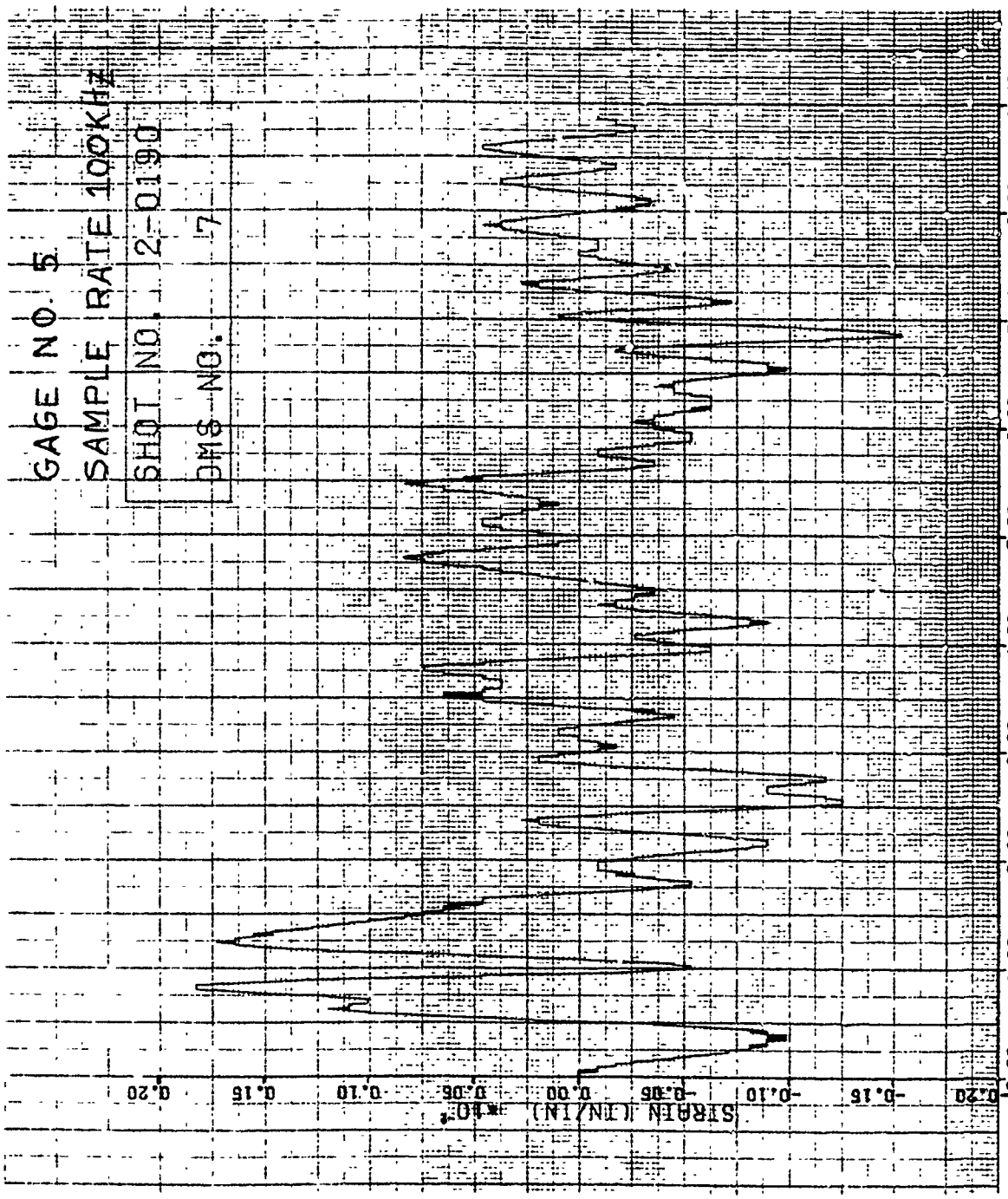

Figure 88. Strain of Shot 2-0190 for Gage #5.

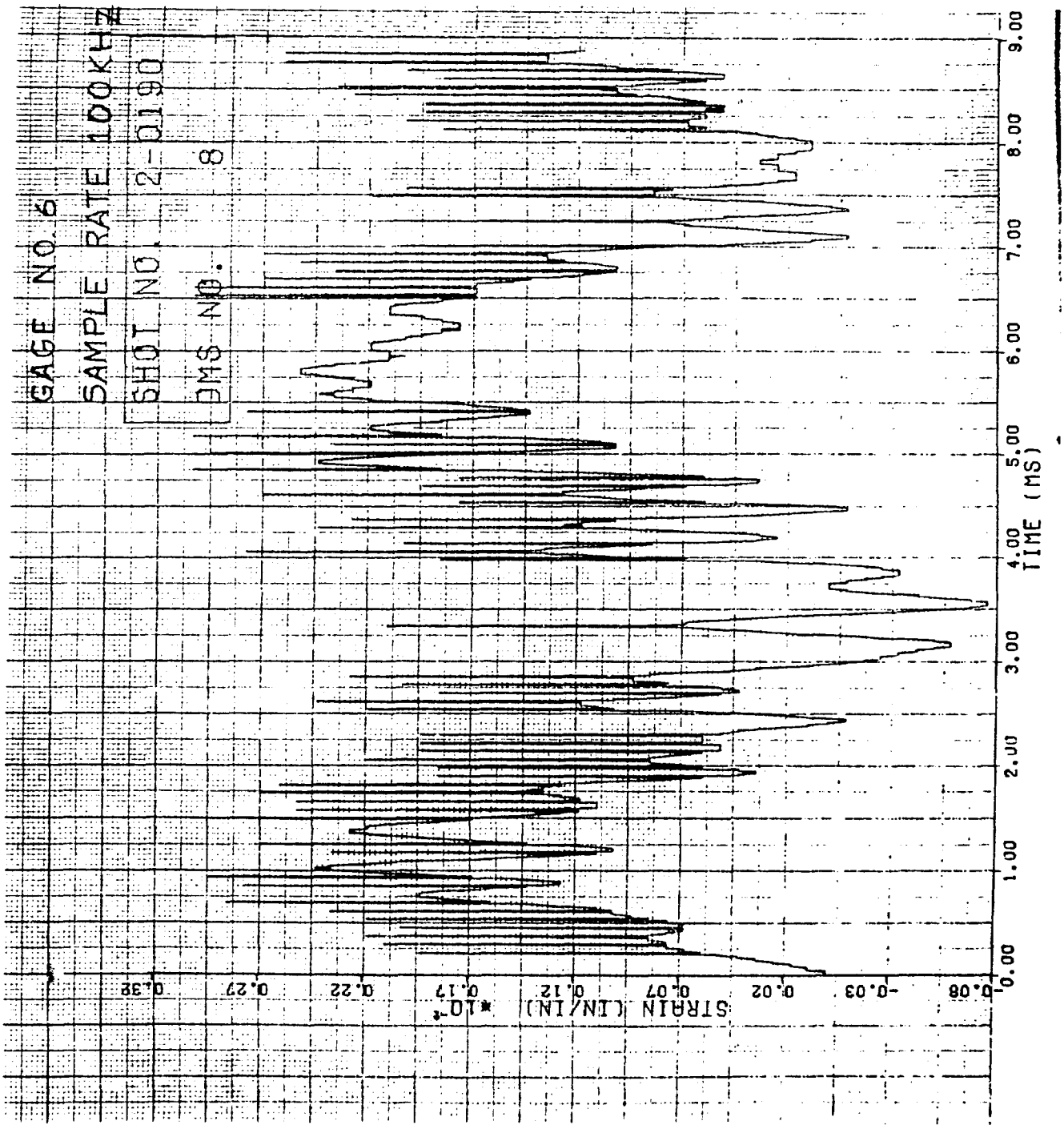

Figure 89. Strain of Shot 2-0190 for Gage #6.

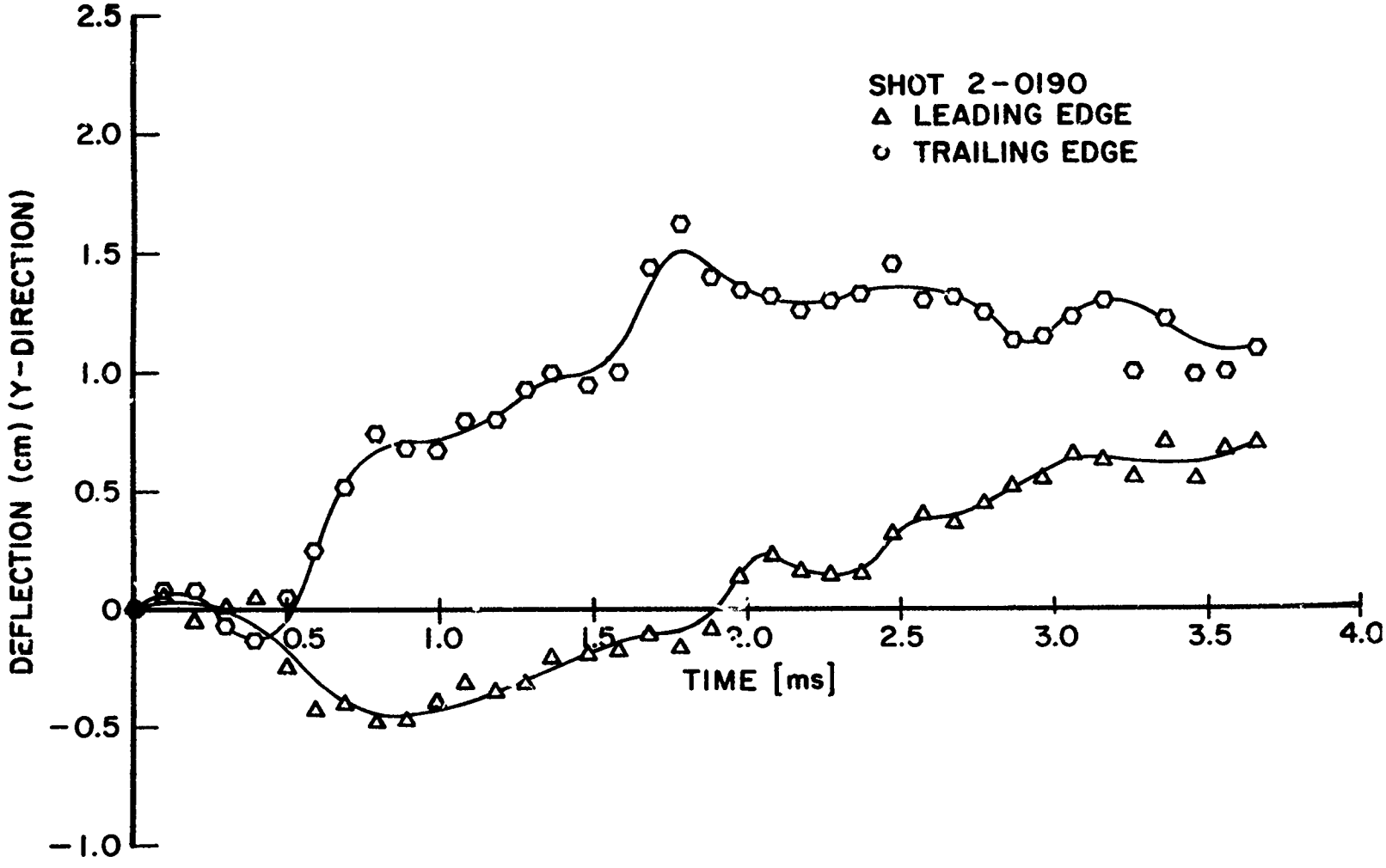

Figure 90. Tip Deflection in "y" Direction for Shot 2-0190.

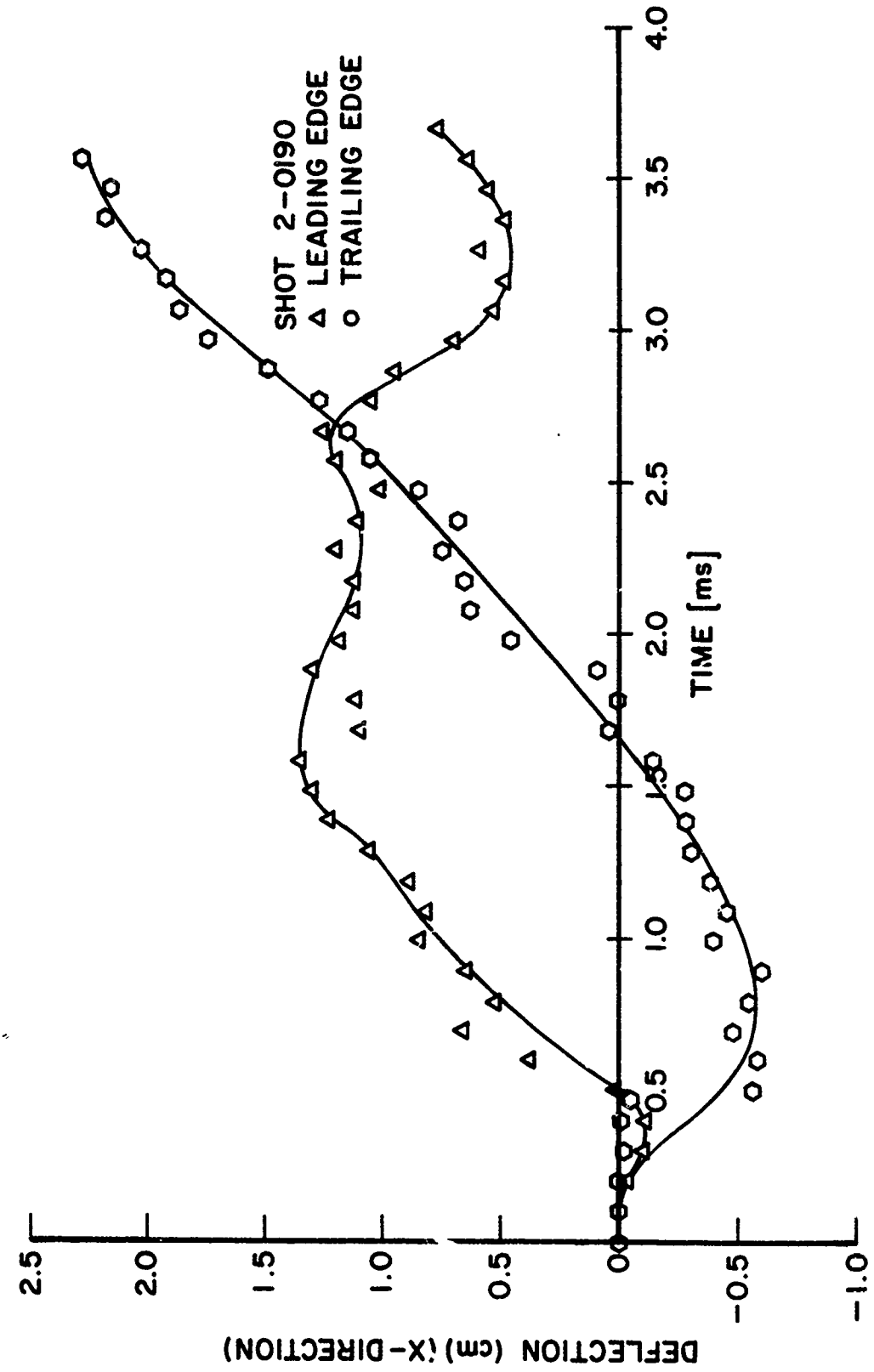

Figure 91. Tip Deflection in "x" Direction for Shot 2-0190.

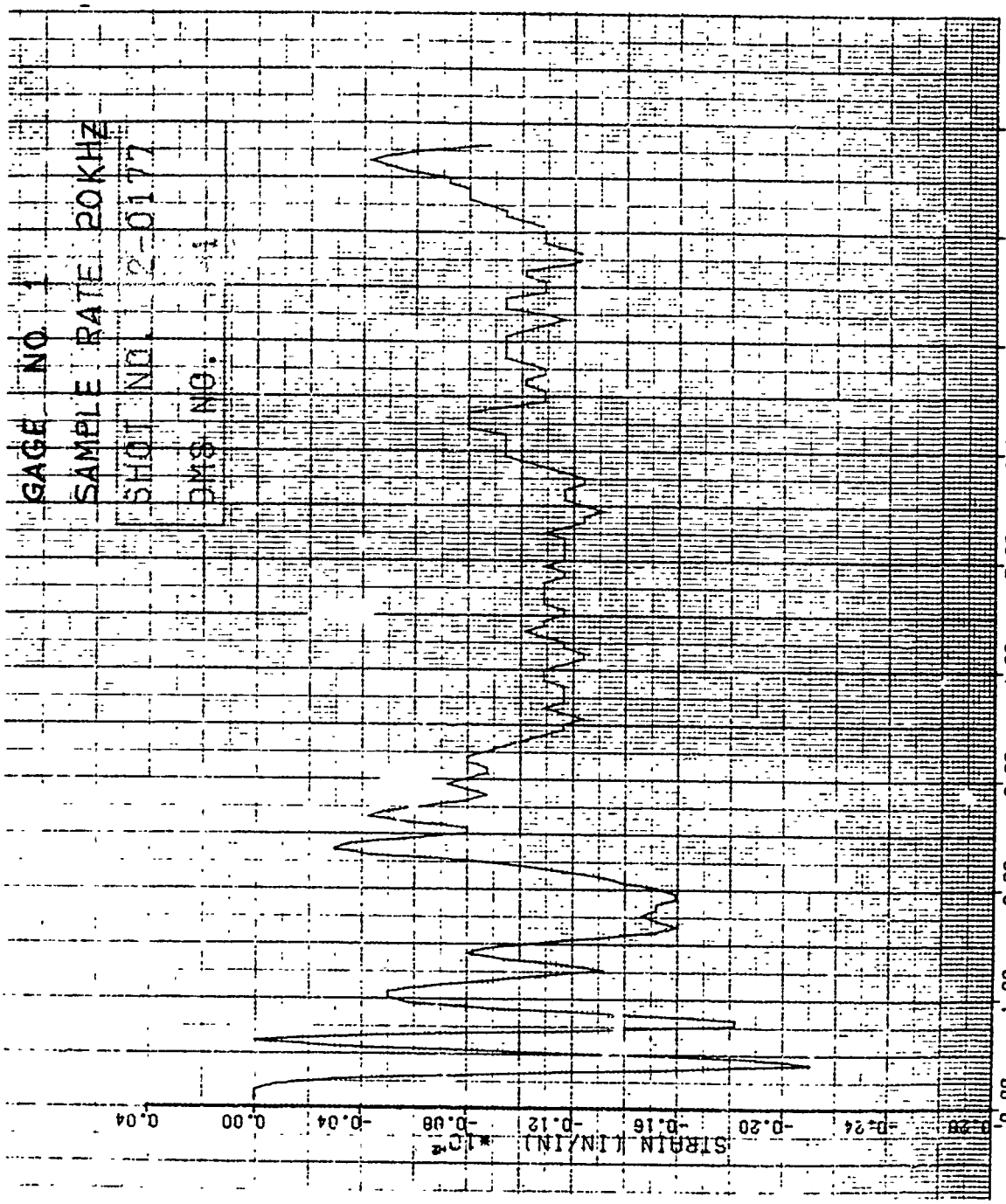

Figure 92. Strain of Shot 2-0177 for Gage #1.

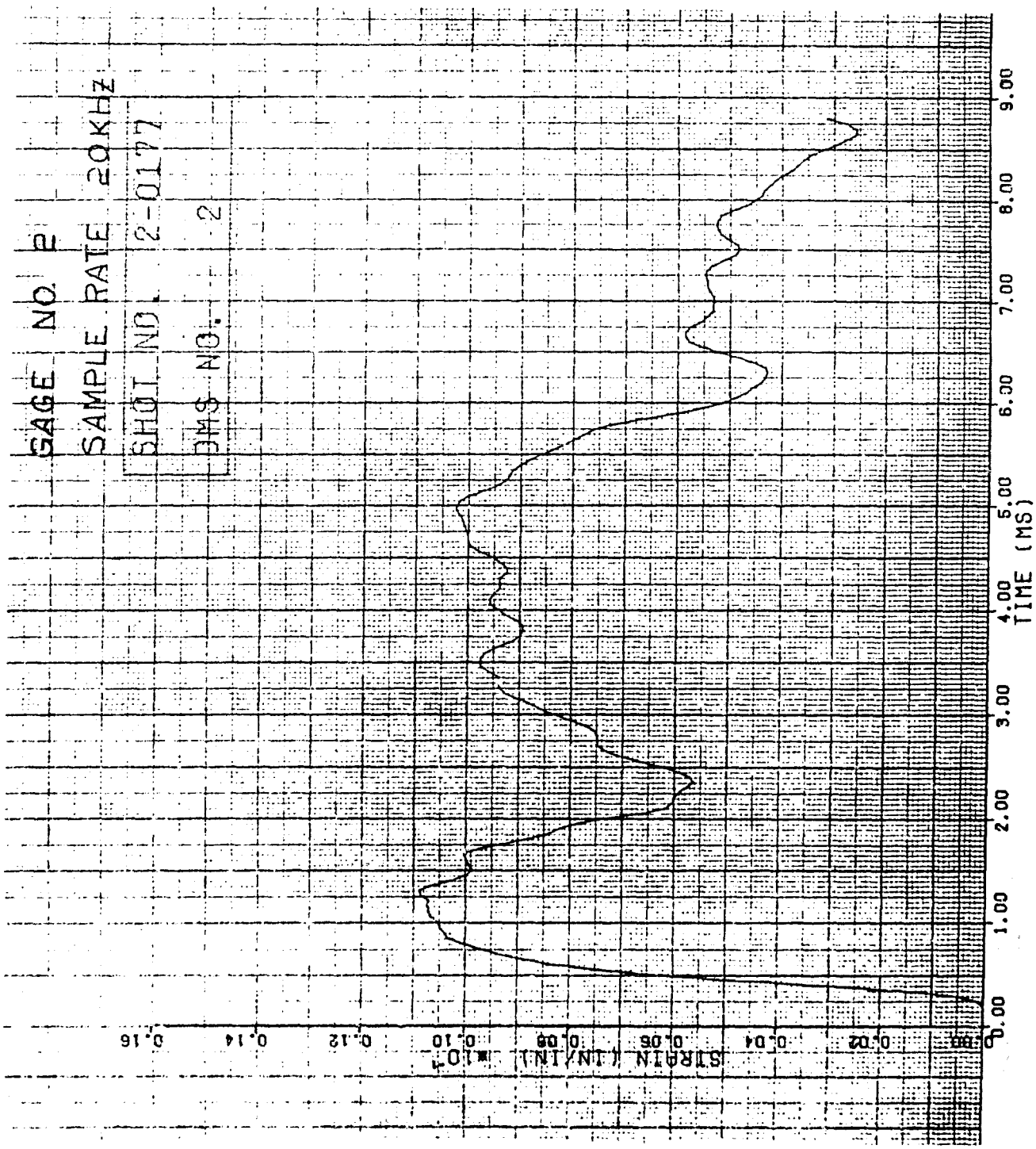

Figure 93. Strain of Shot 2-0177 for Gage #2.

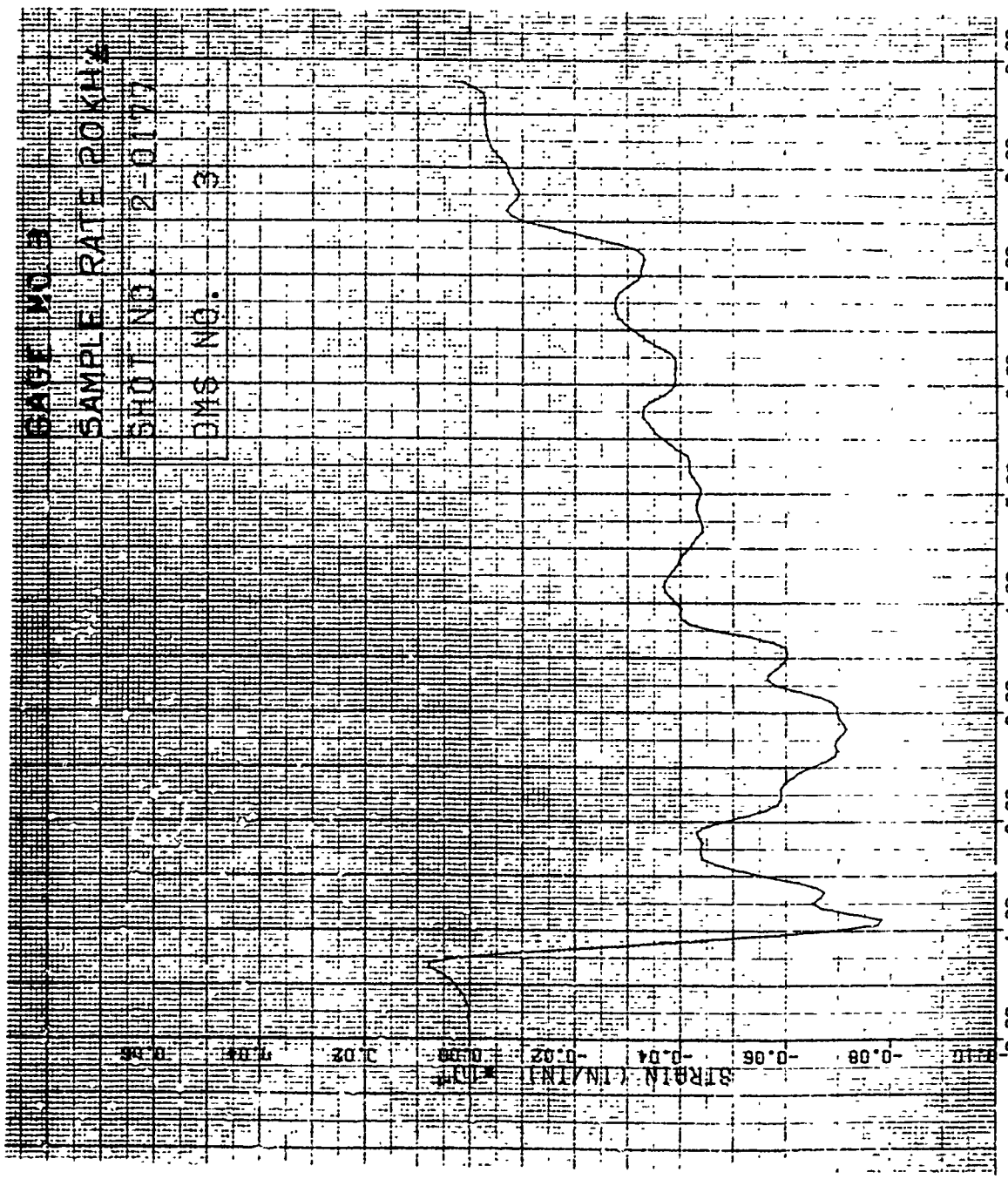

Figure 94. Strain of Shot 2-0177 for Gage #3.

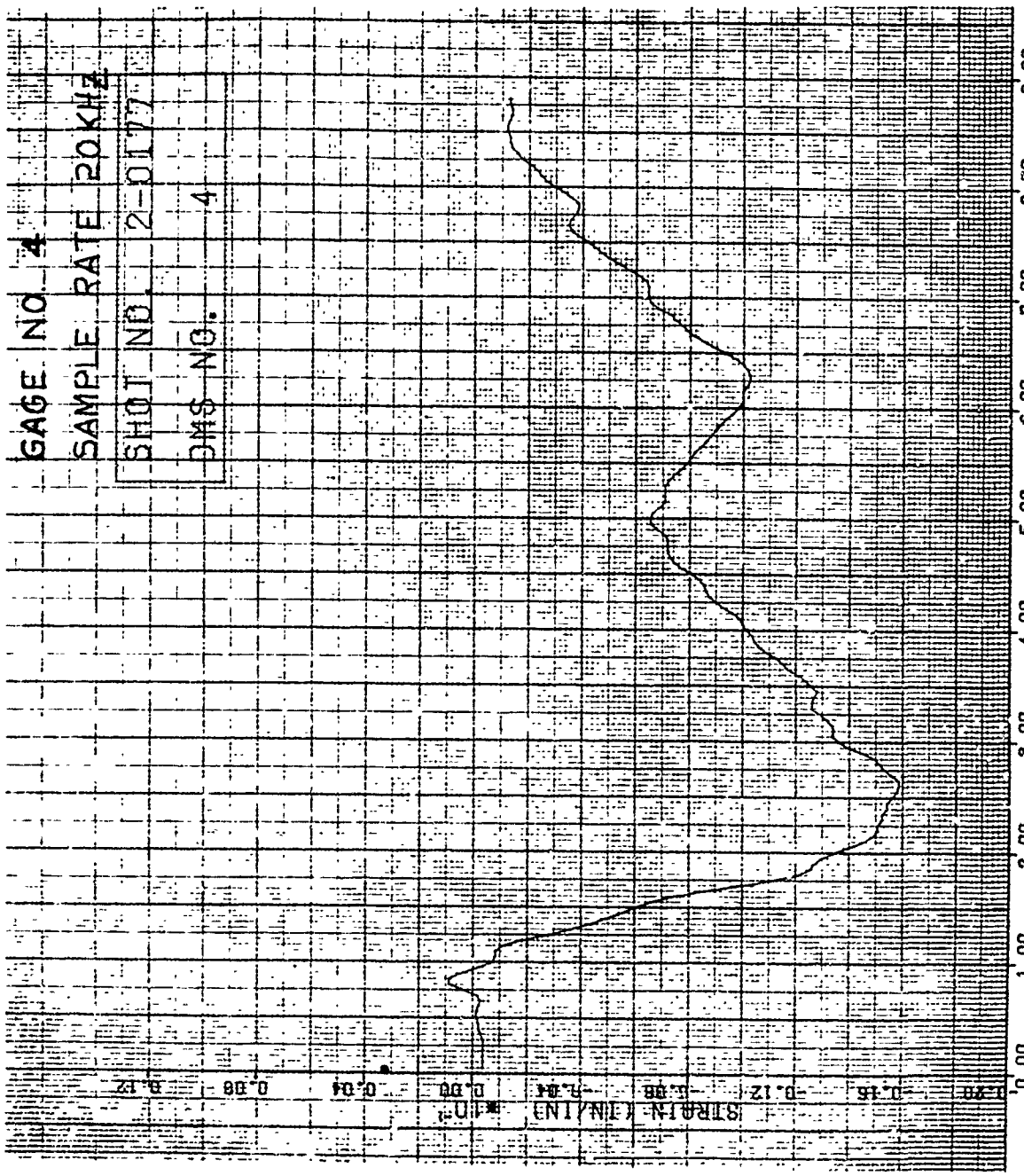

Figure 95. Strain of Shot 2-0177 for Gage #4.

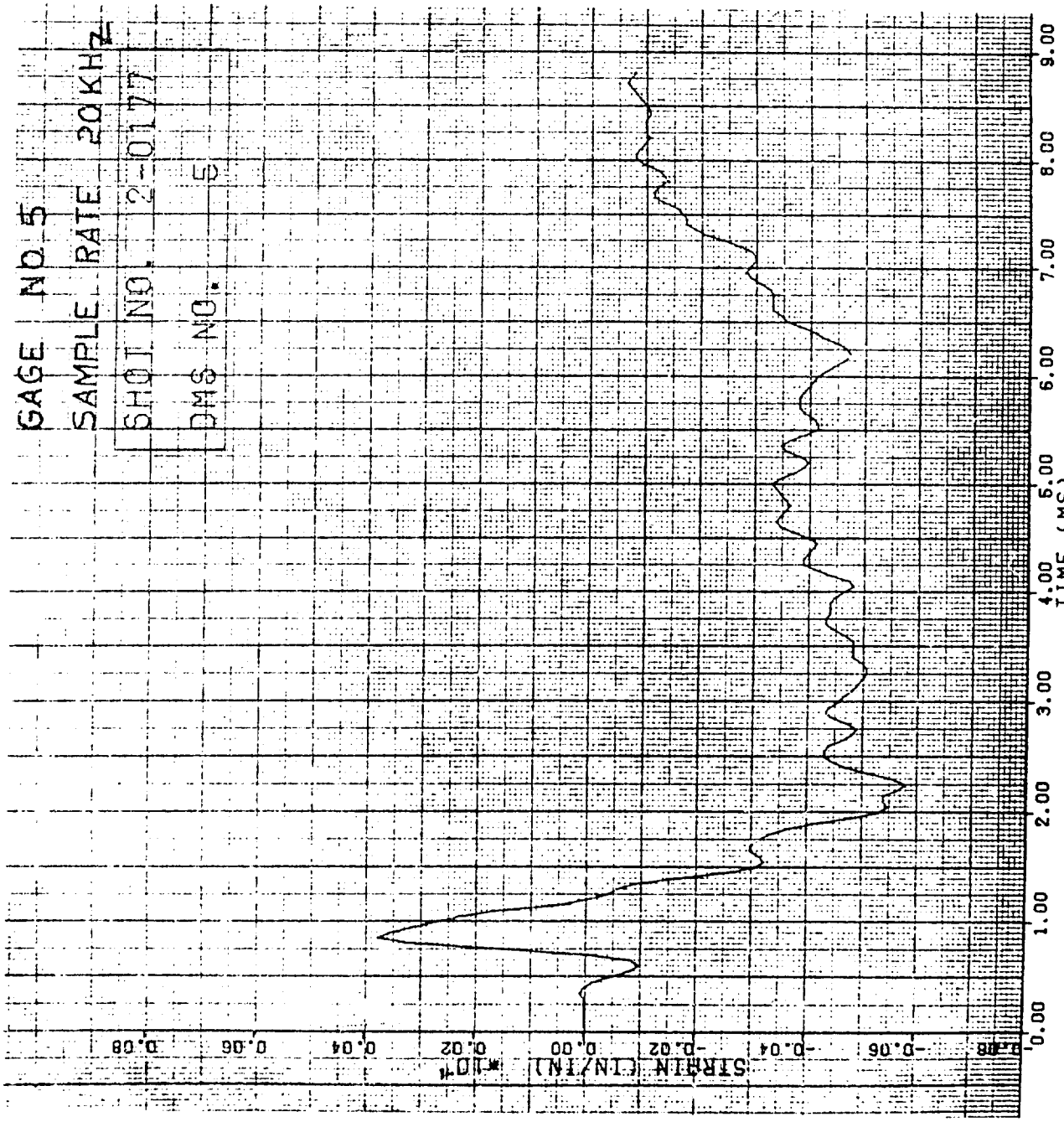

Figure 96. Strain of Shot 2-0177 for Gage #5.

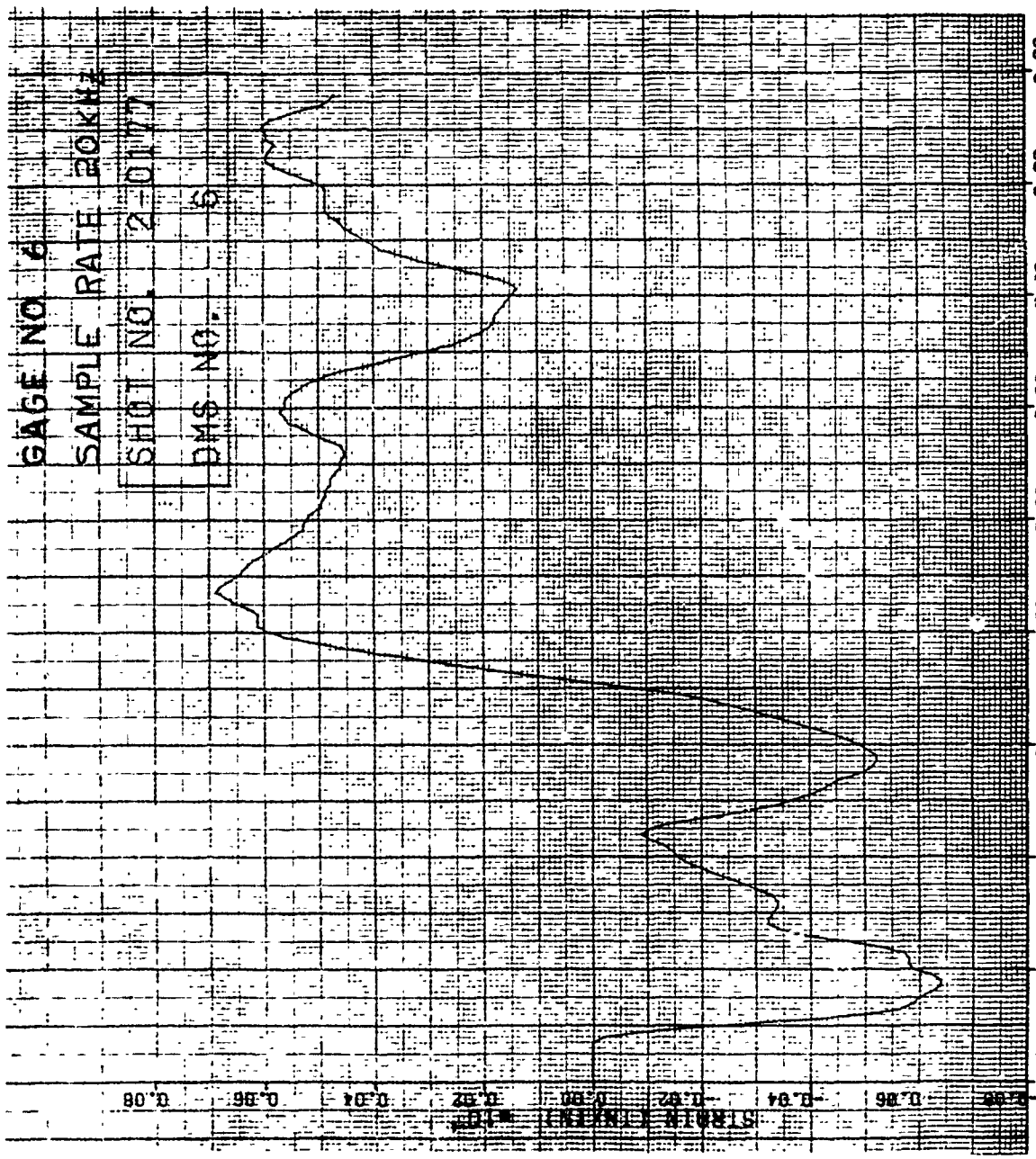

Figure 97. Strain of Shot 2-0177 for Gage #6.

3.1.1.11 Impact Results for Group 11 Specimens

Two Group 11 stainless steel flat plate specimens with a blade-type aspect ratio were impacted by the medium 680 g (1.5 pound) size substitute bird. The impacts were edge (slicing) impacts at the 70 percent span location at an impact angle of 36.4 degrees. An impact velocity of 102 m/s and impact mass of 265.7 g caused the specimen to rock back in the mount. The damage for this impact was bending and plastic deformation at the specimen root with a plastic tip deflection of 17.24 cm on the leading edge and 16.26 cm on the trailing edge.

The second impact was at an impact velocity 54 m/s with an impact mass of 253.8 g. Again, bending and plastic deformation resulted from the impact. The plastic tip deflection measured for this specimen was 7.14 cm.

Typical strain results for these specimens are given in Figures 98 through 103 for Shot 2-0158 which was at the velocity of 54 m/s. Figure 12A of Appendix A gives the strain gage locations for this group. The damage for this impact was given in the previous paragraph. No dynamic displacement data was calculated for this impact.

Figures 24B and 25 B show the damage generated on the specimens of Shots 2-0157 and 2-0158.

3.1.1.12 Impact Results for Group 12 Specimens

Two Group 12 stainless steel specimen impacts were conducted using the medium 680 g (1.5 pound) size artificial bird as the impactor. Again, the impacts were edge (slicing) impacts at the 70 percent span location at an impact angle of 36.4 degrees. One velocity was at 48 m/s and the impact mass was about 300.0 g. No visible damage was observed on the specimen for this impact.

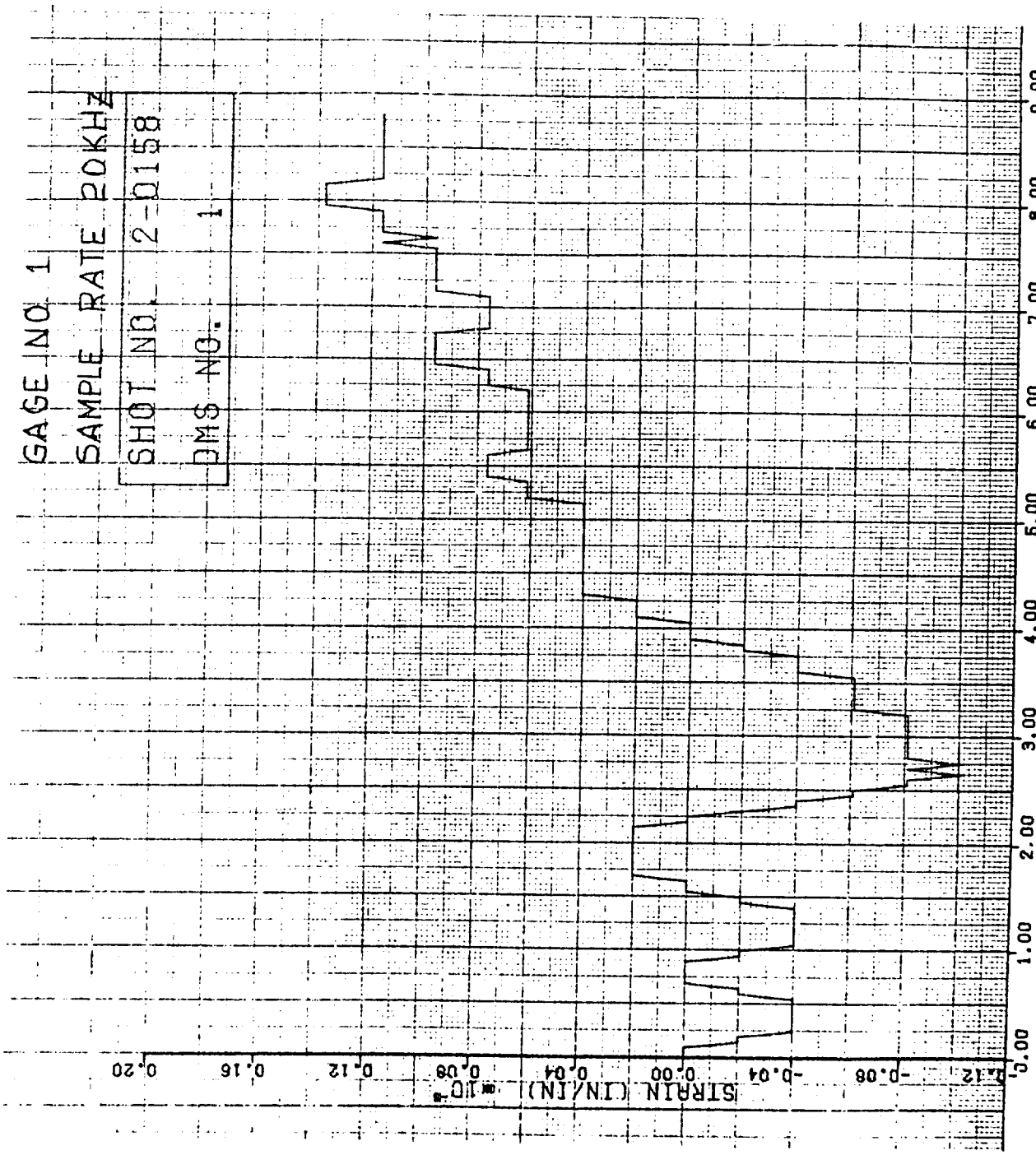

Figure 98. Strain of Shot 2-0158 for Gage #1.

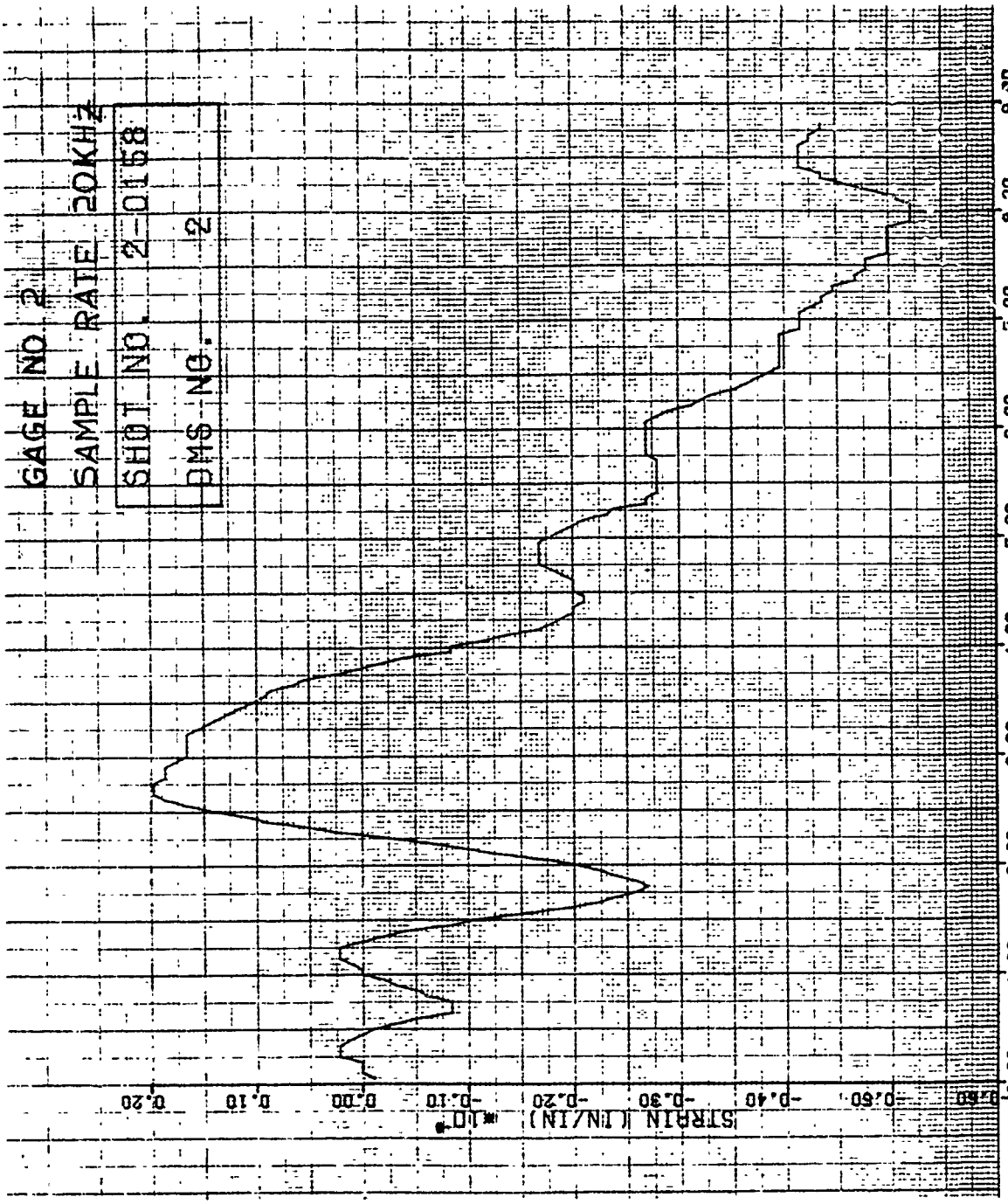

Figure 99. Strain of Shot 2-0158 for Gage #2.

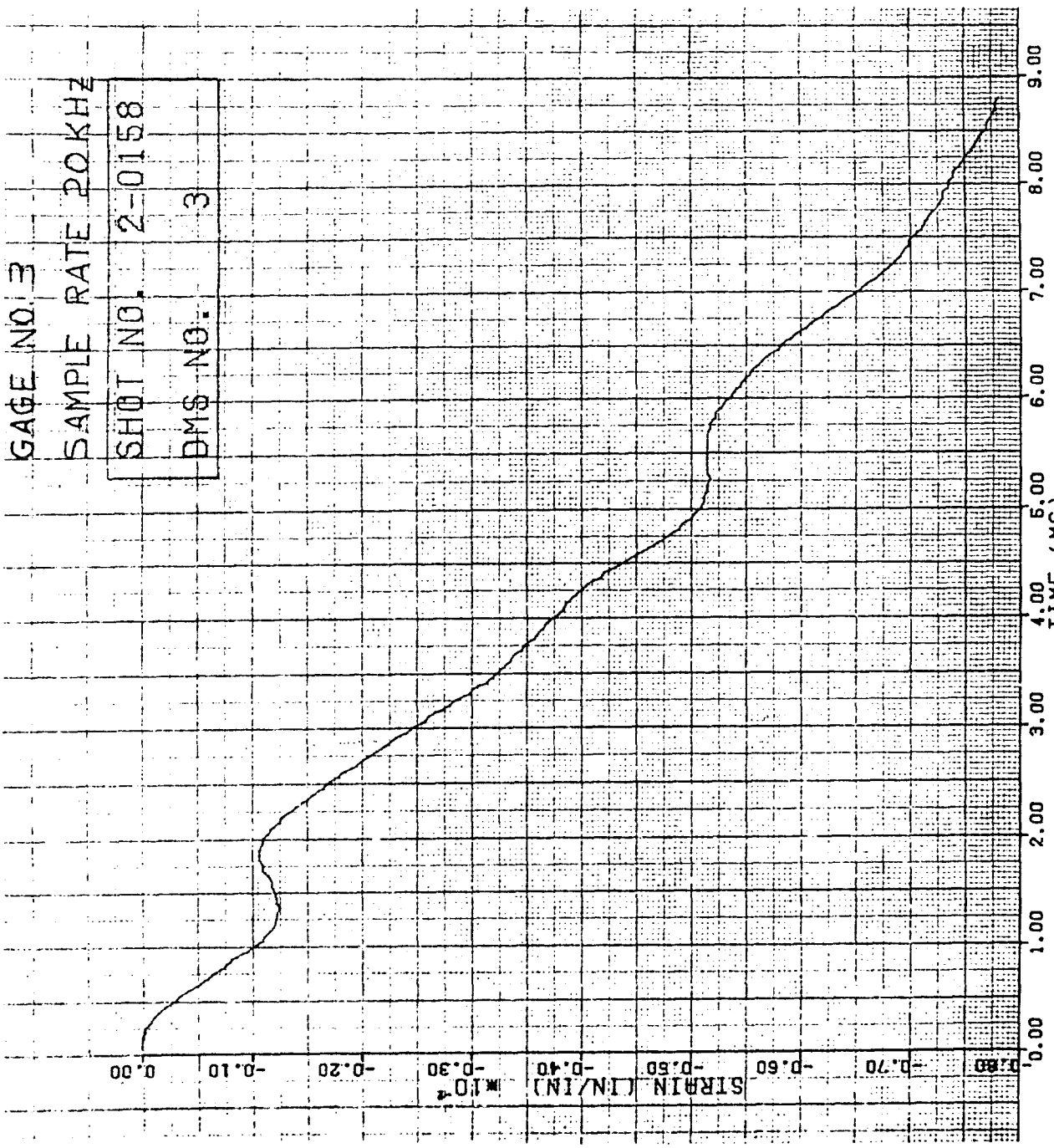

Figure 100. Strain of Shot 2-0158 for Gage #3.

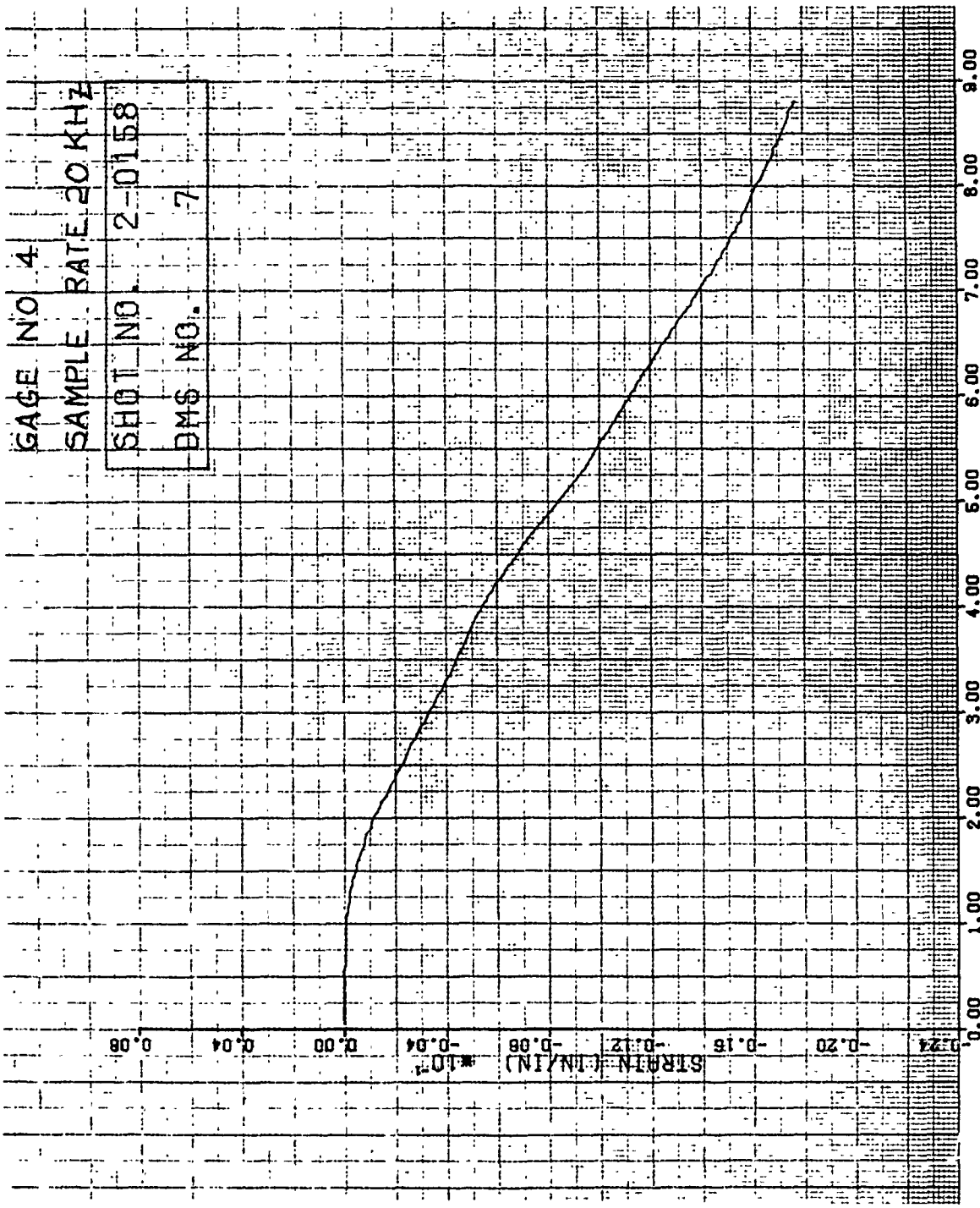

Figure 101. Strain of Shot 2-0158 for Gage #4.

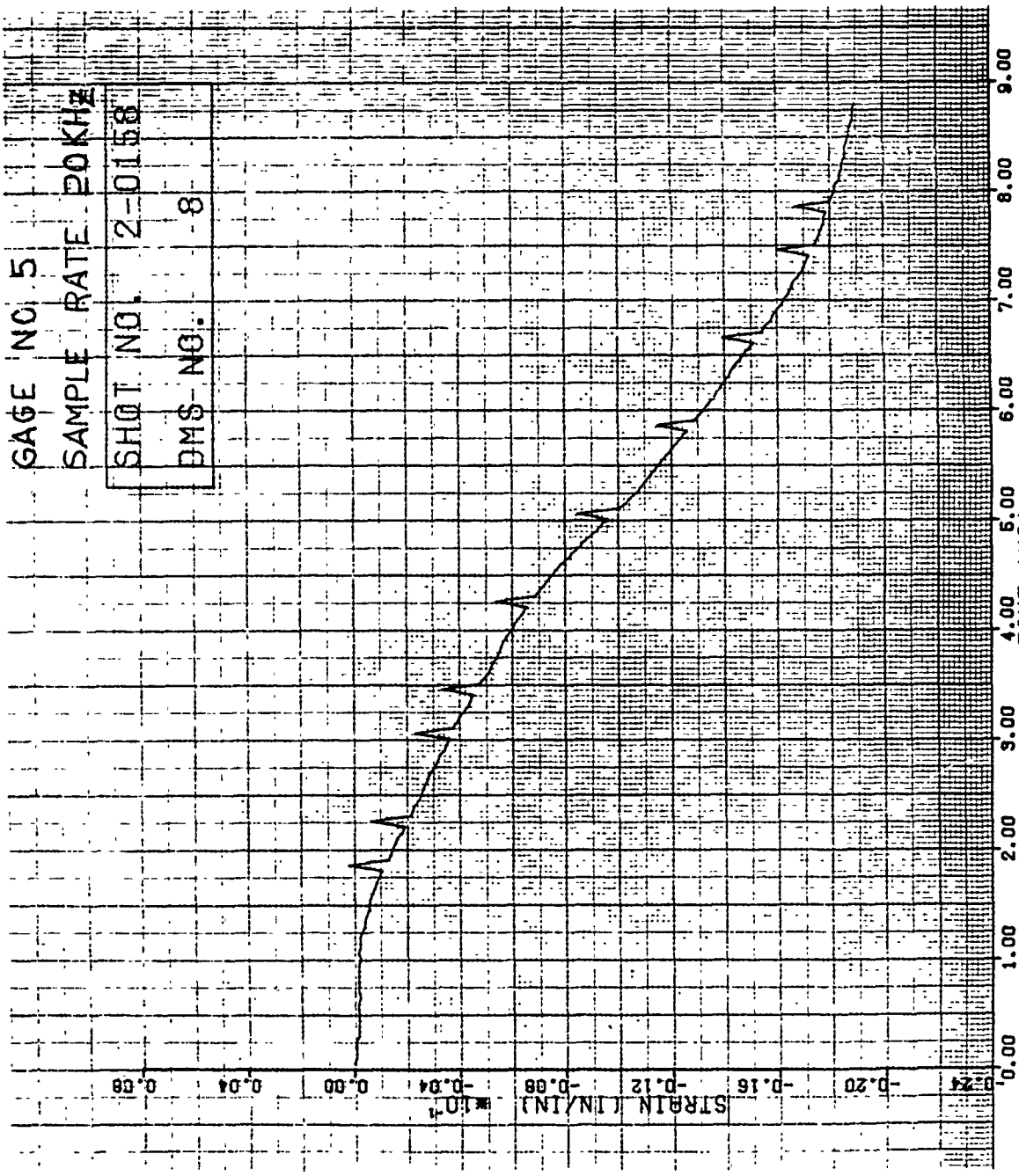

Figure 102. Strain of Shot 2-0158 for Gage #5.

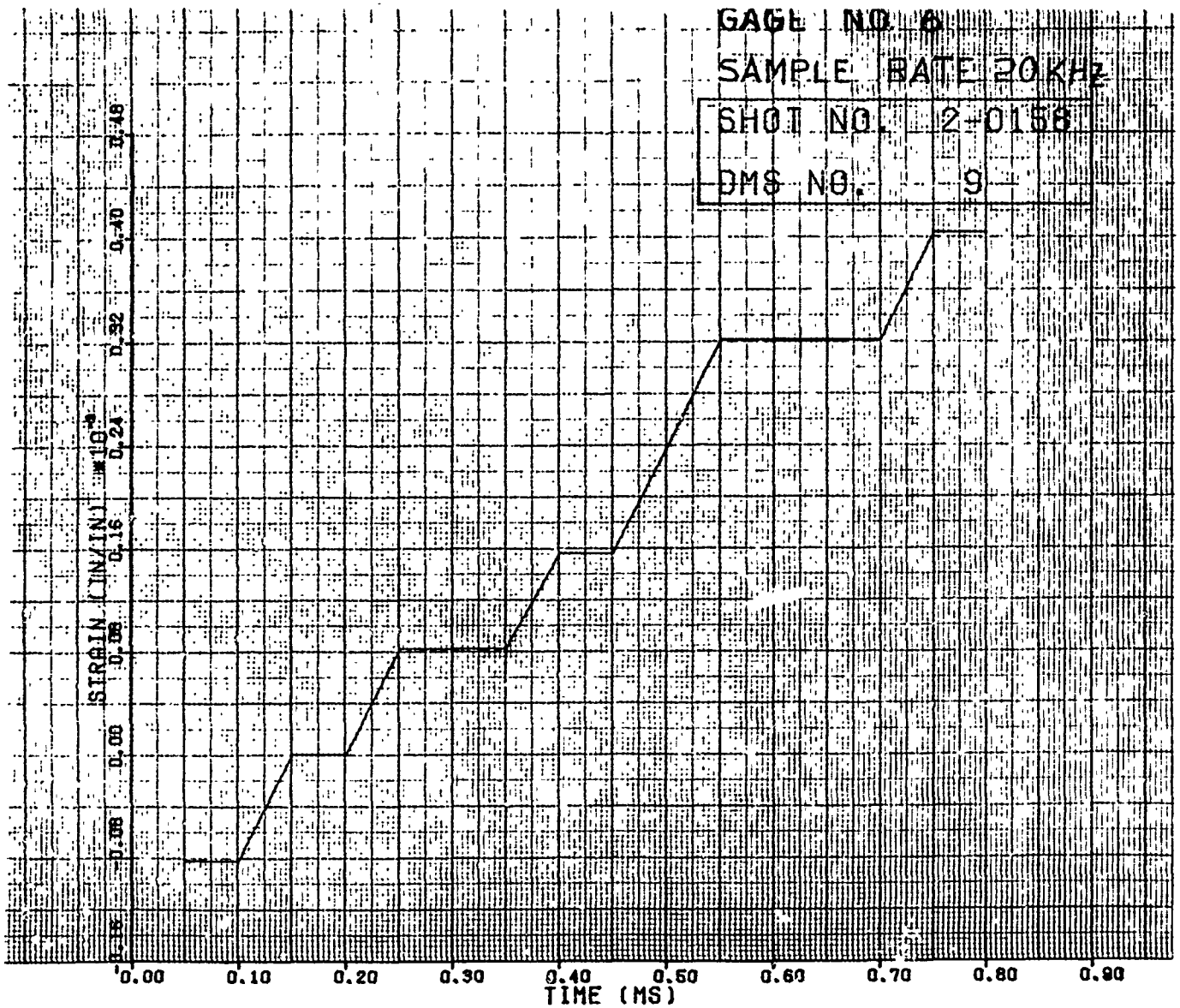

Figure 103. Strain of Shot 2-0158 for Gage #6.

Typical strain results for the second impact are given in Figures 104 through 109 for Shot 2-0163. The impact velocity was 92 m/s and the impact mass 172.3 g. The strain gage locations for this group are given in Figure 12A of Appendix A. The damage for this impact was in the form of bending and plastic deformation at the root giving a tip deflection measurement of 9.84 cm. Dynamic displacement data of the tip is given in Figures 110 through 112 for Shot 2-0163 in the "y", "x", and resultant directions, respectively

Figures 26B and 27B show the damage on the specimens of Shots 2-0159 and 2-0163.

3.1.1.13 Impact Results for Group 13 Specimens

Two Group 13 stainless steel cambered flat plate specimens with a blade-type aspect ratio were impacted using the medium 680 g (1.5 pound) size bird. The impacts were edge (slicing) impacts at the 70 percent span location and the impact angle was 36.4 degrees. The most severe damage by plastic deformation at the root with a tip deflection measurement of 17.78 cm was received for an impact mass of 192.3 g and a velocity of 99 m/s for Shot 2-0162.

Typical strain results are shown in Figures 113 through 118 for Shot 2-0161. In this case, the impact velocity was 64 m/s and the impact mass 148.6 g. Figure 12A of Appendix A gives the strain gage locations for this group of specimens. Damage for this impact was plastic deformation and bending at the root giving a tip deflection of 2.54 cm. Some twist through the span was also visible. Dynamic displacement data for Shot 2-0161 are given in Figures 119 through 121 for the "y", "x", and resultant directions, respectively.

Figures 28B and 29B show the damage received for Shots 2-0161 and 2-0162, respectively.

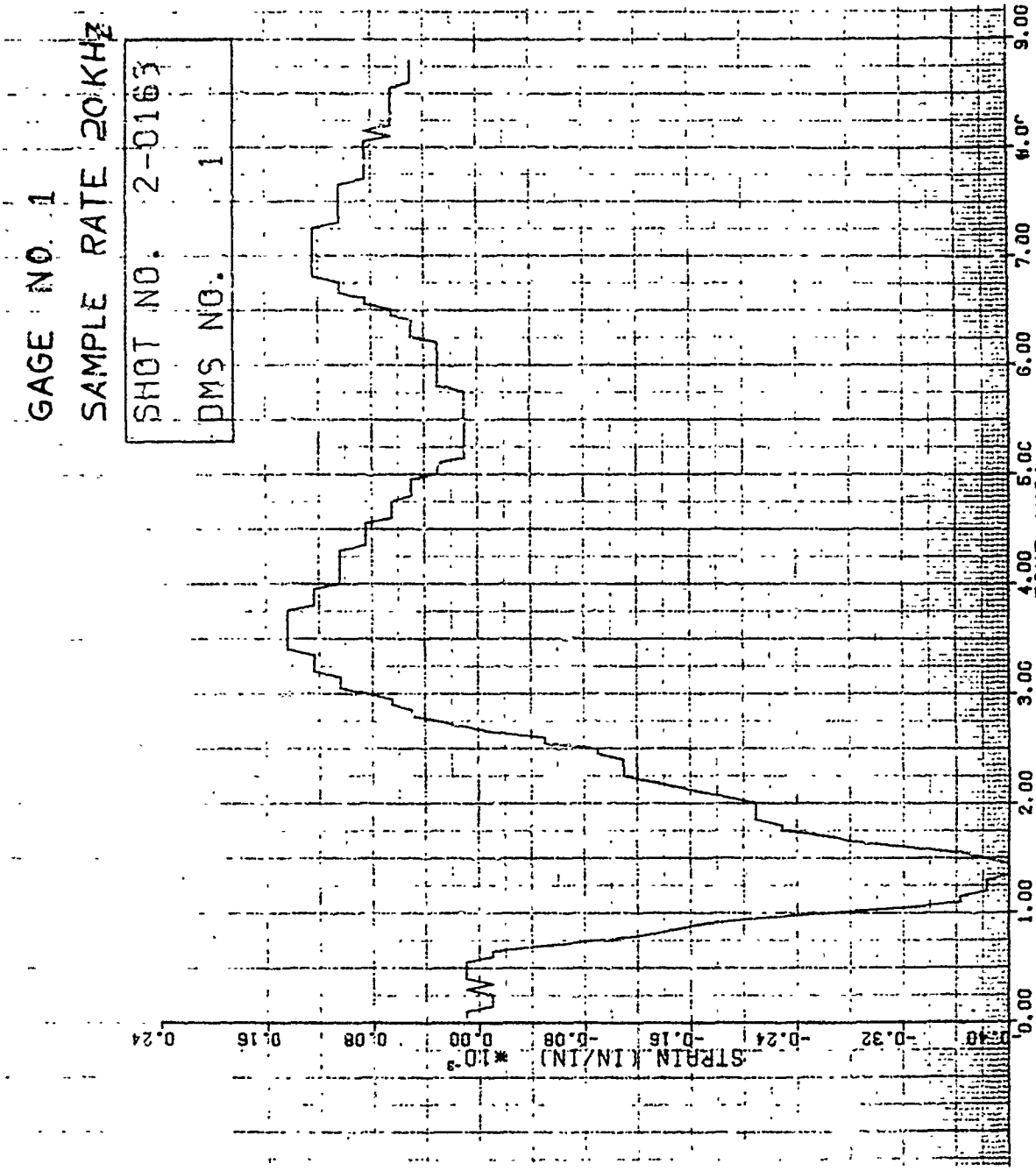

Figure 104. Strain of Shot 2-0163 for Gage #1.

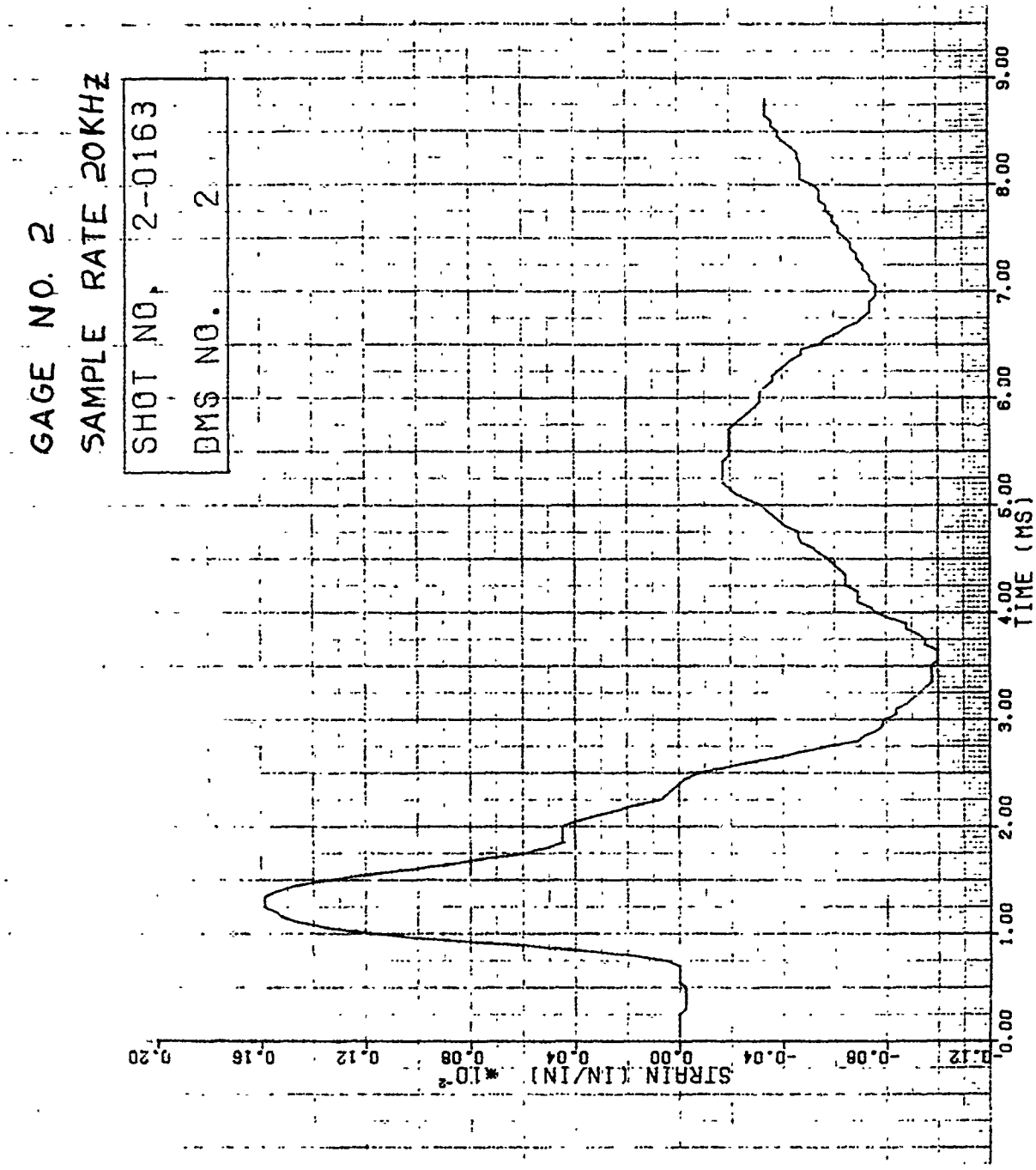

Figure 105. Strain of Shot 2-0163 for Gage #2.

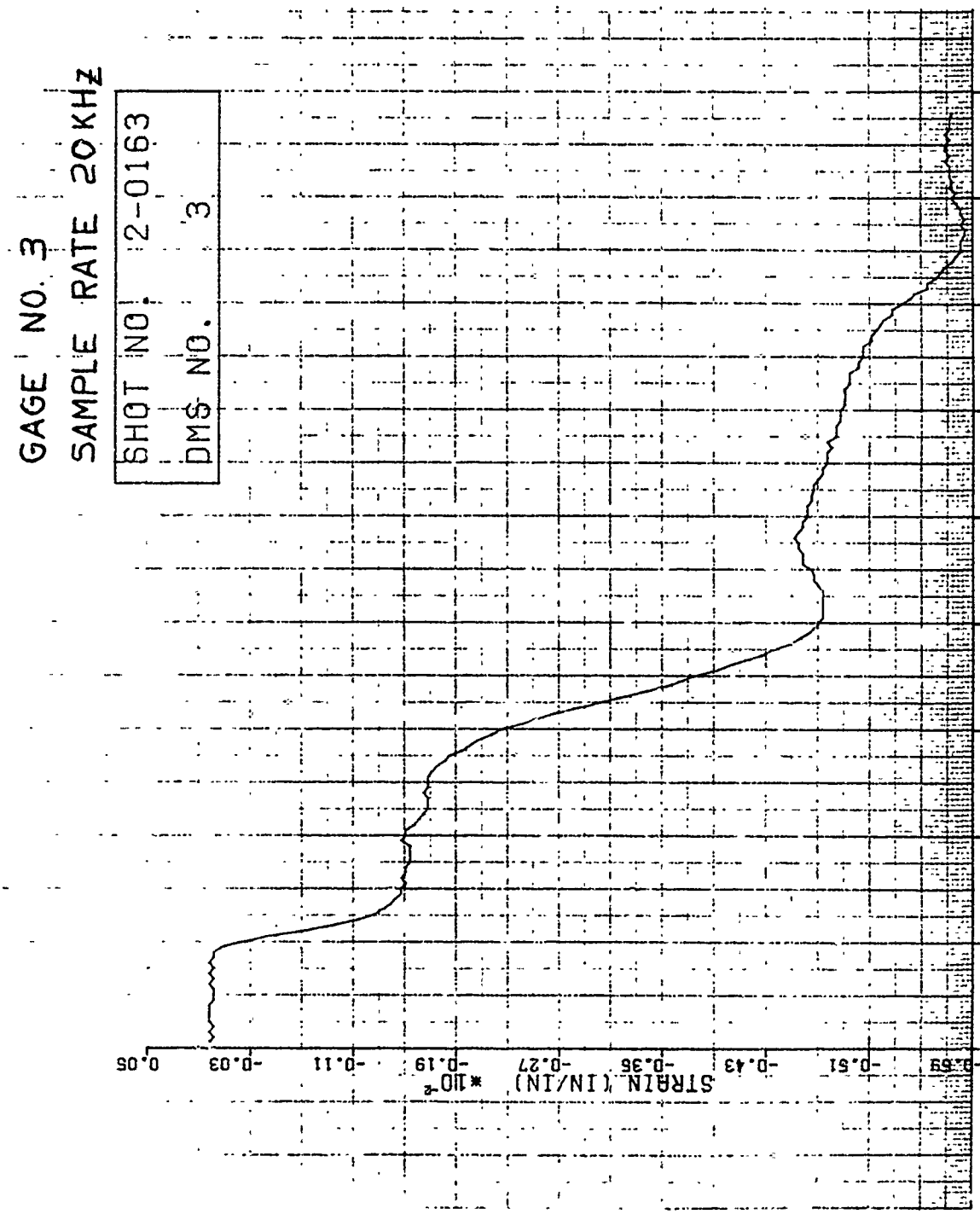

Figure 106. Strain of Shot 2-0163 for Gage #3.

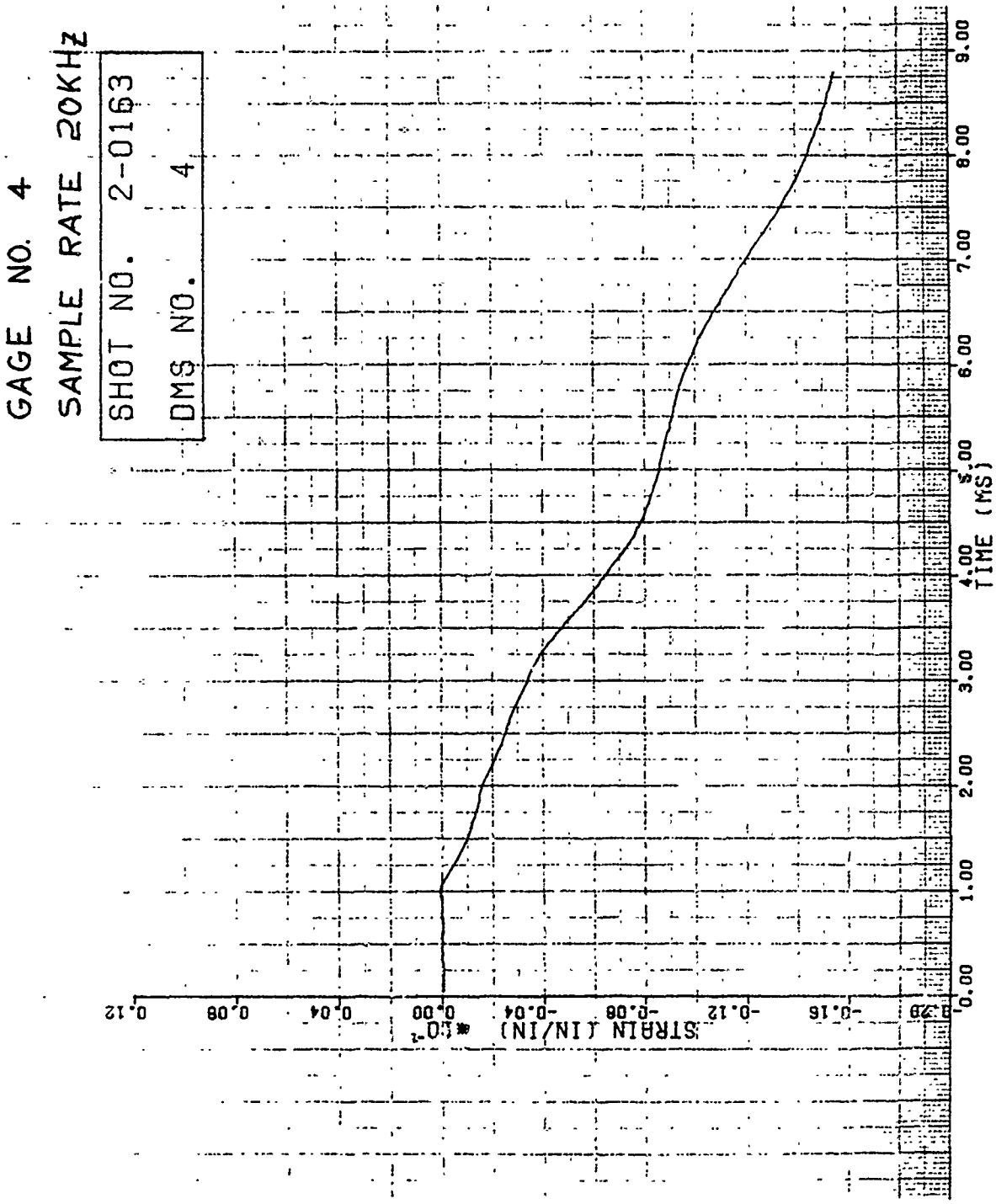

Figure 107. Strain of Shot 2-0163 for Gage #4.

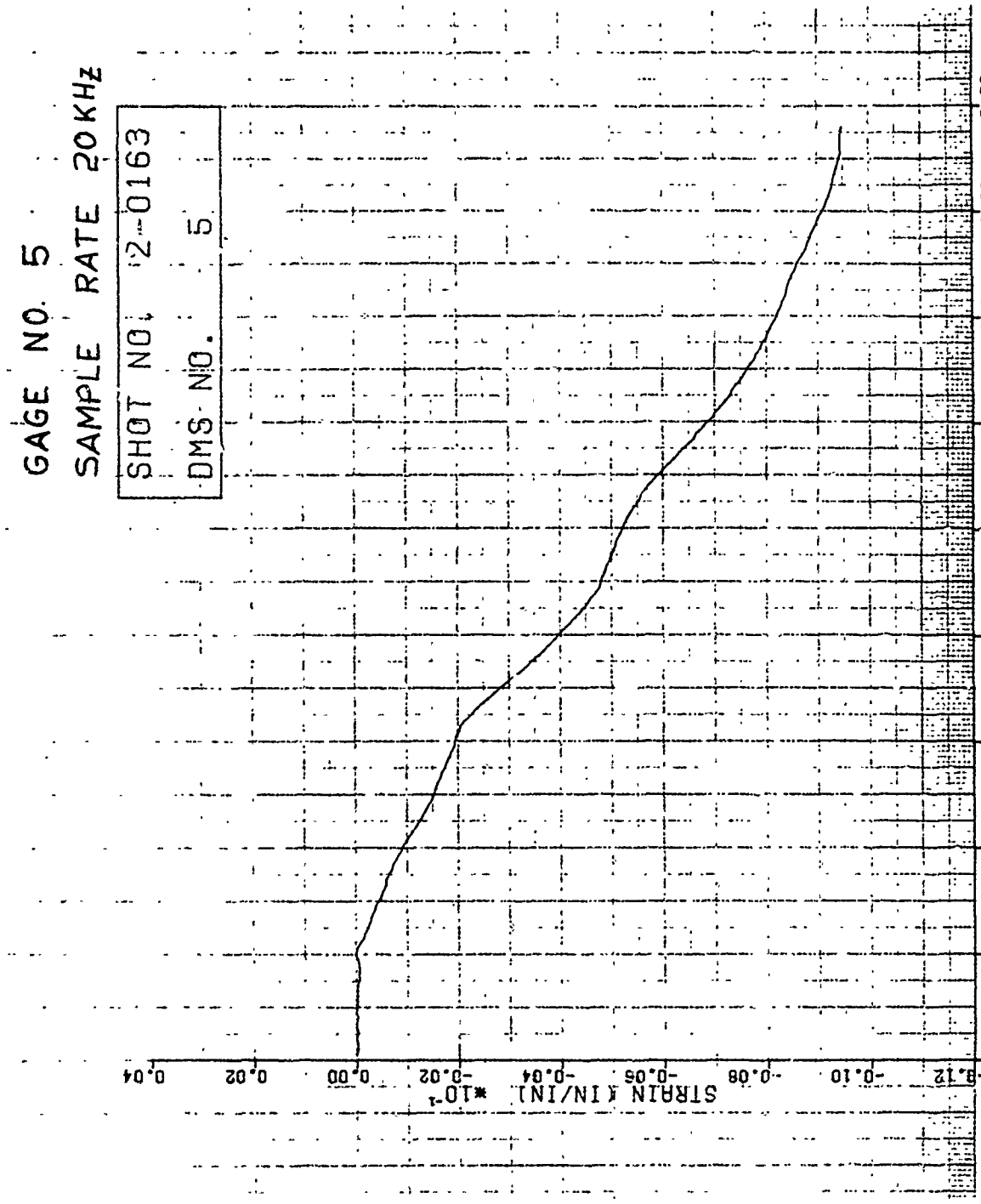

Figure 108. Strain of Shot 2-0163 for Gage #5.

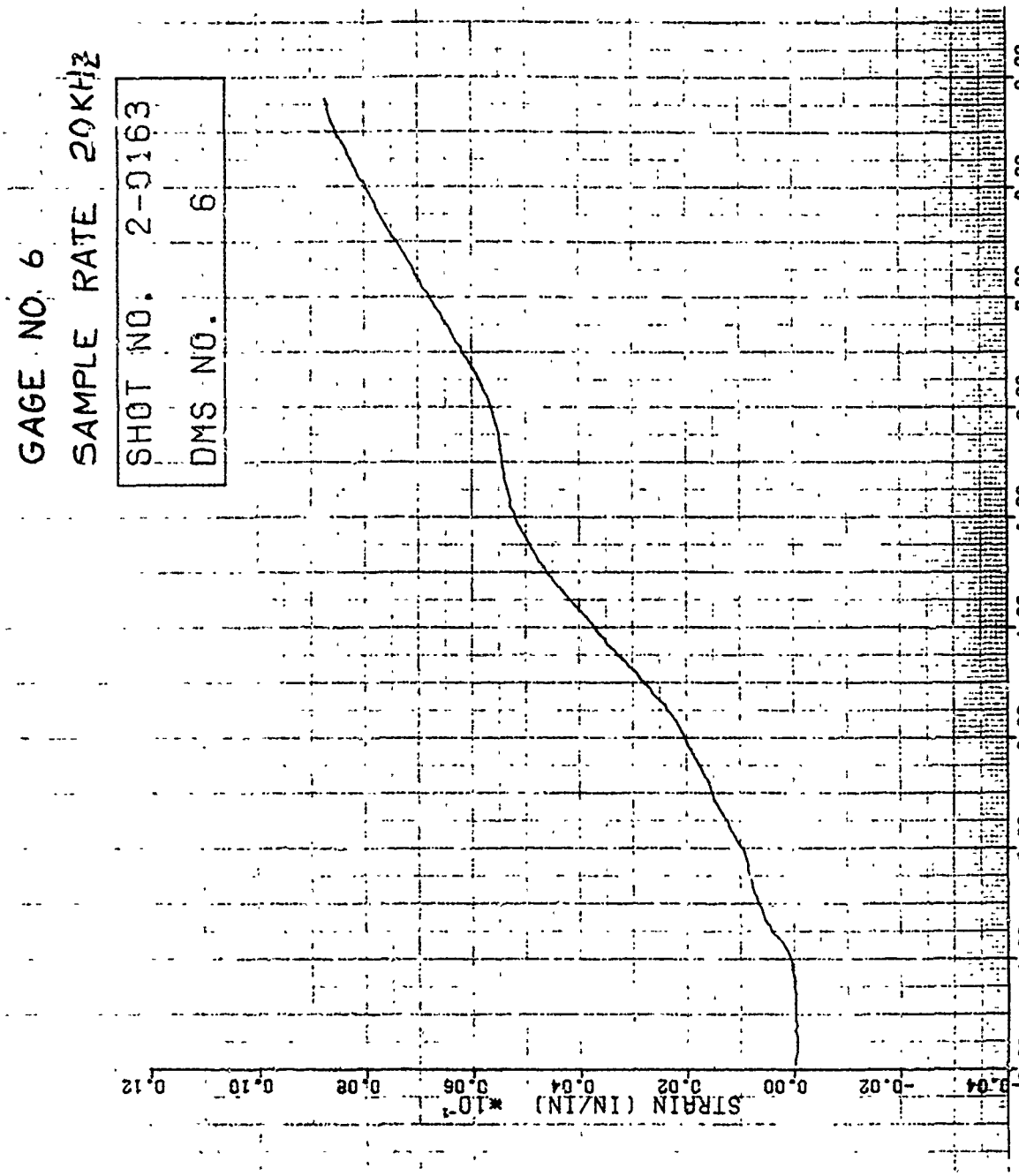

Figure 109. Strain of Shot 2-0163 for Gage #6.

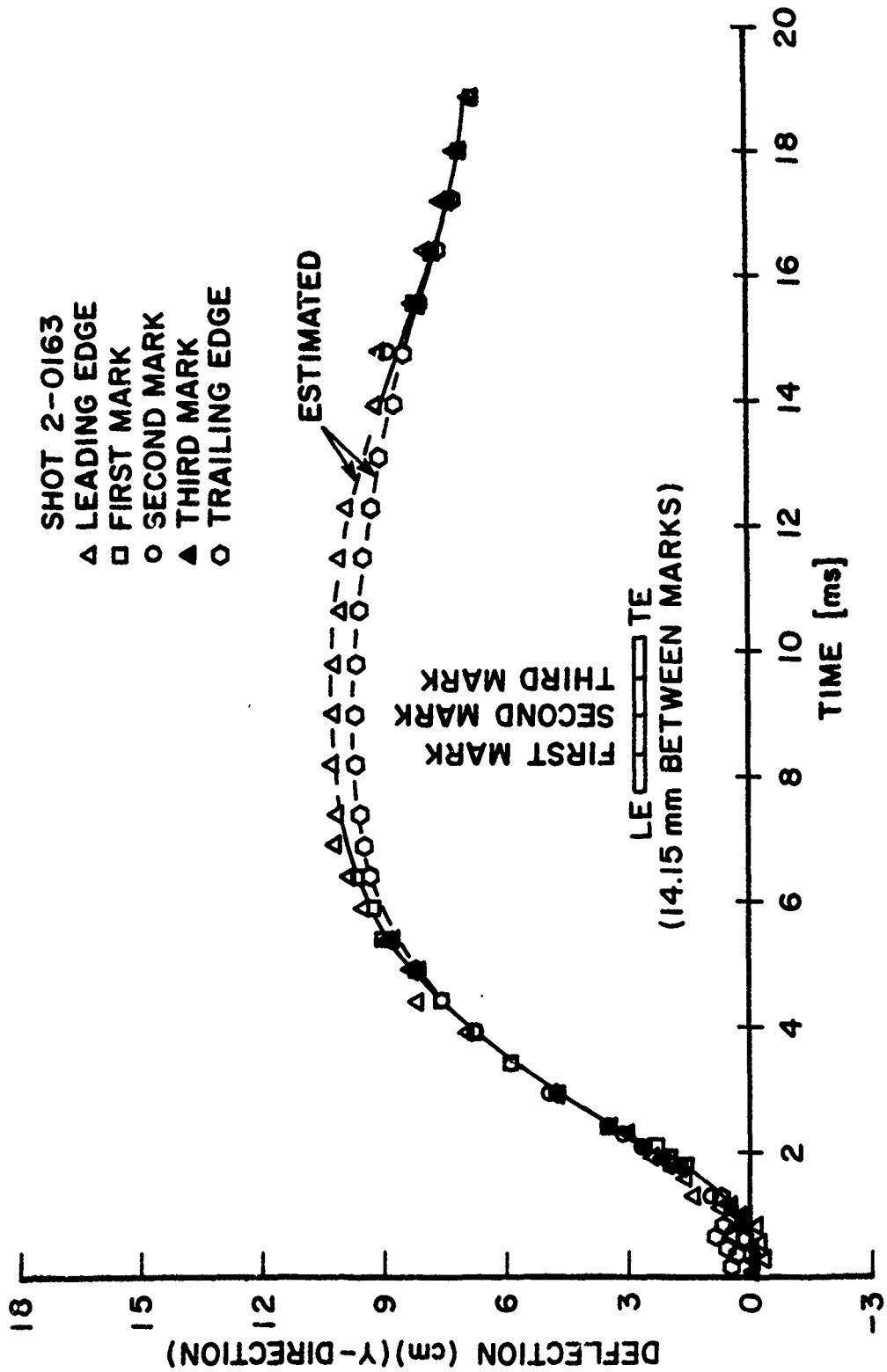

Figure 110. Tip Deflection in "y" Direction for Shot 2-0163.

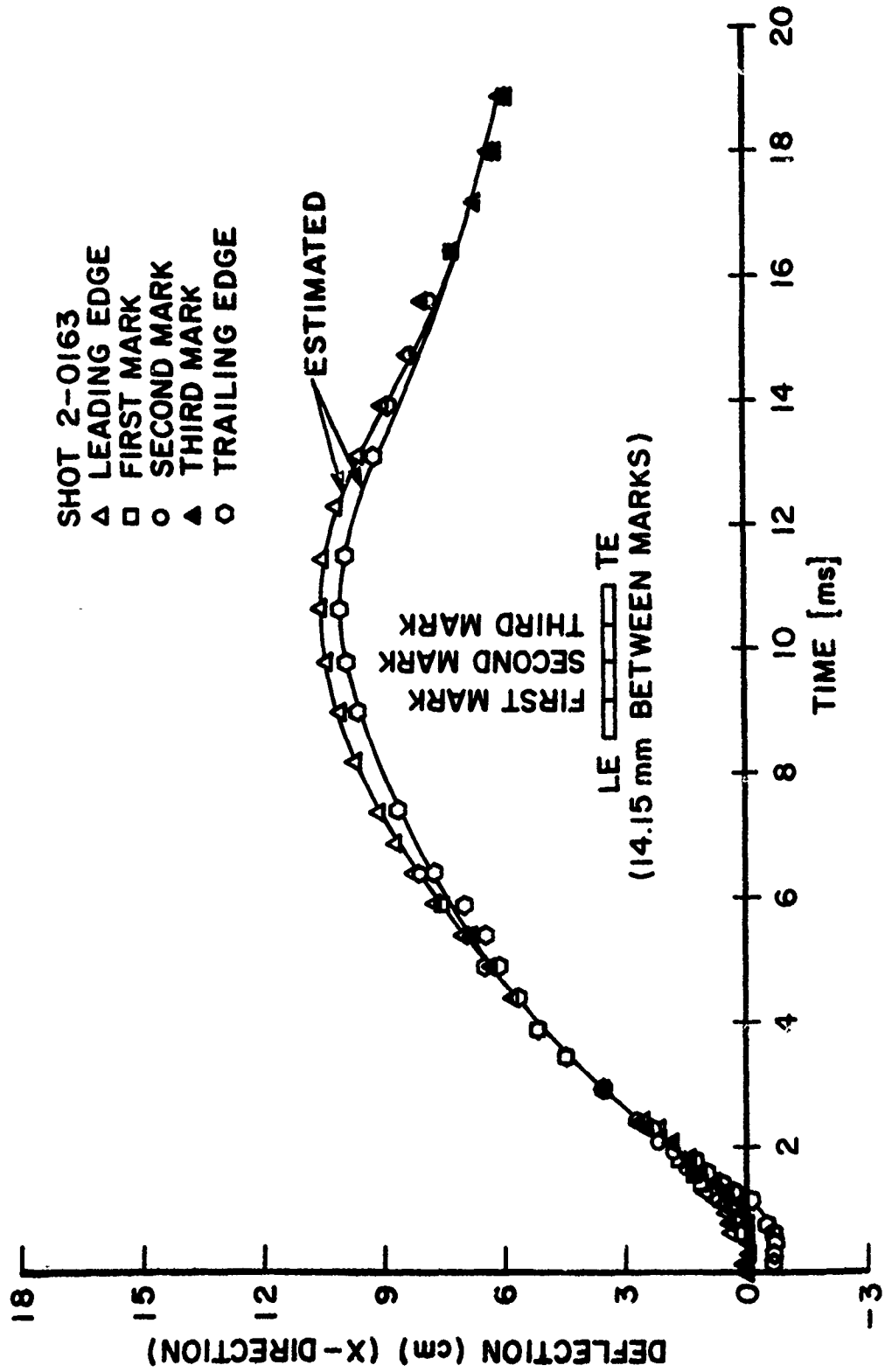

Figure 111. Tip Deflection in "x" Direction for Shot 2-0163.

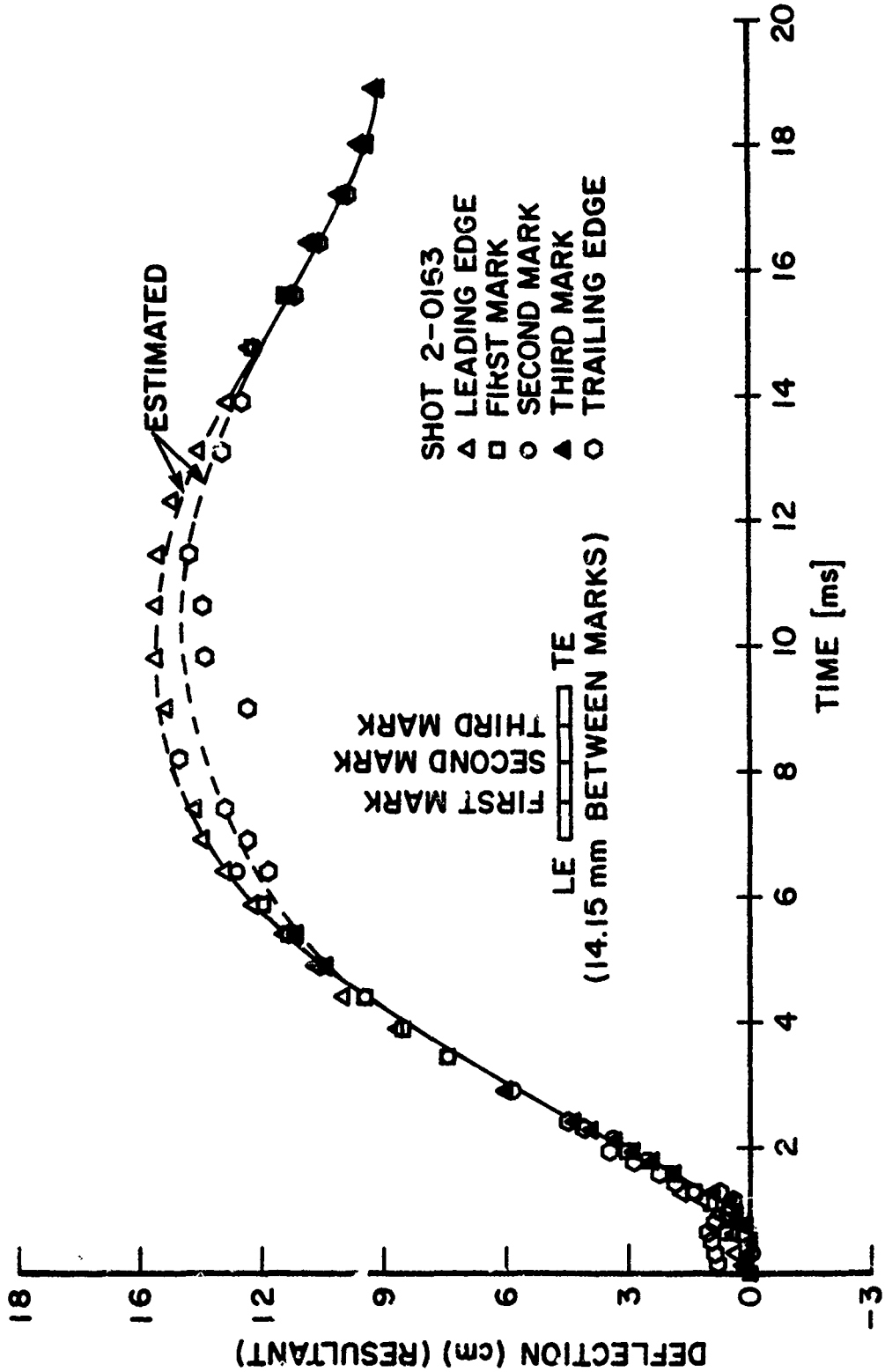

Figure 112. Tip Deflection Resultant for Shot 2-0163.

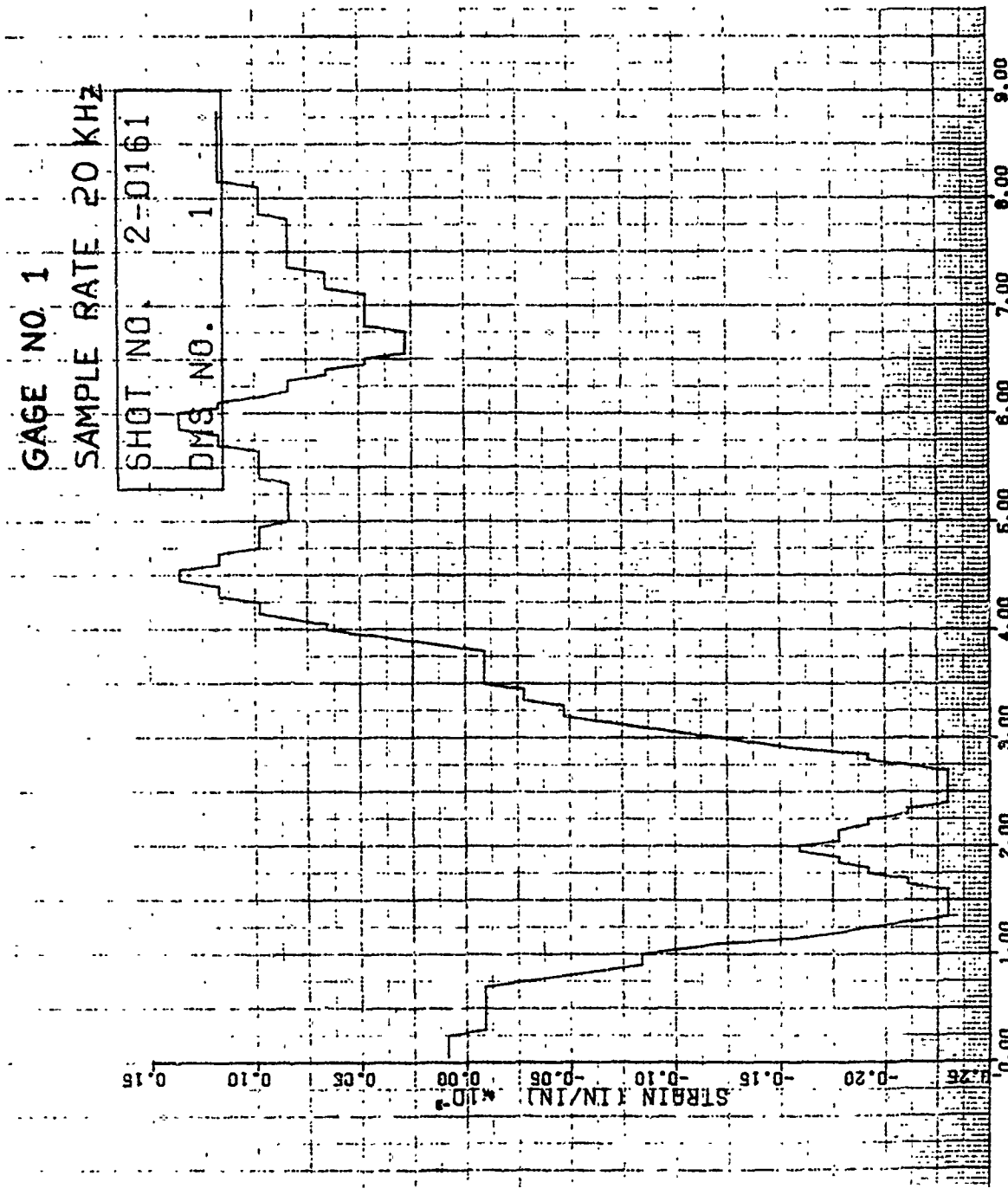

Figure 113. Strain of Shot 2-0161 for Gage #1.

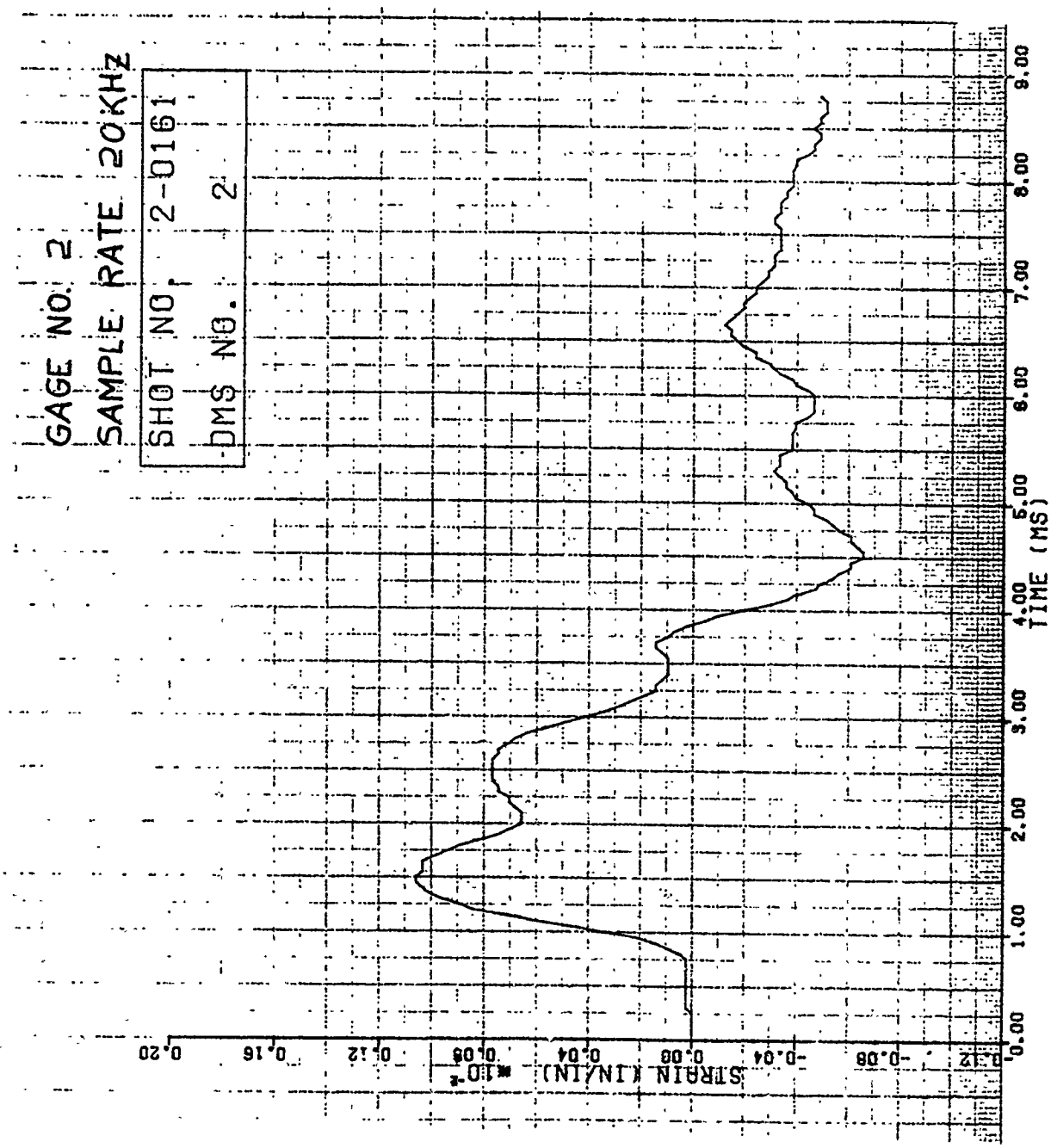

Figure 114. Strain of Shot 2-0161 for Gage #2.

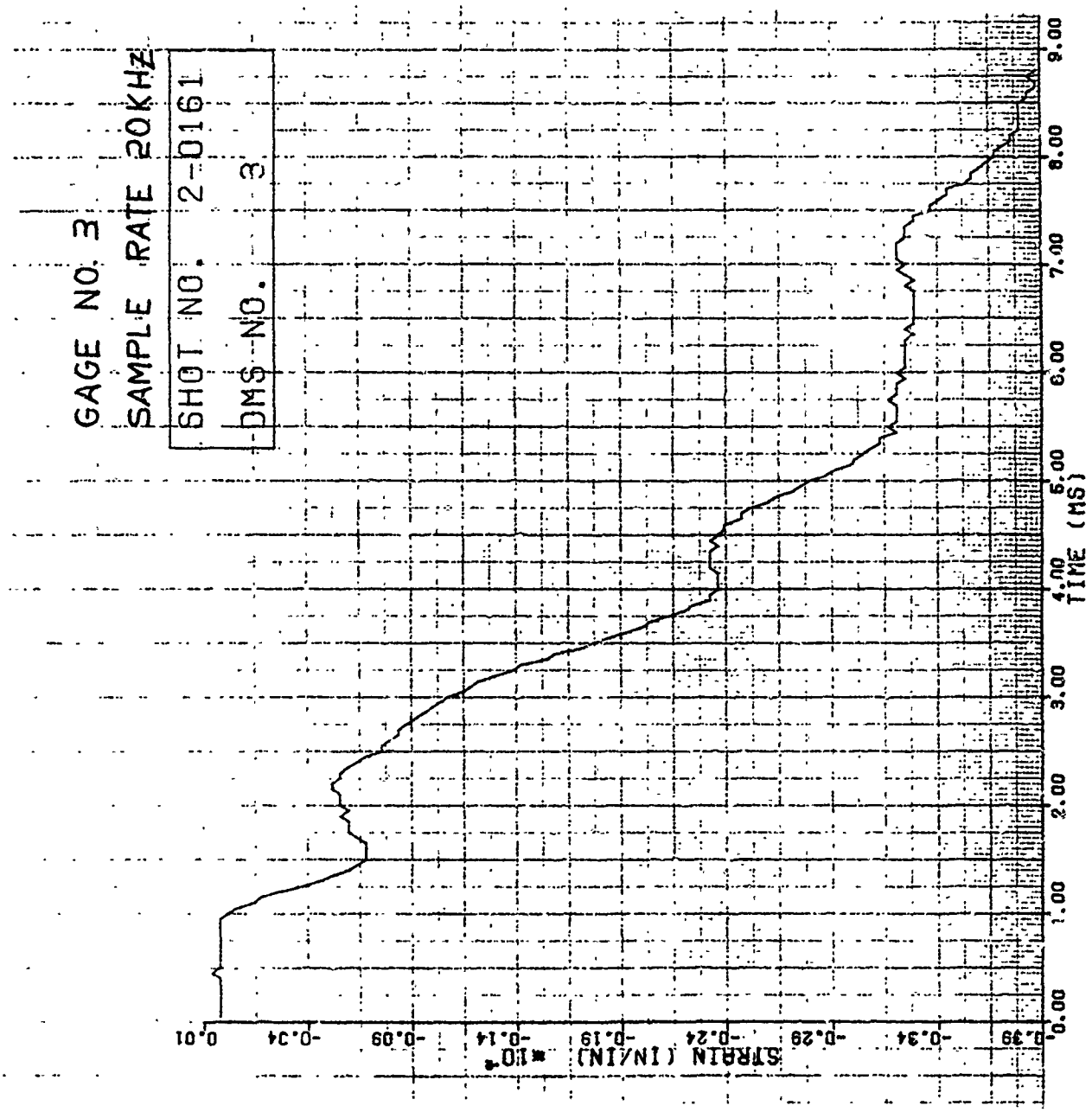

Figure 115. Strain of Shot 2-Q161 for Gage #3.

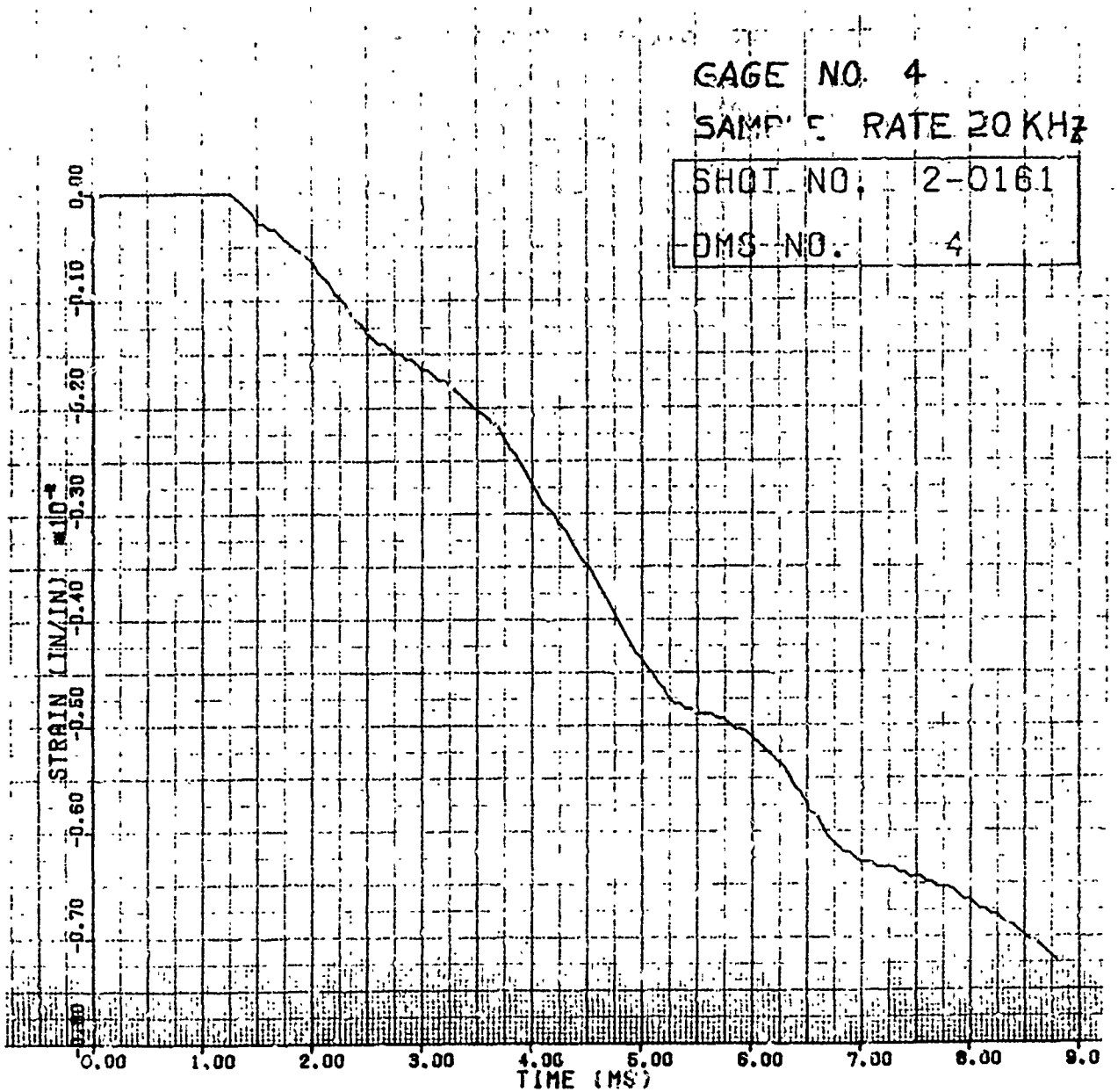

Figure 116. Strain of Shot 2-0161 for Gage #4.

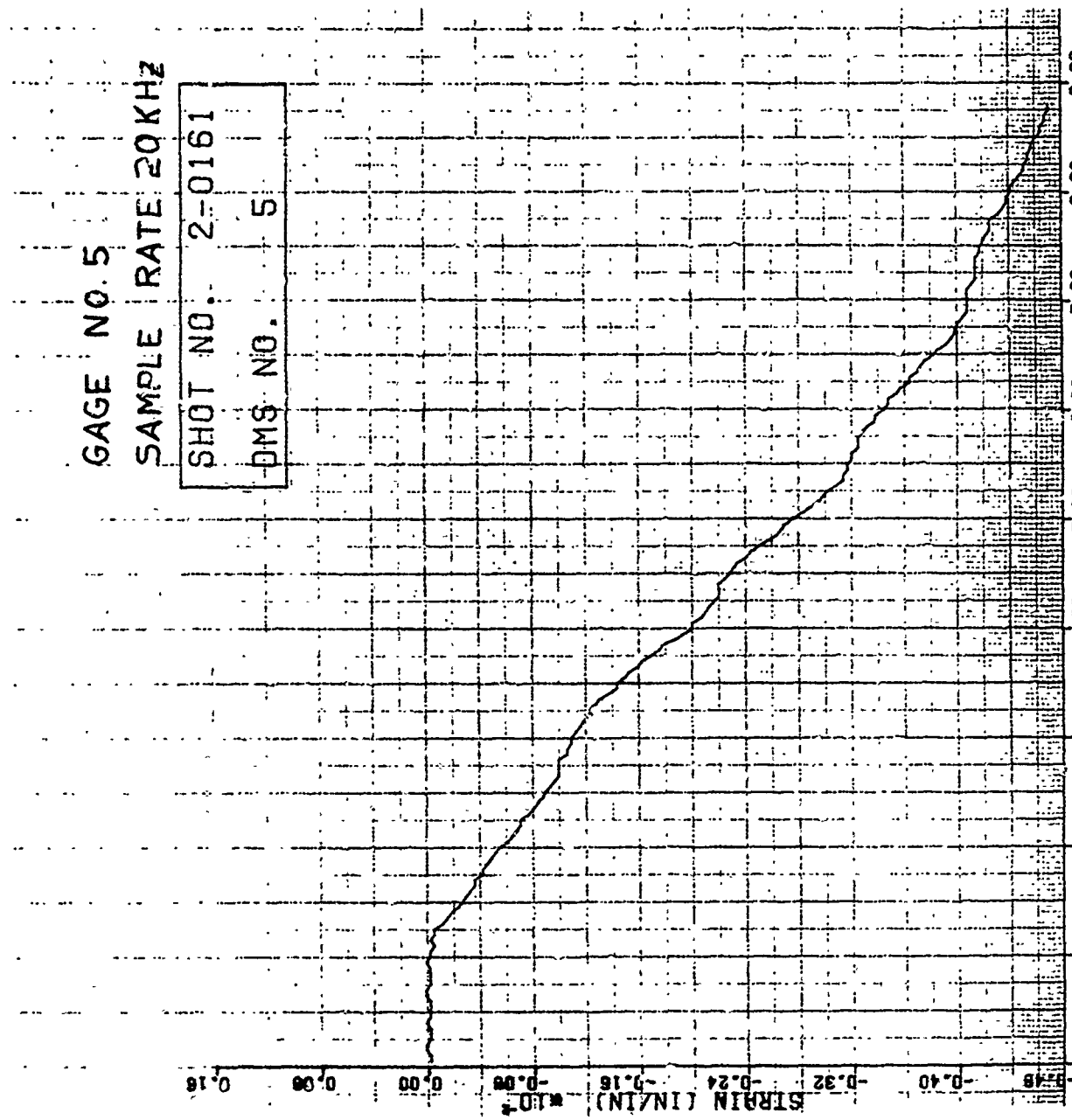

Figure 117. Strain of Shot 2-0161 for Gage #5.

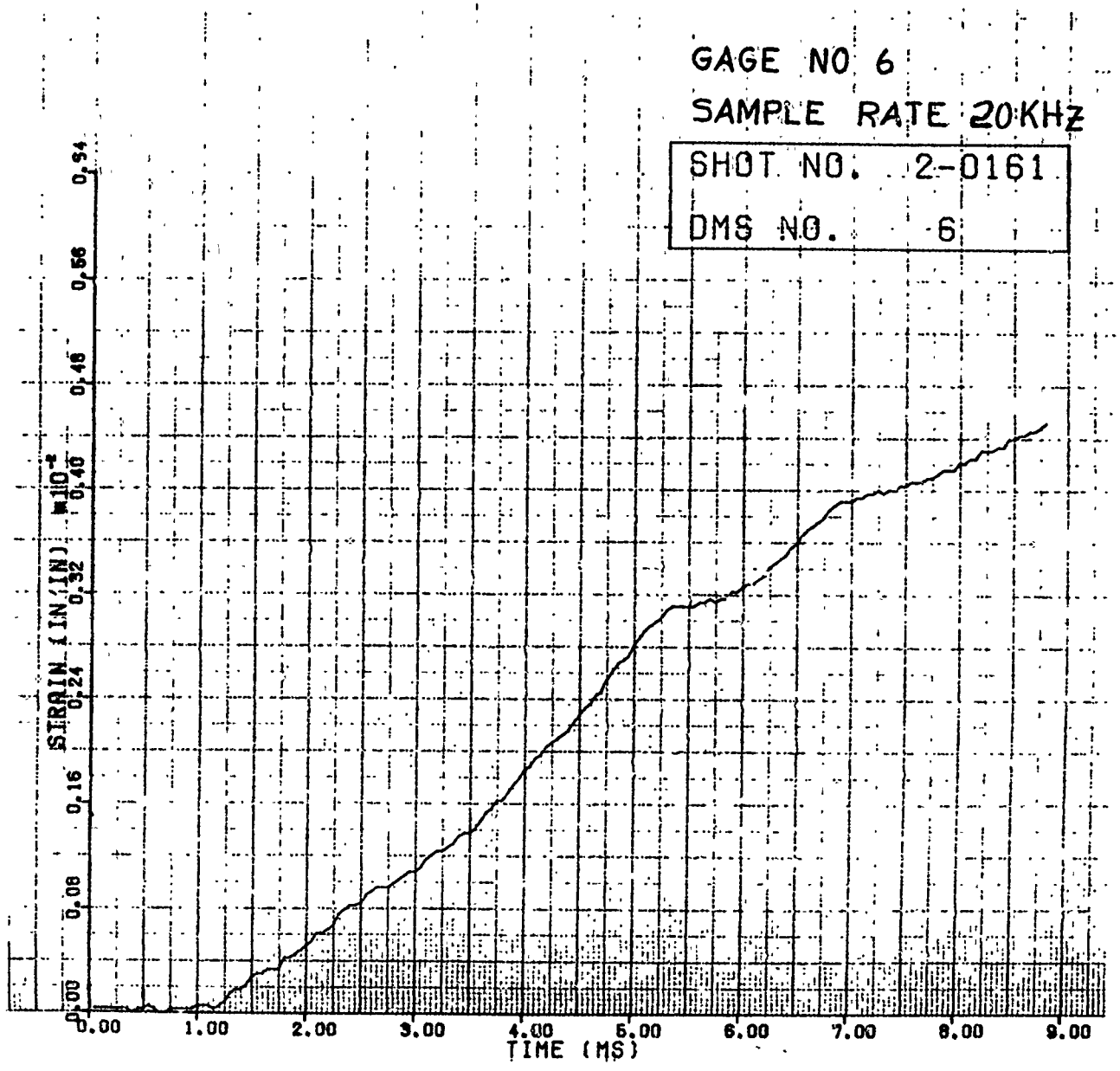

Figure 118. Strain of Shot 2-0161 for Gage #6.

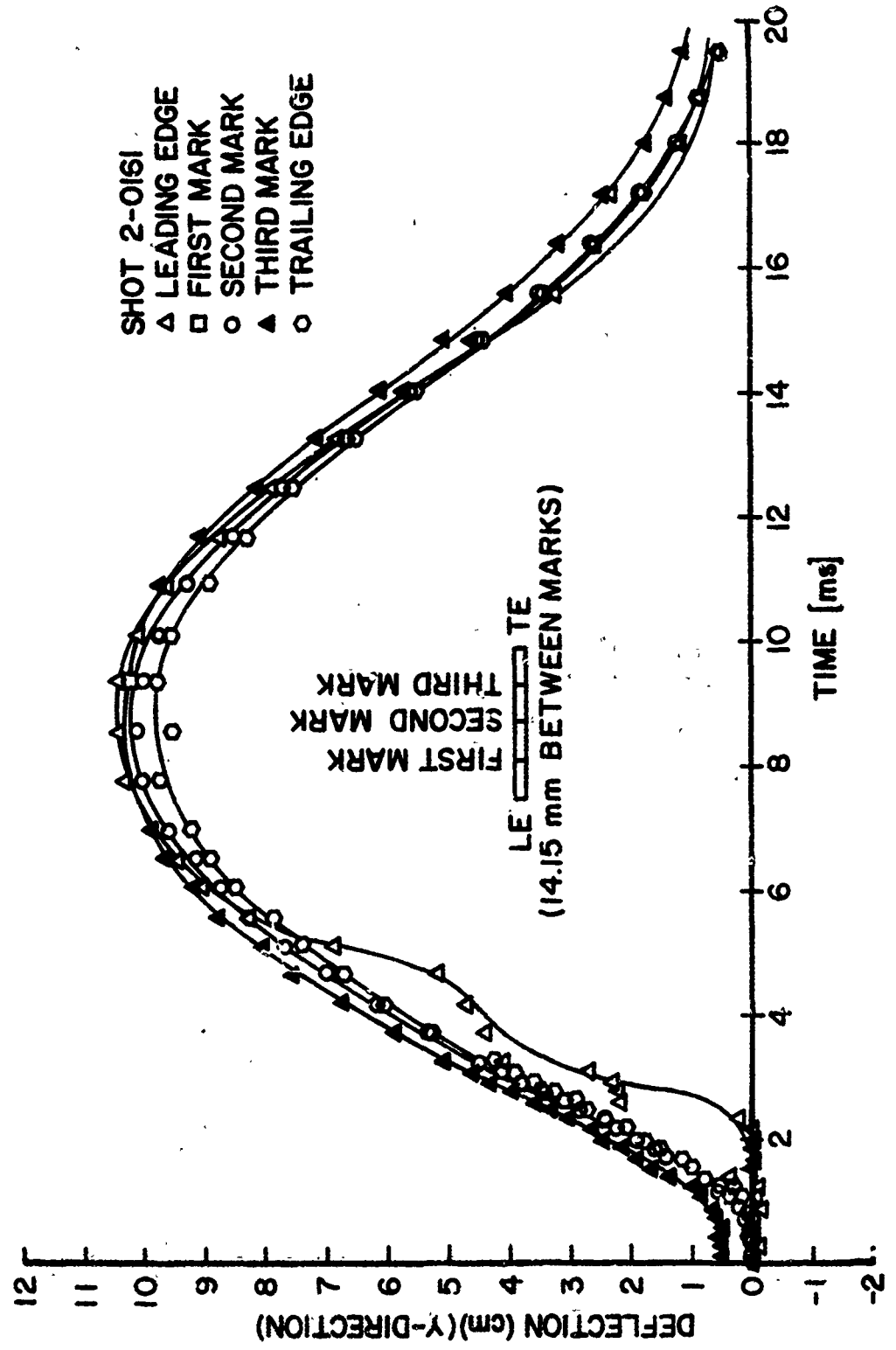

Figure 119. Deflection of Tip in "y" Direction for Shot 2-0161.

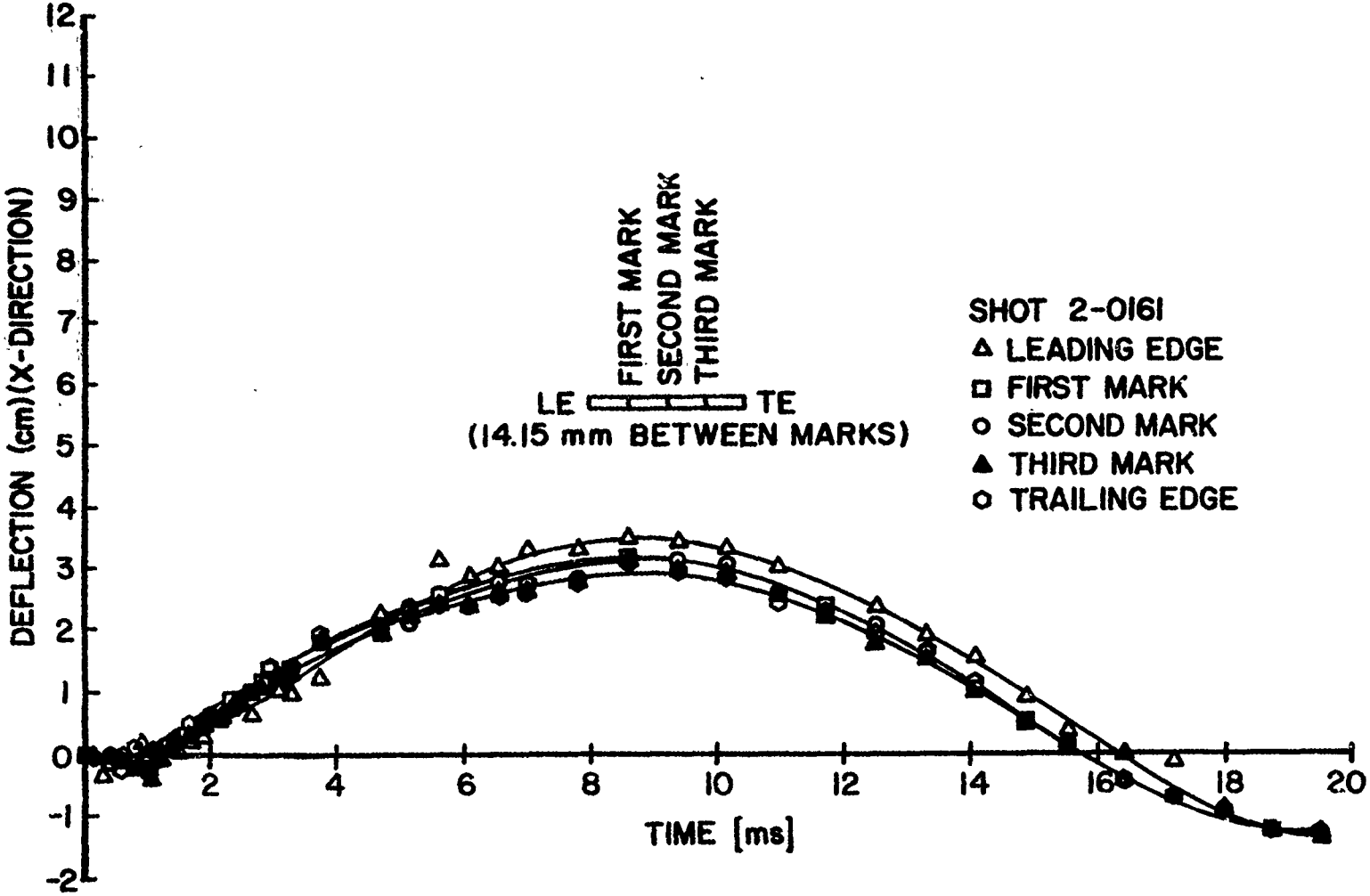

Figure 120. Deflection of Tip in "x" Direction for Shot 2-0161.

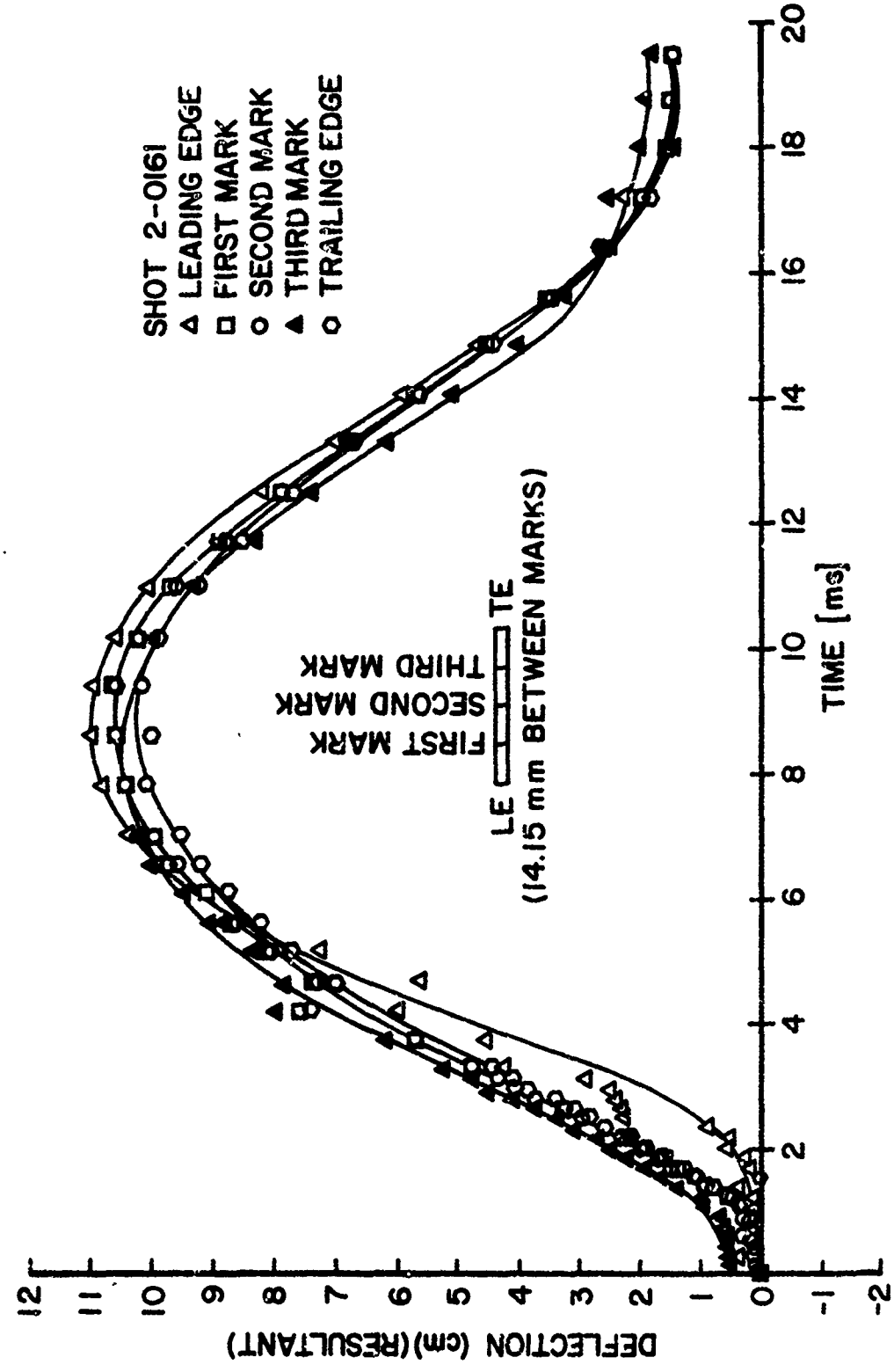

Figure 121. Tip Deflection Resultant for Shot 2-0161.

3.1.1.14 Impact Results for Group 14 Specimens

Seven Group 14 boron/aluminum composite cross ply flat panel specimens with a blade-type aspect ratio were impacted using the small 85 g (3 ounce) bird. The impacts were edge (slicing) impacts at the 70 percent span location with an impact angle of 18.9 degrees. The velocities ranged from a low of 85 to 313 m/s and the impact mass ranged from 8.4 to 20.8 g. The damage generated from the impacts ranged from no visible damage to the specimen breaking off at the root (Shot 2-0139) at the highest impact mass and velocity value.

Typical strain results are given in Figures 122 through 127 for Shot 2-0135. The test conditions for this shot were 185 m/s for the impact velocity and 16.5 g for the impact mass. In this case, the impact resulted in no visible damage on the specimen. The strain gage locations for this group of specimens are given in Figure 13A of Appendix A. Dynamic displacement data of the specimen tip are given in Figures 128 and 129 for the "y" and "x" directions, respectively.

Figure 30B gives the photographs of the root damage for Shot 2-0139. The impact velocity was 313 m/s and the impact mass was 20.8 g for this impact.

3.1.1.15 Impact Results of Group 15 Specimens

Three Group 15 boron/aluminum composite cross ply flat panel specimens with a one-half blade-type aspect ratio were impact tested in the study by the small 85 g (3 ounce) bird. The impacts were edge (slicing) impacts at the 70 percent span location at an impact angle of 18.9 degrees. No visible damage was received for Shot 2-0149 for an impact at a velocity of 185 m/s and an impact mass of about 30 g. The specimens for the remaining two shots (2-0150 and 2-0151) broke off at the root for velocities of 306 and 230 m/s with the impact mass being 23.8 and 46.1, respectively.

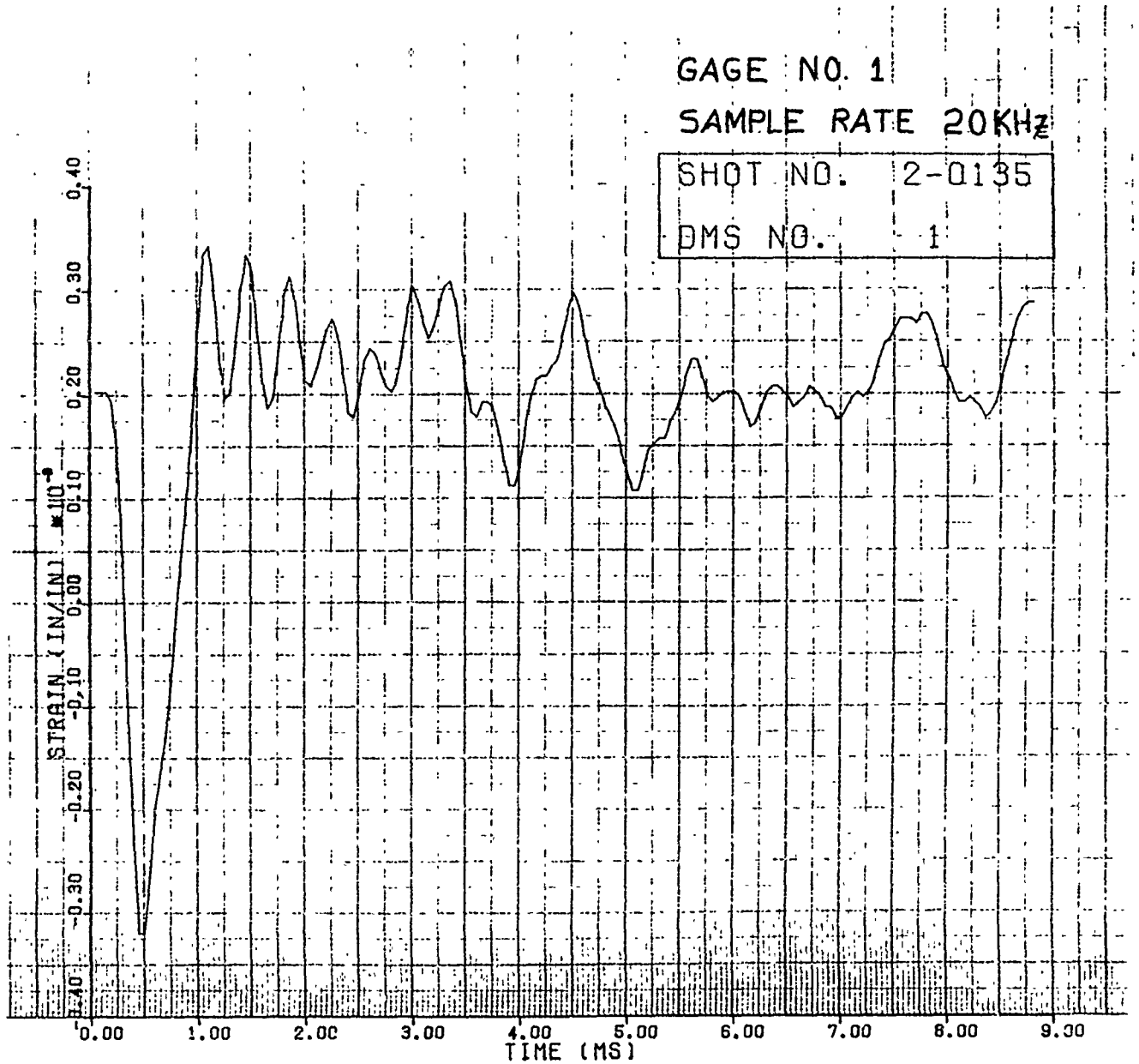

Figure 122. Strain of Shot 2-0135 for Gage #1.

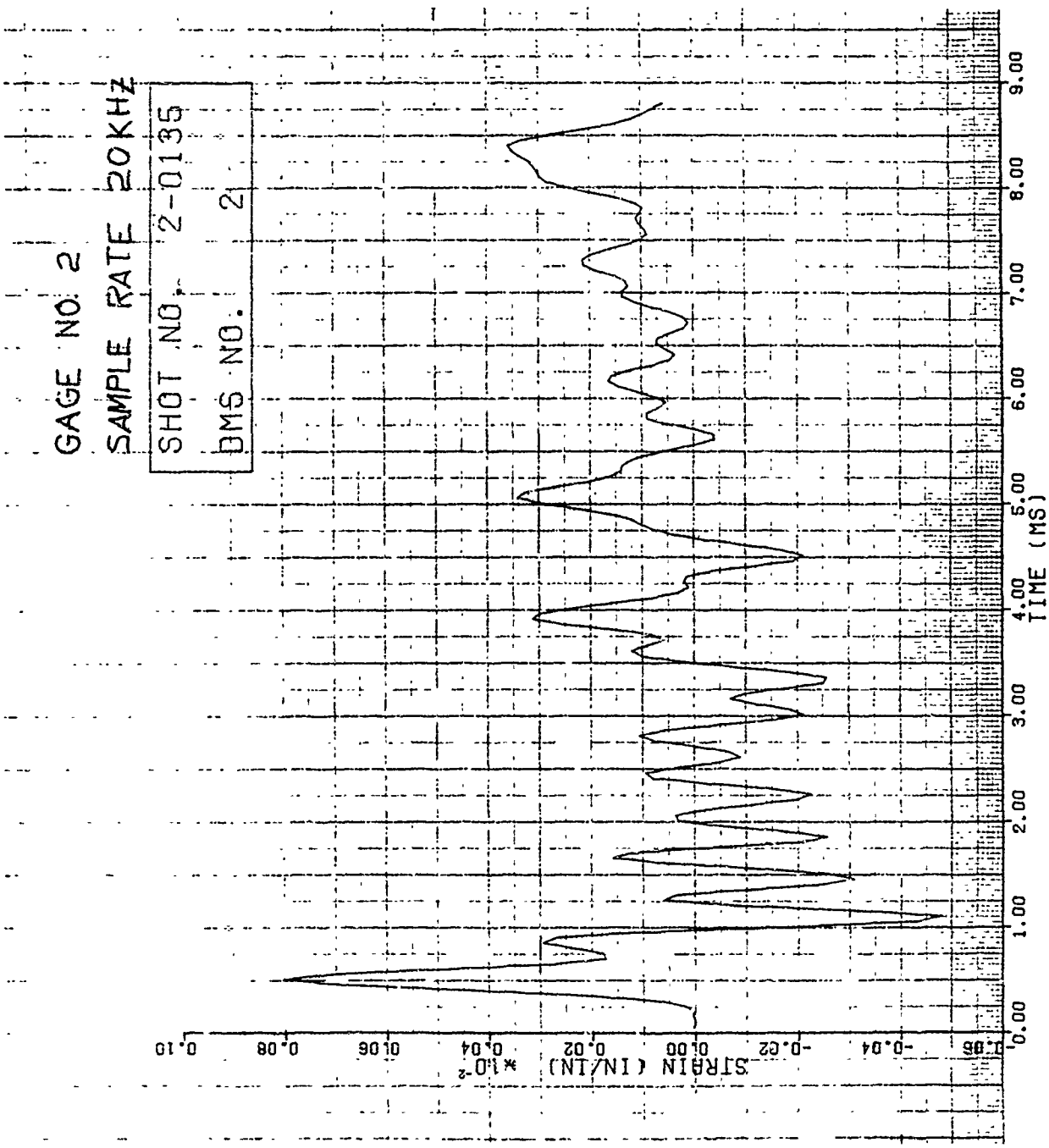

Figure 123. Strain of Shot 2-0135 for Gage #2.

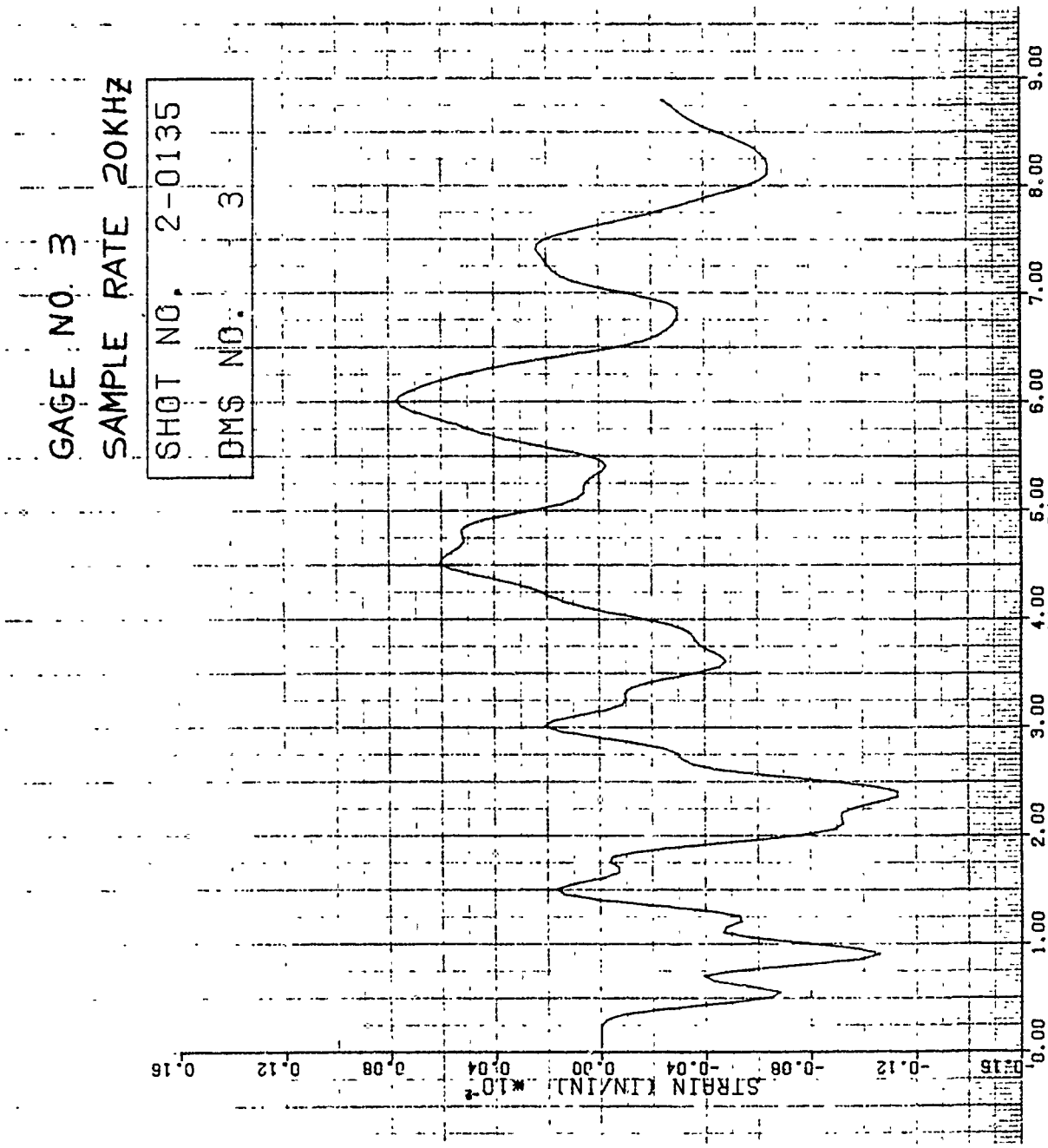

Figure 124. Strain of Shot 2-0135 for Gage #3.

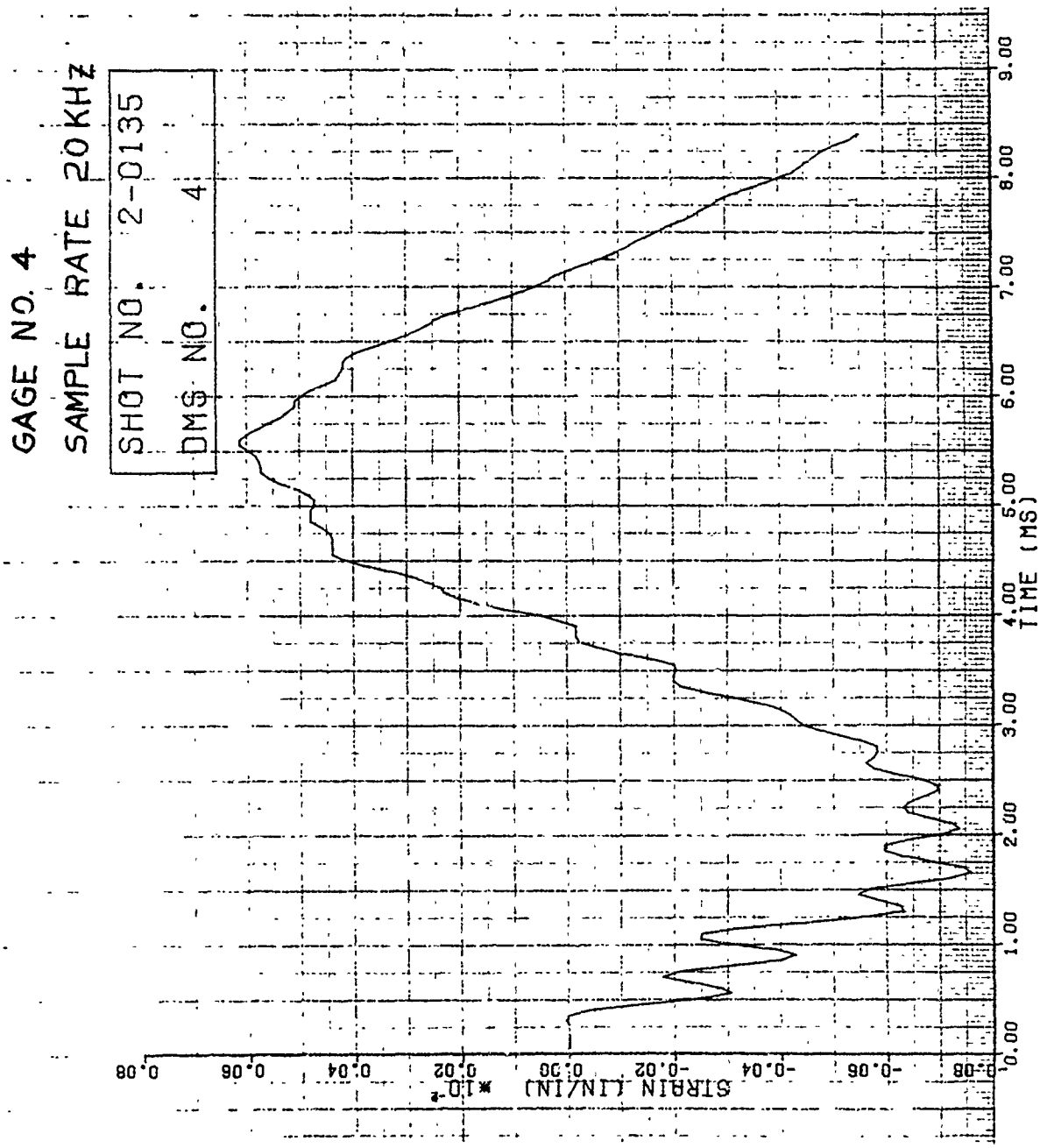

Figure 125. Strain of Shot 2-0135 for Gage #4.

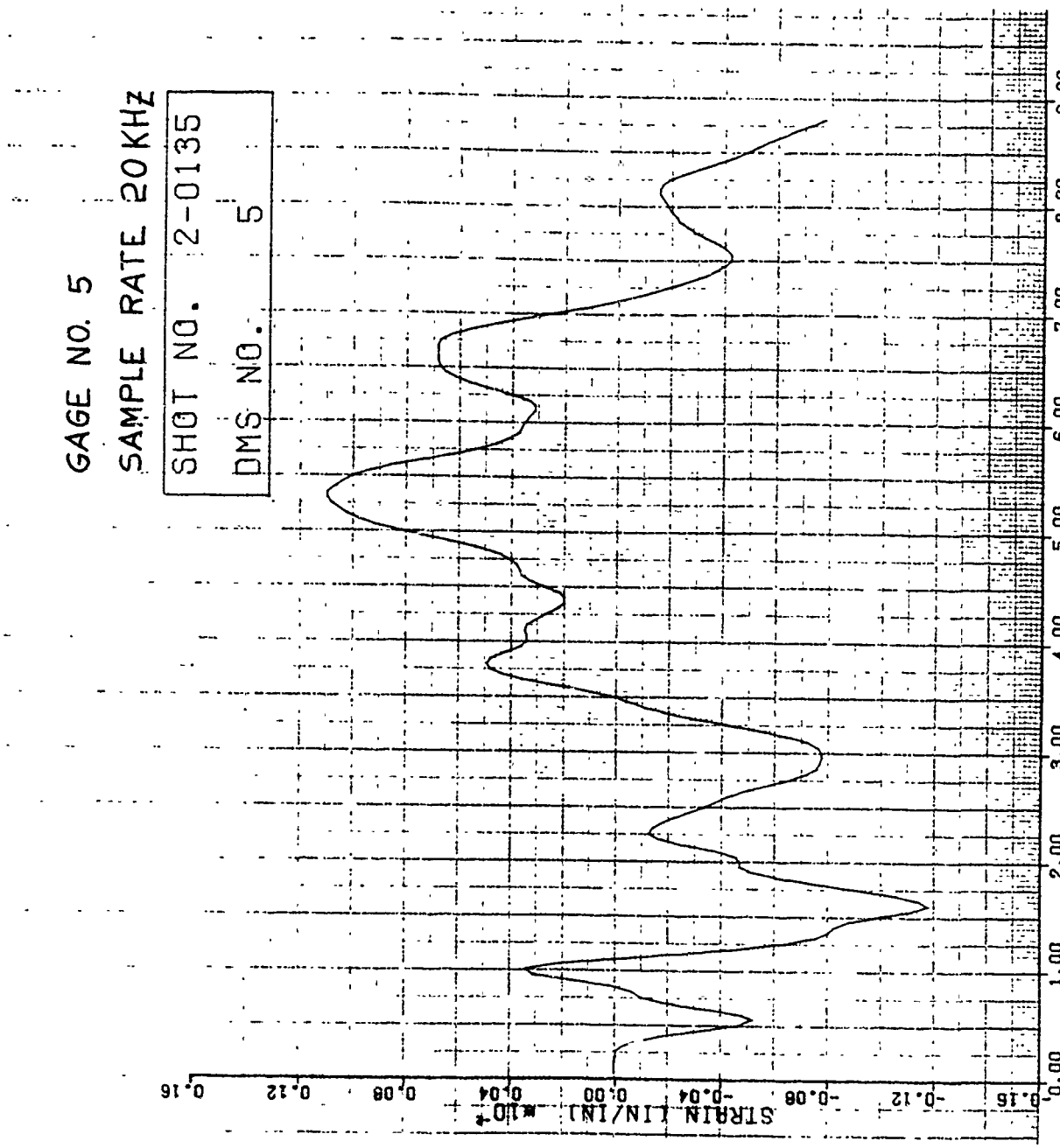

Figure 126. Strain of Shot 2-0135 for Gage #5.

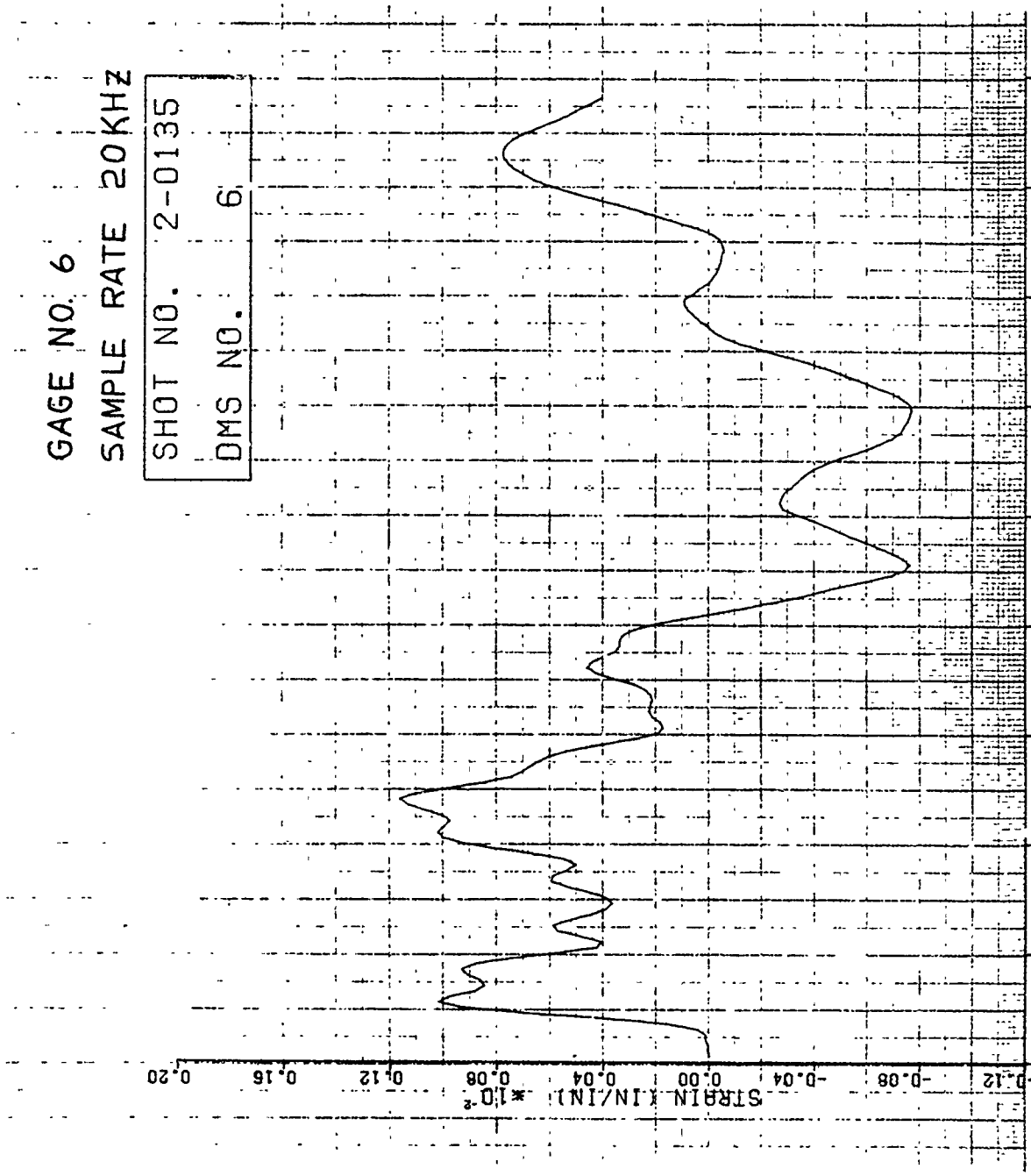

Figure 127. Strain of Shot 2-0135 for Gage #6.

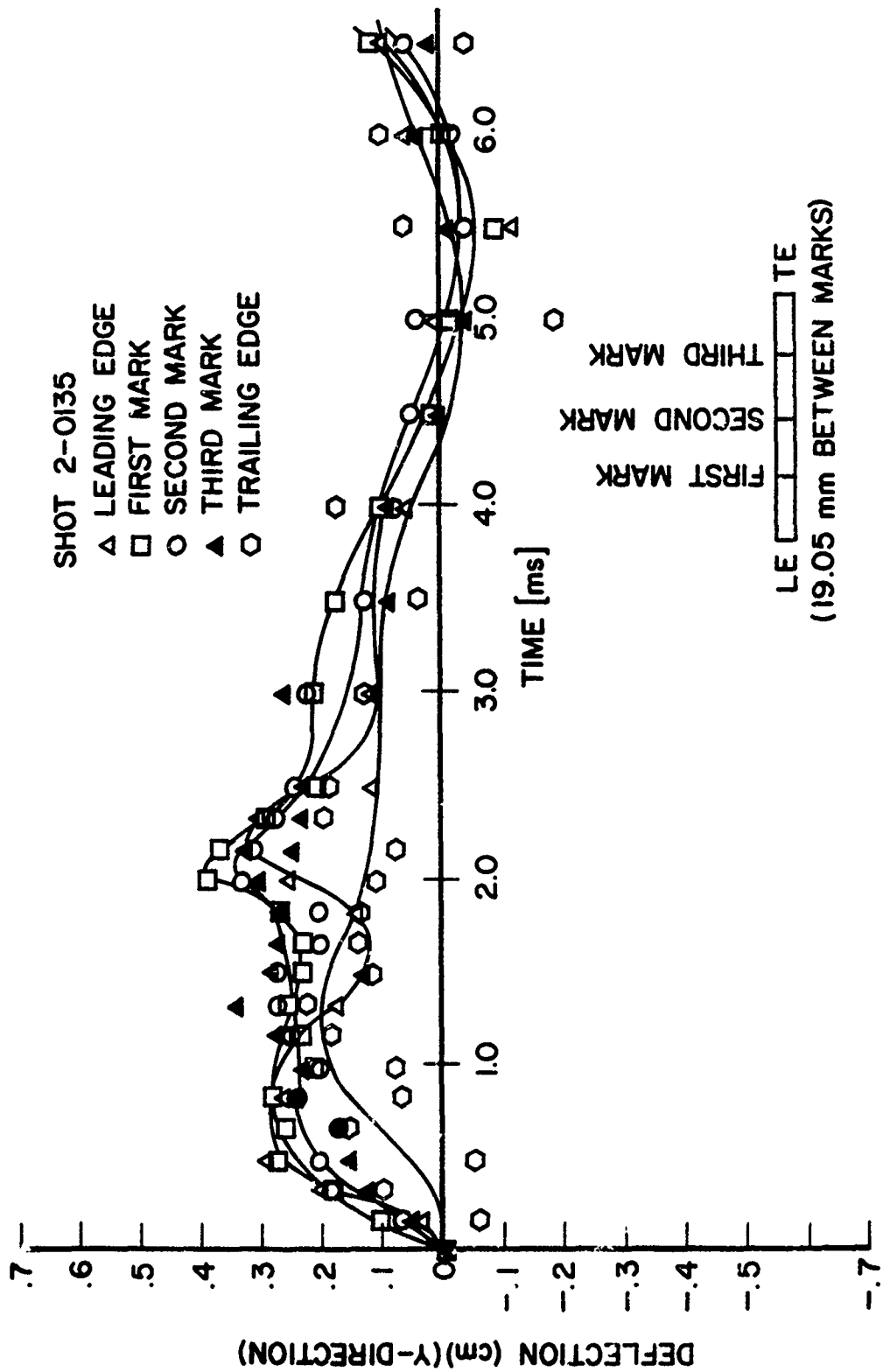

Figure 128. Deflection of Tip in "y" Direction for Shot 2-0135.

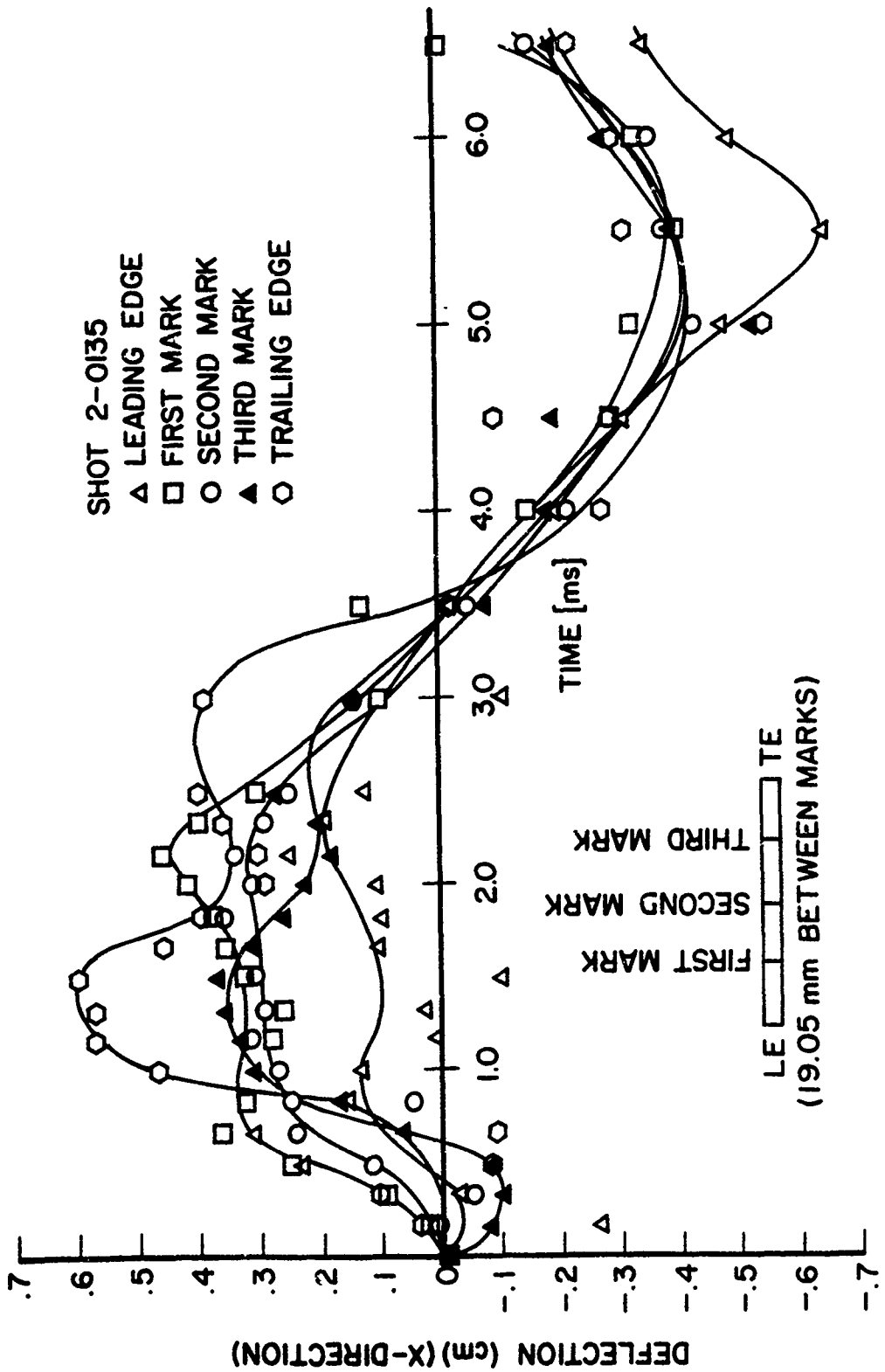

Figure 129. Deflection of Tip in "x" Direction for Shot 2-0135.

The typical strain curves for this group of specimens are given in Figures 130 through 135 for Shot 2-0149. As indicated earlier, no damage was received for this impact at 185 m/s with the bird impact mass of about 30.0 g. The strain gage locations are given in Figure 14A of Appendix A for this group of specimens. No dynamic displacement data from the high speed photography films were calculated for this group of specimens.

Figures 31B through 33B show photographs of the damage for Shots 2-0149, 2-0150, and 2-0151, respectively.

3.1.1.6 Impact Results for Group 16 Specimens

Four Group 16 boron/aluminum composite cross ply flat panel specimens with a blade-type aspect ratio and one-half blade-type thickness to chord ratio were impact tested in the study using the small 85 g (3 ounce) bird. The impacts were edge (slicing) impacts at the 70 percent span location at an impact angle of 18.9 degrees. The damage received ranged from general bending through the free span to breaking off at both the impact site and root. The impact velocities ranged from a low of 73 m/s to a high of 242 m/s. The impact mass ranged from 5.5 to 50.1 g for this series of tests.

Typical strain curves for this group of specimens are given in Figures 136 through 141 for Shot 2-0142. Figure 13A of Appendix A gives the strain gage locations for this group of specimens. The impact velocity of 71 m/s and bird impact mass of 5.5 g generated mild damage of bending through the span giving a plastic deformation of 0.40 cm (measured at the tip). Dynamic displacement data for Shot 2-0142 calculated from the high speed films are given in Figures 142 through 144 for the "y", "x" and resultant directions, respectively.

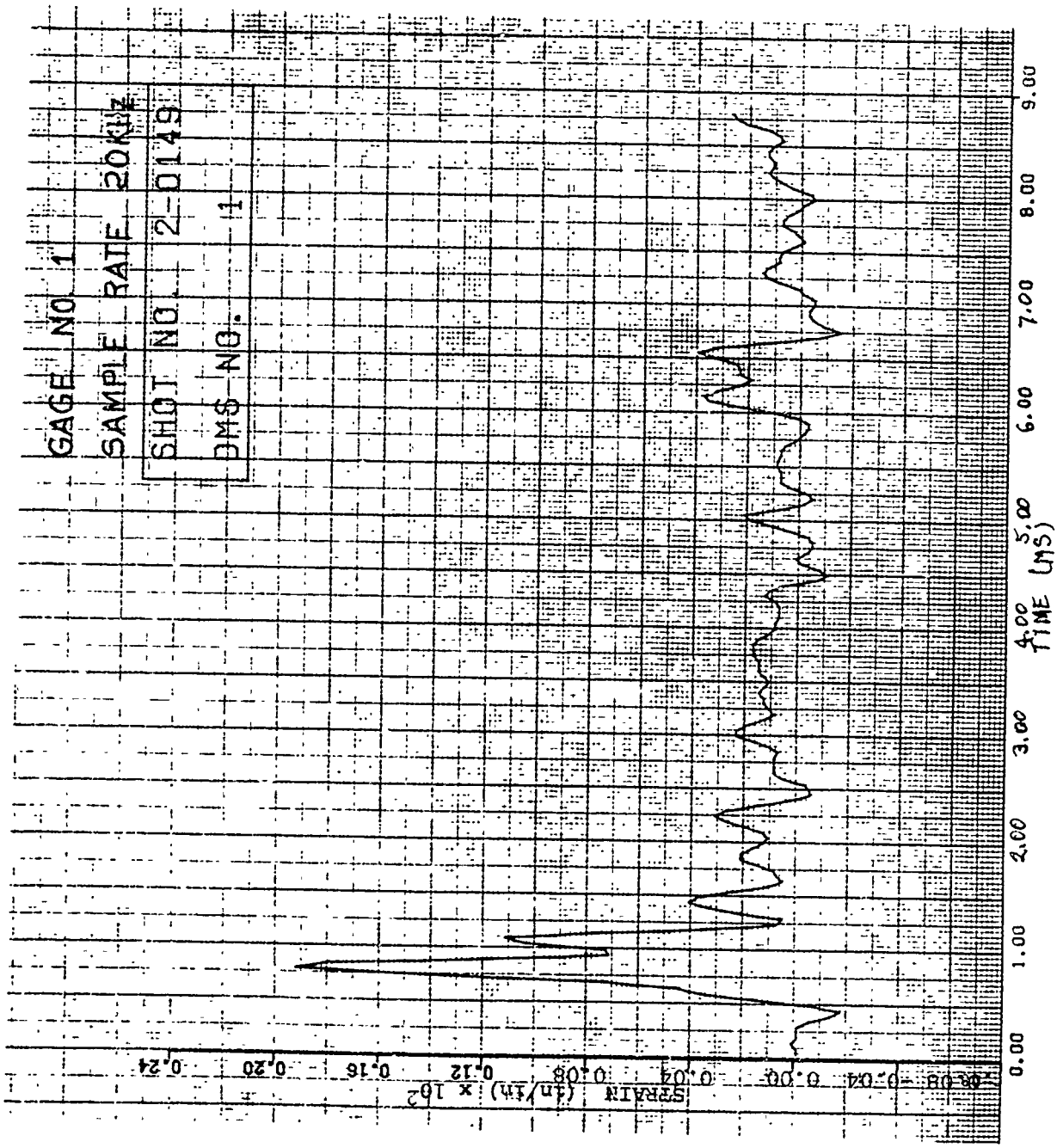

Figure 130. Strain of Shot 2-0149 for Gage #1.

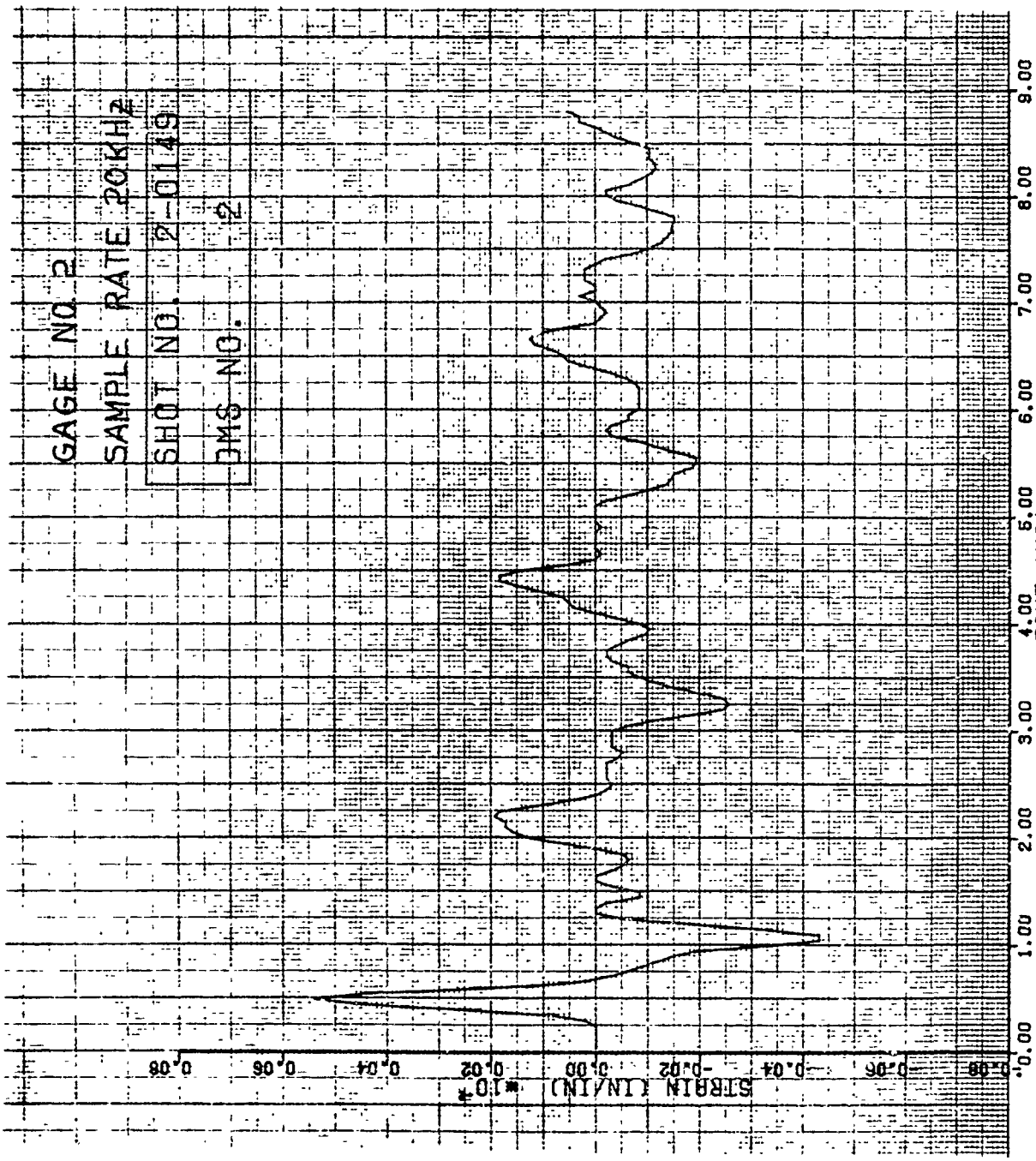

Figure 131. Strain of Shot 2-0149 for Gage #2.

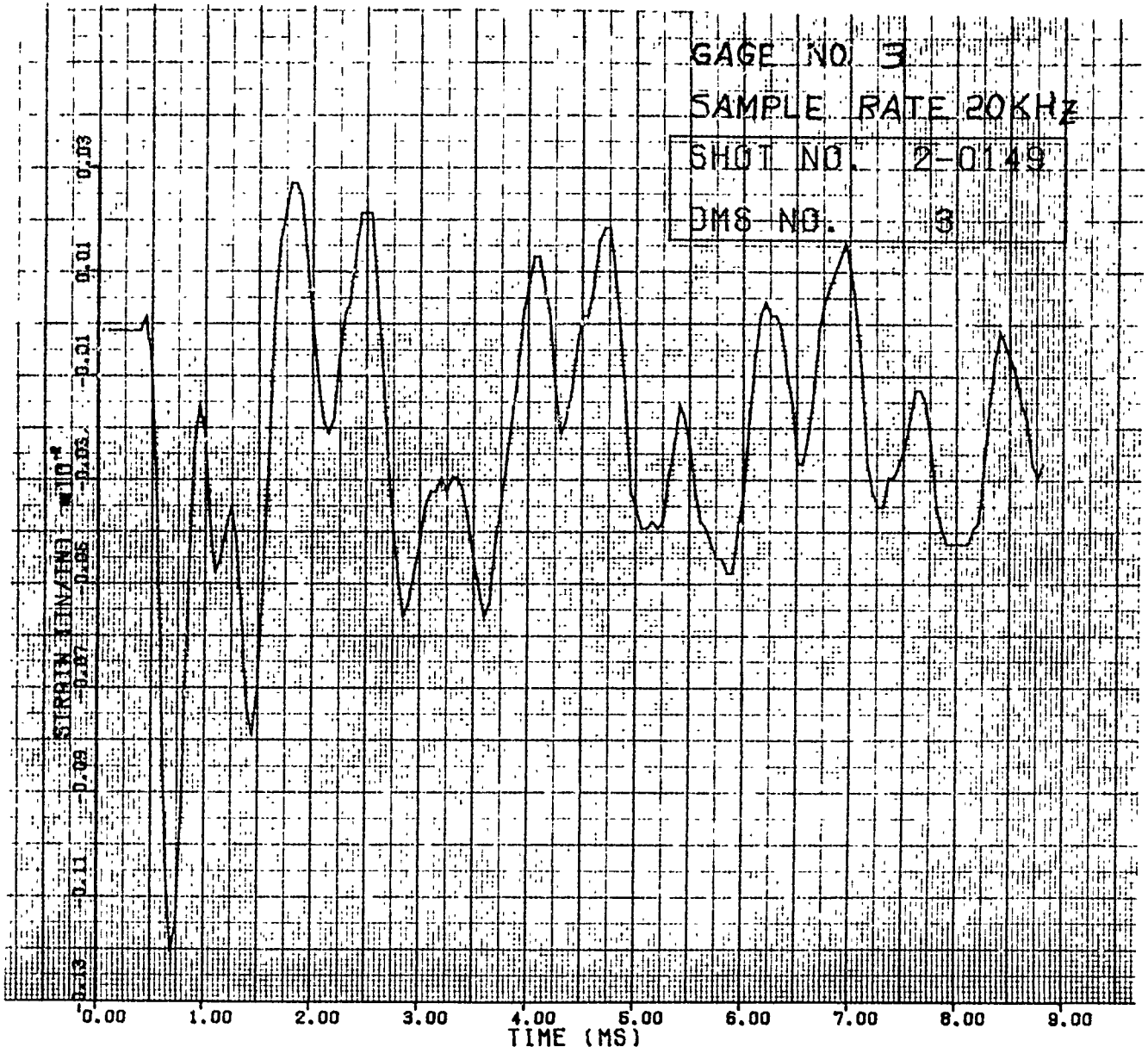

Figure 132. Strain of Shot 2-0149 for Gage #3.

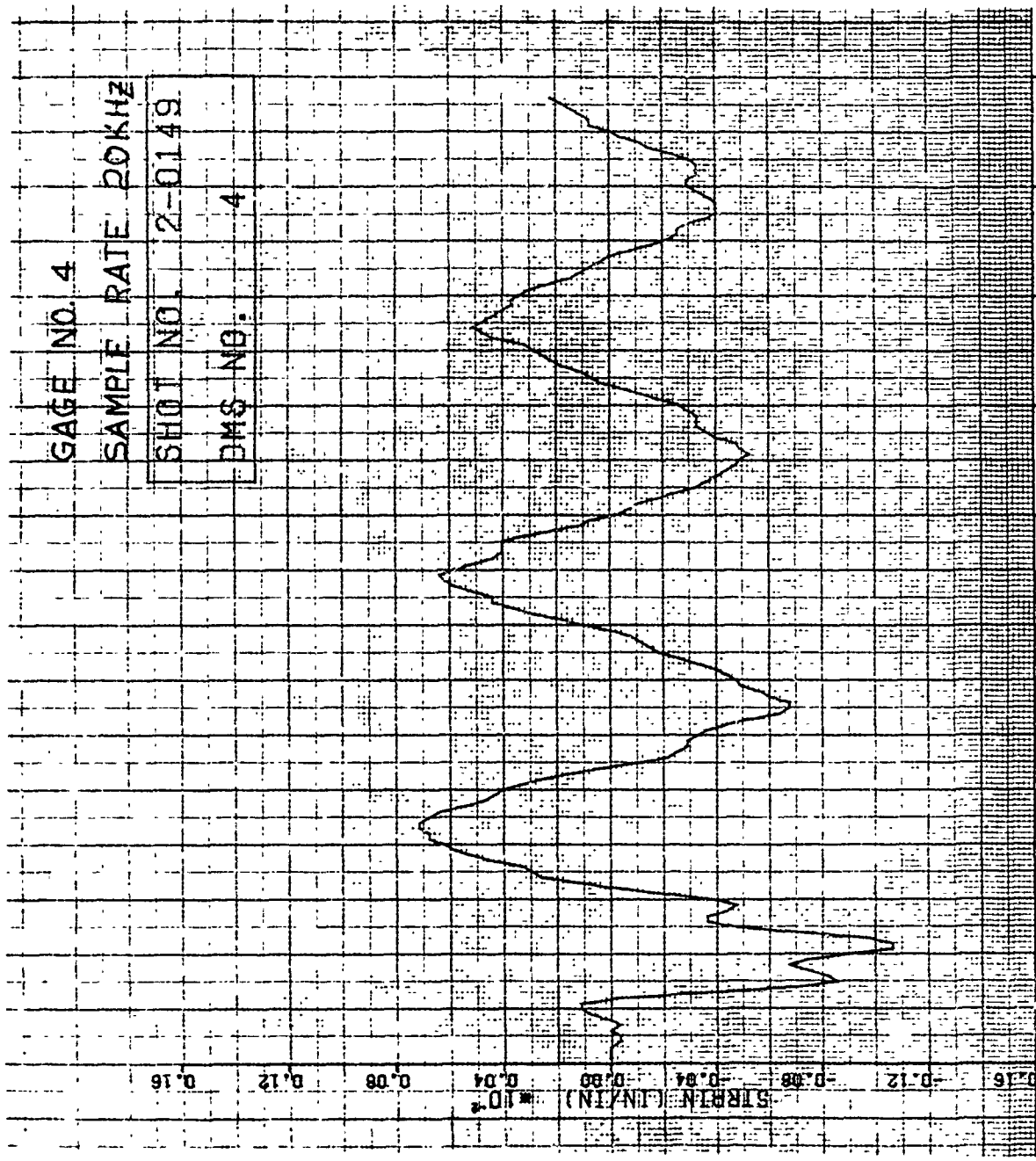

Figure 133. Strain of Shot 2-0149 for Gage #4.

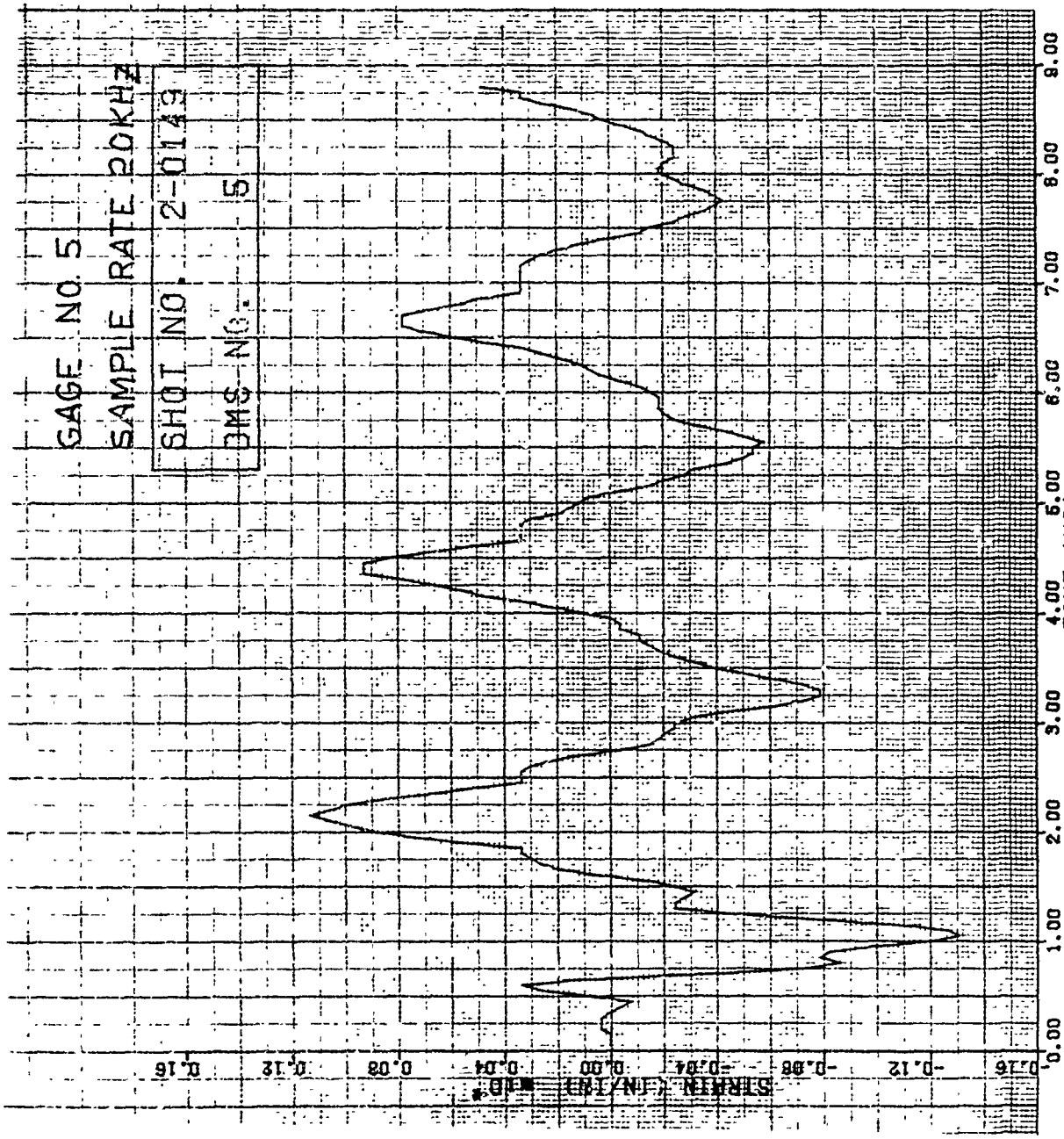

Figure 134. Strain of Shot 2-0149 for Gage #5.

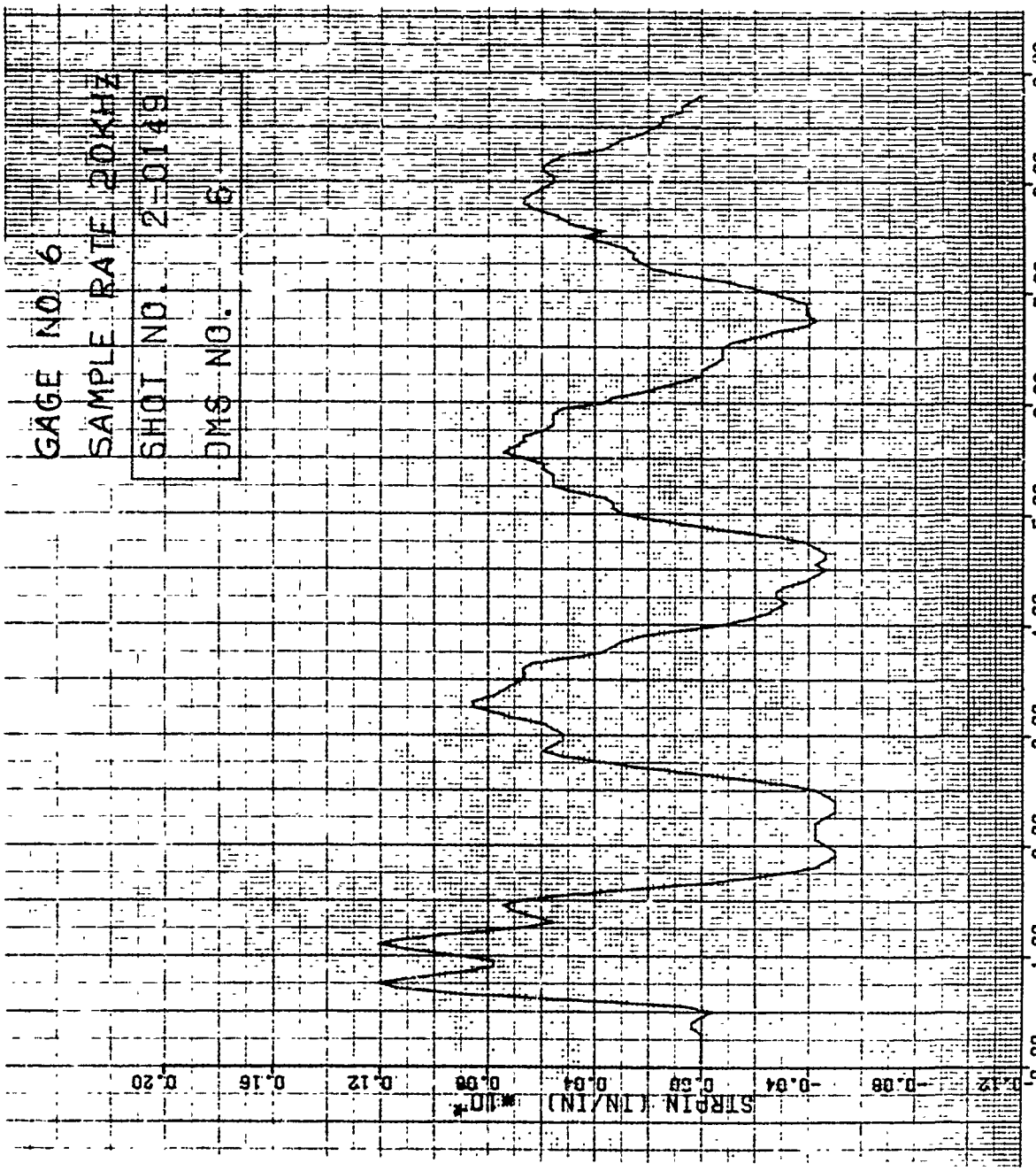

Figure 135. Strain of Shot 2-0149 for Gage #6.

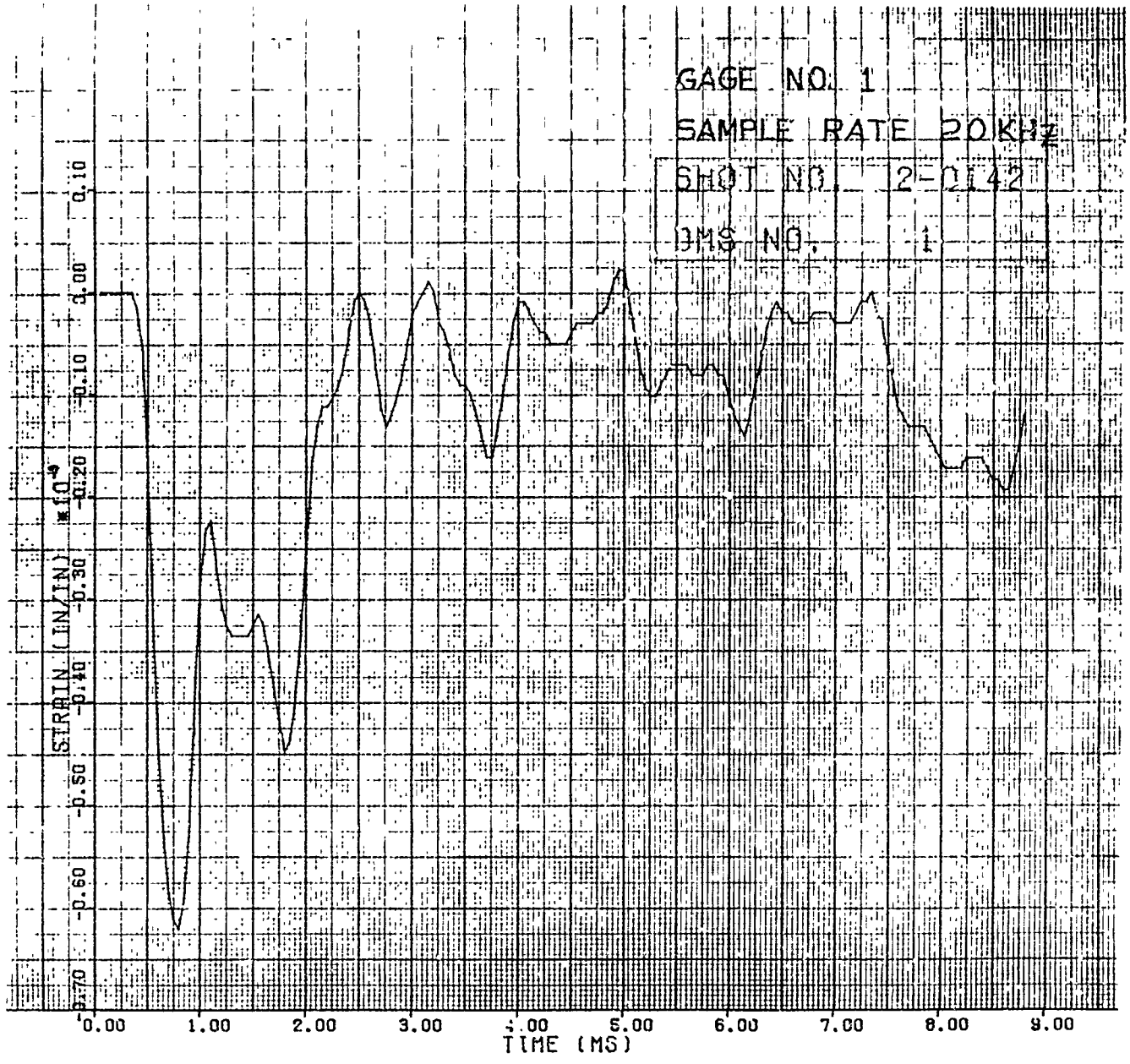

Figure 136. Strain of Shot 2-0142 for Gage #1.

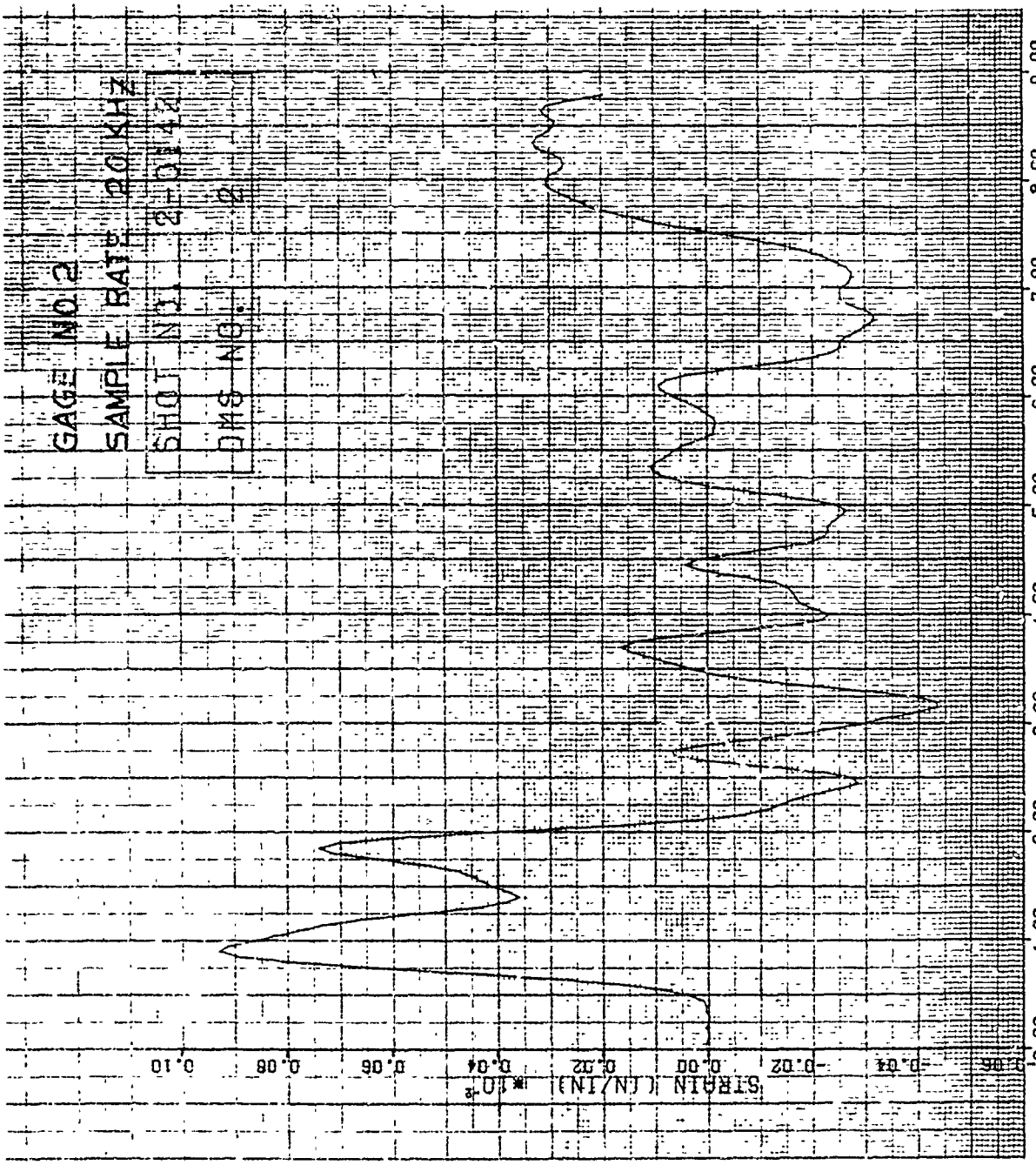

Figure 137. Strain of Shot 2-J142 for Gage #2.

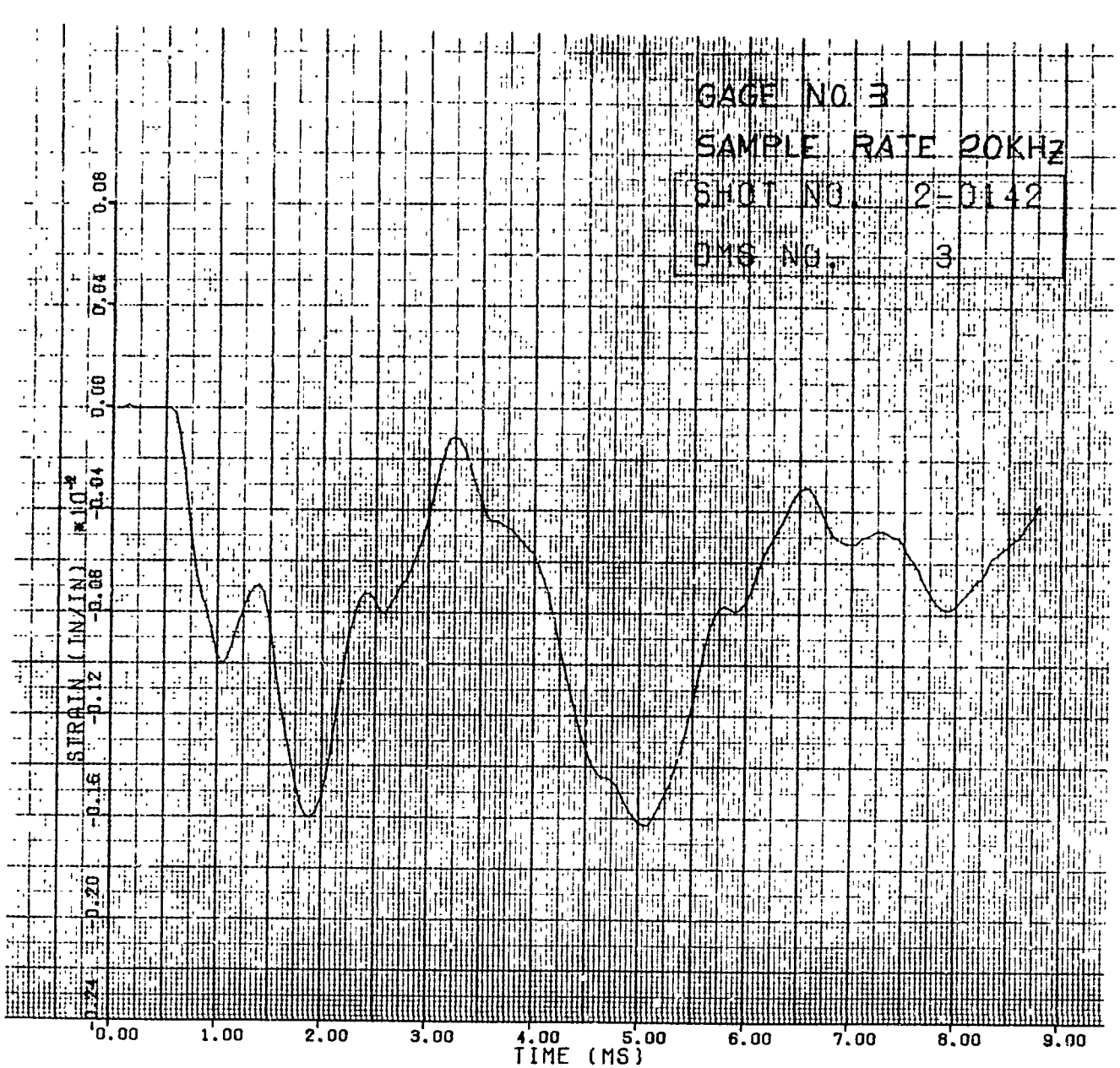

Figure 138. Strain of Shot 2-0142 for Gage #3.

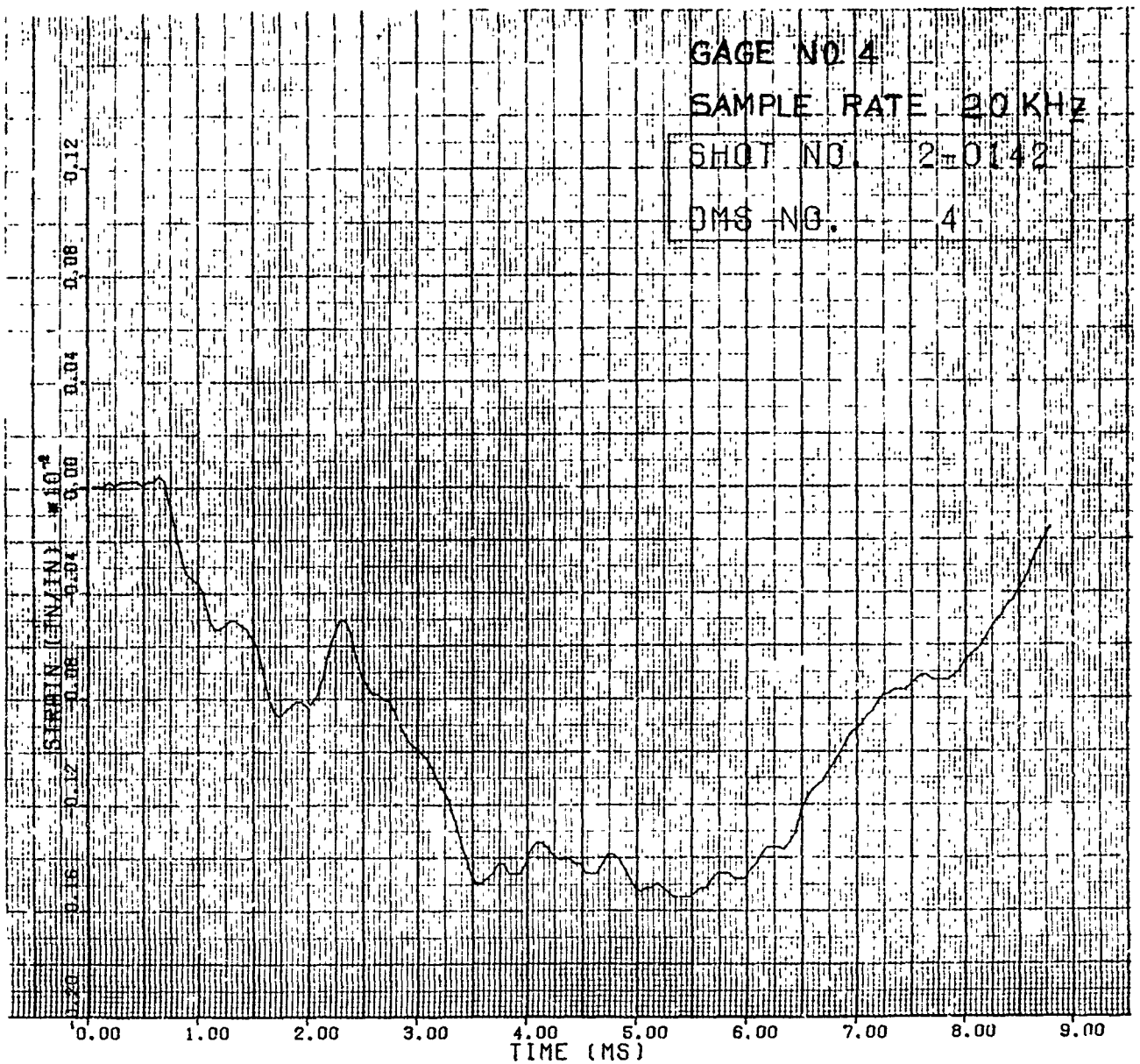

Figure 139. Strain of Shot 2-0142 for Gage #4.

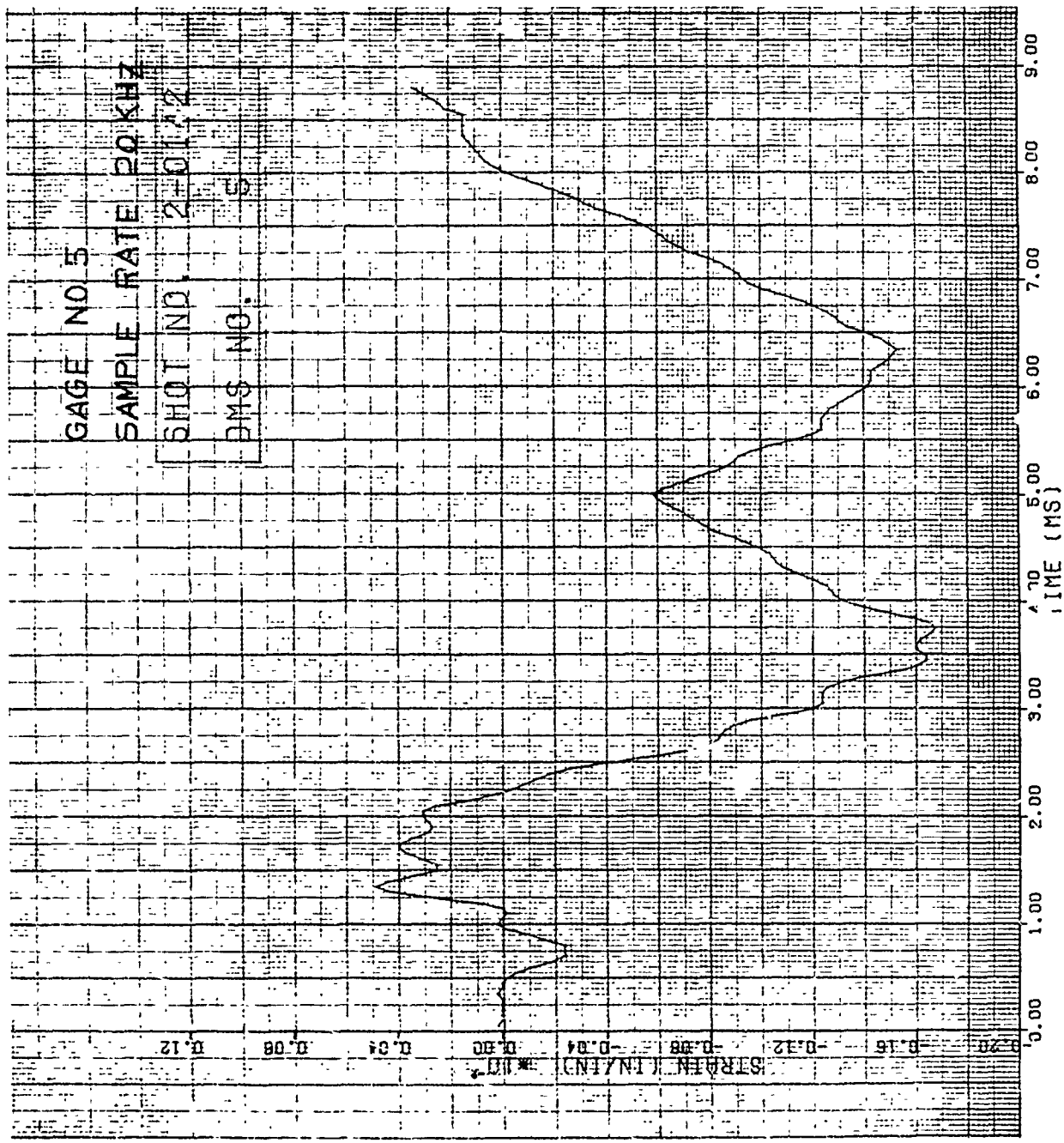

Figure 140. Strain of Shot 2-0142 for Gage #5.

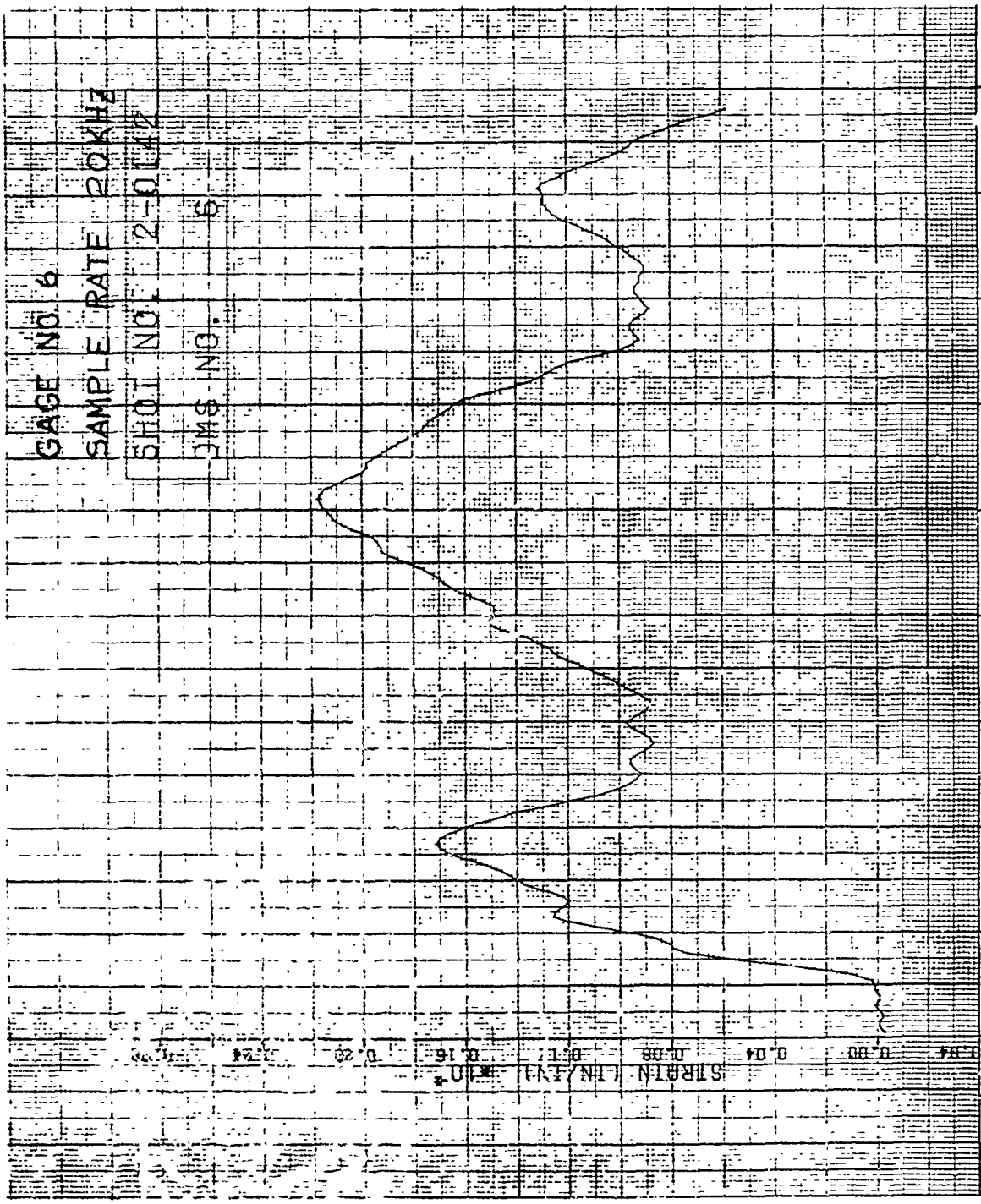

Figure 141. Strain of Shot 2-0142 for Gage #6.

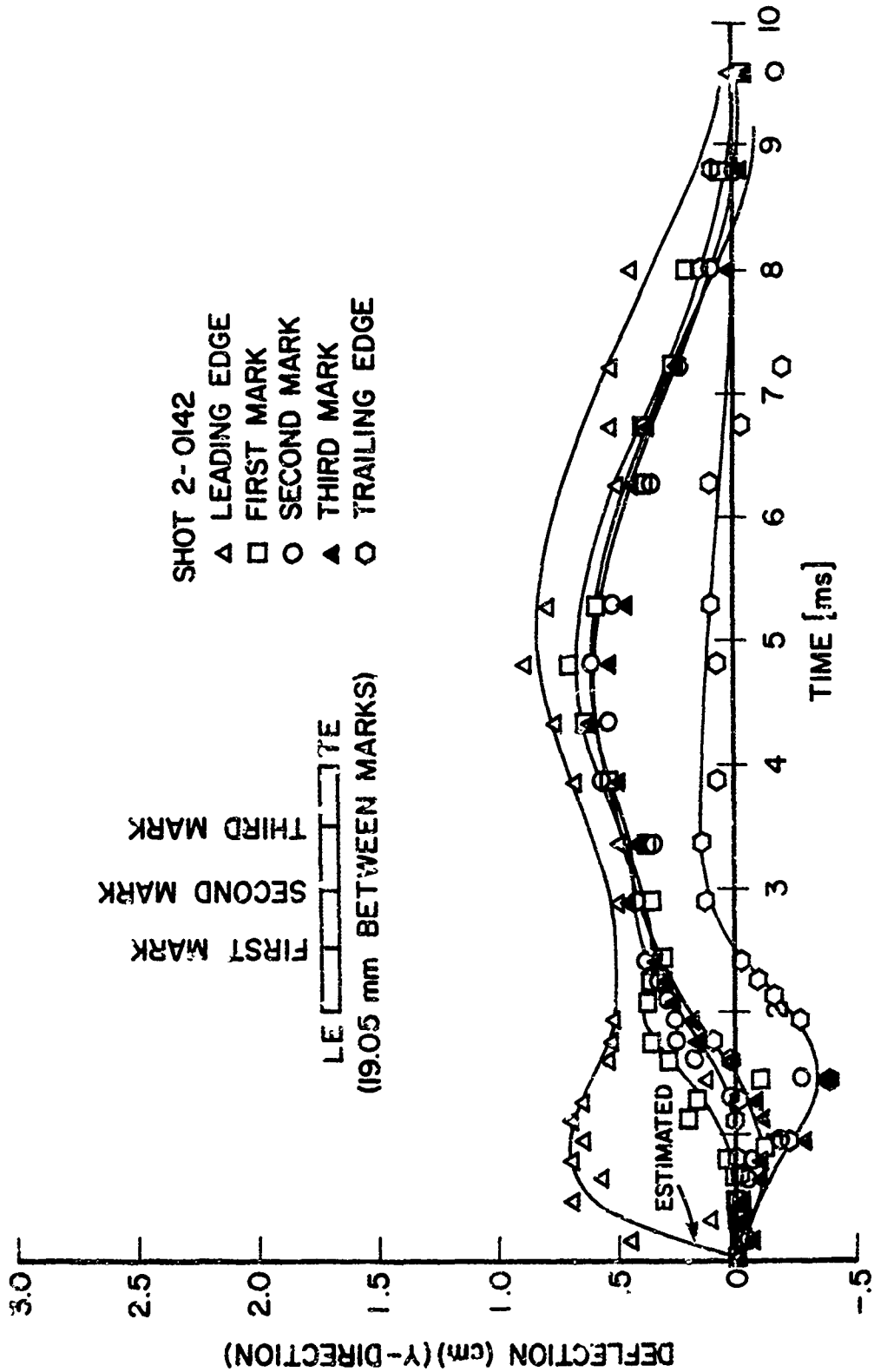

Figure 142. Deflection of Tip in "y" Direction for Shot 2-0142.

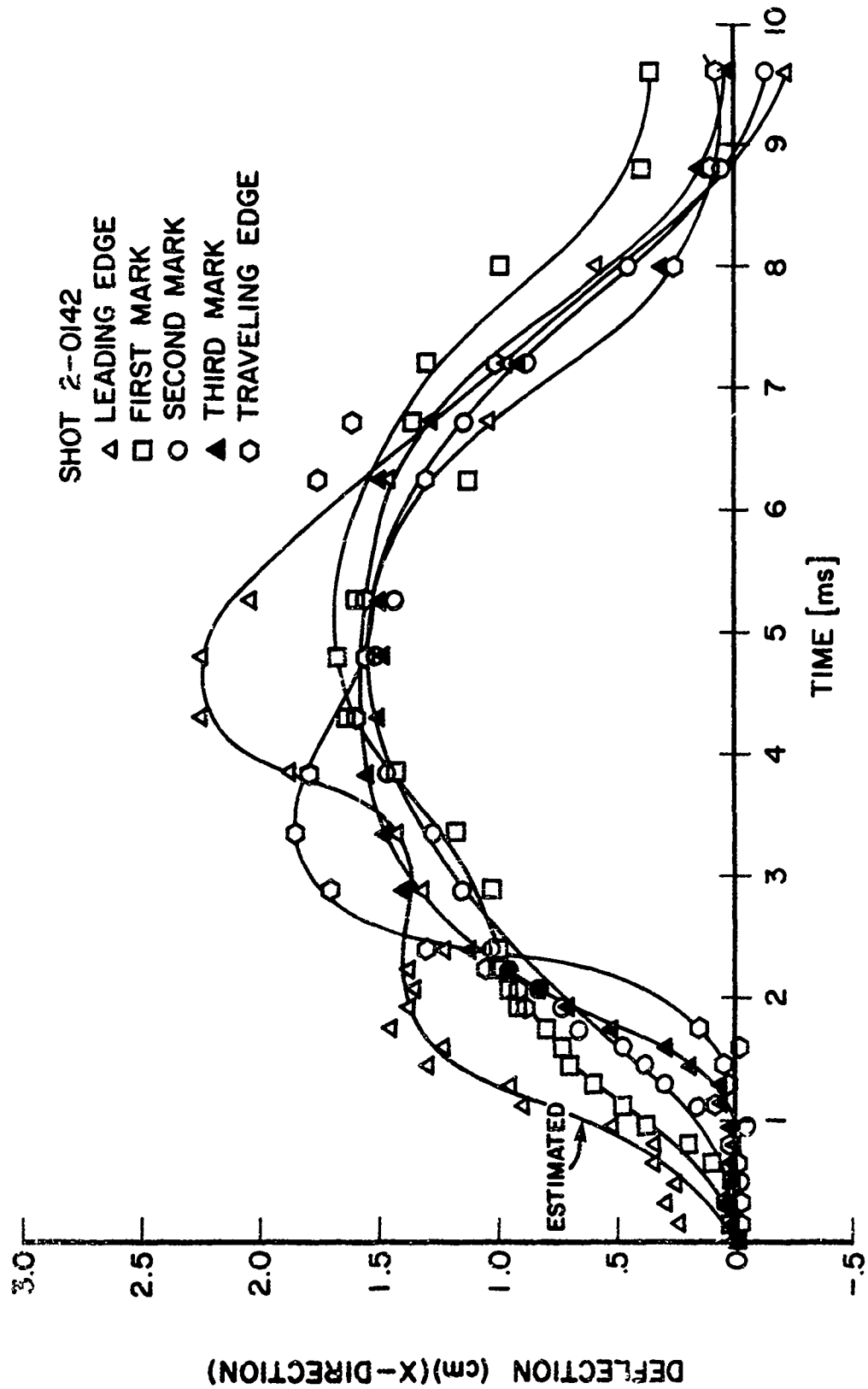

Figure 143. Deflection of Tip in "x" Direction for Shot 2-0142.

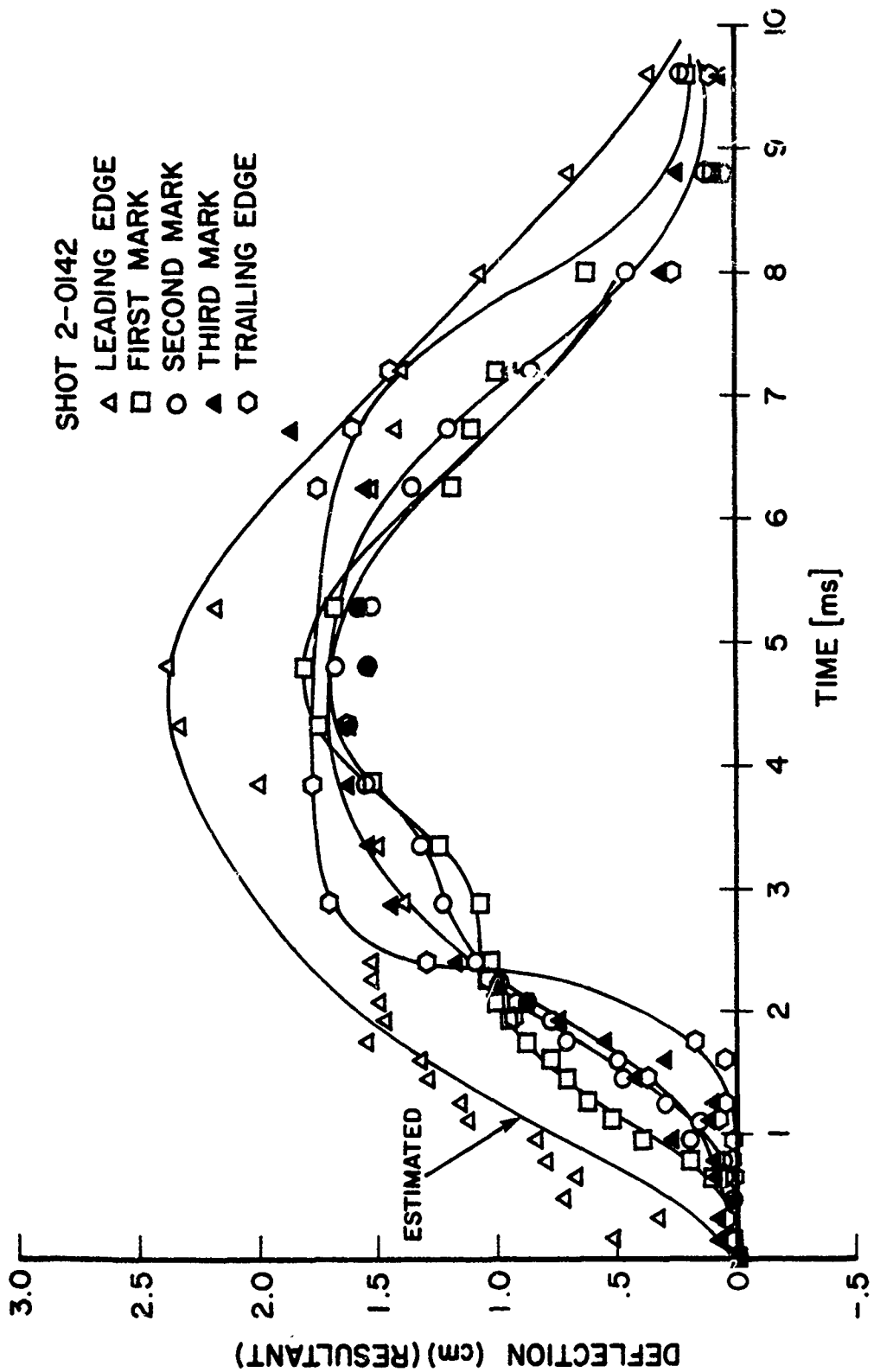

Figure 144. Tip Deflection Resultant for Shot 2-0142.

Figures 34B through 37B give photographs of the damage for the four specimens impacted in this group.

3.1.1.17 Impact Results for Group 17 Specimens

Eight Group 17 boron/aluminum composite cross ply panel specimens with a blade-type aspect ratio and blade-like cross section were impacted by the small 85 g (3 ounce) artificial bird. The impacts were edge (slicing) impacts at the 70 percent span location and at an impact angle of 18.9 degrees. No visible damage on the specimens were received for seven of the impacts ranging in velocities from 79 to 194 m/s and an impact mass as high as 8.0 grams. Very severe damage by the specimen breaking into many pieces at the impact site was received for an impact where the velocity was 247 m/s and the impact mass 31.7 g (Shot 2-0213).

Typical strain curves for this series of impacts are given in Figures 145 through 150 for Shot 2-0212. Figure 15A of Appendix A gives the strain gage locations for this group of specimens. An impact velocity of 194 m/s with an impact mass of 8.0 g (Shot 2-0212) generated no visible damage on the specimen. Figures 151 and 152 give the dynamic displacement plots for the "y" and "x" directions, respectively.

Figure 38B shows the specimen damage received for Shot 2-0213 (247 m/s velocity and 31.7 g impact mass).

3.1.1.18 Impact Results for Group 18 Specimens

Three Group 18 boron/aluminum composite cross ply flat panel specimens with a blade-type aspect ratio and camber were impact tested using the small 85 g (3 ounce) substitute bird for this series of tests. The impacts were edge (slicing) impacts at the 70 percent span location and at an impact angle of 18.9 degrees. No visible damage was received for two of the impacts at impact velocities of 139 and 203 m/s with bird impact masses of 3.1 and 6.7 g, respectively.

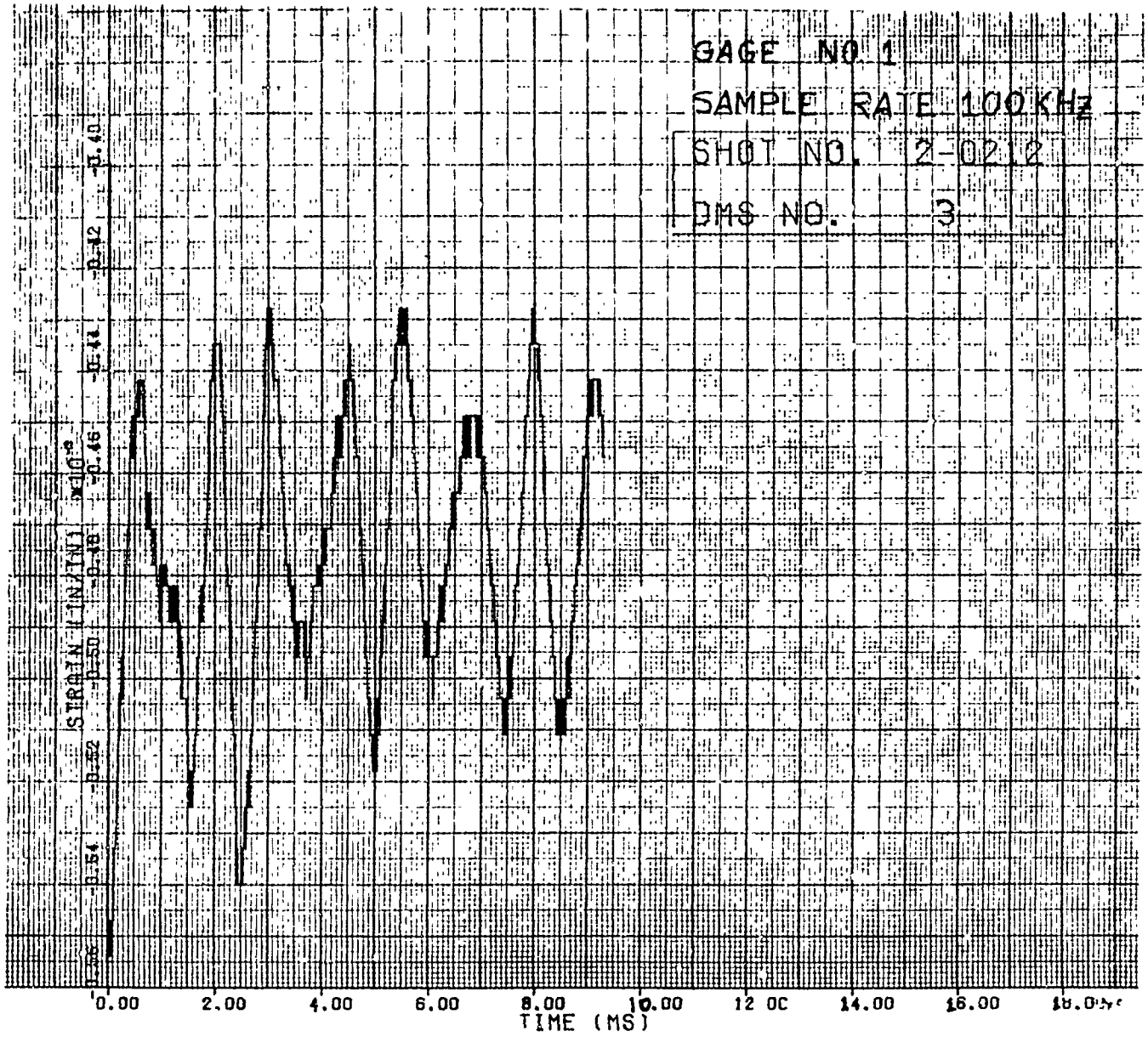

Figure 145. Strain of Shot 2-0212 for Gage #1.

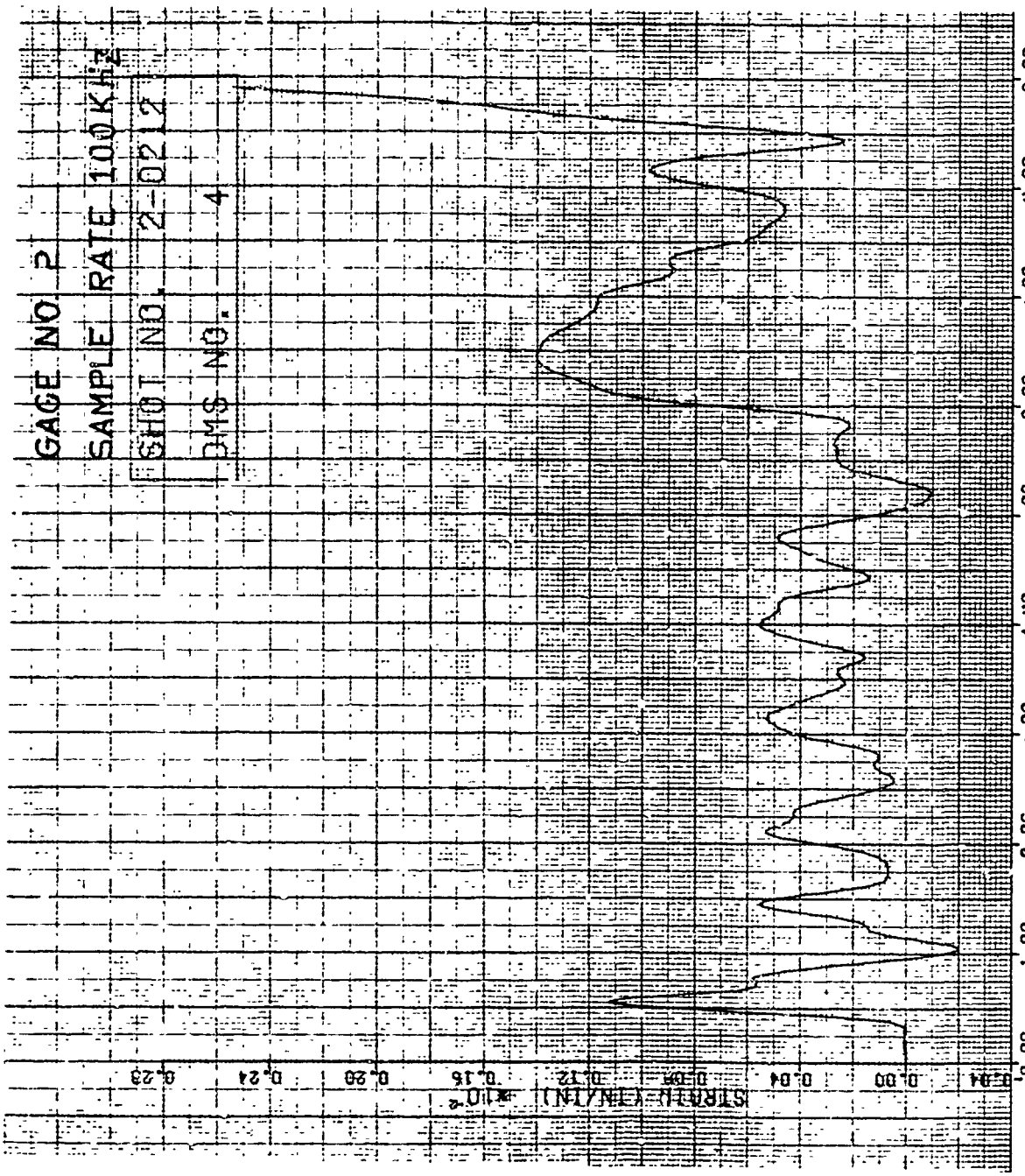

Figure 146. Strain of Shot 2-0212 for Gage #2.

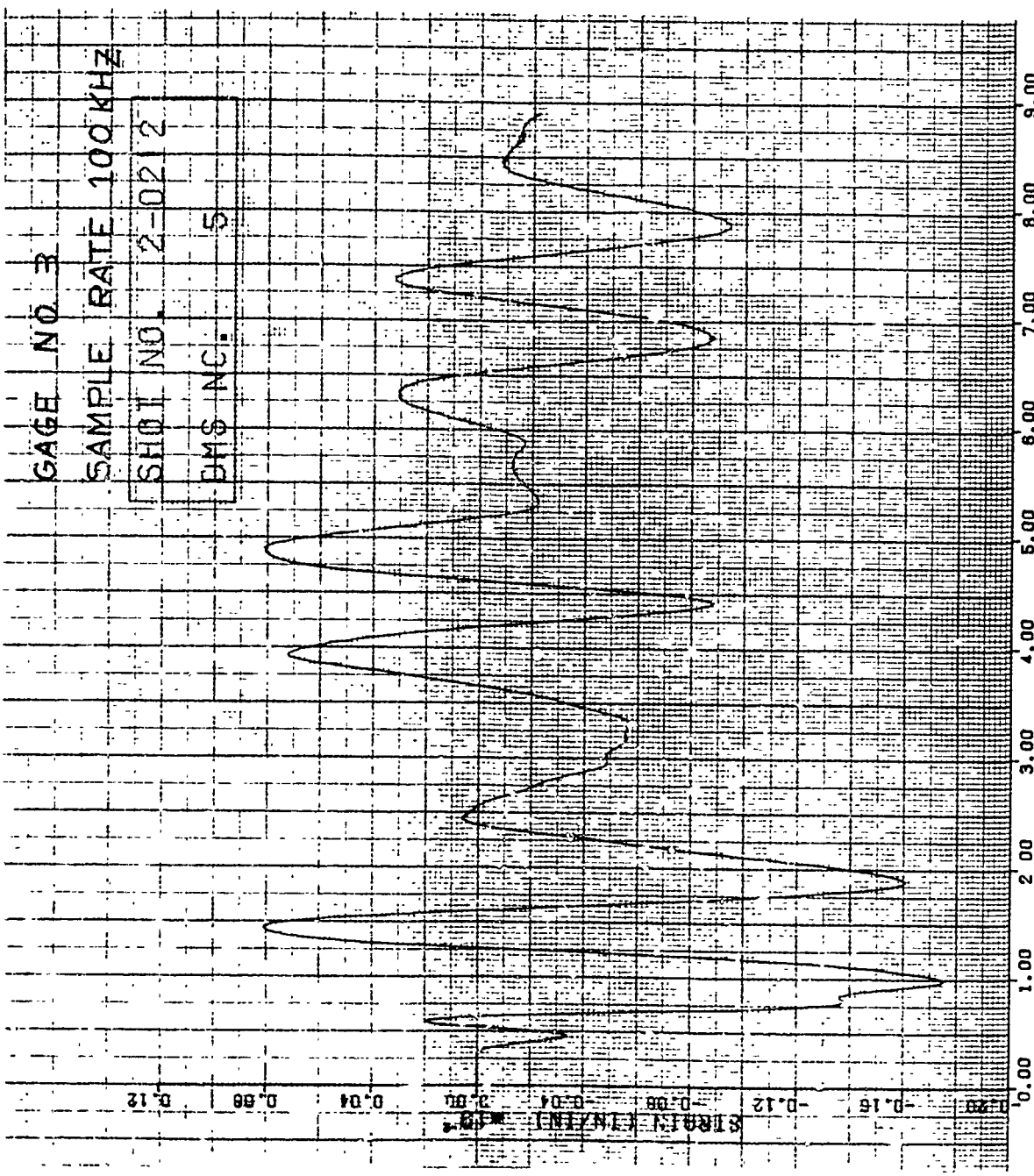

Figure 147. Strain of Shot 2-0212 for Gage #3.

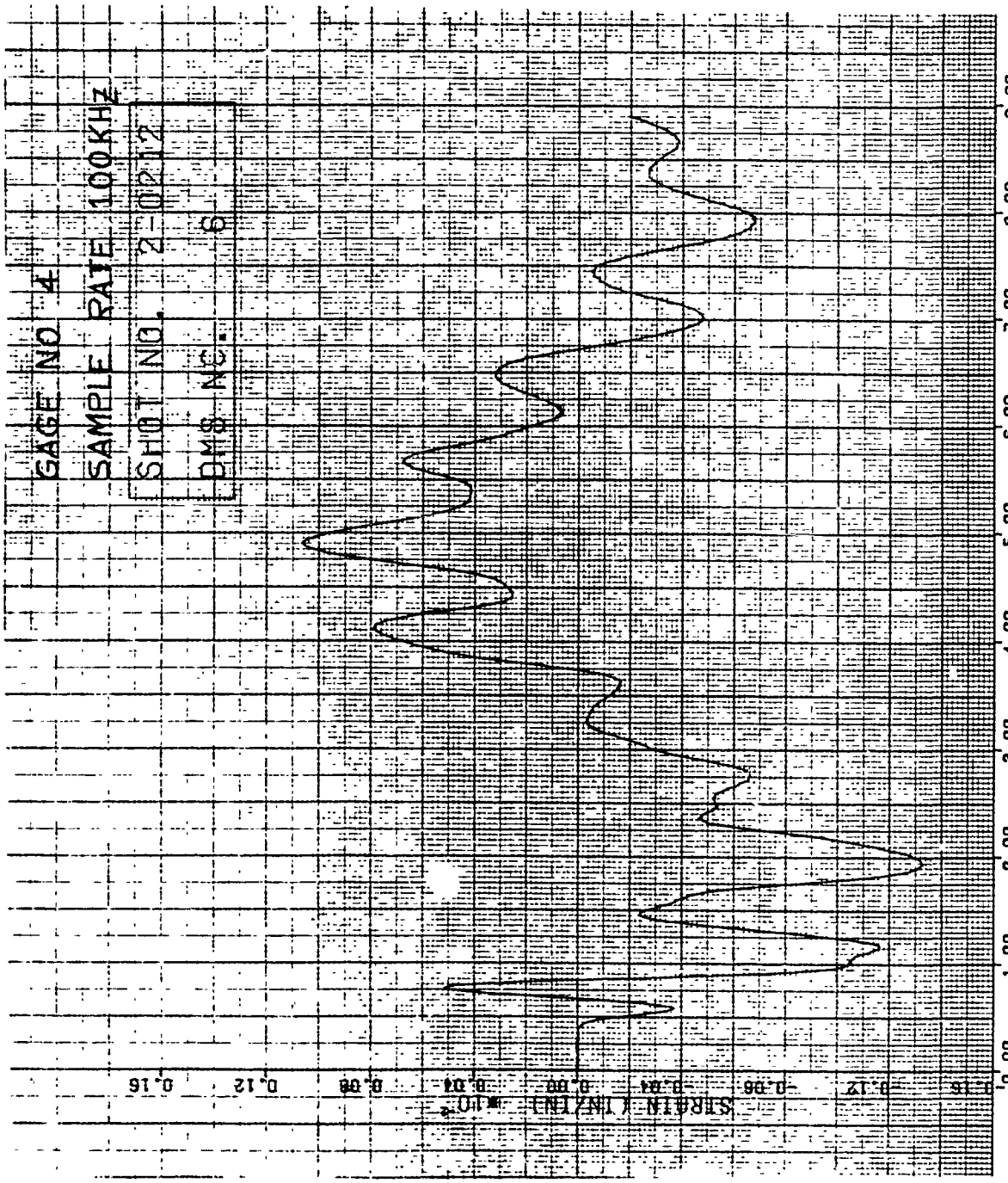

Figure 148. Strain of Shot 2-0212 for Gage #4.

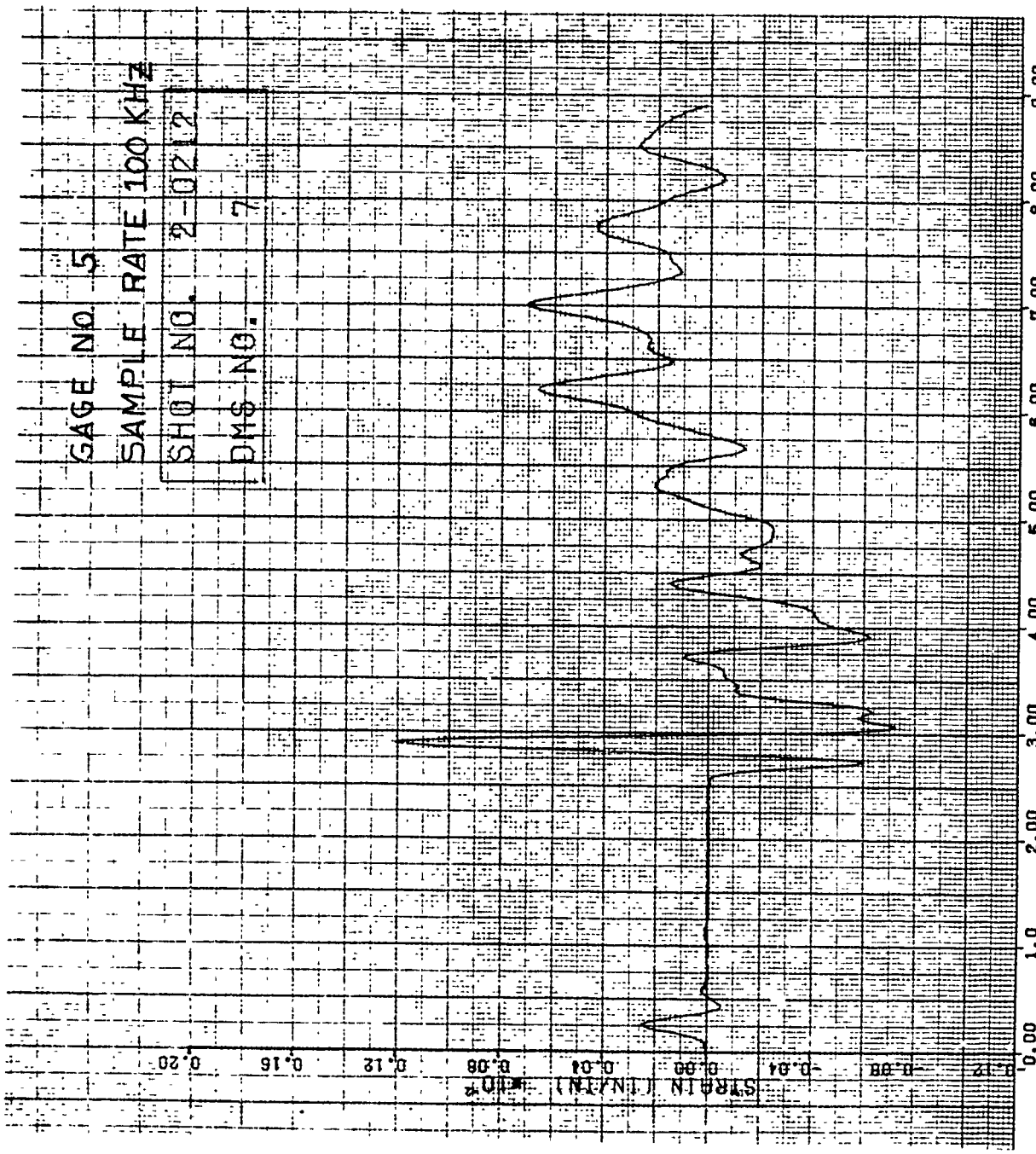

Figure 149. Strain of Shot 2-0212 for Gage #5.

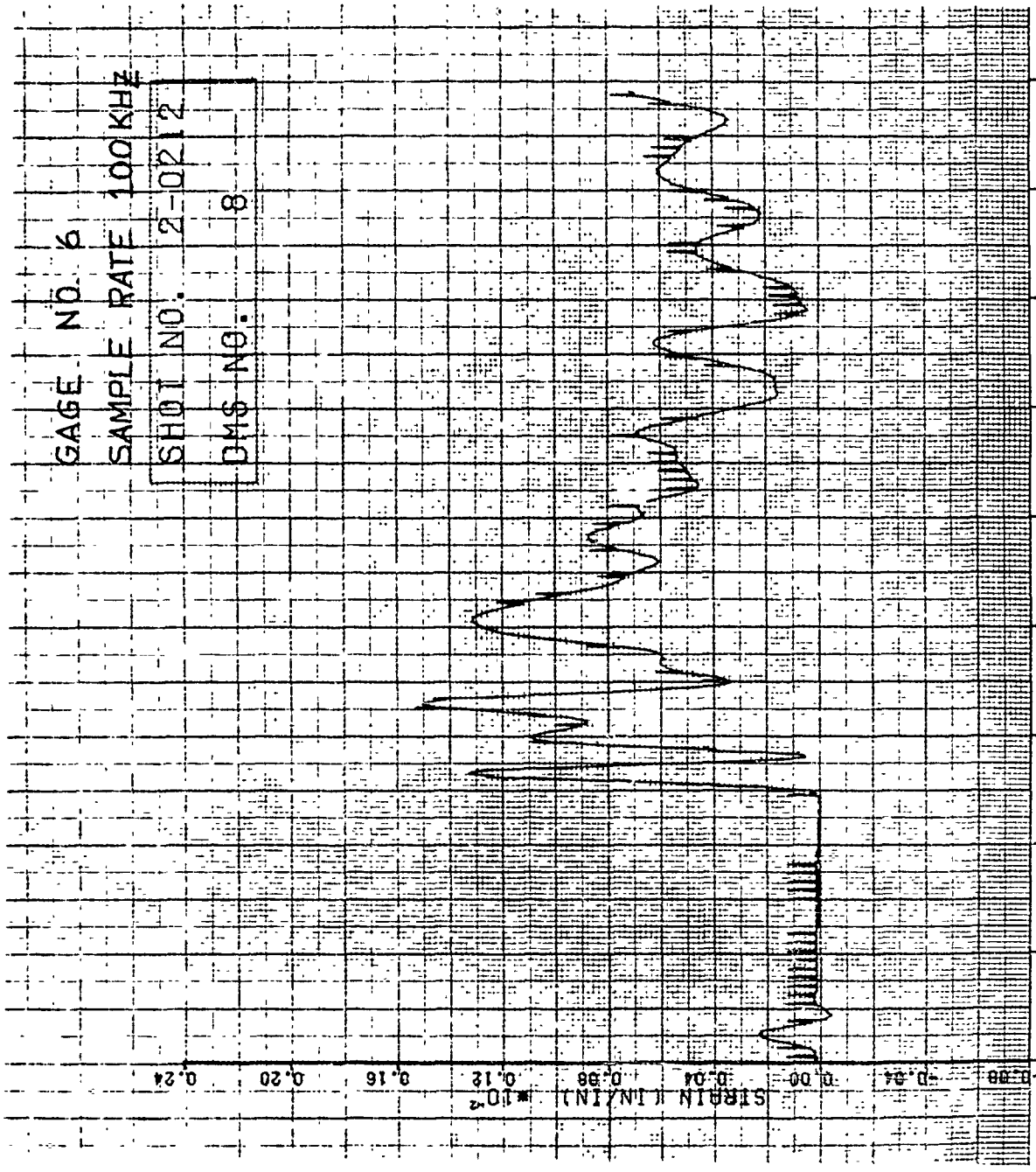

Figure 150. Strain of Shot 2-0212 for Gage #6.

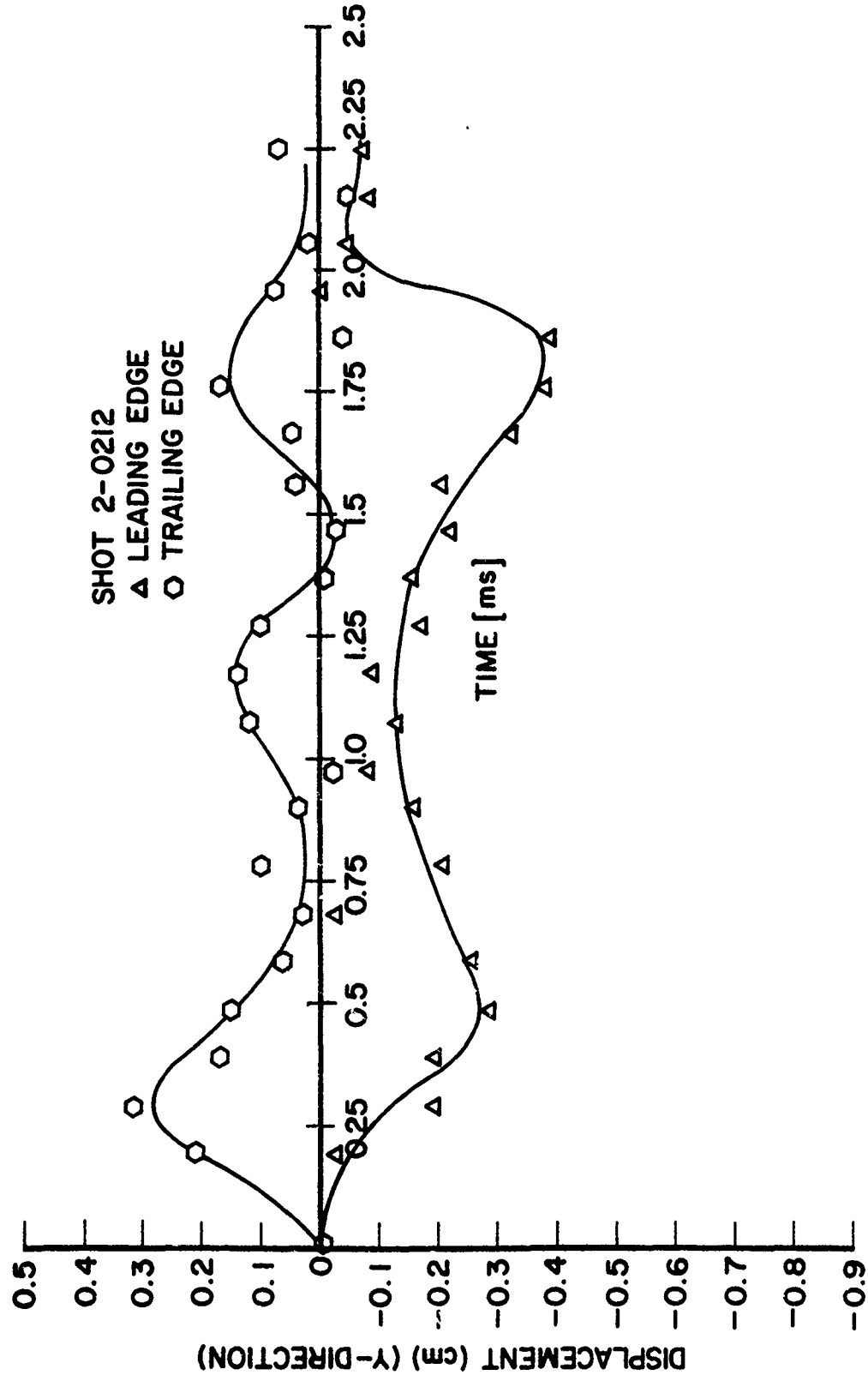

Figure 151. Tip Deflection in "y" Direction for Shot 2-0212.

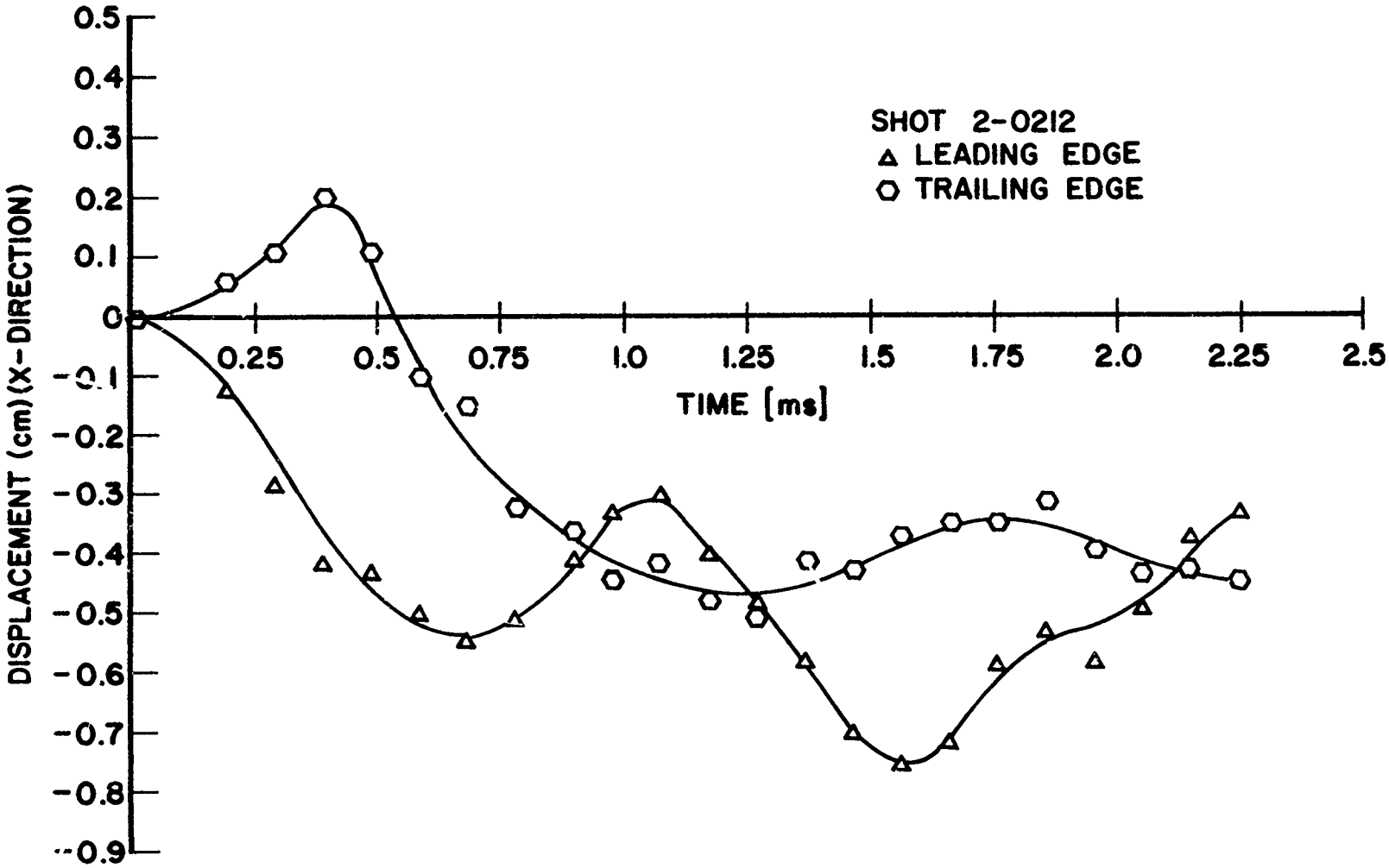

Figure 152. Tip Deflection in "y" Direction for Shot 2-0212.

The specimen that was damaged broke off at the root and also just below the impact site at a velocity of 320 m/s and a bird impact mass of 35.6 g (Shot 2-0145).

The typical strain curves for this series of tests are given in Figures 153 through 158 for Shot 2-0144 (203 m/s velocity and 6.7 g bird mass). Figure 16A of Appendix A gives the strain gage locations for the specimens in this series of tests. As indicated earlier, no visible damage was detected on the specimen for this impact. Dynamic displacement curves calculated from the high speed films are given for Shot 2-0144 in Figures 159 through 161 ("y", "x", and resultant directions, respectively).

Figures 39B and 40B show the specimen damage received from Shots 2-0144 and 2-0145, respectively.

3.1.1.19 Impact Results for Group 19 Specimens

Three Group 19 boron/aluminum composite cross ply flat panel specimens with a blade-type aspect ratio camber and twist were impact tested using the small 85 g (3 ounce) artificial bird for this series of tests. The impacts were edge (slicing) impacts at the 70 percent span location and at an impact angle of 18.9 degrees. Two of the specimens received severe damage by breaking off at the root for Shots 2-0146 and 2-0148. The test conditions were 209 and 186 m/s with impact masses of 47.0 and 33.1 g, respectively. The remaining specimen impact (Shot 2-0147) had no visible damage evident at a velocity of 159 m/s and an impact mass of 11.2 g.

Expanded strain curves for Shot 2-0147 (no damage received) are given in Figures 162 through 167. Figure 16A of Appendix A gives the strain gage locations for this series of specimen impacts. Figures 168 through 170 present dynamic displacement data during the impact event for Shot 2-0147. The curves are plotted for the "y", "x", and resultant directions, respectively.

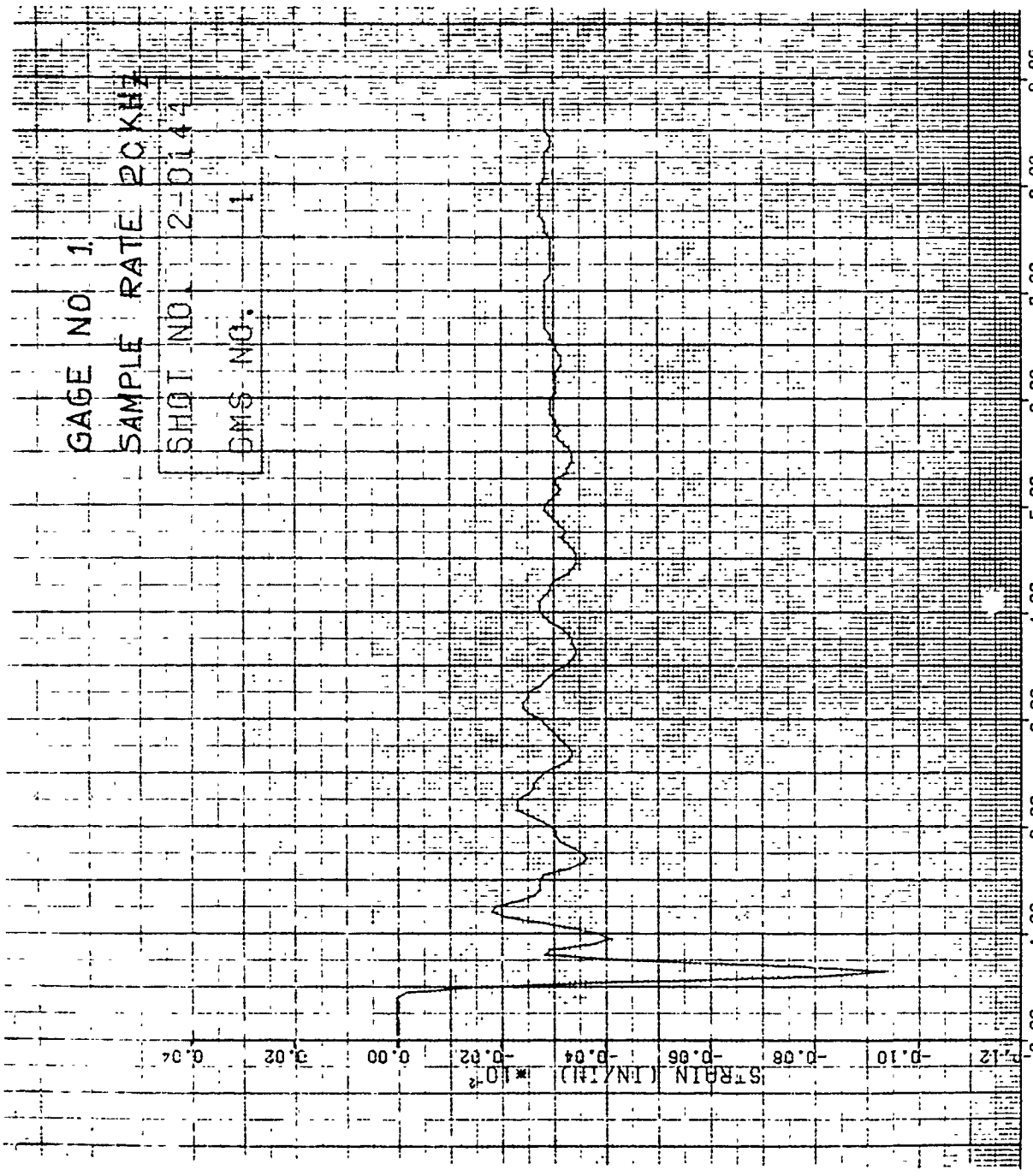

Figure 153. Strain of Shot 2-0144 for Gage #1.

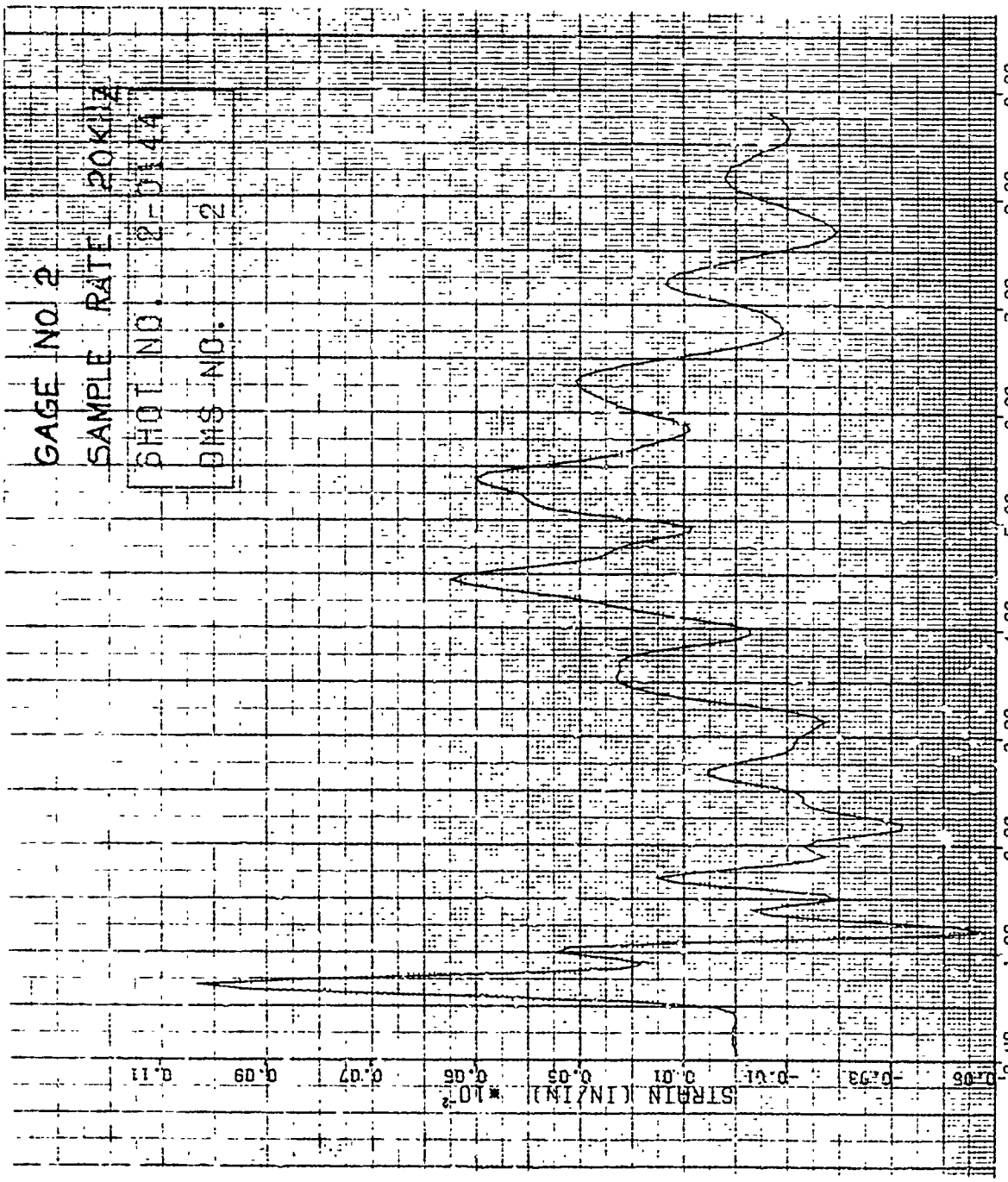

Figure 154. Strain of Shot 2-0144 for Gage #2.

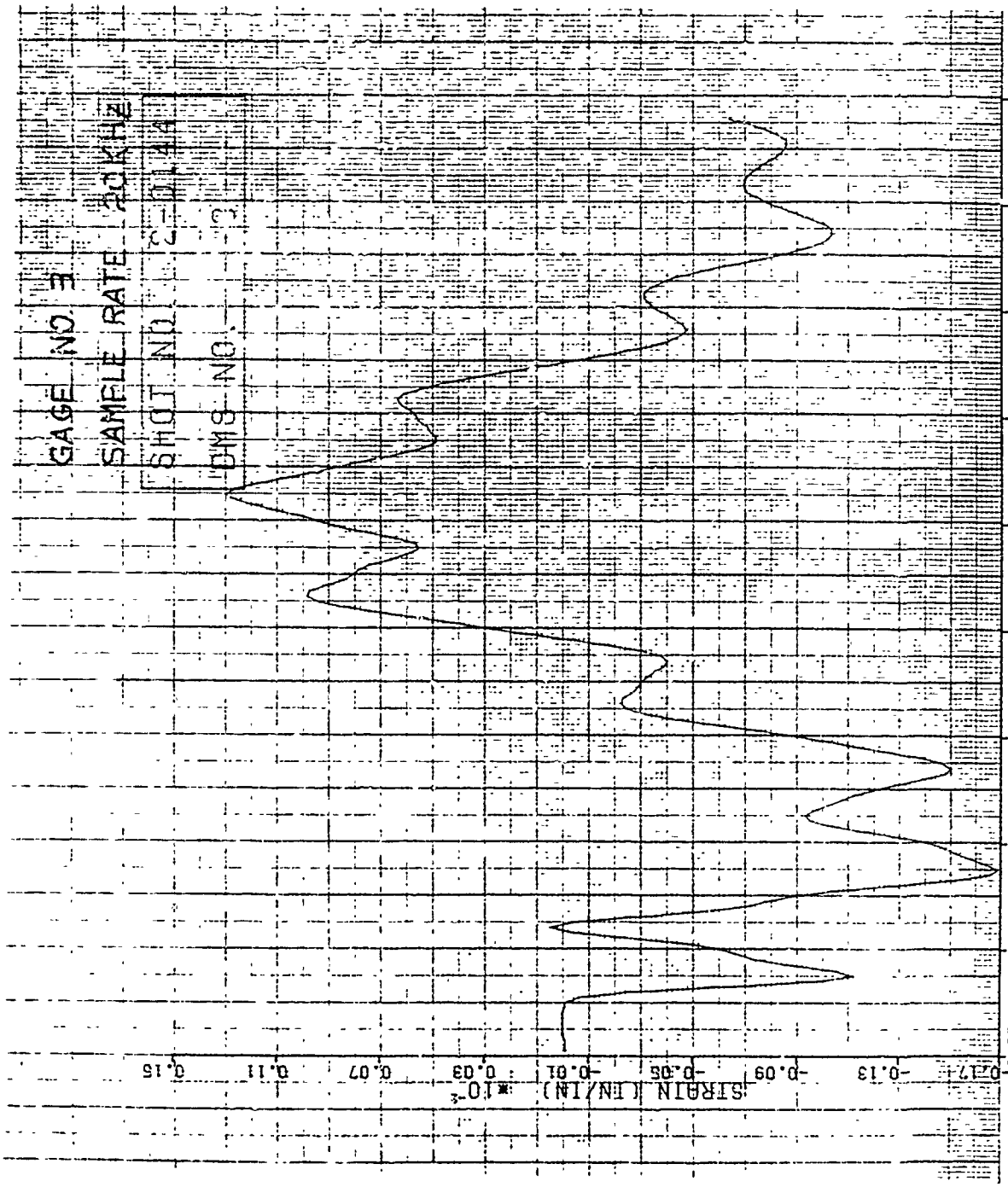

Figure 155. Strain of Shot 2-0144 for Gage #3.

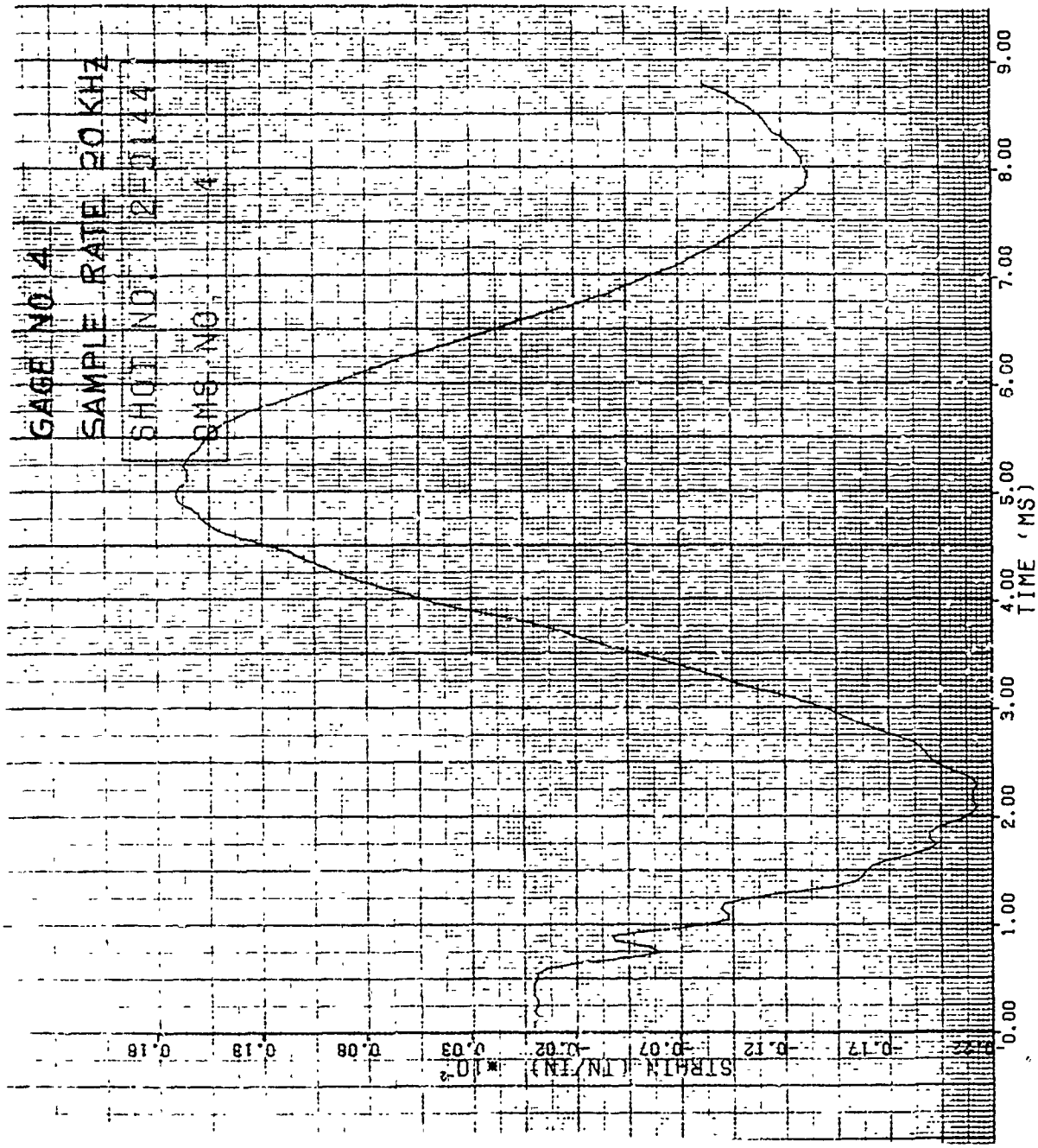

Figure 156. Strain of Shot 2-0144 for Gage #4.

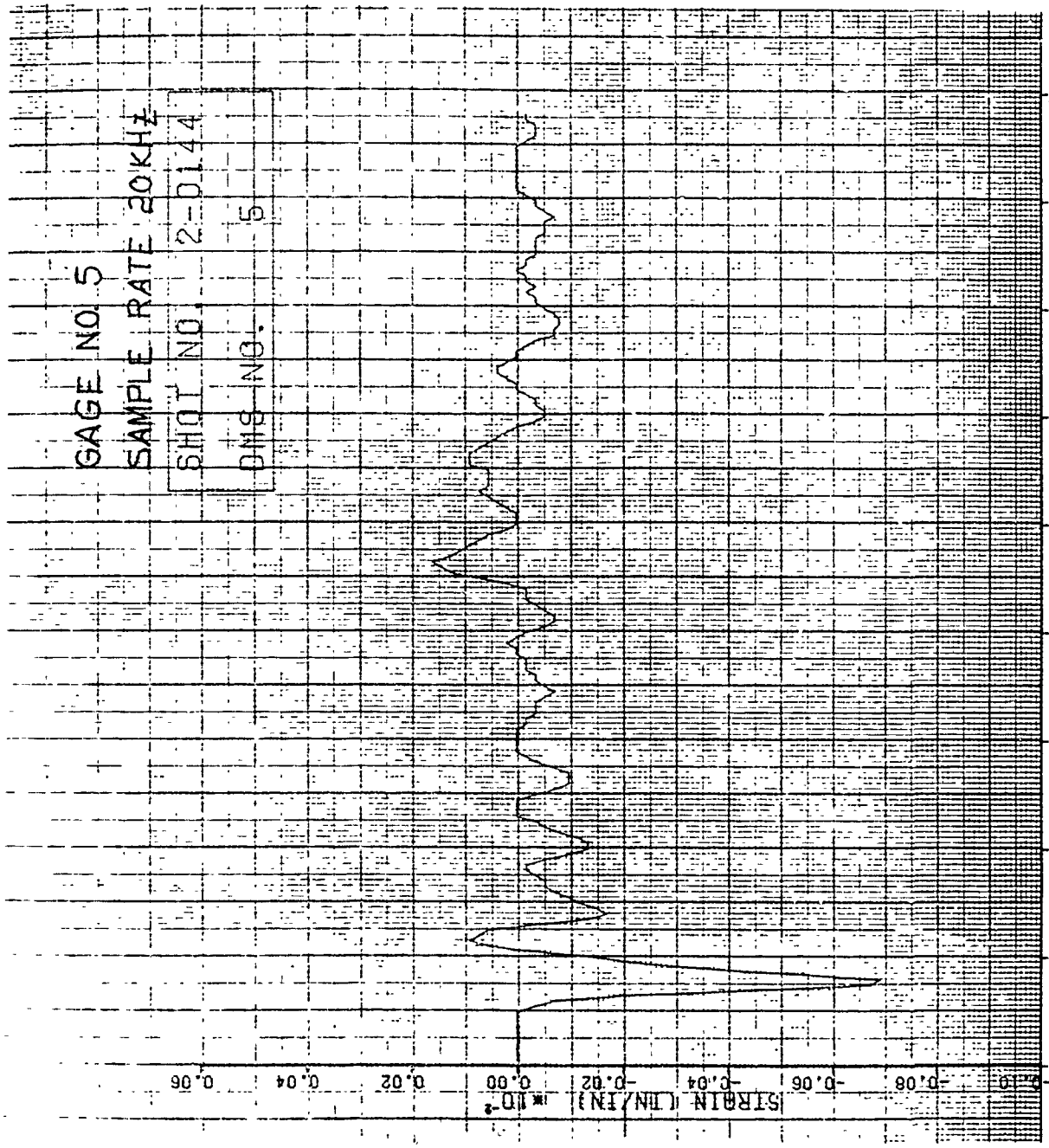

Figure 157. Strain of Shot 2-0144 for Gage #5.

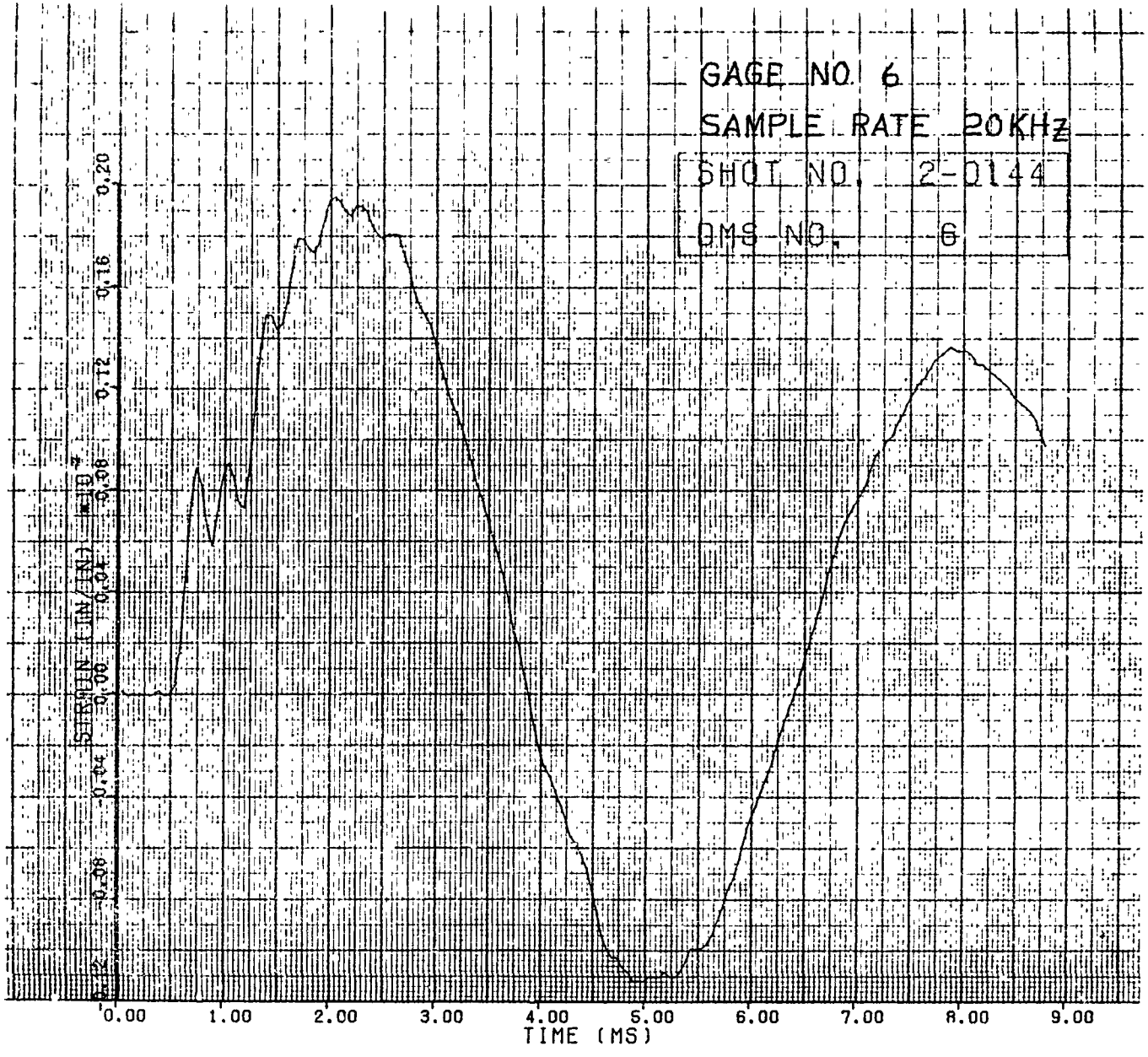

Figure 158. Strain of Shot 2-0144 for Gage #6.

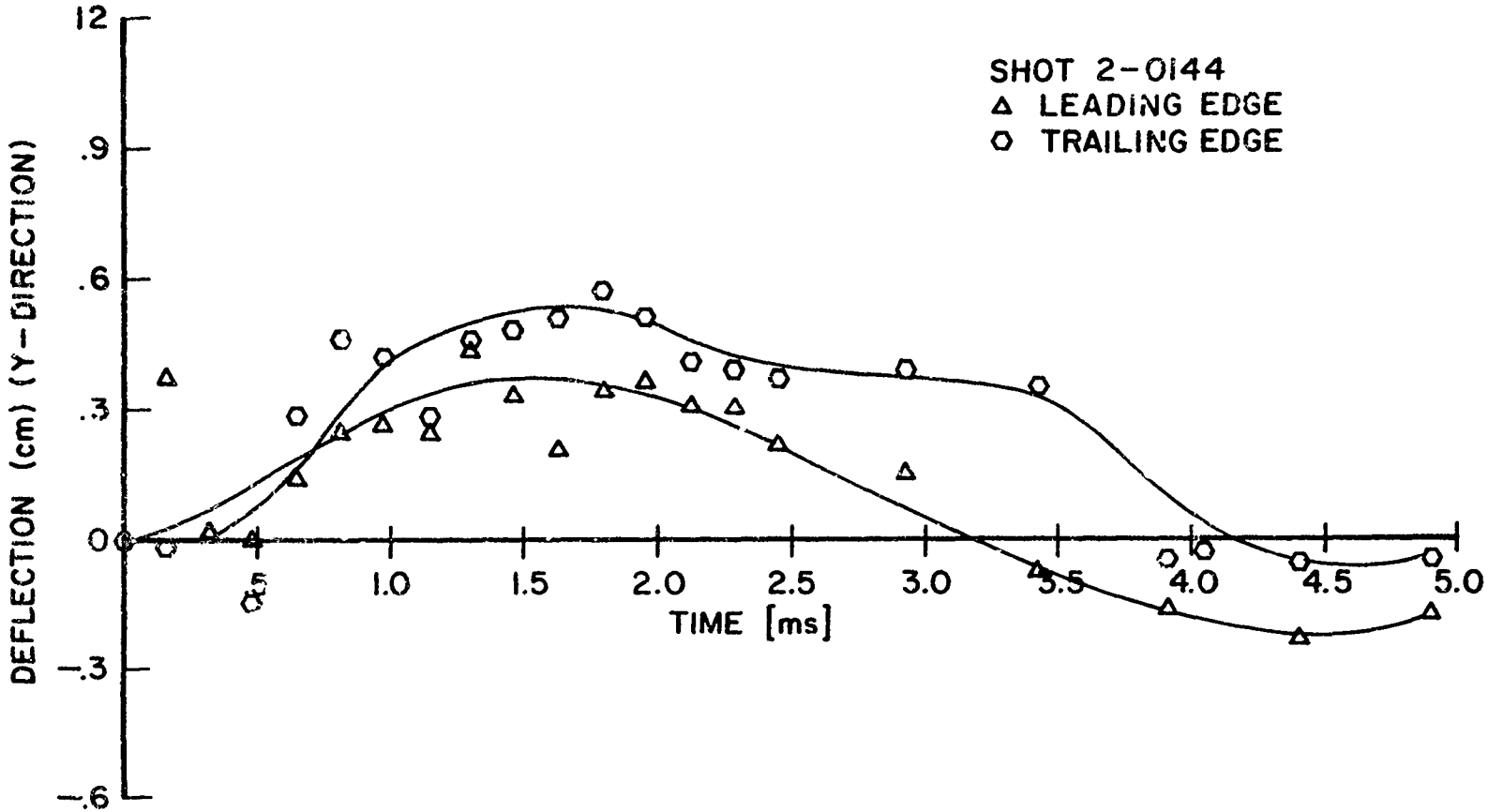

Figure 159. Tip Deflection in "y" Direction for Shot 2-0144.

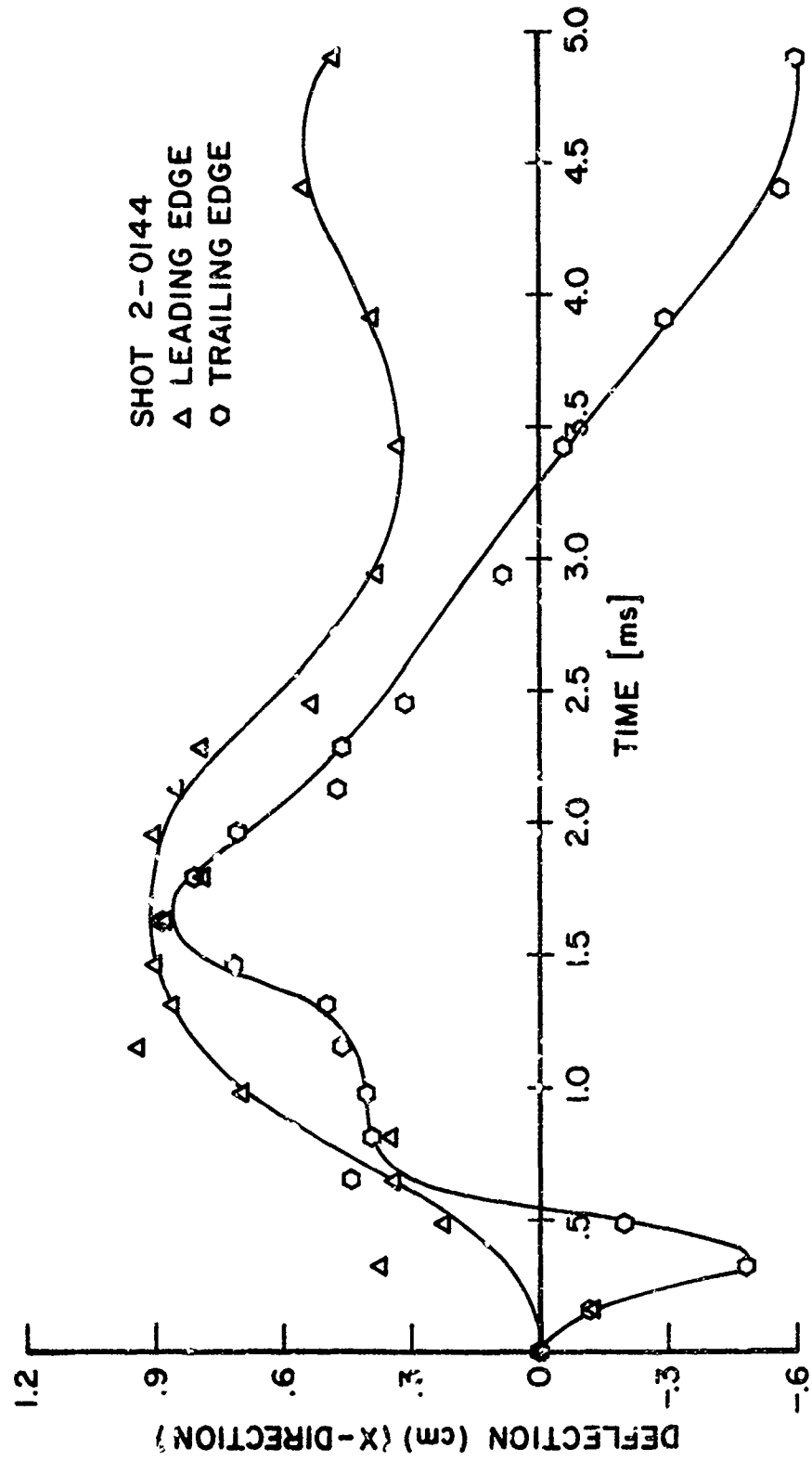

Figure 160. Tip Deflection in "x" Direction for Shot 2-0144.

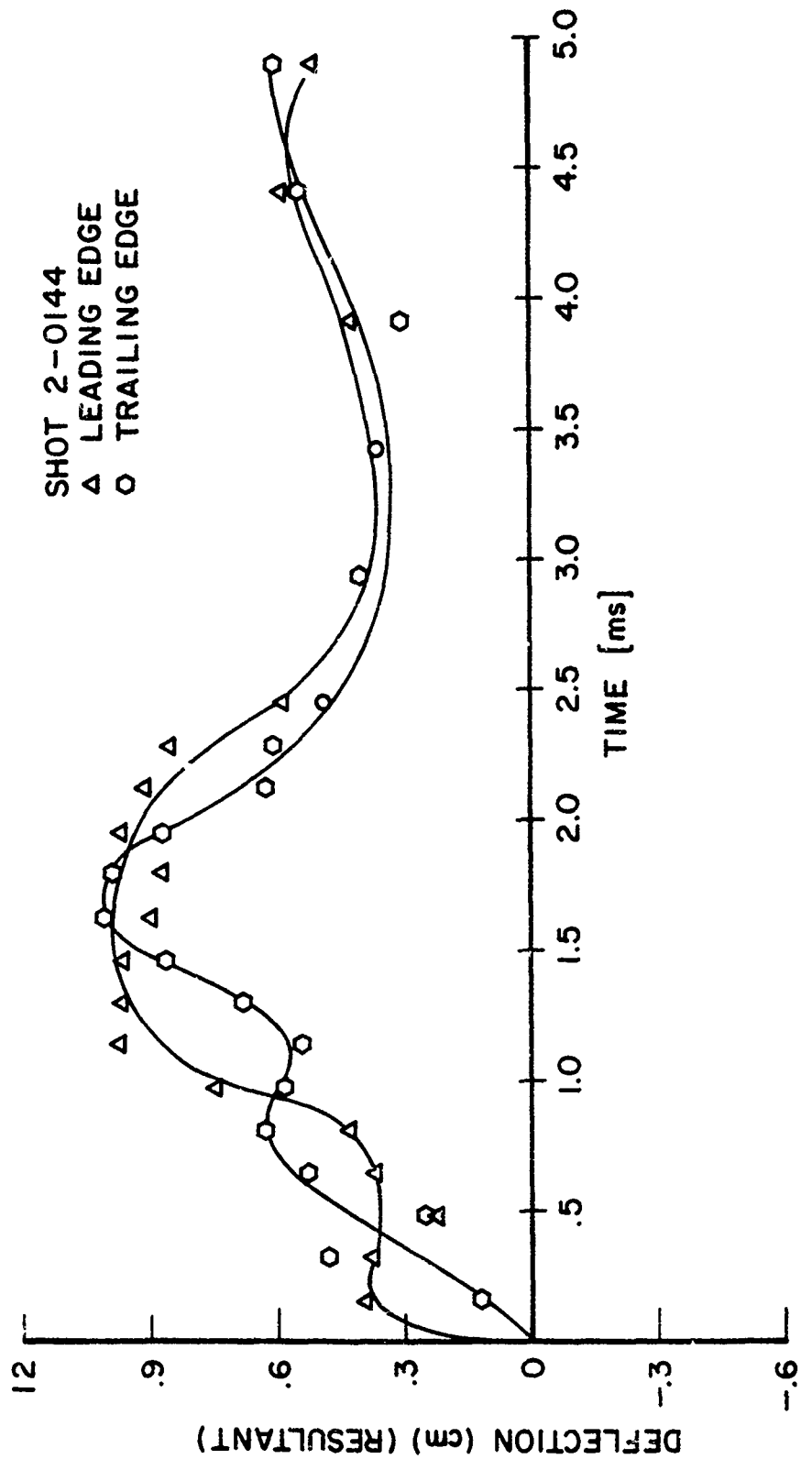

Figure 161. Tip Deflection Resultant for Shot 2-0144.

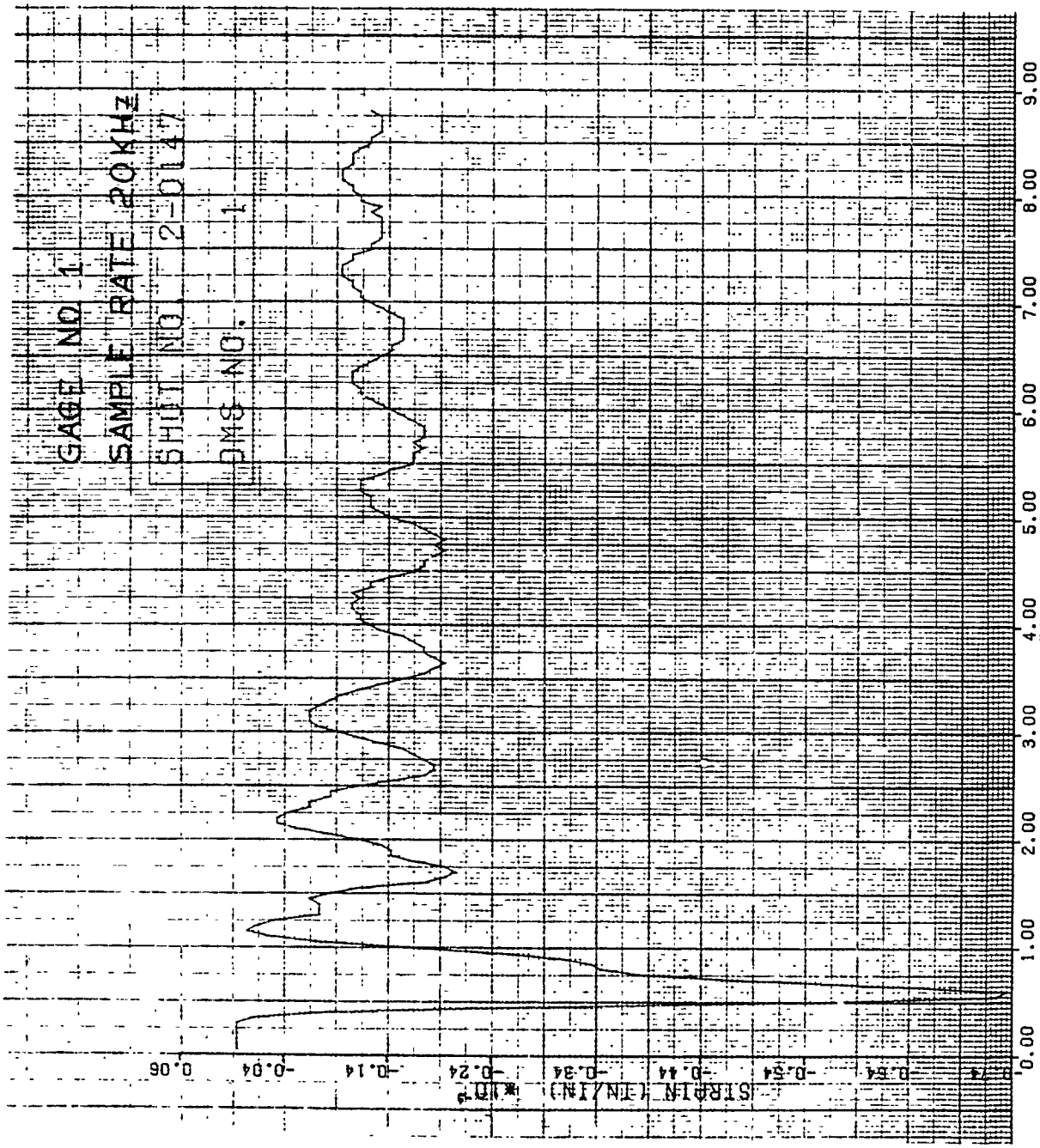

Figure 162. Strain of Shot 2-0147 for Gage #1.

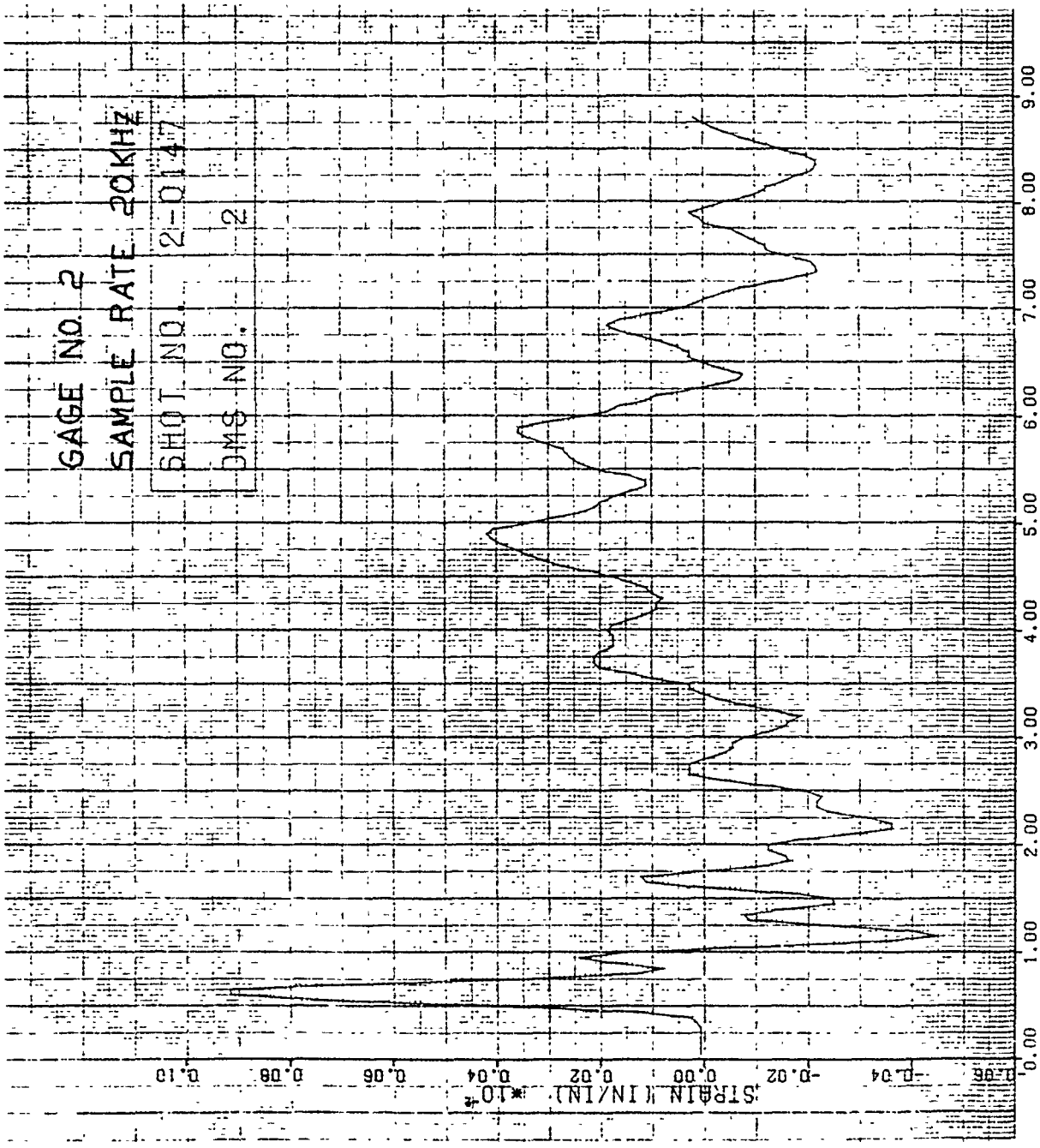

Figure 163. Strain of Shot 2-0147 for Gage #2.

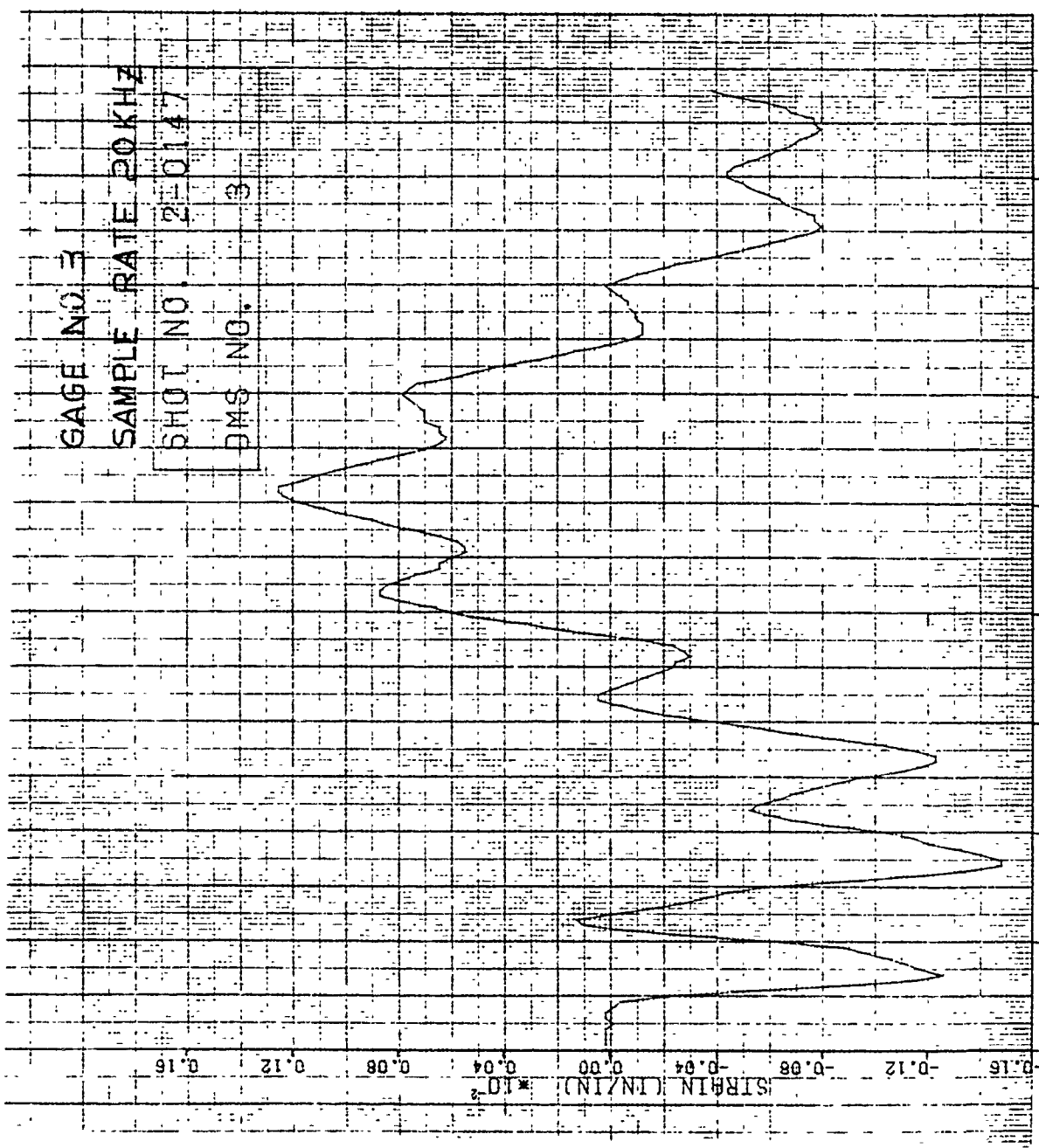

Figure 164. Strain of Shot 2-0147 for Gage #3.

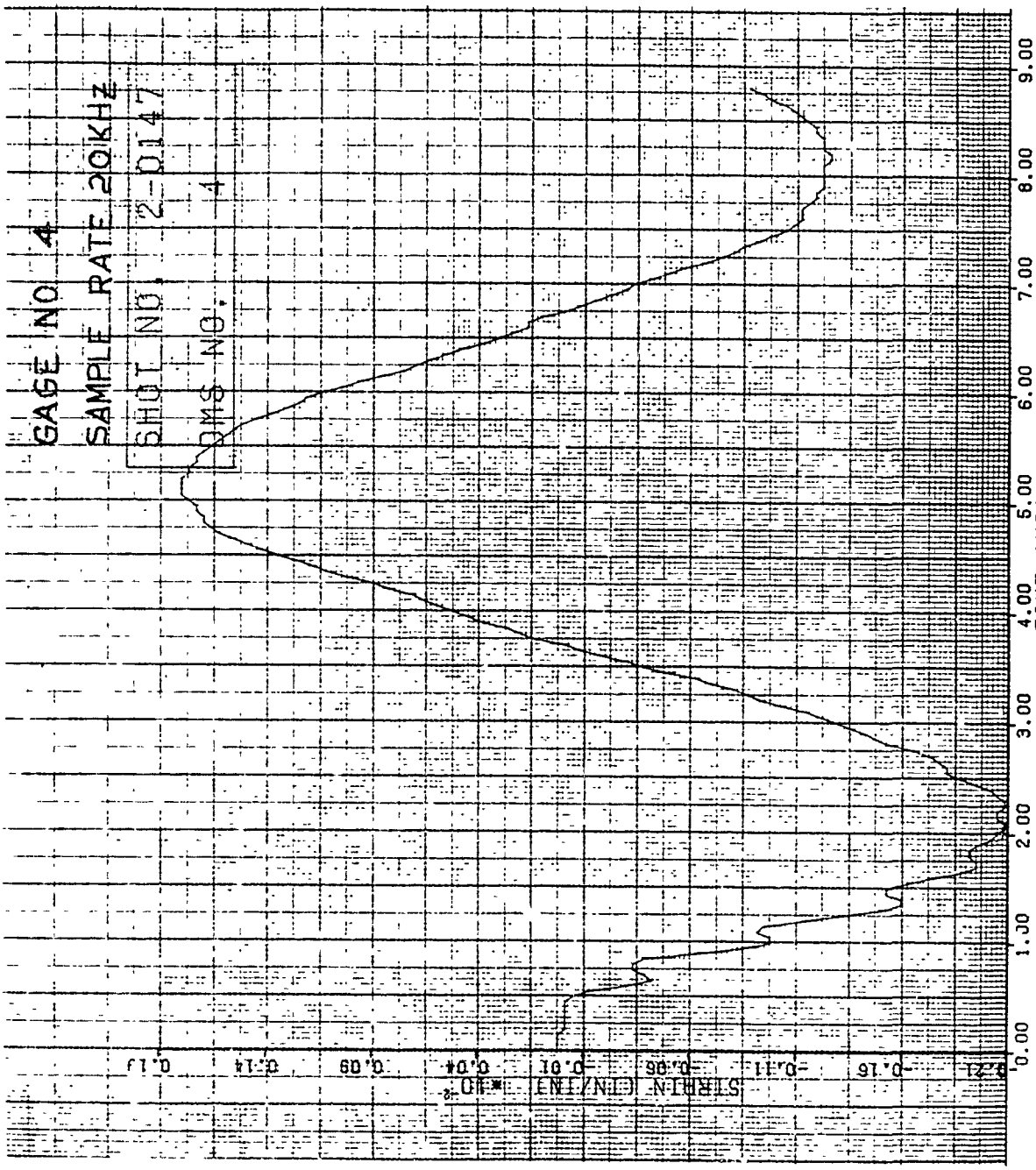

Figure 165. Strain of Shot 2-0147 for Gage #4.

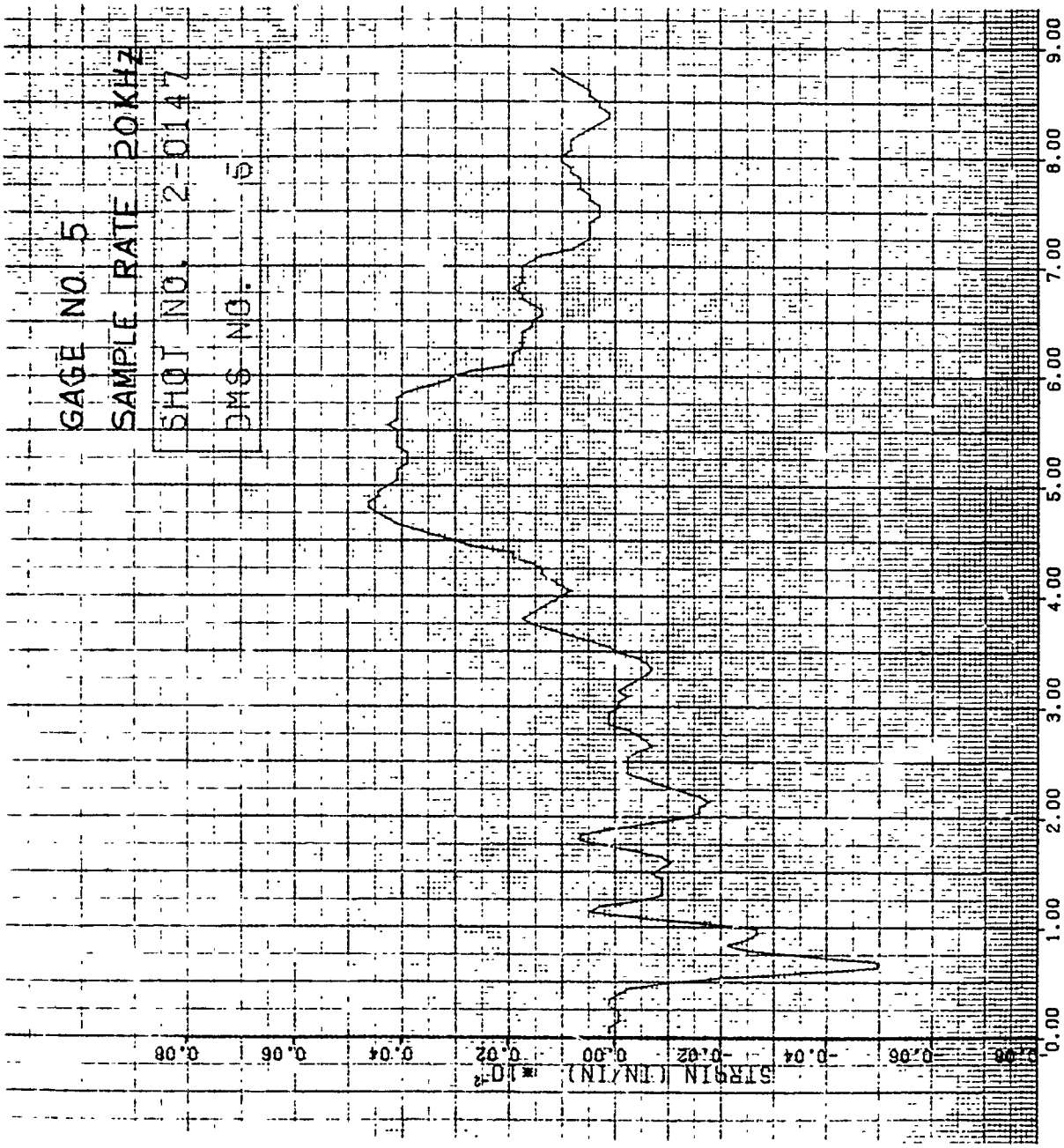

Figure 166. Strain of Shot 2-0147 for Gage #5.

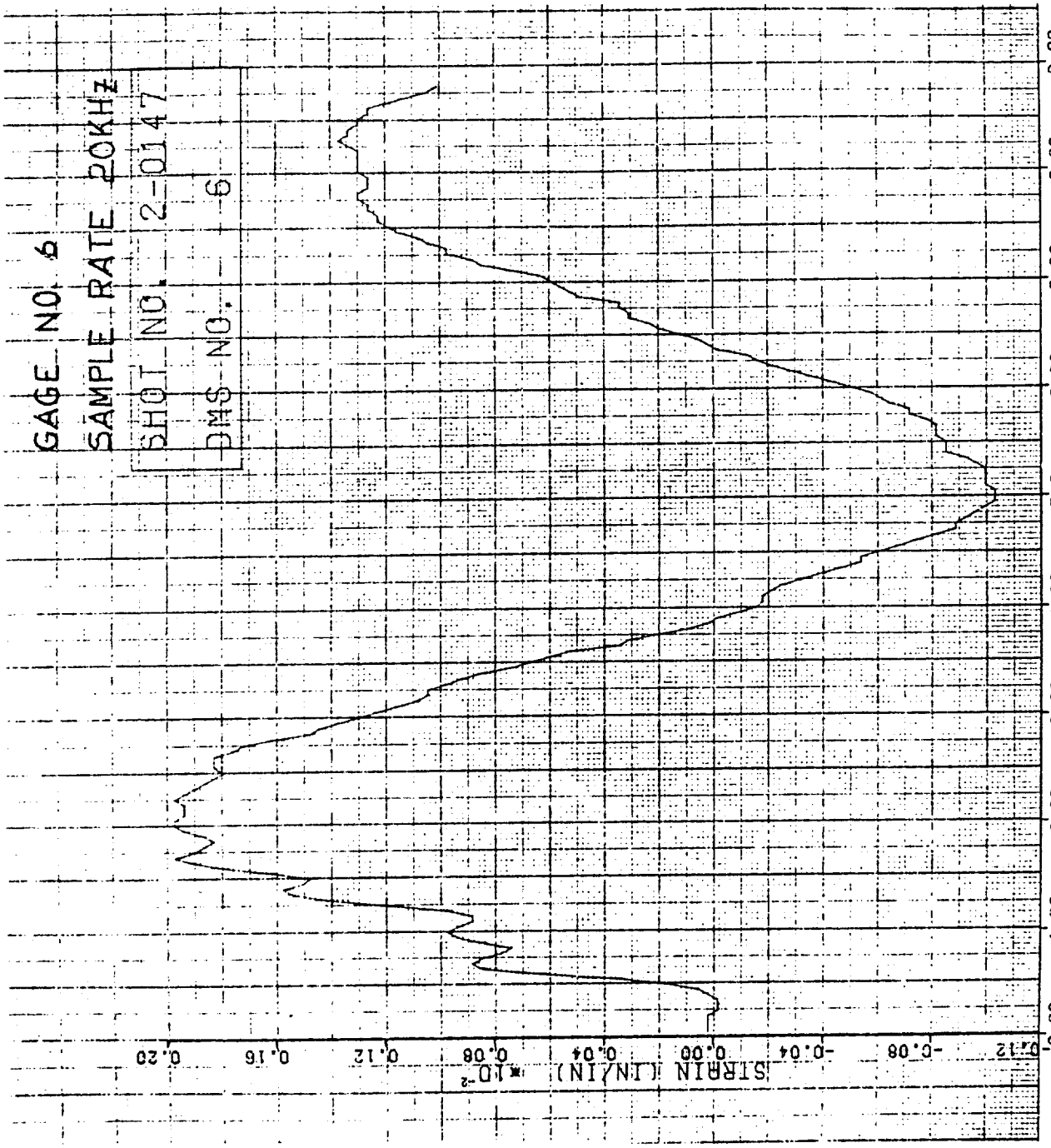

Figure 167. Strain of Shot 2-0147 for Gage #6.

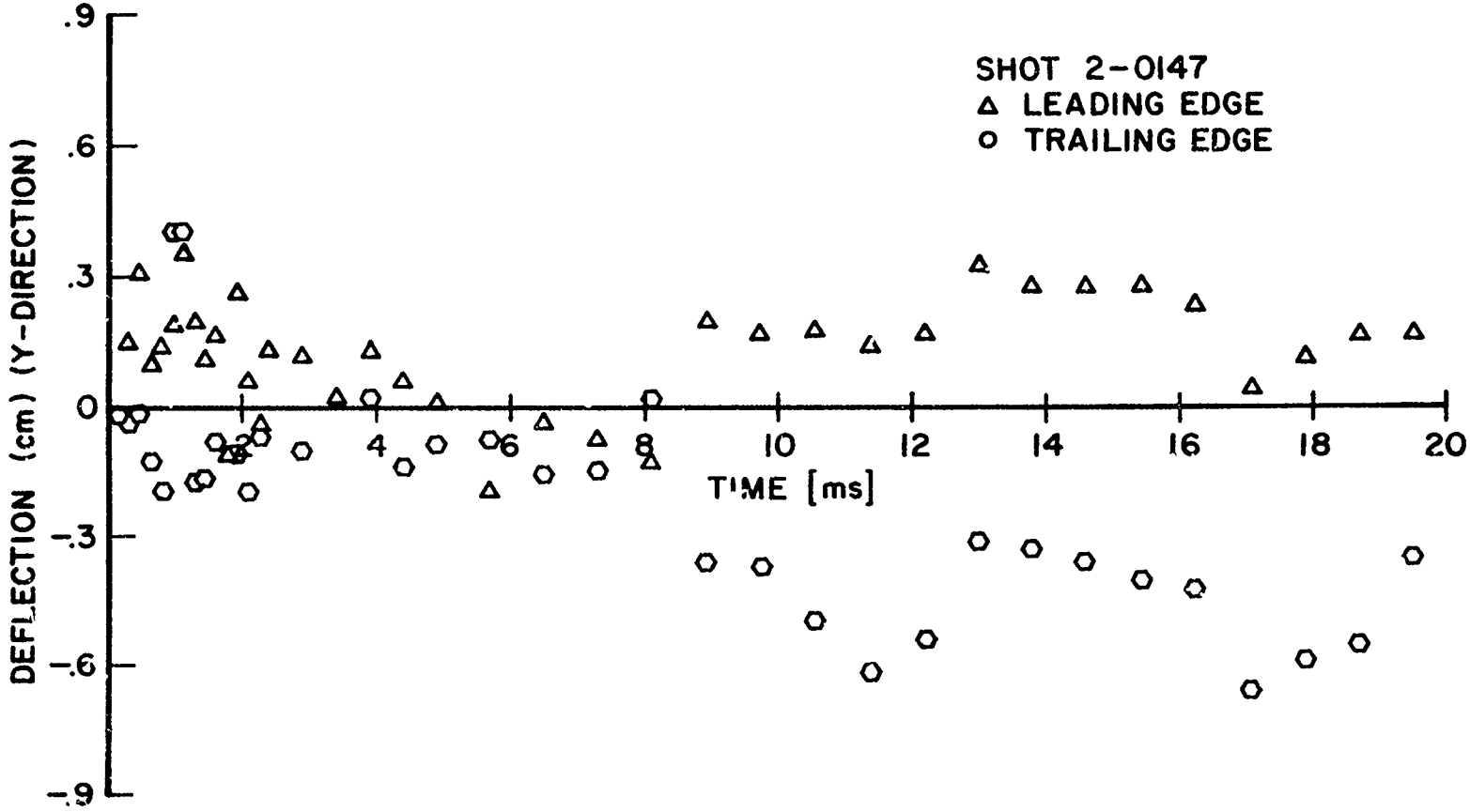

Figure 168. Tip Deflection in "y" Direction for Shot 2-0147.

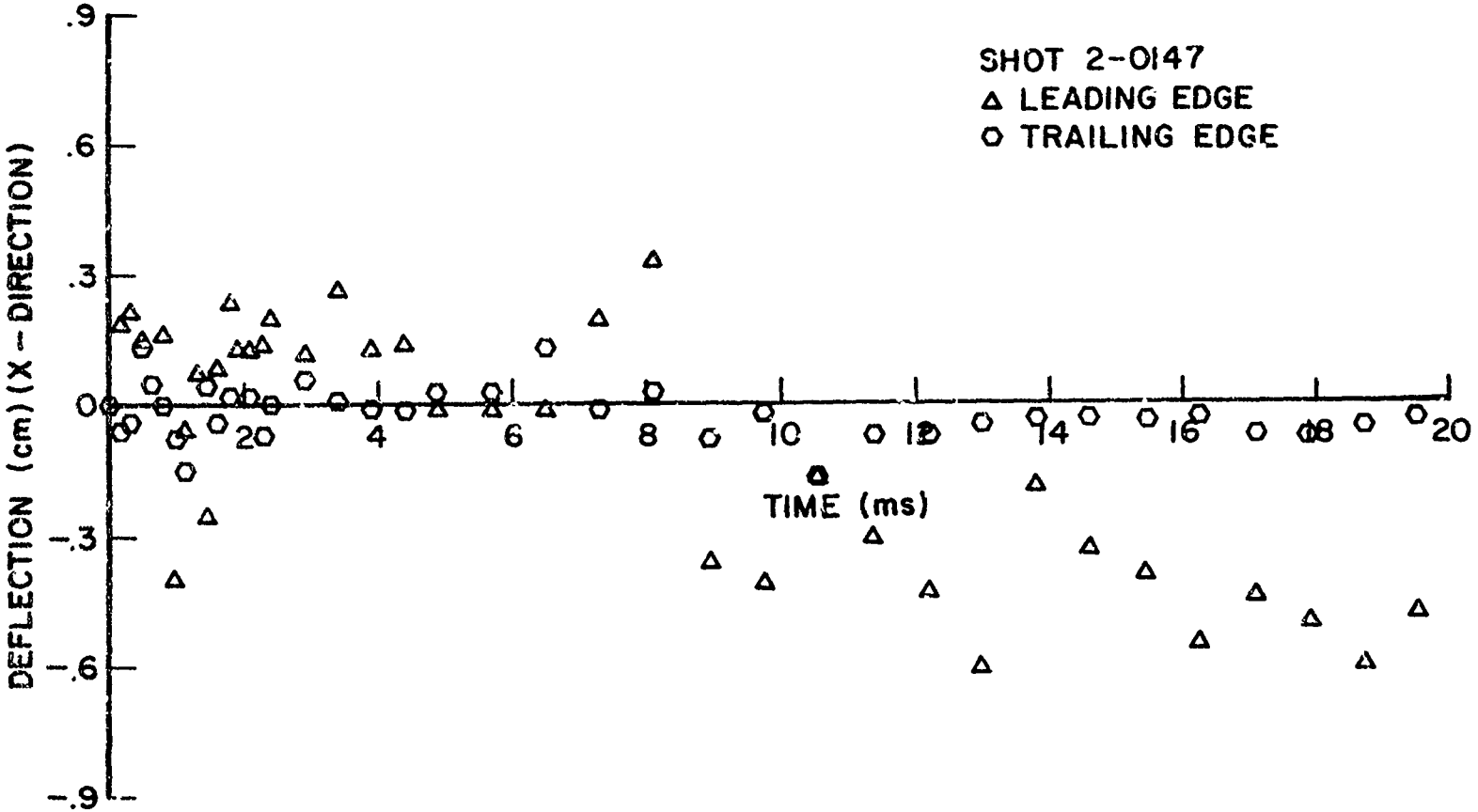

Figure 169. Tip Deflection in "x" Direction for Shot 2-0147.

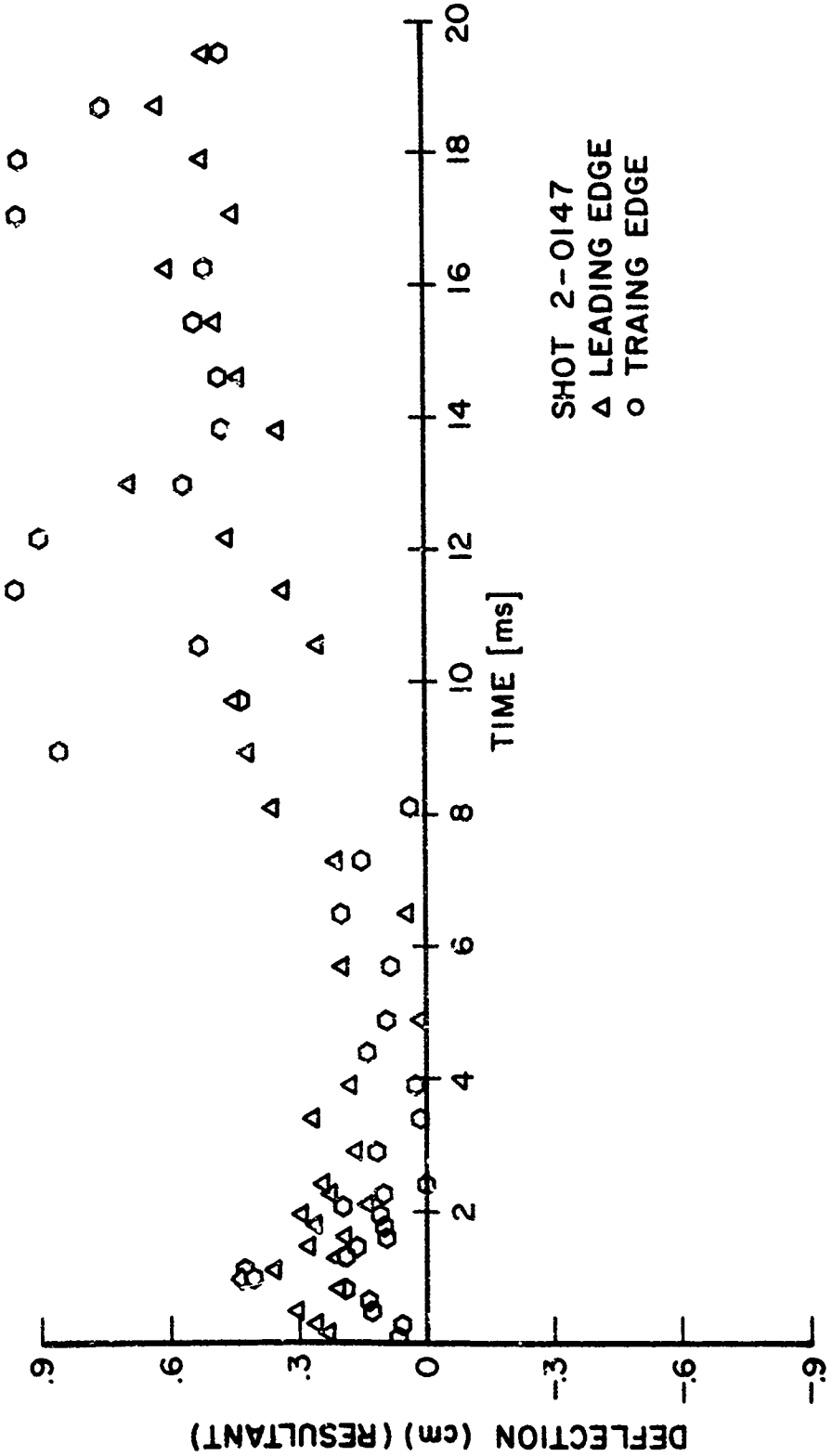

Figure 170. Tip Deflection Resultant for Shot 2-0147.

Figure 41B through 43B of Appendix B show photographs of the damage received for Shots 2-0146, 2-0147, and 2-0148, respectively.

3.2 IMPACT RESULTS ON ACTUAL BLADES

The actual blade tests involved leading-edge impacts and all three blade types were investigated. Various test conditions were used to determine the impact response of the blades. Tests were performed on 15 groups of blades as presented in Table 8 given earlier in this report. The F101 blade using 8-1-1 titanium has a tip shroud which was restrained as shown earlier in Figure 5. The tip shroud was permitted to move in the spanwise direction during the impact event as shown in Figure 5. The strain and strain rate data resulting from the impacts are presented in the Volume II report in the form of strain and strain rate versus time plots. The impactors were either artificial birds or ice projectiles (both slab ice and spheres). Two sizes of birds were utilized in the testing (85 g and 680 g). The 85 g (3 ounce) bird was used to simulate a starling sized bird and the 680 g (1.5 pound) bird would be a seagull sized bird. The test conditions for the small and large bird impacts were presented in Tables 10 and 11, respectively. The ice impactors used in the study were cylinders, 7.62 cm (3.0 inch) in diameter and 17.78 cm (7.0 inches) in length, or 5.08 cm (2.0 inches) diameter spheres. The ice cylinder (mass of 850 g) was used to simulate an ice slab while the ice sphere (mass of 65 g) simulated hail-size ice balls. The impact site was either at the 30 percent or 70 percent span locations.

Table 14 gives the results of the impact tests for the actual blades. The table gives the test conditions, the blade and material type, the proper figure of Appendix A which describes the strain gage locations, the impact velocity and mass, the span location and type of impact, and a description of the damage generated on each blade.

TABLE 14. RESULTS OF STATIC IMPACT TESTING ON ACTUAL BLADES

Group No.	Shot No.	Projectile Type	Projectile Mass (g)	Mass Impacting Target (g)	Target Material and Description	Span Location for Impact (%)	Impact Distance from Platform (cm)	Strain Gauge Locations	Impact Angle (°)	Shroud Restraint	Impact Velocity (m/s)	Damage Description and Comments	High-Speed Camera Type	Camera Framing Rate (frames/sec)	Deformation Plot
1B	2-0017 Blade # KGA00017	Micro-balloon gelatin bird (cylinder) (3.81 cm dia. x 7.62 cm long)	85.0	25.0	8-1-1 Ti F101 blade	Edge impact @ 30% span	8.0	see Fig. 1A	41.0	Yes	269.5	No visible damage specimen.	Dynafax	20,832	No
2B	2-0018 Blade # KGA00172	Micro-balloon gelatin bird (cylinder) (3.81 cm dia. x 7.62 cm long)	85.0	---	8-1-1 Ti F101 blade	Edge impact @ 70% span	18.6	see Fig. 1A	24.4	Yes	353.4	No visible damage on specimen. Unable to determine impact mass.	Dynafax	20,752	No
3B	2-0019 Blade # KGA00017	Micro-balloon gelatin bird (cylinder) (7.62 cm dia. x 15.24 cm long)	672.0	---	8-1-1 Ti F101 blade	Edge impact @ 30% span	8.0	see Fig. 1A	41.0	Yes	259.1E	Sabot impacted blade. Blade damaged slightly by leading edge bow of 0.13 cm. Velocity estimated. Unable to determine impact mass.	Dynafax	20,784	No
4B	2-0020 Blade # KGA00172	Micro-balloon gelatin bird (cylinder) (7.62 cm dia. x 15.24 cm long)	678.0	214.0	8-1-1 Ti F101 blade	Edge impact @ 70% span	18.6	see Fig. 1A	24.4	Yes	259.1E	Blade damaged due to sabot impacting specimen. Velocity estimated. Blade damaged by bowing at impact site. 3.00 cm bow on leading edge and 3.81 cm bow on trailing edge.	Dynafax	20,800	No
4B	2-0196 Blade # KGA01476	Micro-balloon gelatin bird (cylinder) (7.62 cm dia. x 15.24 cm long)	679.7	27.4	8-1-1 Ti F101 blade	Edge impact @ 70% span	18.6	see Fig. 4A	24.4	Yes	106.7E	No visible damage on specimen. Velocity estimated.	Dynafax	20,096	No

TABLE 14. RESULTS OF STATIC IMPACT TESTING ON ACTUAL BLADES (CONTINUED)

Group No.	Shot No.	Projectile Type	Projectile Mass (g)	Mass Impacting Target (g)	Target Material and Description	Span Location for Impact (%)	Impact Distance from Platform (cm)	Strain Gauge Locations	Impact Angle (°)	Shroud Restraint	Impact Velocity (m/s)	Damage Description and Comments	High-Speed Camera Type	Camera Framing Rate (frames/sec)	Deformation Plot
4B	2-0197 Blade# KGA01476	Micro-balloon gelatin bird (cylinder) (7.62 cm dia. x 15.24 cm long)	681.4	64.3	8-1-1 Ti F101 blade	Edge impact @ 70% span	18.6	see Fig. 4	24.4	Yes	117.7	No visible damage on specimen.	Dynafax	20,160	No
B	2-0198 Blade# KGA01476	Micro-balloon gelatin bird (cylinder) (7.62 cm dia. x 15.24 cm long)	681.4	40.7	8-1-1 Ti F101 blade	Edge impact @ 70% span	18.6	see Fig. 4	24.4	Yes	121.3	No visible damage on specimen.	Dynafax	20,288	No
4B	2-0199 Blade# KGA01476	Micro-balloon gelatin bird (cylinder) (7.62 cm dia. x 15.24 cm long)	683.0	124.3	8-1-1 Ti F101 blade	Edge impact @ 70% span	18.6	see Fig. 4	24.4	Yes	187.2	No visible damage on specimen.	Dynafax	20,192	No
4B	2-0200 Blade# KGA01476	Micro-balloon gelatin bird (cylinder) (7.62 cm dia. x 15.24 cm long)	675.2	---	8-1-1 Ti F101 blade	Edge impact @ 70% span	18.6	see Fig. 4	24.4	Yes	230.5	No visible damage on specimen. Unable to determine impact mass.	Dynafax	20,240	No
4B	2-0201 Blade# KGA01476	Micro-balloon gelatin bird (cylinder) (7.62 cm dia x 15.24 cm long)	683.6	105.6	8-1-1 Ti F101 blade	Edge impact @ 70% span	18.6	see Fig. 4	24.4	Yes	183.2	Blade knocked out of bottom fixture. Blade bowed at impact site 1.78 cm.	Dynafax	20,336	No
5B	2-0228 Blade# KGA01582	Ice Cylinder (7.62 cm dia. x 17.78 cm long)	786.8	---	8-1-1 Ti F101 blade	Edge impact @ 70% span	18.6	see Fig. 4	24.4	Yes	95.4	No visible damage on specimen. Ice cylinder broke up upon launch.	Dynafax	20,416	No

TABLE 14. RESULTS OF STATIC IMPACT TESTING ON ACTUAL BLADES (CONTINUED)

Group No.	Shot No.	Projectile Type	Projectile Mass (g)	Mass Impacting Target (g)	Target Material and Description	Span Location for Impact (%)	Impact Distance from Platform (cm)	Strain Gauge Locations	Impact Angle (°)	Shroud Restraint	Impact Velocity (m/s)	Damage Description and Comments	High-Speed Camera Type	Camera Framing Rate (frames/sec)	Deformation Plot
5B	2-0229 Blade# KGA01582	Ice cylinder (7.62 cm dia. x 17.78 cm long)	835.8	---	8-1-1 Ti F101 blade	Edge impact @ 70% span	18.6	see Fig. 4	24.4	Yes	93.9	No visible damage on specimen. Ice cylinder broke up upon launch.	Dynafax	20,368	No
5B	2-0230 Blade# KGA01582	Ice cylinder (7.62 cm dia. x 17.78 cm long)	841.4	---	8-1-1 Ti F101 blade	Edge impact @ 70% span	18.6	see Fig. 4	24.4	Yes	92.7	No visible damage on specimen. Ice cylinder broke up upon launch.	Dynafax	20,560	No
5B	2-0231	Ice cylinder (7.62 cm dia. x 17.78 cm long)	867.1	75.8	8-1-1 Ti F101 blade	Edge impact @ 70% span	18.6	see Fig. 4	24.4	Yes	165.1	Blade bowed at impact site 5.28 cm on leading edge and 6.50 cm on trailing edge.	Dynafax	20,404	Ye
6B	2-0008 Blade #1	Micro-balloon gelatin bird (cylinder) (3.81 cm dia. x 7.62 cm long)	85.6	15.1	403 Stainless steel J79 blade	Edge impact @ 30% span	7.2	see Fig. 2	51.1	No	164.3	No visible damage on specimen.	No film	---	No
6B	2-0009 Blade #1	Micro-balloon gelatin bird (cylinder) (3.81 cm dia. x 7.62 cm long)	84.3	48.1	403 Stainless steel J79 blade	Edge impact @ 30% span	7.2	see Fig. 2	51.1	No	161.3	No visible damage on specimen.	No film	---	No
6B	2-0010 Blade #1	Micro-balloon gelatin bird (cylinder) (3.81 cm dia. x 7.62 cm long)	85.0	48.1	403 Stainless steel J79 blade	Edge impact @ 30% span	7.2	see Fig. 2	51.1	No	200.3	No visible damage on specimen.	Dynafax	20,396	No

TABLE 14. RESULTS OF STATIC IMPACT TESTING ON ACTUAL BLADES (CONTINUED)

Group No.	Shot No.	Projectile Type	Projectile Mass (g)	Mass Impacting Target (g)	Target Material and Description	Span Location for Impact (%)	Impact Distance from Platform (cm)	Strain Gauge Locations	Impact Angle (°)	Shroud Restraint	Impact Velocity (m/s)	Damage Description and Comments	High-Speed Camera Type	Camera Framing Rate (frames/sec)	Deformation Plot
7B	2-0021 Blade #1	Micro-balloon gelatin bird (cylinder) (3.81 cm dia. x 7.62 cm long)	85.0	28.0	403 Stainless steel J79 blade	Edge impact @ 70% span	16.8	see Fig. 2	36.4	No	300.0	Sabot impacted blade. Blade damaged by bowing at impact site. Bow of 5.38 cm at leading edge; 4.08 cm at trailing edge.	Dynafax	20,896	No
8B	2-0011 Blade #1	Micro-balloon gelatin bird (cylinder) (7.62 cm dia. x 15.24 cm long)	679.0	94.9	403 Stainless steel J79 blade	Edge impact @ 30% span	7.2	see Fig. 2	51.1	No	160.7	Blade damaged slightly by bowing at impact site of 0.25 cm.	Dynafax	20,786	No
8B	2-0012 Blade #2	Micro-balloon gelatin bird (cylinder) (7.62 cm dia. x 15.24 cm long)	668.0	---	403 Stainless steel J79 blade	Edge impact @ 30% span	7.2	see Fig. 2	51.1	No	161.6	No visible damage on specimen. No strain gauge data. Unable to determine impact mass.	No film	--	No
8B	2-0013 Blade #2	Micro-balloon gelatin bird (cylinder) (7.62 cm dia. x 15.24 cm long)	678.5	---	403 Stainless steel J79 blade	Edge impact @ 30% span	7.2	see Fig. 2	51.1	No	167.4	No visible damage on specimen. Unable to determine impact mass.	No film	--	No
8B	2-0014 Blade #2	Micro-balloon gelatin bird (cylinder) (7.62 cm dia. x 15.24 cm long)	660.0	37.0	403 Stainless steel J79 blade	Edge impact @ 30% span	7.2	see Fig. 2	51.1	No	170.4	No visible damage on specimen.	Dynafax	20,720	No

TABLE 14. RESULTS OF STATIC IMPACT TESTING ON ACTUAL BLADES (CONTINUED)

Group No.	Shot No.	Projectile Type	Projectile Mass (g)	Mass Impacting Target (g)	Target Material and Description	Span Location for Impact (%)	Impact Distance from Platform (cm)	Strain Gauge Locations	Impact Angle (°)	Shroud Restraint	Impact Velocity (m/s)	Damage Description and Comments	High-Speed Camera Type	Camera Framing Rate (frames/sec)	Deformation Plot
8B	2-0015 Blade #2	Micro-balloon gelatin bird (cylinder) (7.62 cm dia. x 15.24 cm long)	680.0	311.0	403 Stainless steel J79 blade	Edge impact @ 30% span	7.2	see Fig. 2	51.1	No	170.7	Blade severely damaged by being knocked from fixture. General bowing through free span with tip deflection of 8.15 cm.	No film	--	No
9B	2-0024 Blade #3	Micro-balloon gelatin bird (cylinder) (7.62 cm dia. x 15.24 cm long)	680.0	161.0	403 Stainless steel J79 blade	Edge impact @ 70% span	16.8	see Fig. 2	36.4	No	254.0	Blade severely damaged by being knocked from fixture. Specimen hit target tank. Large amount of bow damage of 9.8 cm at impact site.	Dynafax	20,800	Yes
10B	2-0219 Blade #1-1	Ice ball (5.08 cm dia. sphere)	65.6	∿32.8	403 Stainless steel J79 blade	Edge impact @ 30% span	7.2	see Fig. 6	51.1	No	88.7	No visible damage on specimen. Impact mass estimate to be half of ice sphere.	Dynafax	20,384	Yes
10B	2-0220 Blade #1-1	Ice ball (5.08 cm dia. sphere)	65.0	∿32.5	403 Stainless steel J79 blade	Edge impact @ 30% span	7.2	see Fig. 6	51.1	No	139.4	No visible damage on specimen. Impact mass estimated to be half of ice sphere.	Dynafax	20,384	No
10B	2-0221 Blade #1-2	Ice ball (5.08 cm dia. sphere)	63.5	∿31.8	403 Stainless steel J79 blade	Edge impact @ 30% span	7.2	see Fig. 6	51.1	No	182.3	No visible damage on specimen. Ice ball broke up upon launch. Impact mass estimated to be half of ice sphere.	Dynafax	20,288	No
10B	2-0222 Blade #1-1	Ice ball (5.08 cm dia. sphere)	65.2	∿32.6	403 Stainless steel J79 blade	Edge impact @ 30% span	7.2	see Fig. 6	51.1	No	247.9	General bending from root to tip through free span. Tip deflection of 2.24 cm. Impact mass estimated to be half of ice sphere.	Dynafax	20,336	No

TABLE 14. RESULTS OF STATIC IMPACT TESTING ON ACTUAL BLADES (CONTINUED)

Group No.	Shot No.	Projectile Type	Projectile Mass (g)	Mass Impacting Target (g)	Target Material and Description	Span Location for Impact (%)	Impact Distance from Platform (cm)	Strain Gauge Locations	Impact Angle (°)	Shroud Restraint	Impact Velocity (m/s)	Damage Description and Comments	High-Speed Camera Type	Camera Framing Rate (frames/sec)	Deformation Plot
10B	2-0226 Blade #1-2	Ice ball (5.08 cm dia. sphere)	64.6	32.3	403 Stainless steel J79 blade	Edge impact @ 30% span	7.2	see Fig. 6	51.1	No	324.7	Plastic deformation of bowing at impact site. Bow of 1.58 cm along leading edge. Tip deflection of 5.13 cm at leading edge and 8.49 cm at trailing edge. Impact mass estimated to be half of ice sphere.	Dynafax	20,368	No
11B	2-0232 Blade #1-3	Ice cylinder (7.62 cm dia. x 17.78 cm long)	686.5	147.8	403 Stainless steel J79 blade	Edge impact @ 30% span	7.2	see Fig. 6	51.1	No	99.4	No visible damage on specimen.	No film	--	No
11B	2-0234 Blade #1-4	Ice cylinder (7.62 cm dia. x 17.78 cm long)	758.5	207.4	403 Stainless steel J79 blade	Edge impact @ 30% span	7.2	see Fig. 6	51.1	No	97.6	No visible damage on specimen.	Dynafax	20,288	Yes
11B	2-0235 Blade #1-4	Ice cylinder (7.62 cm dia. x 17.78 cm long)	688.6	158.4	403 Stainless steel J79 blade	Edge impact @ 30% span	7.2	see Fig. 6	51.1	No	133.6	Plastic deflection of bowing at impact site. Tip deflection of 14.70 cm along leading edge and 15.49 cm along trailing edge.	Dynafax	20,240	No
12B	2-0016 Blade #082	Micro-balloon gelatin bird (cylinder) (3.81 cm dia. x 7.62 cm long)	85.0	16.0	Boron/ aluminum APSI blade	Edge impact @ 30% span	4.4	see Fig. 3	38.8	No	259.16	Local damage at impact site by breaking off material along leading edge. Affected area was 7.13 cm long and 1.80 cm maximum width.	No film	--	No

TABLE 14. RESULTS OF STATIC IMPACT TESTING ON ACTUAL BLADES (CONTINUED)

Group No.	Shot No.	Projectile Type	Projectile Mass (g)	Mass Impacting Target (g)	Target Material and Description	Span Location for Impact (%)	Impact Distance from Platform (cm)	Strain Gauge Locations	Impact Angle (°)	Shroud Restraint	Impact Velocity (m/s)	Damage Description and Comments	High-Speed Camera Type	Camera Framing Rate (frames/sec)	Deformation Plot
12B	2-0023 Blade #073	Micro-balloon gelatin bird (cylinder) (3.81 cm dia. x 7.62 cm long)	85.0	---	Boron/ aluminum APSI blade	Edge impact @ 30% span	4.4	see Fig. 3	38.8	No	418.9	Blade cracked along platform across chord 5.08 cm starting at leading edge side. Sabot also impacted blade. Unable to determine impact mass	Dynafax	20,912	Yes
13B	2-0022 Blade #059	Micro-balloon gelatin bird (cylinder) (3.81 cm dia. x 7.62 cm long)	85.0	---	Boron/ aluminum APSI blade	Edge impact @ 70% span	10.8	see Fig. 3	18.9	No	406.1	Blade broke off along platform close to root area. Also broke out material at tip 10.16 cm down along leading edge and 2.29 cm width. Unable to determine impact mass.	Dynafax	20,784	Yes
14B	2-0214 Blade #076	Ice ball (5.08 cm dia. sphere)	62.0	∿31.0	Boron/ aluminum APSI blade	Edge impact @ 30% span	4.4	see Fig. 5	38.8	No	133.8	No visible damage on blade. Projectile broke up upon launch. Impact mass estimated to be half of initial ice ball mass.	No film	--	No
14B	2-0215 Blade #076	Ice ball (5.08 cm dia. sphere)	65.3	∿32.7	Boron/ aluminum APSI blade	Edge impact @ 30% span	4.4	see Fig. 5	38.8	No	198.8	Blade bowed 0.25 cm on leading edge at impact site. Projectile broke up upon launch. Impact mass estimated to be half of initial ice ball mass.	Dynafax	20,224	No
14B	2-0216 Blade #046	Ice ball (5.08 cm dia. sphere)	65.4	∿32.7	Boron/ aluminum APSI blade	Edge impact @ 30% span	4.4	see Fig. 5	38.8	No	132.3	Severe damage by breaking out 6.60·1.27 cm (length·width) section of leading edge at impact site. Impact mass estimated to be half of initial ice ball mass.	No film	--	No

TABLE 14. RESULTS OF STATIC IMPACT TESTING ON ACTUAL BLADES (CONCLUDED)

Group No.	Shot No.	Projectile Type	Projectile Mass (g)	Mass Impacting Target (g)	Target Material and Description	Span Location for Impact (%)	Impact Distance from Platform (cm)	Strain Gauge Locations	Impact Angle (°)	Shroud Restraint	Impact Velocity (m/s)	Damage Description and Comments	High-Speed Camera Type	Camera Framing Rate (frames/sec)	Deformation Plot
14B	2-0217 Blade #040	Ice ball (5.08 cm dia. sphere)	69.8	~34.9	Boron/ aluminum APSI blade	Edge impact @ 30% span	4.4	see Fig. 5	38.8	No	79.0	No visible damage on blade, projectile broke up upon launch. No strain gauge data. Impact mass estimated to be half of initial ice ball mass.	No film	---	No
14B	2-0218 Blade #040	Ice ball (5.08 cm dia. sphere)	68.3	~34.2	Boron/ aluminum APSI blade	Edge impact @ 30% span	4.4	see Fig. 5	38.8	No	92.7	Severe damage by breaking out 5.08·1.27 cm (length·width) section of leading edge at impact site. Impact mass estimated to be half of initial ice ball mass.	Dynafax	20,160	No
15B	2-0233 Blade #068	Ice cylinder (7.62 cm dia. x 17.78 cm long)	716.1	135.7	Boron/ aluminum APSI blade	Edge impact @ 30% span	4.4	see Fig. 5	38.8	No	96.0	Severe damage by breaking off at platform close to root arc and breaking out 9.65·[illegible] cm (length·width) section of leading edge at impact site.	Dynafax	20,304	No

As indicated earlier, 41 impacts were conducted on actual blades. All of the blades were instrumented with six strain gages. The sampling rate for the actual blade shots was 100 kHz; 20 kHz low-pass filters were used. Frequency checks were also made on the blades before and after each test on selected shots. Any difference between the pretest and post-test frequency checks may be attributed to damage on the blade. These frequency checks were conducted at a sampling rate of 20 kHz with 4 kHz low-pass filters to attenuate frequencies above 4 kHz.

The impact velocity was also varied for the blade tests from a low velocity range to generate elastic deformation response (no visible damage), to a medium range to generate plastic deformation (threshold damage), and finally a high velocity range, where plastic/tear deformations were produced (severe damage). High speed photography was used in every test to permit determining the dynamic tip deflection of the blades (except for the F101 blades which have a tip shroud) versus time.

In all cases, photographs of the damaged blades were taken to document the damage. Typical photographs of the damage generated in the bird and ice impacts are presented in Appendix B.

The amount of data generated for the 41 actual blade shots was enormous; therefore it is not practical to expand on each impact. The strain gage results are described in detail on selected shots in this report; however, the Volumee II report contains all of the strain and strain rate versus time plots. Tension is characterized as a positive strain value while compression is a negative strain for all cases unless noted. For the shots described in detail, the strain and strain rate versus time plots are expanded to the first 9 ms of the impact event. Dynamic tip deflection versus time plots were developed for selected shots.

The following paragraphs describe the results of the impact tests on each group of the blades.

3.2.1 Impact Results for Group 1B Blades

The impact testing of a Group 1B F101 titanium blade was conducted at an impact velocity of 270 m/s and impact angle of 41.0 degrees (Shot 2-0017). The impactor was an 85 g (3 ounce) bird. The impact mass was 25.0 g for the leading edge impact at the 30 percent span location. No visible damage resulted from the impact. The tip shroud was also restrained as shown in Figure 5 given earlier in this report. The strain data was not expanded for this impact; however, the Volume II report contains the strain data for this shot. The strain gage locations for this impact is given in Figure 1A of Appendix A. Tension is denoted as a negative strain and compression as a positive strain for the strain data for this shot.

3.2.2 Impact Results for Group 2B Blades

The impact test of a Group 2B F101 titanium blade was conducted at an impact velocity of 353 m/s and impact angle of 24.4 degrees (Shot 2-0018). The impact mass of the 85 g (3 ounce) bird was unable to be determined for this leading edge impact at the 70 percent span location. No visible damage resulted from this impact. Again, the tip shroud was restrained. The strain gage locations are given in Figure 1A of Appendix A. For this impact (Shot 2-0018), the strain data was expanded as shown in Figures 171 through 176. In this shot, tension is denoted as a negative strain and compression is a positive strain.

3.2.3 Impact Results for Group 3B Blades

The impact testing of a F101 titanium Group 3B blade (Shot 2-0019) was conducted at a velocity of 259 m/s and an impact angle of 41.0 degrees. The impact mass of the 680 g (1.5 pound) bird could not be determined because of the projectile breakup upon impact. The impact was a leading edge impact at the 30 percent span location. The blade was restrained at the tip shroud. The balsa wood sabot ejected

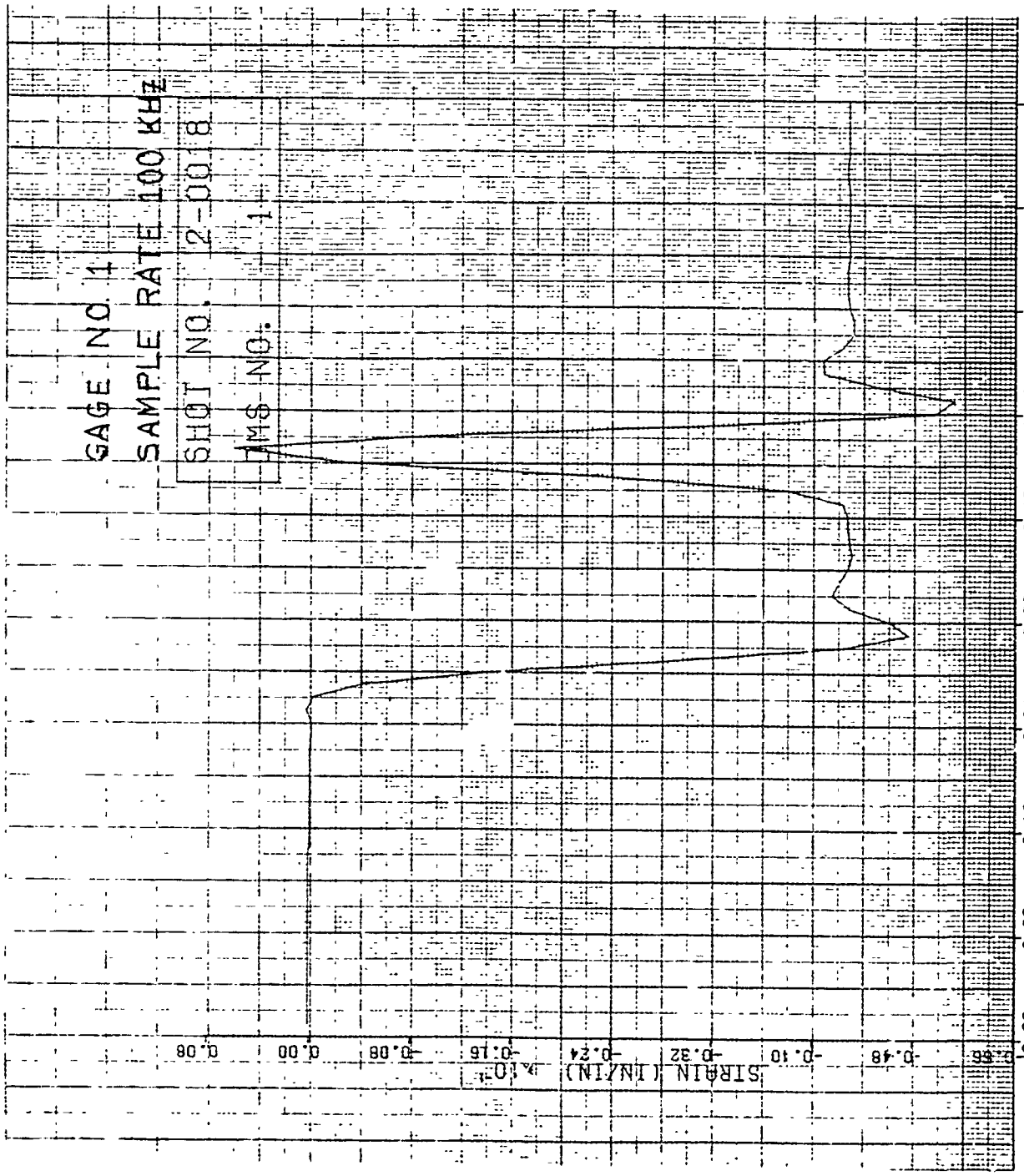

Figure 171. Strain of Shot 2-0018 for Gage #1.

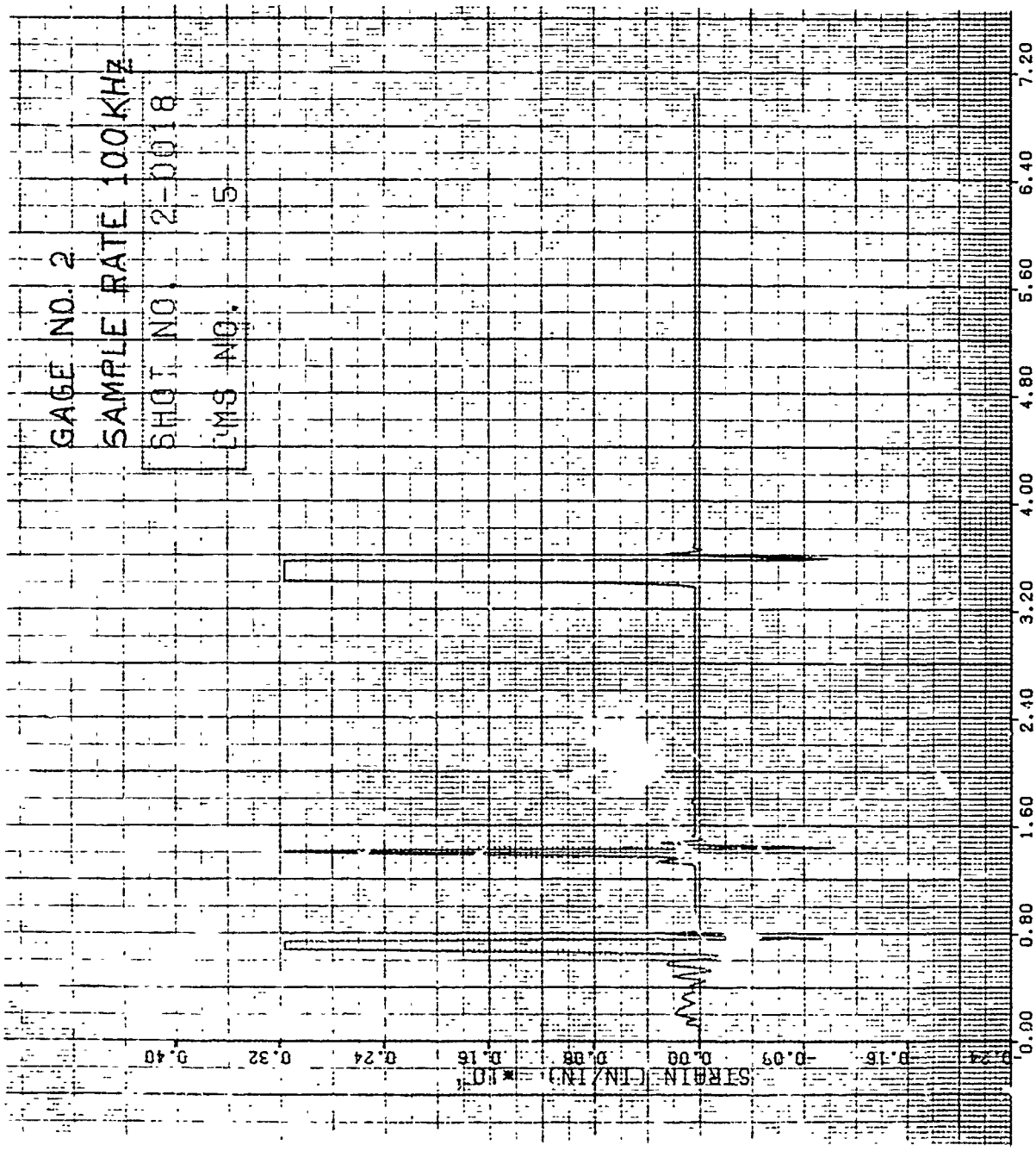

Figure 172. Strain of Shot 2-0018 for Gage #2.

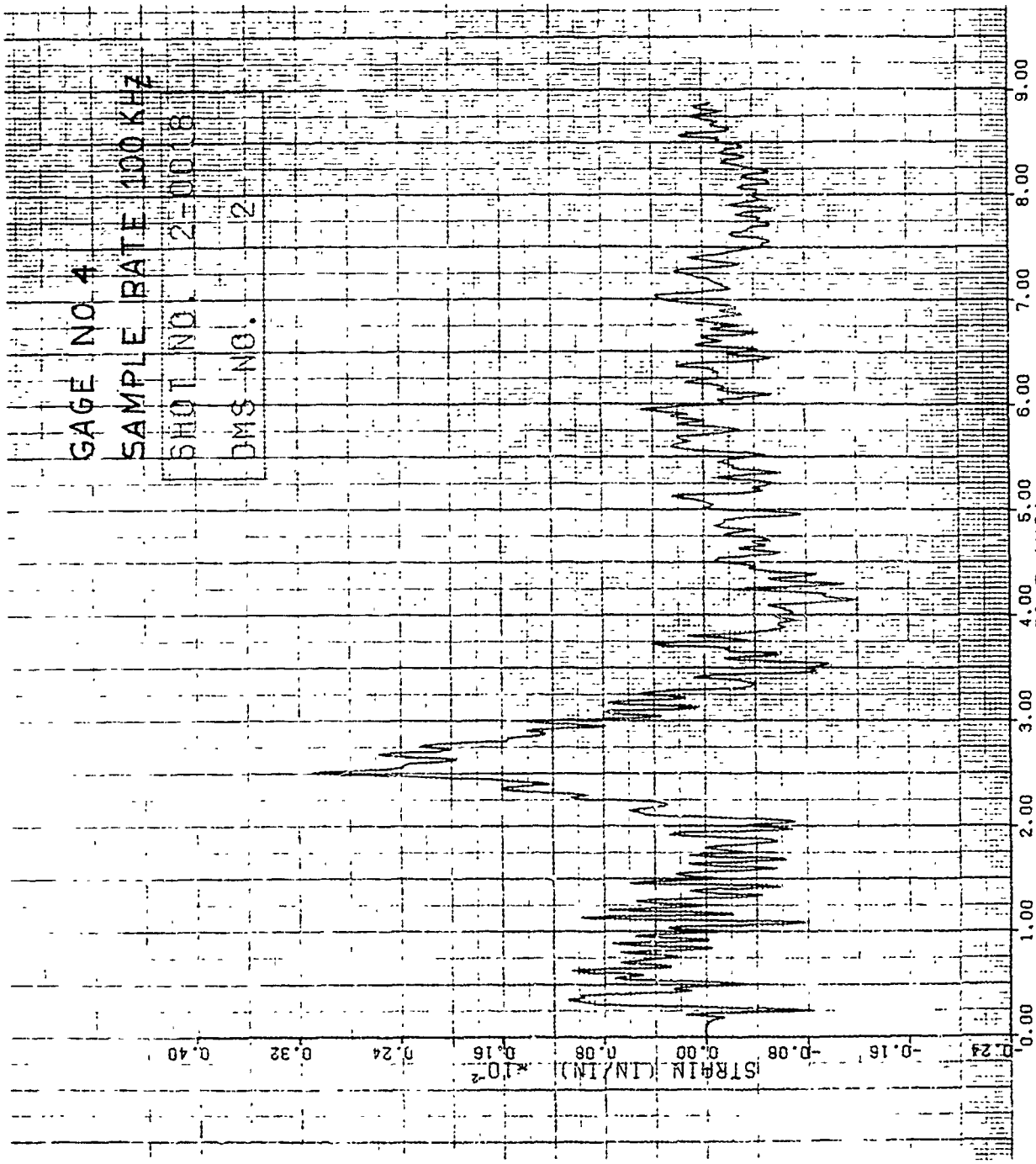

Figure 173. Strain of Shot 2-0018 for Gage #4.

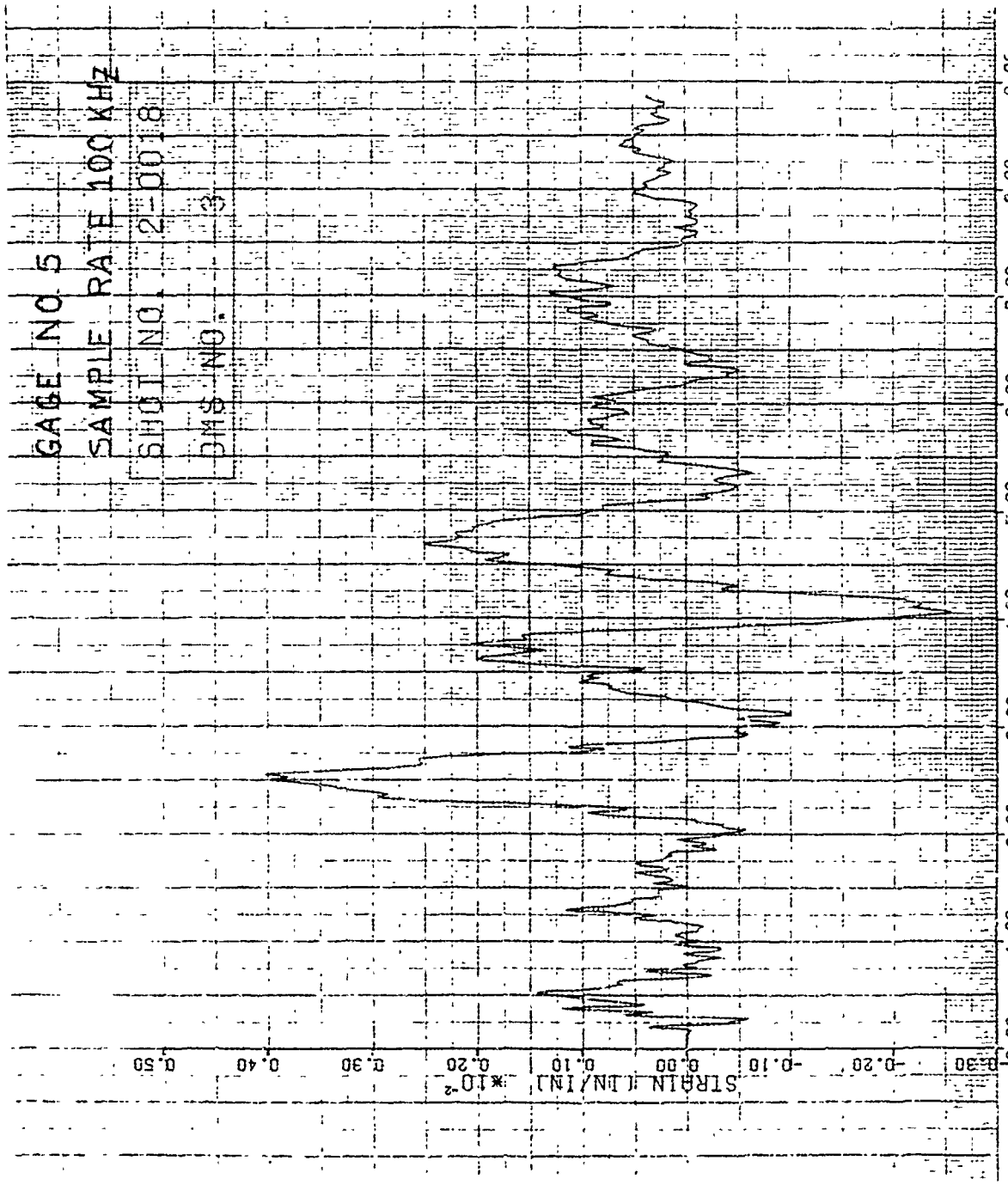

Figure 174. Strain of Shot 2-0018 for Gage #5.

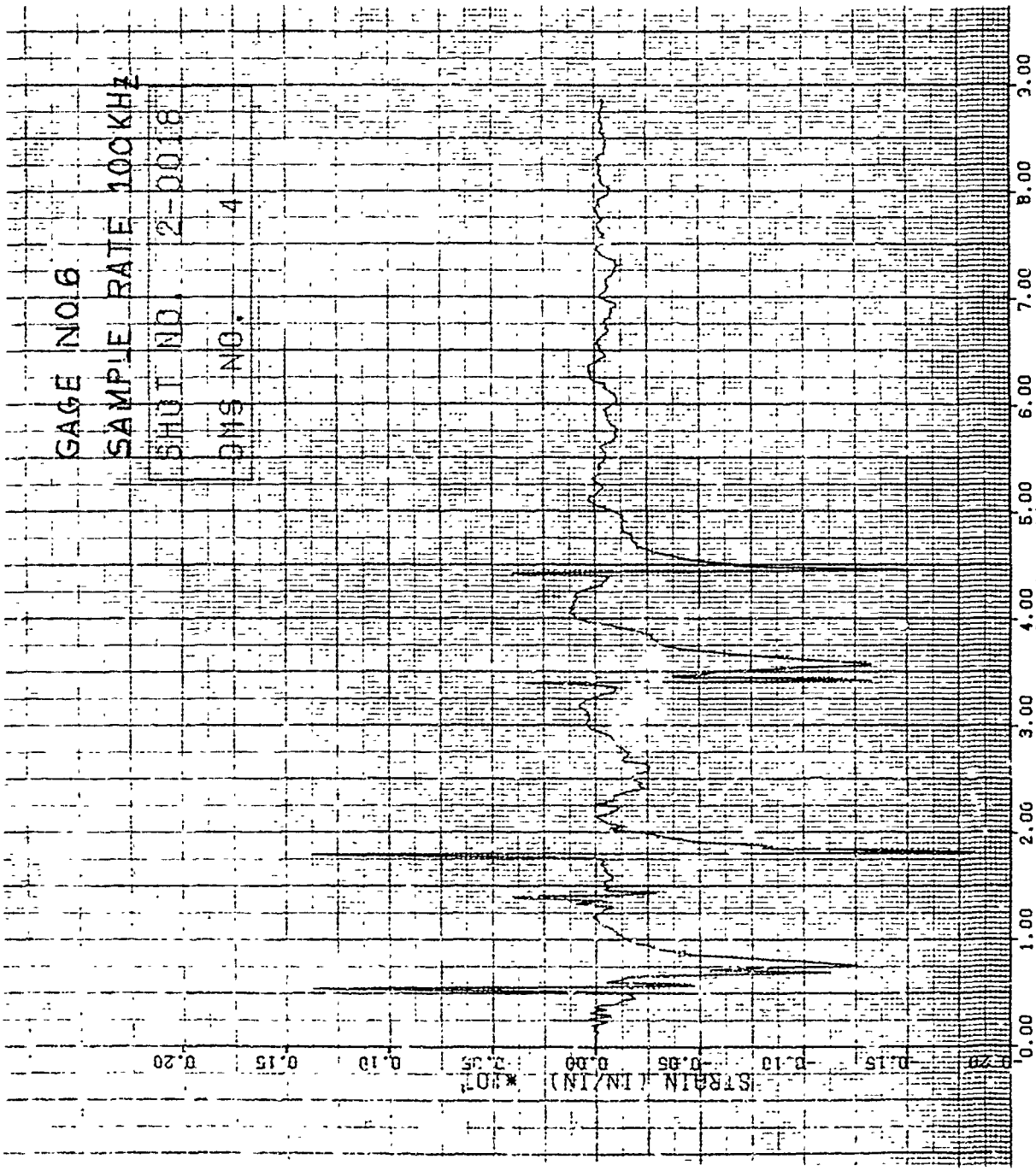

Figure 175. Strain of Shot 2-0018 for Gage #6.

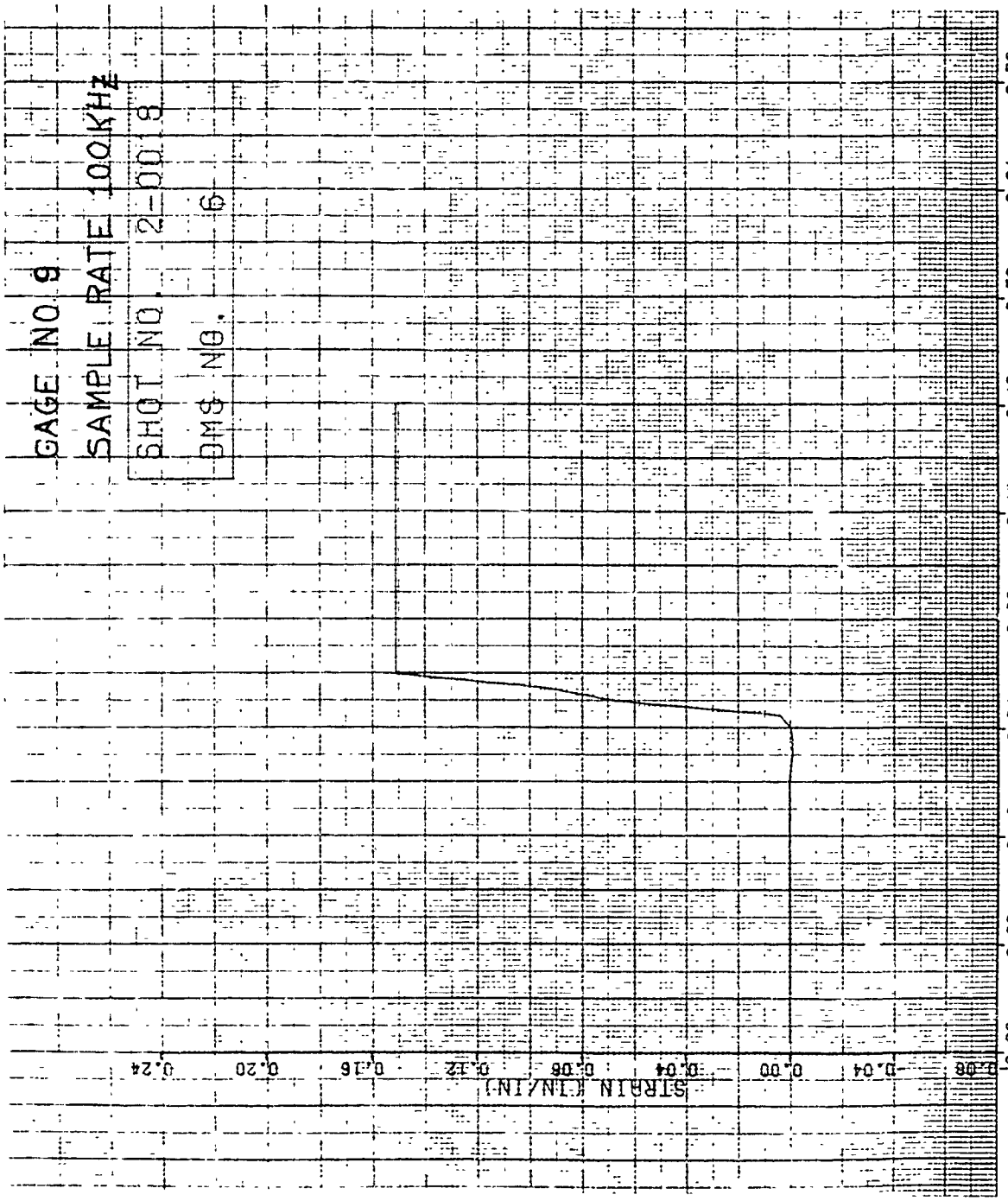

Figure 176. Strain of Shot 2-0018 for Gage #9.

the blade after the bird hi.. A slight leading edge bow of 0.13 cm was measured after impact. The strain data was not expanded for this impact; however, the strain data is contained in the Volume II report. The strain gage locations are given in Figure 1A of Appendix A. Tension is denoted as a negative strain and compression is denoted as a positive strain in the strain data. The highest strain rate for the impact was 341 in/in/sec for the gage located at the tip as identified in the strain and strain rate plots of Figures 177 and 178, respectively.

Figure 44B of Appendix B show photographs of the blade after impact.

3.2.4 Impact Results for Group 4B Blades

The impact testing on the F101 titanium Group 4B blades consisted of seven impacts of the 680 g (1.5 pound) bird at the 70 percent span location. The impacts were leading edge impacts at an impact angle of 24.4 degrees. Again, the blade tip was restrained by the method shown in Figure 5. The strain data of Shot 2-0020 is given in Figures 179 through 184 for the strain gage locations as shown in Figure 1A of Appendix A. Tension is denoted as a negative strain and compression as a positive strain for this impact. The impact velocity was estimated to be 259 m/s and the impact mass was 214.0 g. The highest strain rate value for this large bird impact was 367 in/in/sec as identified in Figures 184 and 185. This strain rate was for the gage location at the tip along the leading edge in the spanwise direction. It is borderline whether it is real data or noise. Figure 45B shows the damage received for this blade. The damage was in the form of bowing at the impact site with a value of 3.0 cm for the leading edge and 3.81 cm for the trailing edge.

Additional impacts (Shots 2-0196 through 2-0200) for this group of blades generated no damage for five specimens for a velocity up to 321 m/s; however, it was not possible to determine the impact mass for this impact. For one case at a velocity of 183 m/s (Shot 2-0201), the blade was bowed at

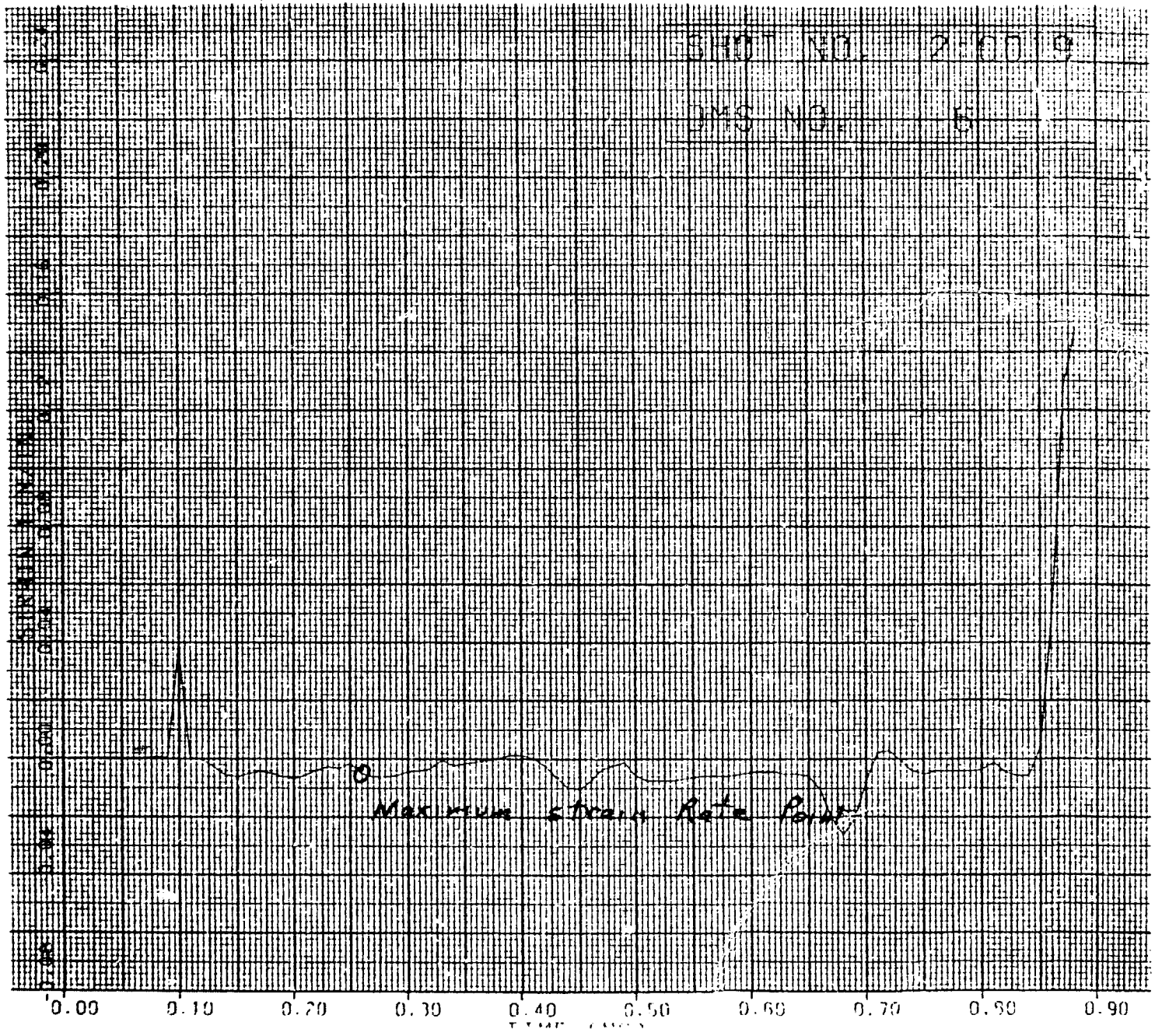

Figure 177. Strain of Shot 2-0019 for Gage #9.

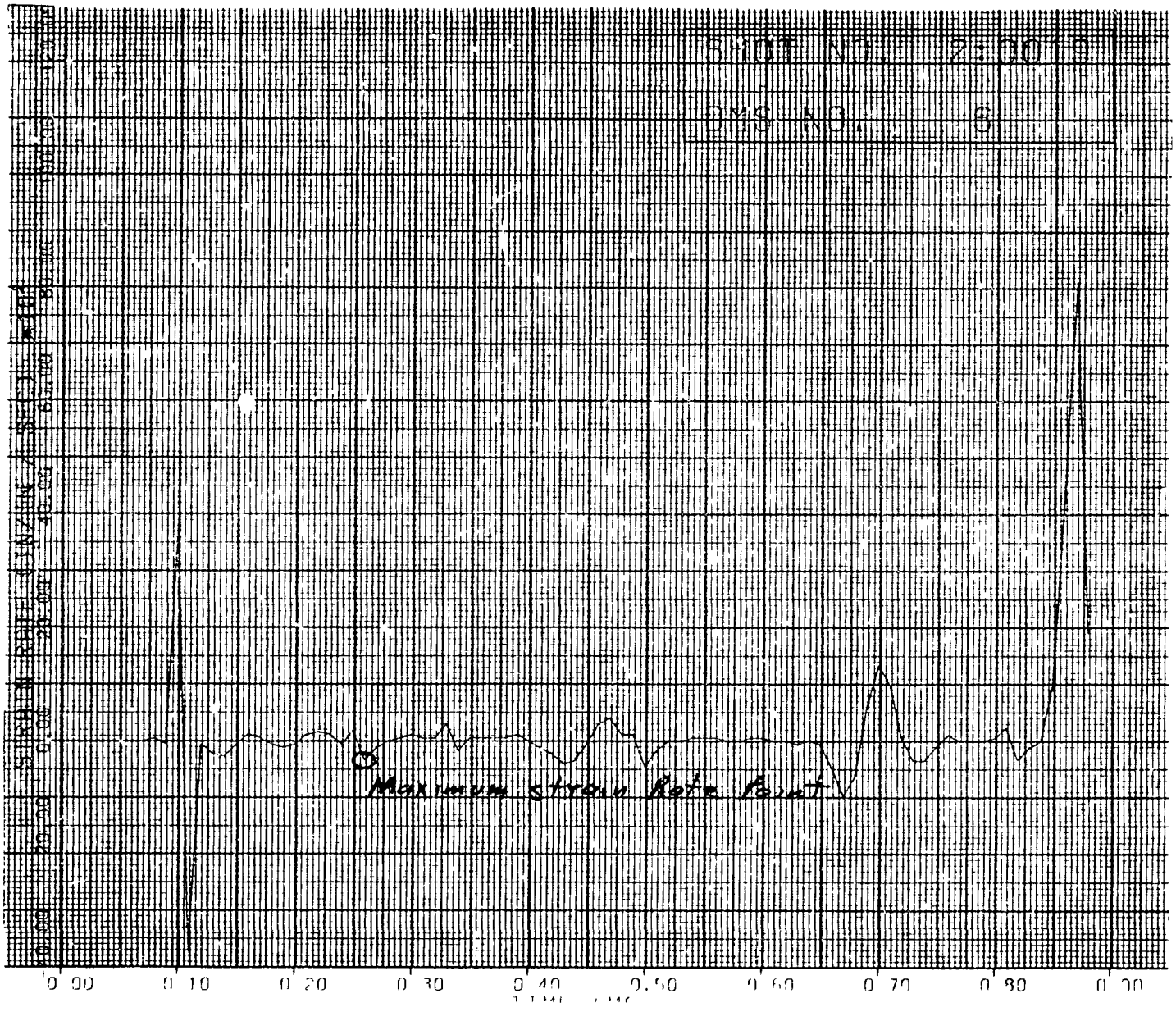

Figure 178. Strain Rate of Shot 2-0019 for Gage #9.

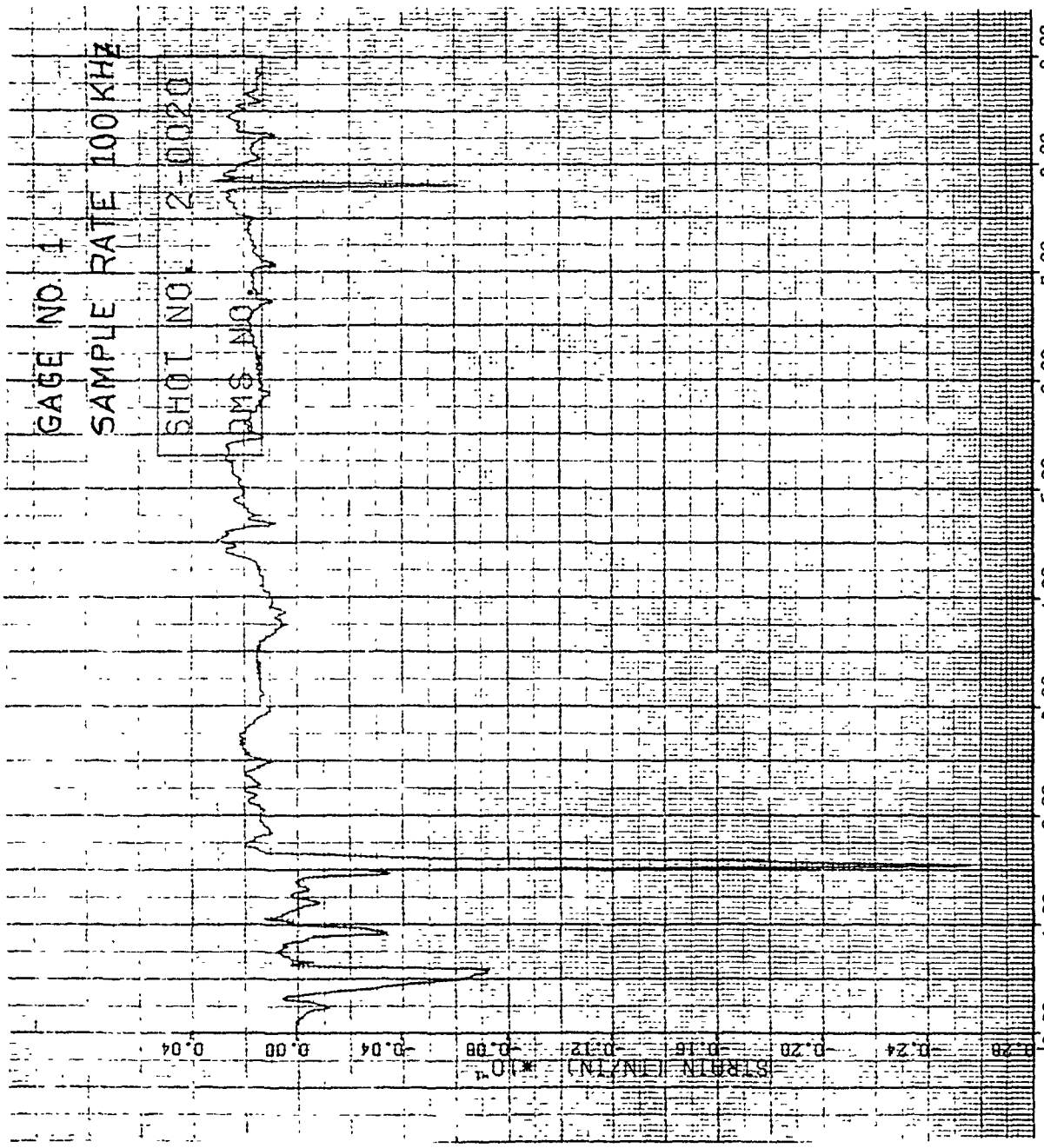

Figure 179. Strain of Shot 2-0020 for Gage #1.

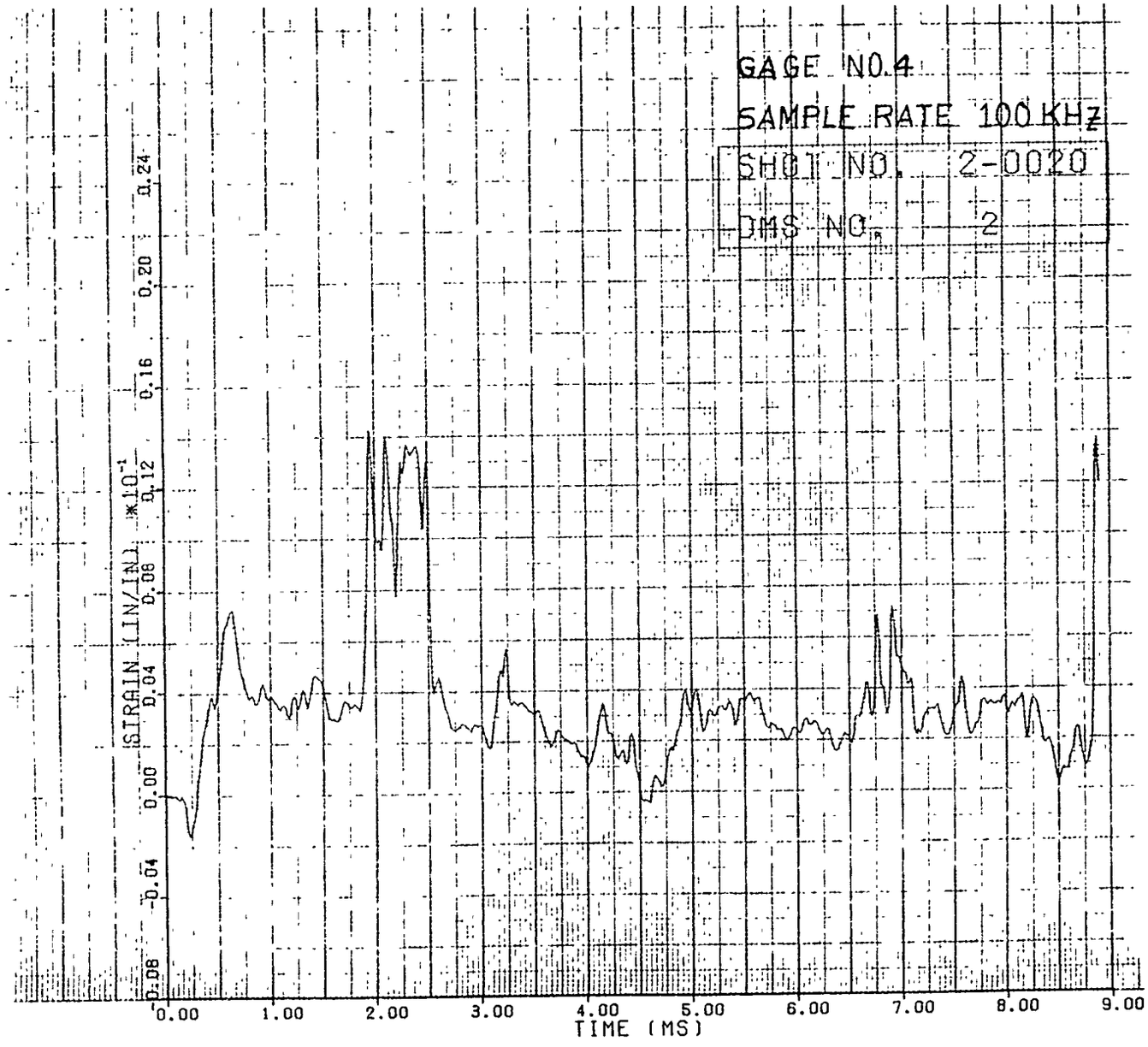

Figure 180. Strain of Shot 2-0020 for Gage #4.

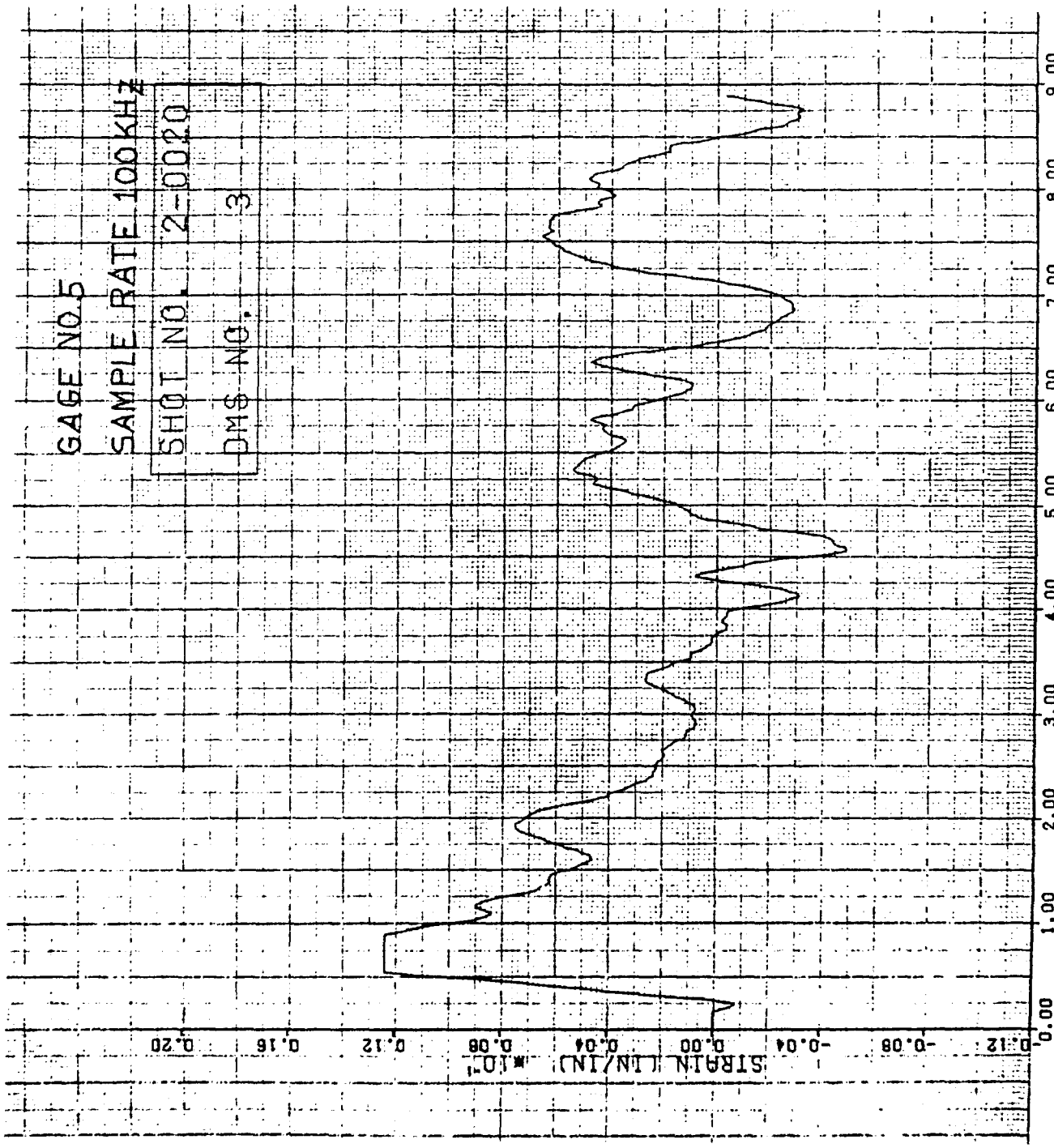

Figure 181. Strain of Shot 2-0020 for Gage #5.

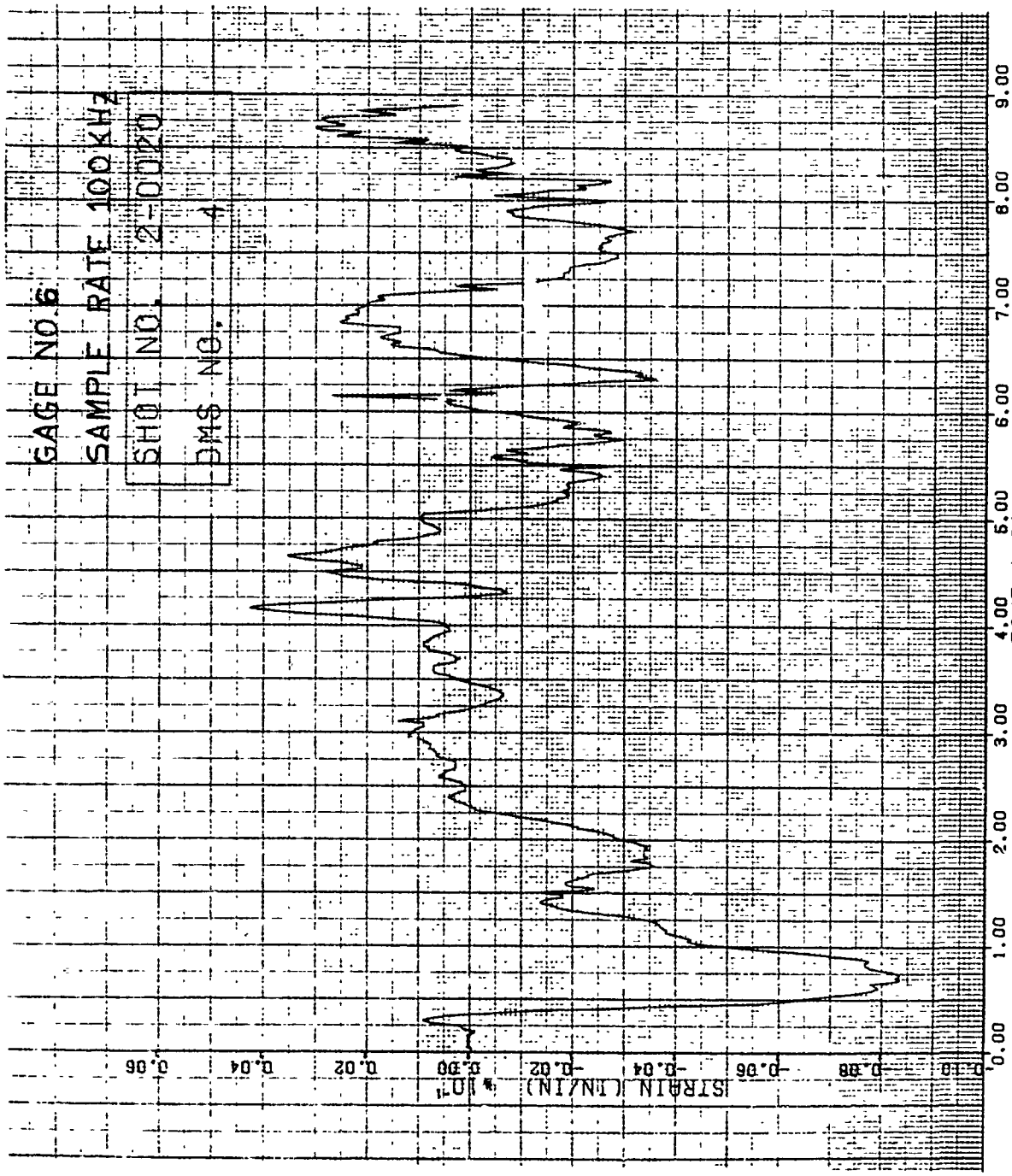

Figure 132. Strain of Shot 2-0020 for Gage #6.

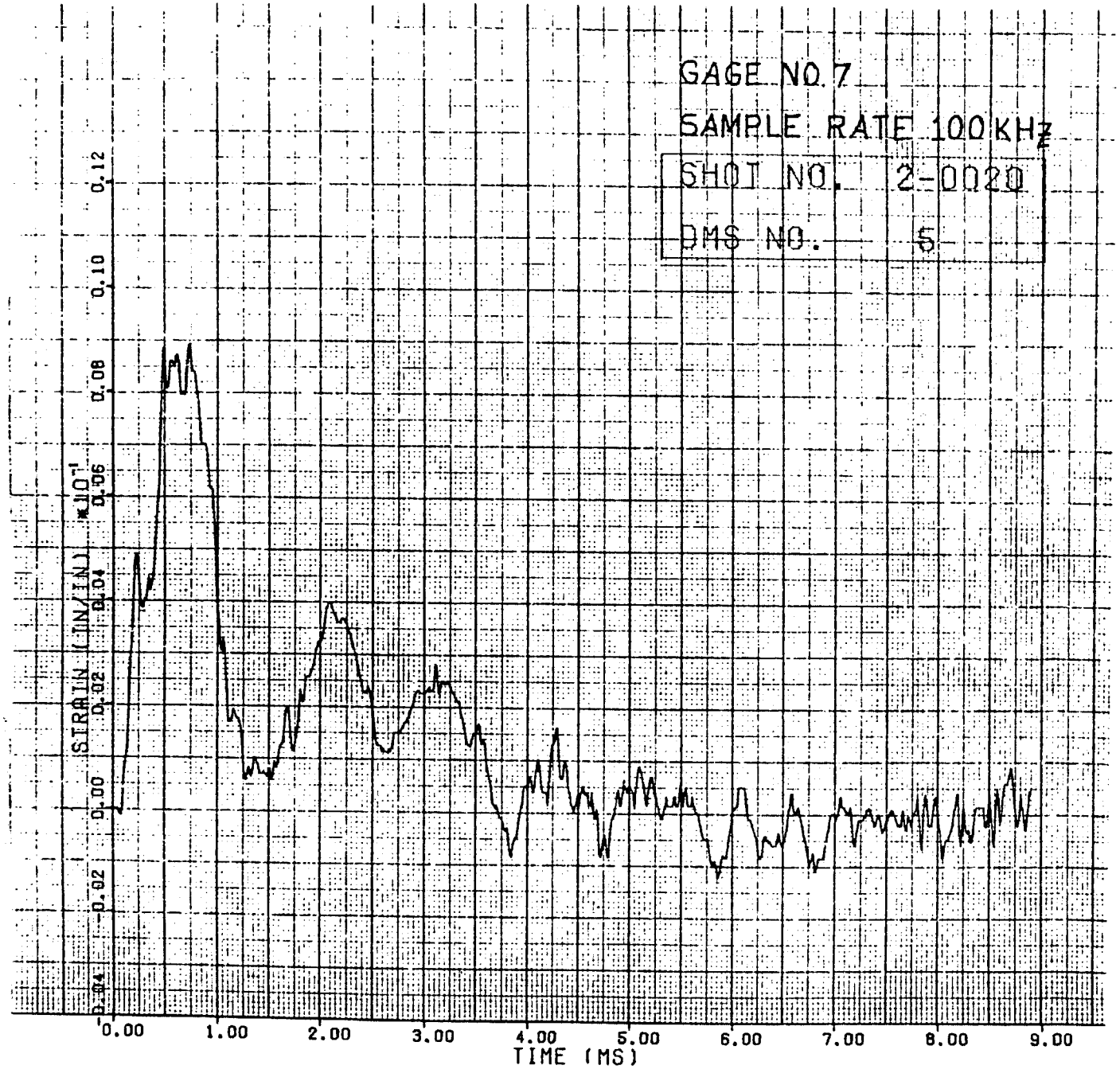

Figure 183. Strain of Shot 2-0020 for Gage #7.

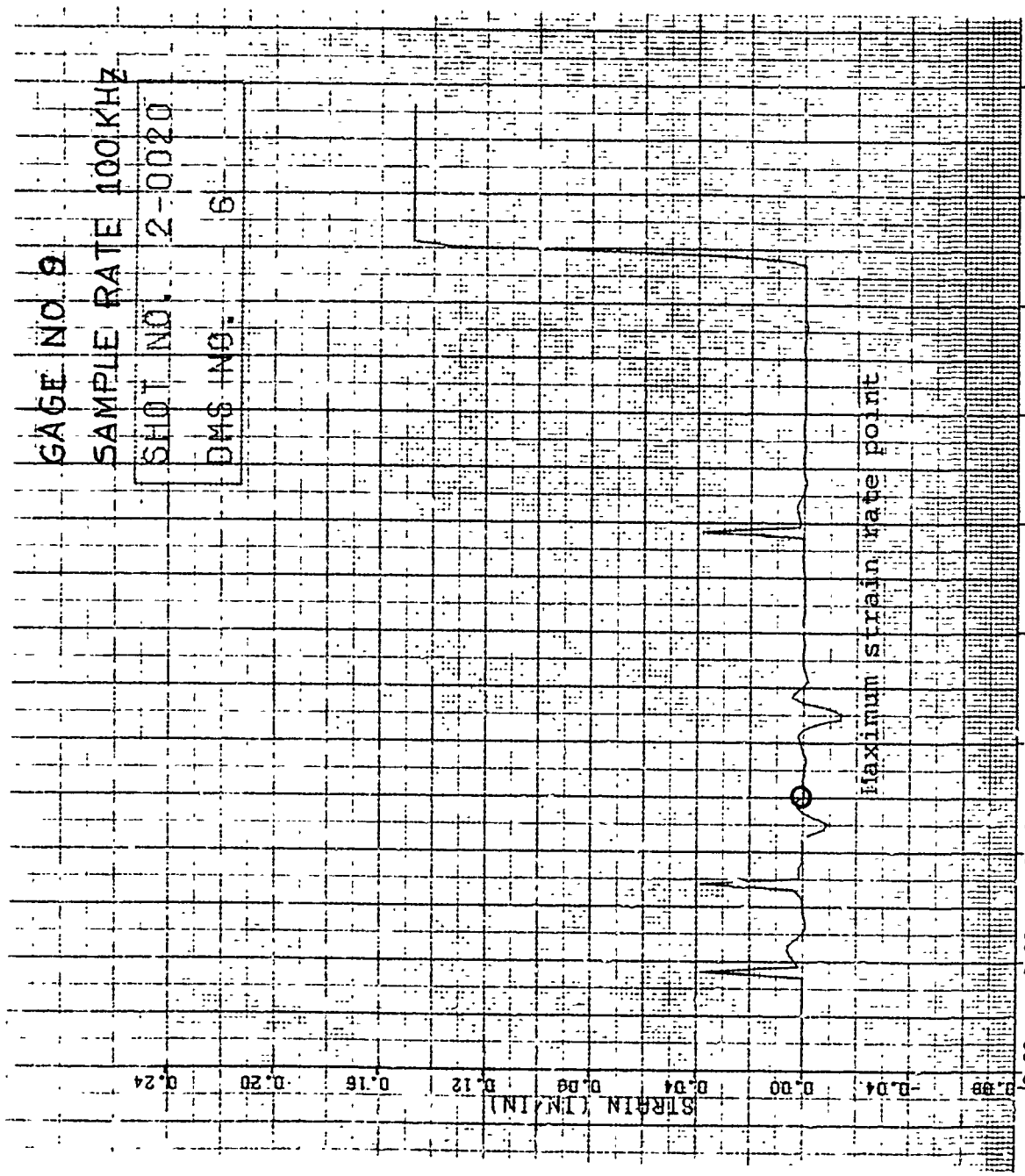

Figure 184. Strain of Shot 2-0020 for Gage #9.

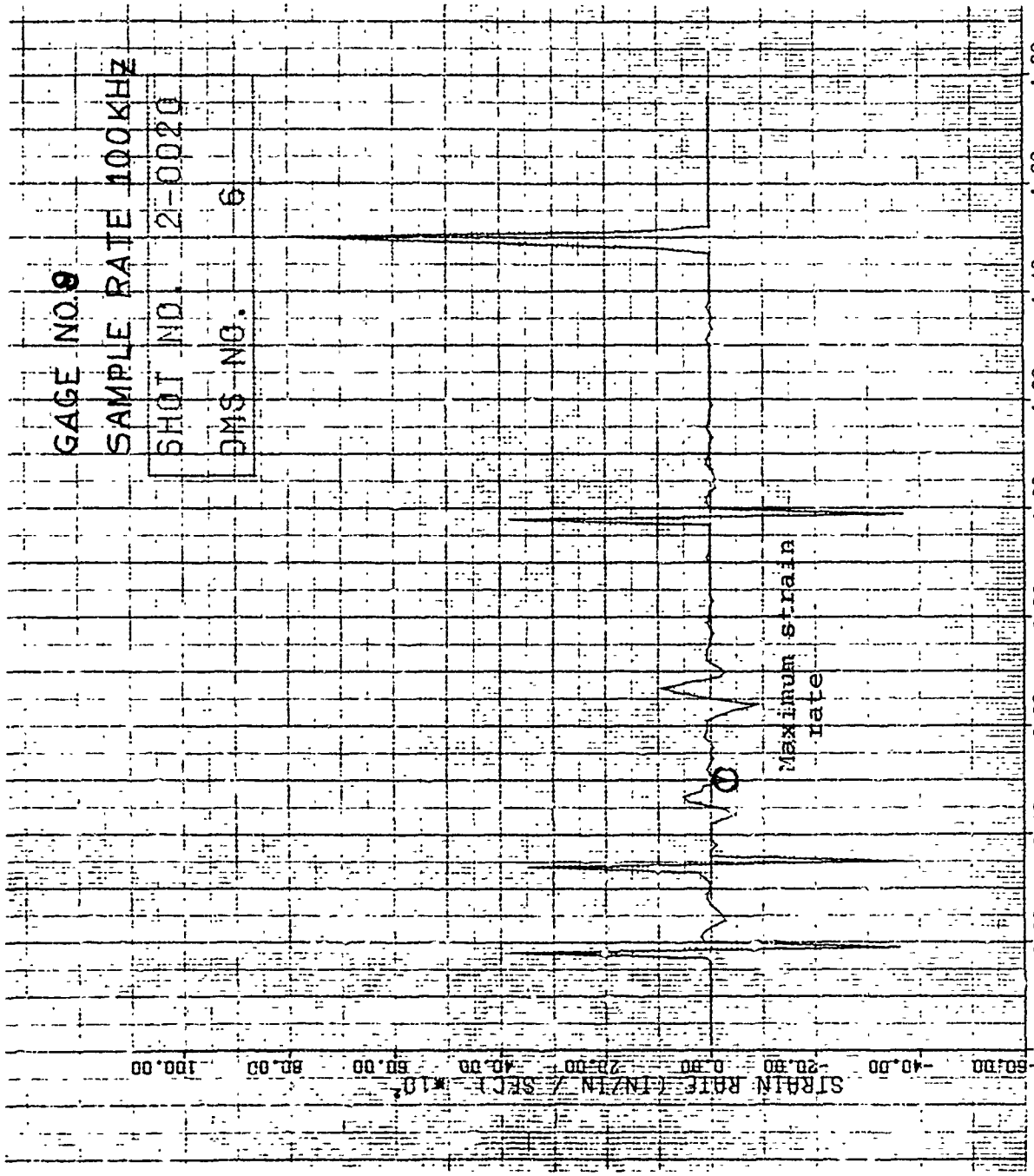

Figure 185. Strain Rate of Shot 2-0020 for Gage #9.

the impact site 1.78 cm for an impact mass of 105.6 g. Figure 46B shows the damage for Shot 2-0201. The strain data for Shot 2-0201 are given in Figures 186 through 191. The strain gage location for these impacts are given in Figure 4A of Appendix A. Tension for these impacts is denoted as a positive strain and compression as a negative strain.

Typical strain curves are given in Figures 192 through 197 for Shot 2-0198. No visible damage was received for this impact at a velocity of 121 m/s and impact mass of 40.7 g.

3.2.5 Impact Results for Group 5B Blades

Four leading edge impacts of slab ice (7.62 cm diameter x 17.78 cm long) on F101 titanium Group 5B blades generated damage on only one blade (Shot 2-0231). The impact velocity for this shot at the 70 percent span location was 185 m/s and the impact mass was 75.8 grams. The angle of incidence for the impacts was 24.4 degrees. The blade tip was restrained as shown in Figure 5. The damage for Shot 2-0231 was in the form of bowing at the impact site 5.28 cm on the leading edge and 6.50 cm on the trailing edge.

The strain versus time curves for Shot 2-0231 are given in Figures 198 through 203. Tension is denoted by a positive strain and compression by a negative strain. The location of the strain gages is given in Figure 4A of Appendix A. Photographs of the damage of Shot 2-0231 are given in Figure 47B.

3.2.6 Impact Results for Group 6B Blades

Three leading edge impacts of the small 85 g (3 ounce) bird on the J79 stainless steel blades resulted in generating no damage on the blades. The impact velocities ranged from 161 to 200 m/s for the 30 percent span location impacts and the impact mass ranged from 15.1 to 48.1 g. The angle of incidence for the impacts was 51.1 degrees.

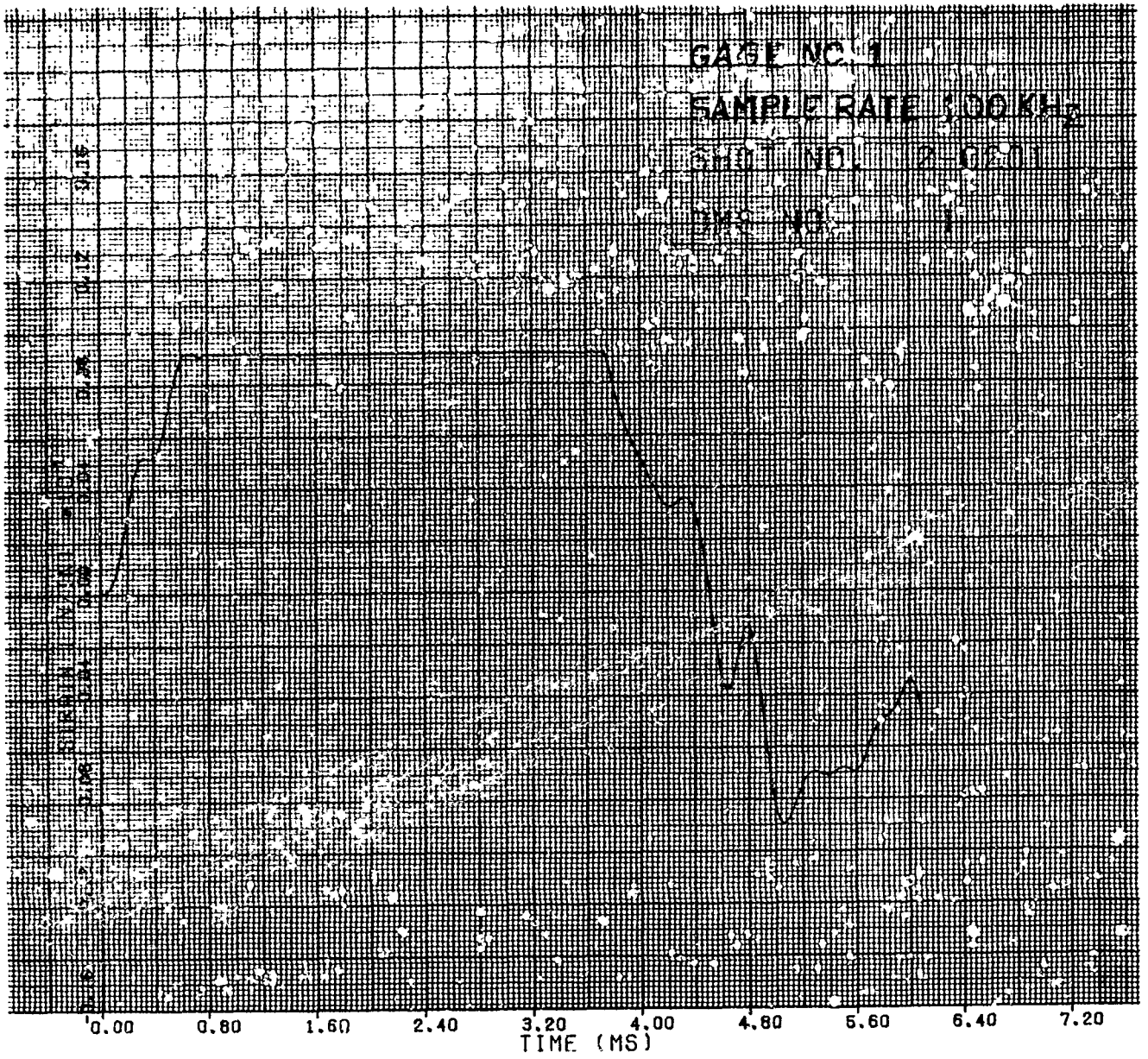

Figure 186. Strain of Shot 2-0201 for Gage #1.

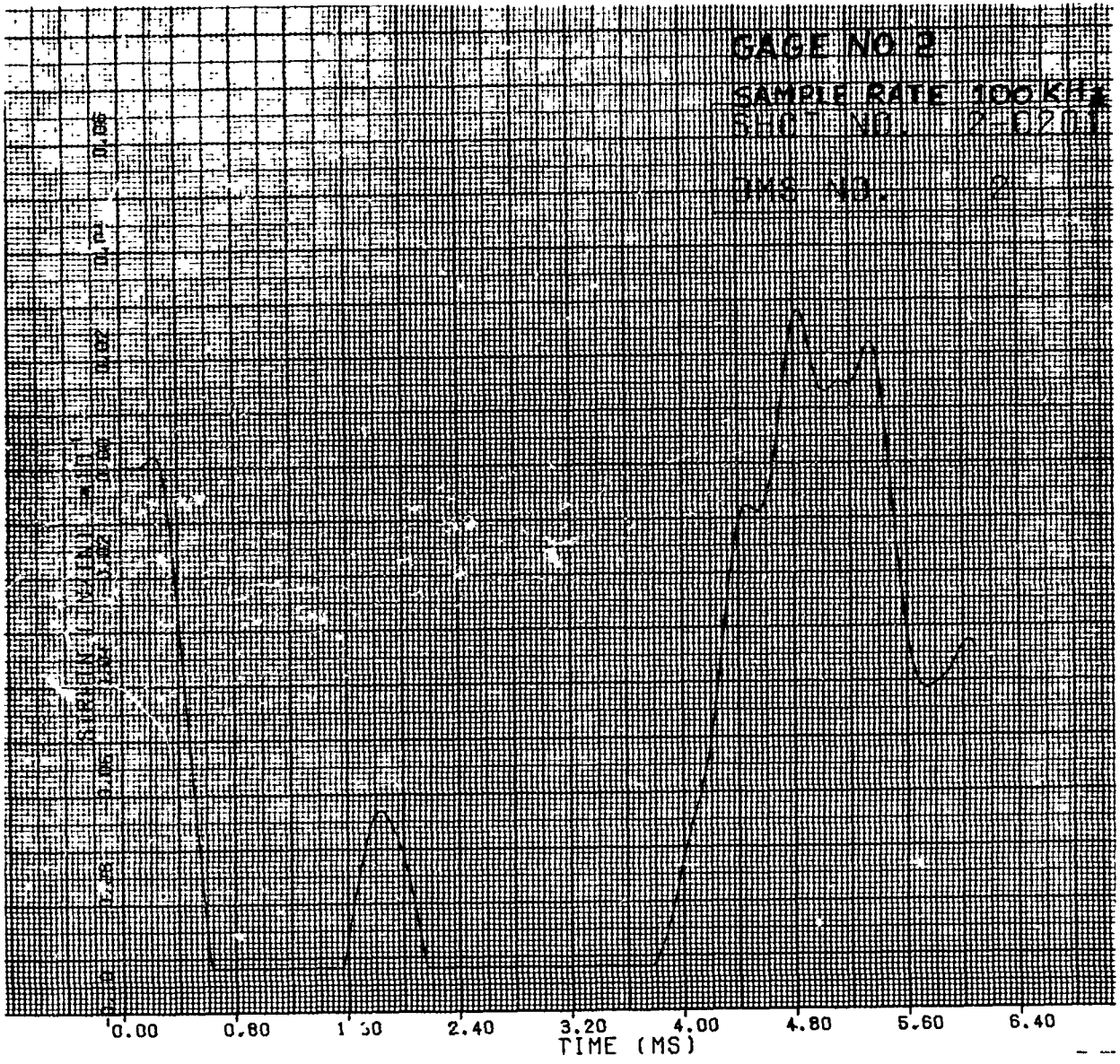

Figure 187. Strain of Shot 2-0201 for Gage #2.

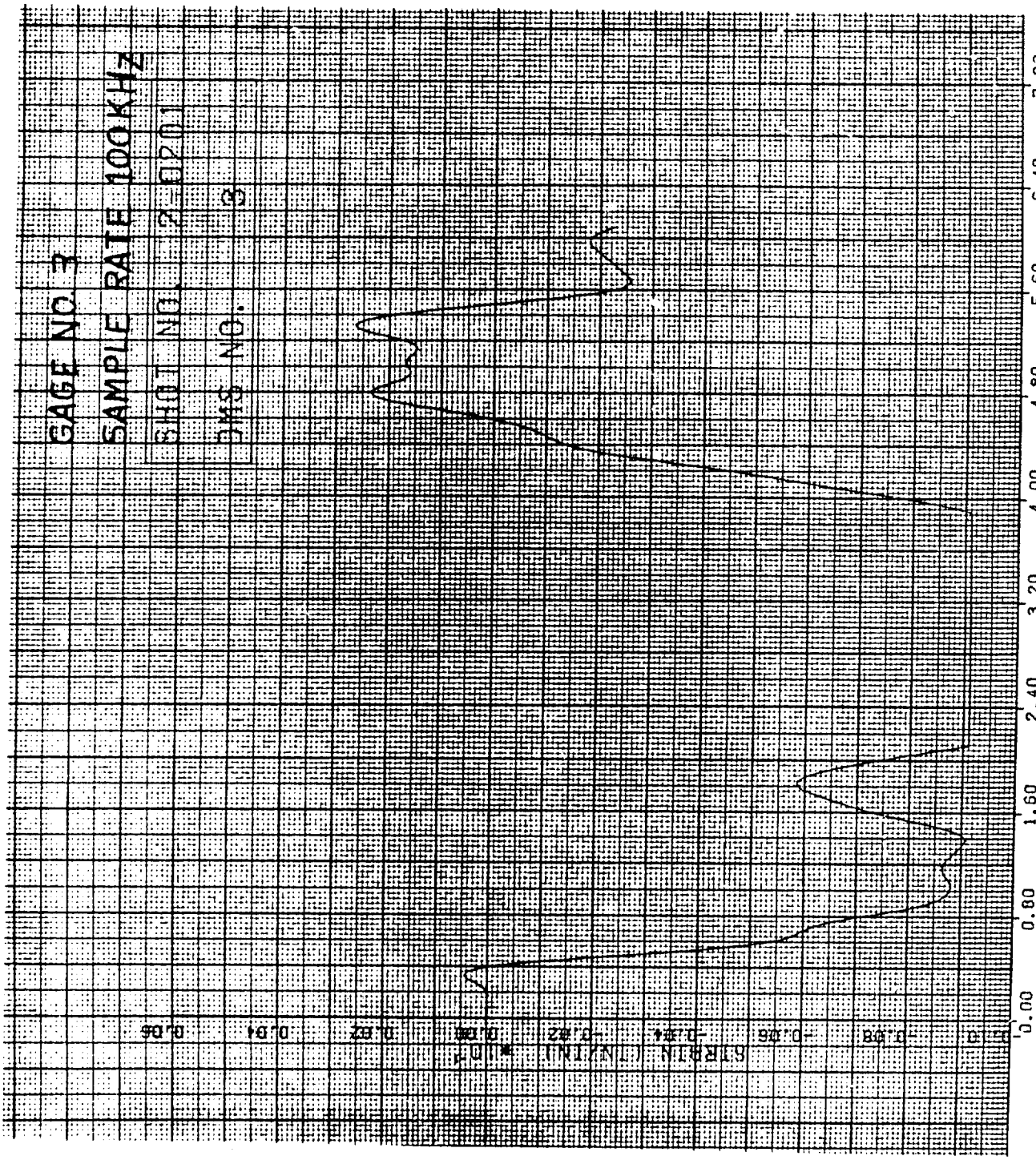

Figure 188. Strain of Shot 2-0201 for Gage #3.

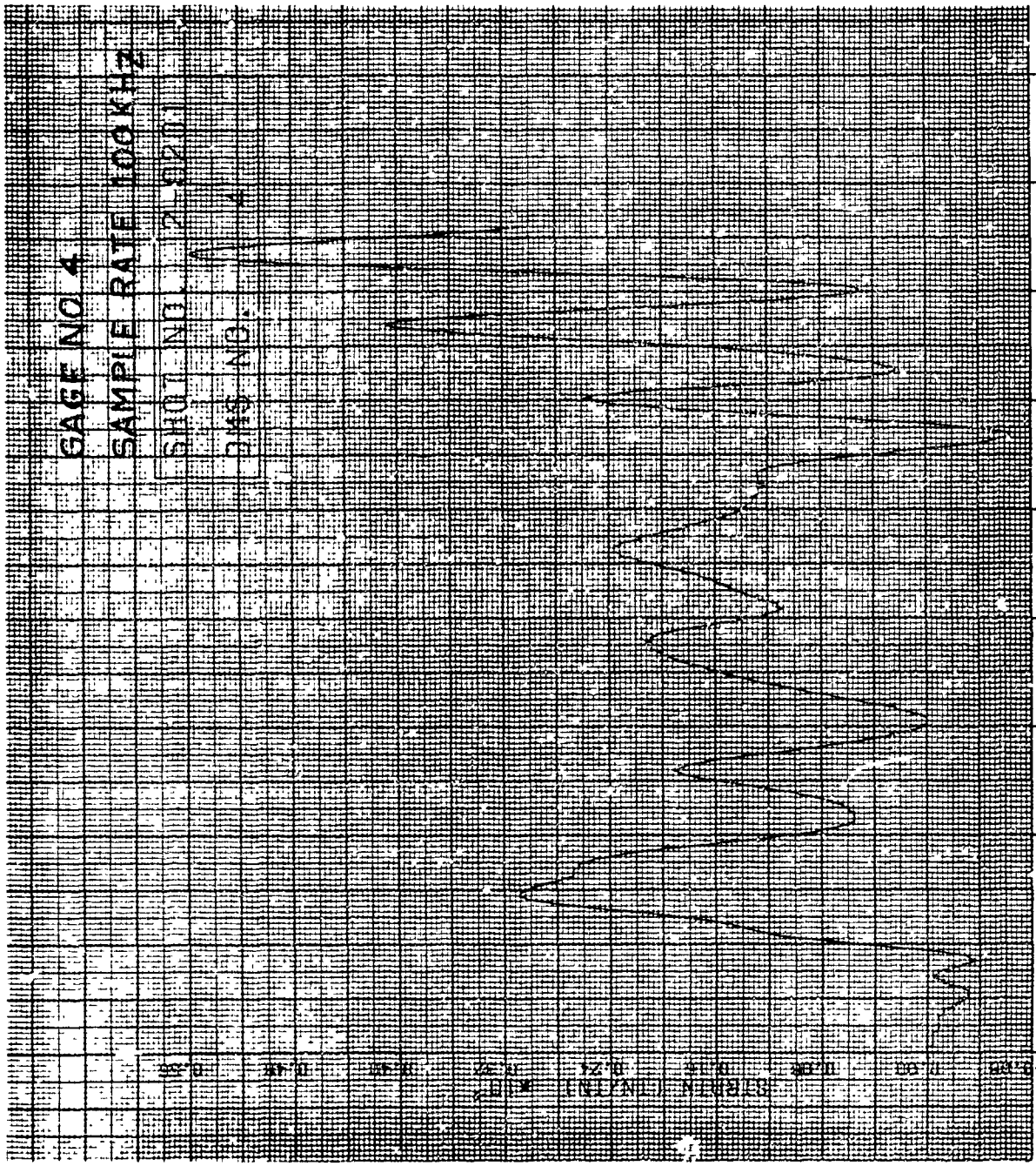

Figure 189. Strain of Shot 2-0201 for Gage #4.

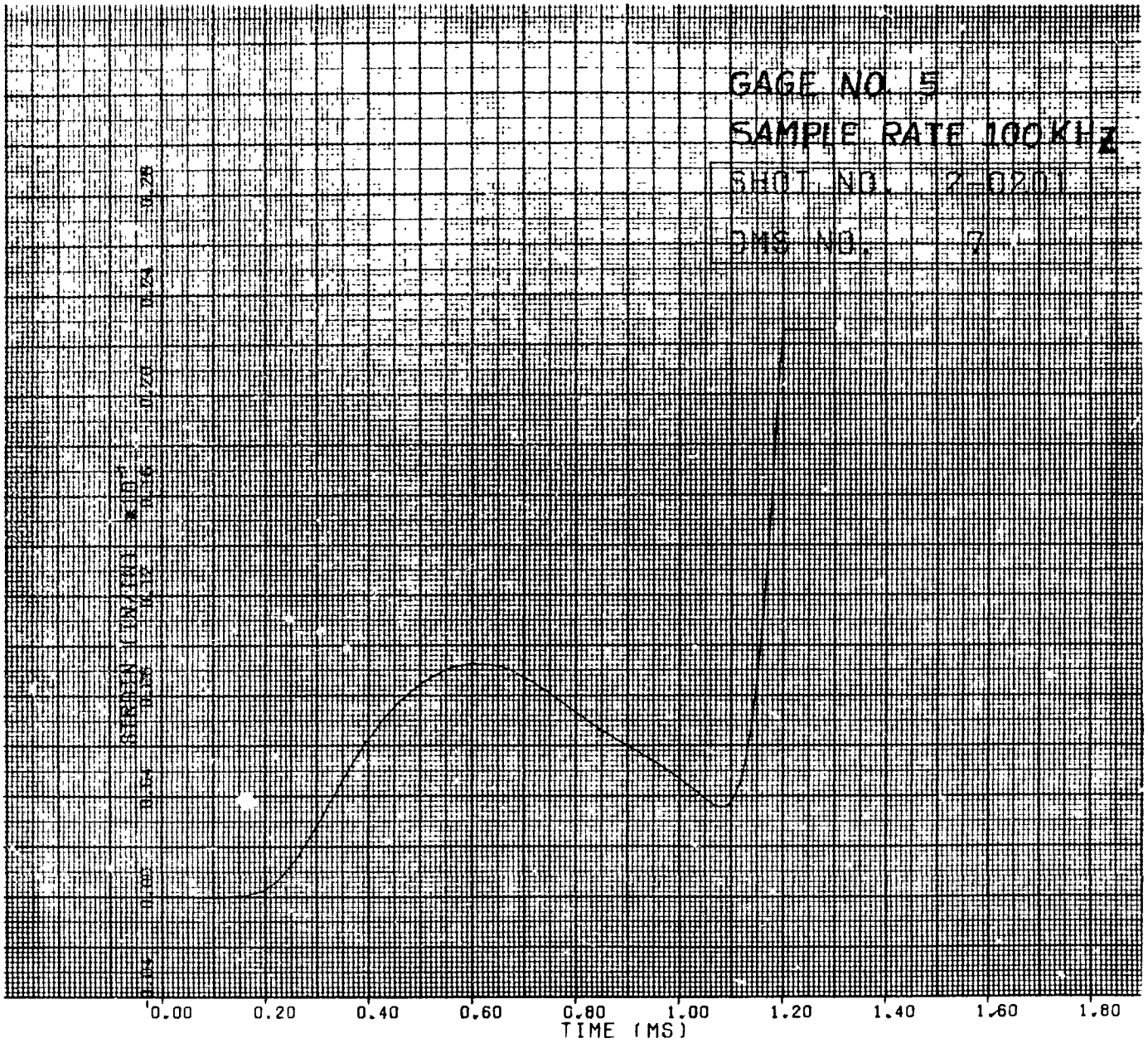

Figure 190. Strain of Shot 2-0201 for Gage #5.

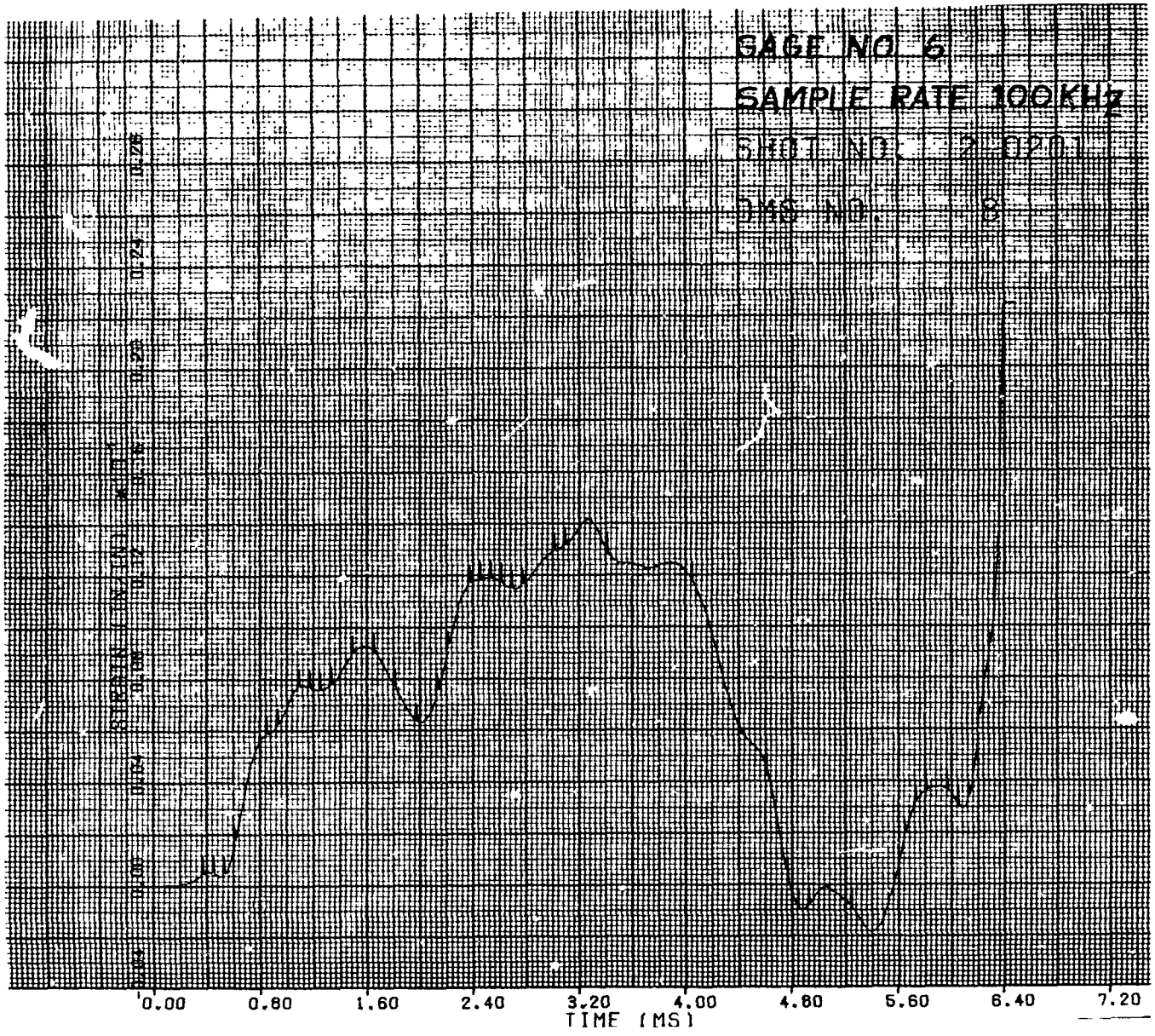

Figure 191. Strain of Shot 2-0201 for Gage #6.

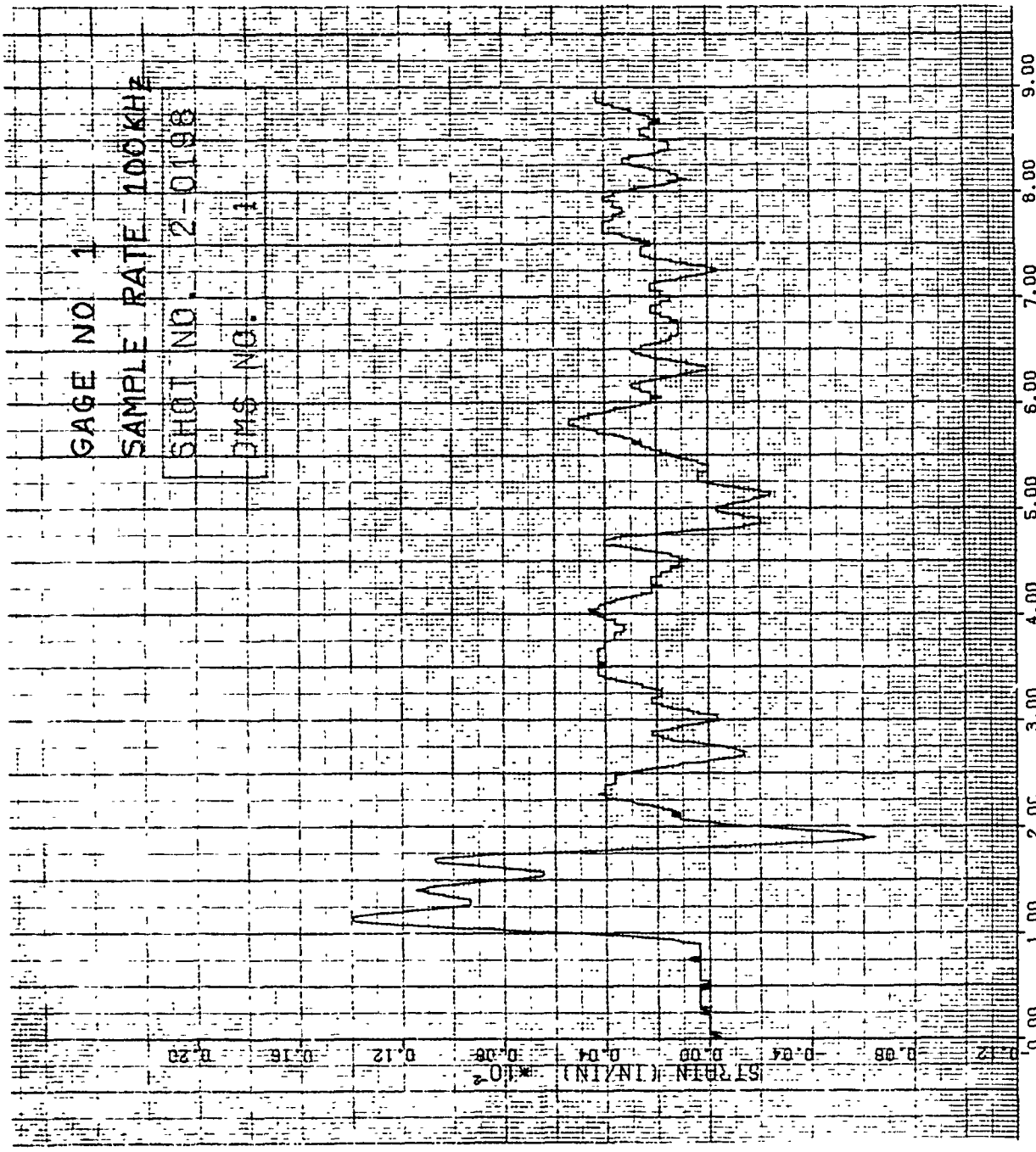

Figure 192. Strain of Shot 2-0198 for Gage #1.

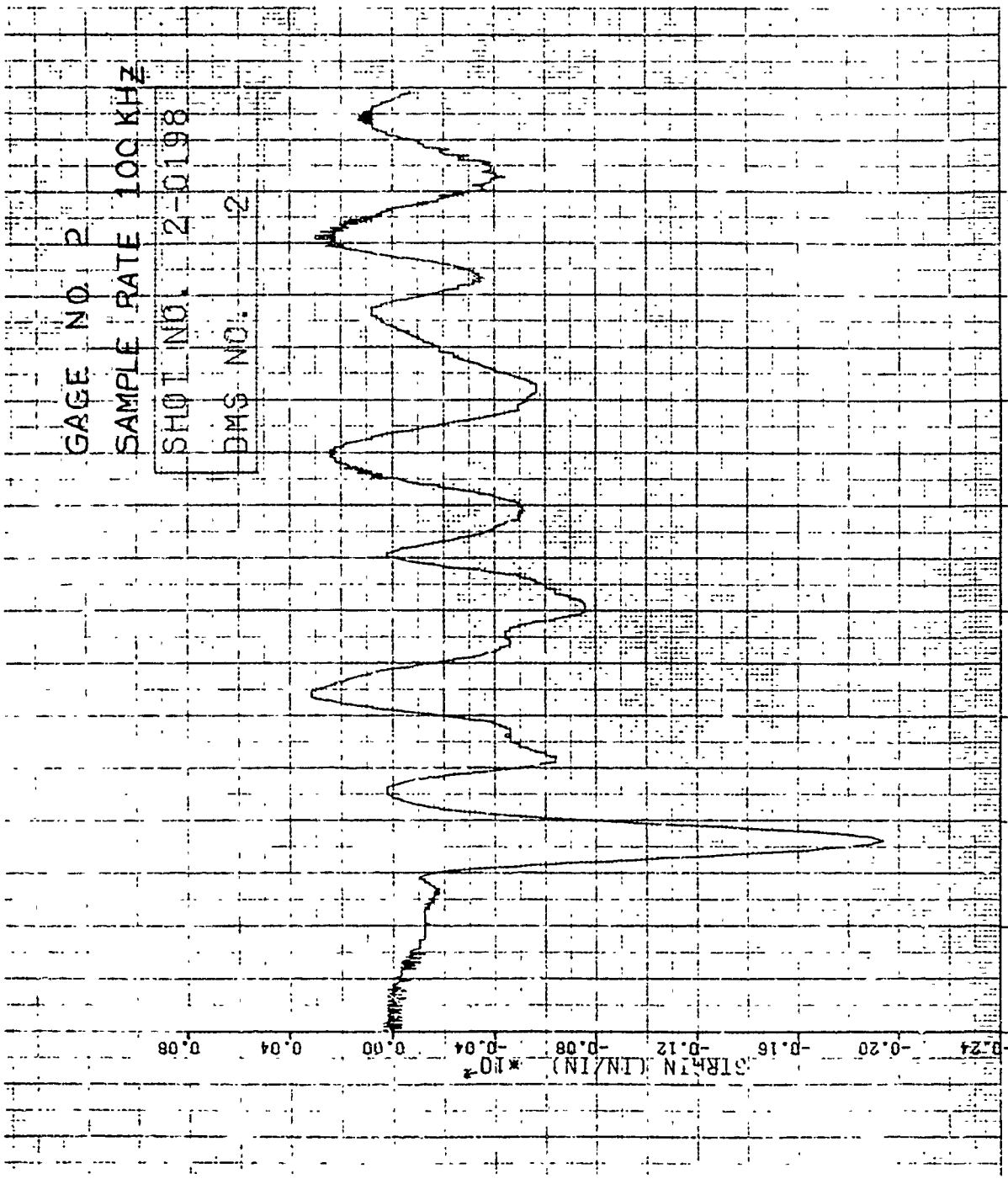

Figure 193. Strain of Shot 2-0198 for Gage #2.

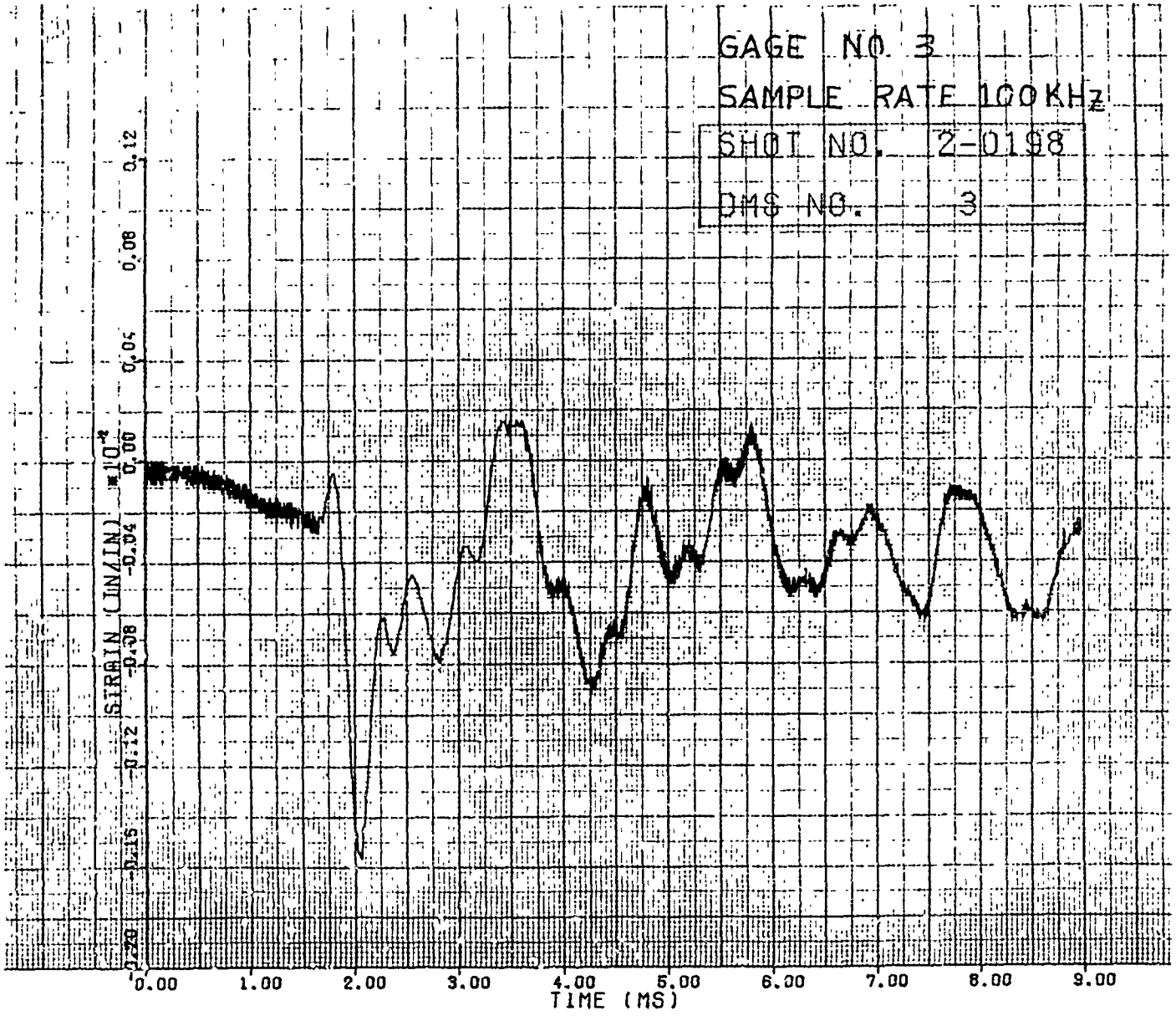

Figure 194. Strain of Shot 2-0198 for Gage #3.

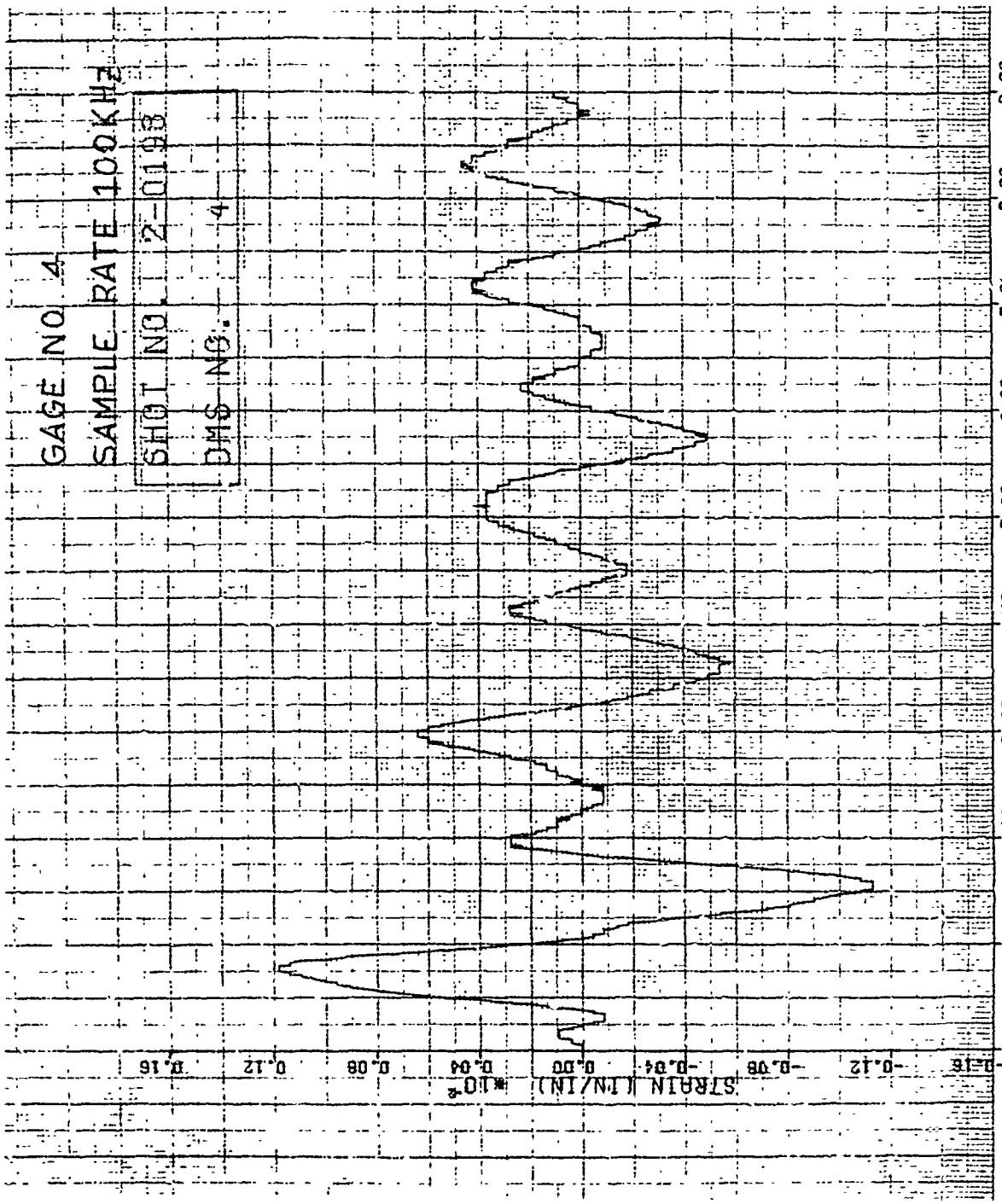

Figure 195. Strain of Shot 2-0198 for Gage #4.

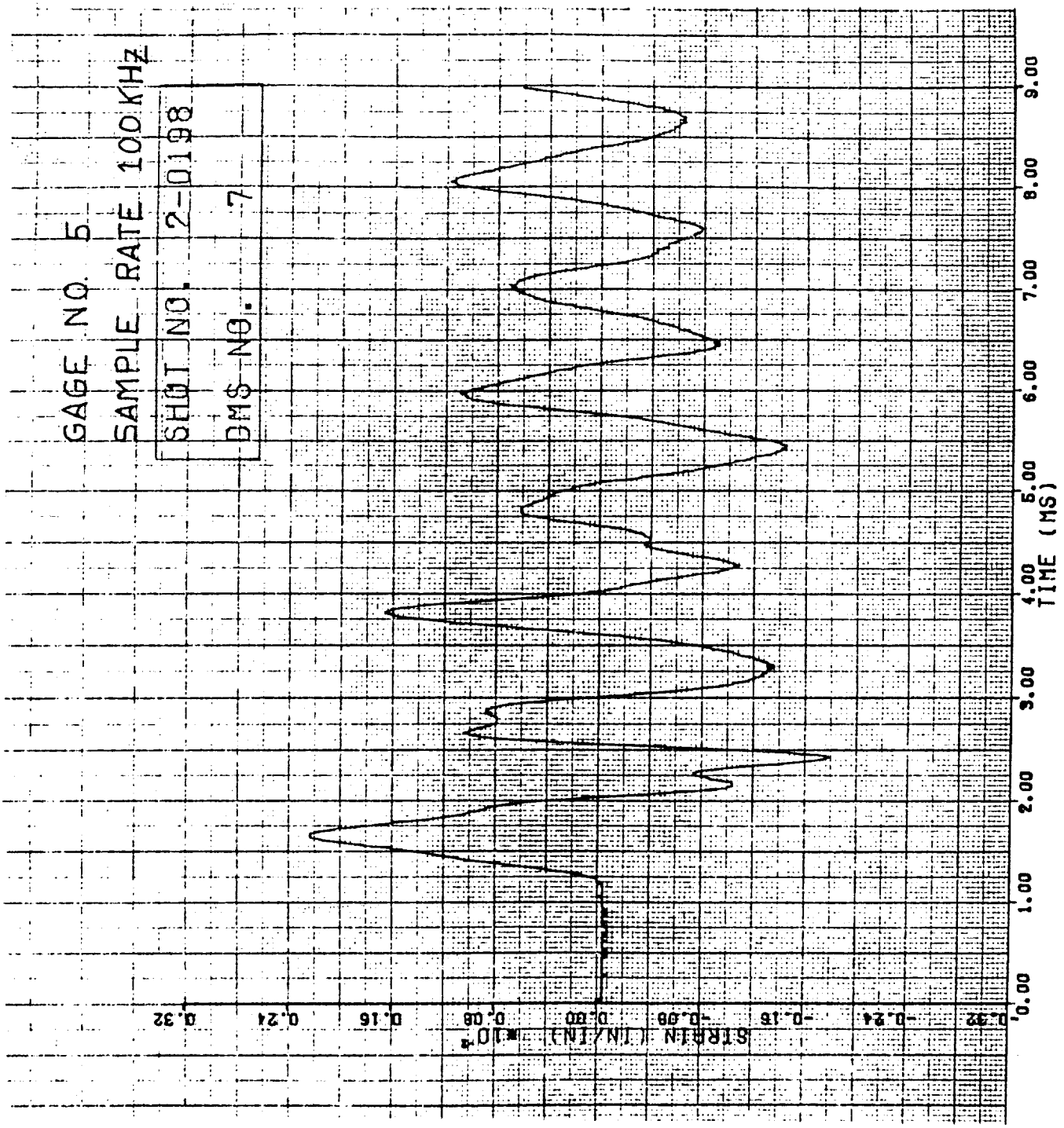

Figure 196. Strain of Shot 2-0198 for Gage #5.

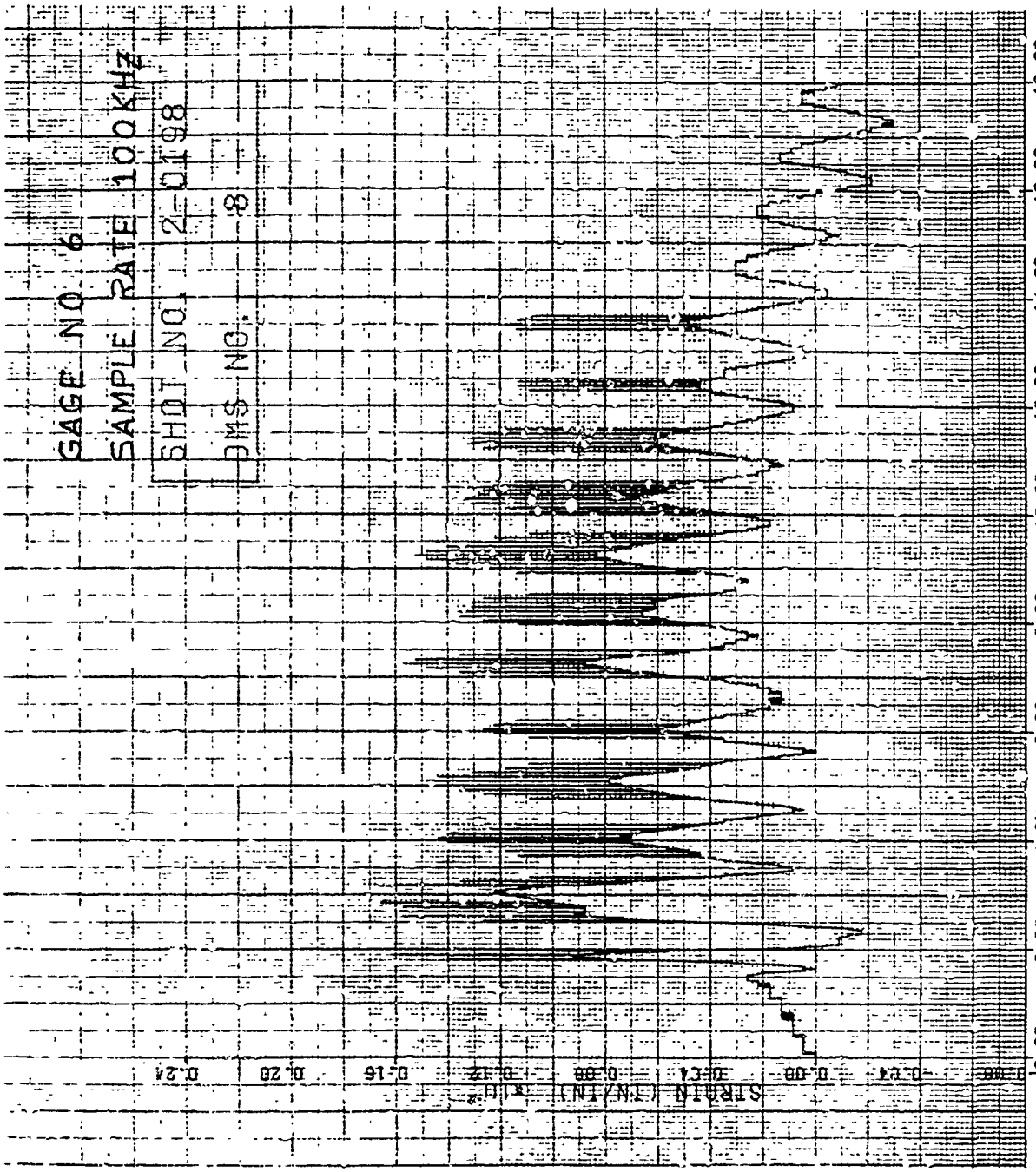

Figure 197. Strain of Shot 2-0198 for Gage #6.

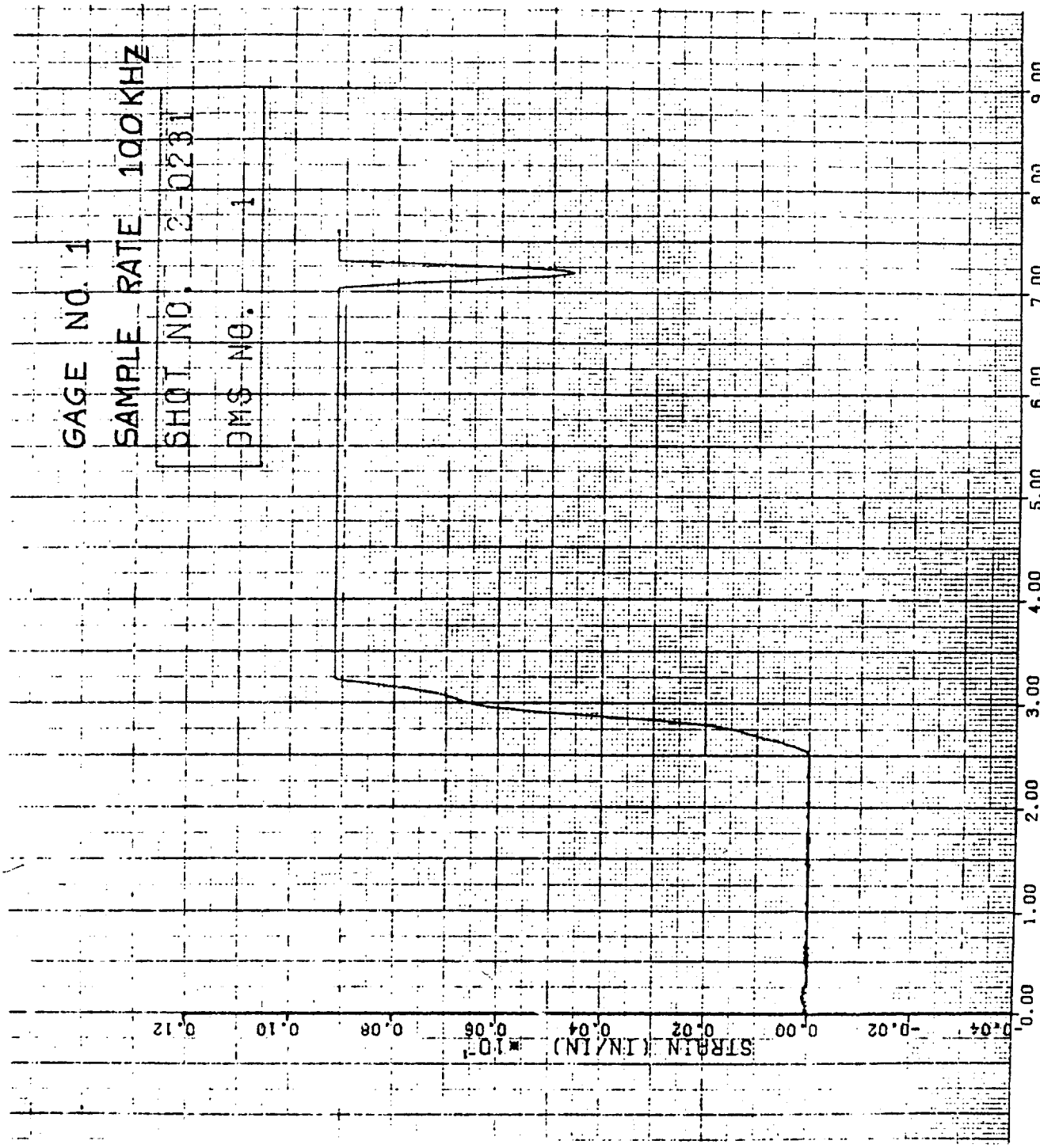

Figure 198. Strain of Shot 2-0231 for Gage #1.

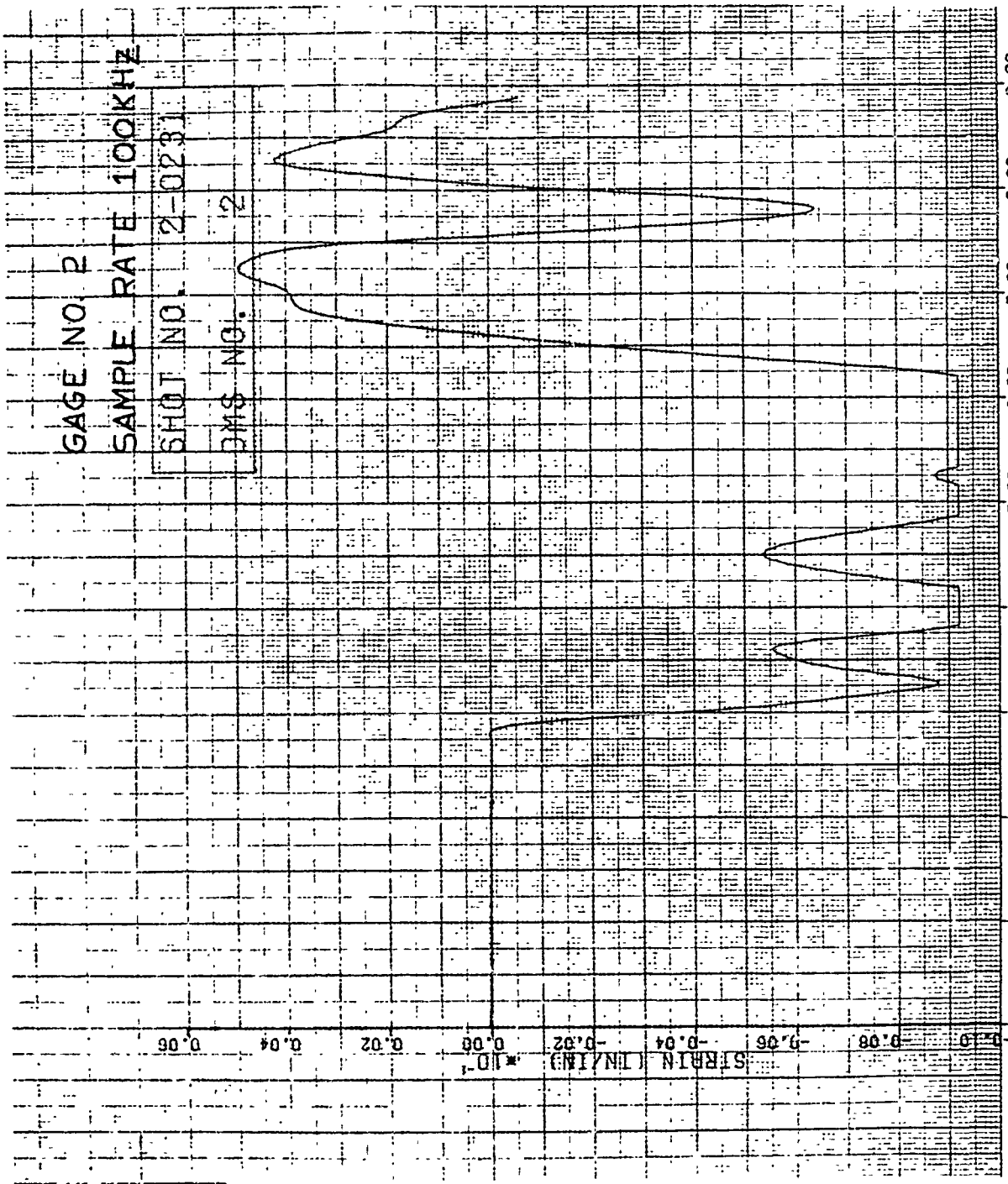

Figure 199. Strain of Shot 2-0231 for Gage #2.

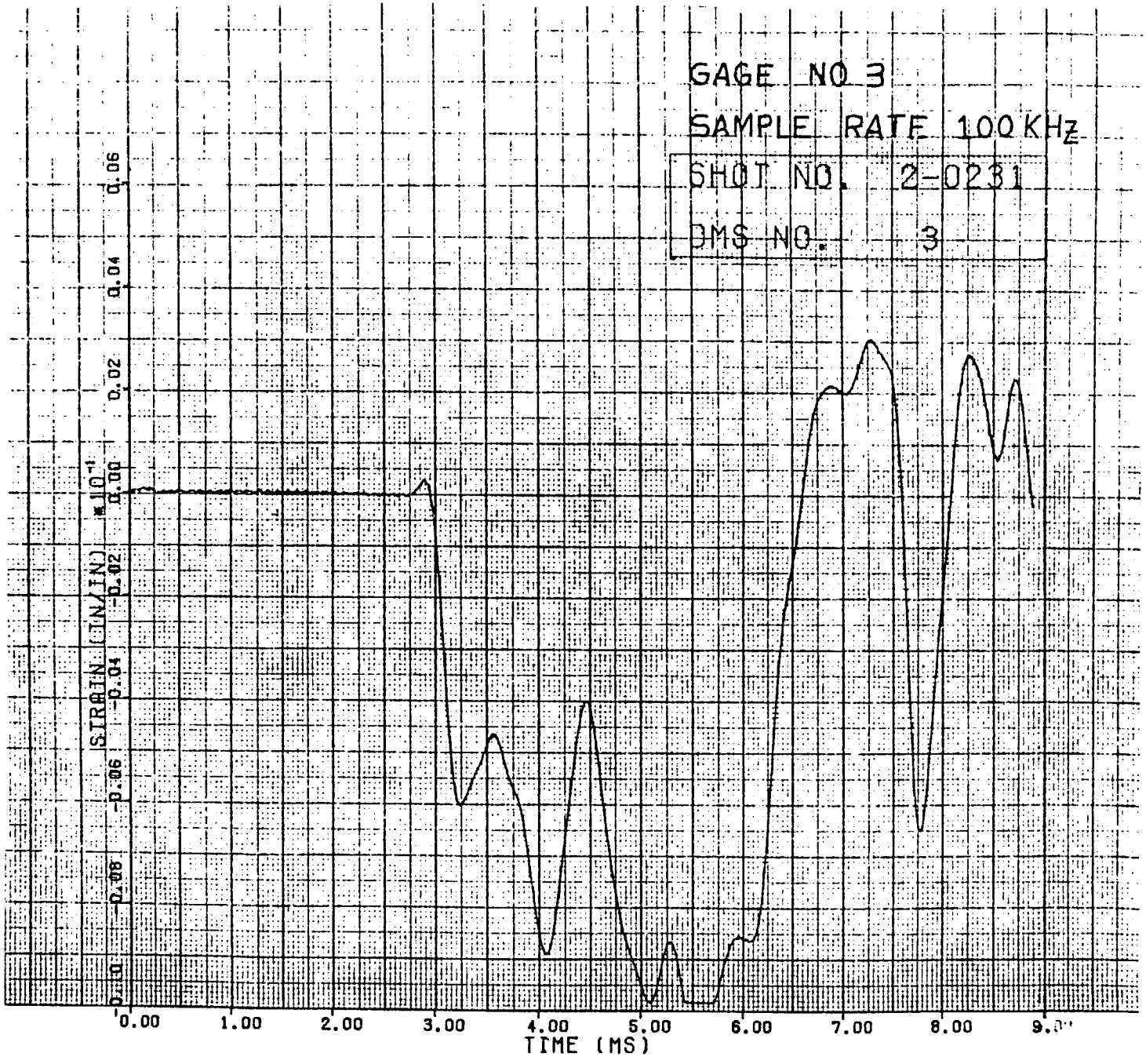

Figure 200. Strain of Shot 2-0231 for Gage #3.

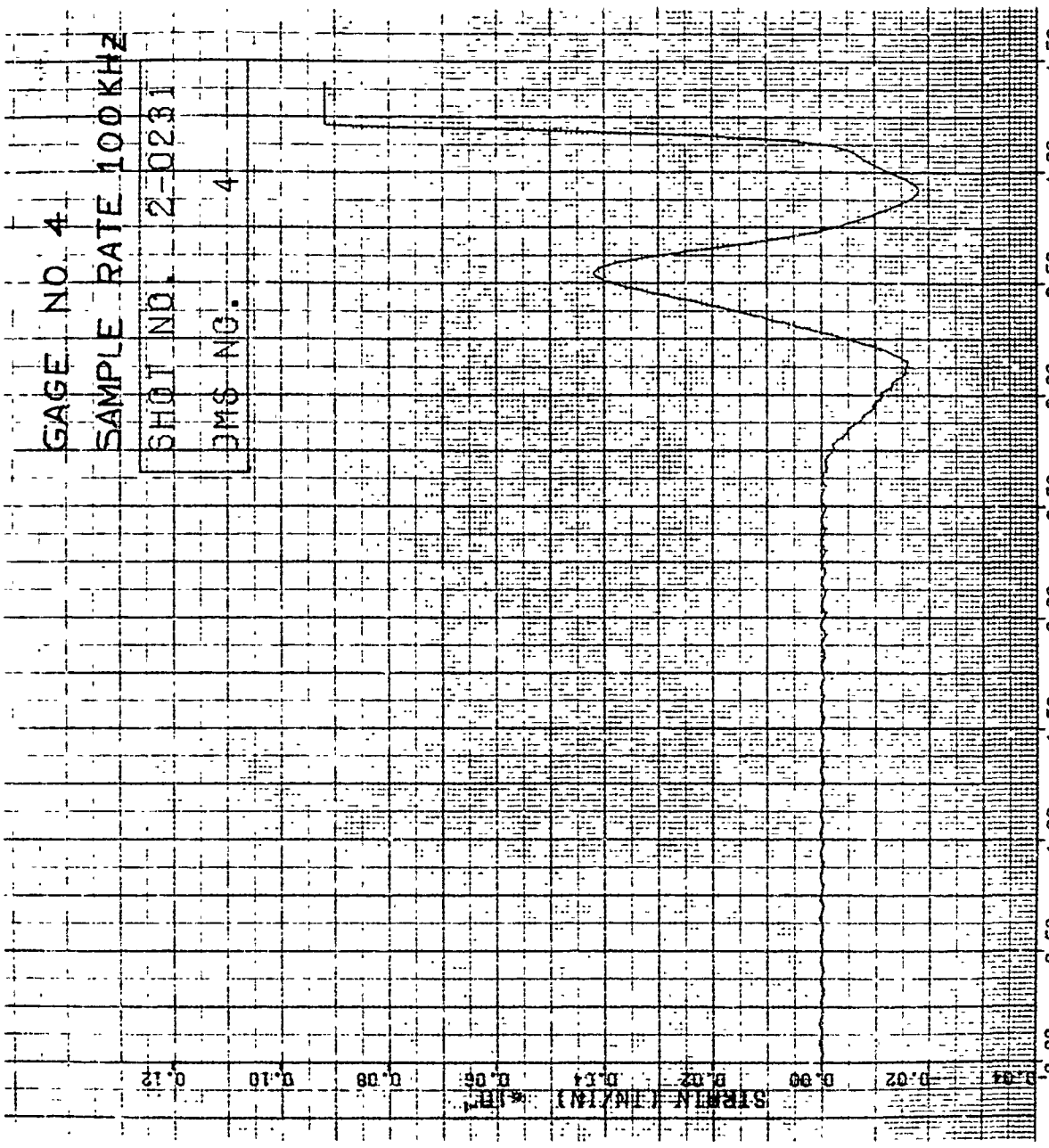

Figure 201. Strain of Shot 2-0231 for Gage #4.

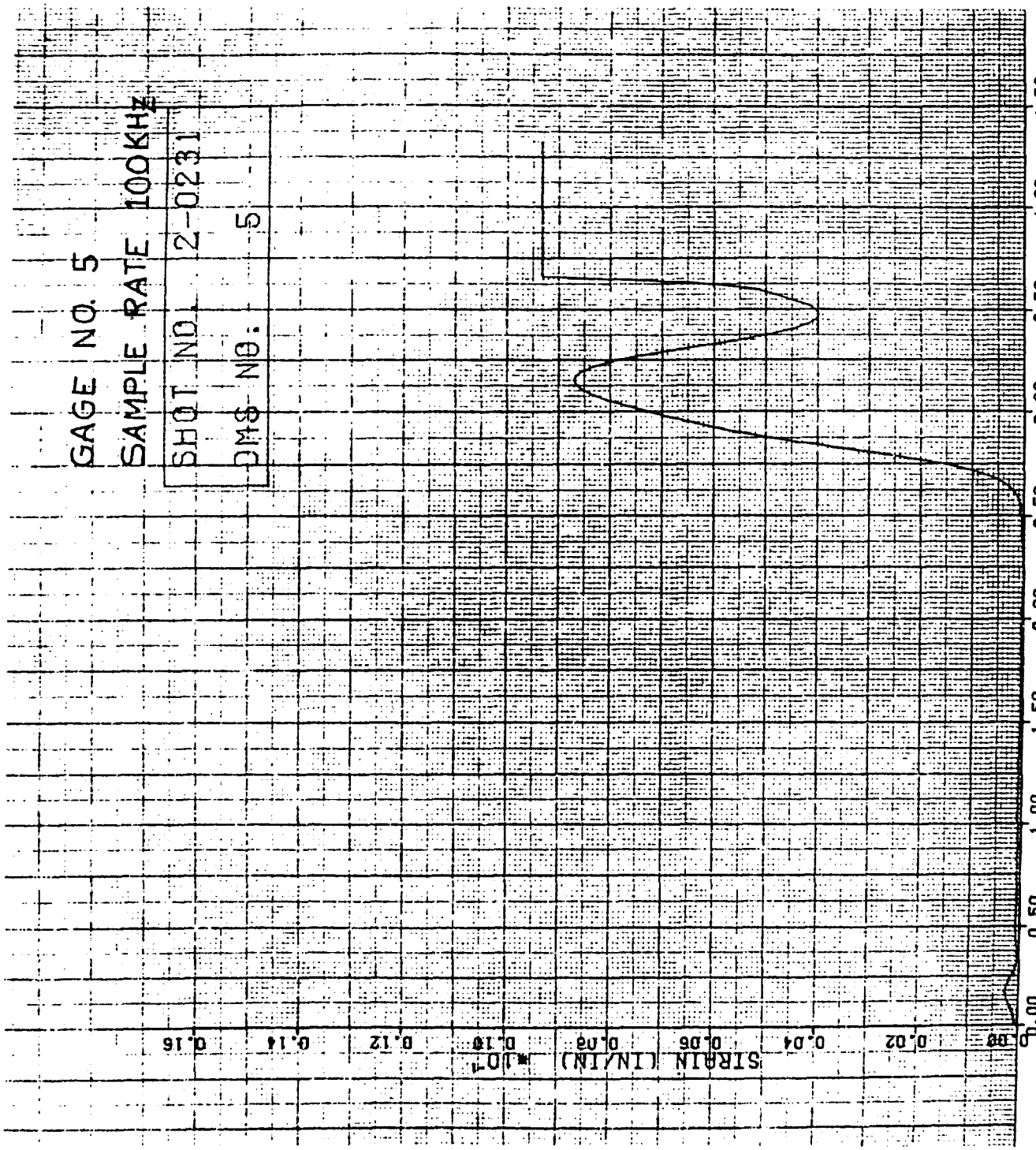

Figure 202. Strain of Shot 2-0231 for Gage #5.

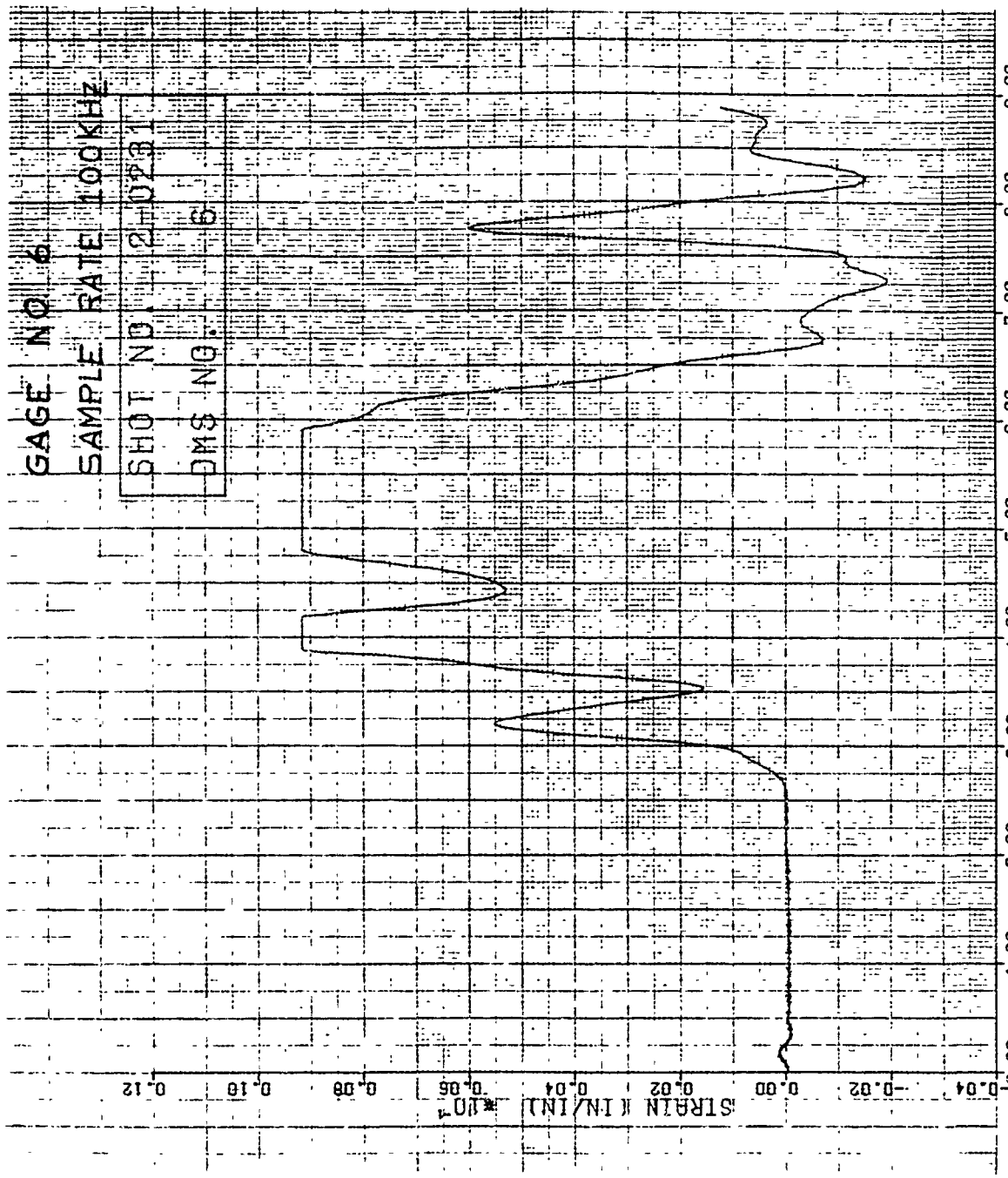

Figure 203. Strain of Shot 2-0231 for Gage #6.

Typical strain data for this group of blades are given in Figures 204 through 209 for Shot 2-0009. The strain gage locations for this blade group is given in Figure 2A of Appendix A. Tension is denoted as a negative strain and compression as a positive strain for all impacts in this series of tests. As indicated above, no visible damage was received for Shot 2-0009 for an impact velocity of 161 m/s and an impact mass of 48.1 g.

Strain versus time data are also given in Figures 210 through 215 for Shot 2-0010 for an impact velocity of 200 m/s and impact mass of 48.1 g. The strain for this higher velocity shot is considerably greater than for the lower velocity shot.

3.2.7 Impact Results for Group 7B Blades

One leading edge impact (Shot 2-0021) using the small 85 g (3 ounce) size bird generated damage on the J79 stainless steel blade in the form of bowing at the impact site. The balsa wood sabot also hit the blade. The impact velocity for the 70 percent span location impact was 300 m/s and the impact mass was 28.0 grams. The angle of incidence was 36.4 degrees.

The strain versus time curves for Shot 2-0021 are given in Figures 216 through 221. The strain gage locations are given in Figure 2A of Appendix A. Tension is denoted as a negative strain and compression as a positive strain in the strain data curves. Figure 48B shows the damage received on the J79 blade from Shot 2-0021.

3.2.8 Impact Results for Group 8B Blades

Five leading edge impacts using the 680 g (1.5 pound) bird were conducted on J79 stainless steel blades at a velocity of about 170 m/s. The impact mass ranged from a low of 37.0 g to a high of 311.0 g. The impact site was at the 30 percent span location of the blades. The angle of incidence for these impacts was 51.1 degrees.

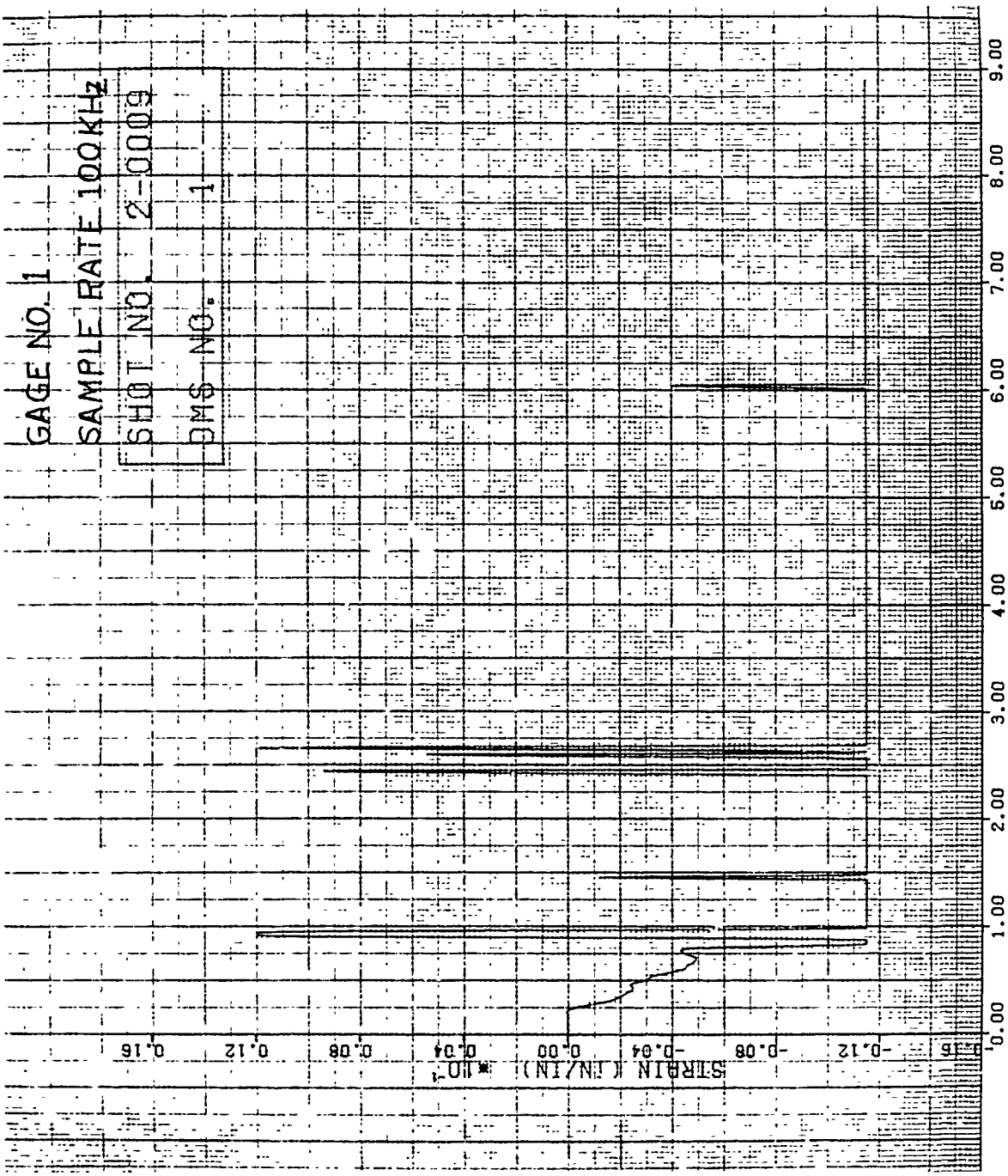

Figure 204. Strain of Shot 2-0009 for Gage #1.

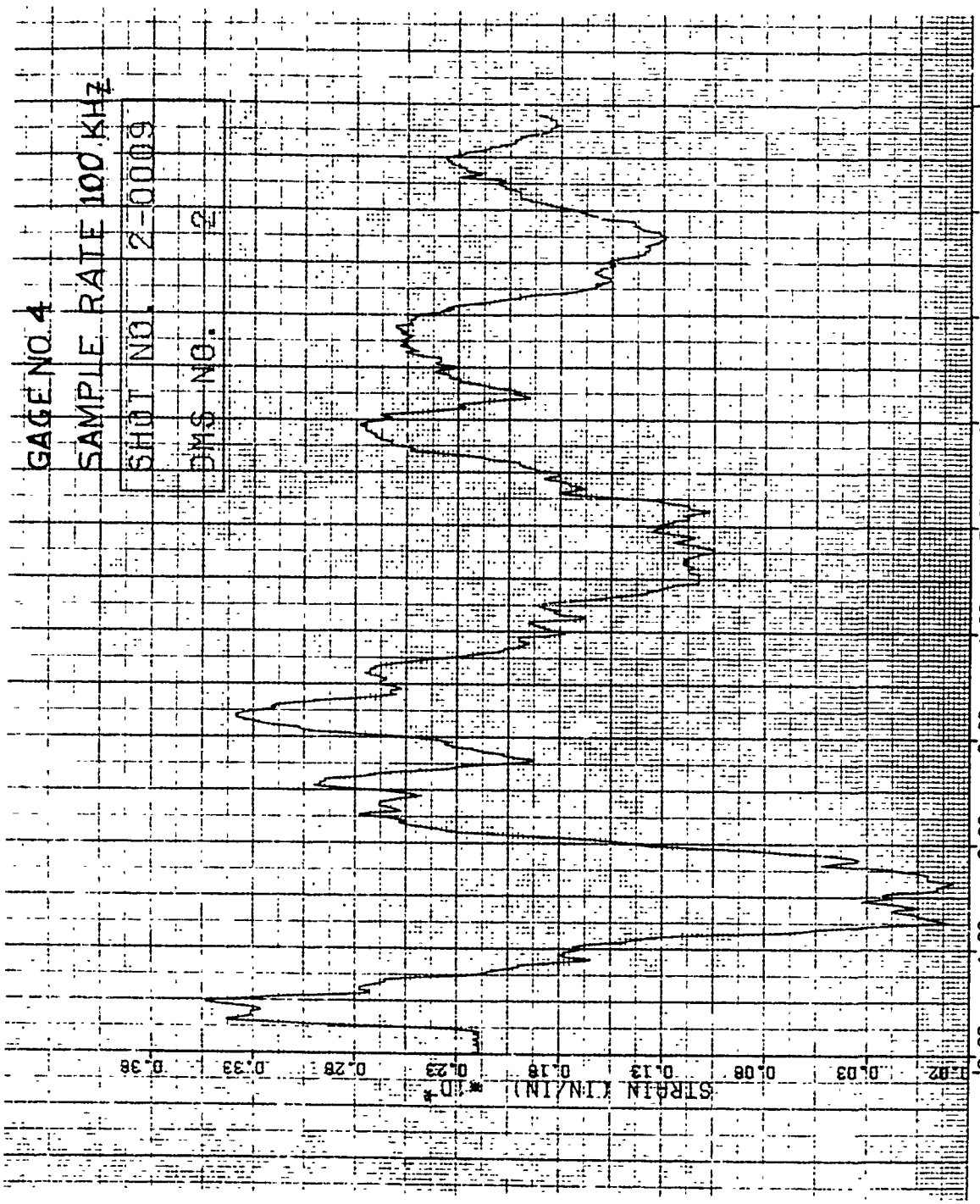

Figure 205. Strain of Shot 2-0009 for Gage #4.

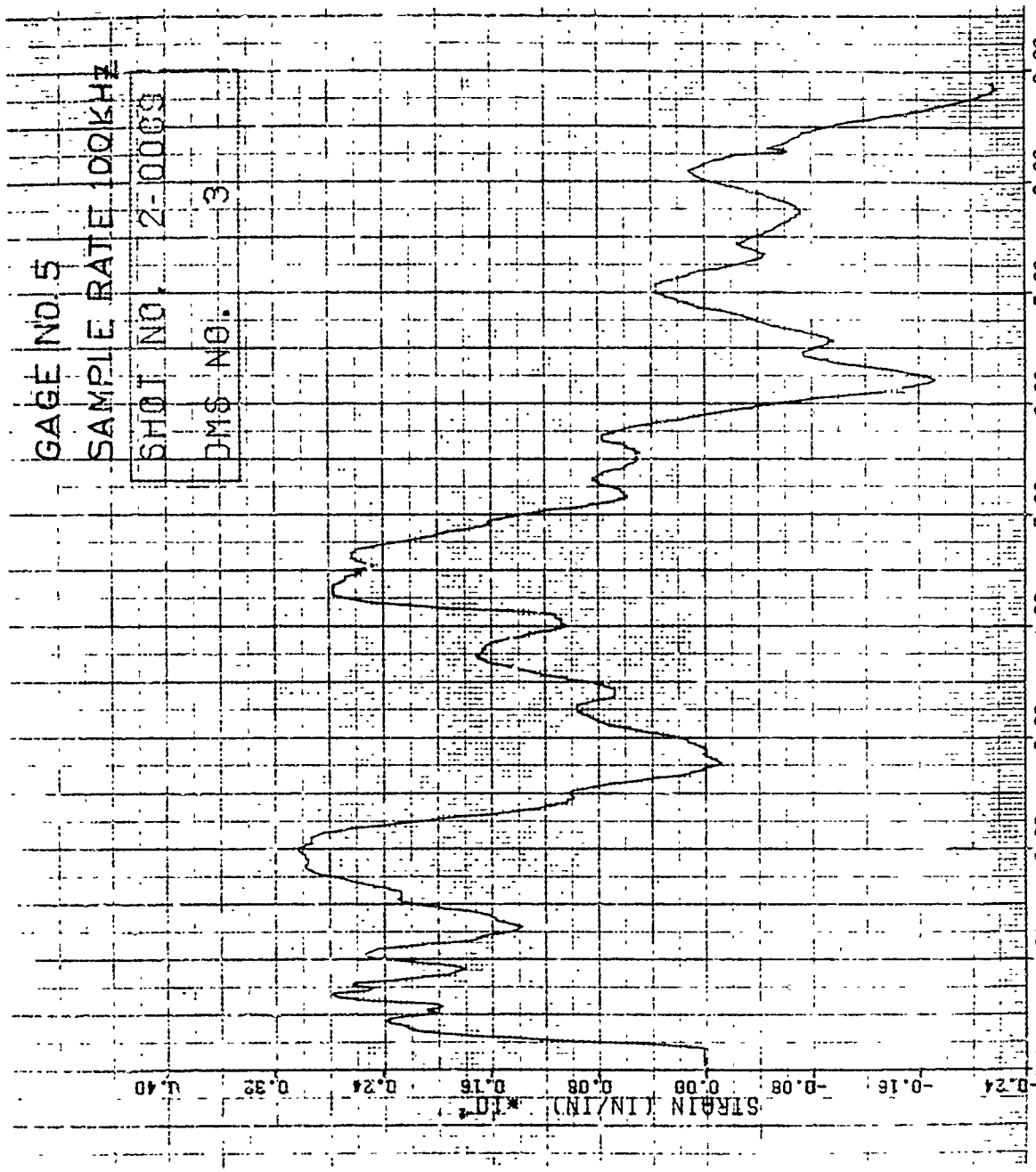

Figure 206. Strain of Shot 2-0009 for Gage #5.

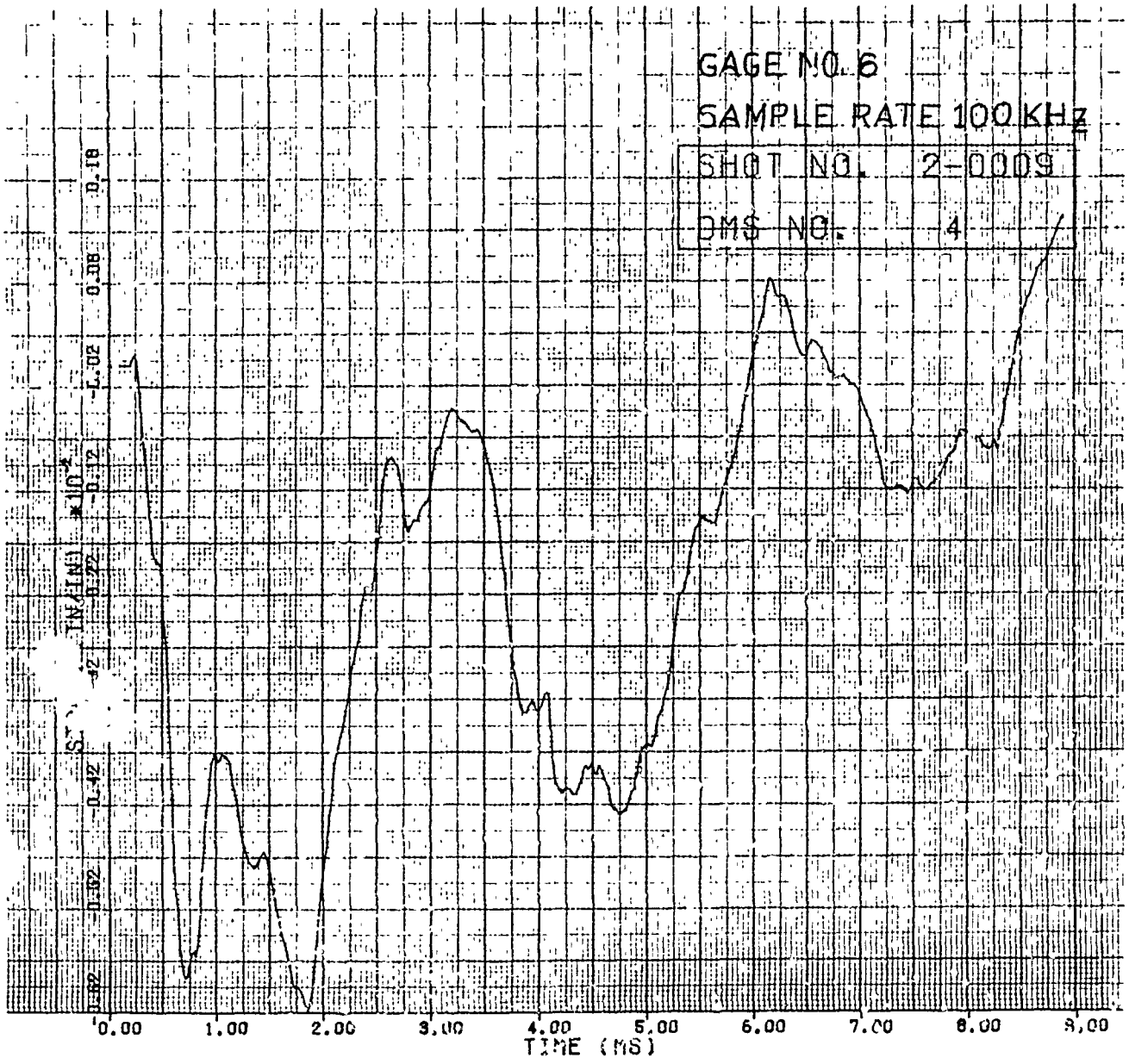

Figure 207. Strain of Shot 2-0009 for Cage #6.

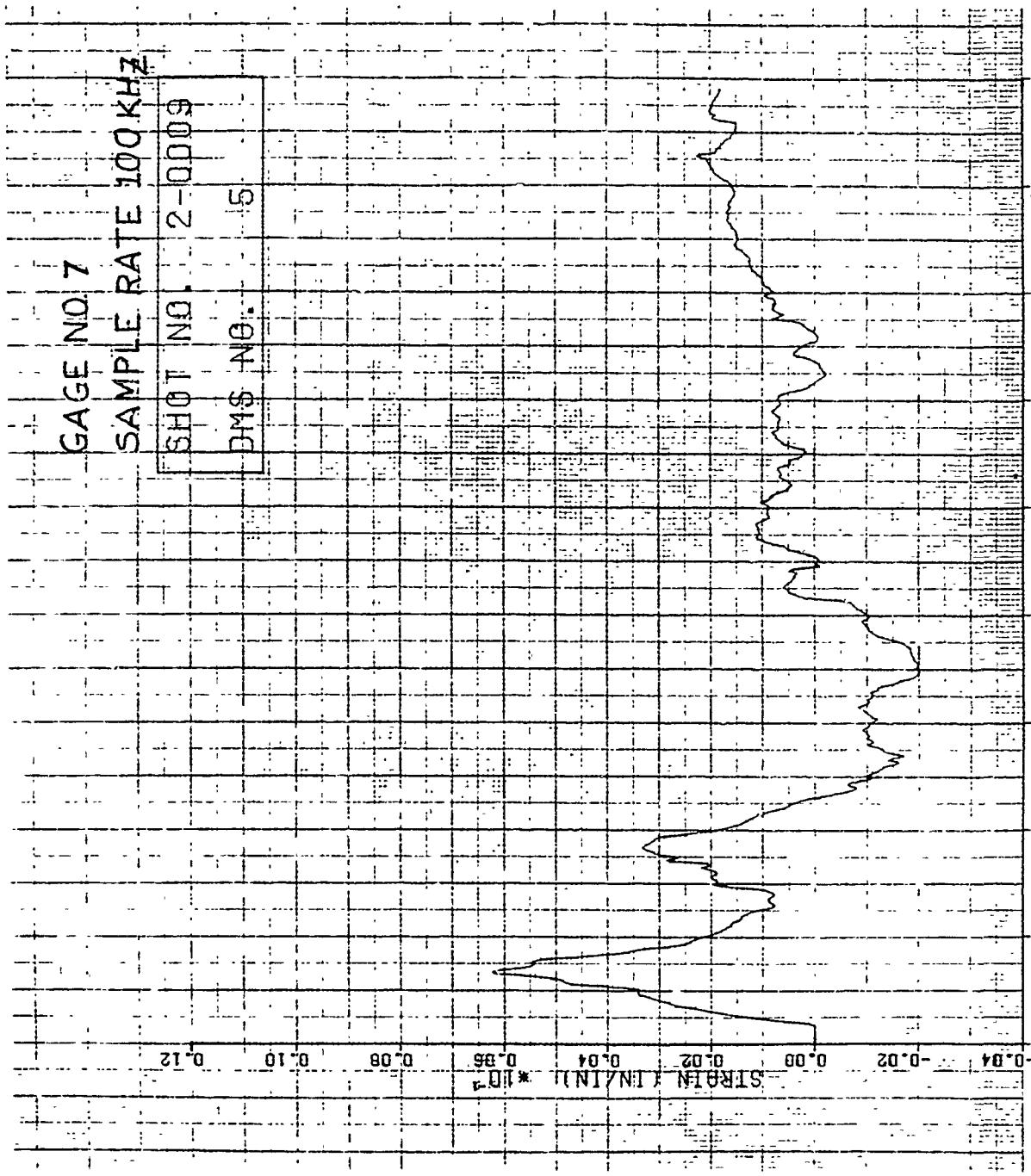

Figure 208. Strain of Shot 2-0009 for Gage #7.

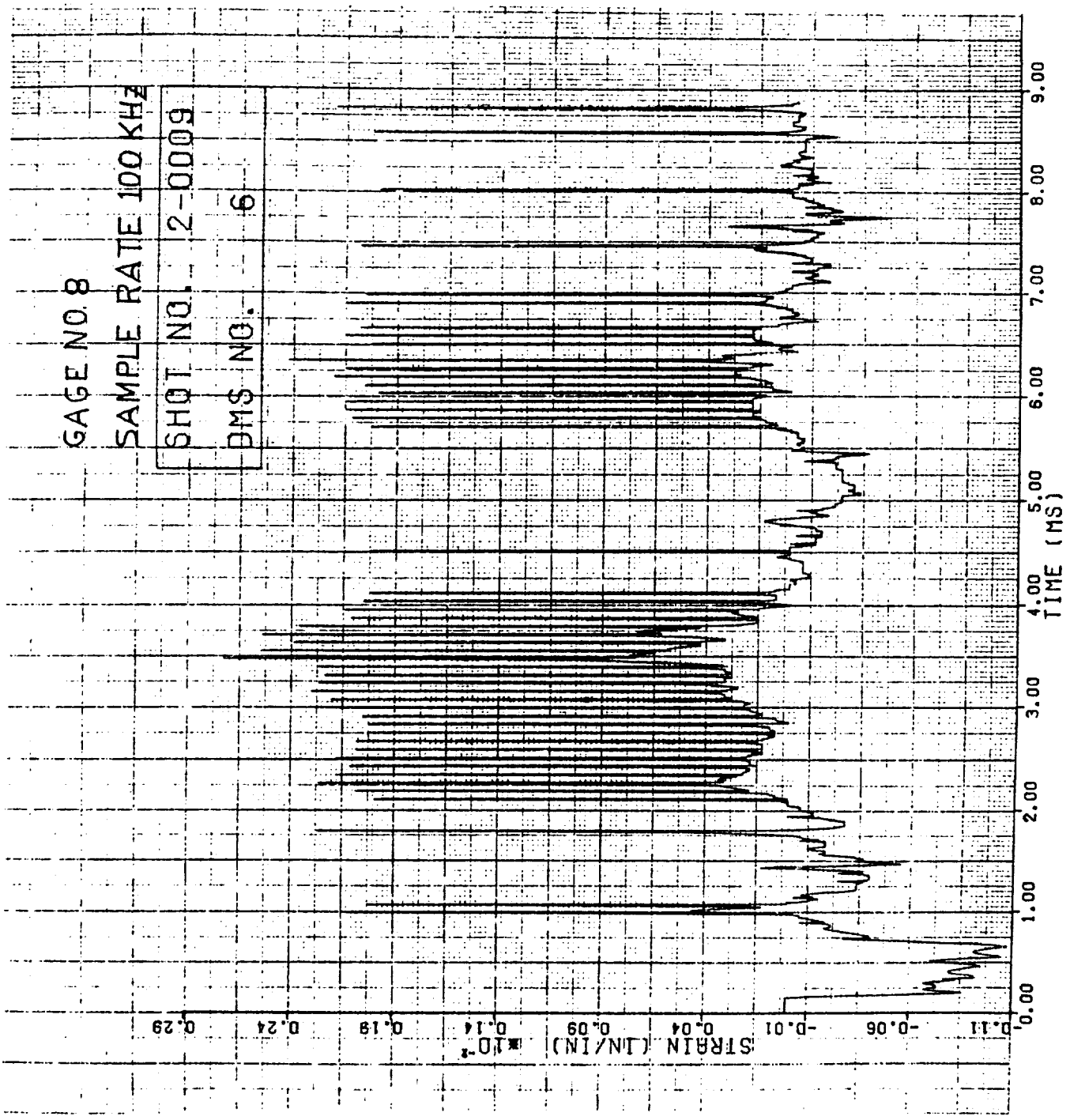

Figure 209. Strain of Shot 2-0009 for Gage #8.

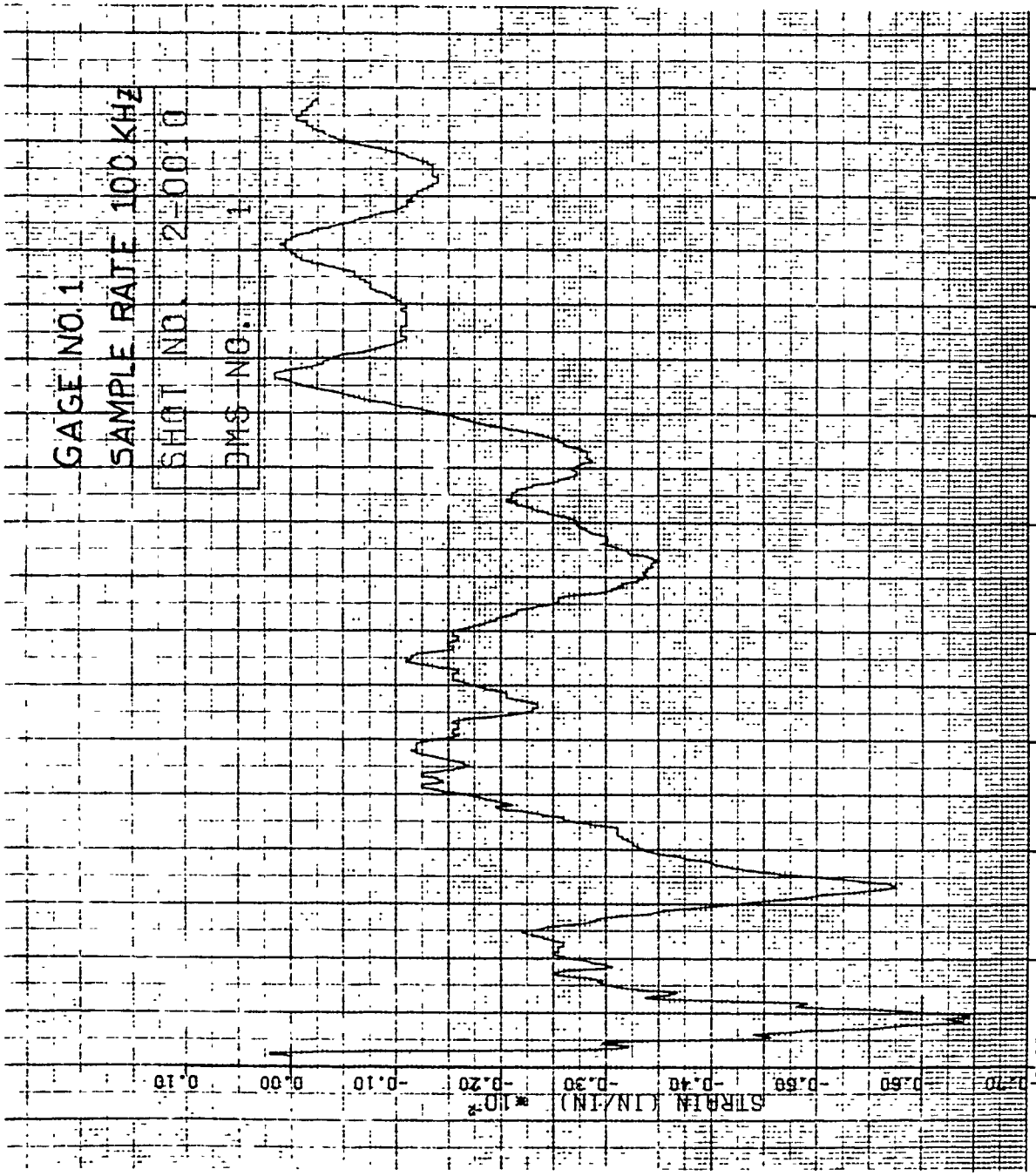

Figure 210. Strain of Shot 2-0010 for Gage #1.

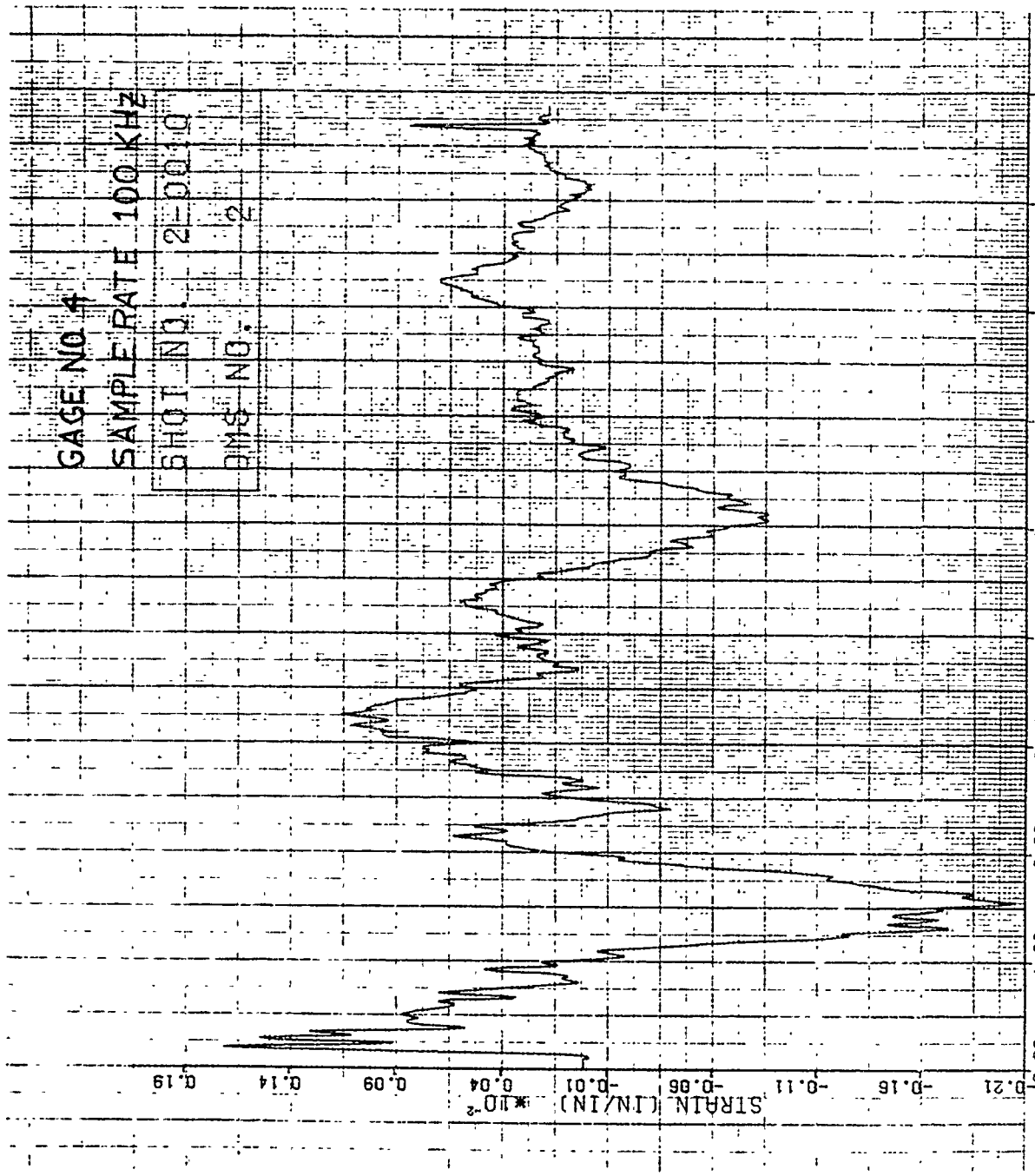

Figure 211. Strain of Shot 2-0010 for Gage #4.

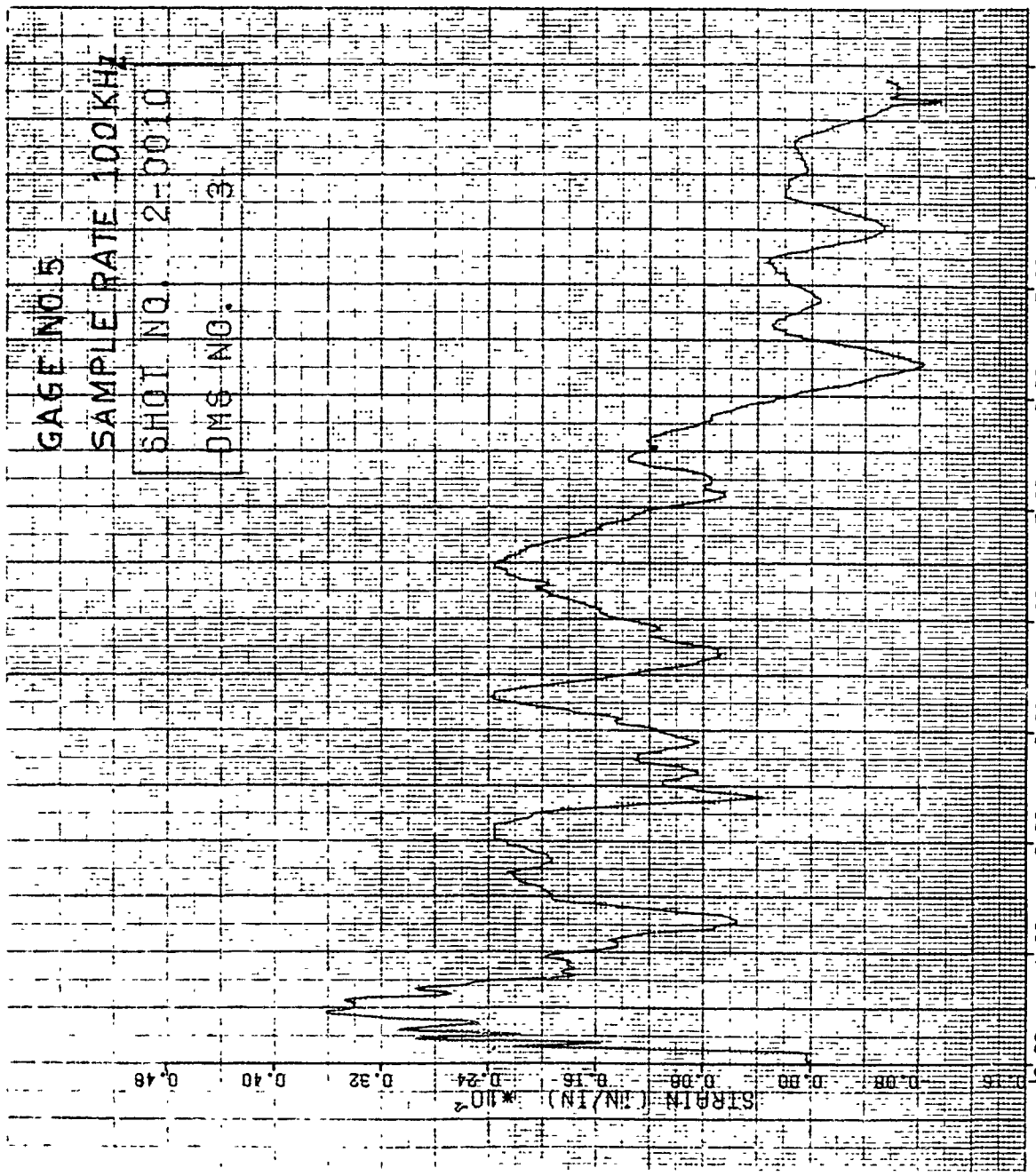

Figure 212. Strain of Shot 2-0010 for Gage #5.

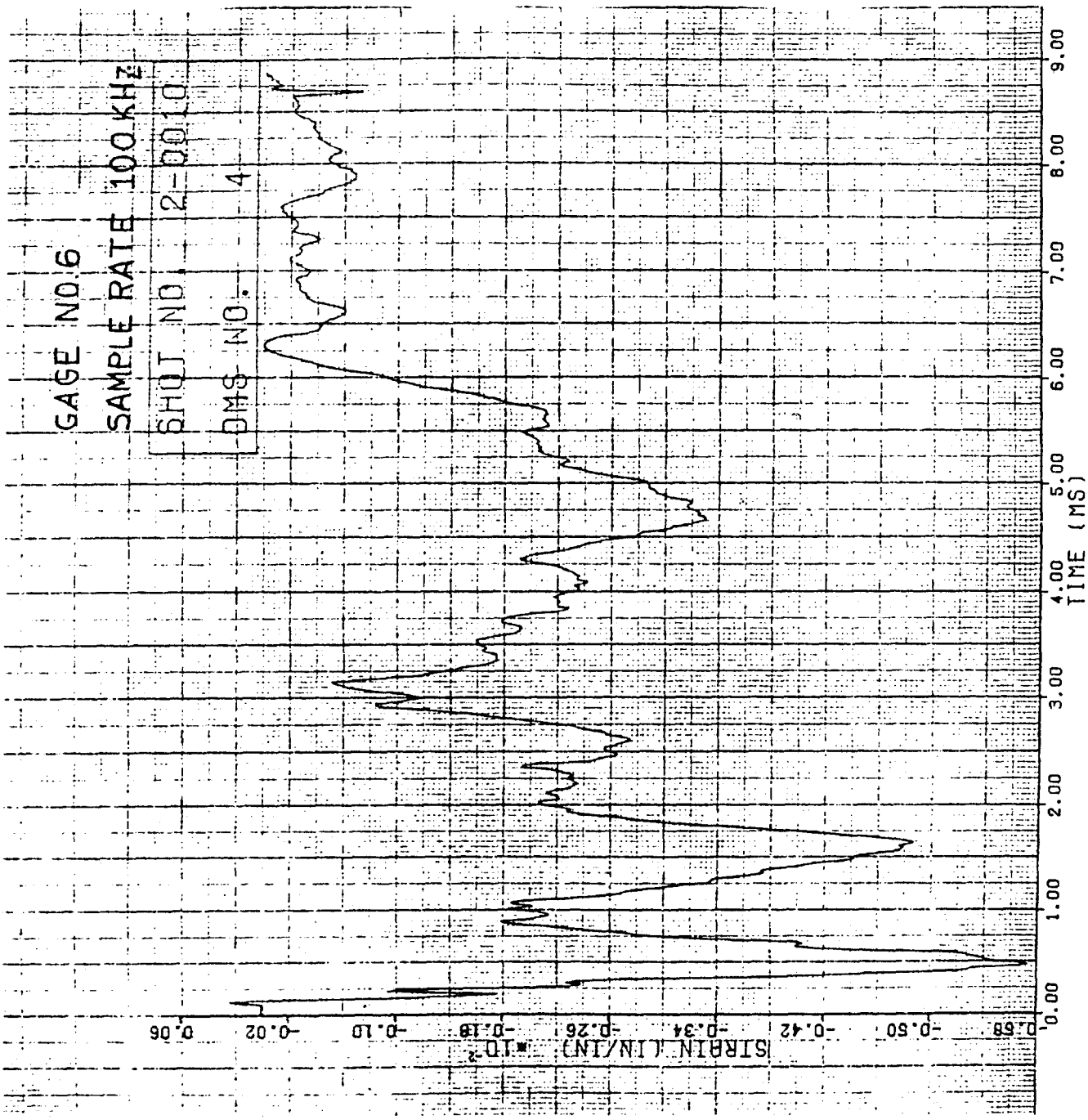

Figure 213. Strain of Shot 2-0010 for Gage #6.

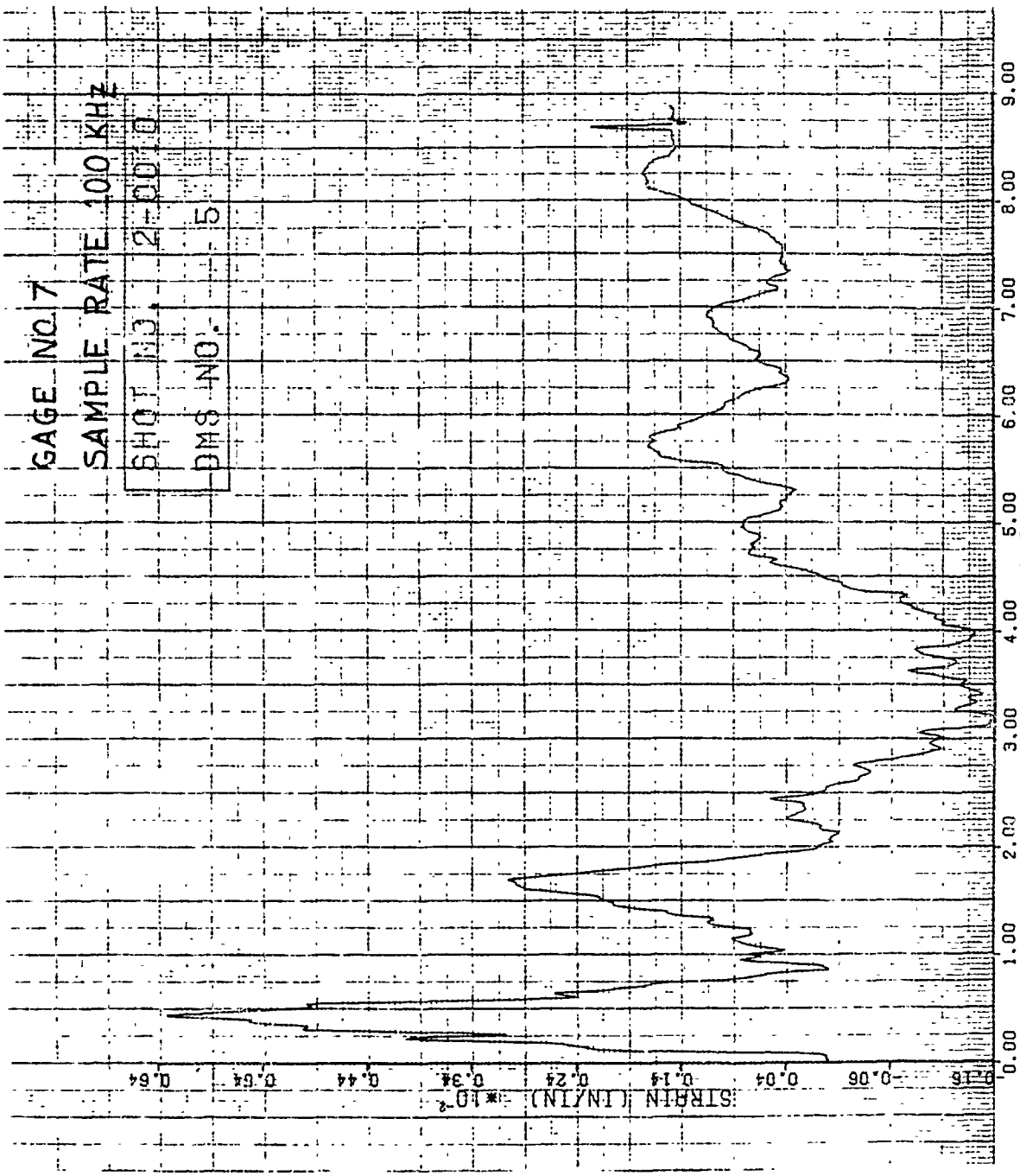

Figure 214. Strain of Shot 2-0010 for Gage #7.

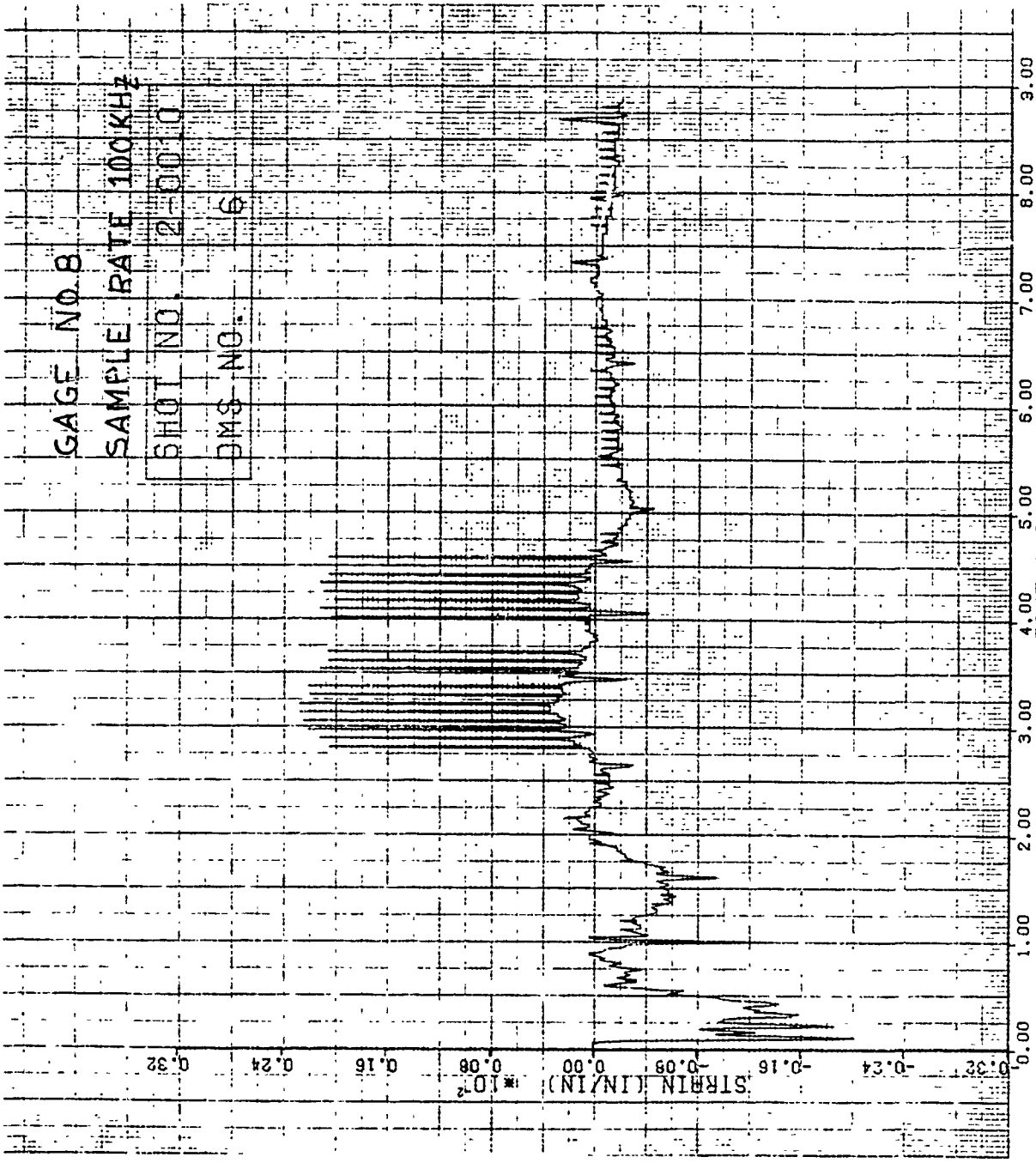

Figure 215. Strain of Shot 2-0010 for Gage #8.

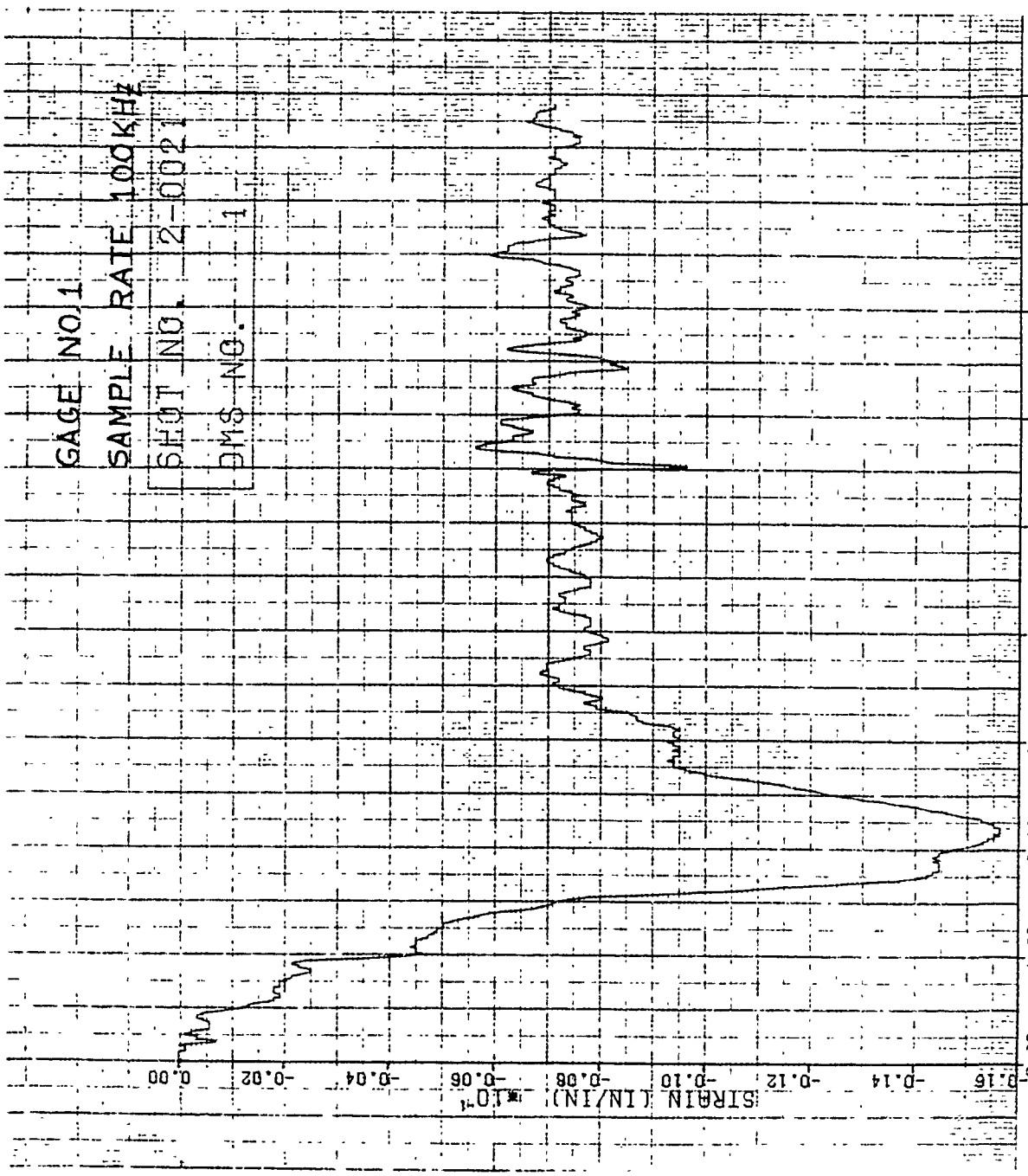

Figure 216. Strain of Shot 2-0021 for Gage #1.

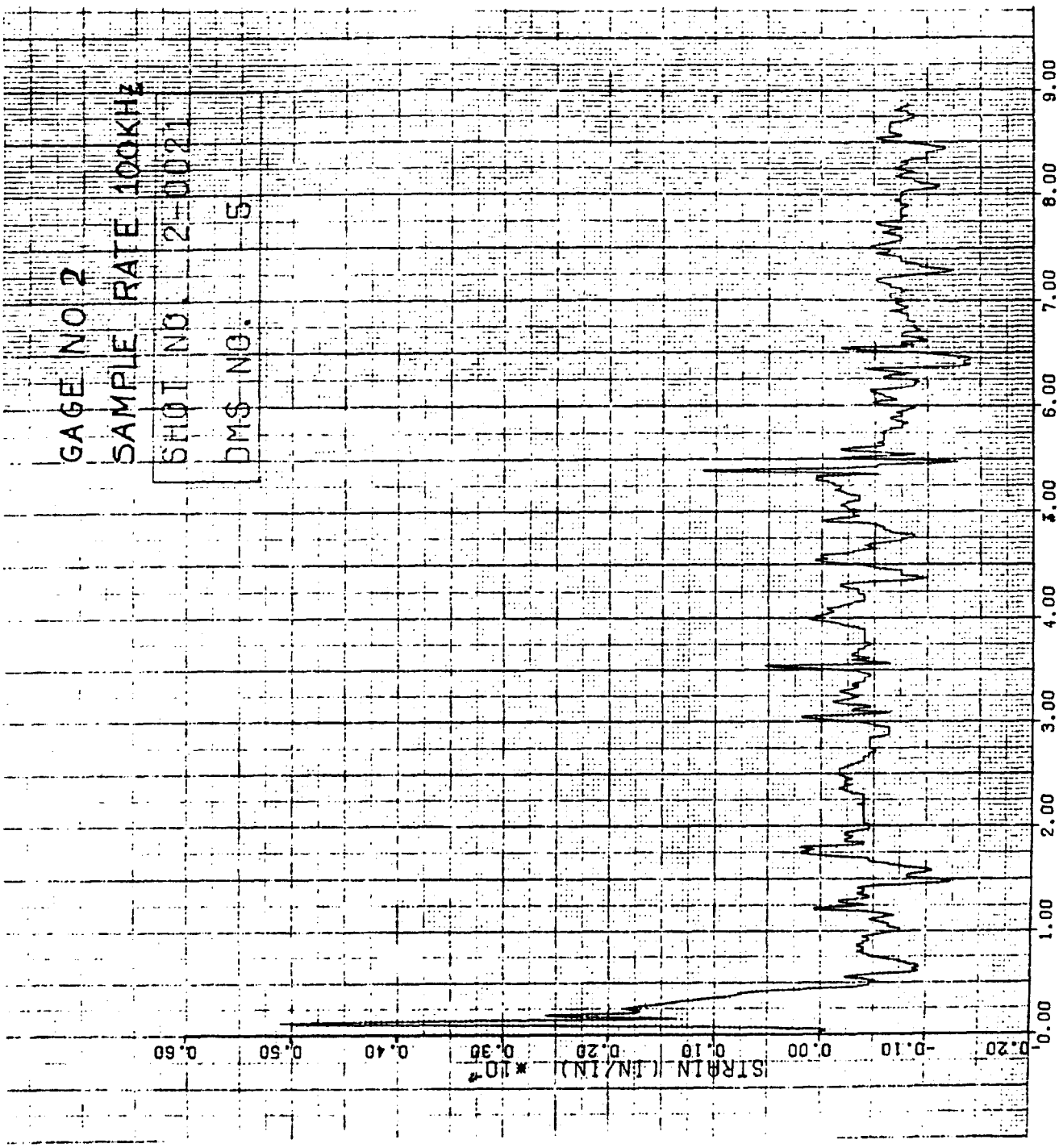

Figure 217. Strain of Shot 2-0021 for Gage #2.

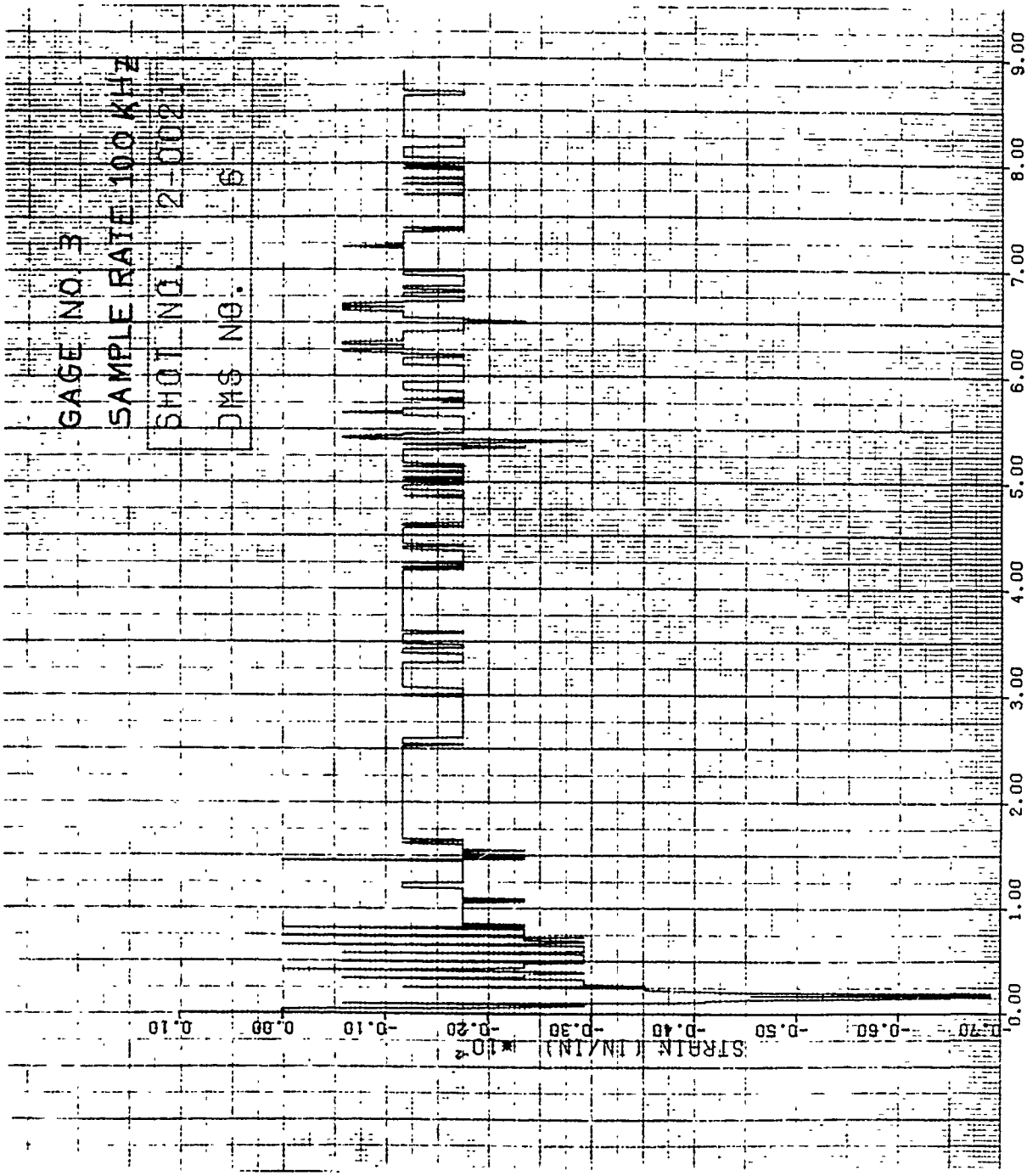

Figure 218. Strain of Shot 2-0021 for Gage #3.

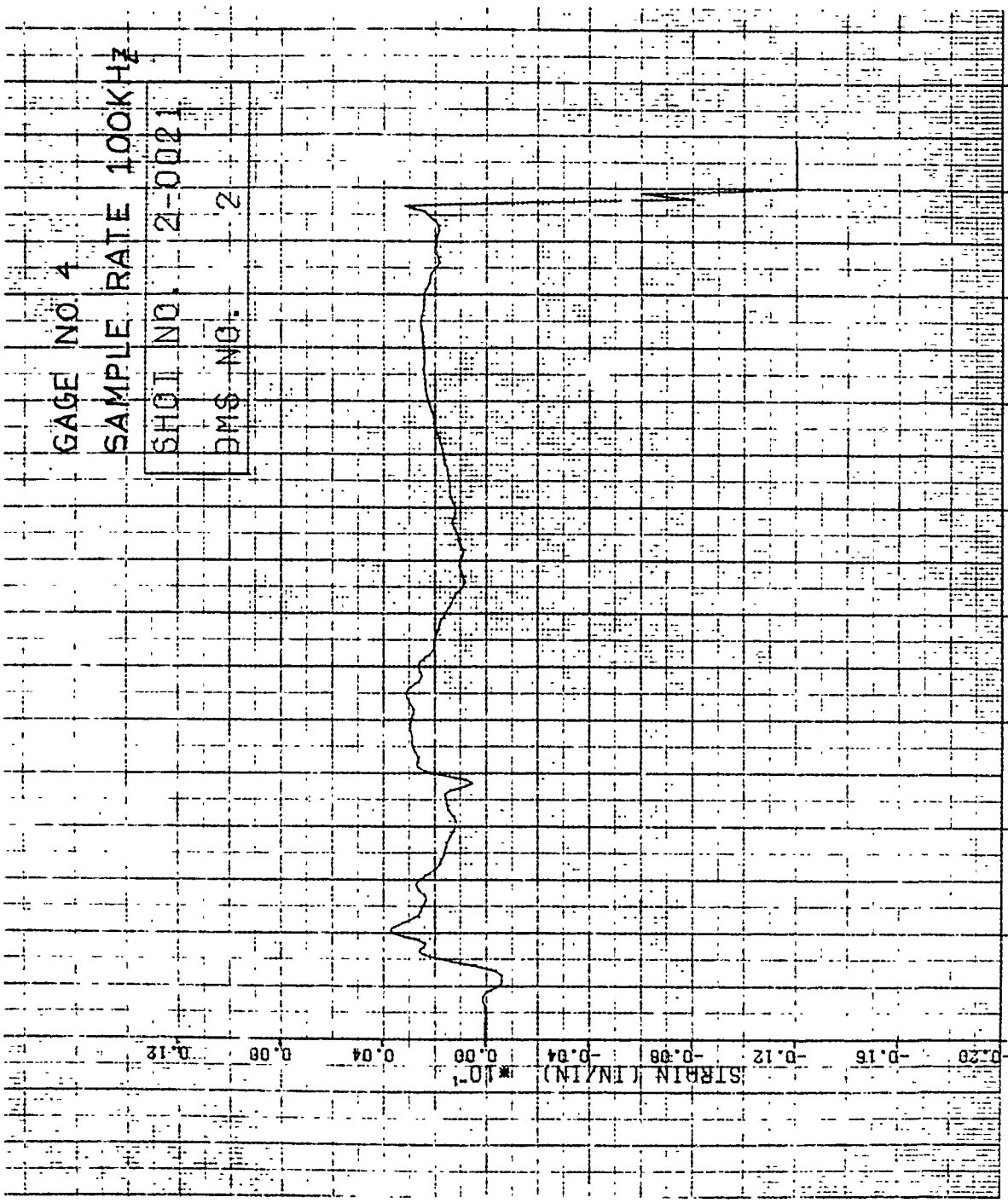

Figure 219. Strain of Shot 2-0021 for Gage #4.

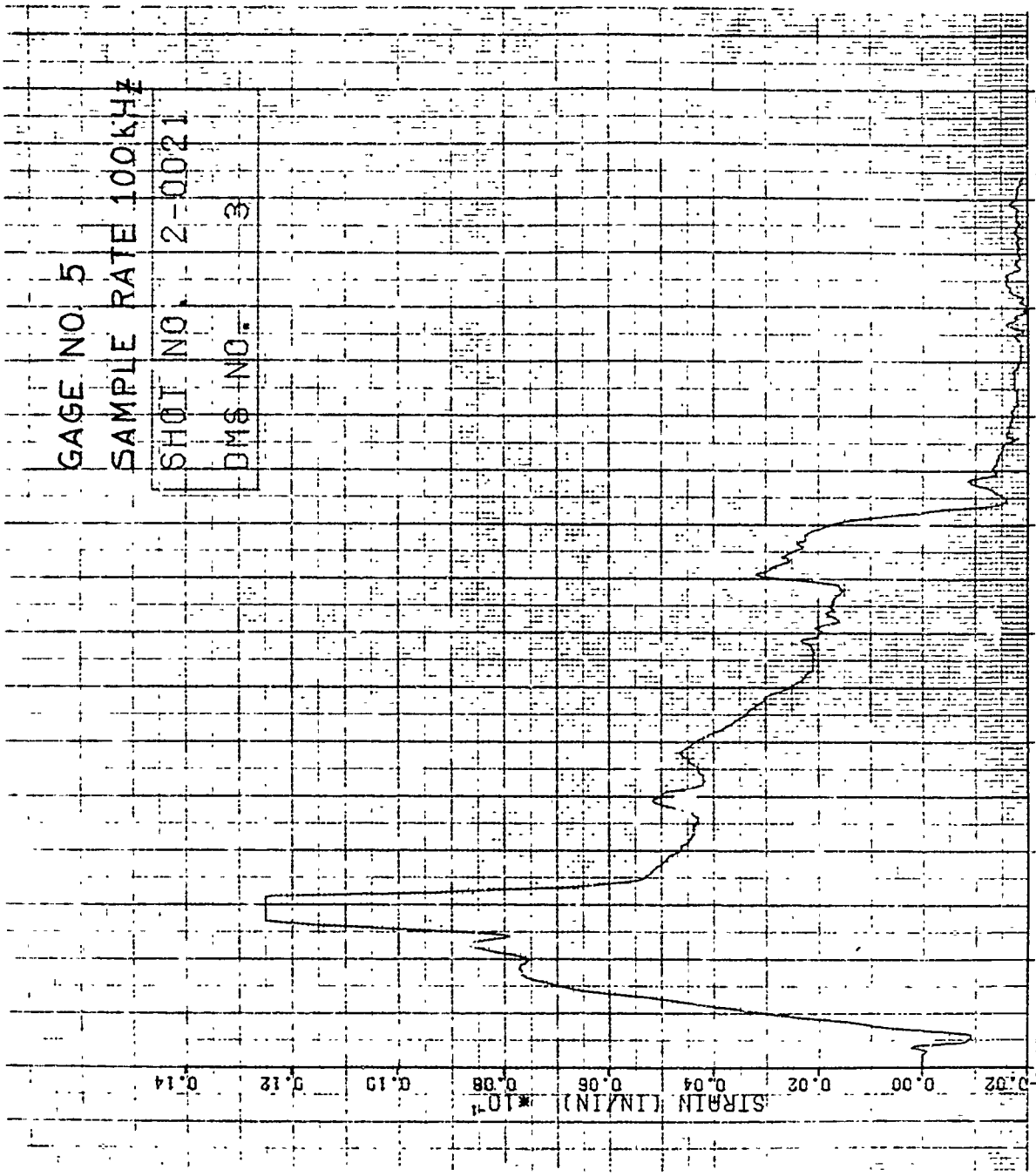

Figure 220. Strain of Shot 2-0021 for Gage #5.

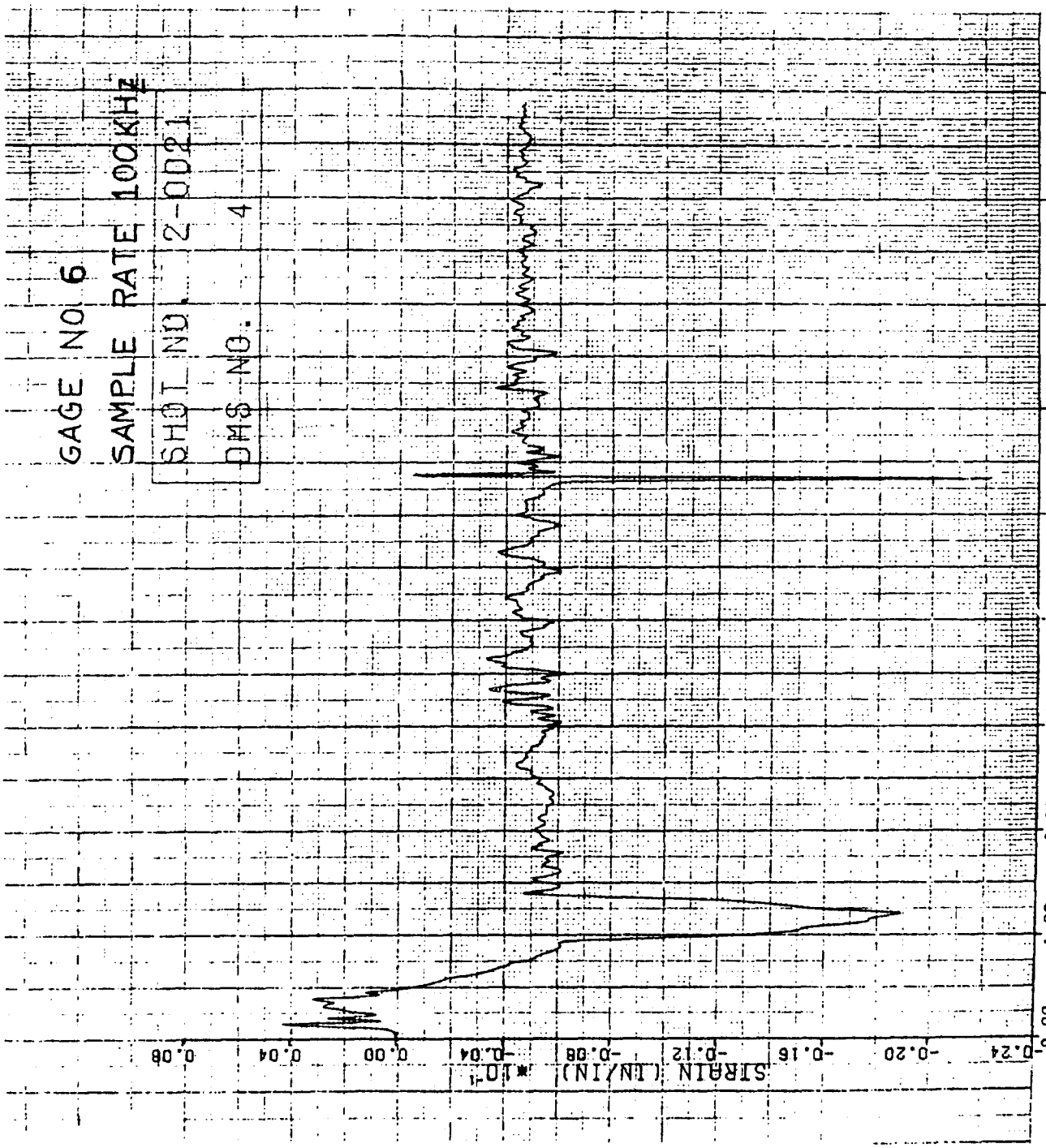

Figure 221. Strain of Shot 2-0021 for Gage #6.

No visible damage was received for Shots 2-0012, 2-0013, and 2-0014. A slight amount of damage of bowing at the impact site of 0.25 cm was received for Shot 2-0011 at a velocity of 161 m/s and an impact mass of 94.9 g. The most severe damage was received for Shot 2-0015 with general bowing through the span of the blade giving a plastic tip deflection of 8.15 cm. In this shot, the blade was knocked out of the mounting fixture.

For Shot 2-0014 at a velocity of 170 m/s and impact mass of 37.0 g, the highest strain rate for the 30 percent span impacts was 372 in/in/sec for the 680 g (1.5 pound) bird as identified in Figures 222 and 223. Figure 222 gives the strain versus time plot while Figure 223 gives the strain rate versus time plot. The strain data for this impact is contained in the Volume II report. This strain rate value was for a gage located on the midchord at the blade root in the spanwise direction. The strain gage locations are given in Figure 2A of Appendix A. No visible damage was received by the blade for this impact.

Typical strain versus time curves are given in Figures 224 through 229 for Shot 2-0011. The impact velocity was 161 m/s and impact mass of 94.9 g generated slight damage on the blade. Tension is denoted as a negative strain and compression as a positive strain in the strain data curves for all the impacts in this blade group.

Figure 49B gives the damage received by the blade for Shot 2-0015.

3.2.9 Impact Results for Group 9B Blades

One leading edge impact (Shot 2-0024) using the 680 g (1.5 pound) bird generated severe damage in the form of bowing 9.8 cm at the impact site. The blade was knocked out of its mounting fixture and hit the back of the target tank. The impact velocity for the 70 percent span impact was 254 m/s.

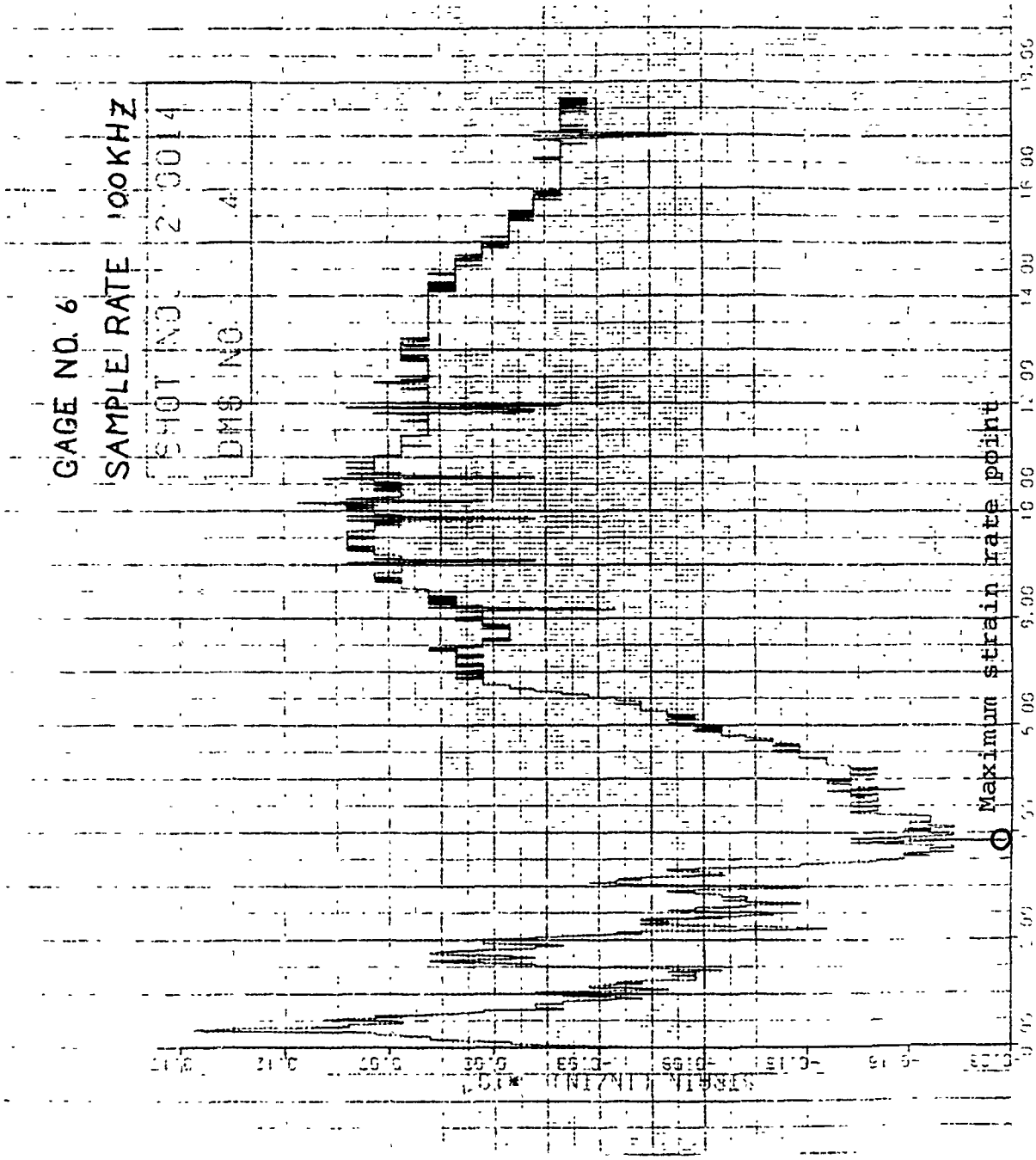

Figure 222. Strain of Shot 2-0014 for Gage #6.

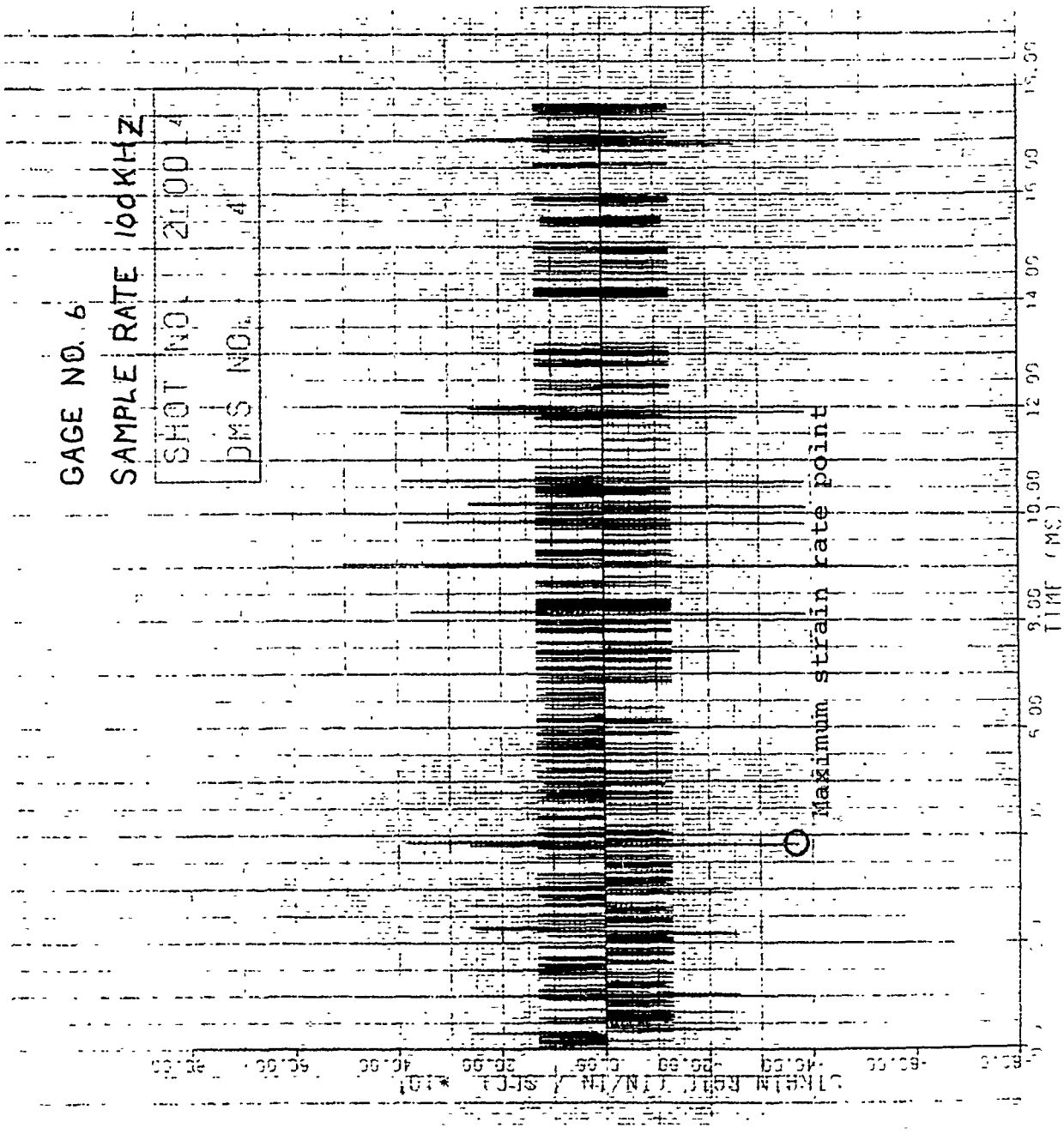

Figure 223. Strain Rate of Shot 2-0014 for Gage #6.

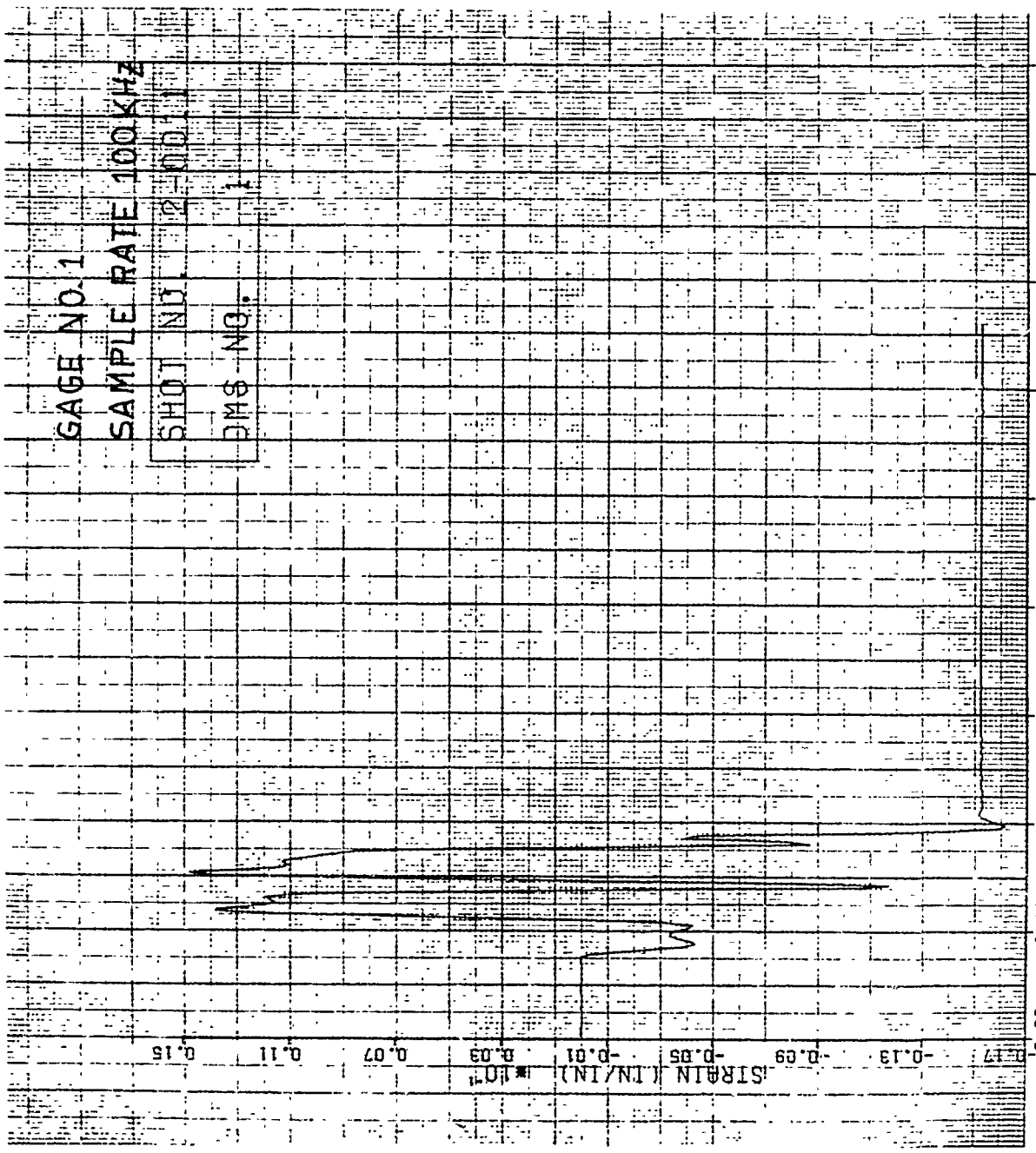

Figure 224. Strain of Shot 2-0011 for Gage #1.

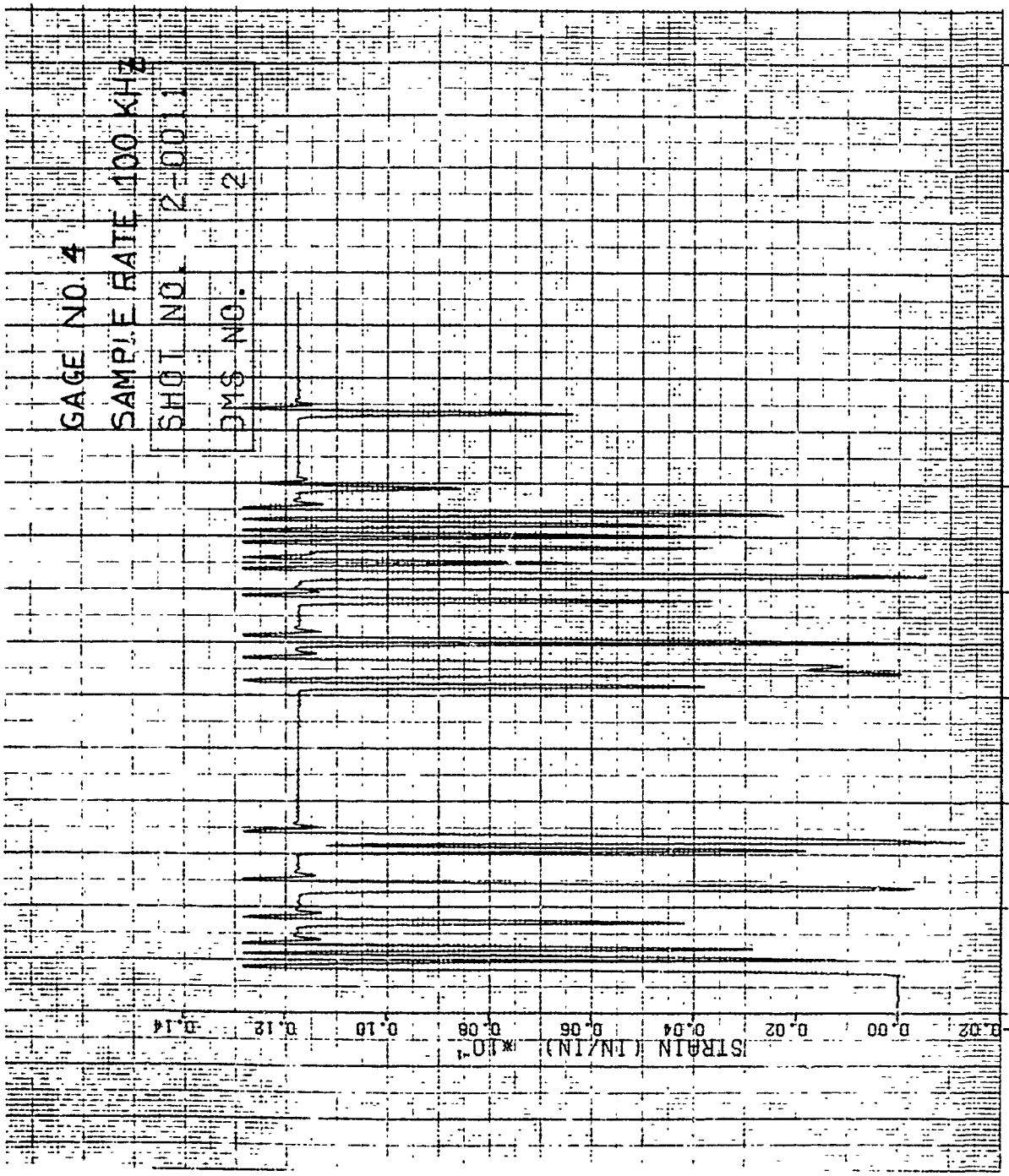

Figure 225. Strain of Shot 2-0011 for Gage #4.

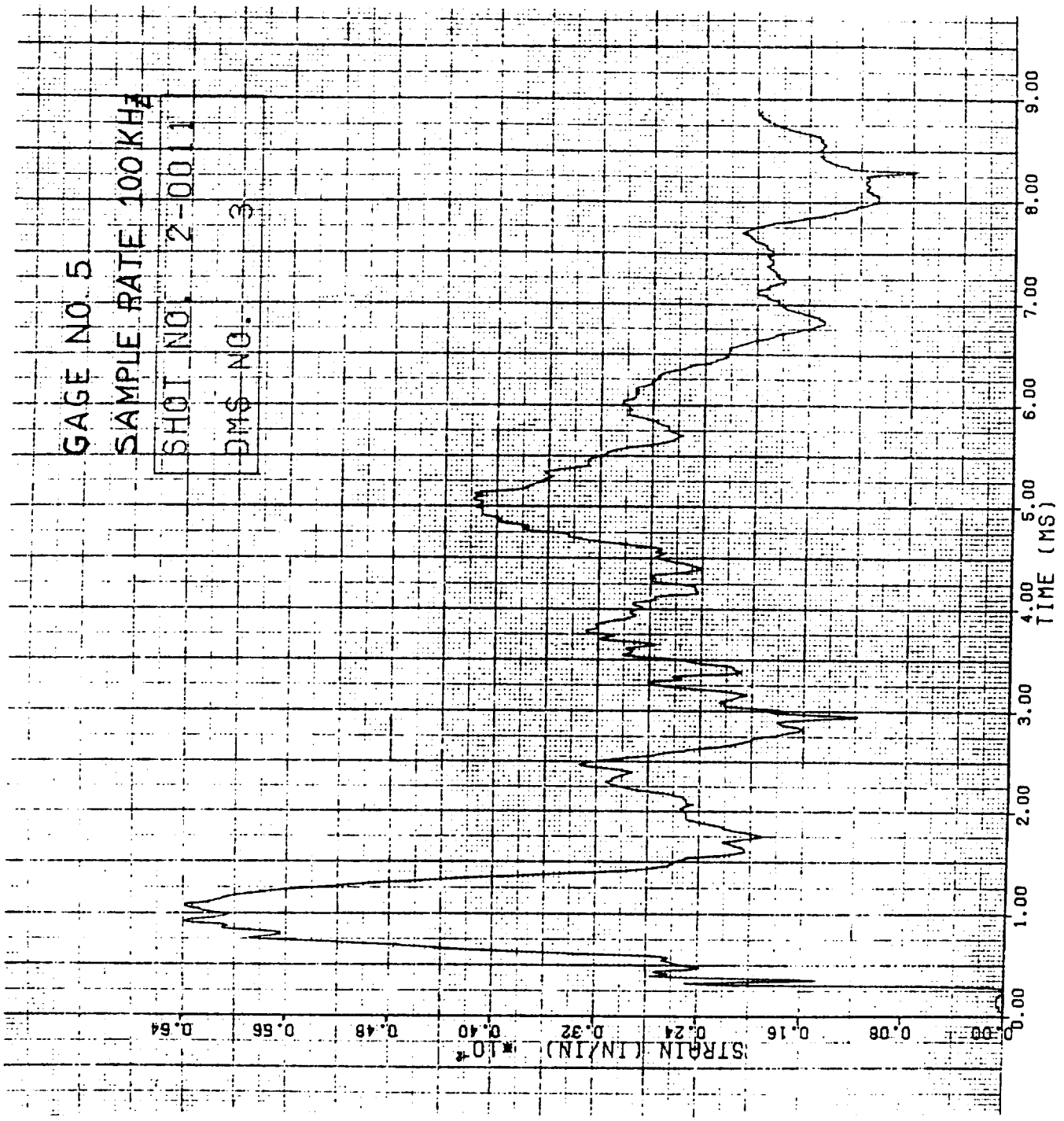

Figure 226. Strain of Shot 2-0011 for Gage #5.

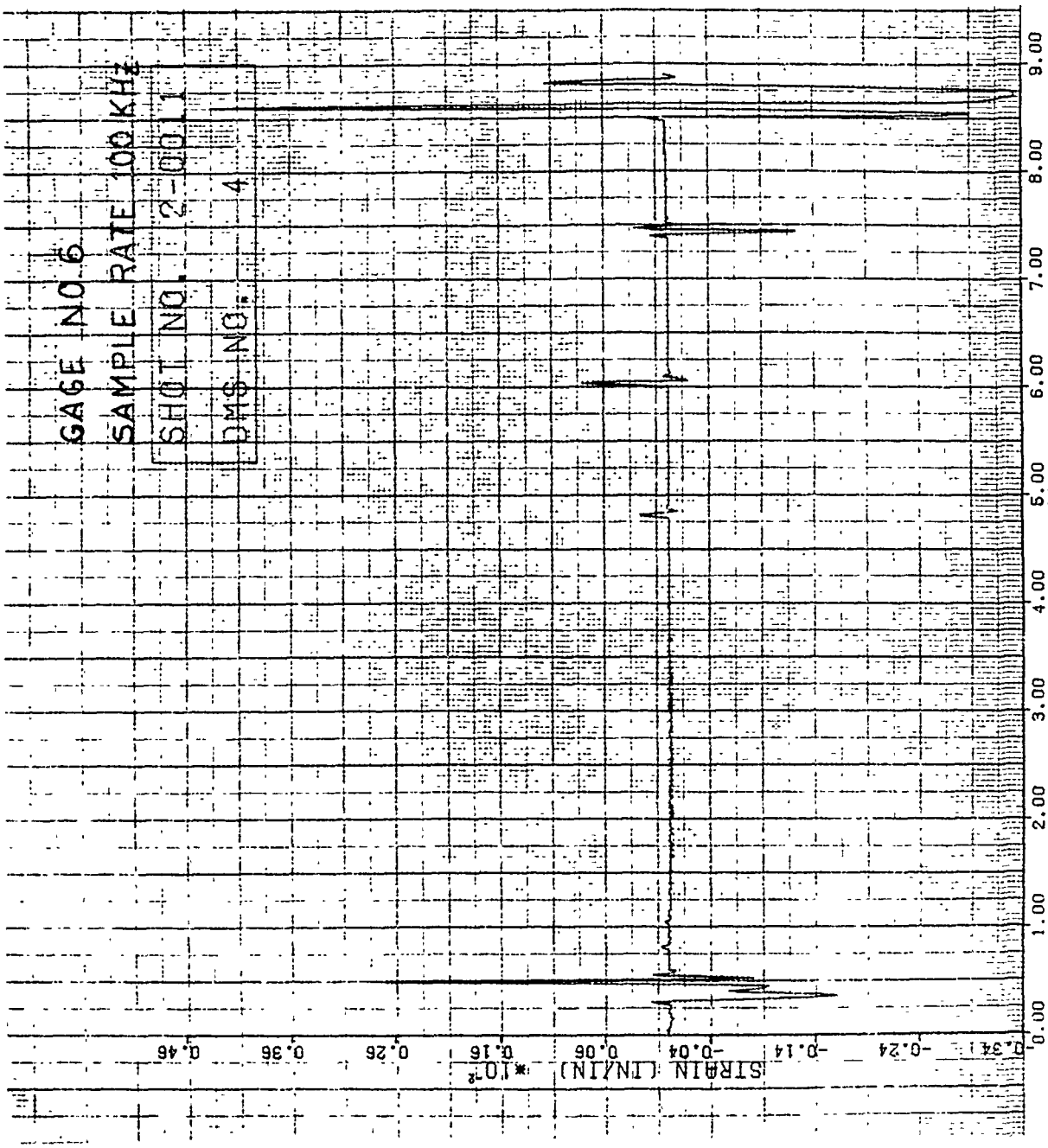

Figure 227. Strain of Shot 2-0011 for Gage #6.

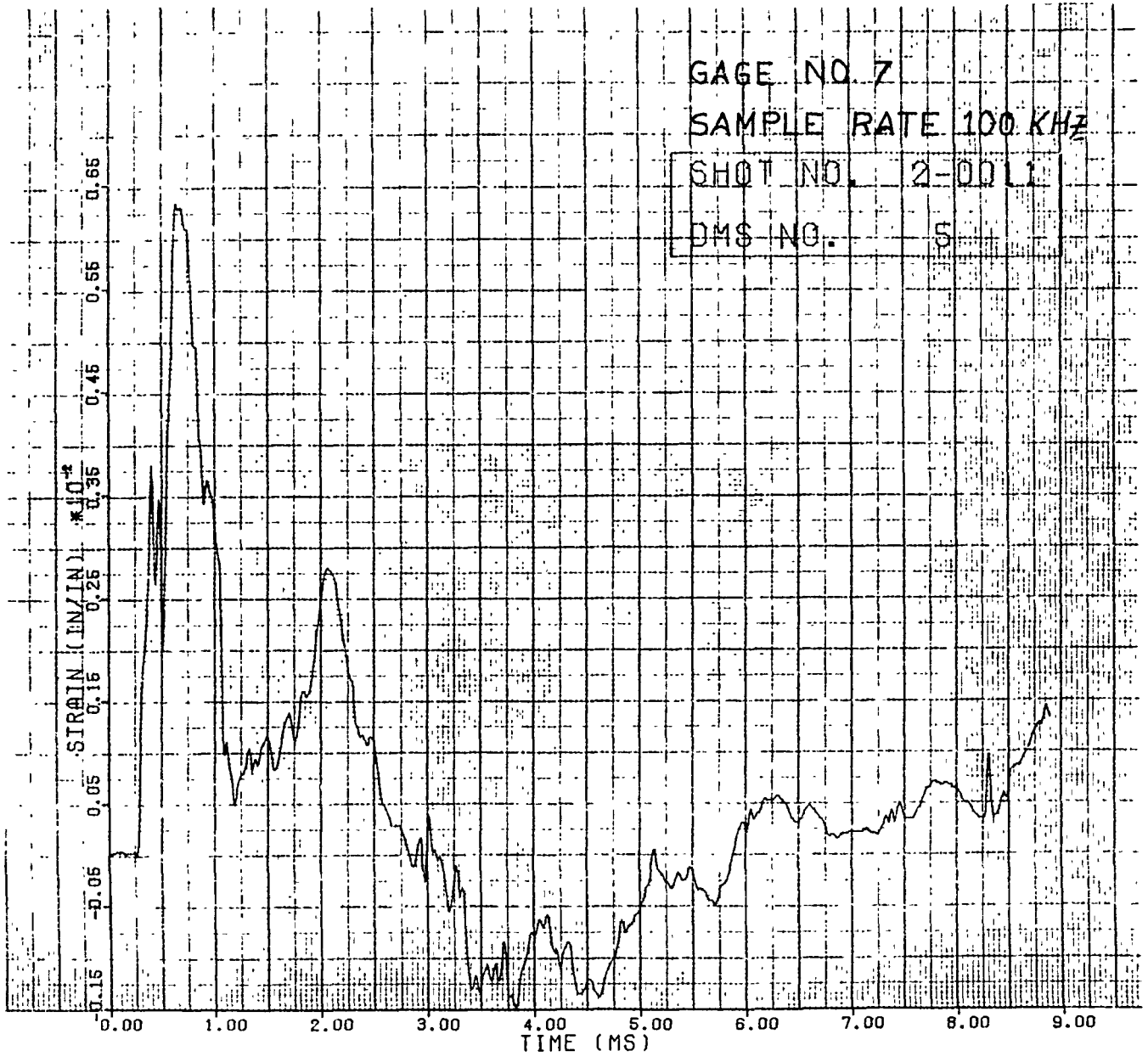

Figure 228. Strain of Shot 2-0011 for Gage #7.

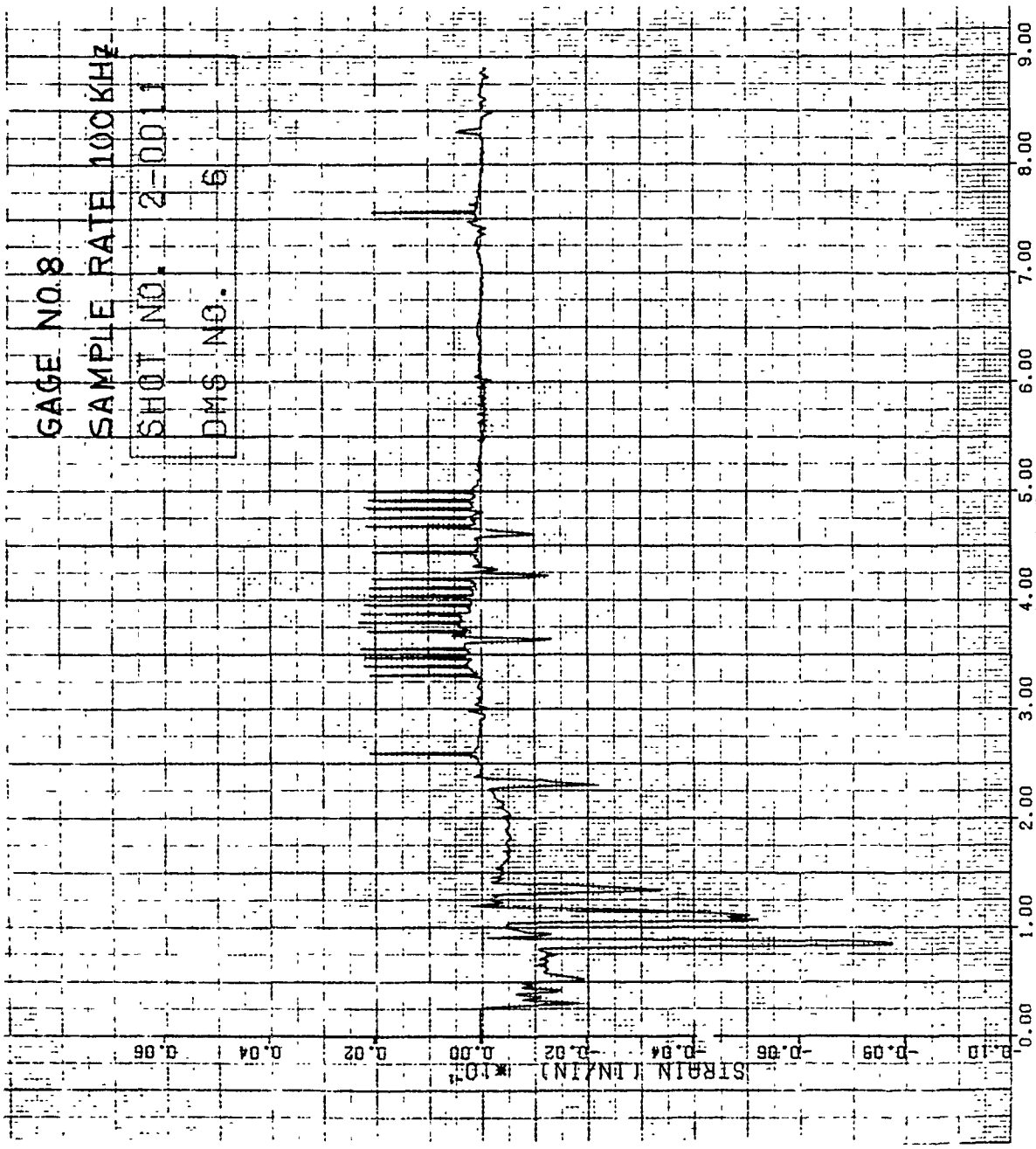

Figure 229. Strain of Shot 2-0011 for Gage #8.

The impact mass was 161.0 g and the angle of incidence was 36.4 degrees.

The strain versus time data curves for Shot 2-0024 are given in Figures 230 through 235. The strain gage locations are given in Figure 2A of Appendix A. Tension is denoted as a negative strain and compression as a positive strain for the curves. The highest strain rate was 395 in/in/sec for Gage #3 as identified in Figures 232 and 236. This gage was located directly behind the impact site and its orientation was in the chordwise direction.

Figures 237 through 240 present dynamic tip deflection data for the impact event for Shot 2-0024. Figures 237 and 238 give the deflection versus time curves for the "y" and "x" directions for the blade leading edge. Figures 239 and 240 give the displacement curves for the "y" and "x" directions for the trailing edge of the blade.

Figure 50B gives photographs of the blade damage for Shot 2-0024. Note that much of the damage may have been caused by the blade hitting the target tank when it dismounted the mounting fixture.

3.2.10 Impact Results for Group 10B Blades

Five leading edge impacts using the 5.08 cm (2.0 inch) diameter ice spheres were conducted on the J79 stainless steel blades at velocities ranging from 89 to 325 m/s. The blades were mounted such that the ice balls would be sliced into equal parts and only one-half of the sphere would actually load the blades. The initial mass of the ice balls is about 65 g; therefore, 32.5 g would impact the blades. The impact site was at the 30 percent span location of the blades. The angle of incidence for these impacts was 51.1 degrees.

No visible damage was received on three of the impacts up to a velocity of 182 m/s. Slight damage in the form of general bending from the root to the tip through the

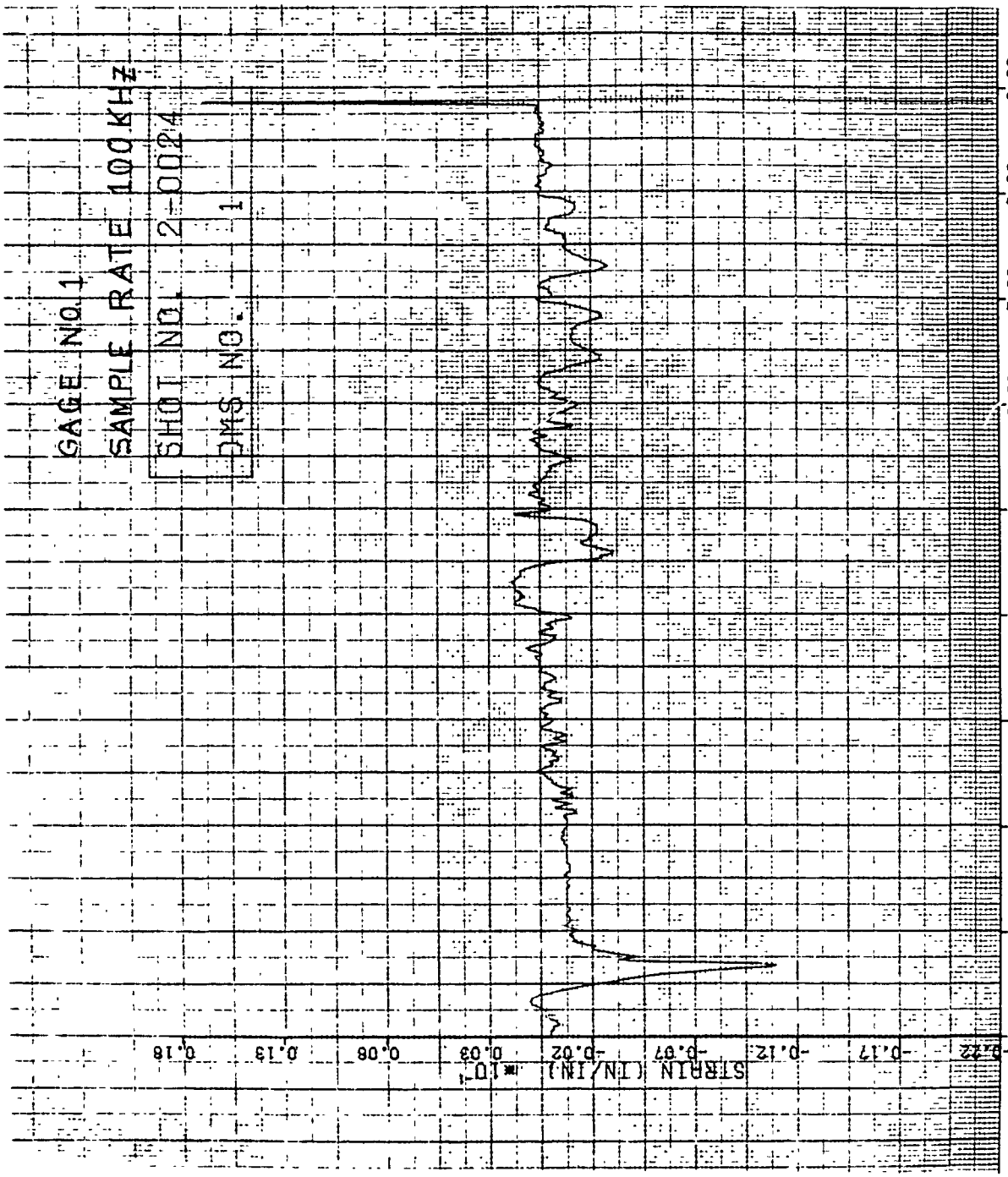

Figure 230. Strain of Shot 2-0024 for Gage #1.

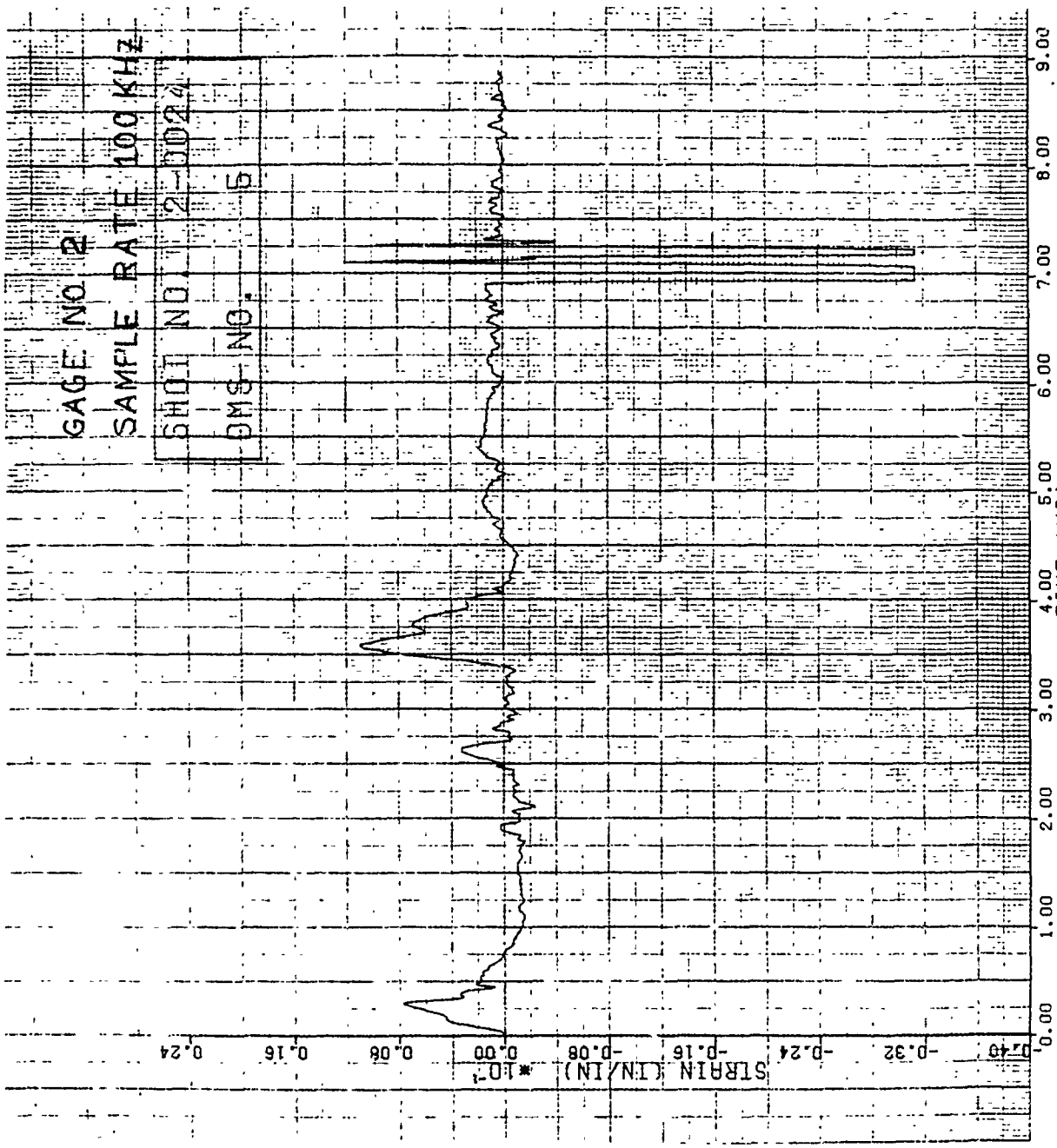

Figure 231. Strain of Shot 2-0024 for Gage #2.

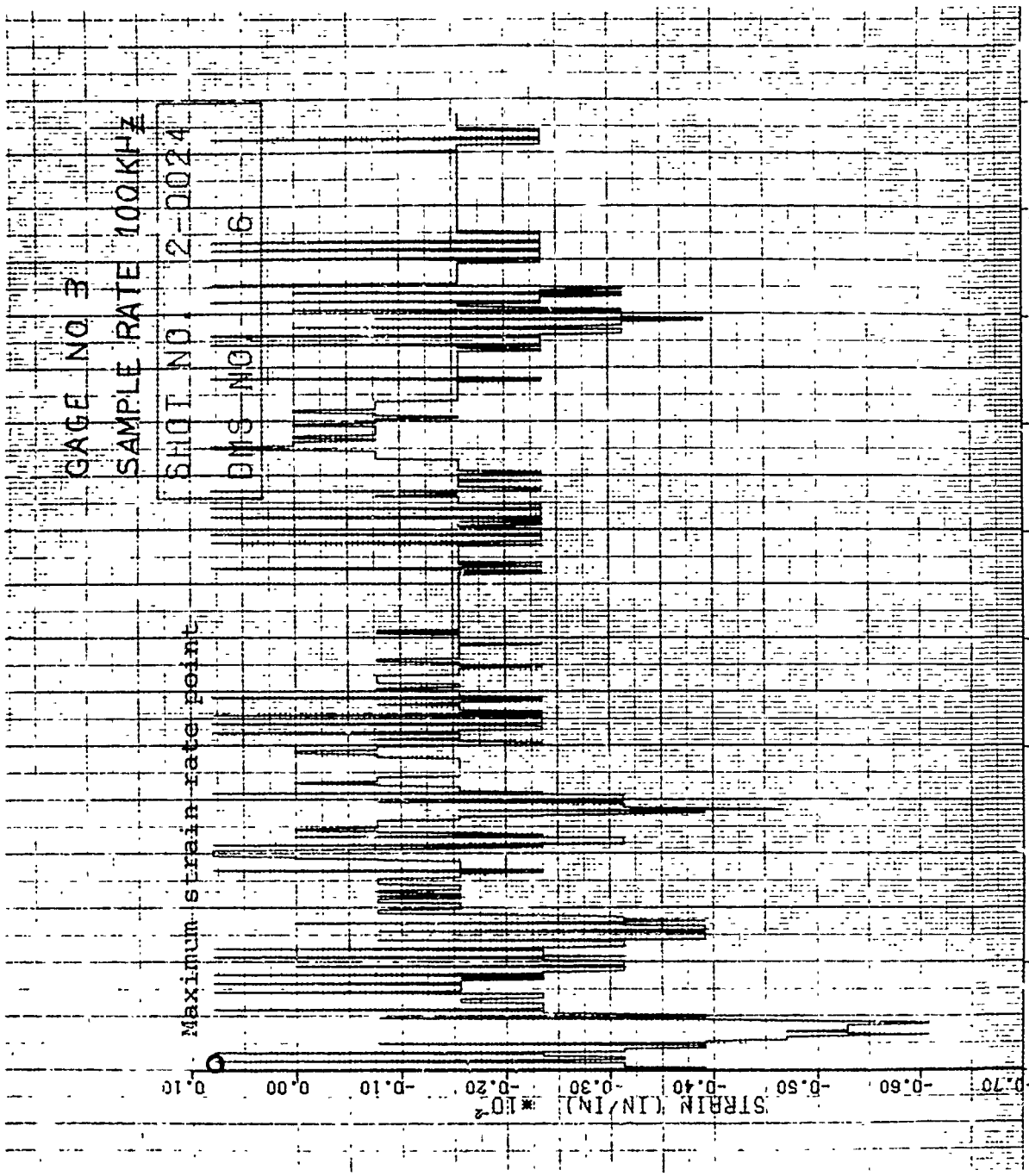

Figure 232. Strain of Shot 2-0024 for Gage #3.

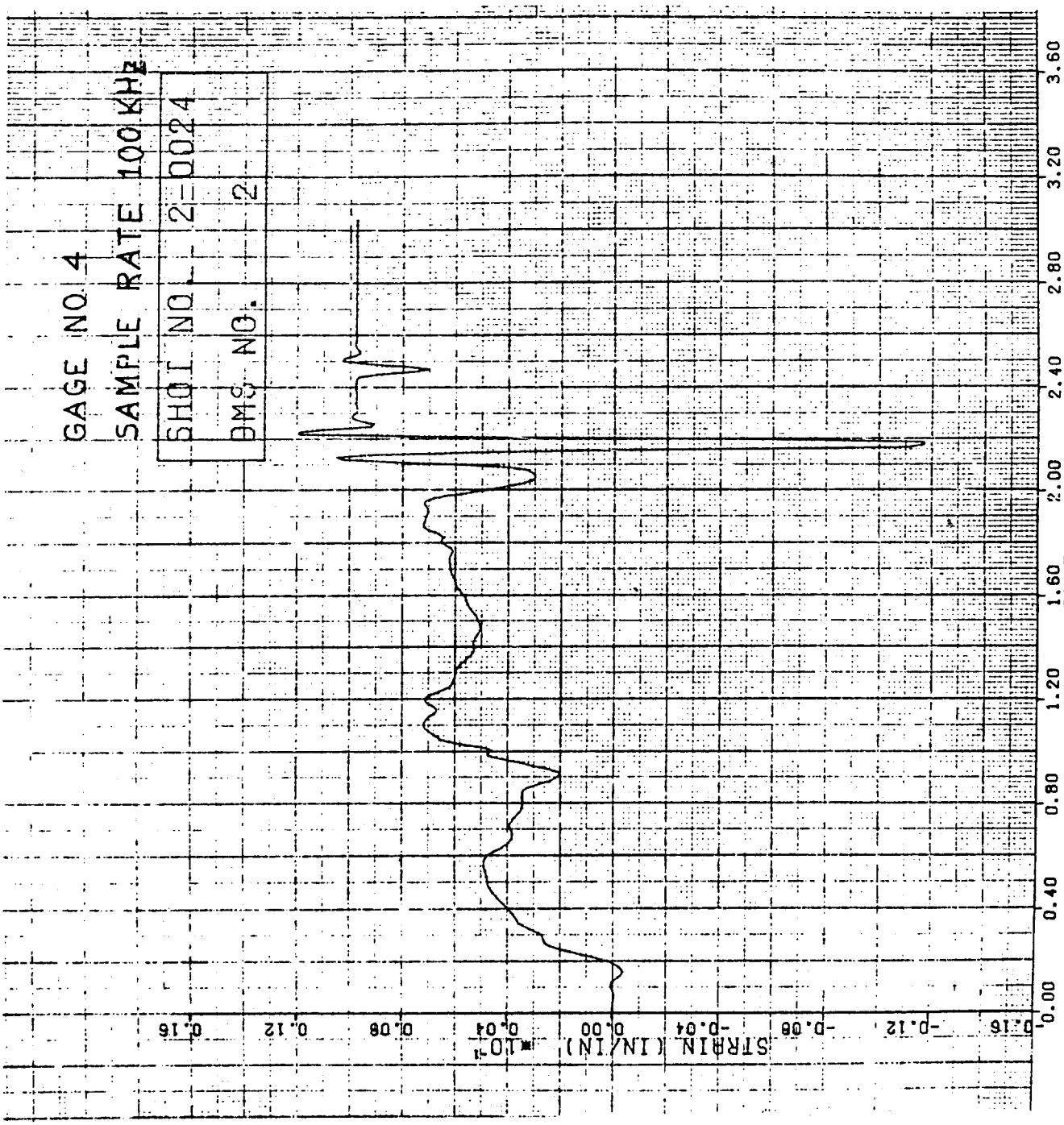

Figure 233. Strain of Shot 2-0024 for Gage #4.

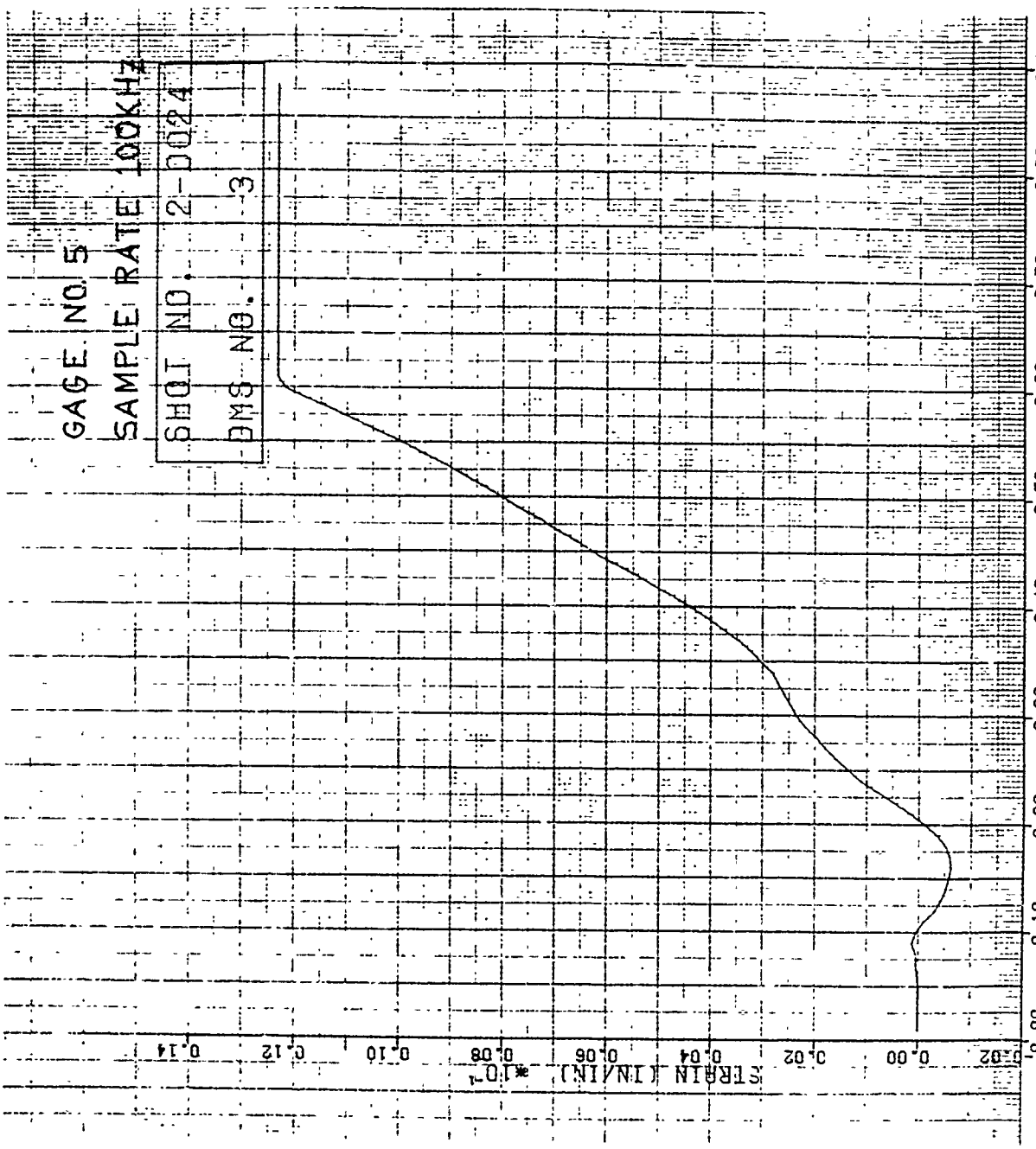

Figure 234. Strain of Shot 2-0024 for Gage #5.

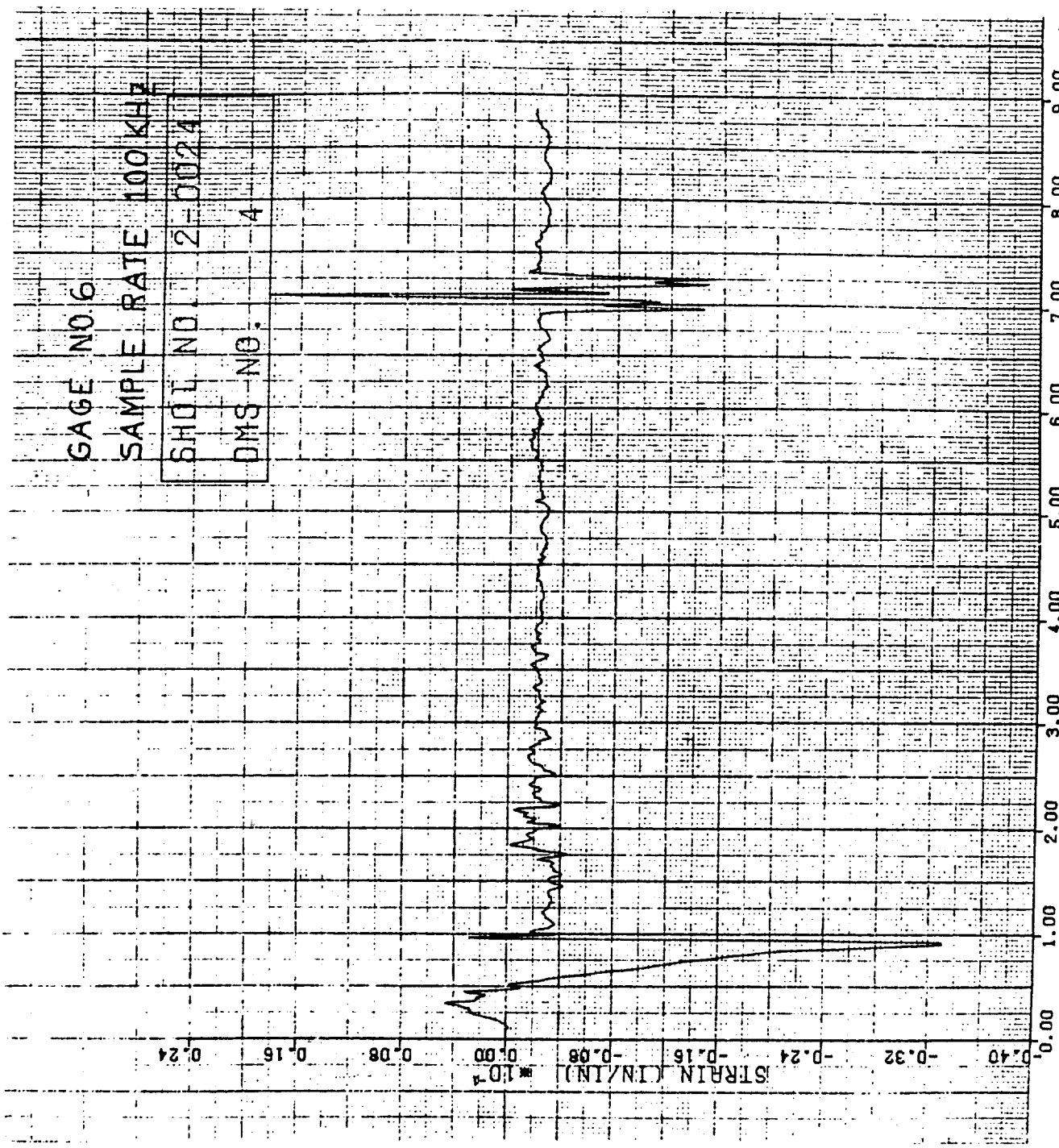

Figure 235. Strain of Shot 2-0024 for Gage #6.

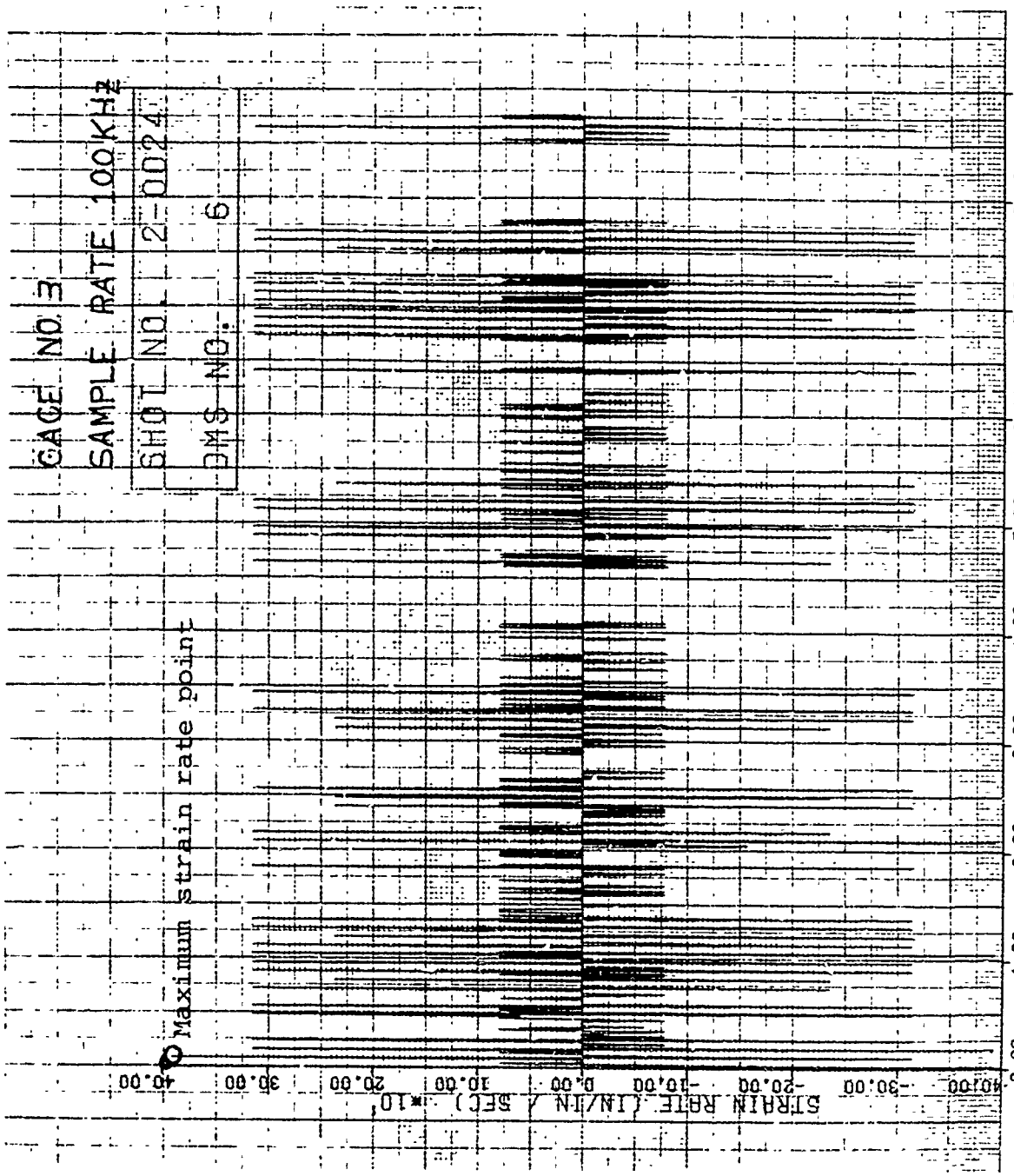

Figure 236. Strain Rate of Shot 2-0024 for Gage #3.

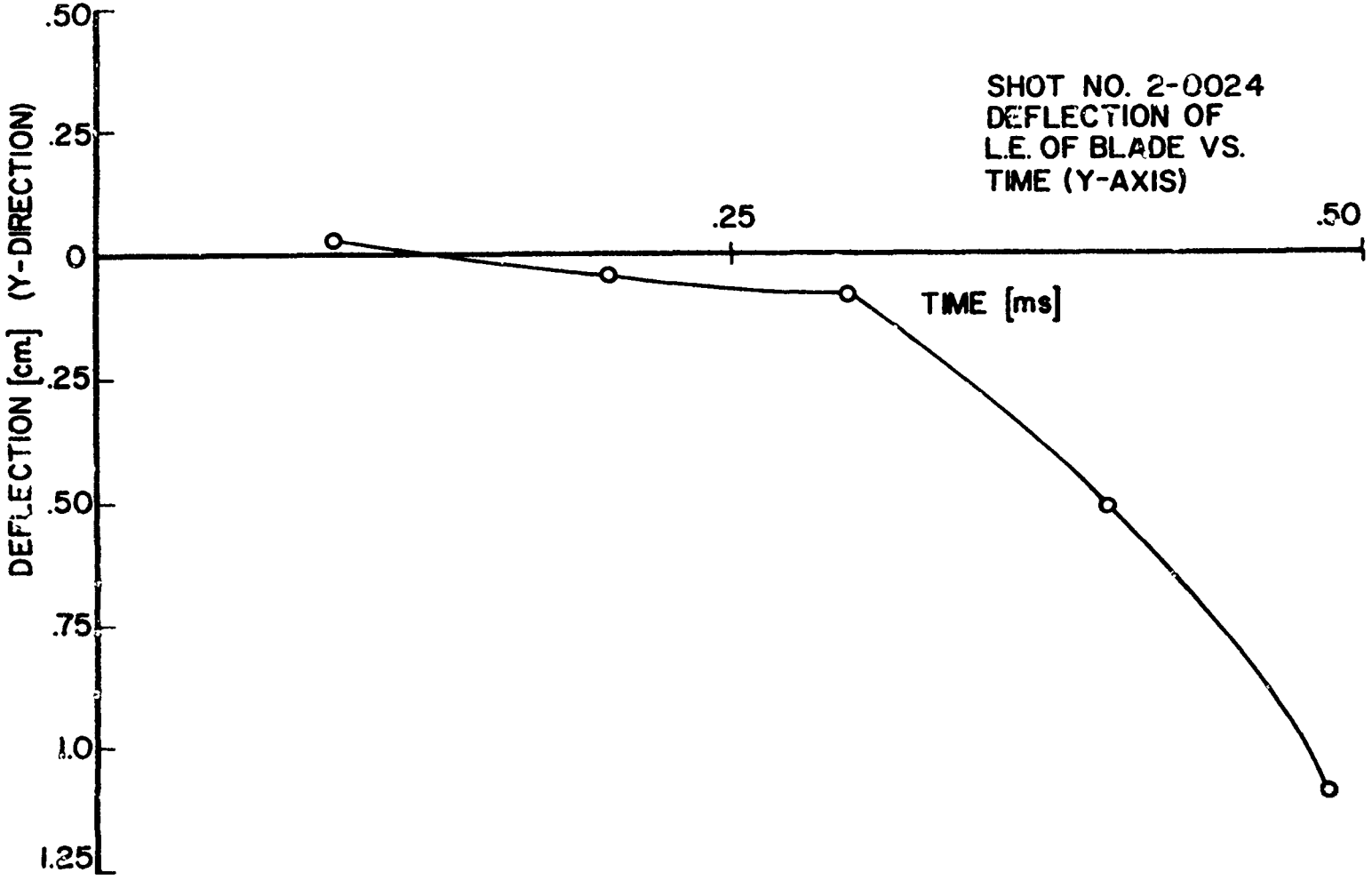

Figure 237. Leading Edge Tip Deflection in "y" Direction for Shot 2-0024.

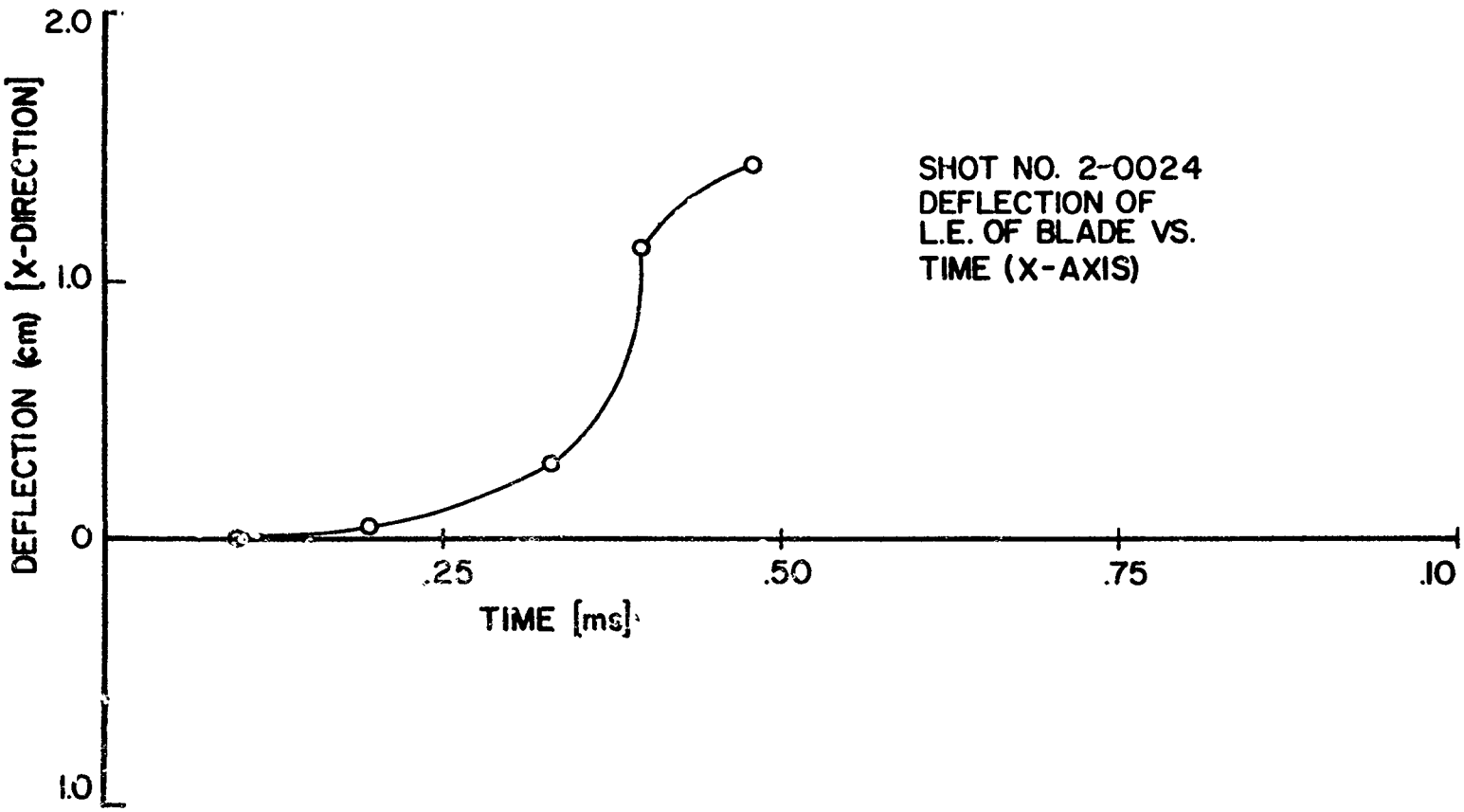

Figure 238. Leading Edge Tip Deflection in "x" Direction for Shot 2-0024.

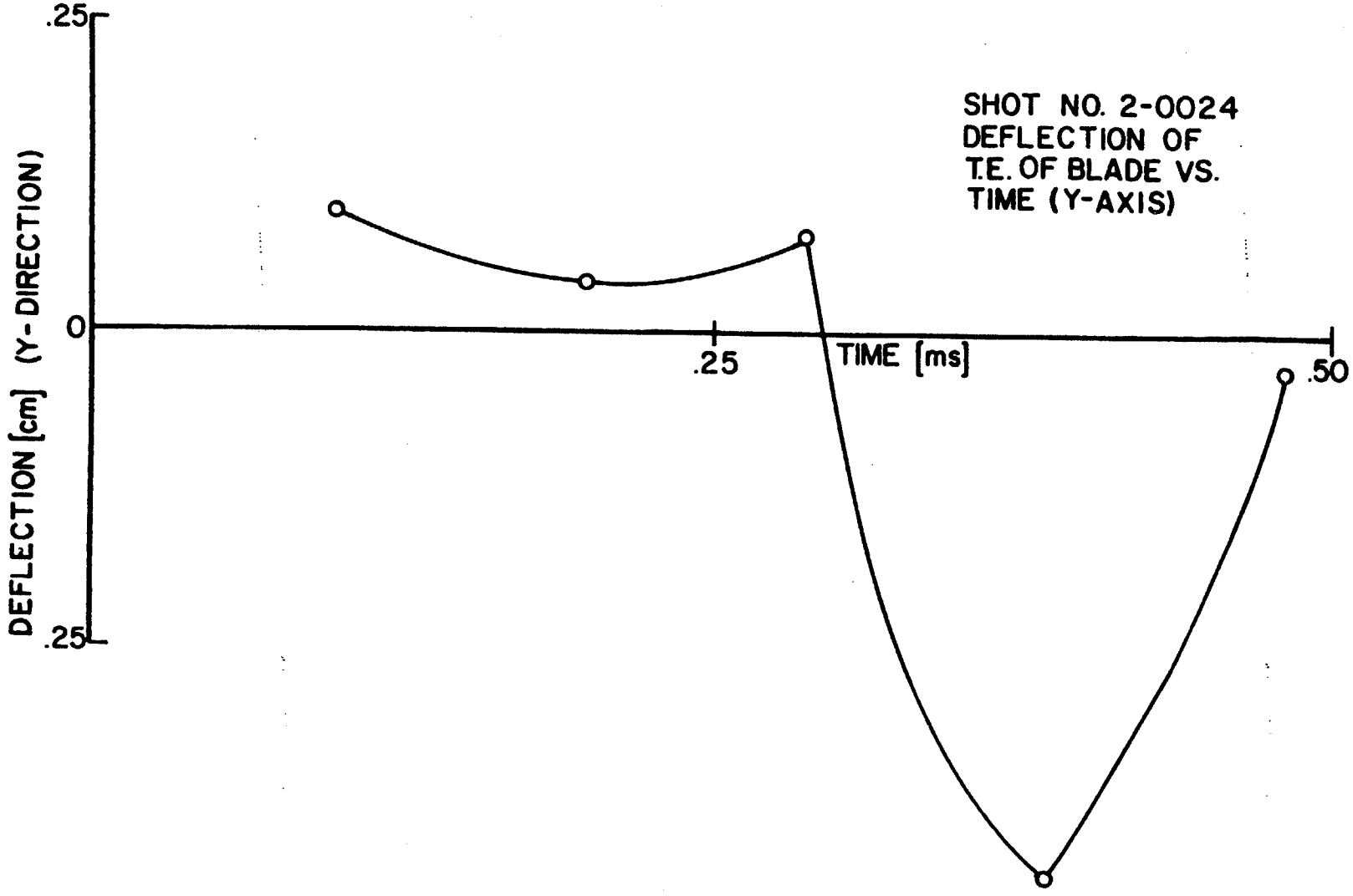

Figure 239. Trailing Edge Tip Deflection in "y" Direction for Shot 2-0024.

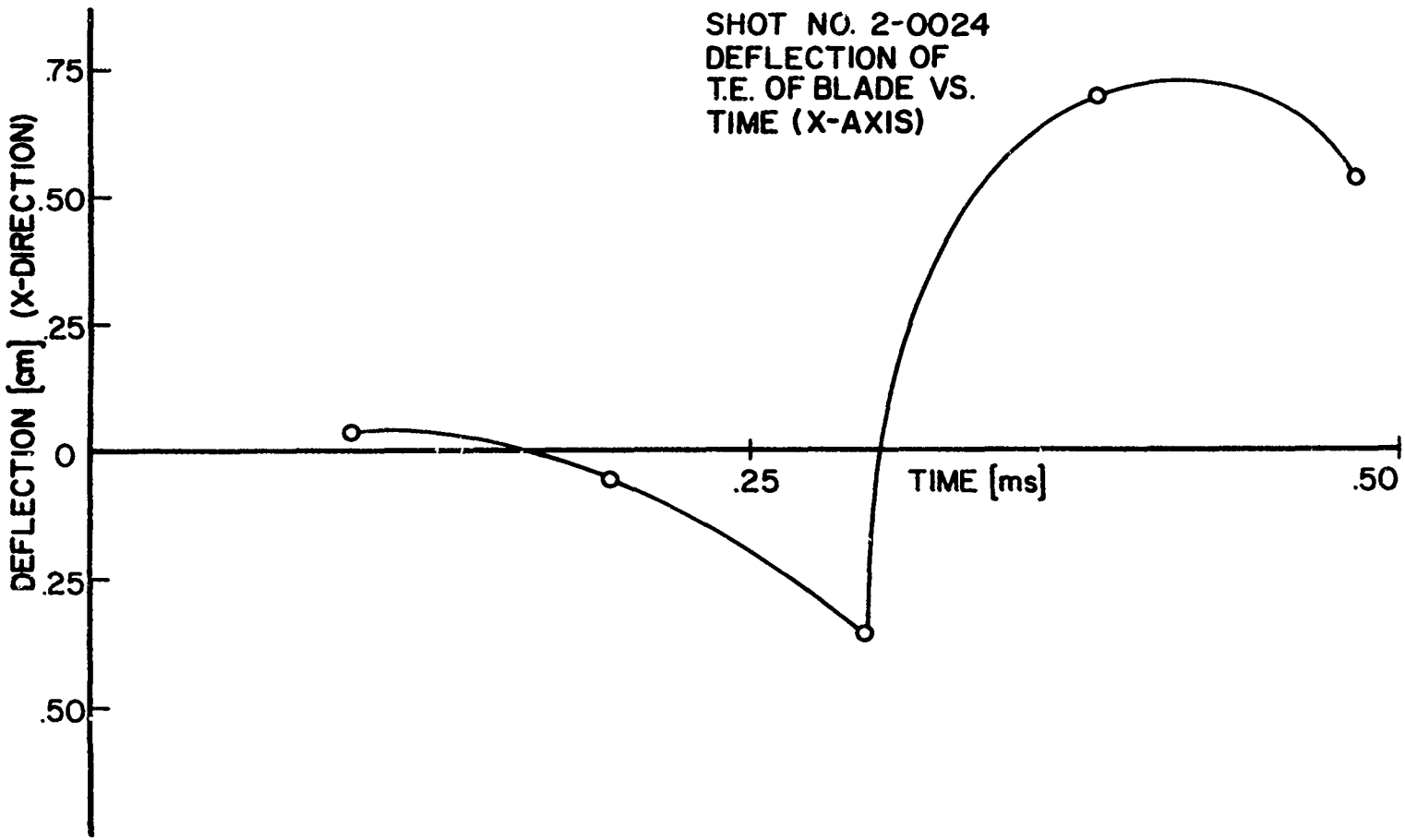

Figure 240. Trailing Edge Tip Deflection in "x" Direction for Shot 2-0024.

free span was received for Shot 2-0222 at a velocity of 248 m/s. The tip displacement measured for this impact was 2.24 cm. Figure 51B gives photographs of the damage of Shot 2-0222.

Severe damage in the form of bowing at the impact site was received for Shot 2-0226 at a velocity of 325 m/s. The leading edge bow was measured to be 1.58 cm. The tip displacement for this impact was 5.13 cm for the leading edge and 8.48 cm for the blade trailing edge. Figure 52B gives the damage for Shot 2-0226.

Strain versus time curves are given in Figures 241 through 246 for Shot 2-0219. This impact had a velocity of 89 m/s and no damage was received by the specimen. Figure 6A of Appendix A gives the strain gage locations for this group of blades. In the curves, tension is denoted as a positive strain and compression as a negative strain for all impacts of this blade group. Figures 247 and 248 give dynamic tip deflection versus time curves for the "y" and "x" directions, respectively.

3.2.11 Impact Results for Group 11B Blades

Three leading edge impacts using an ice cylinder (7.62 cm diameter and 17.78 cm long) to simulate slab ice were conducted on J79 stainless steel blades at the 30 percent span location. The impact velocity ranged from 98 to 134 m/s and the impact mass 147.8 to 207.4 g. The impact angle for the impacts was 51.1.

No visible damage on the blades was received for two of the impacts (Shots 2-0232 and 2-0234). The impact conditions for Shot 2-0232 was a velocity of 99 m/s and an impact mass of 147.8 g while 98 m/s and 207.4 g were the conditions for Shot 2-234.

Severe damage was received for Shot 2-0235 at a velocity of 134 m/s and a mass of 158.4 g. The damage was in the form of bowing at the impact site. The tip displacement measurement of the damage was 14.74 cm for the leading

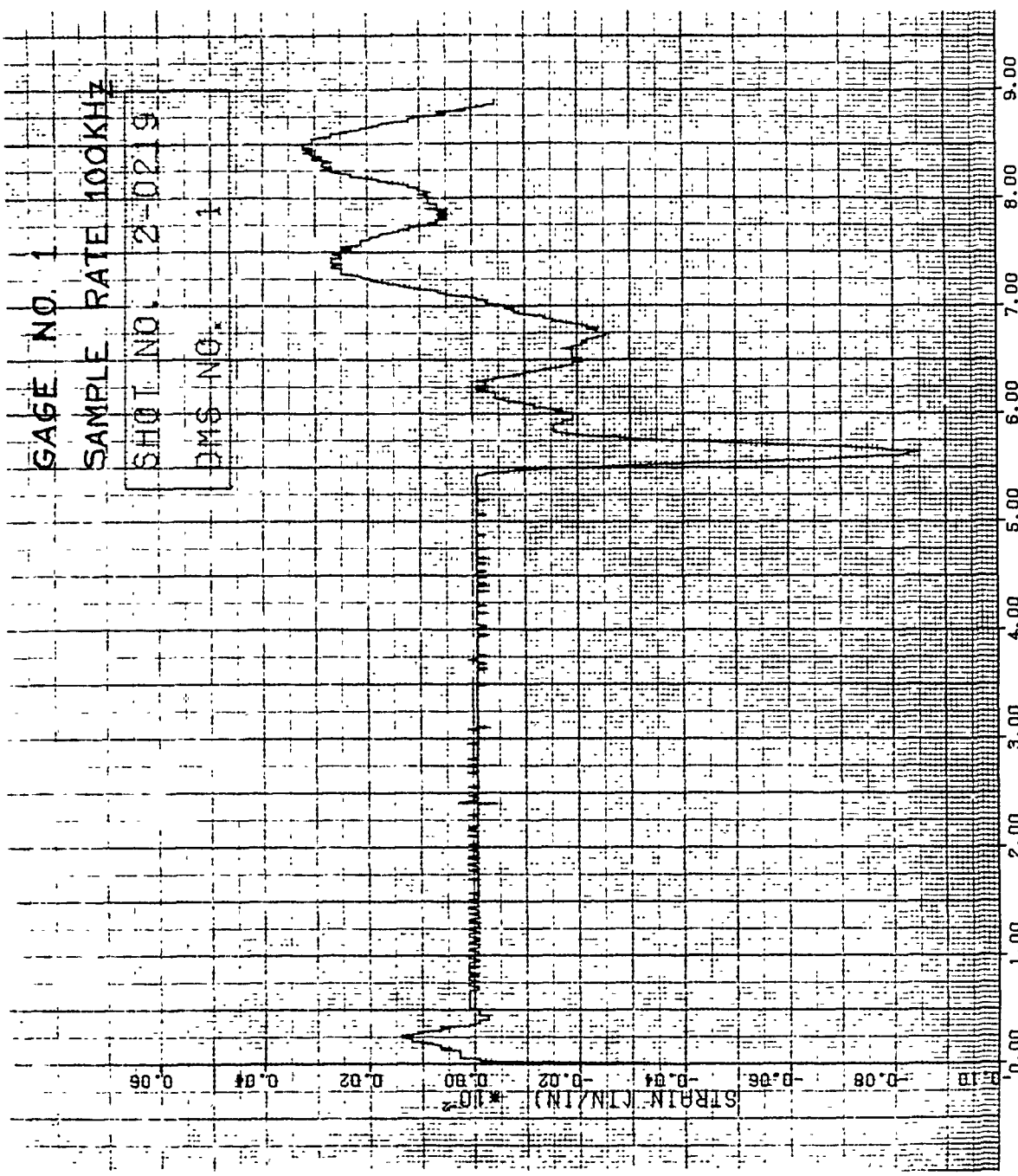

Figure 241. Strain of Shot 2-0219 for Gage #1.

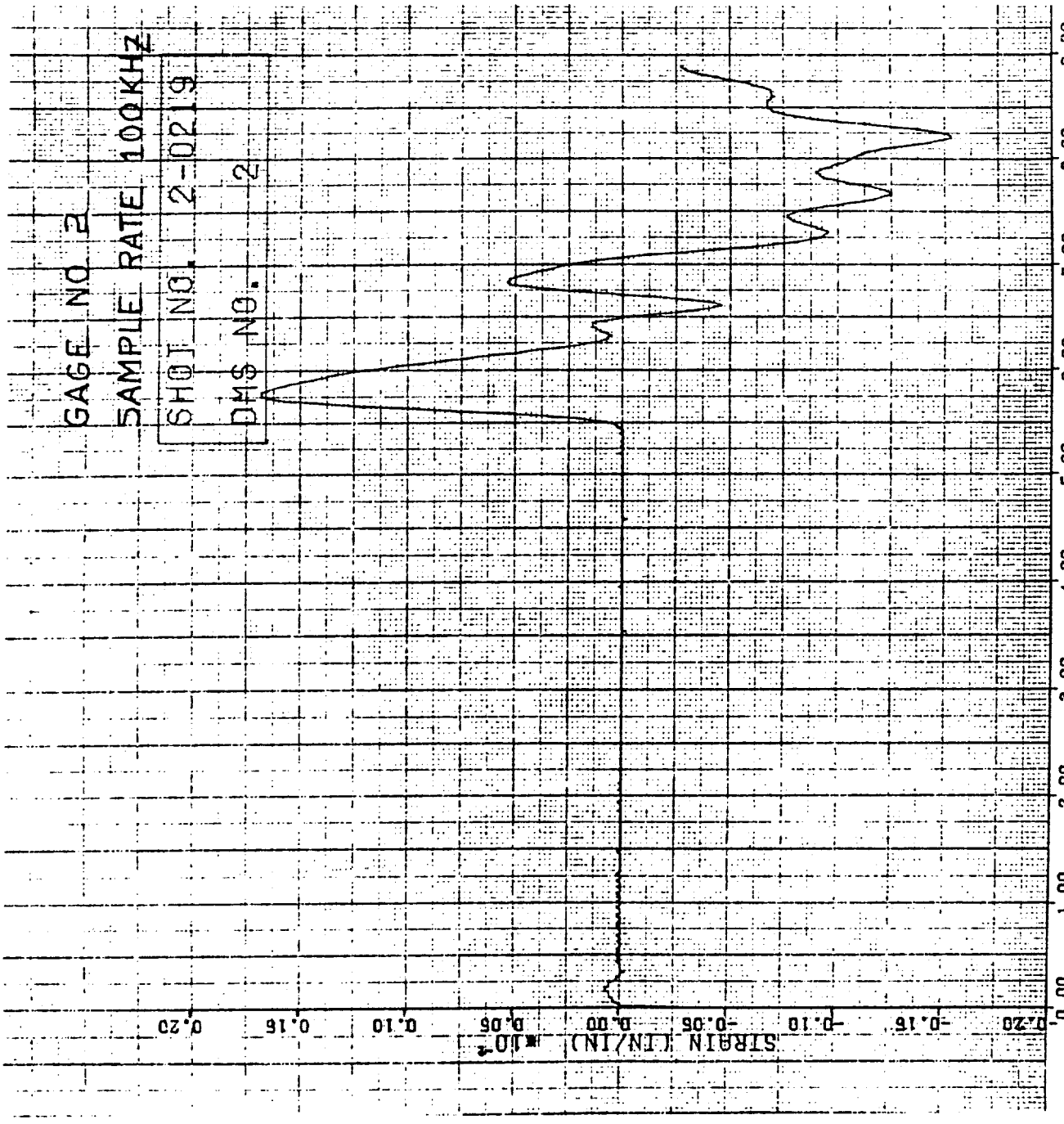

Figure 242. Strain of Shot 2-0219 for Gage #2.

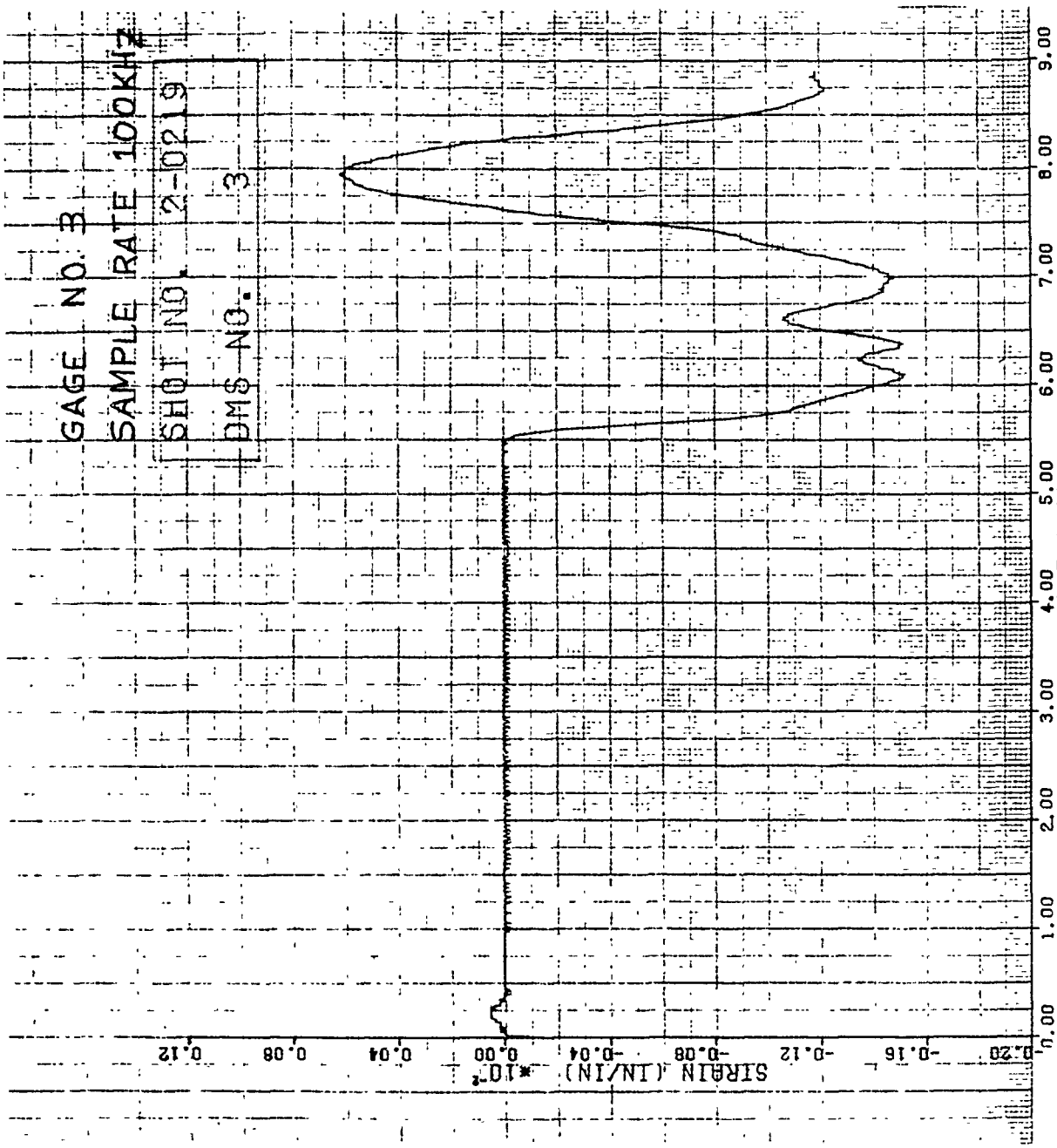

Figure 243. Strain of Shot 2-0219 for Gage #3.

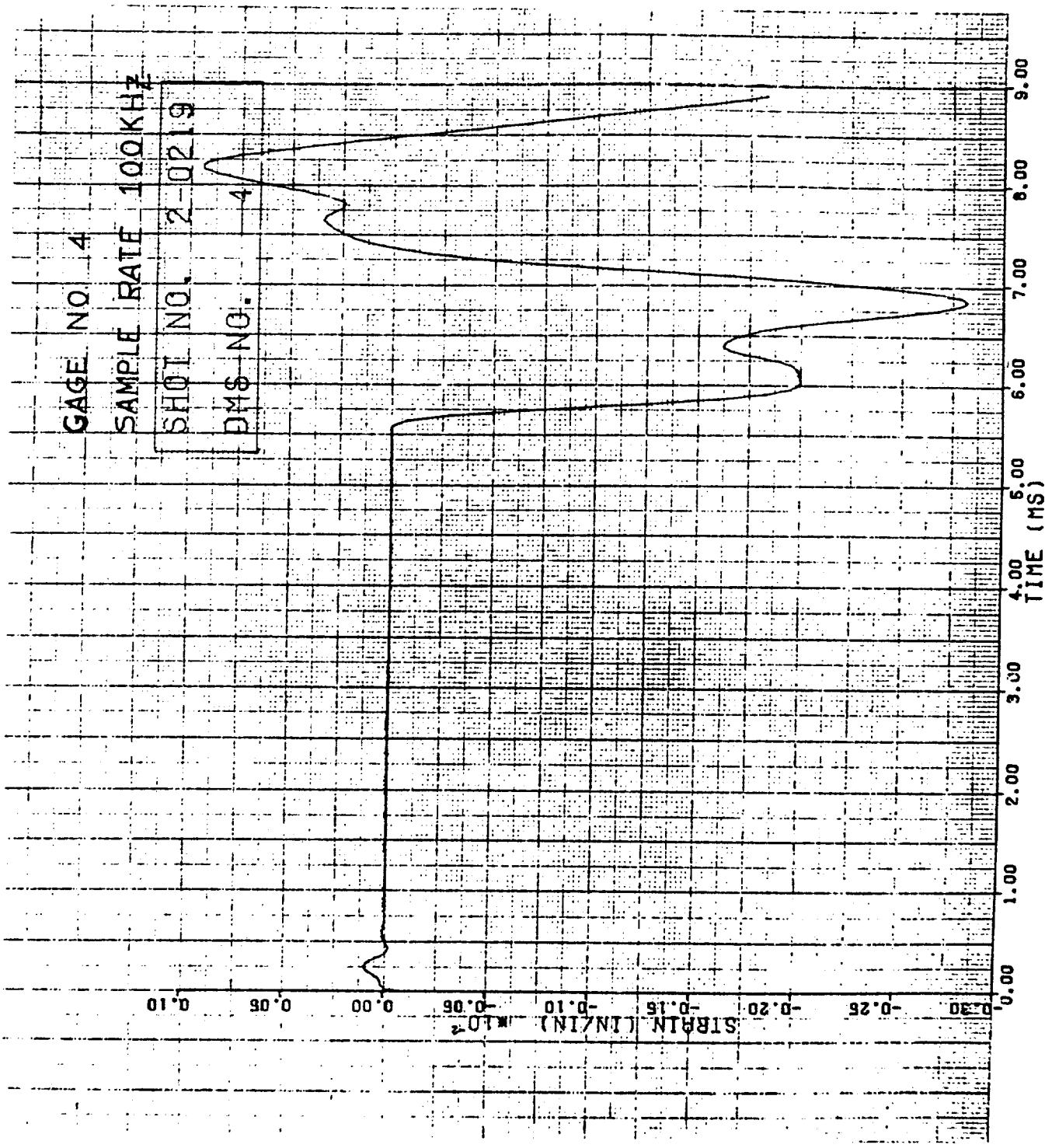

Figure 244. Strain of Shot 2-0219 for Gage #4.

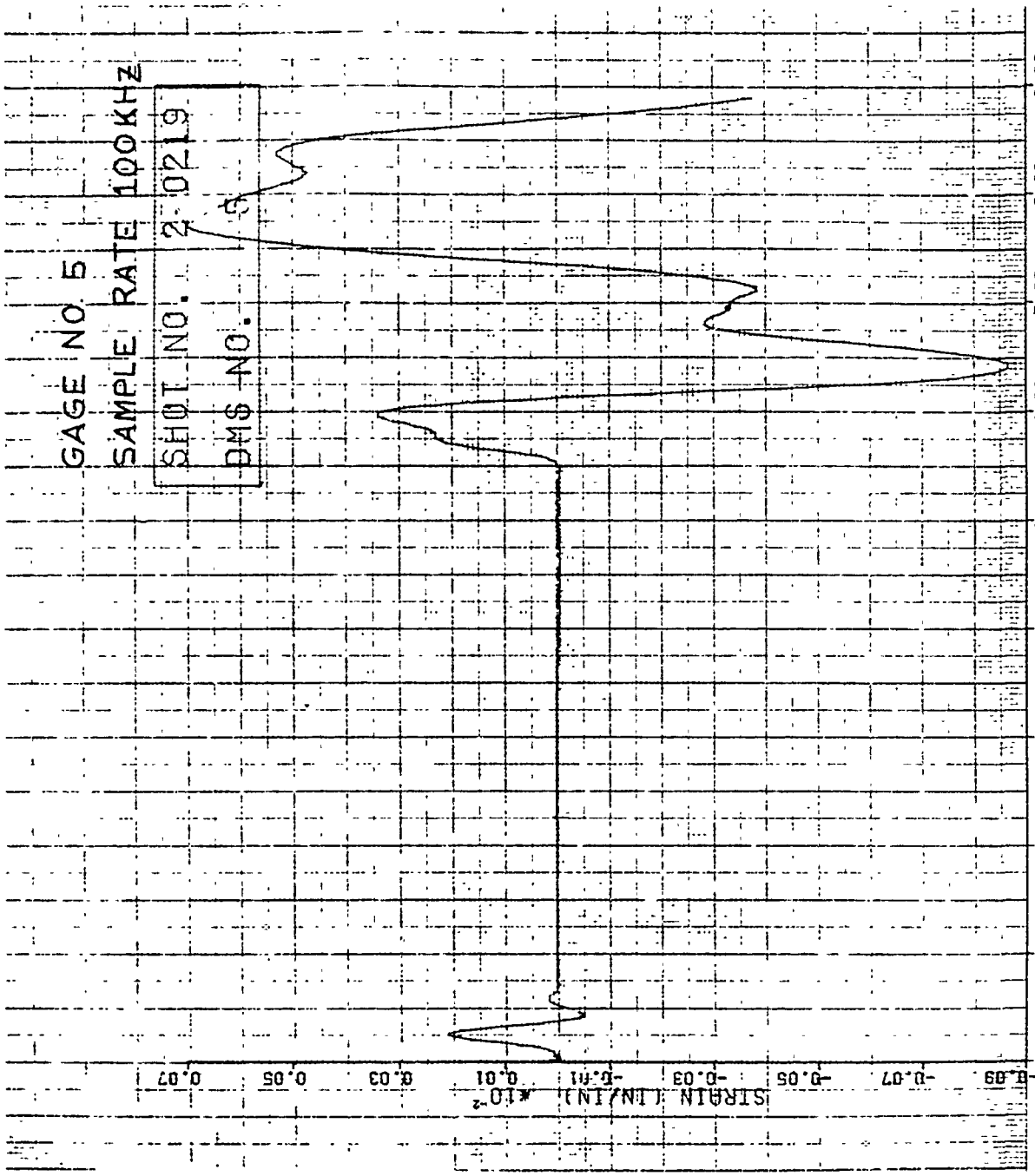

Figure 245. Strain of Shot 2-0219 for Gage #5.

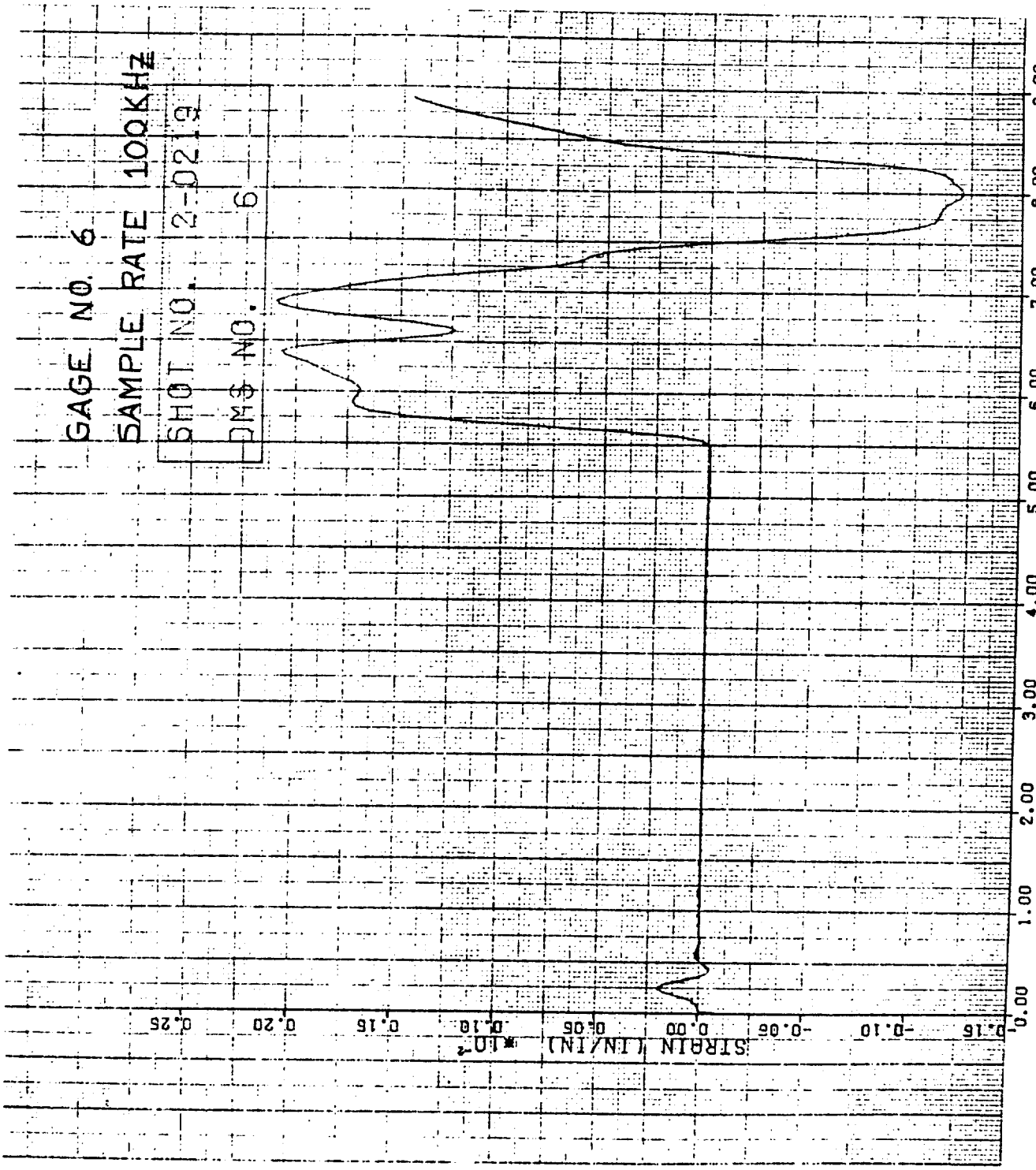

Figure 246. Strain of Shot 2-0219 for Gage #6.

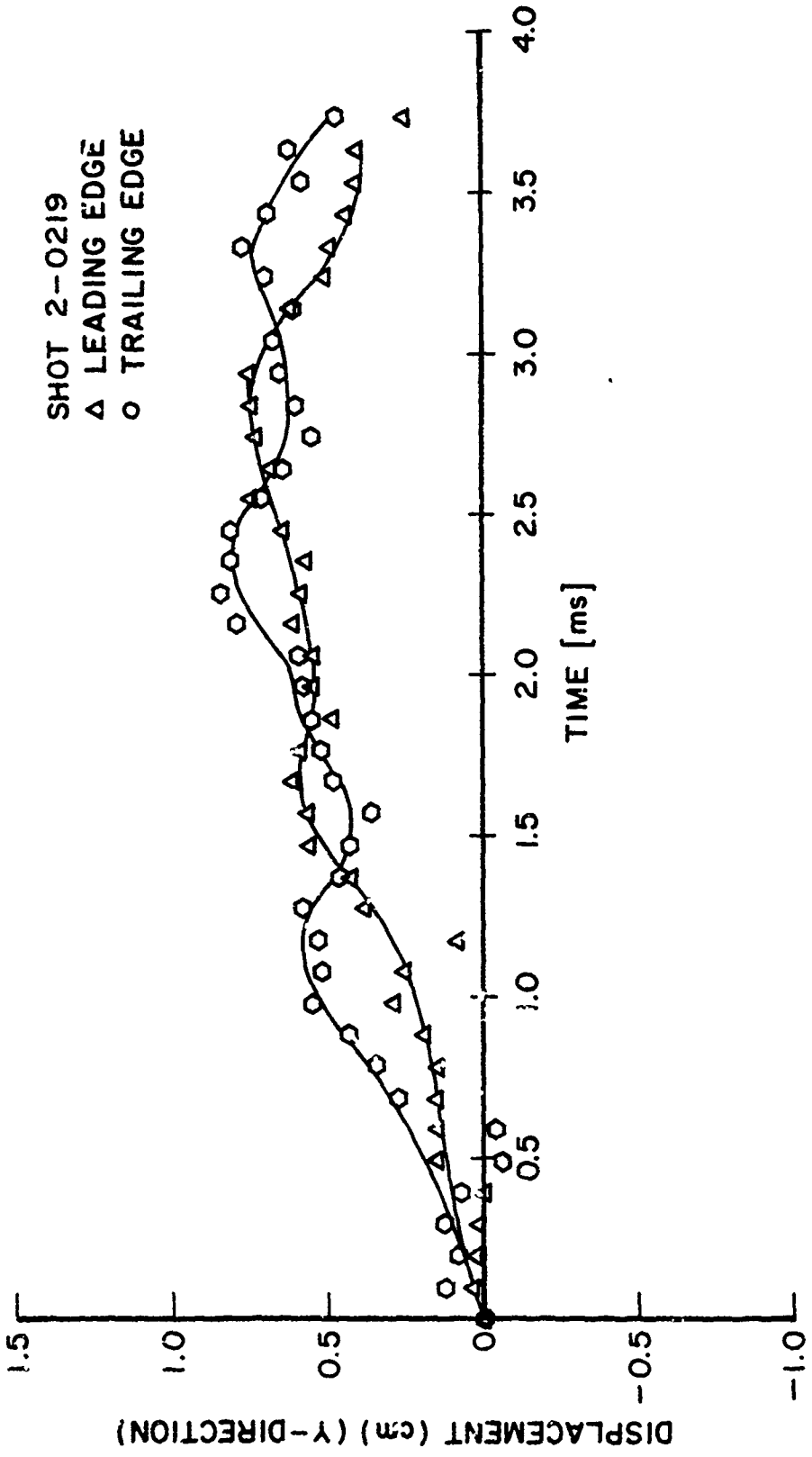

Figure 247. Tip Deflection in "y" Direction for Shot 2-0219.

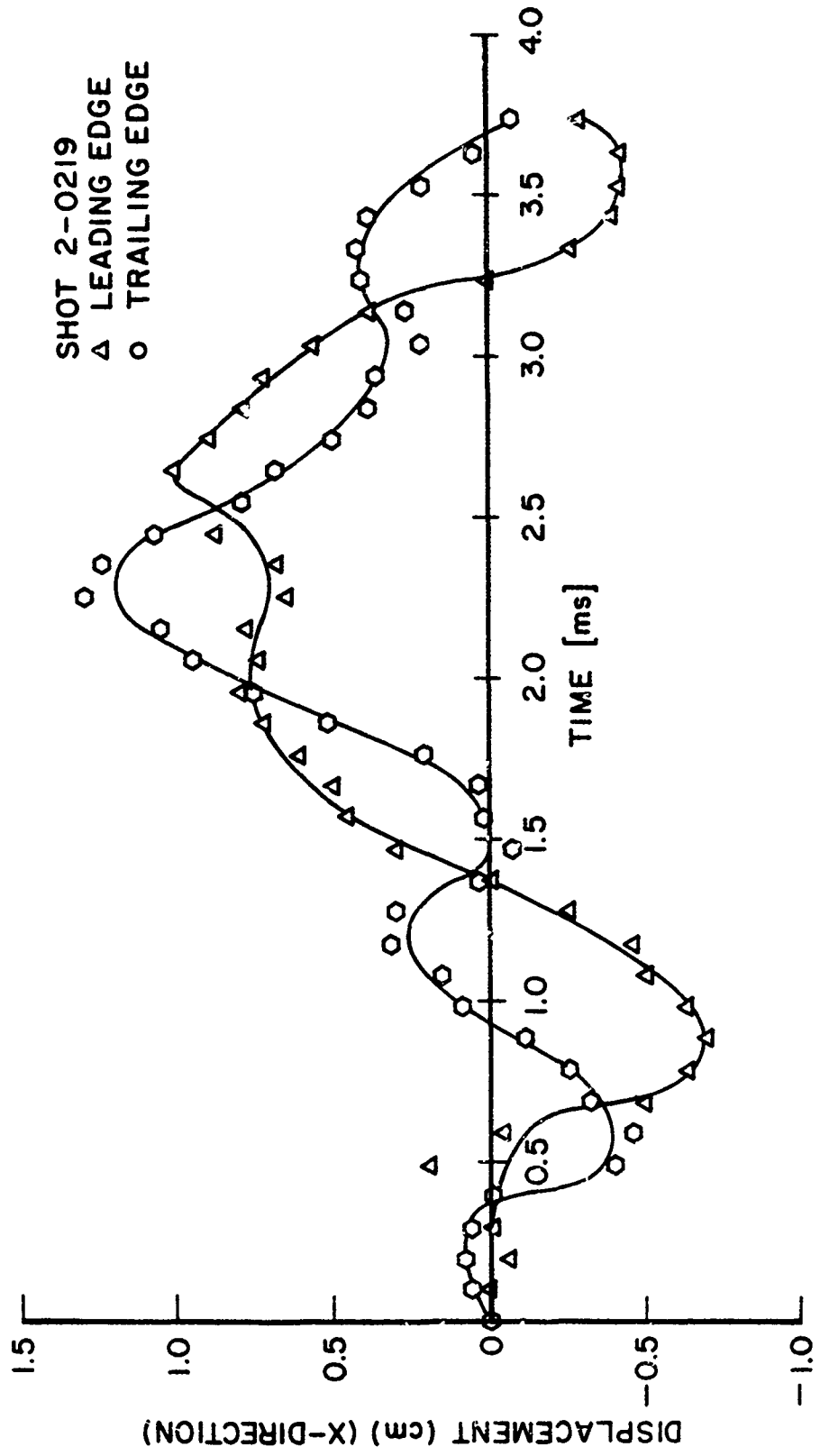

Figure 248. Tip Deflection in "x" Direction for Shot 2-0219.

edge and 15.49 cm for the trailing edge. Figure 53B gives photographs of the damage for this impact.

Strain versus time curves are presented in Figures 249 through 254 for Shot 2-0234. No damage resulted from an impact at a velocity of 98 m/s and impact mass of 207.4 g. Figure 6A of Appendix A gives the strain gage locations of this group of blades. Tension is denoted as a positive strain and compression as a negative strain. Dynamic tip deflection curves for the impact event of Shot 2-0234 are given in Figures 255 and 256 for the "y" and "x" directions, respectively.

3.2.12 Impact Results for Group 12B Blades

Two leading edge impacts using the 85 g (3 ounce) artificial bird were conducted on boron/aluminum composite blades (APSI) at the 30 percent span location. Both impacts generated damaged on the blades. The incidence angle for this group of blades was 38.8 degrees. Shot 2-0016 fired at a velocity of about 259 m/s (estimated) generated local damage at the impact site with an impact mass of 16.0 g. The damage for this impact was in the form of breaking off material along the leading edge at the impact site. The affected area was 7.13 cm long and 1.80 cm maximum width. Figure 54B shows the damage received for Shot 2-0016.

Shot 2-0023 at a velocity of 419 m/s generated damage in the form of a crack across the chord 5.08 cm long starting from the leading edge surface. The impact mass could not be determined for this impact. Also, the balsa wood sabot hit the target after the bird. Figures 257 through 262 give strain versus time curves for the impact. Figure 2A of Appendix A gives the gage locations for this series of tests. Tension is denoted as a negative strain and compression as a positive strain for this group of blades. It was impossible to determine the maximum strain rate because of noise in the data. Figures 263 through 266 show the tip deflection versus time results for Shot 2-0023 during the impact event. Figure 261 shows the

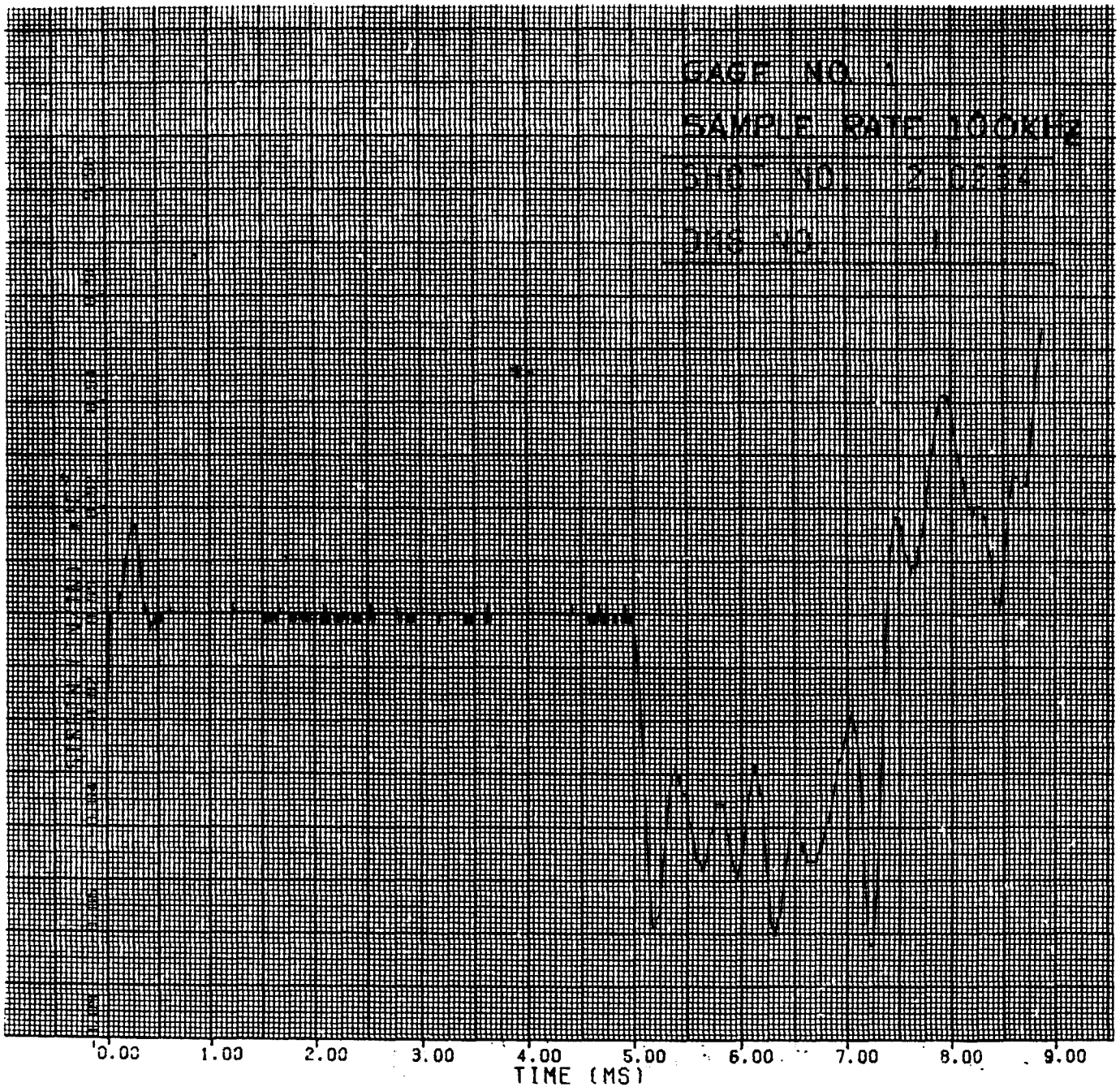

Figure 249. Strain of Shot 2-0234 for Gage #1.

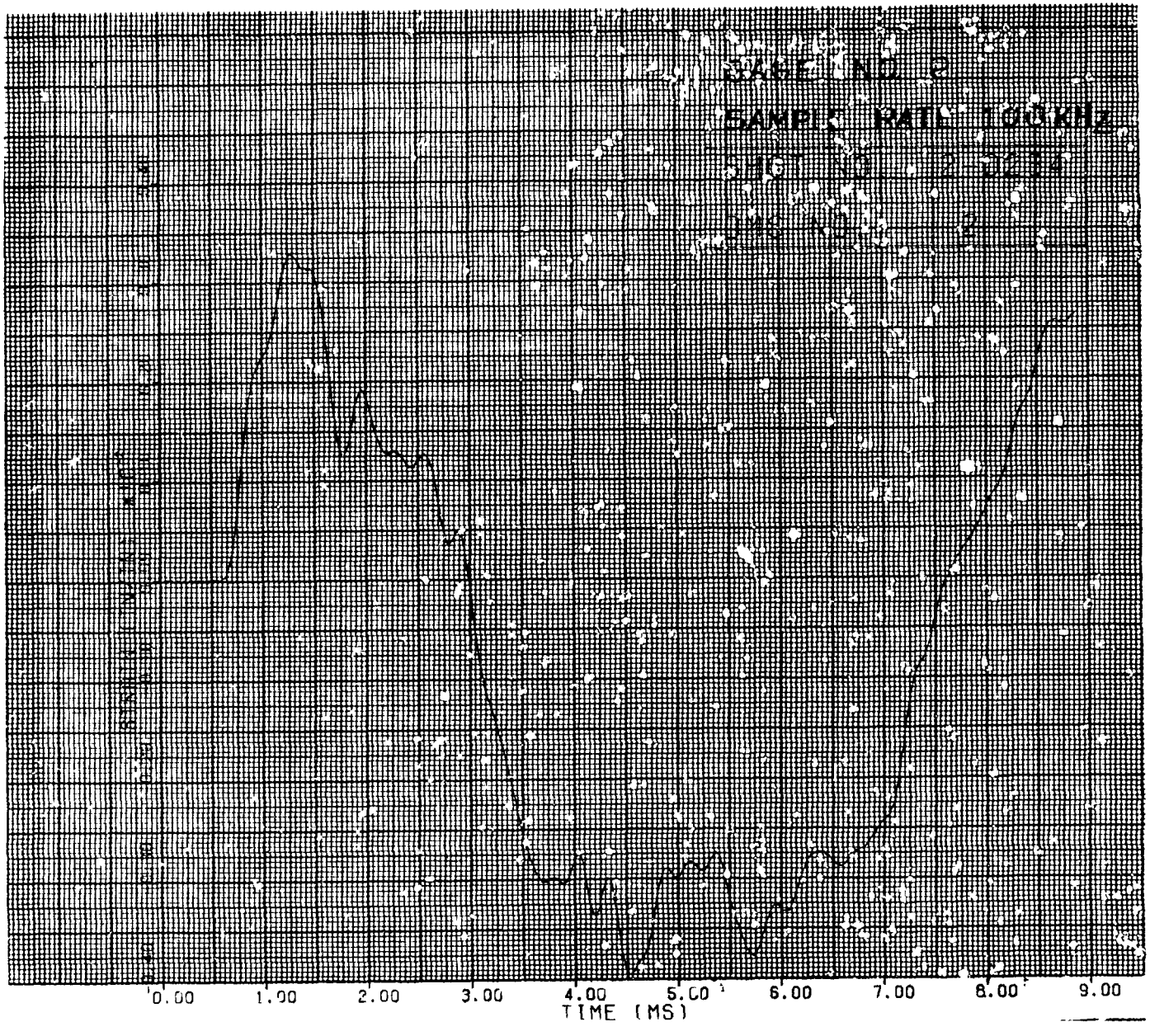

Figure 250. Strain of Shot 2-0234 for Gage #2.

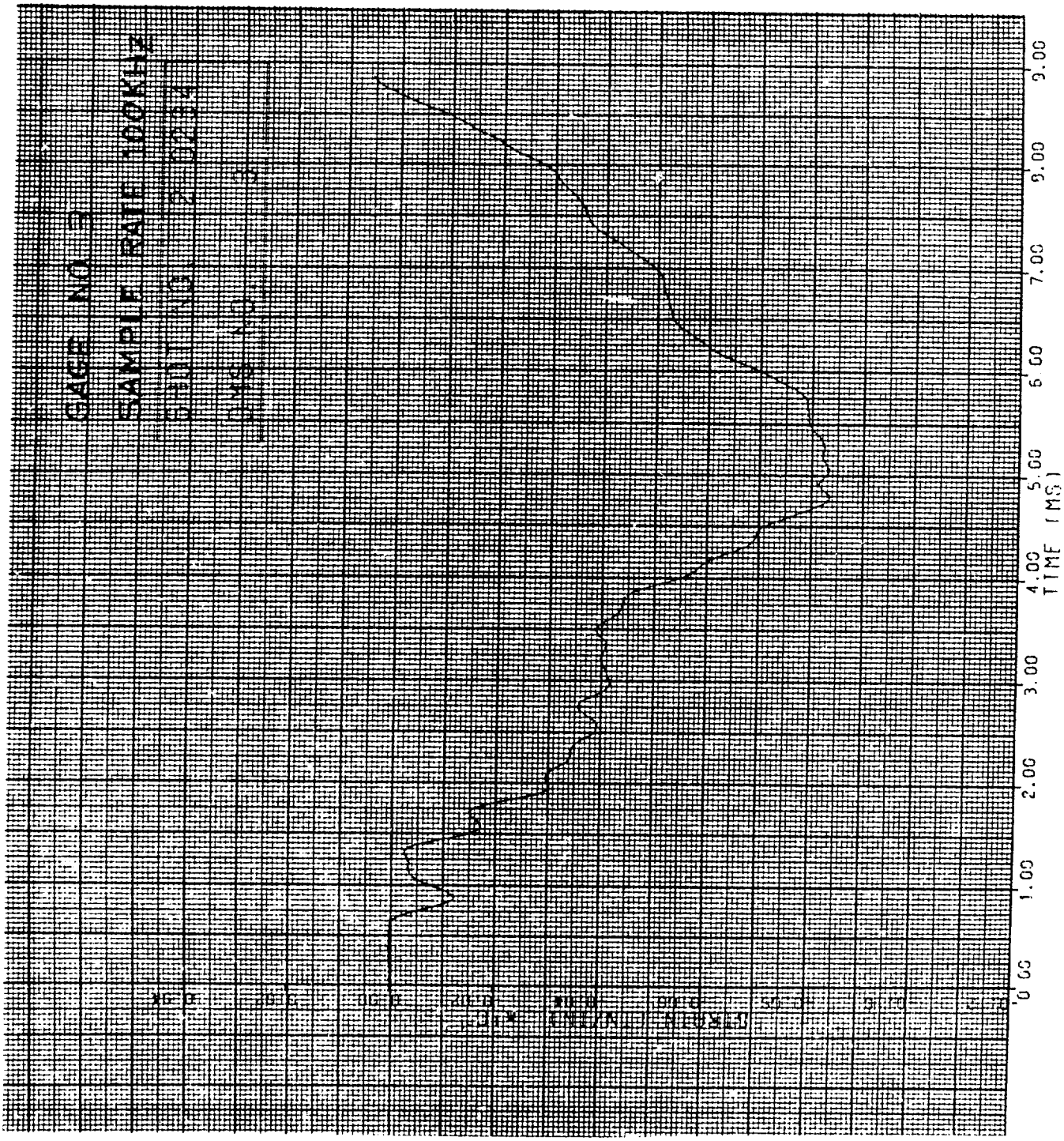

Figure 251. Strain of Shot 2-0234 for Gage #3.

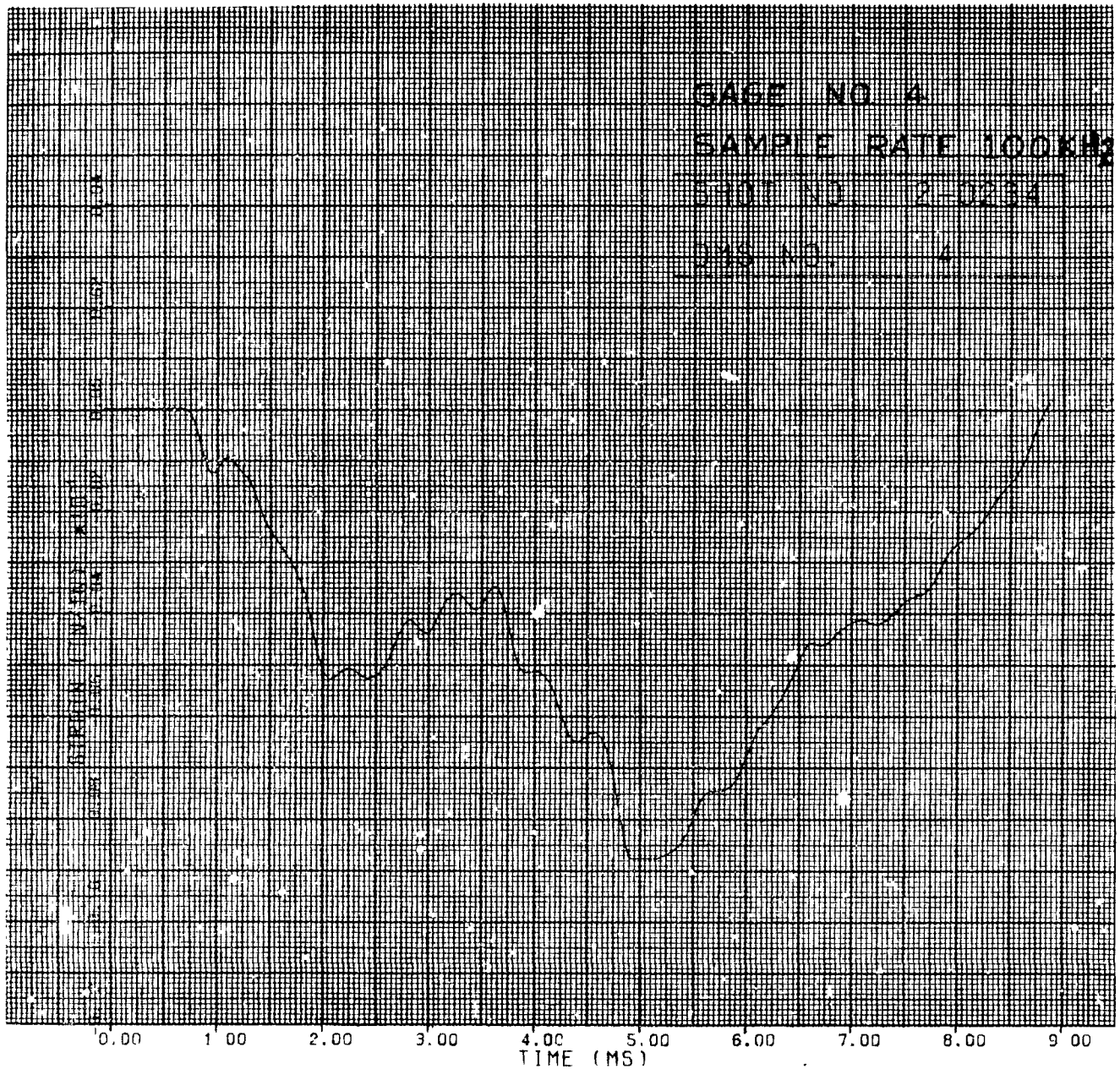

Figure 252. Strain of Shot 2-0234 for Gage #4.

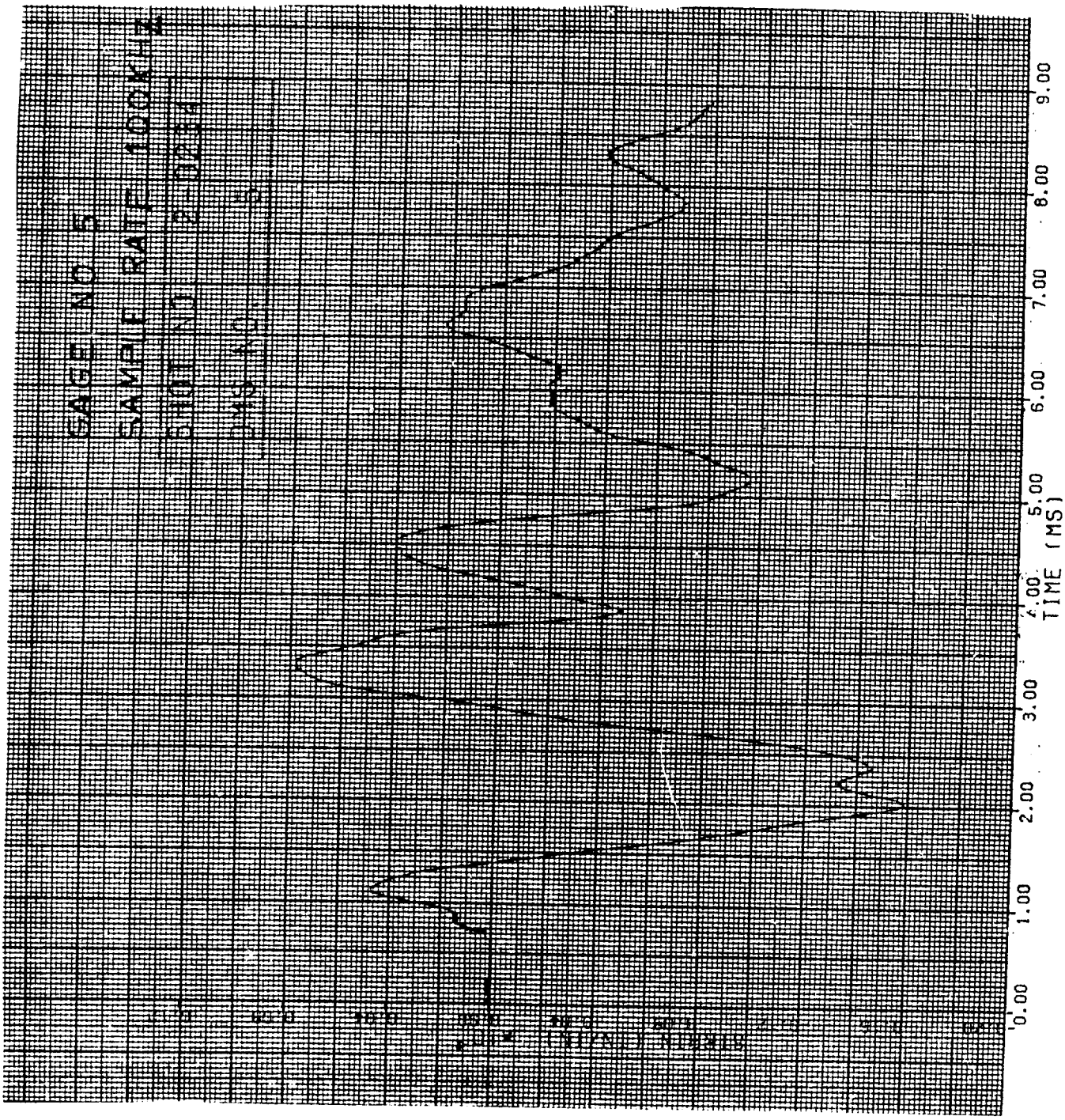

Figure 253. Strain of Shot 2-0234 for Gage #5.

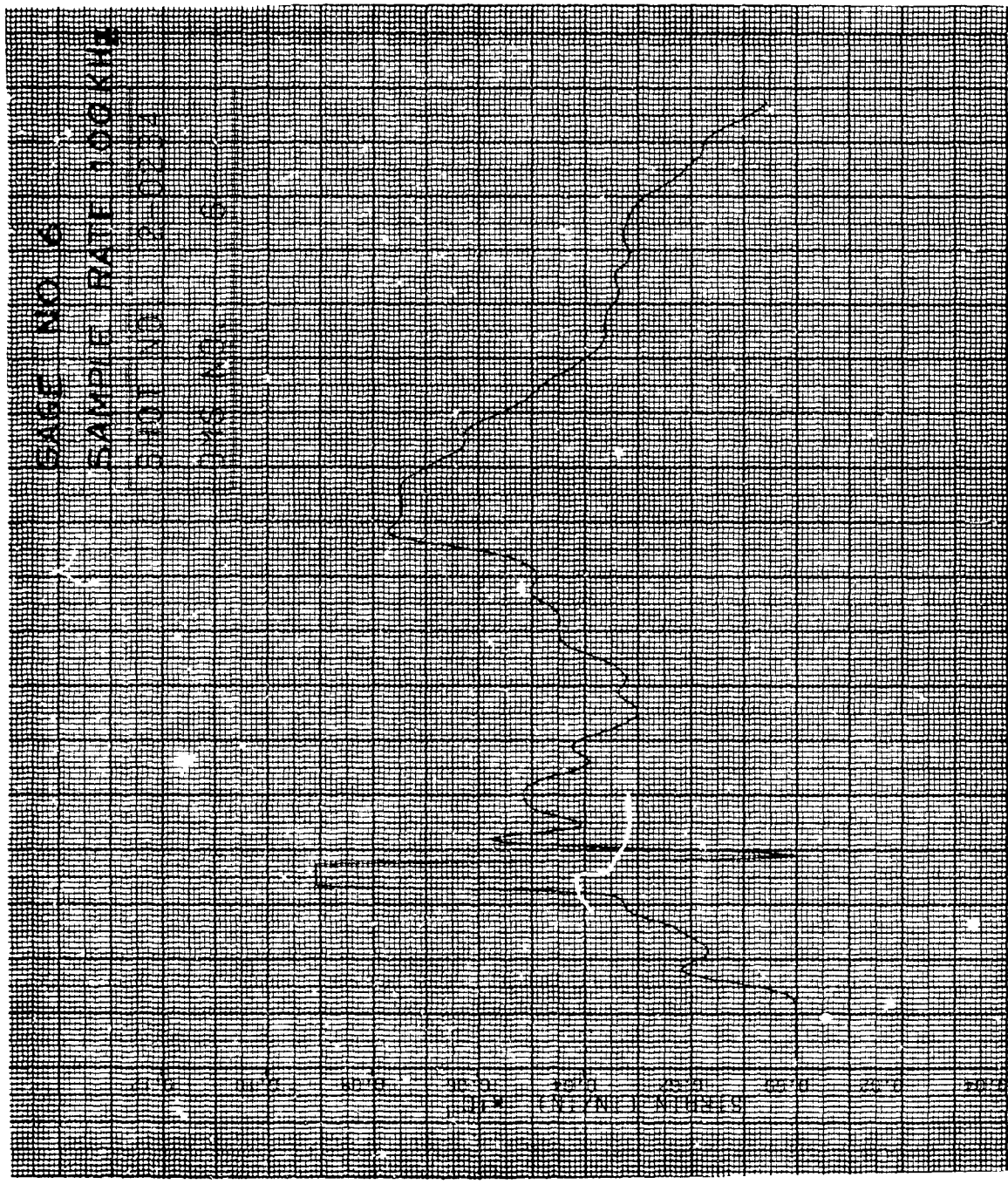

Figure 254. Strain of Shot 2-0234 for Gage #6.

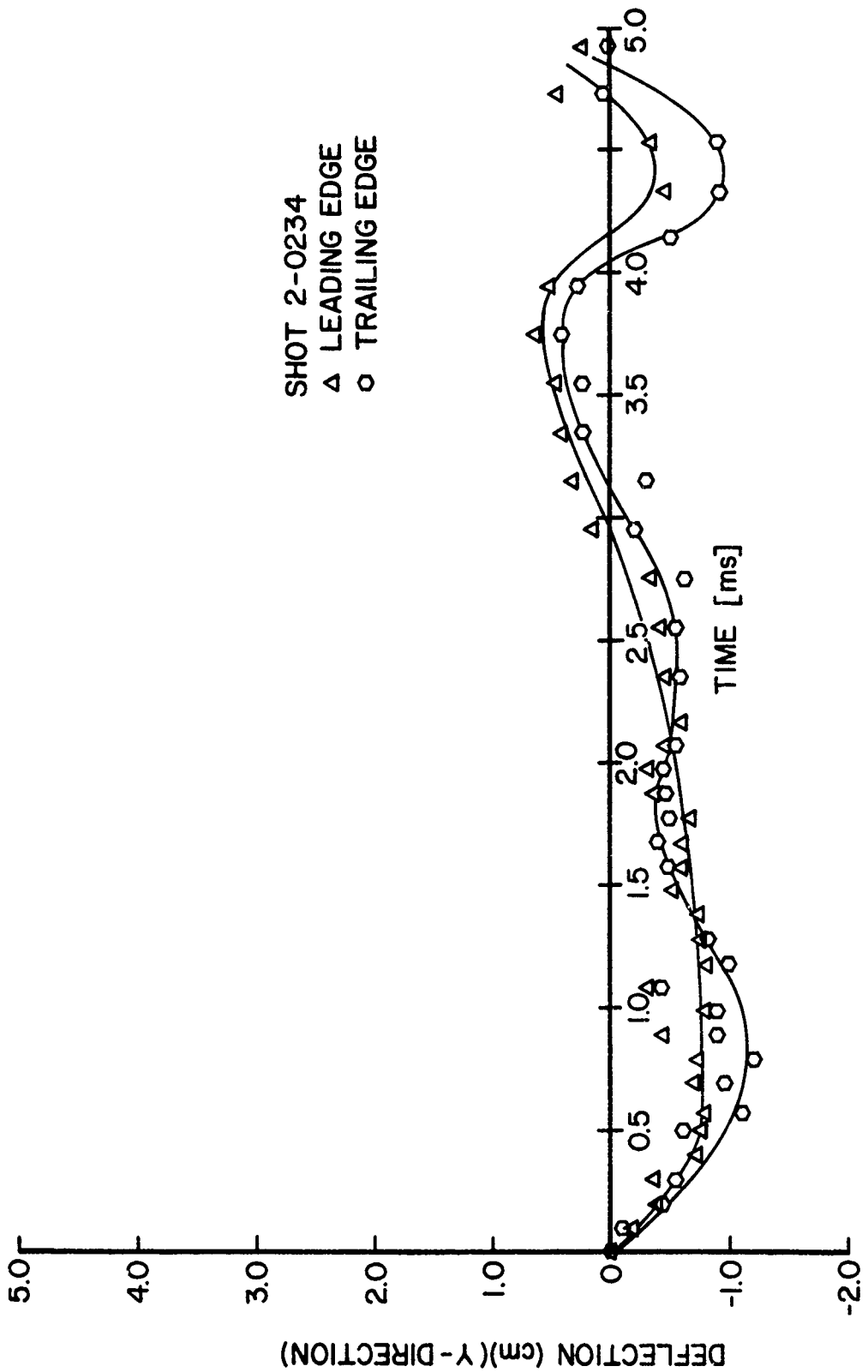

Figure 255. Tip Deflection in "y" Direction for Shot 2-0234.

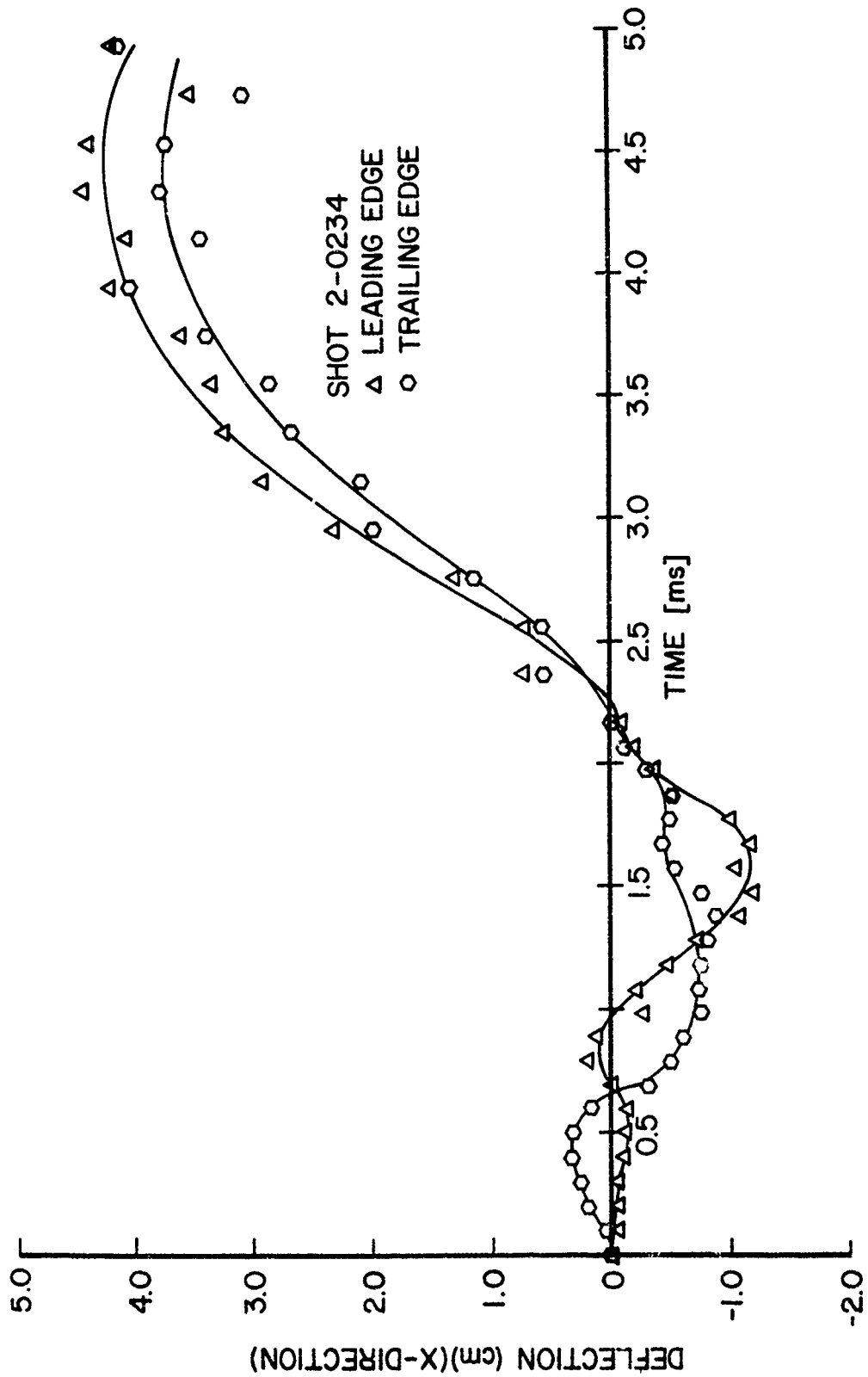

Figure 256. Tip Deflection in "x" Direction for Shot 2-0234.

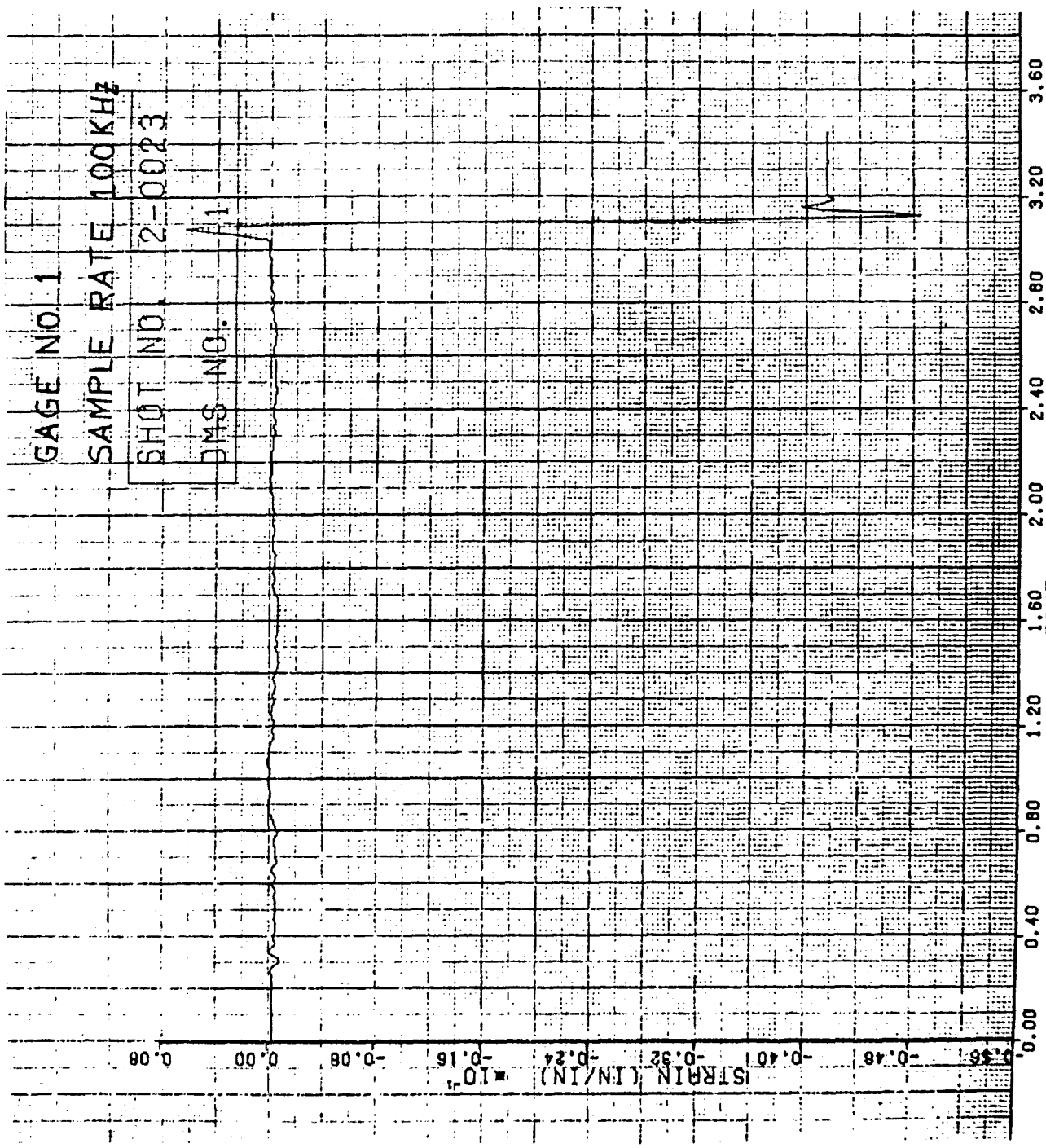

Figure 257. Strain of Shot 2-0023 for Gage #1.

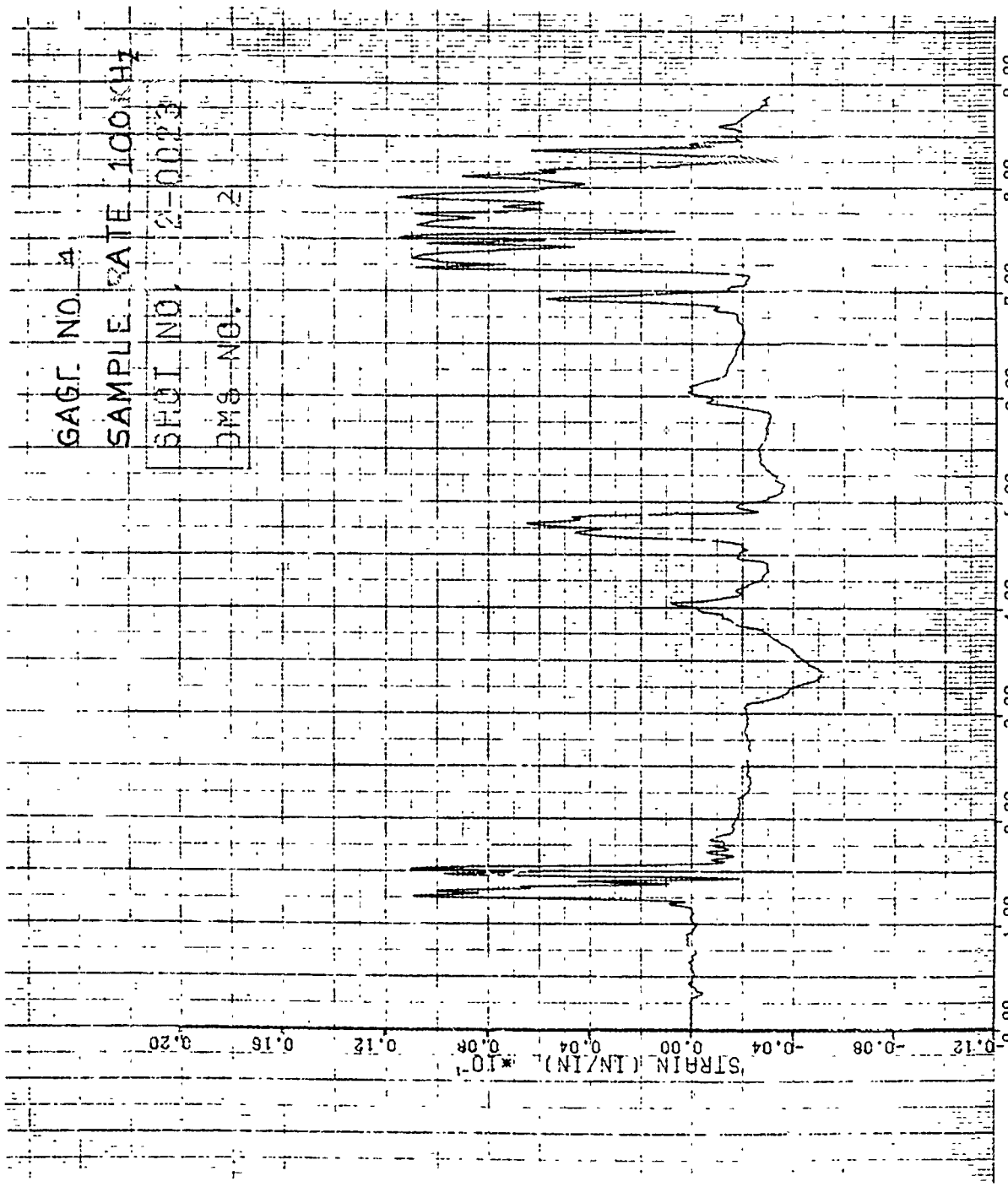

Figure 258. Strain of Shot 2-0023 for Gage #4.

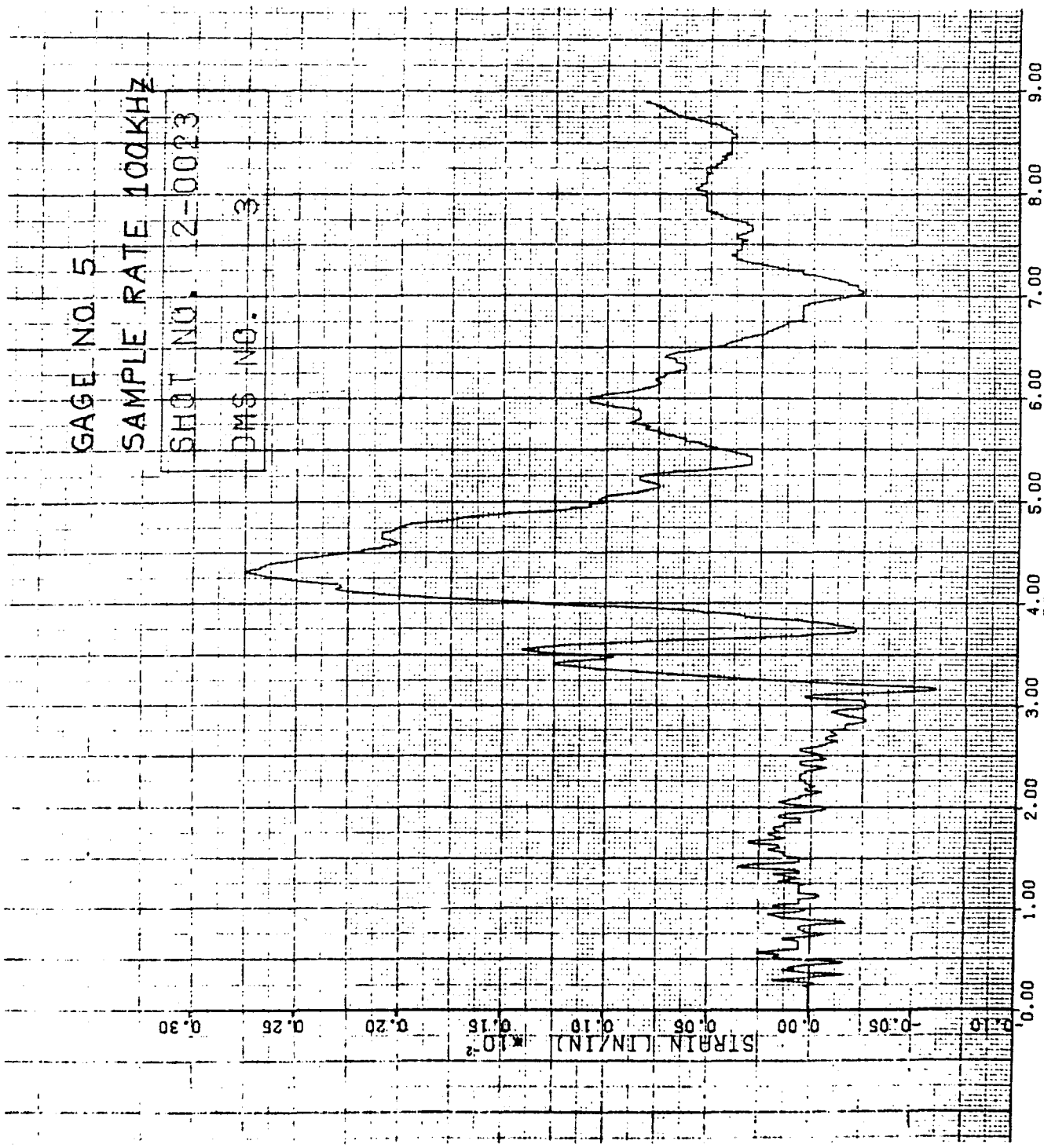

Figure 259. Strain of Shot 2-0023 for Gage #5.

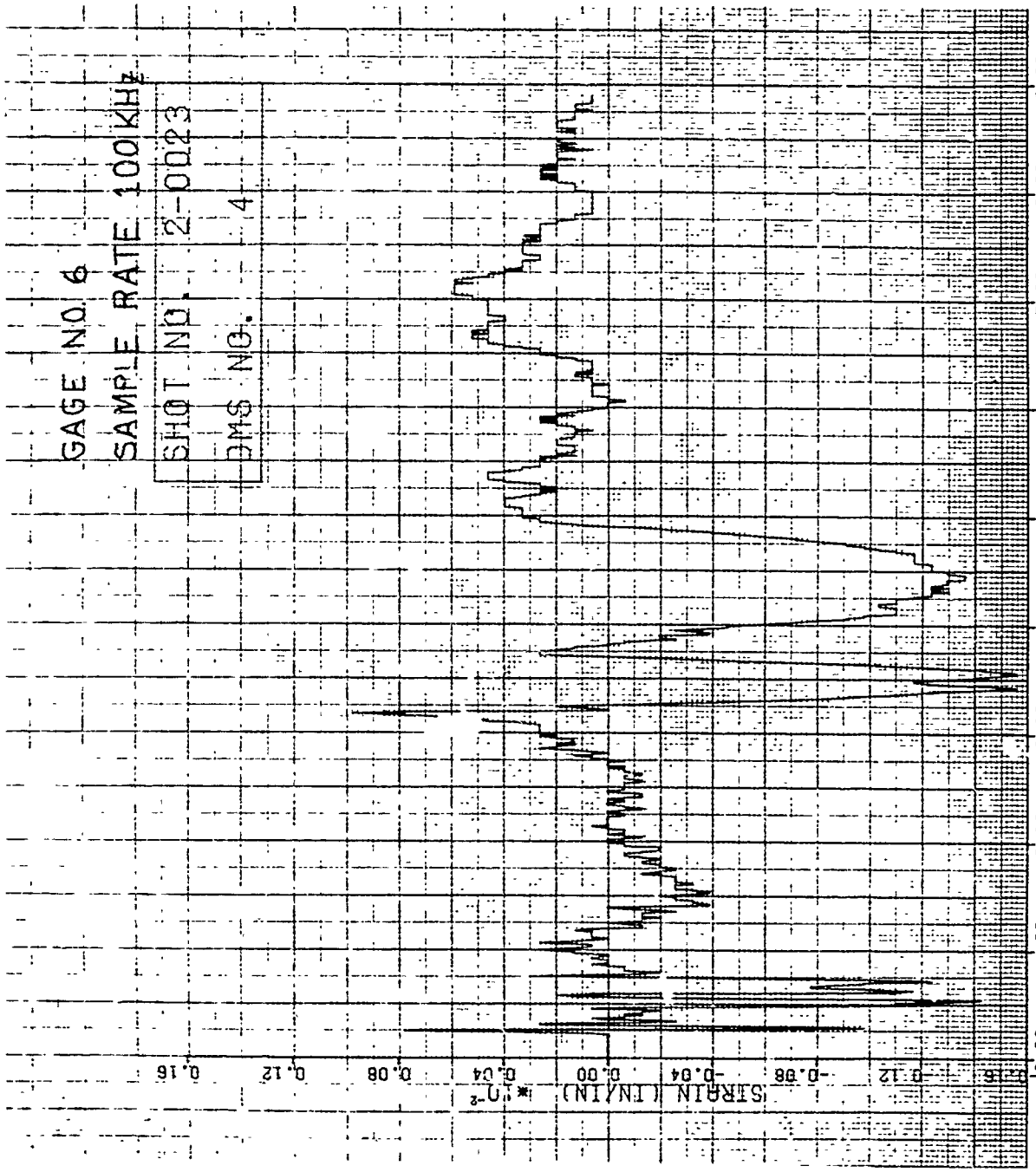

Figure 260. Strain of Shot 2-0023 for Gage #6.

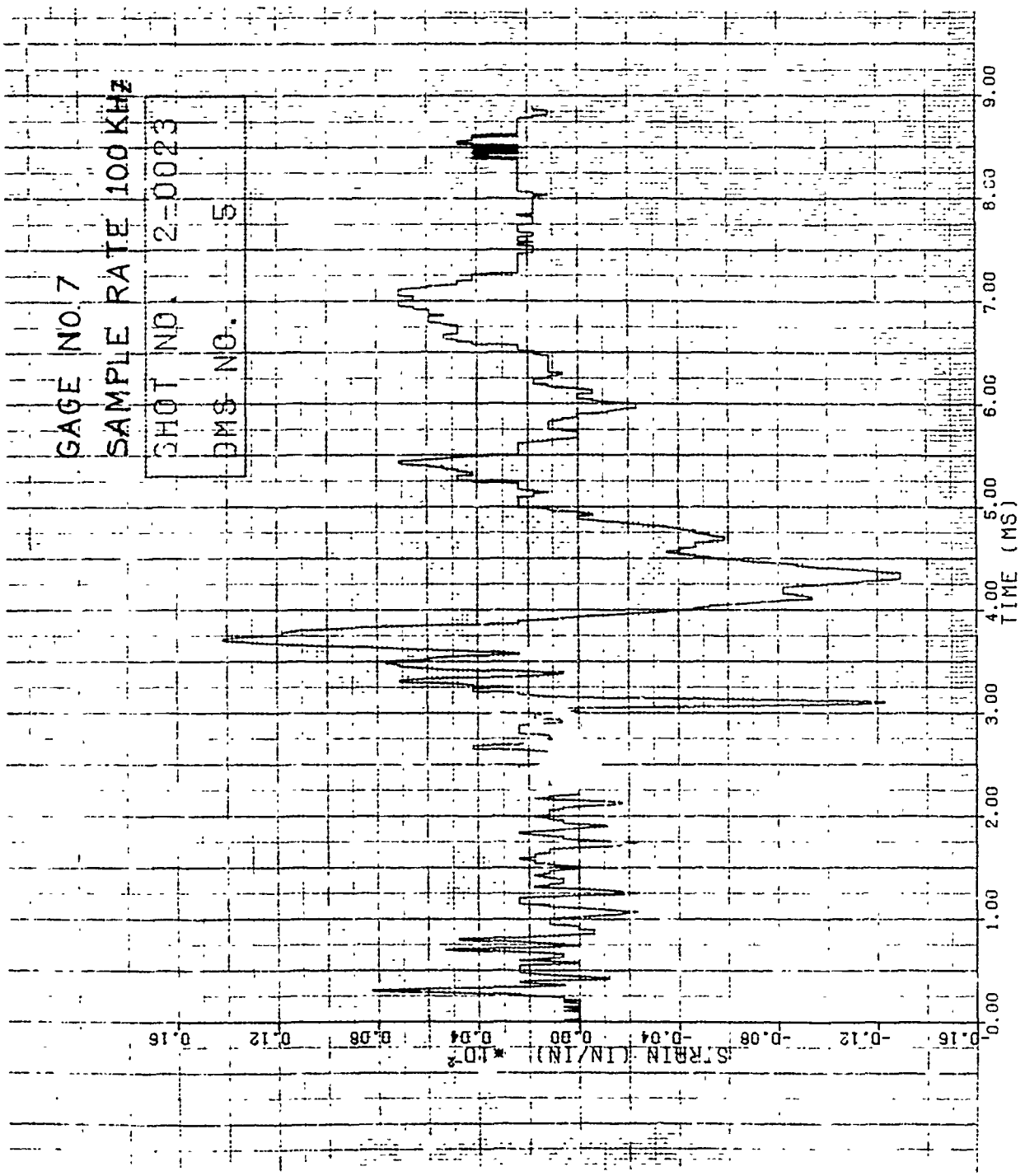
GAGE NO. 7
SAMPLE RATE 100 KHz
SHOT NO. 2-0023
DMS NO. 5
STRAIN (IN/IN) *10^-2
-0.16
-0.12
-0.08
-0.04
0.00
0.04
0.08
0.12
0.16
TIME (MS)
0.00
1.00
2.00
3.00
4.00
5.00
6.00
7.00
8.00
9.00

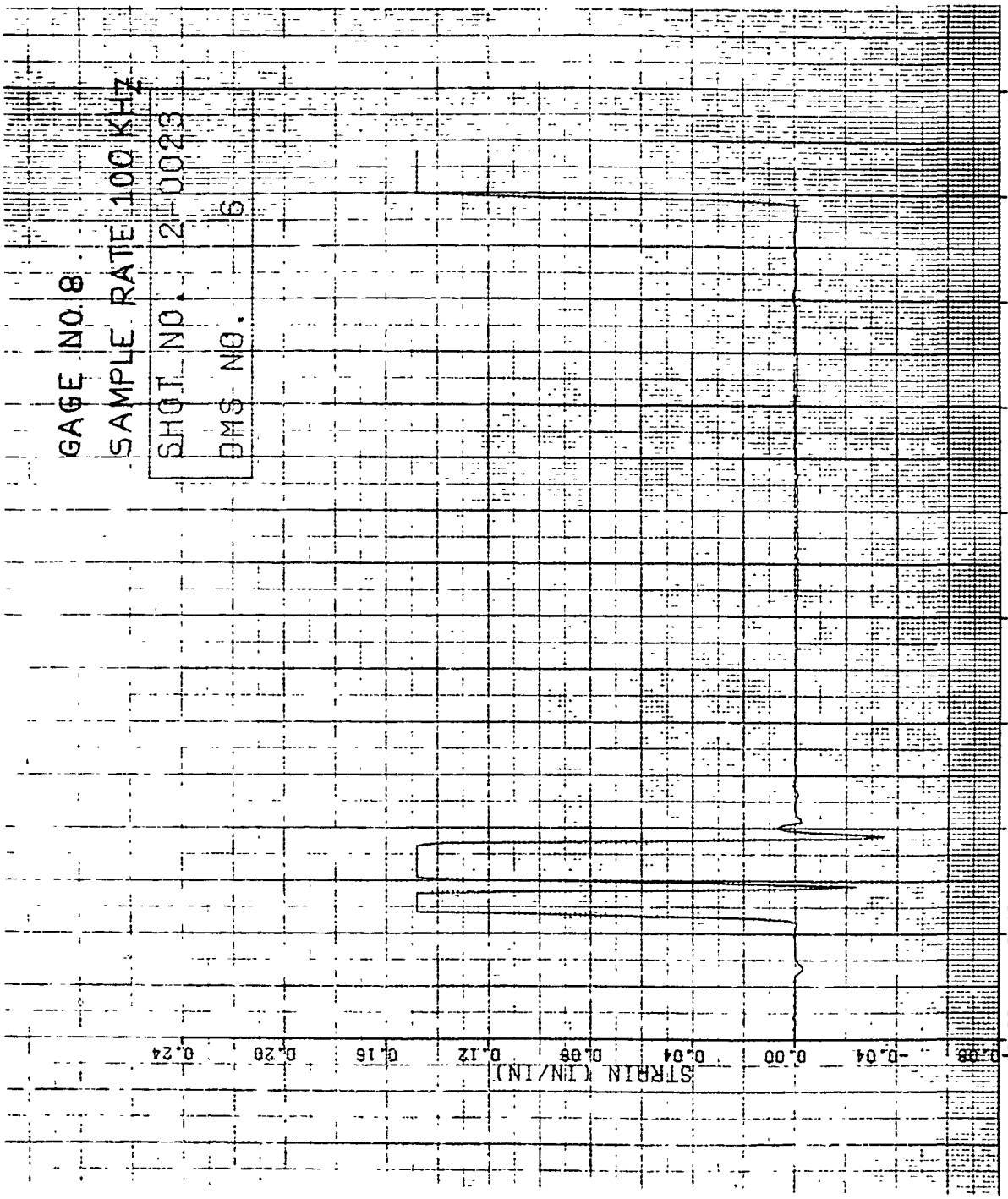

Figure 262. Strain of Shot 2-0023 for Gage #8.

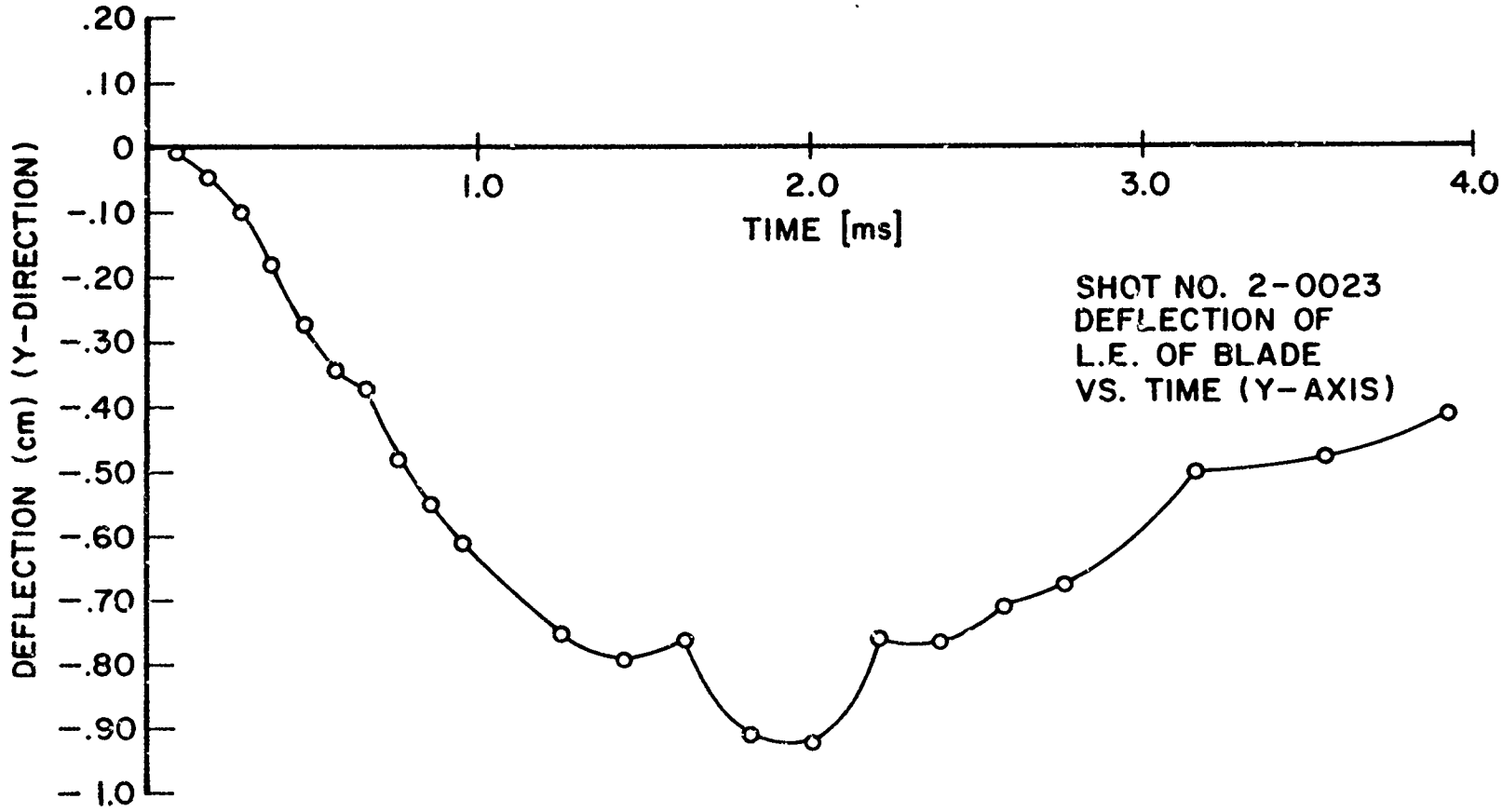

Figure 263. Leading Edge Tip Deflection in "y" Direction for Shot 2-0023.

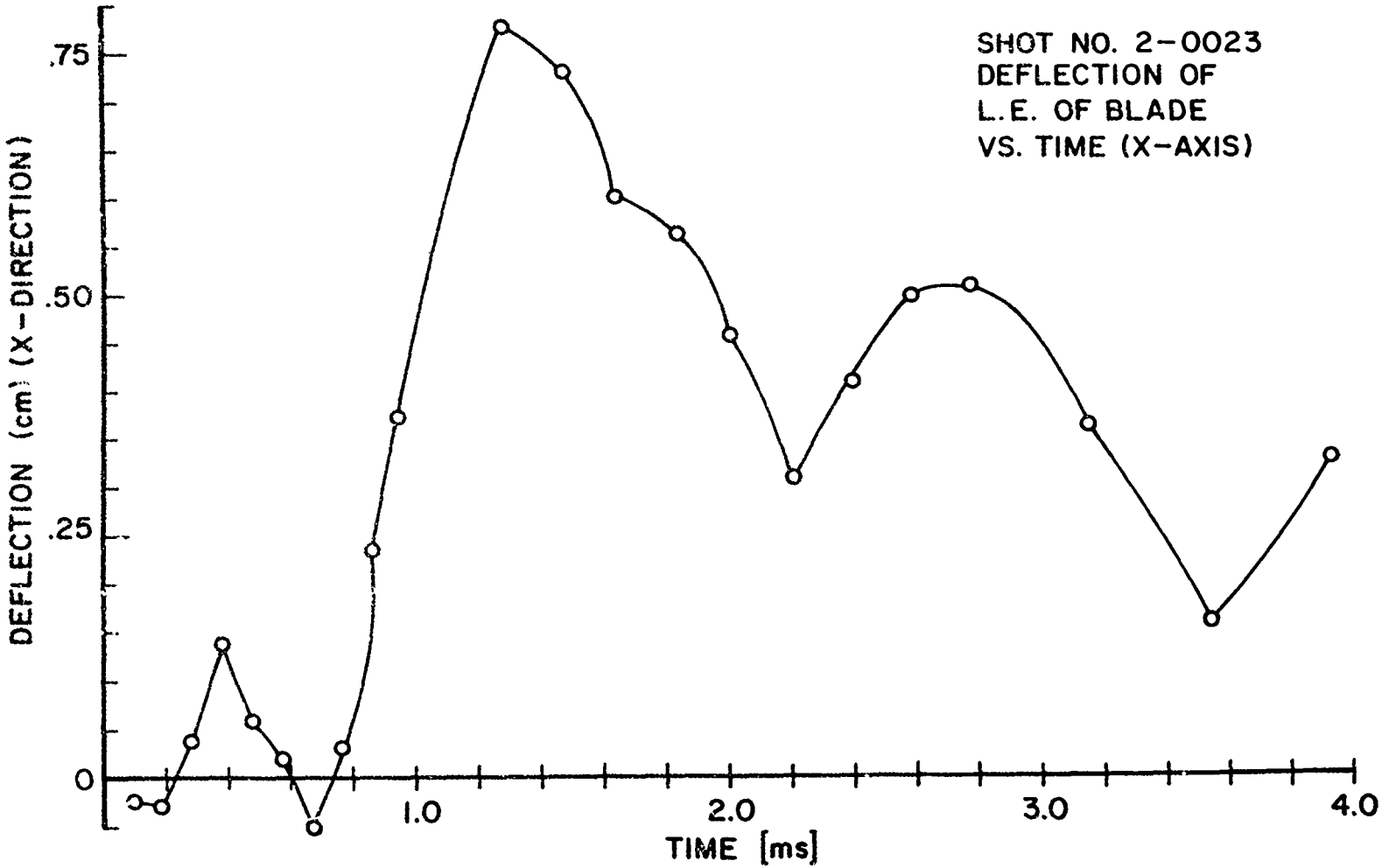

Figure 264. Leading Edge Tip Deflection in "x" Direction for Shot 2-0023.

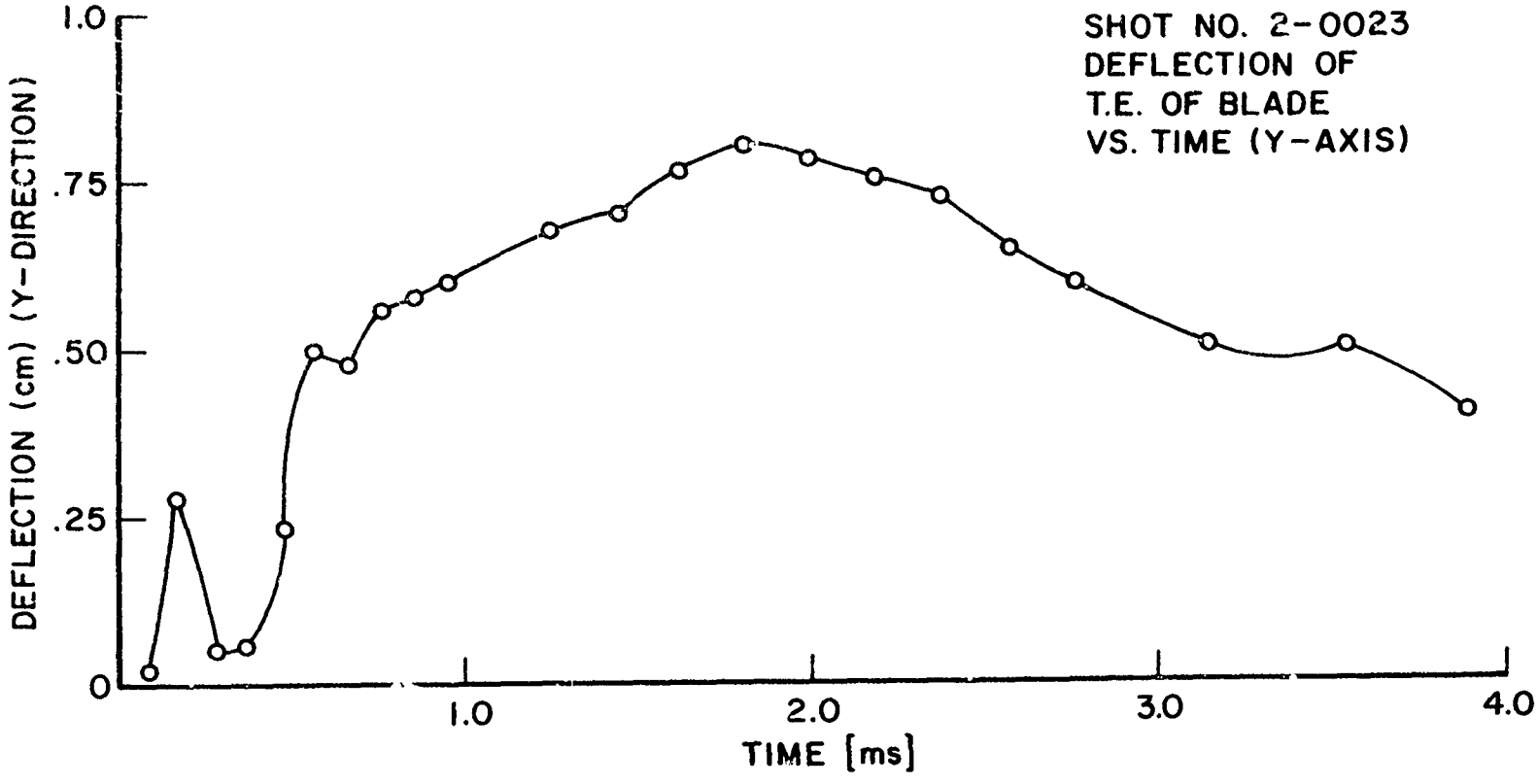

Figure 265. Trailing Edge Tip Deflection in "y" Direction for Shot 2-0023.

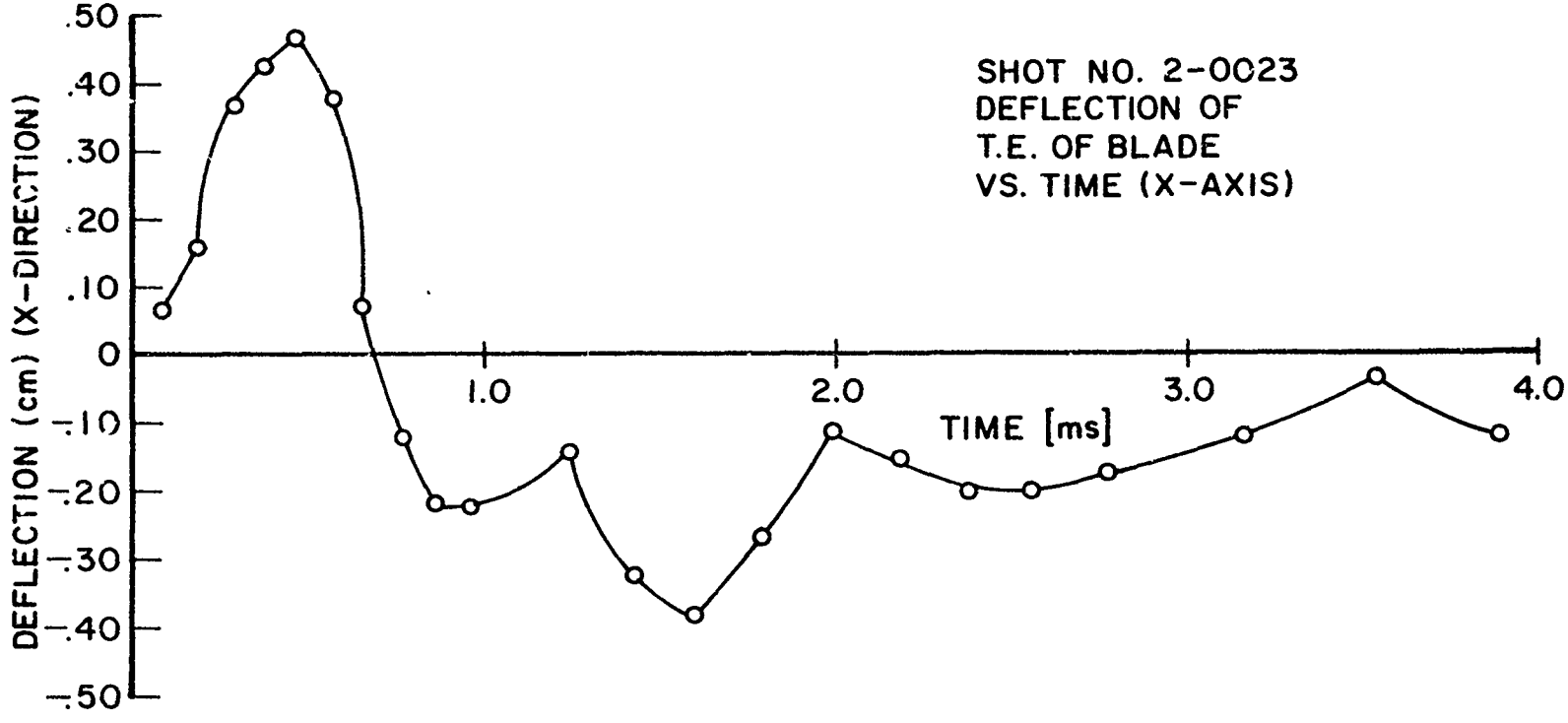

Figure 266. Trailing Edge Tip Deflection in "x" Direction for Shot 2-0023.

shows the dynamic tip deflection of the leading edge for the "y" direction while Figure 264 gives the leading edge deflection of the tip in the "x" direction. Figure 265 shows the deflection of the trailing edge tip in the "y" direction and Figure 266 shows the trailing edge results for the "x" direction. Figure 55B shows the damage received for Shot 2-0023.

3.2.13 Impact Results for Group 13B Blades

One leading edge impact using the 85 g (3 ounce) artificial bird was conducted on a boron/aluminum composite blade (APSI) at the 70 percent span location. The impact angle for the impact was 18.9 degrees. Shot 2-0022 at a velocity of 406 m/s generated severe damage on the blade. The blade broke off along the platform close to the root area. Material also broke out at the impact site starting at the rip running 10.16 cm down along the leading edge. The maximum width of the break out was 2.29 cm. The impact mass could not be determined due to the high velocity causing the slice to break up into many pieces. Figure 56B shows the damage received for the impact.

Strain versus time curves for the impact are presented in Figures 267 through 272. Figure 3A of Appendix A gives the strain gage locations for the impact. Tension is denoted as a negative strain and compression as a positive strain in the curves. The highest strain rate for the APSI blade shots was 366 in/in/sec for this impact as identified in Figures 272 and 273. This high strain rate occurred at the gage location at the midchord of the root orientated in the spanwise direction. Dynamic tip deflection curves during the impact event are shown in Figures 274 through 277. Figures 274 and 276 are curves for the "y" direction for the leading and trailing edge, respectively. Figures 275 and 277 give the results for the "x" direction for the leading and trailing edge, respectively.

3.2.14 Impact Results for Group 14B Blades

Five leading edge impacts using the 5.08 cm (2.0 inch) diameter ice spheres were conducted on the boron/

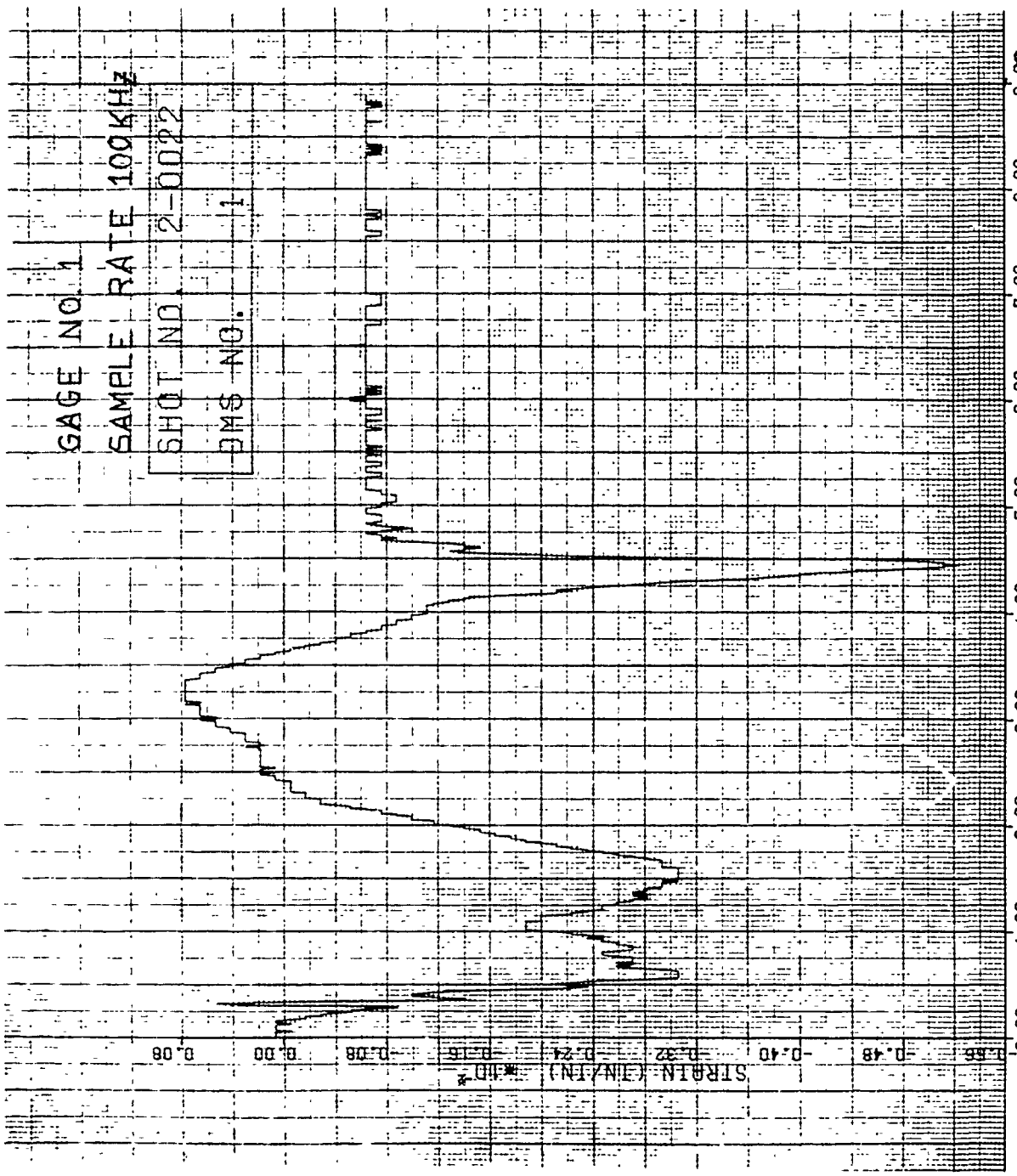

Figure 267. Strain of Shot 2-0022 for Gage #1.

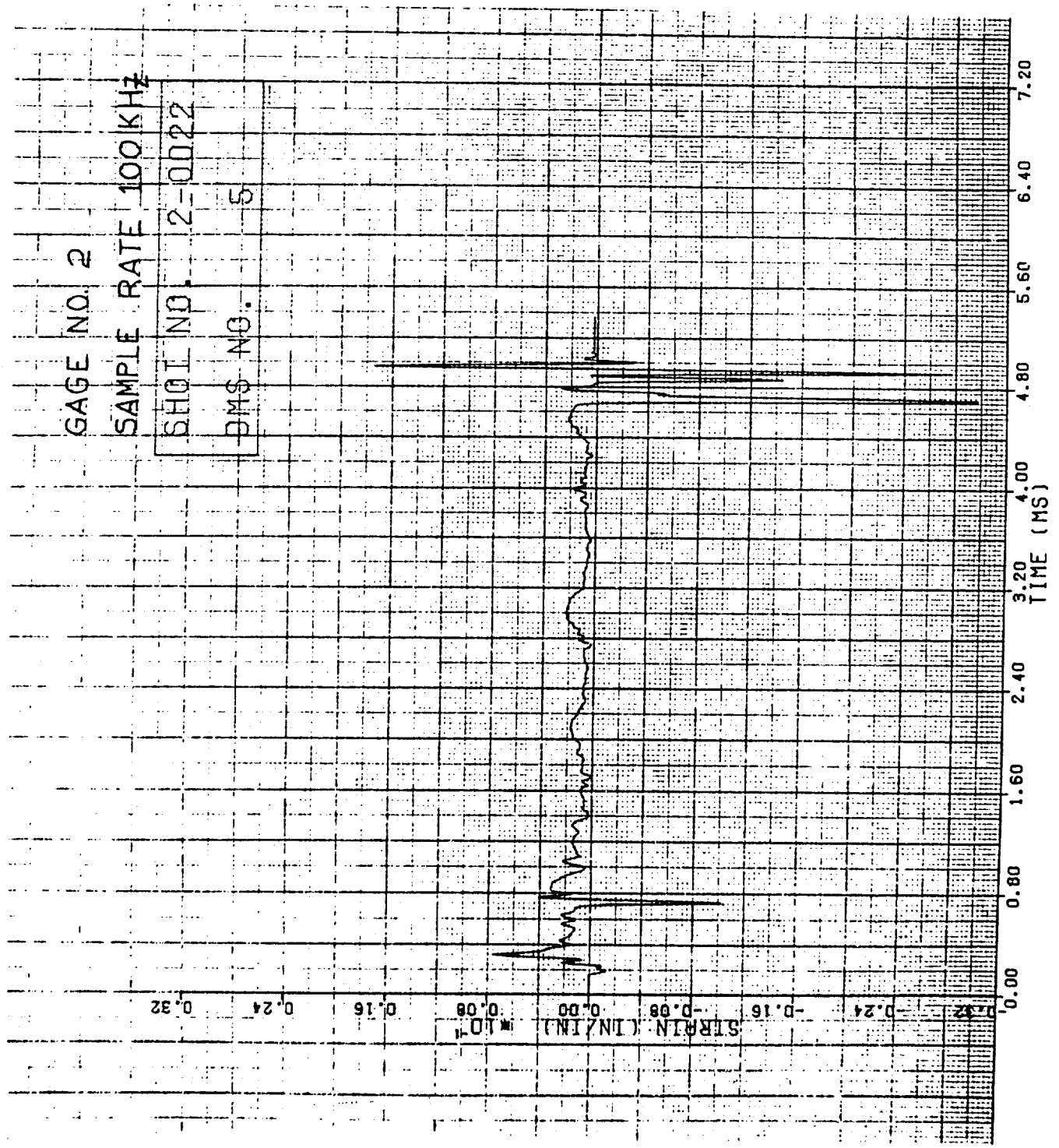

Figure 268. Strain of Shot 2-0022 for Gage #2.

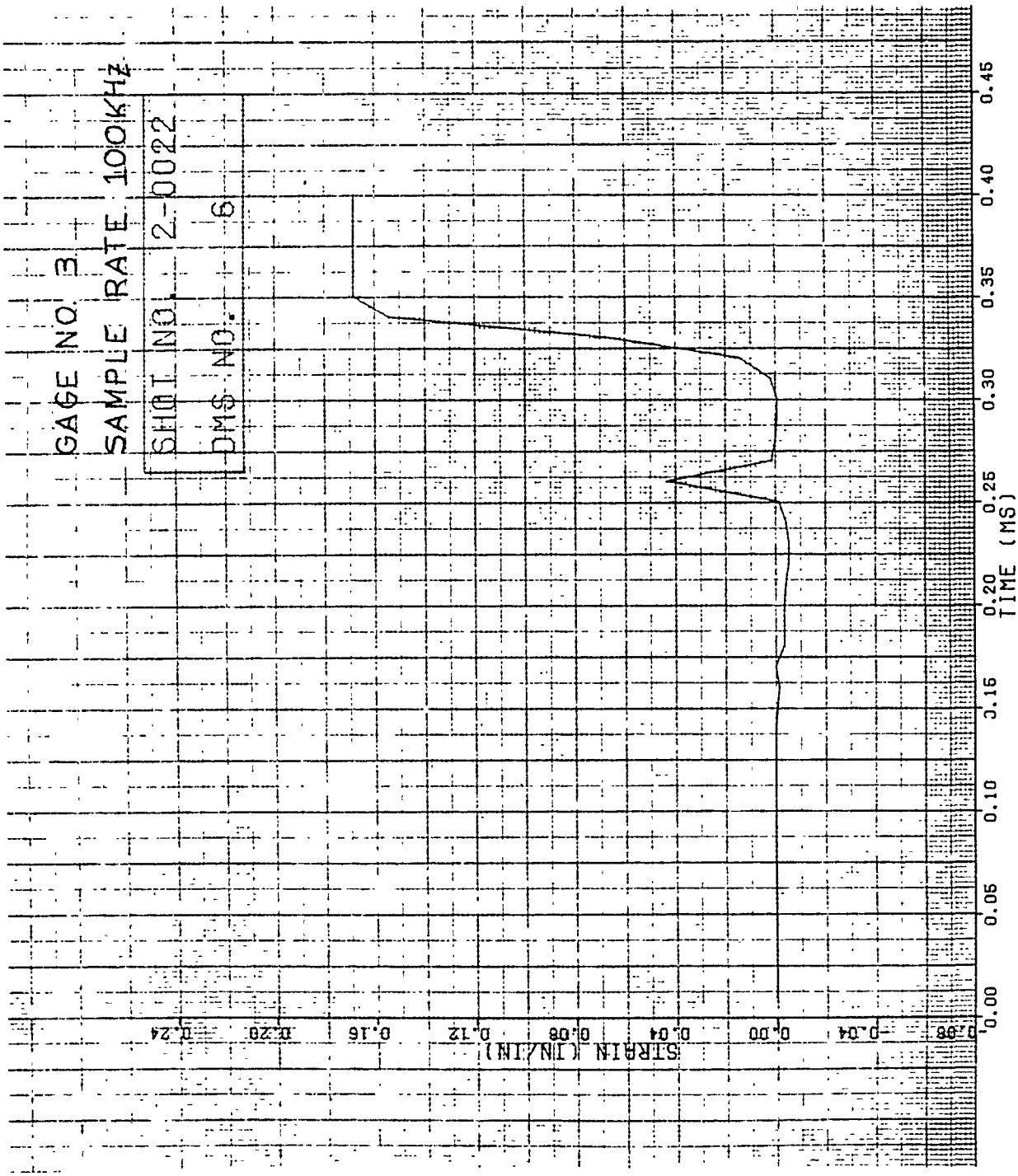

Figure 269. Strain of Shot 2-0022 for Gage #3.

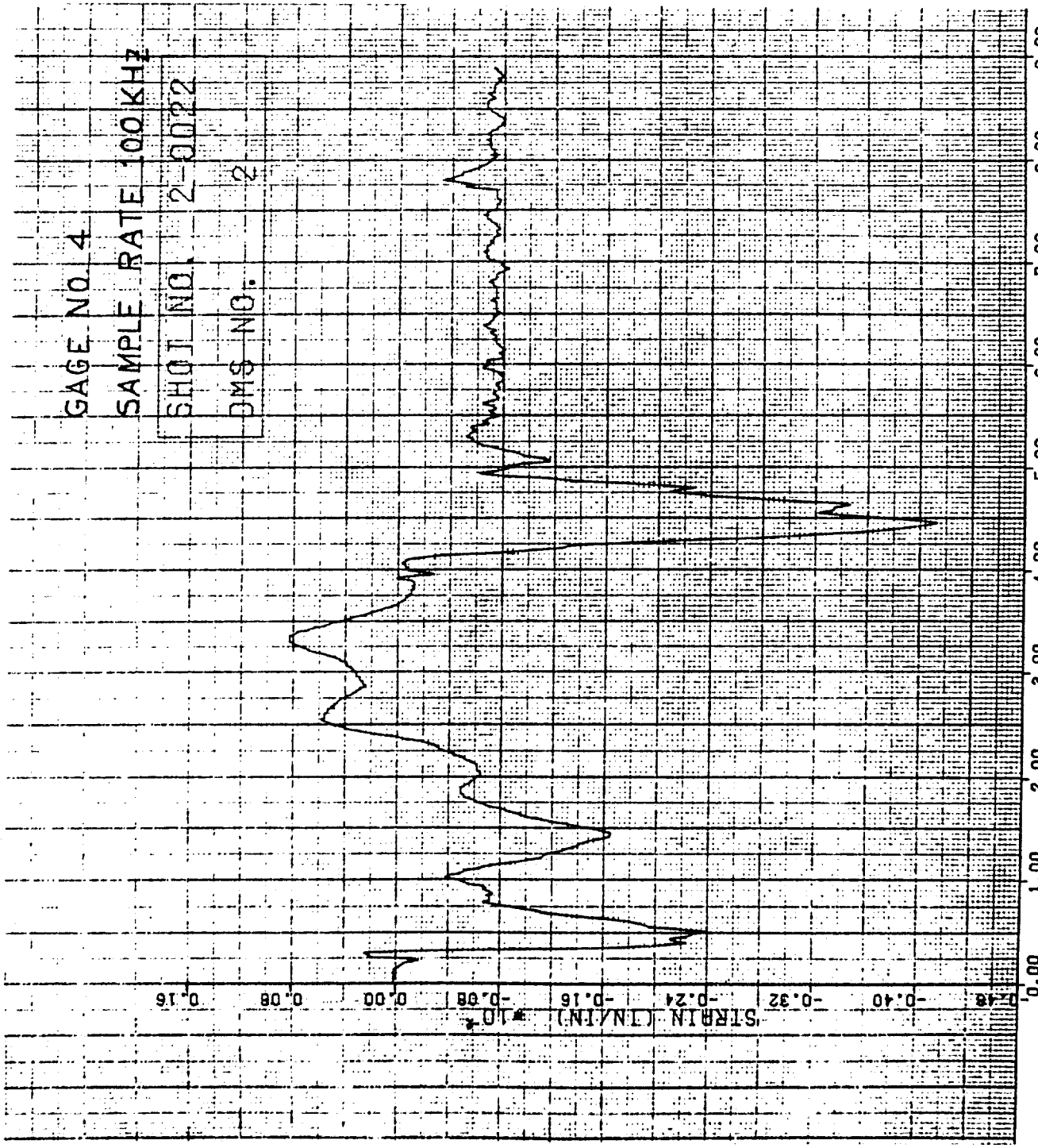

Figure 270. Strain of Shot 2-0022 for Gage #4.

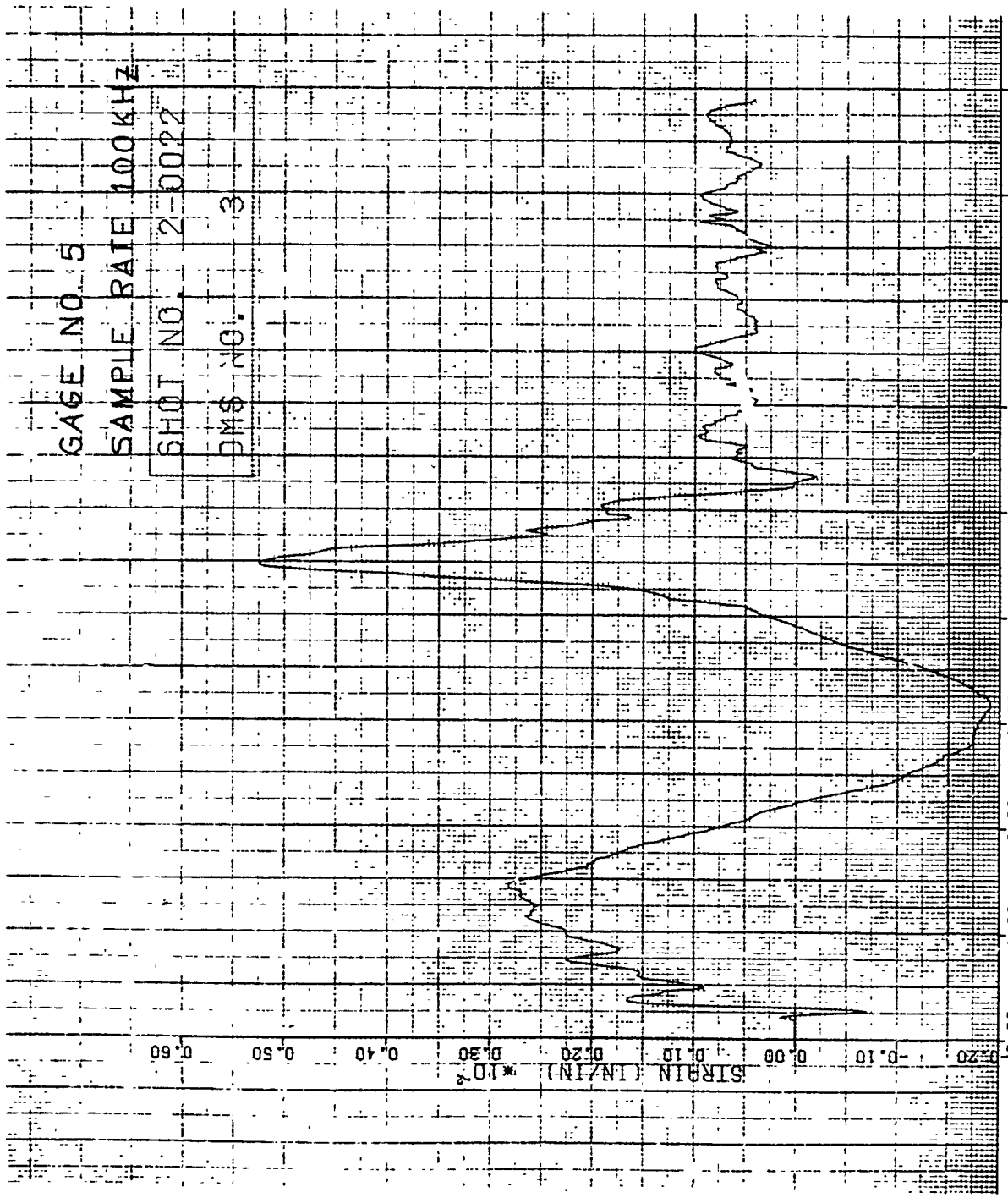

Figure 271. Strain of Shot 2-0022 for Gage #5.

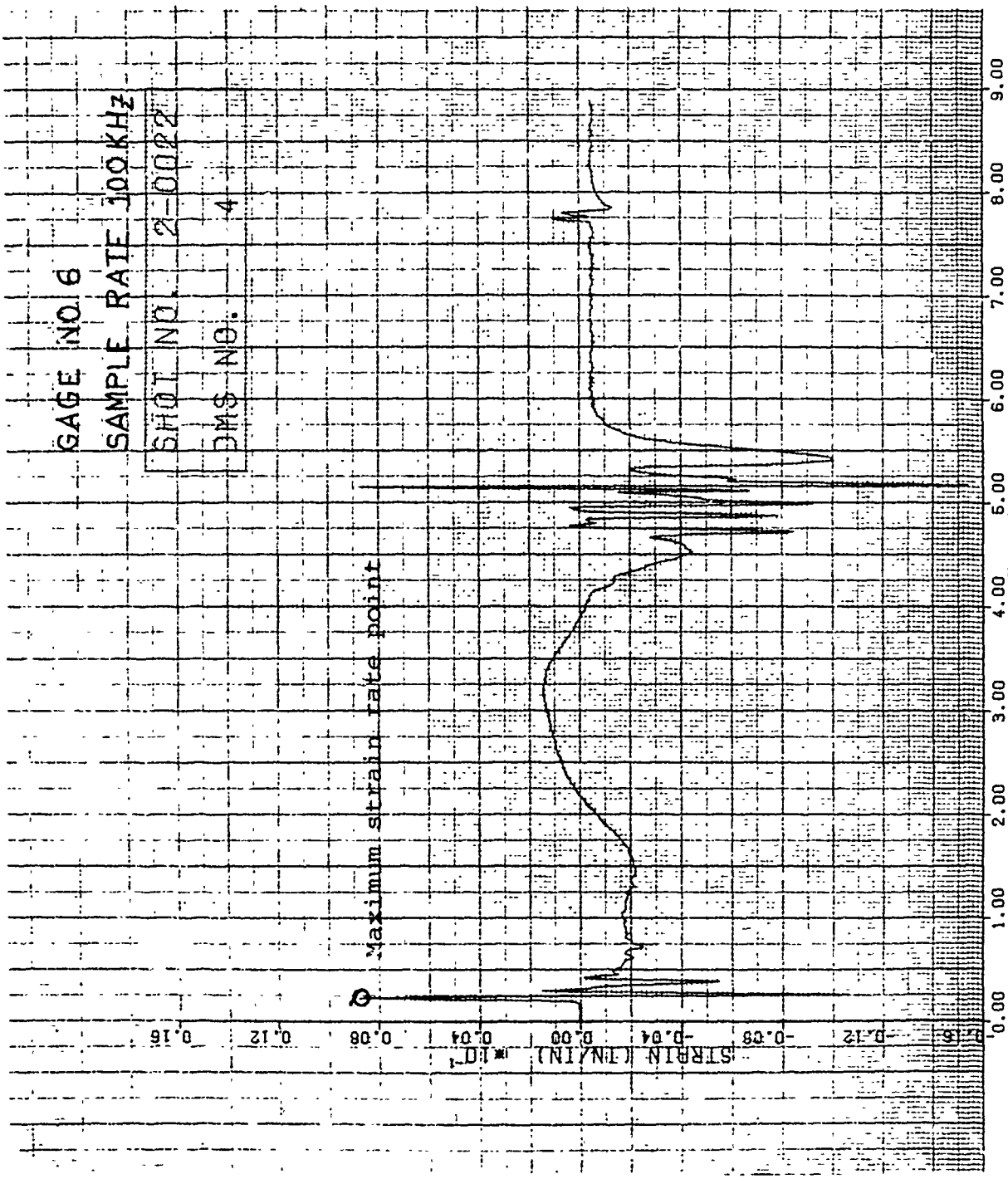

Figure 272. Strain of Shot 2-0022 for Gage #6.

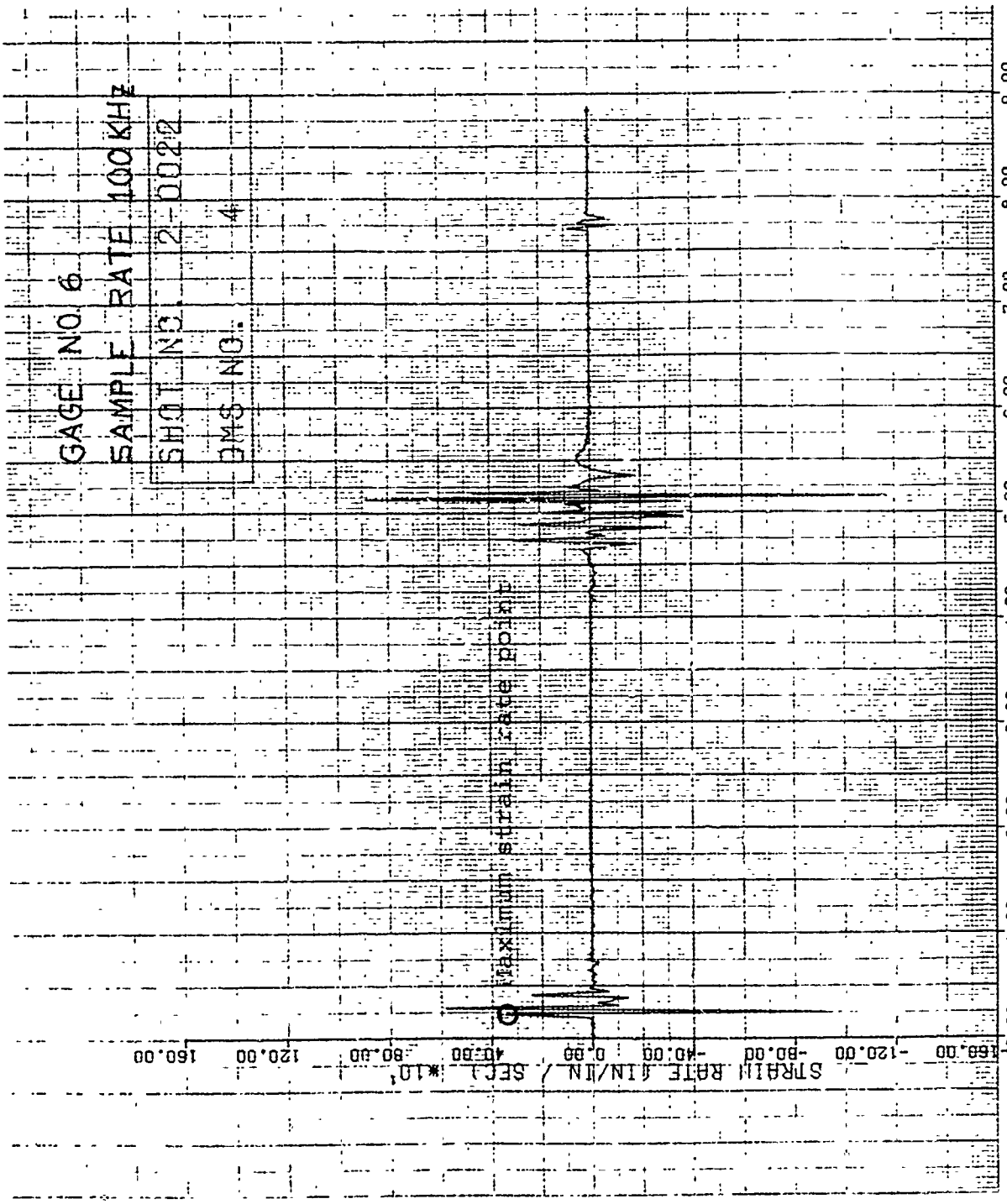

Figure 273. Strain Rate of Shot 2-0022 for Gage #6.

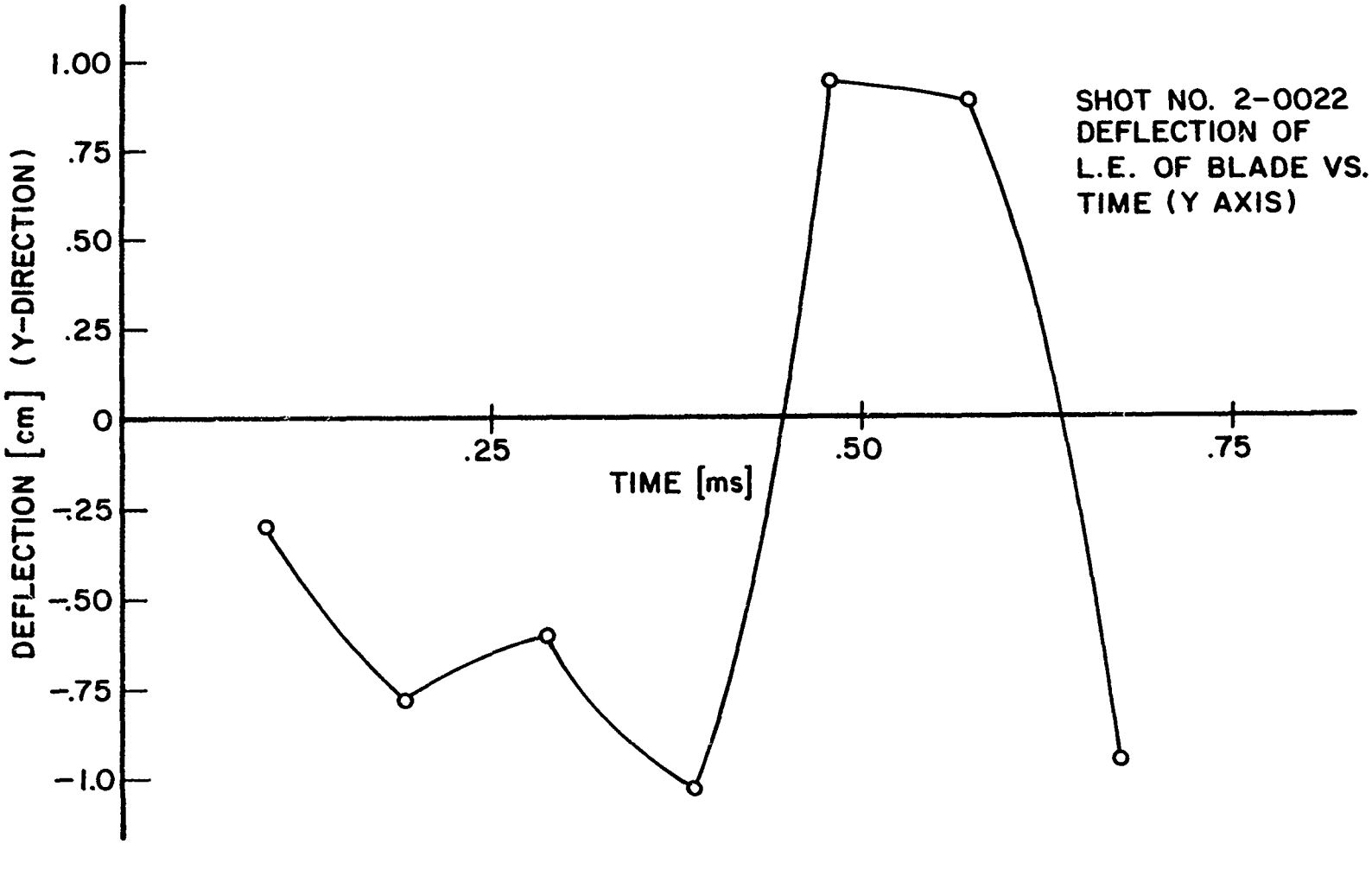

Figure 274. Leading Edge Tip Deflection in "y" Direction for Shot 2-0022.

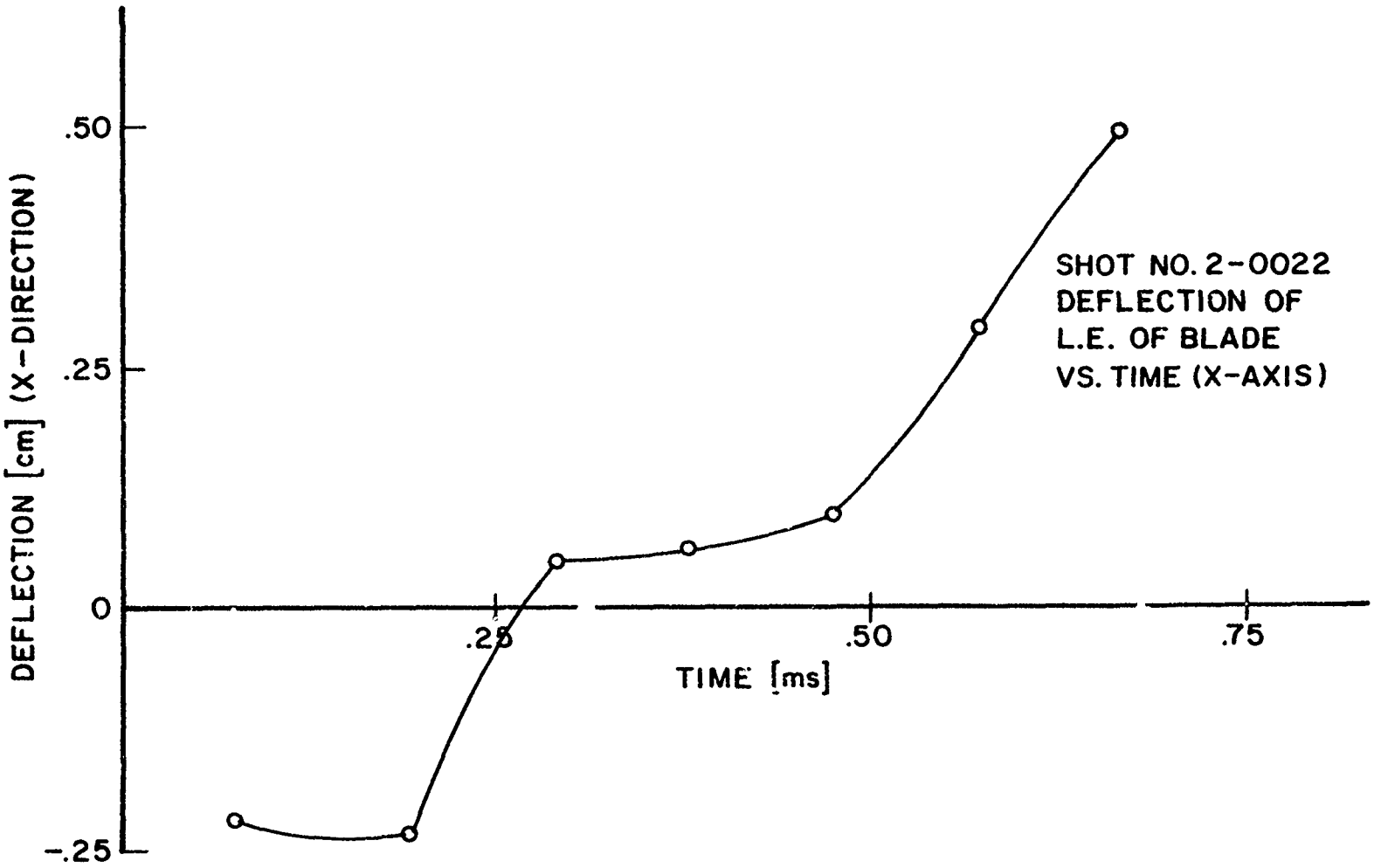

Figure 275. Leading Edge Tip Deflection in "x" Direction for Shot 2-0022.

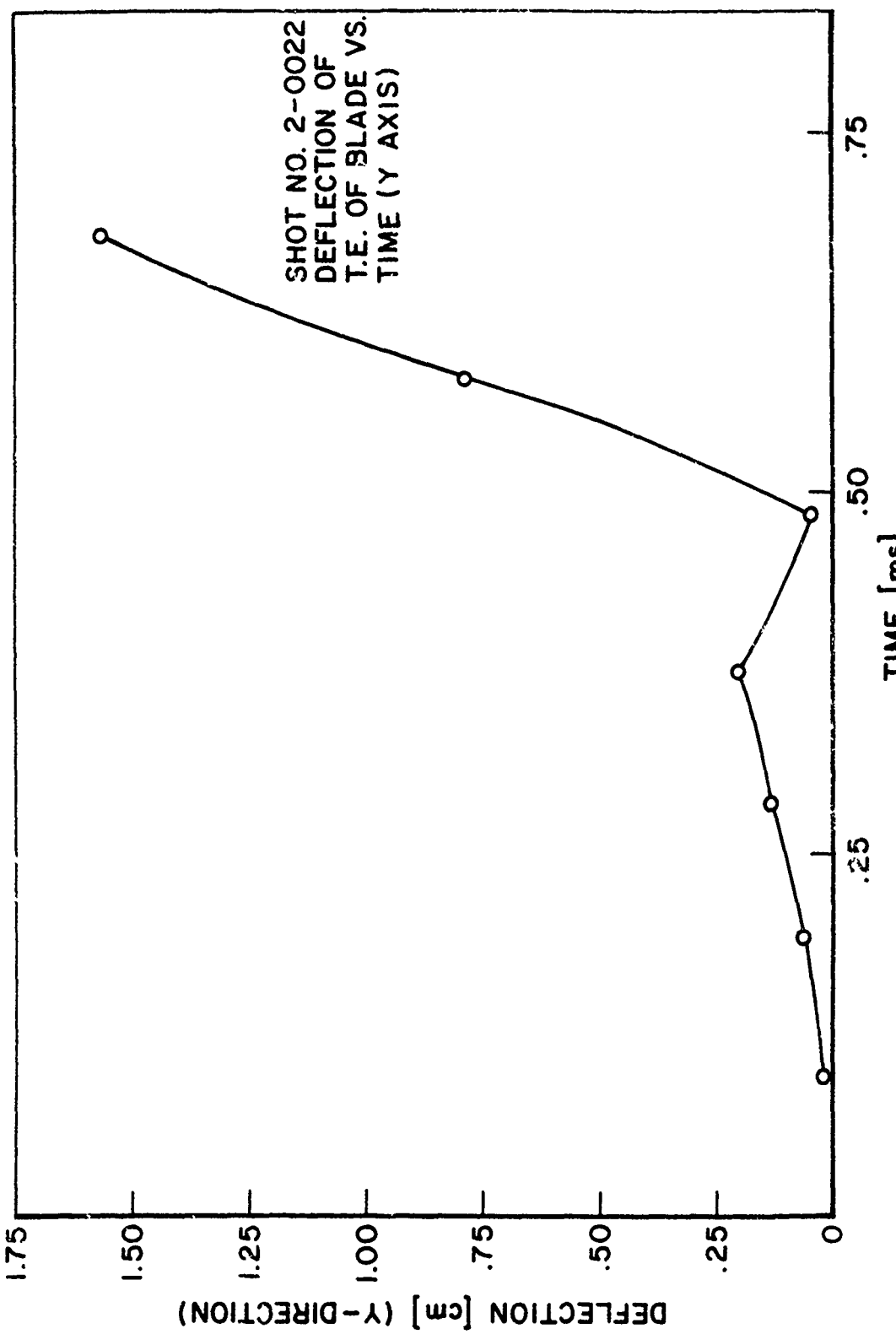

Figure 276. Trailing Edge Tip Deflection in "y" Direction for Shot 2-0022.

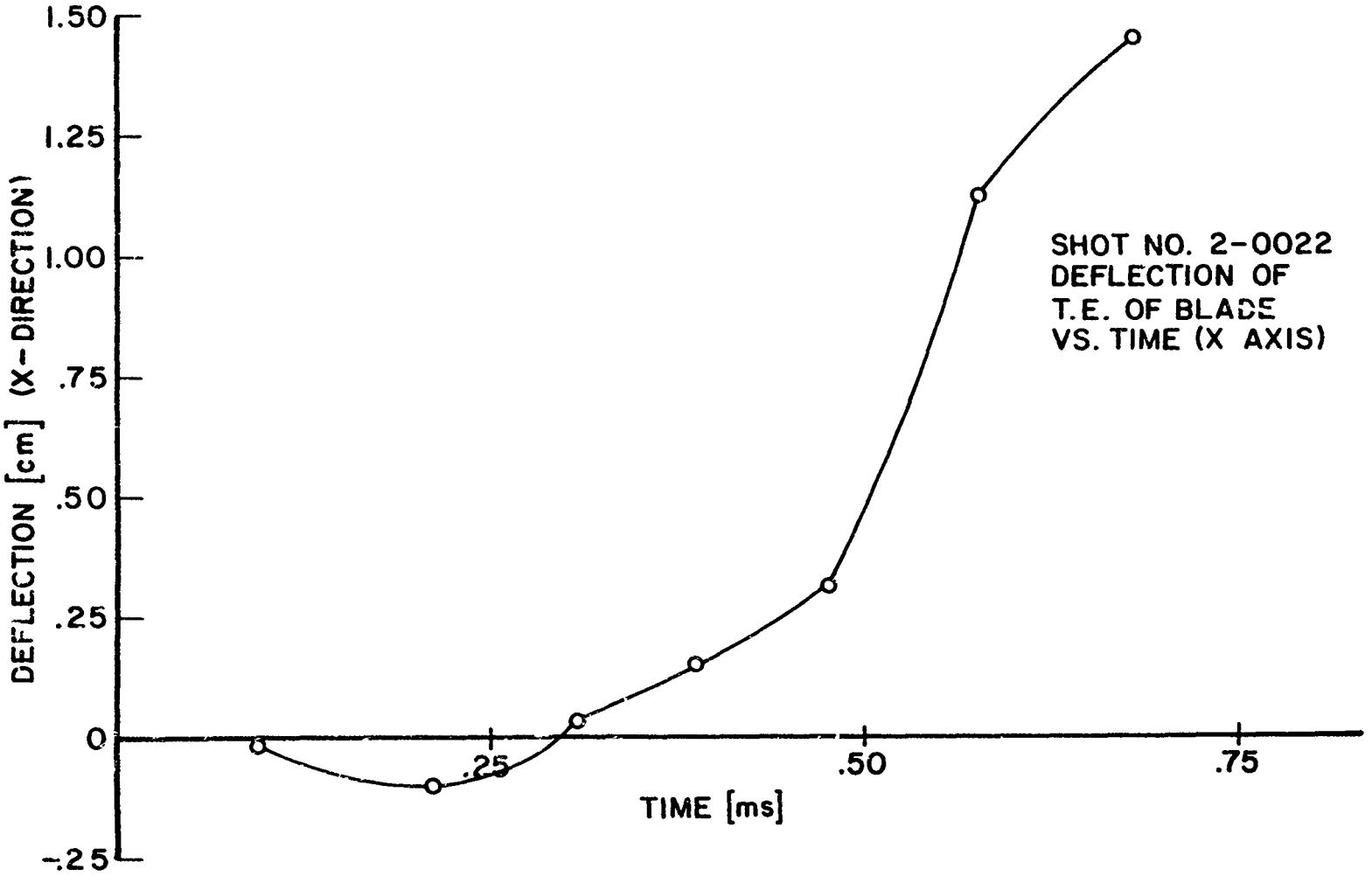

Figure 277. Trailing Edge Tip Deflection in "x" Direction for Shot 2-0022.

aluminum composite APSI blades at velocities ranging from 79 to 199 m/s. The blades were mounted such that the ice balls would be sliced into equal parts allowing one-half of the sphere to actually load the blades. The initial mass of the ice balls is about 65 g; therefore, 32.5 g would impact the blades. The impact site was at the 30 percent span location and the impact angle was 38.8 degrees.

Two of the five impacts caused no visible damage on the blades. Shots 2-0214 and 2-0217 at velocities of 134 and 79 m/s, respectively, generated no damage on the blades. The ice sphere for both impacts broke up upon launch which may explain why do damage occurred at this velocity.

The ice sphere of Shot 2-0215 generated slight damage on the blade in the form of bowing 0.25 cm on the leading edge at the impact site. The impact velocity for this impact was high at 199 m/s; however, the sphere broke up upon launch.

Severe damage was received by two blades where the ice sphere was intact upon impact. This damage in the form of breaking out a section of the leading edge at the impact site was received for Shots 2-0216 and 2-0218. For Shot 2-0216 at a velocity of 132 m/s, the blade break out was 6.60 cm long and 1.27 cm wide. The blade break out for Shot 2-0218 was 5.08 cm long and 1.27 cm wide for an impact velocity of 93 m/s. Figures 57B and 58B show the damage generated for Shots 2-0216 and 2-0218, respectively.

The strain curves for the impacts of this group of blades are contained in the Volume II report. The strain gage locations for this blade group are given in Figure 5A of Appendix A.

3.2.15 Impact Results for Group 15B Blades

One impact (Shot 2-0233) at a velocity of 96 m/s and impact mass of 135.7 g of an ice cylinder (7.62 cm diameter

and 17.78 cm long) caused severe damage on the blade. The ice cylinder (used to simulate slab ice) impact broke off the blade at the platform close at the root area and also broke out a section of the leading edge at the impact site 9.65 cm long and 1.52 cm wide. Figure 59B shows the damage generated for Shot 2-0233.

The strain data for this impact are contained in the Volume II report. Figure 5A of Appendix A gives the strain gage locations for this blade group.

SECTION 4
SUMMARY AND CONCLUSIONS

The experimental program (Task VI) involved conducting non-rotating bench impact tests on test specimens ranging from simple cantilevered beams and plates to real blades. The response of the test specimens to impacts of substitute birds or ice was determined in the testing. The data collected included accurate impact conditions, dynamic displacement of the specimens at discreet points, strain/time histories local to the impact site and at critical blade stress regions identified from the structure response models, and damage assessment. The simple elements, such as beams or plates, were tested with progressive introduction of airfoil geometric parameters to validate experimentally the analytical predictions of Tasks V and VIII of the overall program and to derive a correlation between structural elemented specimens and full-scale blades.

Three types of blade materials, geometries, and sizes were investigated using ice and substitute birds as the impactors. The three blade types investigated in the study were the F101 blade using 8Al-1Mo-IV (8-1-1) titanium, the J79 blade using 403 stainless steel, and the APSI metal matrix boron/aluminum blade. The geometries of the test specimens were similar to the geometries at the 50 percent span location of the three blade types investigated.

A baseline series of tests was conducted on the titanium material, a supplimentary series was conducted on the stainless steel material, and a more complete series was conducted on the advanced composite material. The geometry effects which were believed to effect impact response were independently introduced in the testing and analysis. These effects included the aspect ratio, thickness to chord ratio, shape, shrouds, camber, and twist.

Four impactors were used in the testing which included 85 g (3-ounce) and 680 g (1.5-pound) artificial birds, a 50.8 mm (2-ounce) ice ball, and 750 g (1.65-pound) ice cylinders to simulate slab ice. The impactors were gun launched to impact the leading edge of the test specimens in the majority of the testing.

A total of 92 impacts were conducted on the simple element test specimens. All of the specimens were strain gaged (except for the Moiré fringe shots) to obtain strain/time histories of the specimens local to the impact site and at critical blade stress regions for an impact. The impact velocity for the impacts was varied to obtain no damage, threshold damage, and severe damage on the specimens. The damage assessment portion of the data collected in the study included determining the mode of damage and measuring the extent of damage.

In several impacts, the Moiré fringe device was used to accurately measure the deflection of cantilevered flat plates. Two thicknesses of flat plates were investigated. One was a flat plate with a blade-type aspect ratio and nominal thickness of the actual F101 blade at the 50 percent span level. The second was a flat plate with a blade-type aspect ratio and one-half blade-type thickness to chord ratio of the actual blade at the 50 percent span location. Dynamic deflection versus span location curves (relative to the impact site) were obtained at various times after impact.

High speed photography coverage was also used in the majority of the testing. Dynamic tip deflection versus time curves were determined by using the high speed movie films.

In addition to impact testing of simple element specimens, a number of impact tests (41 shots) were also conducted on full scale component blades. This impact testing of the actual blades was coordinated with the full scale blade testing of Task IVA where impact tests were conducted to establish the strain rate limits for the material property tests of Task IVA.

The impact velocities used in the Task IVA tests corresponded to those which would be typical of an impact at 70 percent span and 30 percent span locations at full power settings of the engine during takeoff for each of the blade types. Impacts at the 70 percent span level are representative of the highest velocity impacts experienced by a blade. Impacts at the 30 percent span level are typical of those in the highest stress regions of the blade where it is most vulnerable to the effects of impact degradation. The impact tests of Task IVA indicated that the highest strain rates developed were less than 400 in/in/sec in any of the types of blades tested (J79, F101, and APSI).

For the J79 impacts, the highest strain rate for the 30 percent span impact was 372 in/in/sec for the 680 g (1.5 pound) bird impact. This value was for a gage located on the midchord at the root in the spanwise direction. For the 70 percent span impact of the J79 blade, the highest strain rate was 395 in/in/sec which was also for the 680 g (1.5 pound) bird impact. This value was for a gage directly behind the impact site which was oriented in the chordwise direction.

The highest strain rate for the 30 percent span impacts of the tip restrained F101 blade was 341 in/in/sec. For the 70 percent span impacts of this blade, the highest strain rate was 367 in/in/sec. Both strain rates were for the 680 g (1.5 pound) bird impacts and for a gage location at the tip along the leading edge in the spanwise direction.

For the APSI blade, the highest strain rate developed was 366 in/in/sec for the 70 percent impact of a 85 g (3 ounce) substitute bird. This occurred at a gage location at the midchord of the root in the spanwise direction.

In the case for the Task VI blade impacts, the impact velocity was varied to obtain no damage, threshold damage, and severe damage of the blade.

The strain data for all of the shots where strain gages were utilized are contained in the Volume II report. Photographs of typical damage received from the impacts are given in Appendix B of this report.

REFERENCES

1. Barber, J. P., H. R. Taylor, and J. S. Wilbeck, "Characterization of Bird Impacts on a Rigid Plate: Part I," AFFDL-TR-75-5, January 1975.

2. Peterson, R. L. and J. P. Barber, "Bird Impact Forces in Aircraft Windshield Design," AFFDL-TR-75-150, March 1976.

3. Barber, J. P., J. S. Wilbeck, and H. R. Taylor, "Bird Impact Forces and Pressures on Rigid and Compliant Targets," AFFDL-TR-77-60, May 1978.

4. Wilbeck, J. S., "Impact Behavior of Low Strength Projectiles," AFML-TR-77-134, July 1978.

5. Piekutowski, A. J., "A Device to Determine the Out-of-Plane Displacement of a Surface Using a Moiré Fringe Technique," AFWAL-TR-81-3005, March 1981.

APPENDIX A

STRAIN GAGE LOCATIONS

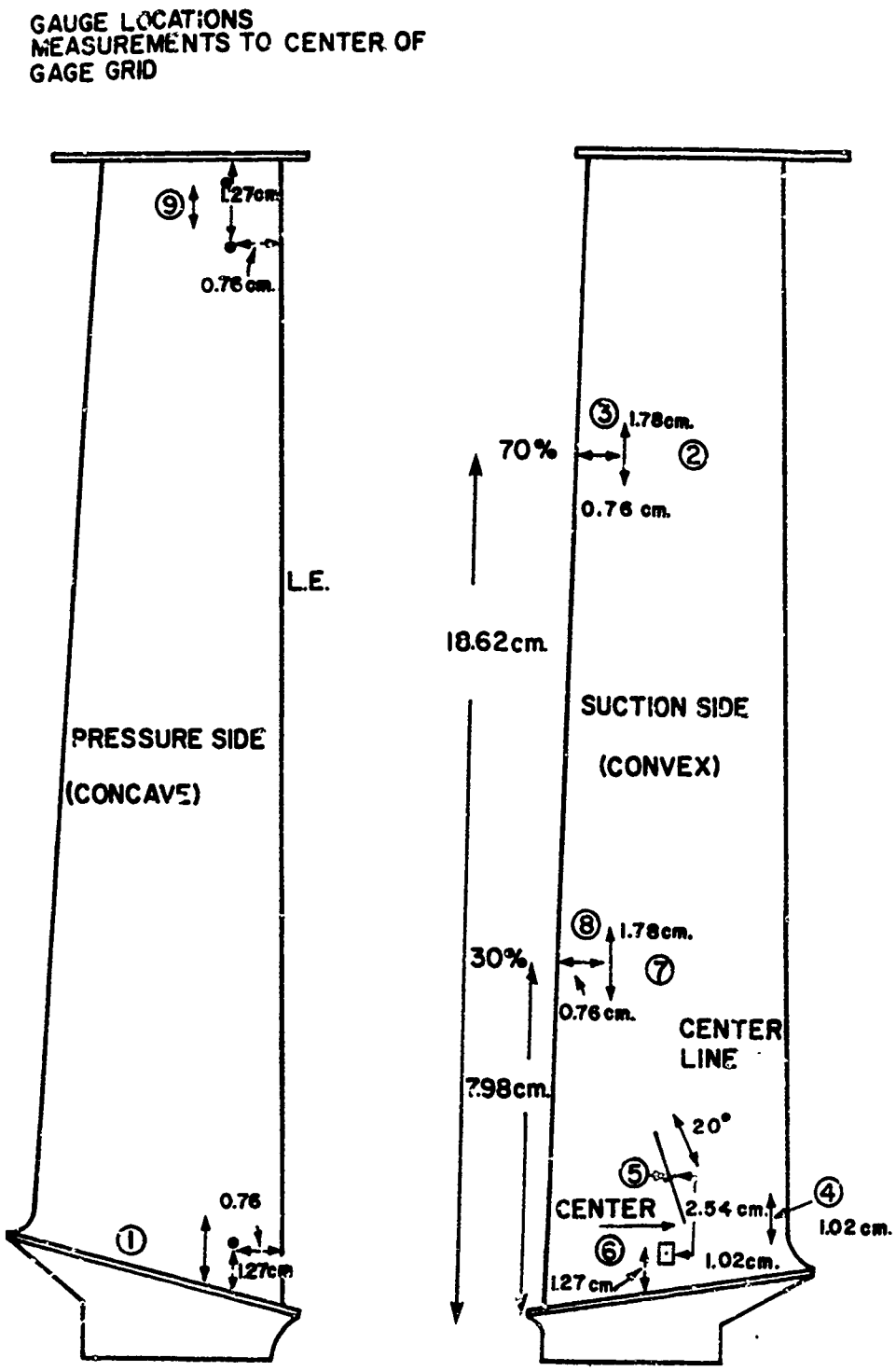

Figure 1A. Strain Gage Locations for Group 1B, 2B, 3B, and 4B Blades.

GAUGE LOCATIONS
MEASUREMENTS TO CENTER OF
GAGE GRID

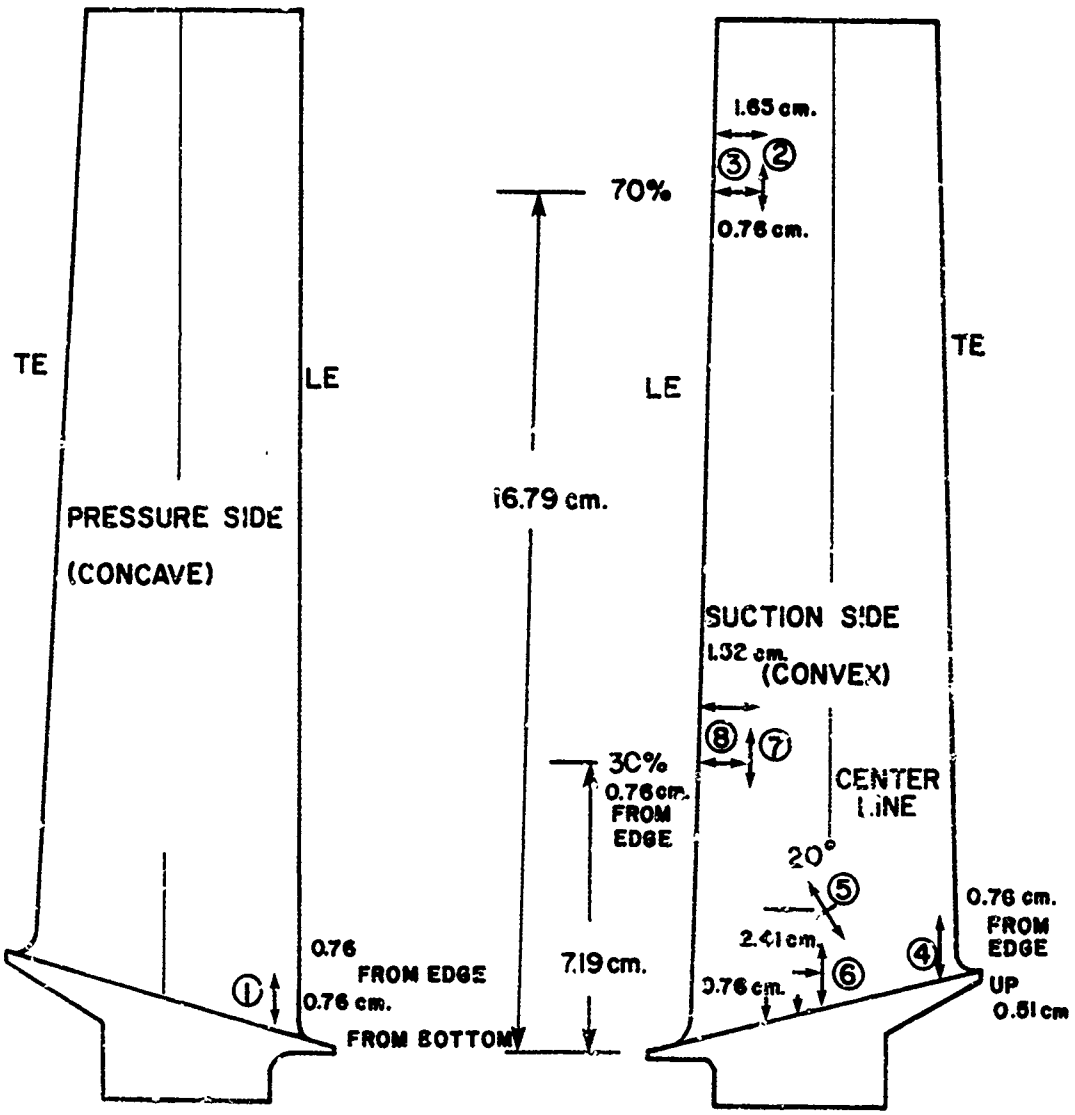

Figure 2A. Strain Gage Locations for Group 6B, 7B, 8B, and 9B Blades.

GAUGE LOCATIONS
MEASUREMENTS TO CENTER OF
GAGE GRID

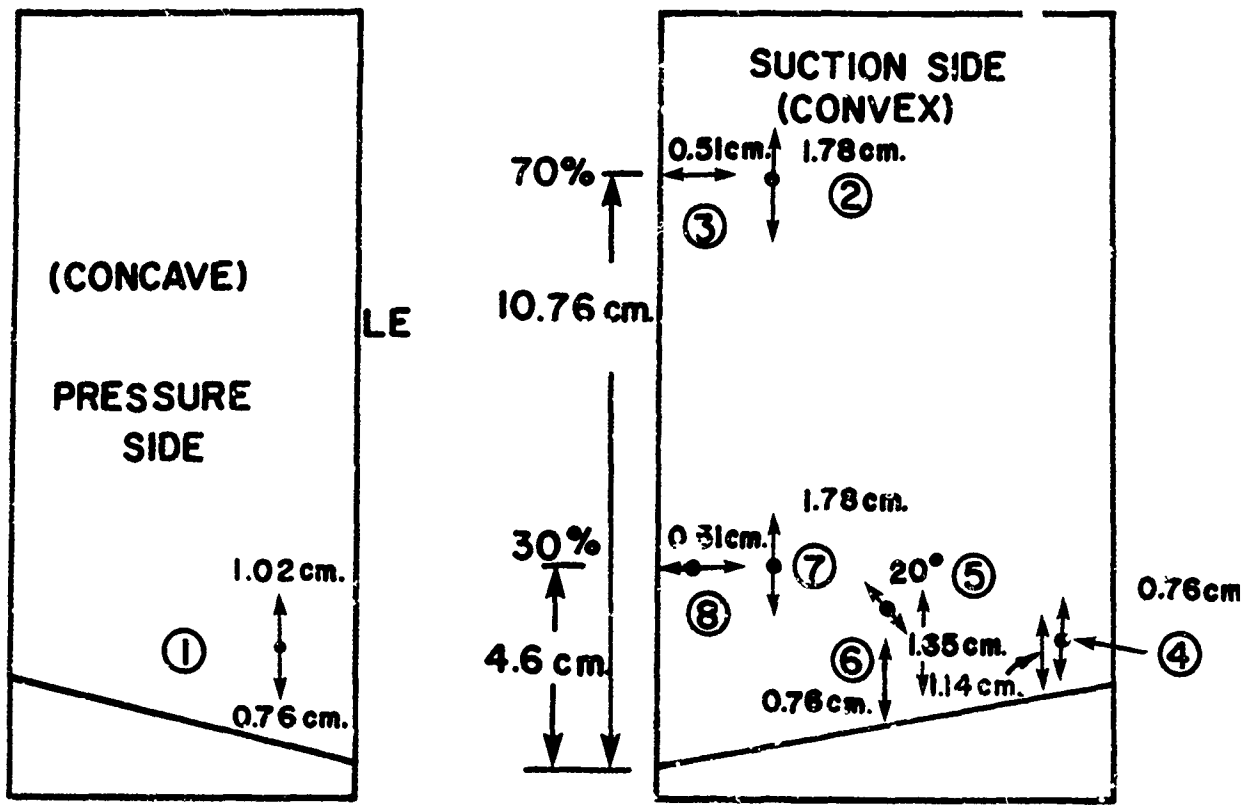

Figure 3A. Strain Gage Locations for Group 12B and 13B Blades.

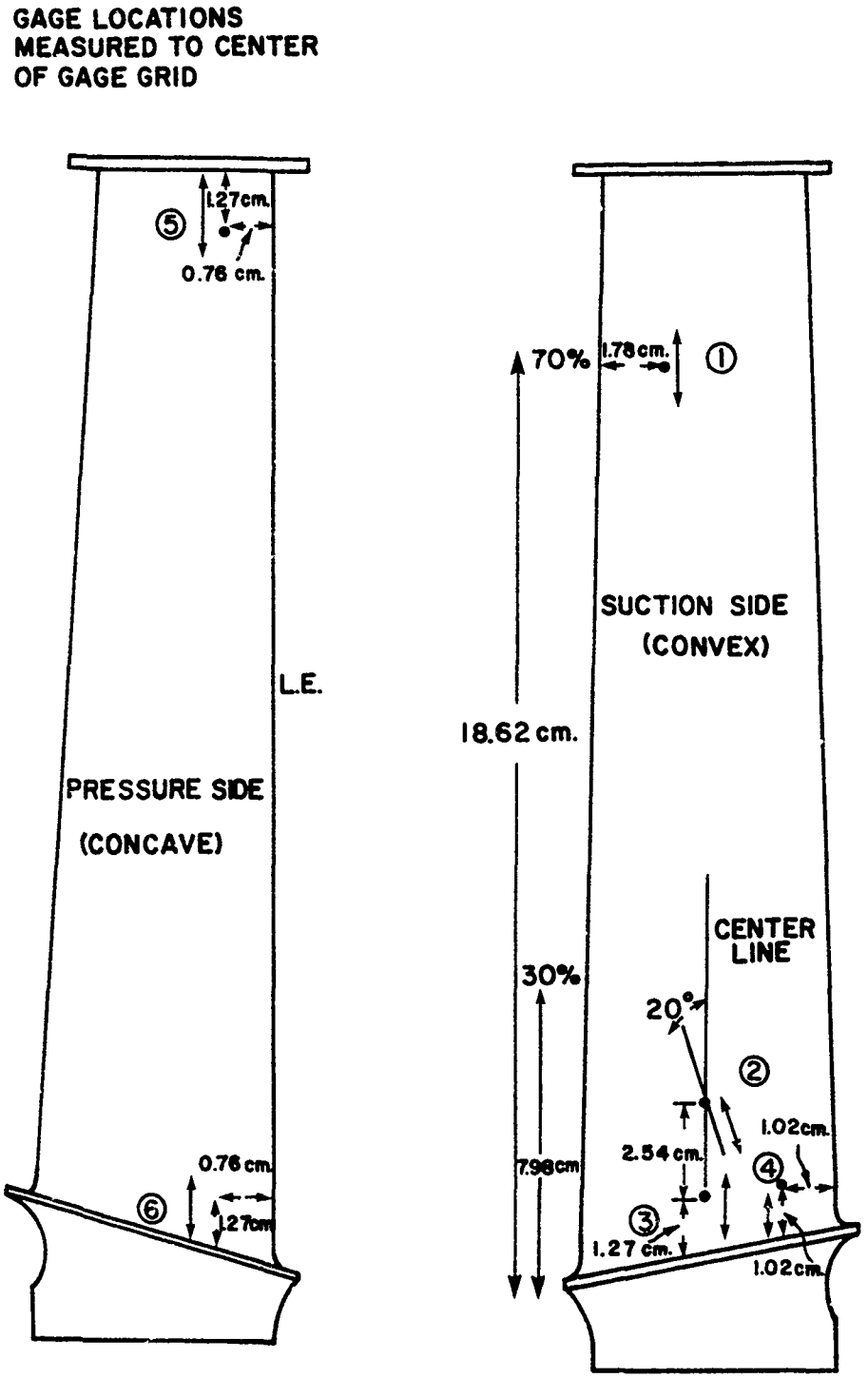

Figure 4A. Strain Gage Locations for Group 4B and 5B Blades.

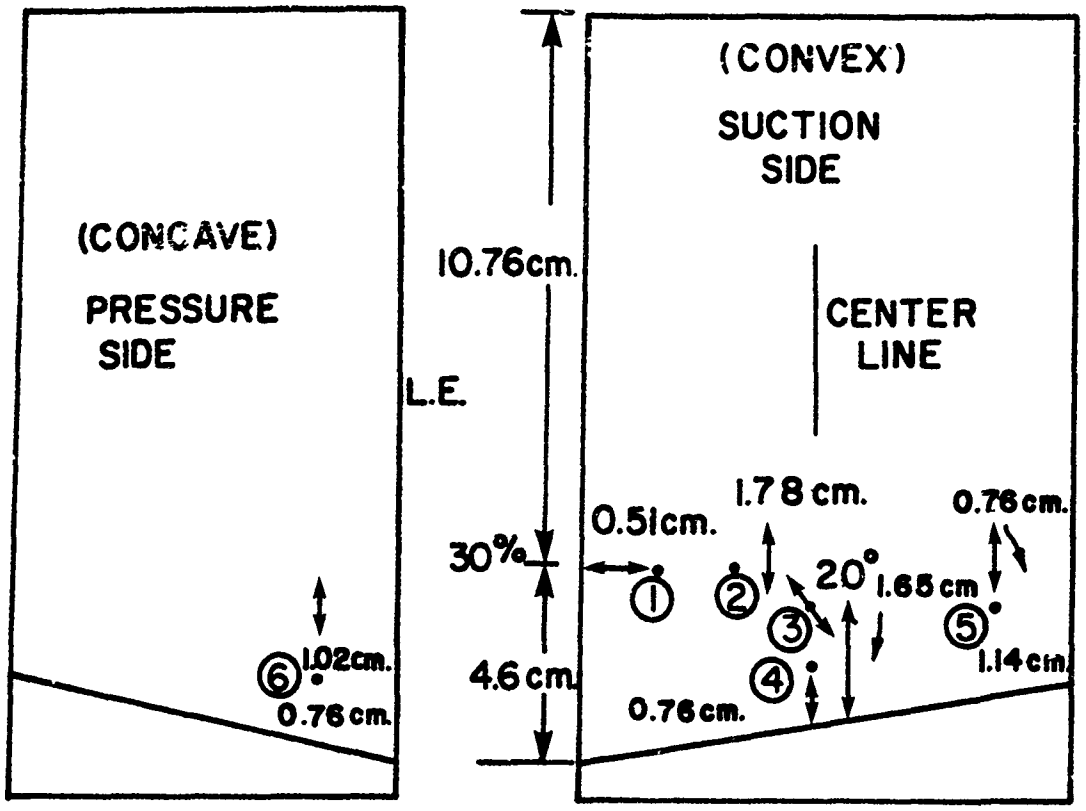

Figure 5A. Strain Gage Locations for Group 14B and 15B Blades.

GAUGE LOCATIONS
MEASUREMENTS TO CENTER OF
GAGE GRID

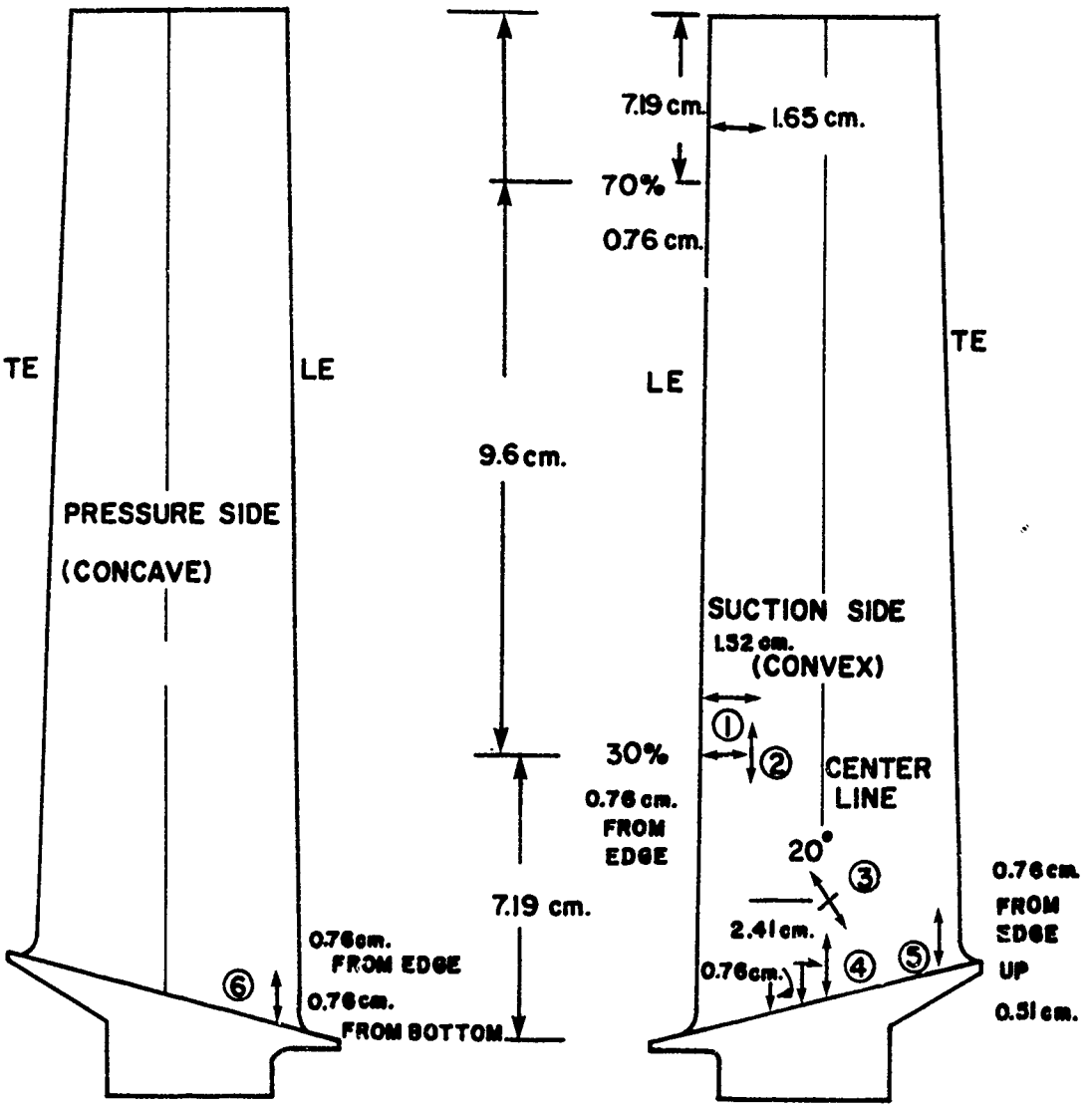

Figure 6A. Strain Gage Locations for Group 10B and 11B Blades.

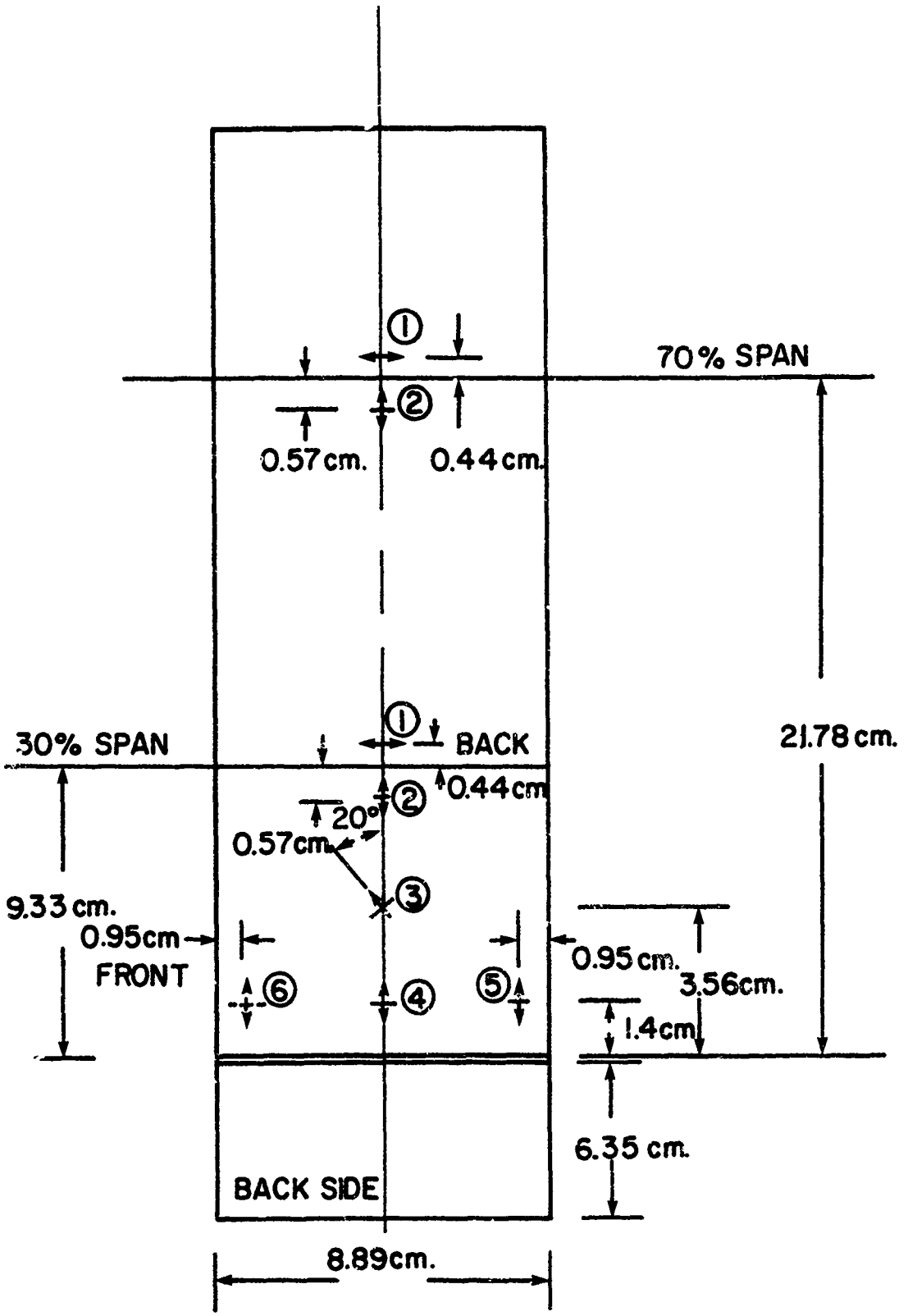

Figure 7A. Strain Gage Locations for Group 1, 2, and 6 Structrual Element Test Specimens.

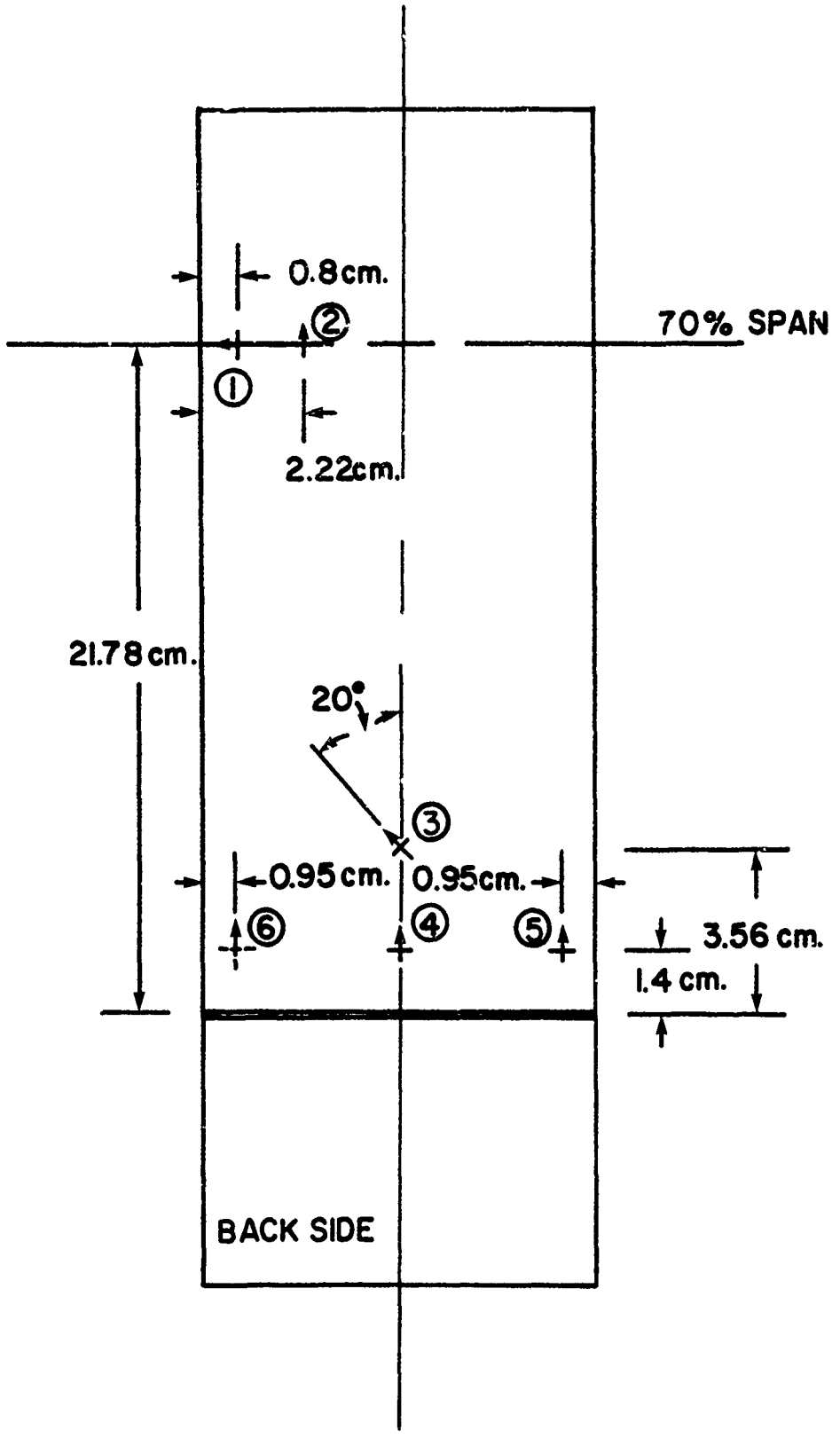

Figure 8A. Strain Gage Locations for Group 3, 7, 8, and 9 Structural Element Test Specimens.

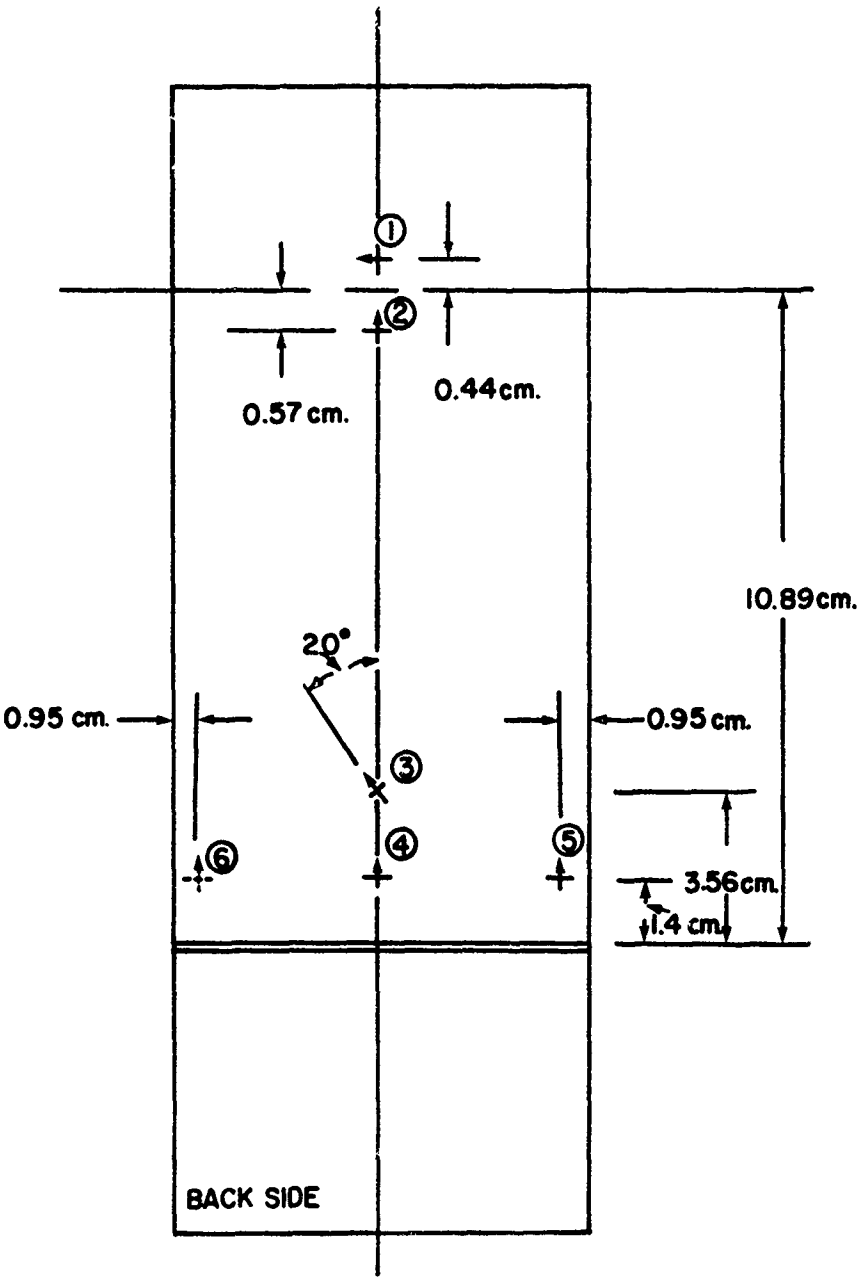

Figure 9A. Strain Gage Locations for Group 4 Structural Element Test Specimens.

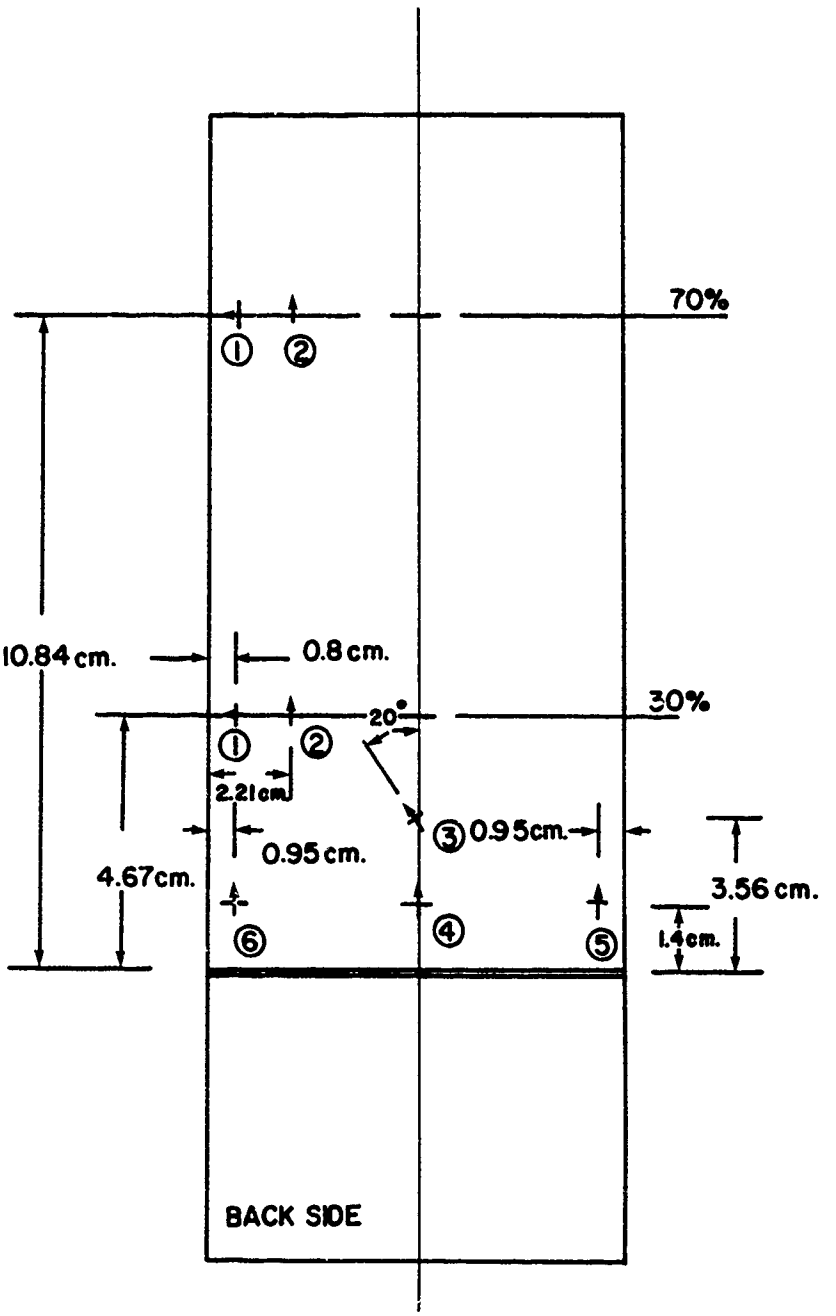

Figure 10A. Strain Gage Locations for Group 5 Structural Element Test Specimens.

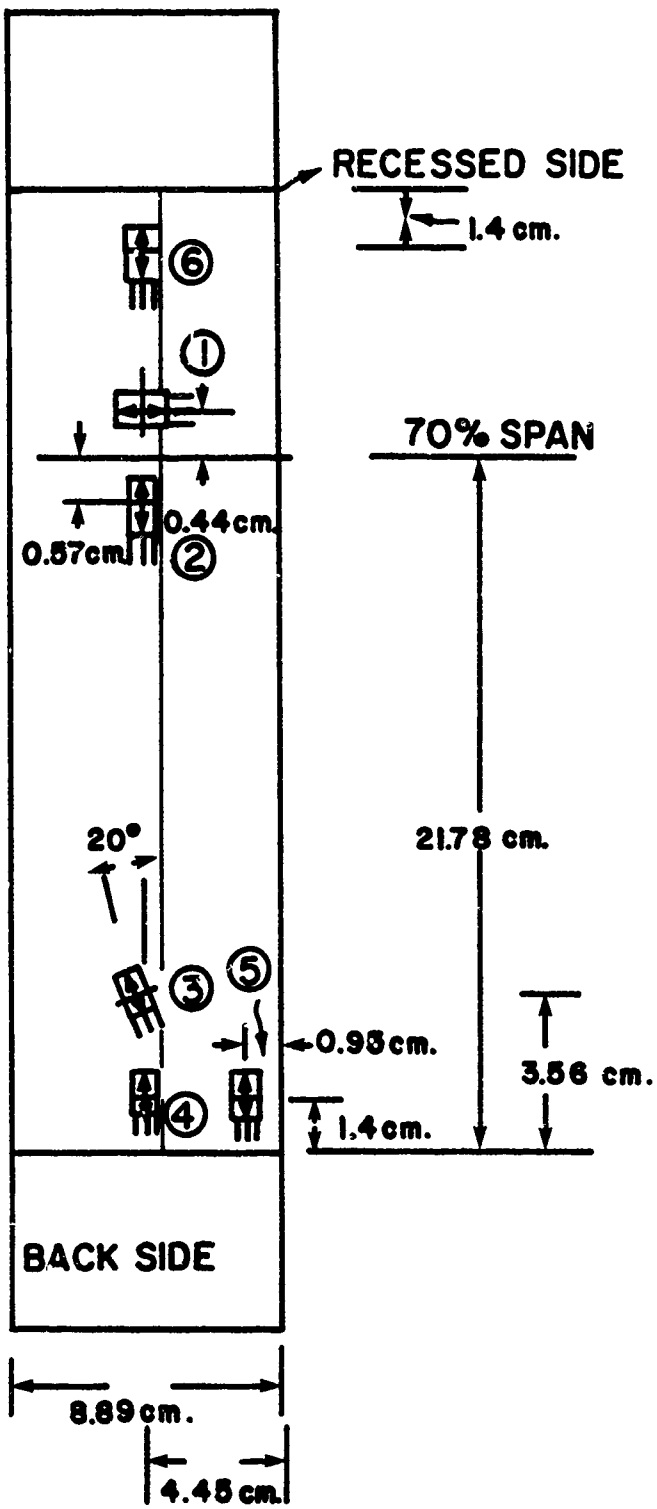

Figure 11A. Strain Gage Locations for Group 10 Structural Element Test Specimens.

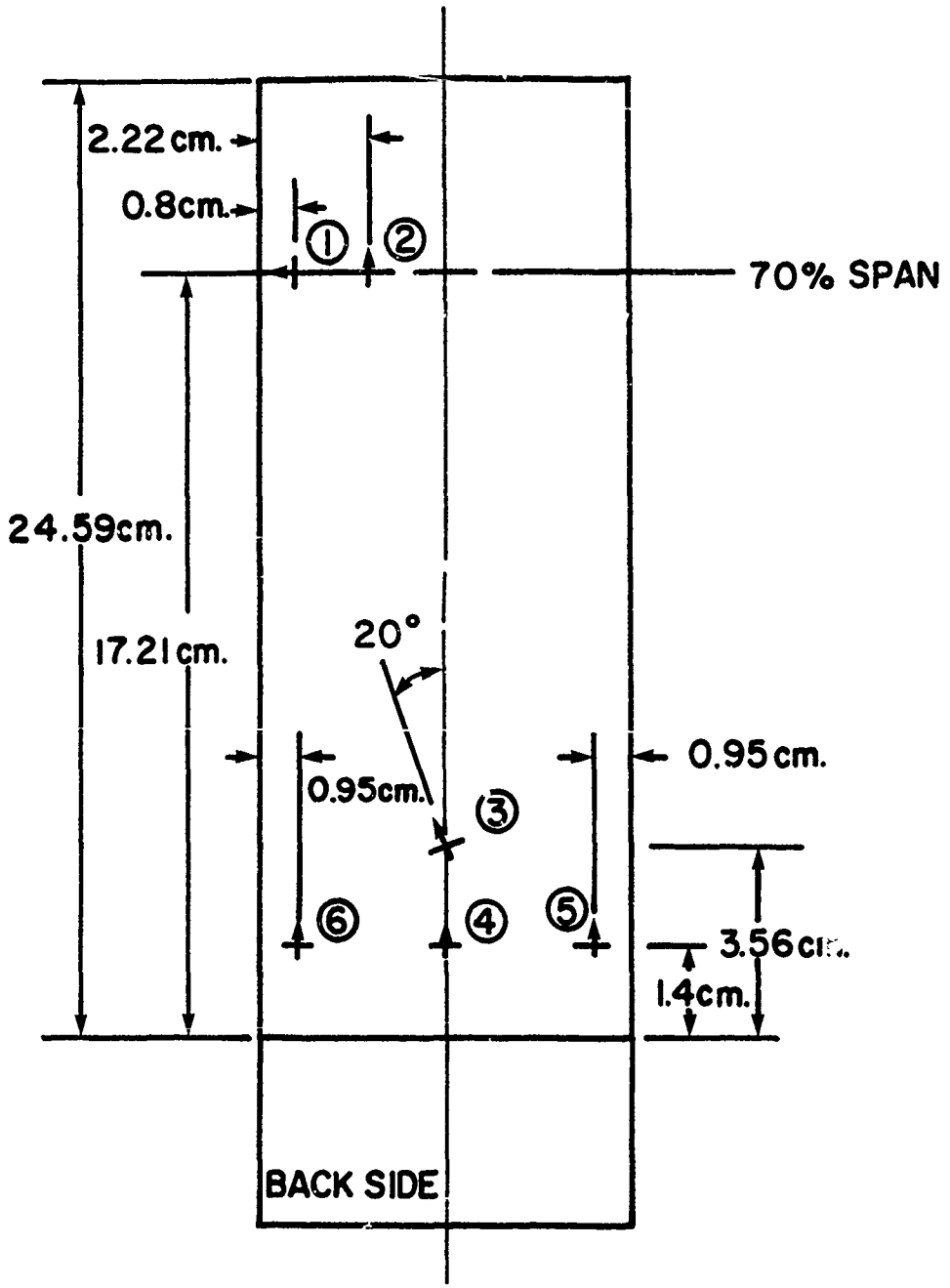

Figure 12A. Strain Gage Locations for Group 11, 12, and 13 Structural Element Test Specimens.

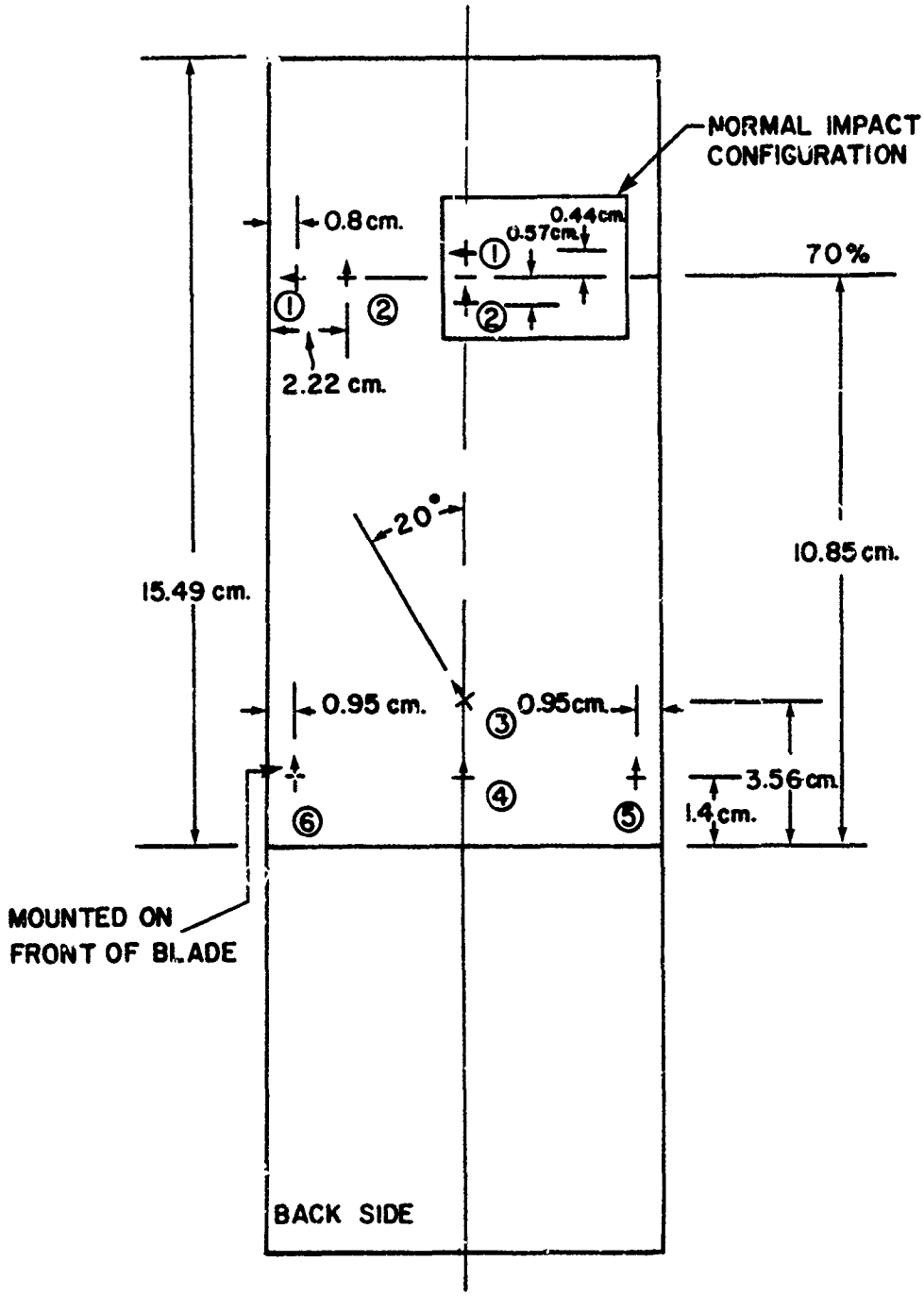

Figure 13A. Strain Gage Locations for Group 14 and 16 Structural Element Test Specimens.

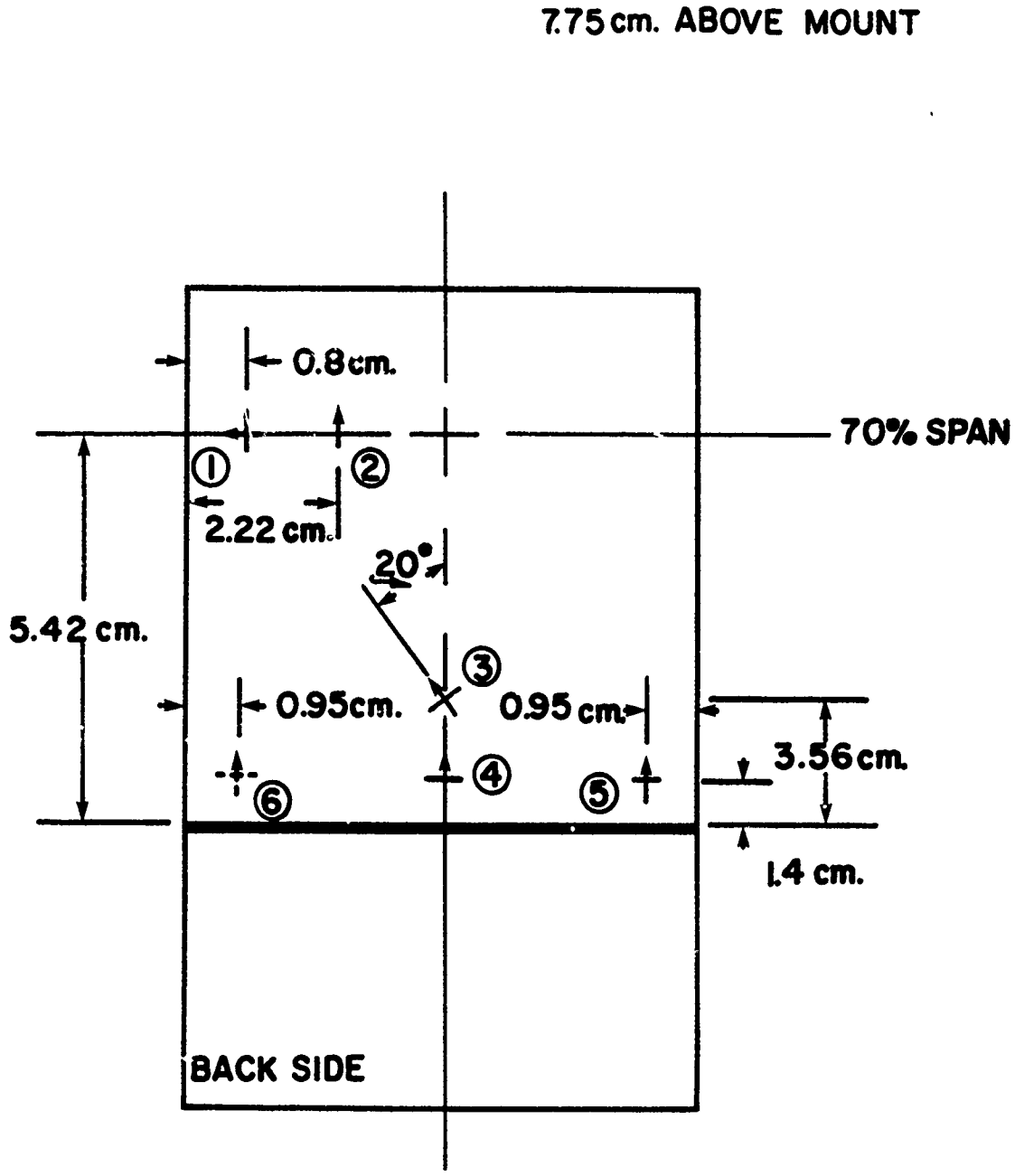

Figure 14A. Strain Gage Locations for Group 15 Structural Element Test Specimens.

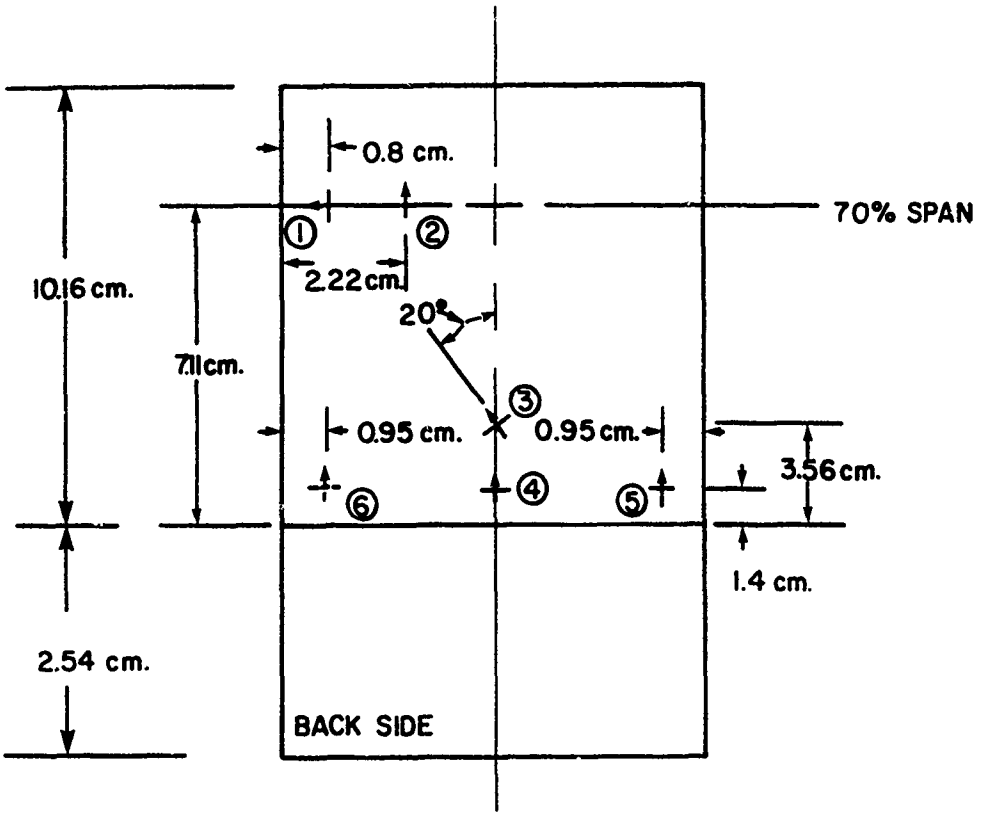

Figure 15A. Strain Gage Locations for Group 17 Structural Element Test Specimens.

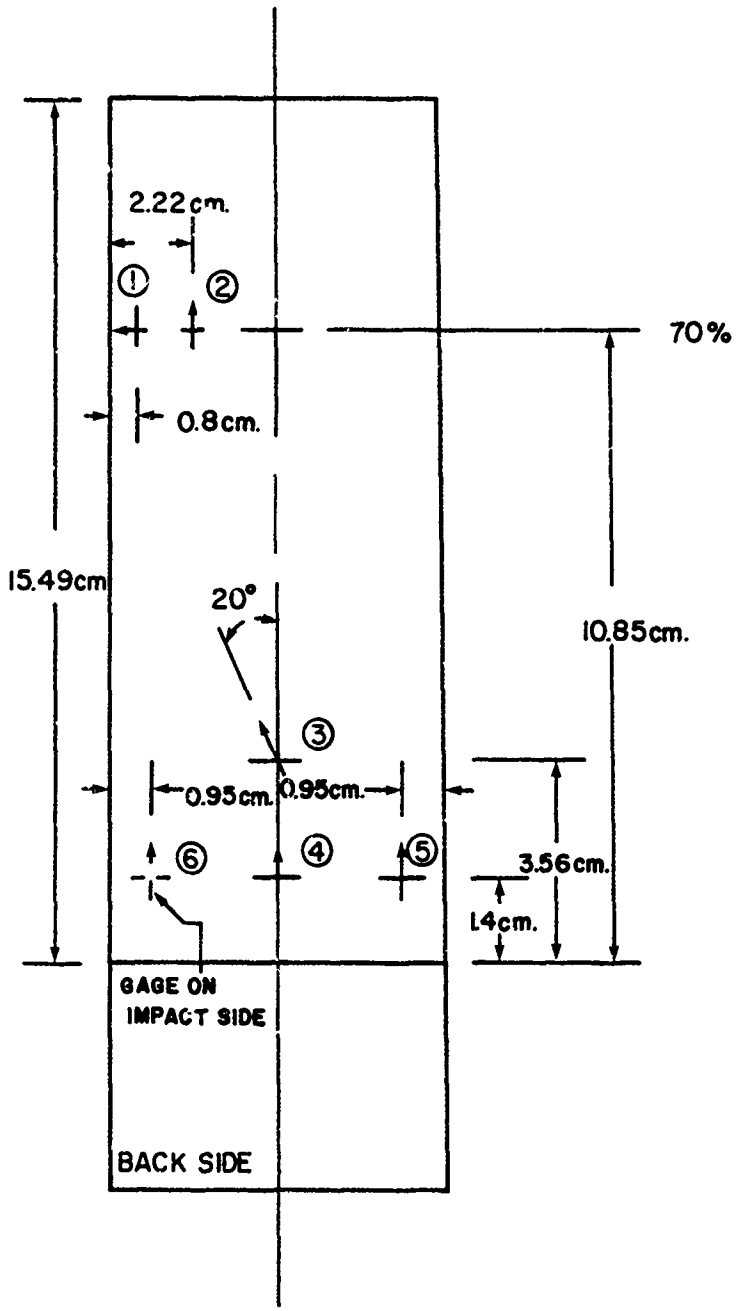

Figure 16A. Strain Gage Locations for Group 18 and 19 Structural Element Test Specimens.

APPENDIX B

TYPICAL DAMAGE FROM IMPACTS

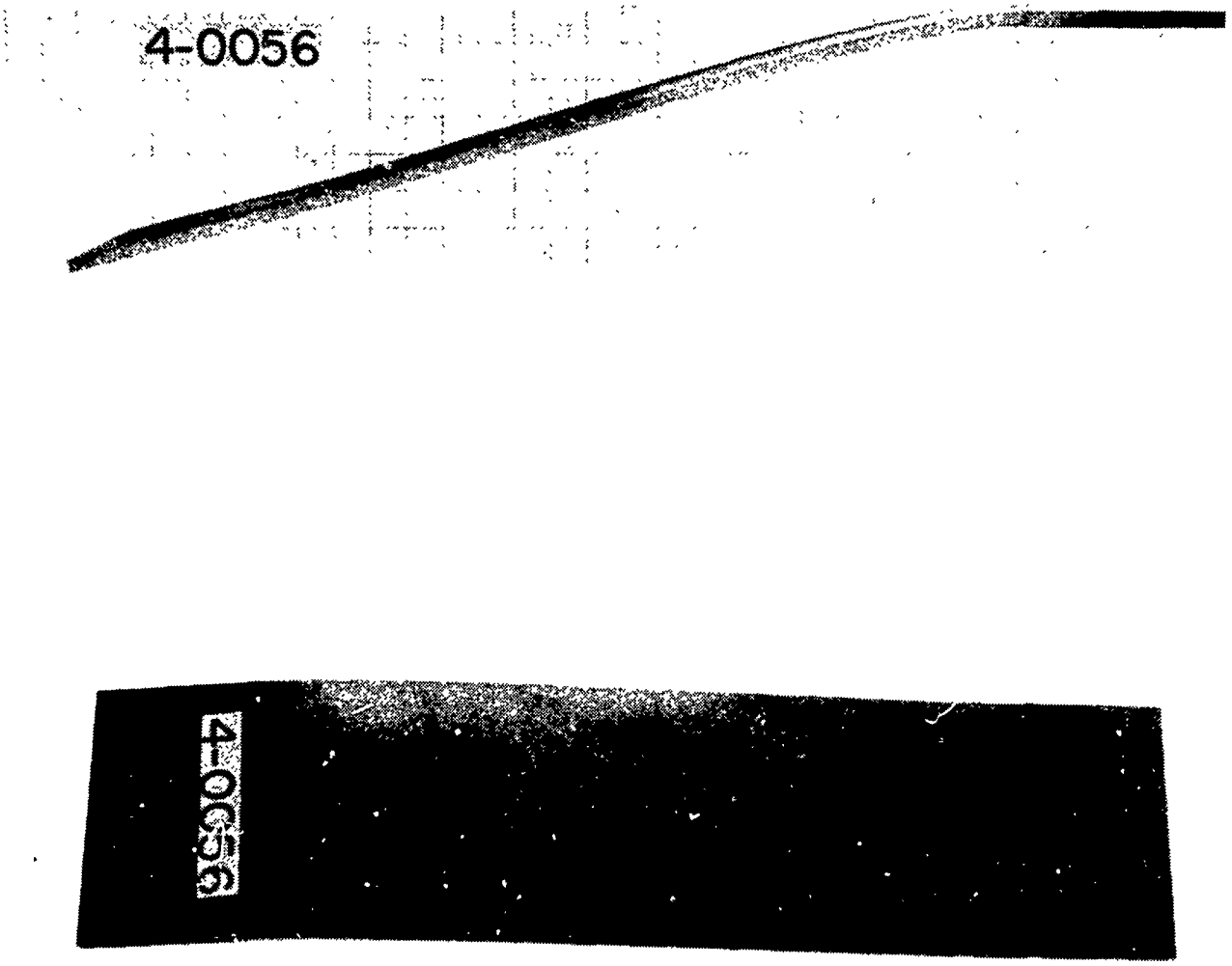

Figure 1B. Damage for Group 1 Titanium Specimen Due to 85 g (3 ounce) Artificial Bird Impact (Shot 4-0056).

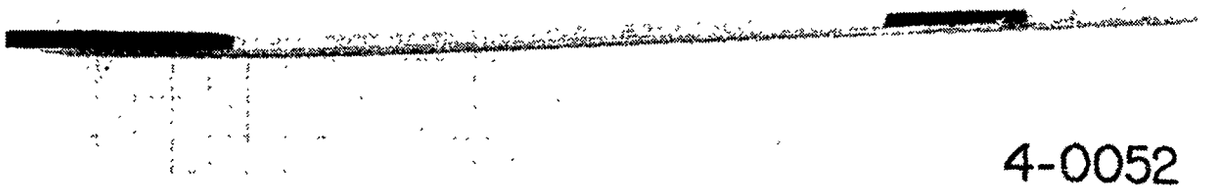

Figure 2B. Damage for Group 1 Titanium Specimen for 85 g (3 ounce) Artificial Bird Impact (Shot 4-0052).

Figure 3B. Specimen Due to 85 g (3 ounce) Artificial Bird Impact (Shot 2-0131).

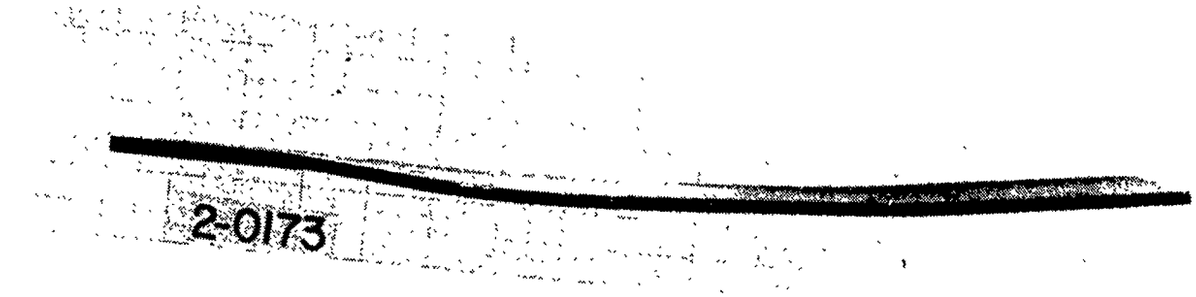

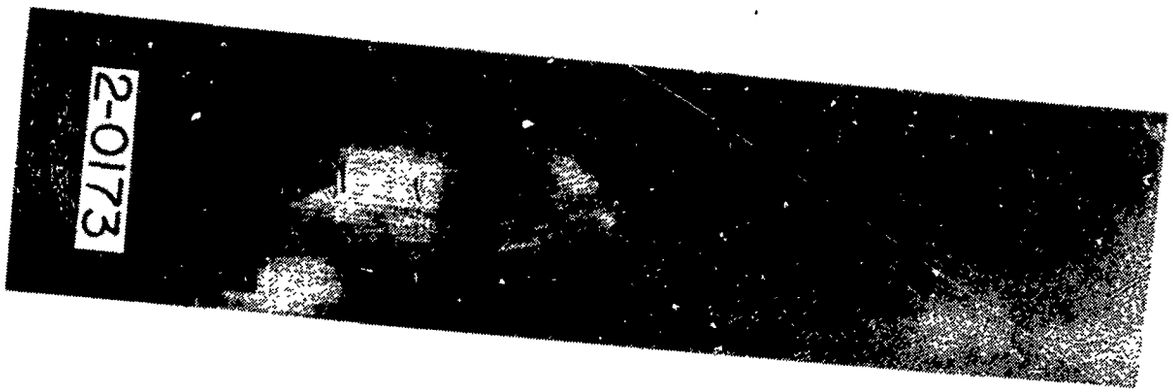

Figure 4B. Damage for Group 2 Titanium Specimen for 5.08 cm Diameter Ice Ball Impact (Shot 2-0173).

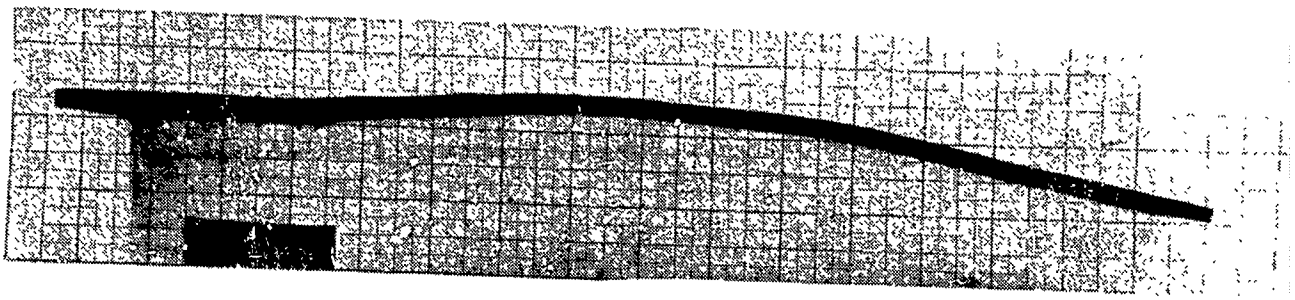

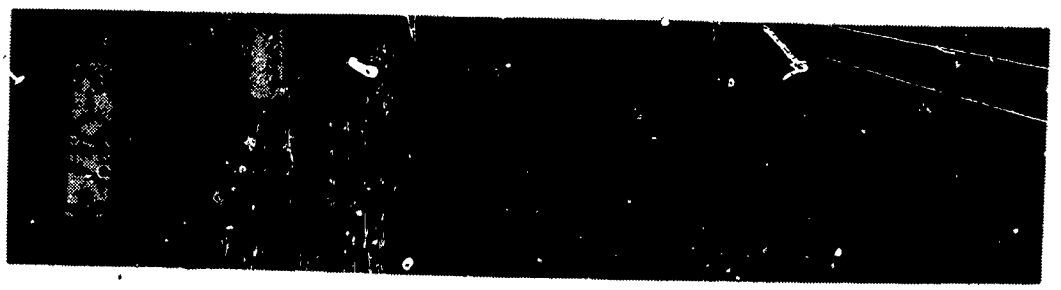

Figure 5B. Damage for Group 2 Titanium Specimen for 5.08 cm Diameter Ice Ball Impact (Shot 2-0174).

2-0127

Figure 6B. Damage for Group 3 Titanium Specimen for 85 g (3 ounce) Artificial Bird Impact (Shot 2-0127).

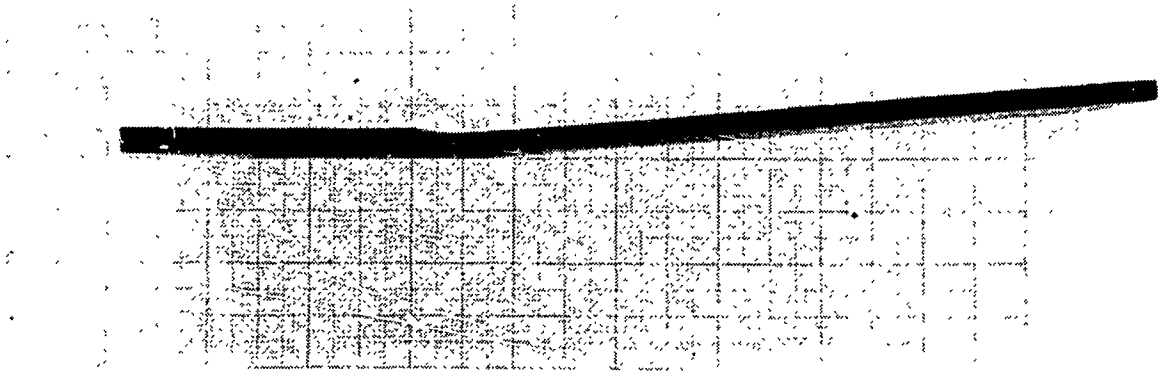

2-0096

Figure 7B. Damage for Group 4 Titanium Specimen for 85 g (3 ounce) Artificial Bird Impact (Shot 2-0096).

2-0097

Figure 8B. Damage for Group 4 Titanium Specimen for 85 g (3 ounce) Artificial Bird Impact (Shot 2-0097).

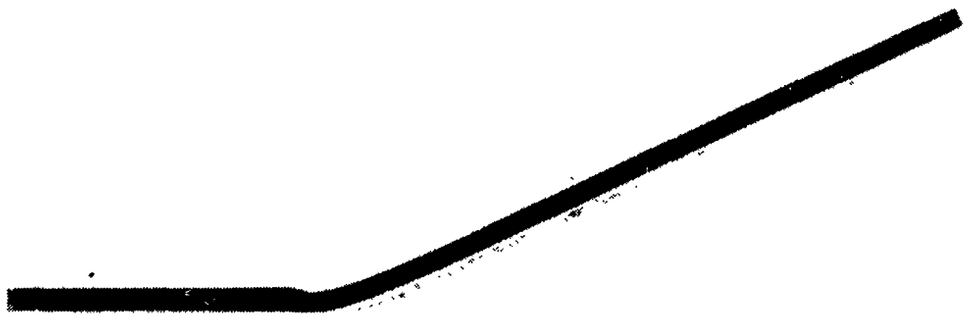

2-0098

Figure 9B. Damage for Group 4 Titanium Specimen for 85 g (3 ounce) Artificial Bird Impact (Shot 2-0098).

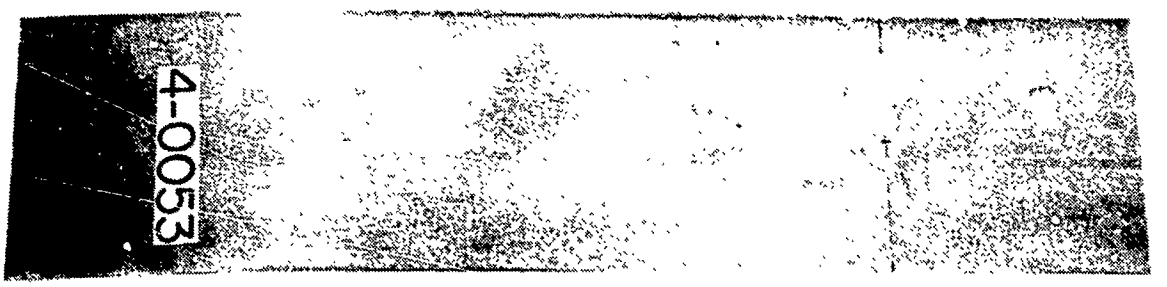

4-0053

Figure 10B. Damage for Group 6 Titanium Specimen for 85 g (3 ounce) Artificial Bird Impact (Shot 4-0053).

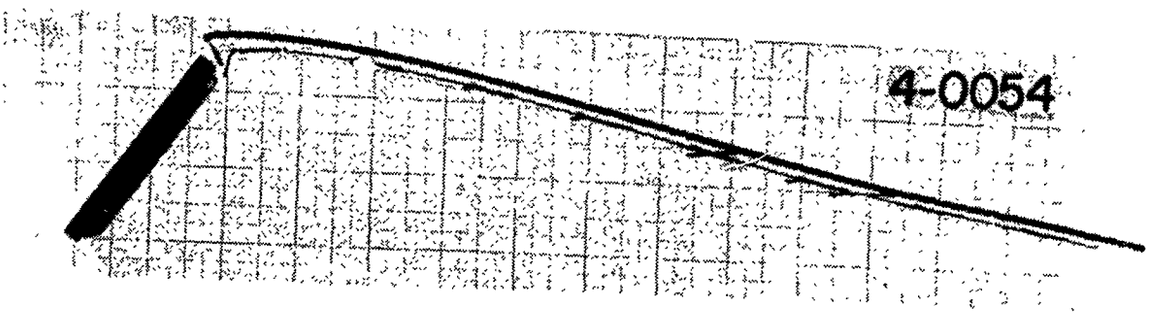

Figure 11B. Damage for Group 6 Titanium Specimen for 85 g (3 ounce) Artificial Bird Impact (Shot 4-0054).

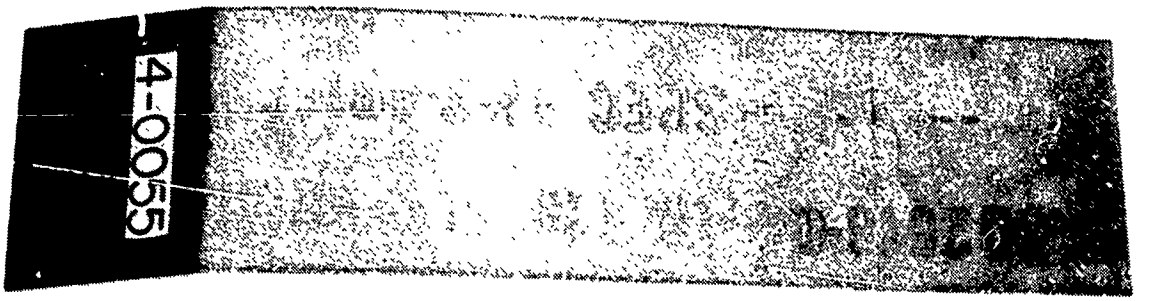

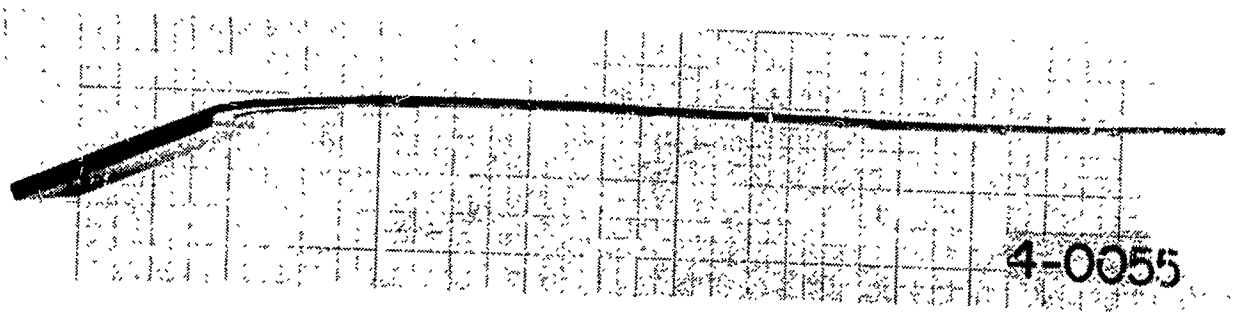

Figure 12B. Damage for Group 6 Titanium Specimen for 85 g (3 ounce) Artificial Bird Impact (Shot 4-0055).

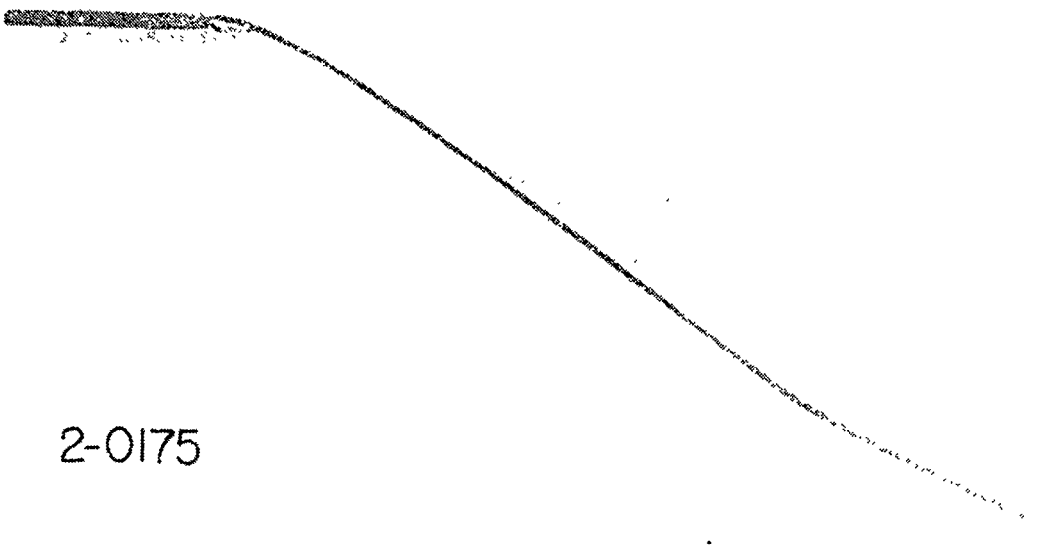

Figure 13B. Damage for Group 6 Titanium Specimen for 85 g (3 ounce) Artificial Bird Impact (Shot 2-0175).

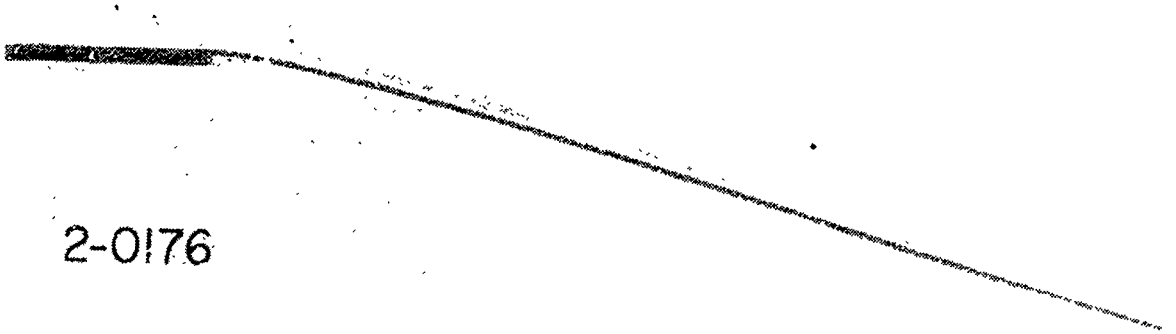

Figure 14B. Damage for Group 6 Titanium Specimen for 85 g (3 ounce) Artificial Bird Impact (Shot 2-0176).

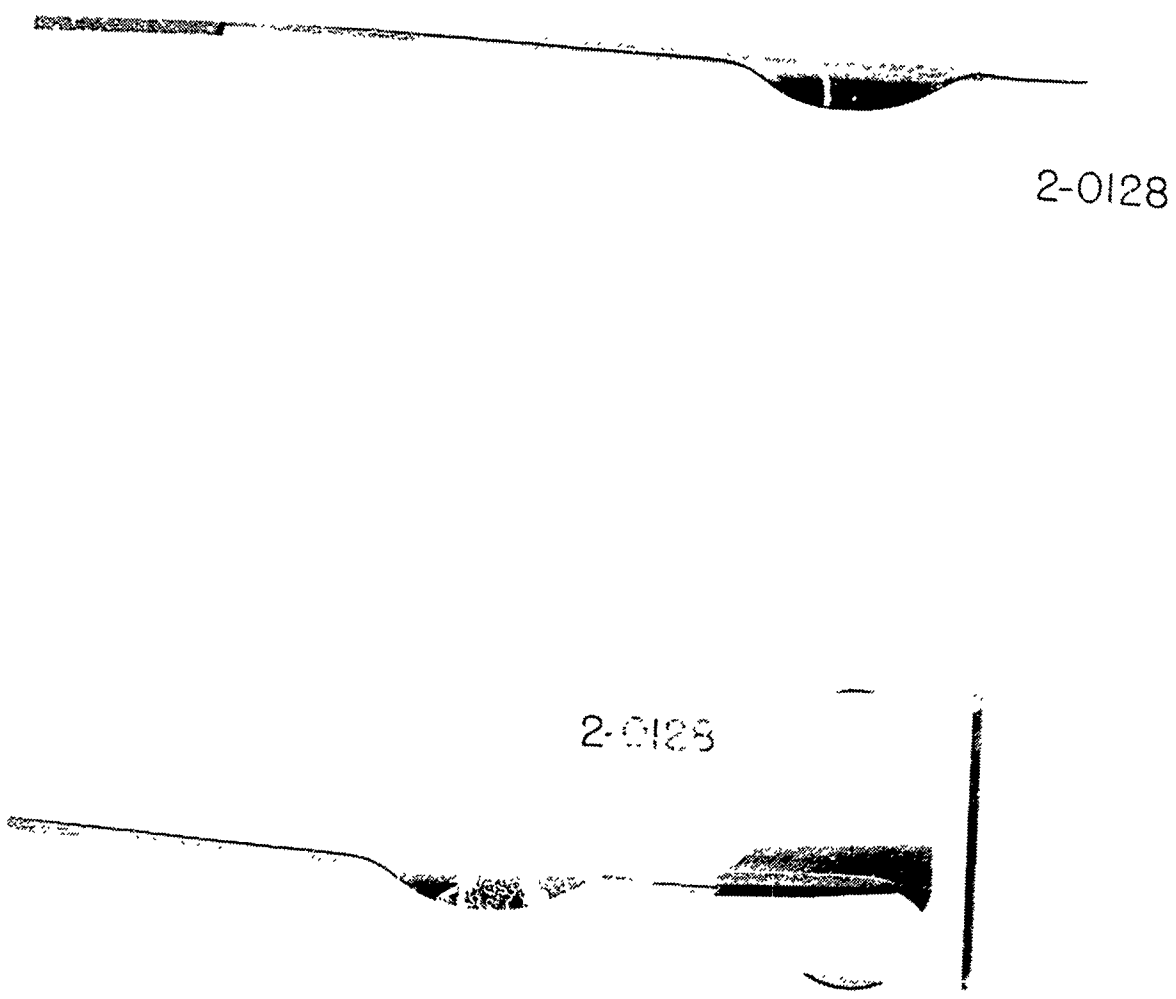

Figure 15B. Damage for Group 7 Titanium Specimen Due to 85 g (3 ounce) Artificial Bird Impact (Shot 2-0128).

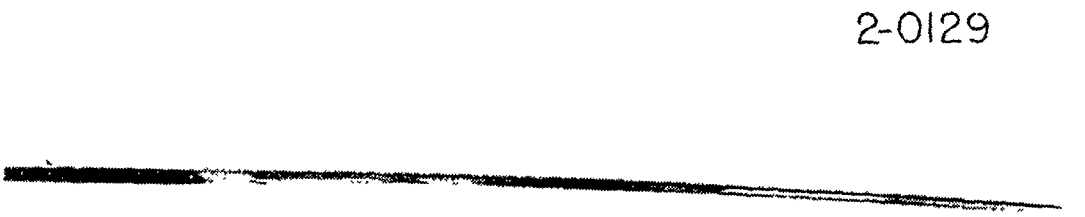

Figure 16B. Damage for Group 7 Titanium Specimen Due to 85 g (3 ounce) Artificial Bird Impact (Shot 2-0129).

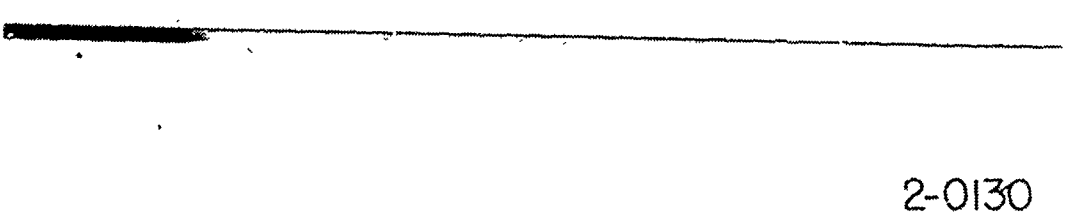

Figure 17B. Damage for Group 7 Titanium Specimen Due to 85 g (3 ounce) Artificial Bird Impact (Shot 2-0130).

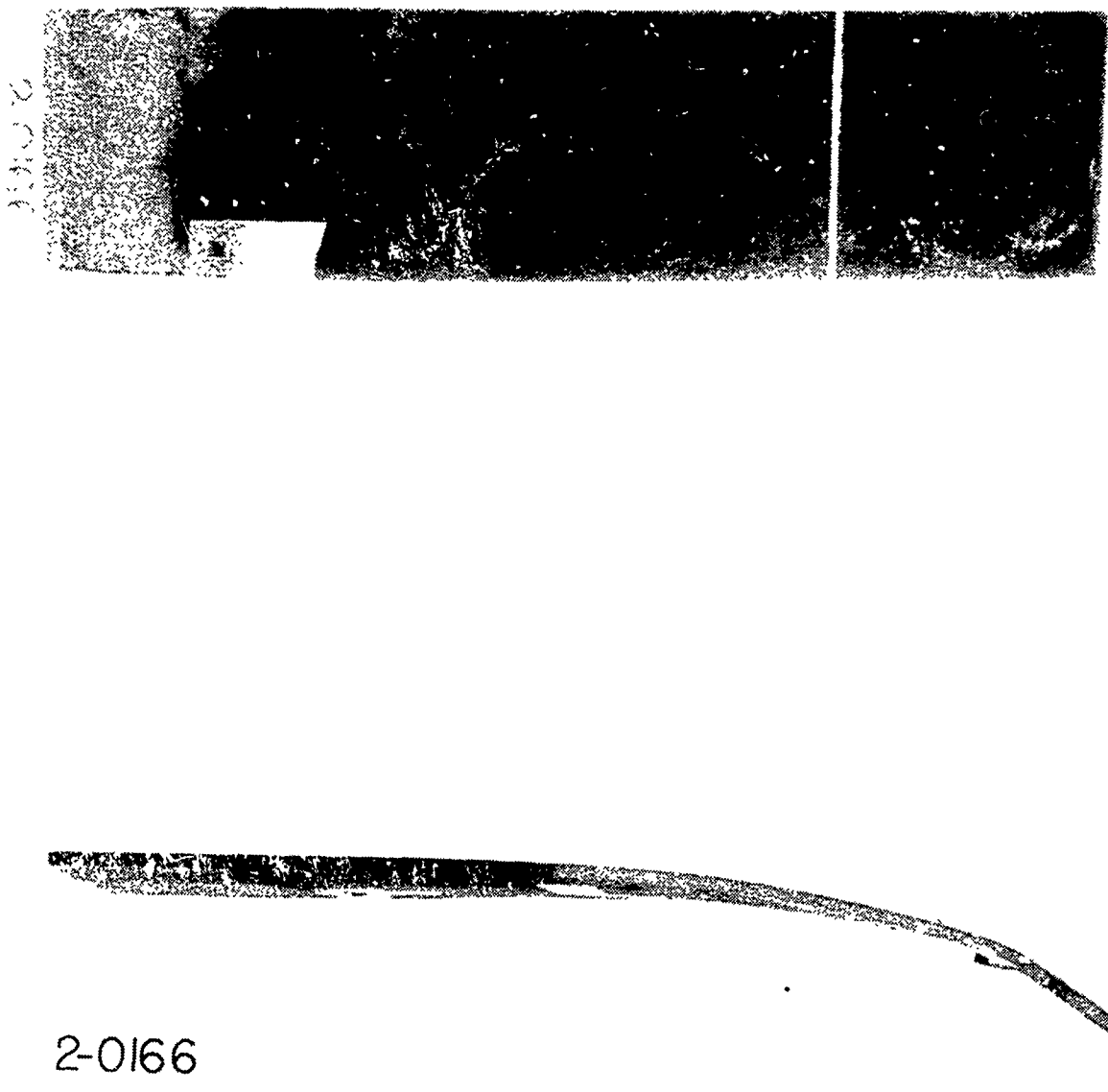

Figure 18B. Damage for Group 8 Titanium Specimen Due to 85 g (3 ounce) Artificial Bird Impact (Shot 2-0166).

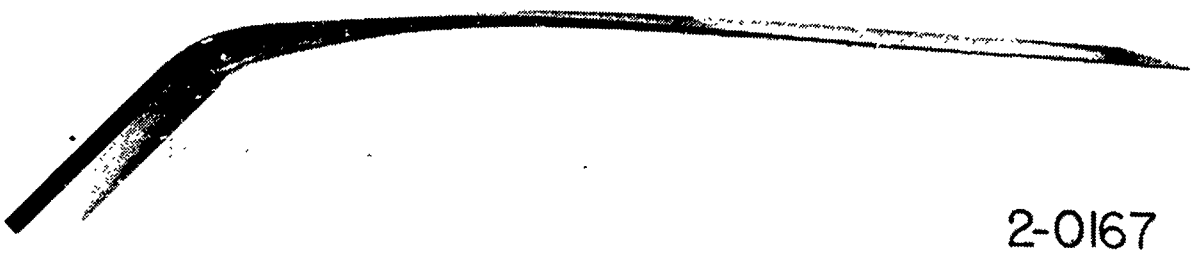

Figure 19B. Damage for Group 8 Titanium Specimen Due to 85 g (3 ounce) Artificial Bird Impact (Shot 2-0167).

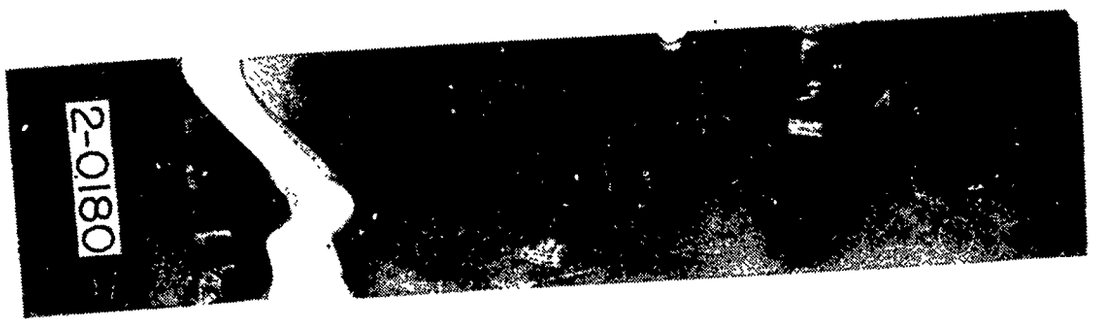

Figure 20B. Damage for Group 9 Titanium Specimen Due to 680 g (1.5 pound) Artificial Bird Impact (Shot 2-0180).

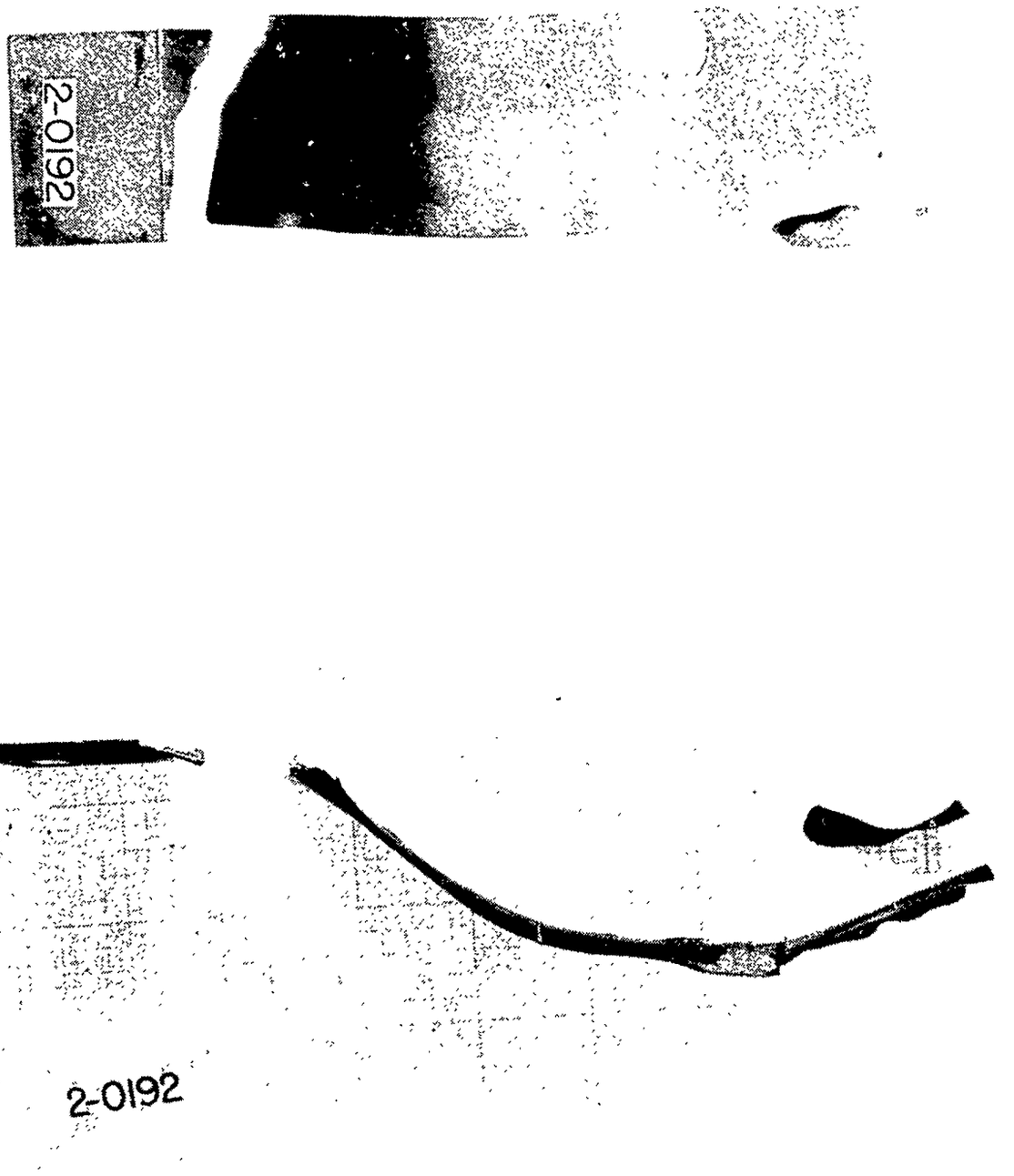

Figure 21B. Damage for Group 9 Titanium Specimen Due to 680 g (1.5 pound) Artificial Bird Impact (Shot 2-0192).

Figure 22B. Damage for Group 10 Titanium Specimen Due to 85 g (3 ounce) Artificial Bird Impact (Shot 2-0177).

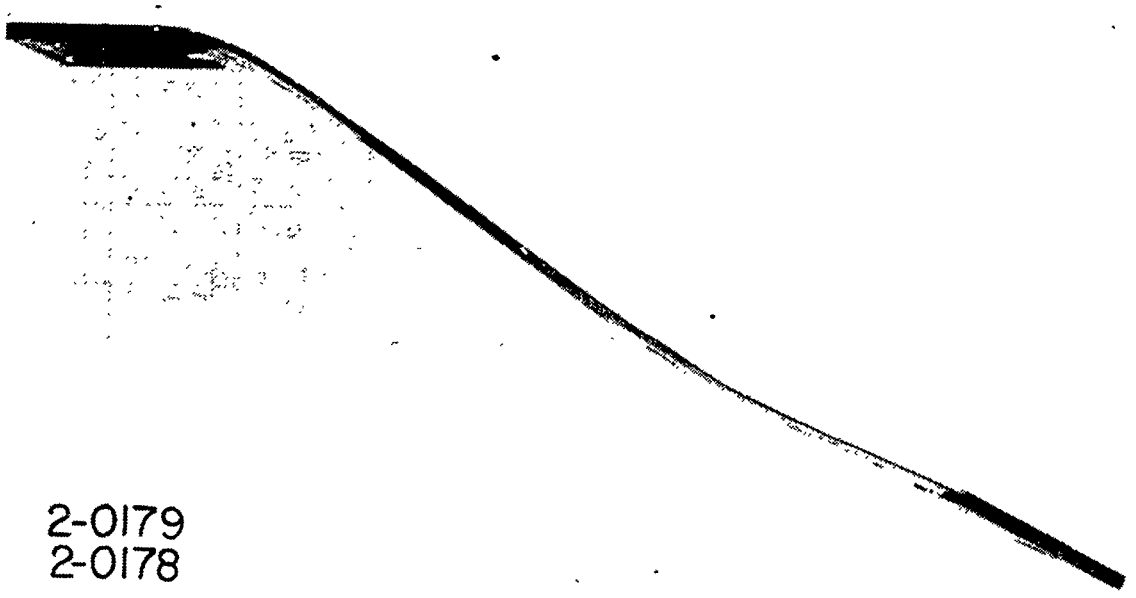

Figure 23B. Damage for Group 10 Titanium Specimen Due to 85 g (3 ounce) Artificial Bird Impact (Shot 2-0179).

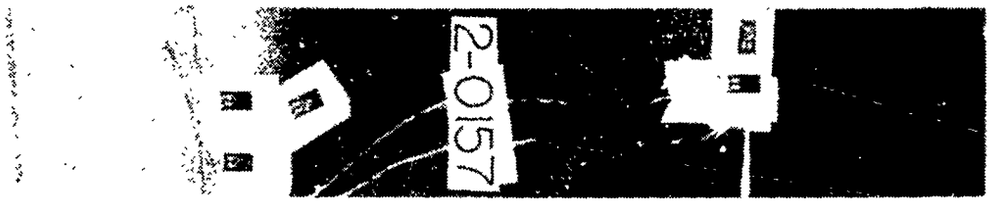

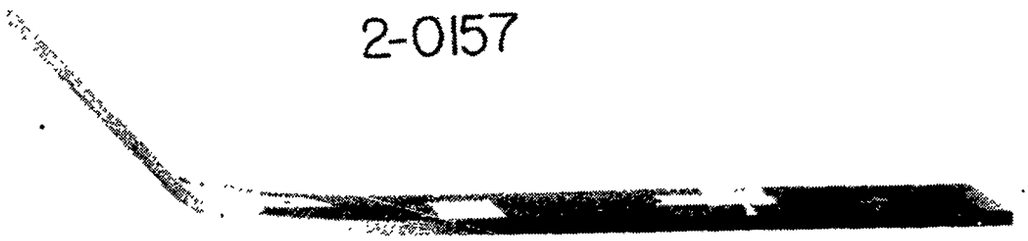

Figure 24B. Damage for Group 11 Stainless Steel Specimen Due to 680 g (1.5 pound) Artificial Bird Impact (Shot 2-0157).

Figure 25B. Damage for Group 11 Stainless Steel Specimen Due to 680 g (1.5 pound) Artificial Bird Impact (Shot 2-0158).

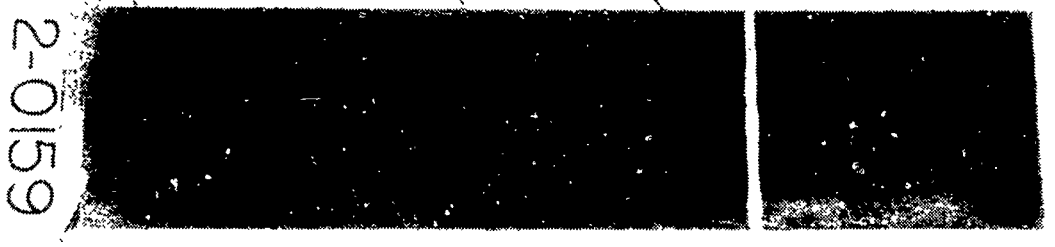

2-0159

Figure 26B. Damage for Group 12 Stainless Steel Specimen Due to 680 g (1.5 pound) Artificial Bird Impact (Shot 2-0159).

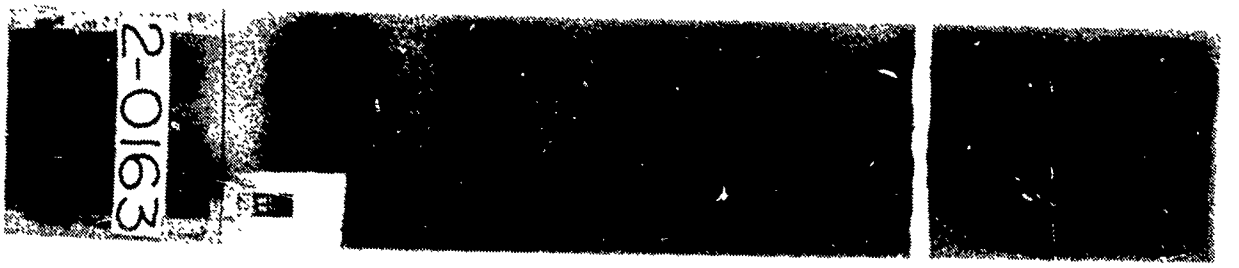

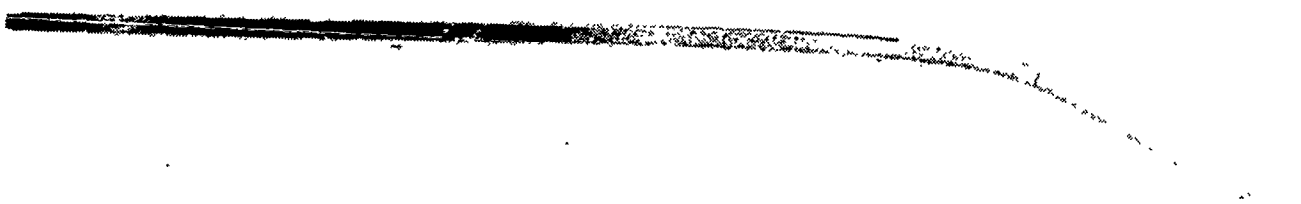

2-0163

Figure 27B. Damage for Group 12 Stainless Steel Specimen Due to 680 g (1.5 pound) Artificial Bird Impact (Shot 2-0163).

2-0161

Figure 28B. Damage for Group 13 Stainless Steel Specimen Due to 680 g (1.5 pound) Artificial Bird Impact (Shot 2-0161).

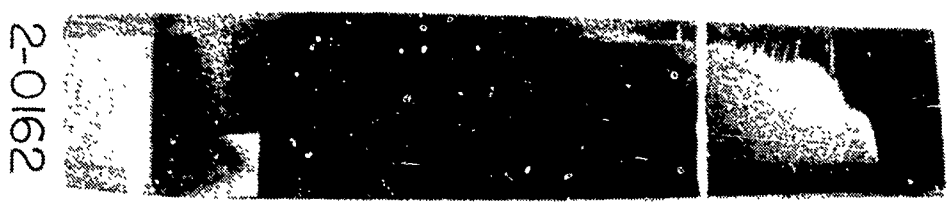

Figure 29B. Damage for Group 13 Stainless Steel Specimen Due to 680 g (1.5 pound) Artificial Bird Impact (Shot 2-0162).

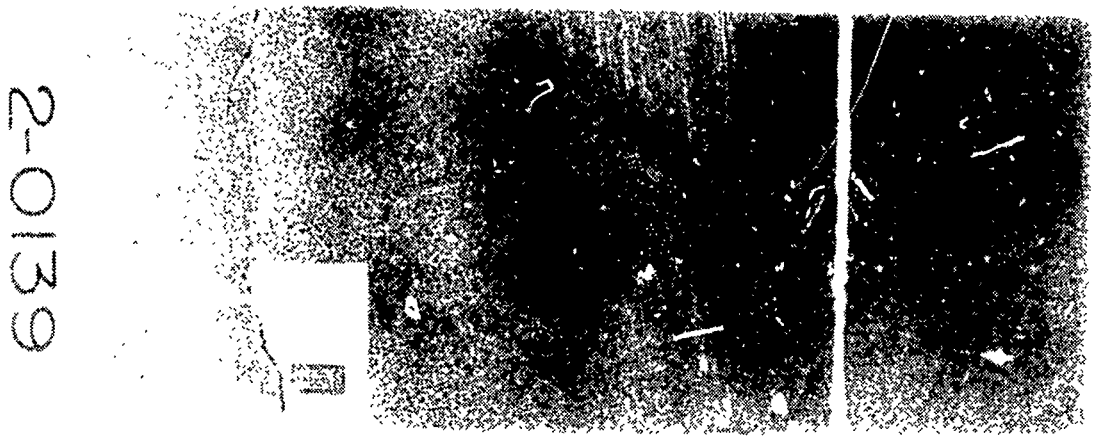

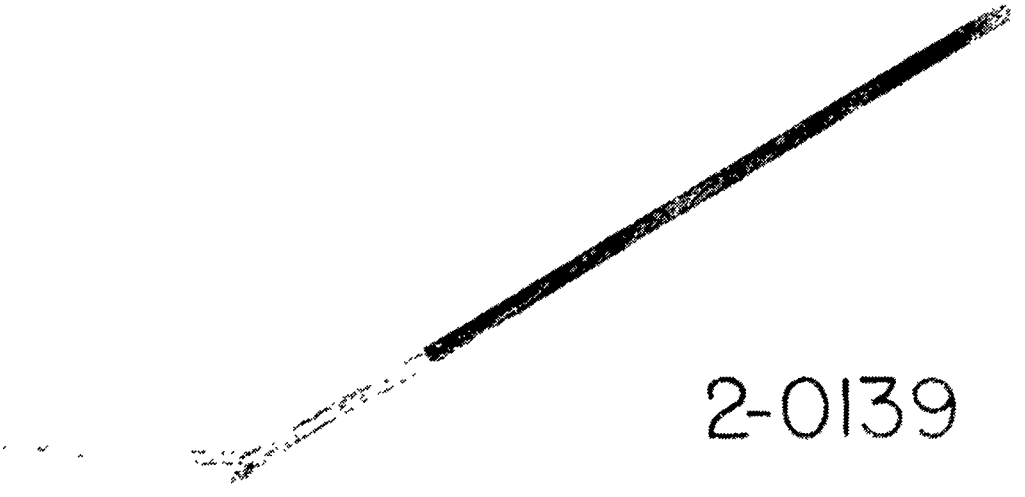

Figure 30B. Damage for Group 14 Boron/Aluminum Co[illegible]te Specimen Due to 85 g (3 ounce) Artificial Bird Impact (Shot 2-0139).

2-0149

2-0149

Figure 31B. Damage for Group 15 Boron/Aluminum Composite Specimen Due to 85 g (3 ounce) Artificial Bird Impact (Shot 2-0149).

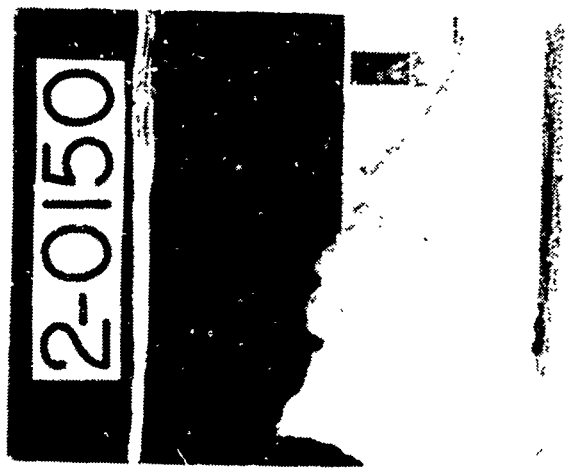

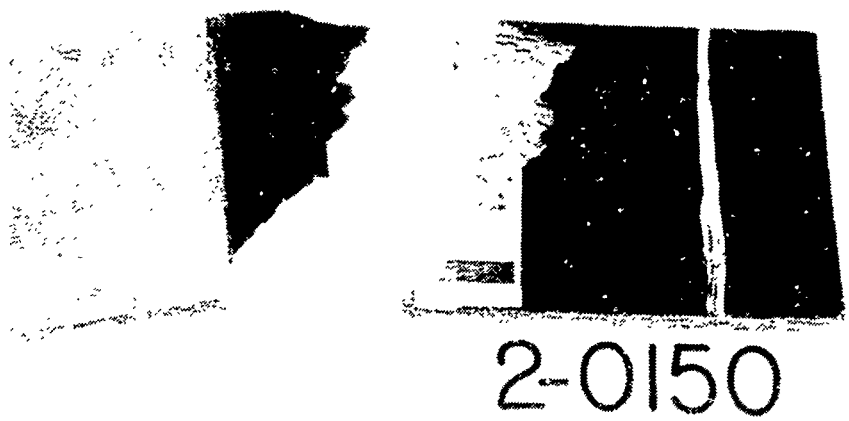

Figure 32B. Damage for Group 15 Boron/Aluminum Composite Specimen Due to 85 g (3 ounce) Artificial Bird Impact (Shot 2-0150).

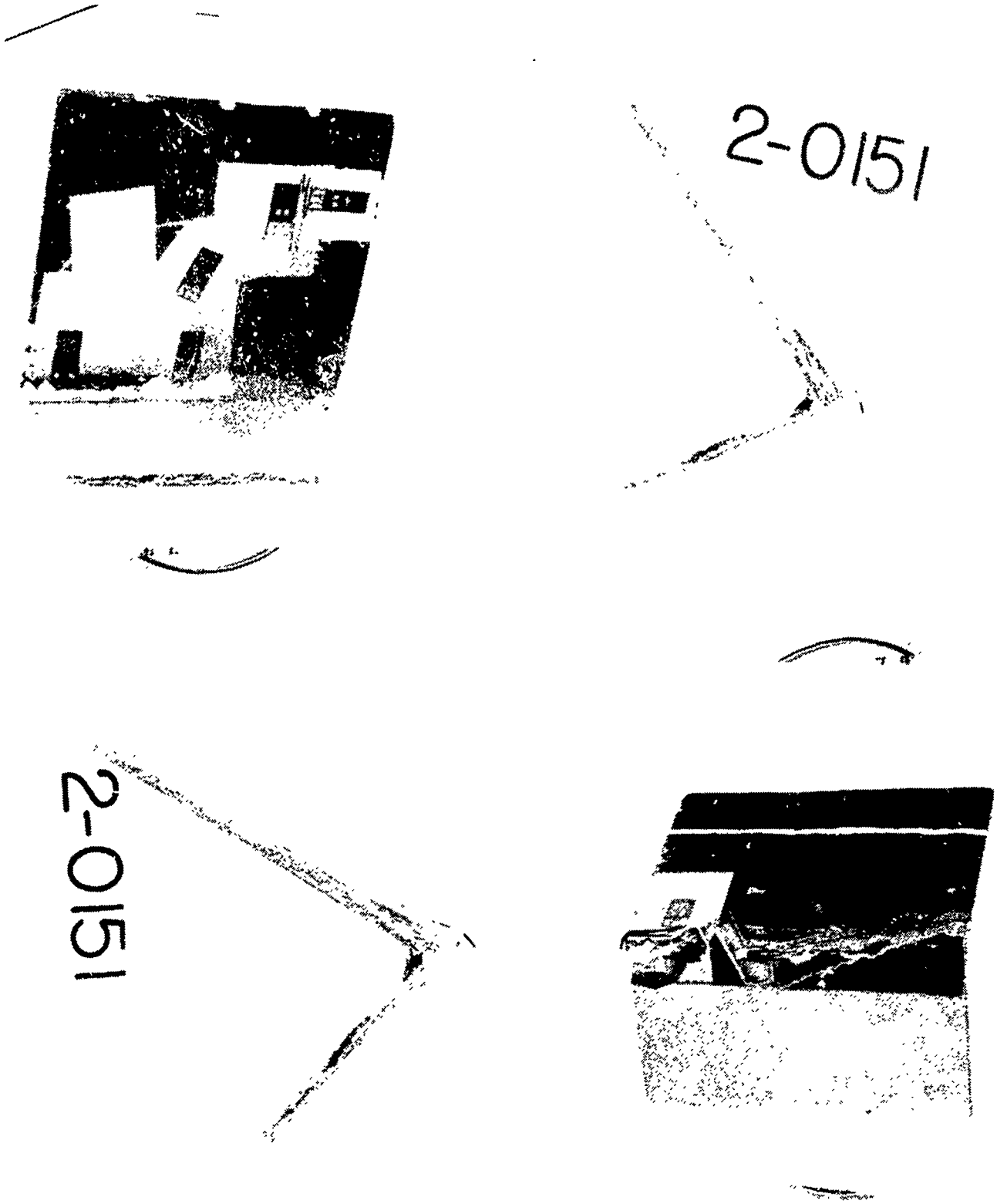

Figure 33B. Damage for Group 15 Boron/Aluminum Composite Specimen Due to 85 g (3 ounce) Artificial Bird Impact (Shot 2-0151).

Figure 34B. Damage for Group 16 Boron/Aluminum Composite Specimen Due to 85 g (3 ounce) Artificial Bird Impact (Shot 2-0138).

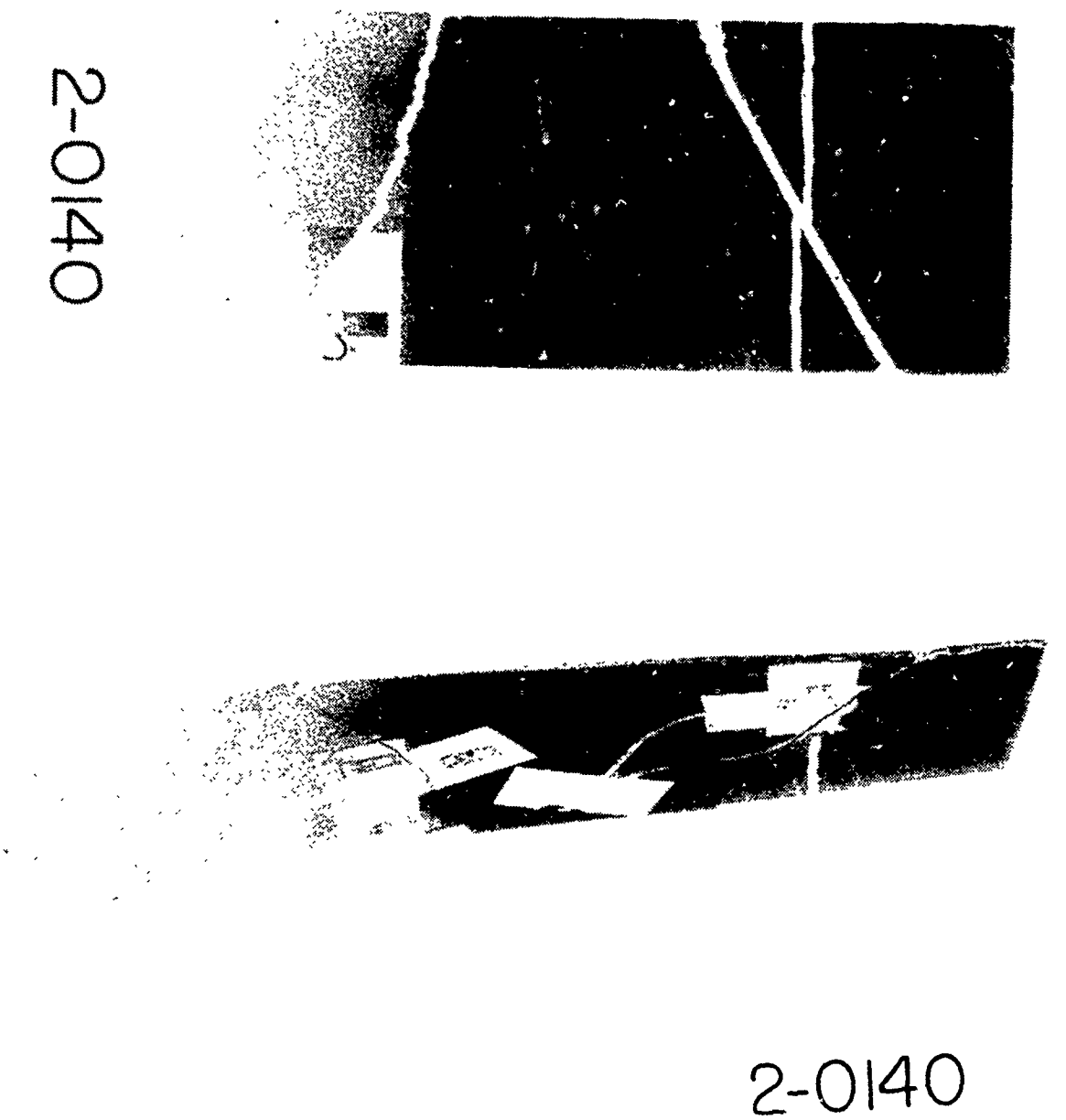

Figure 35B. Damage for Group 16 Boron/Aluminum Composite Specimen Due to 85 g (3 ounce) Artificial Bird Impact (Shot 2-0140).

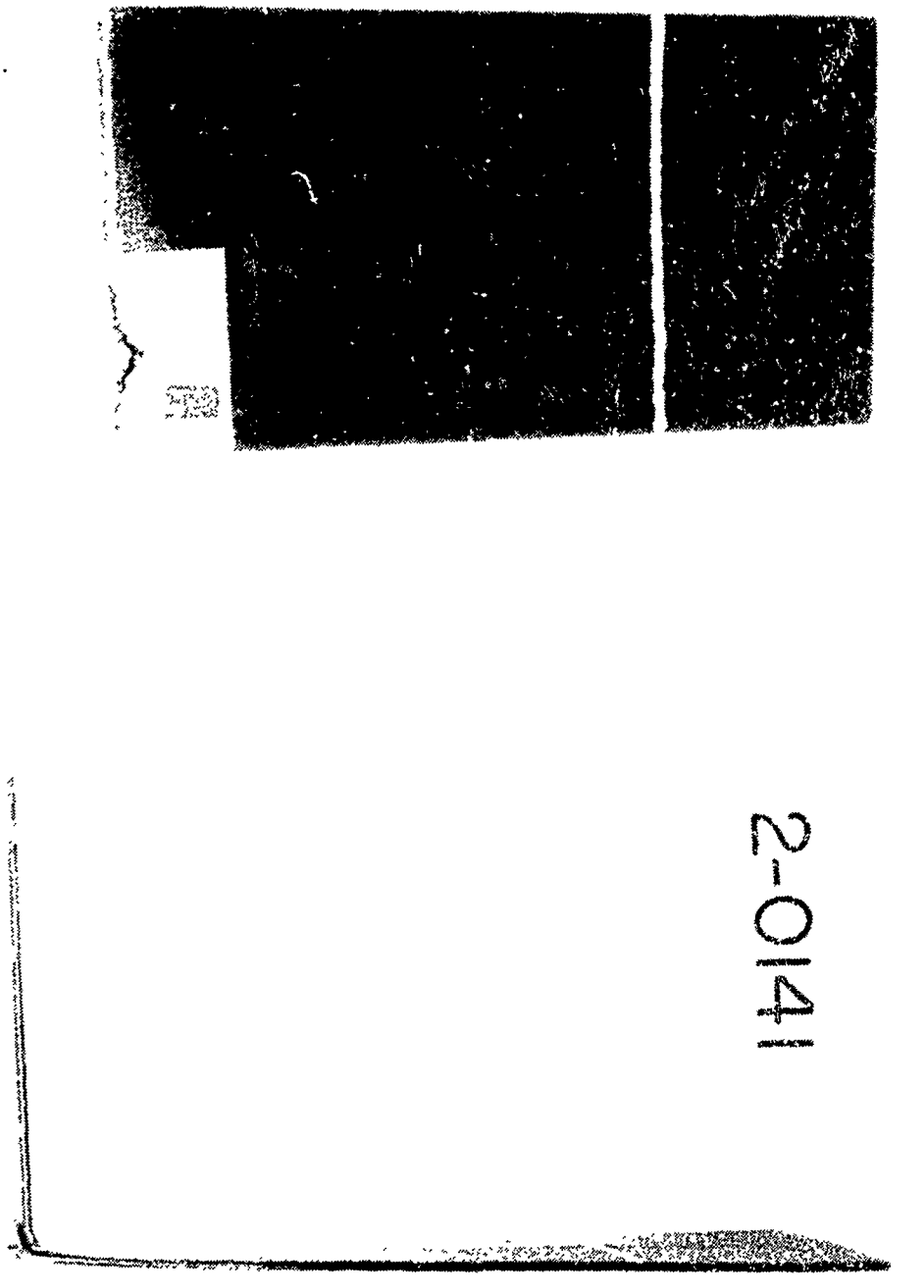

Figure 36B. Damage for Group 16 Boron/Aluminum Composite Specimen Due to 85 g (3 ounce) Artificial Bird Impact (Shot 2-0141).

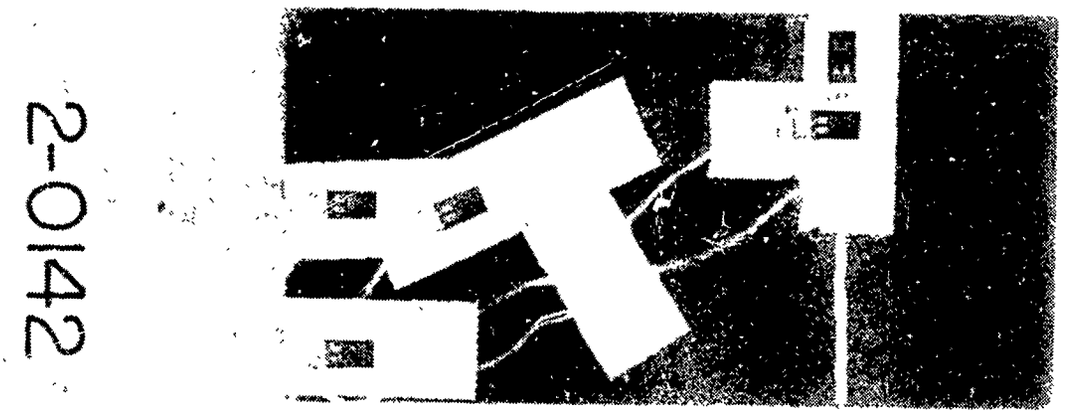

2-0142

Figure 37B. Damage for Group 16 Boron/Aluminum Composite Specimen Due to 85 g (3 ounce) Artificial Bird Impact (Shot 2-0142).

2-0213

2-0213

Figure 38B. Damage for Group 17 Boron/Aluminum Composite Specimen Due to 85 g (3 ounce) Artificial Bird Impact (Shot 2-0213).

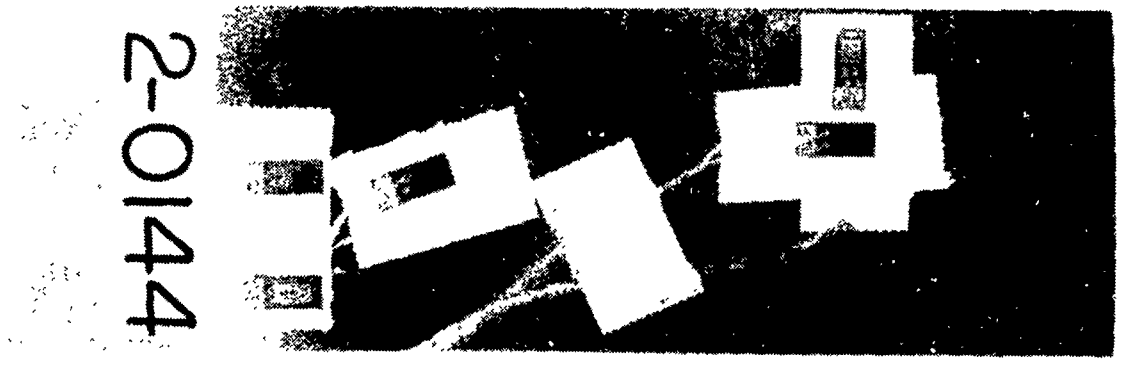

Figure 39B. Damage for Group 18 Boron/Aluminum Composite Specimen Due to 85 g (3 ounce) Artificial Bird Impact (Shot 2-0144).

2-0145

2-0145

Figure 40B. Damage for Group 18 Boron/Aluminum Composite Specimen Due to 85 g (3 ounce) Artificial Bird Impact (Shot 2-0145).

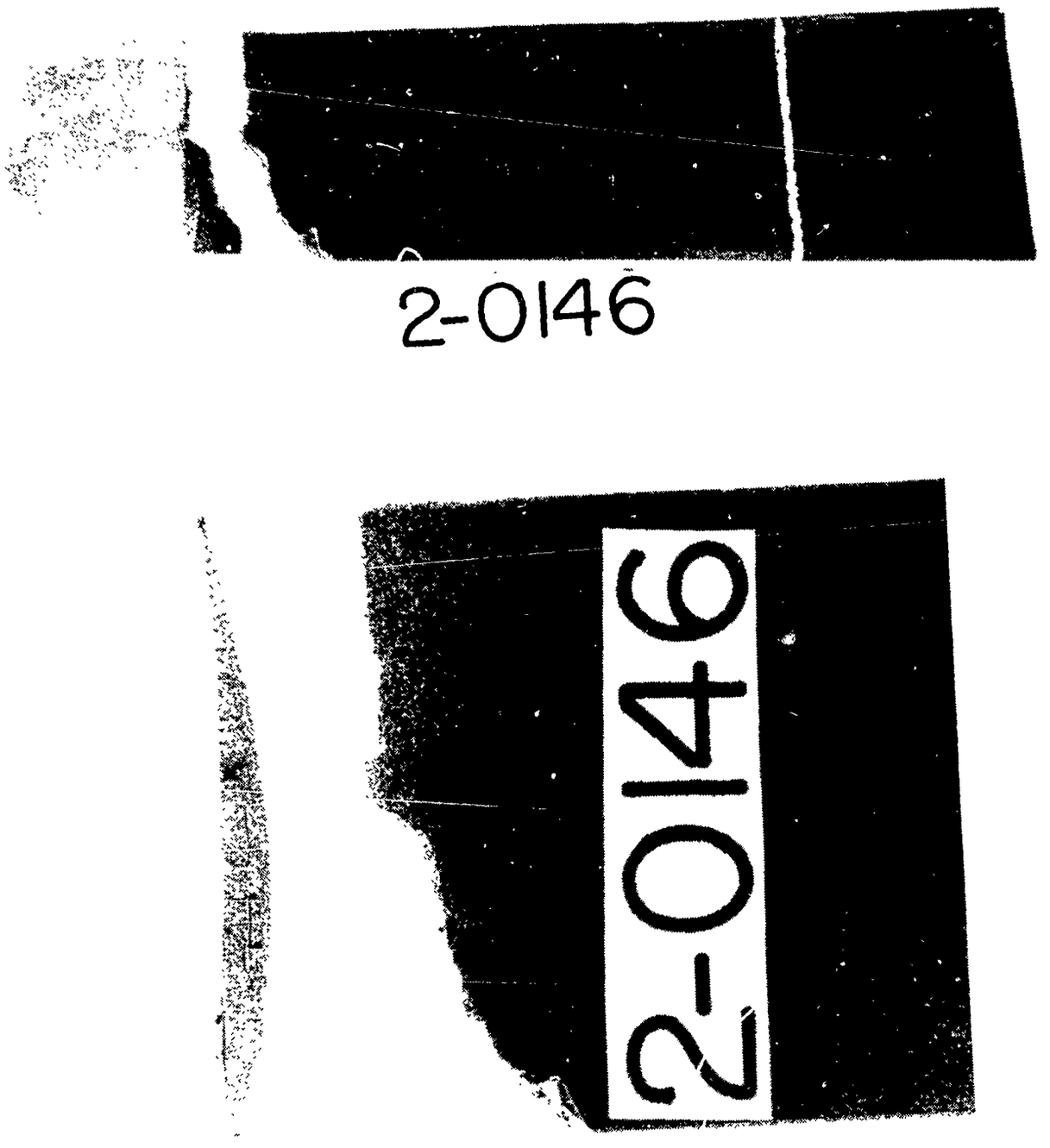

Figure 41B. Damage for Group 19 Boron/Aluminum Composite Specimen Due to 85 g (3 ounce) Artificial Bird Impact (Shot 2-0146).

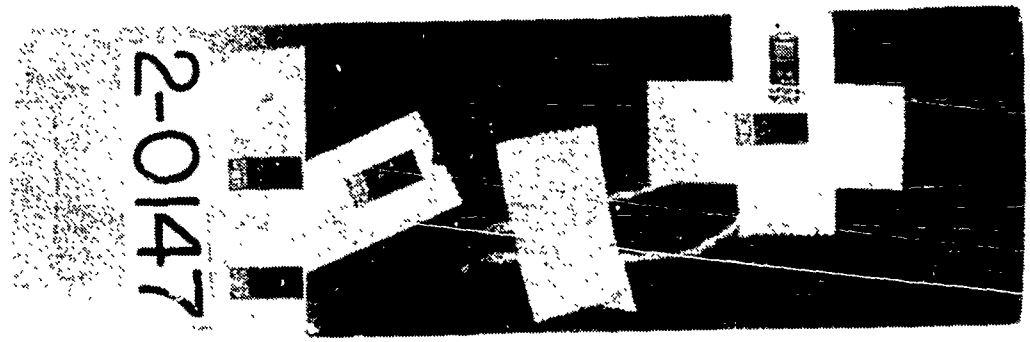

Figure 42B. Damage for Group 19 Boron/Aluminum Composite Specimen Due to 85 g (3 ounce) Artificial Bird Impact (Shot 2-0147).

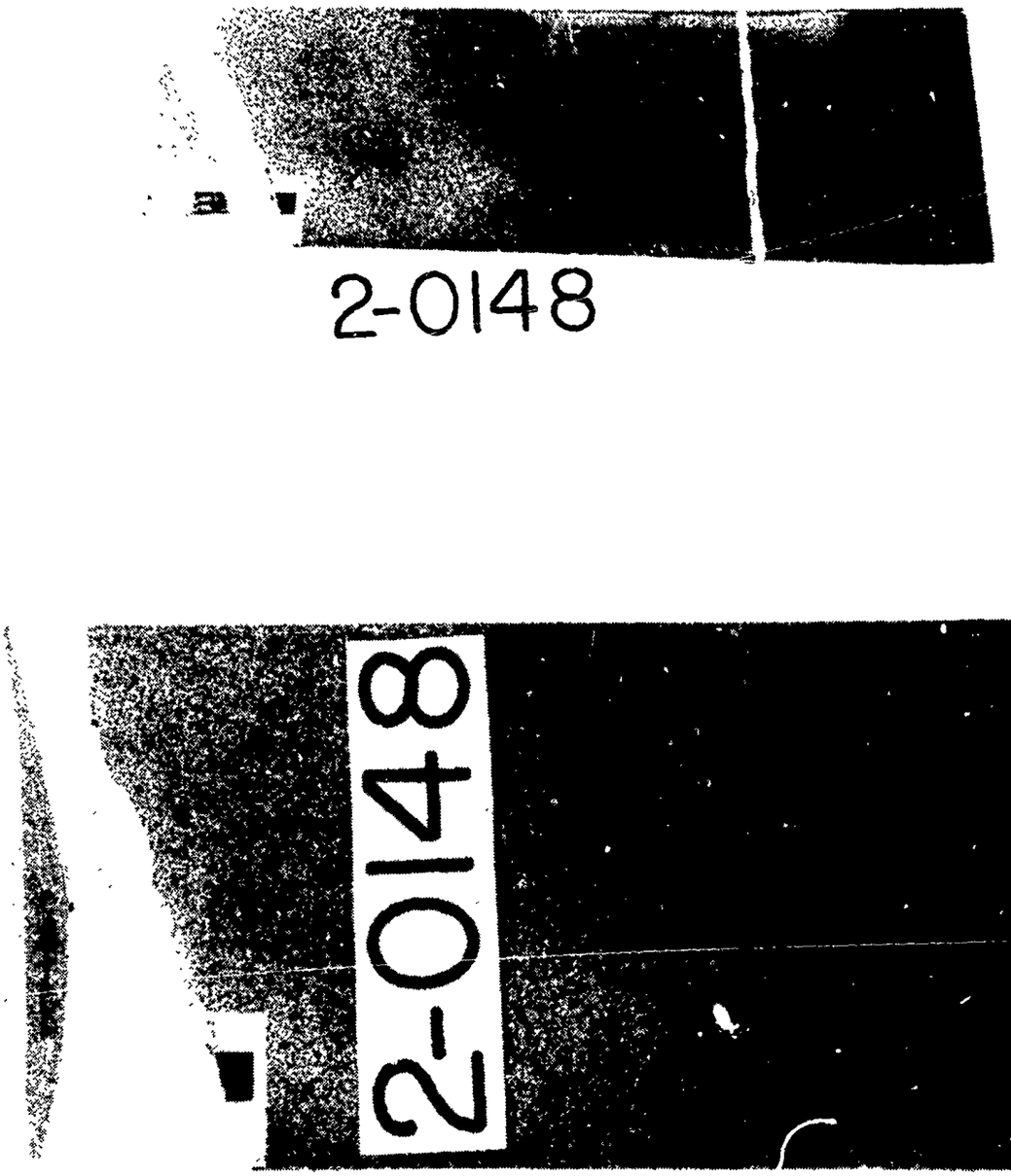

Figure 43B. Damage for Group 19 Boron/Aluminum Composite Specimen Due to 85 g (3 ounce) Artificial Bird Impact (Shot 2-0148).

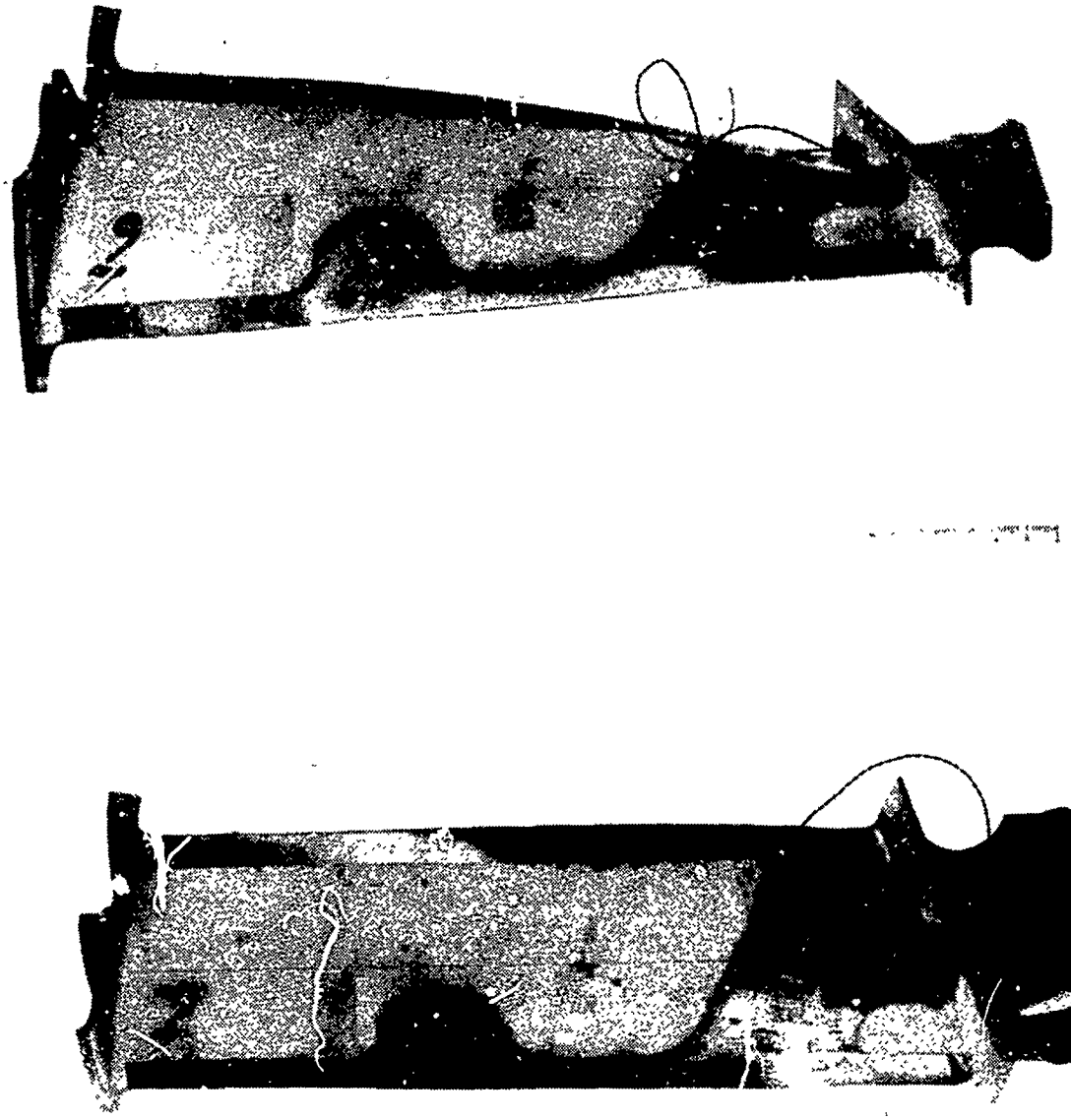

Figure 44 B. Damage for Group 3B F101 Titanium Blade Due to 680 g (1.5 pound) Artificial Bird Impact (Shot 2-0019).

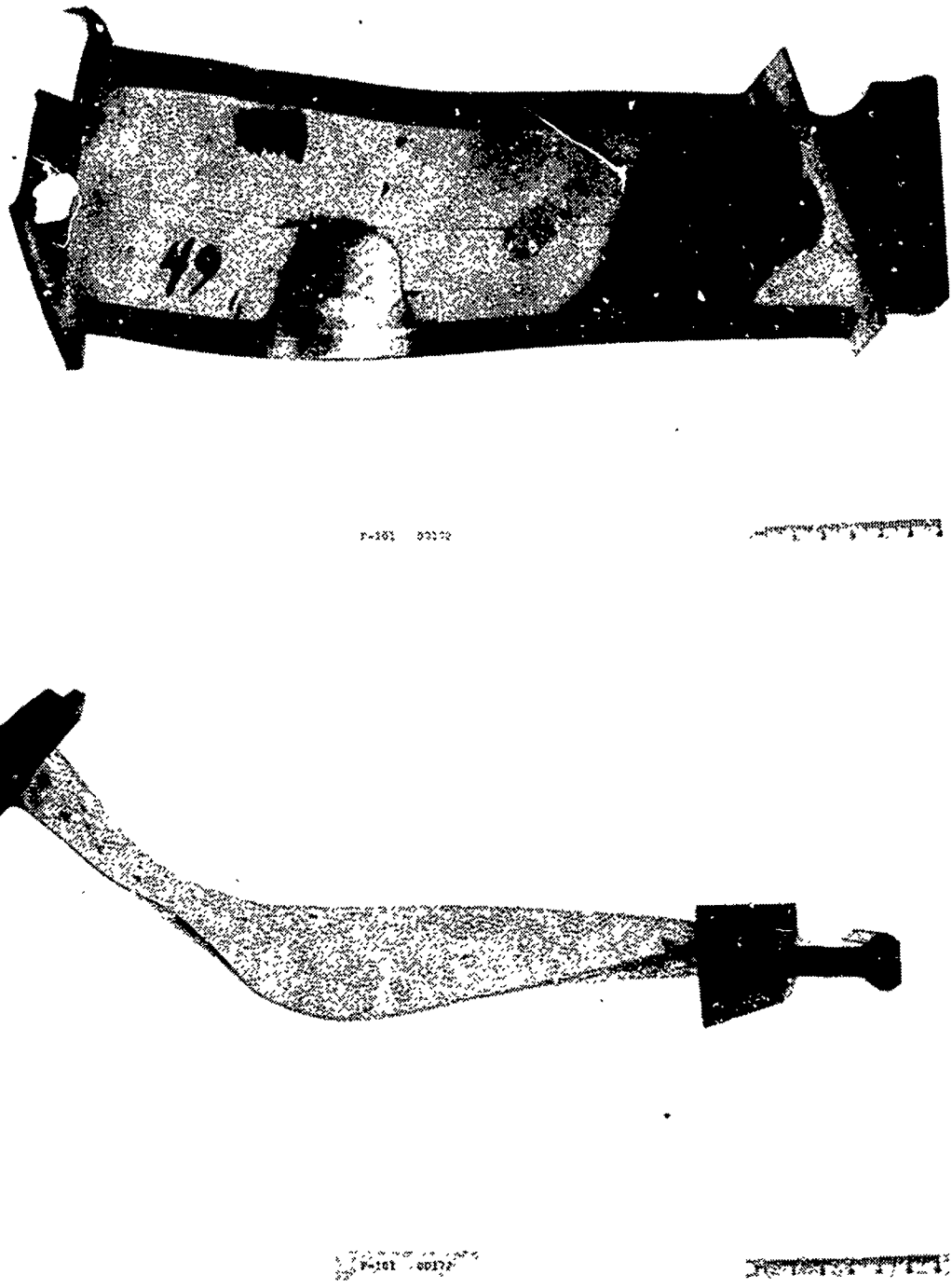

Figure 45B. Damage for Group 4B F101 Titanium Blade Due to 680 g (1.5 pound) Artificial Bird Impact (Shot 2-002Q).

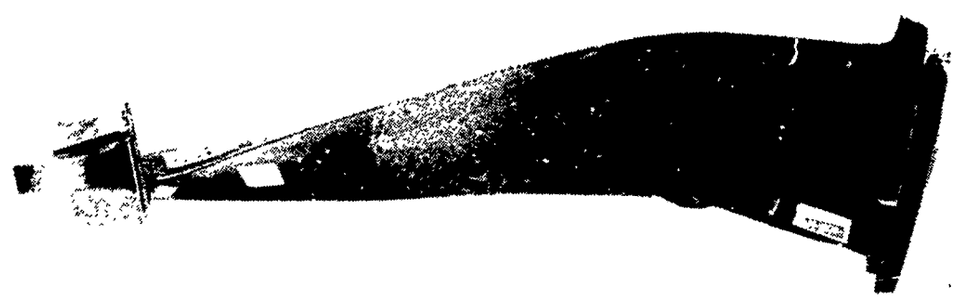

2-0201

2-0201

Figure 46B. Damage for Group 4B F101 Titanium Blade Due to 680 g (1.5 pound) Artificial Bird Impact (Shot 2-0201).

2-0231

2-0231

Figure 47B. Damage for Group 5B F101 Titanium Blade Due to Ice Cylinder (Slab Ice) Impact (Shot 2-0231).

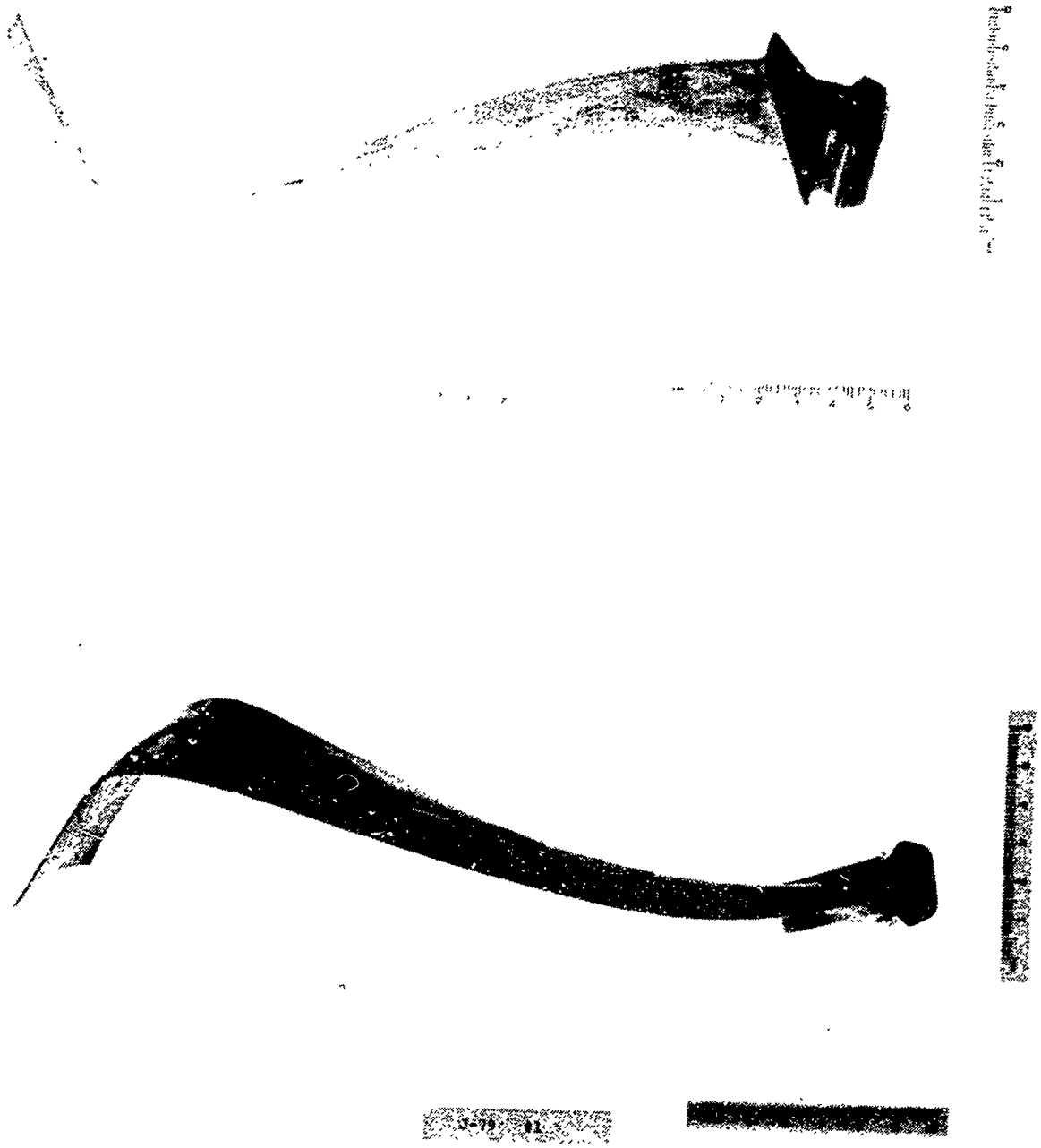

Figure 48B. Damage for Group 7B J79 Stainless Steel Blade Due to 85 g (3 ounce) Artificial Bird Impact (Shot 2-0021).

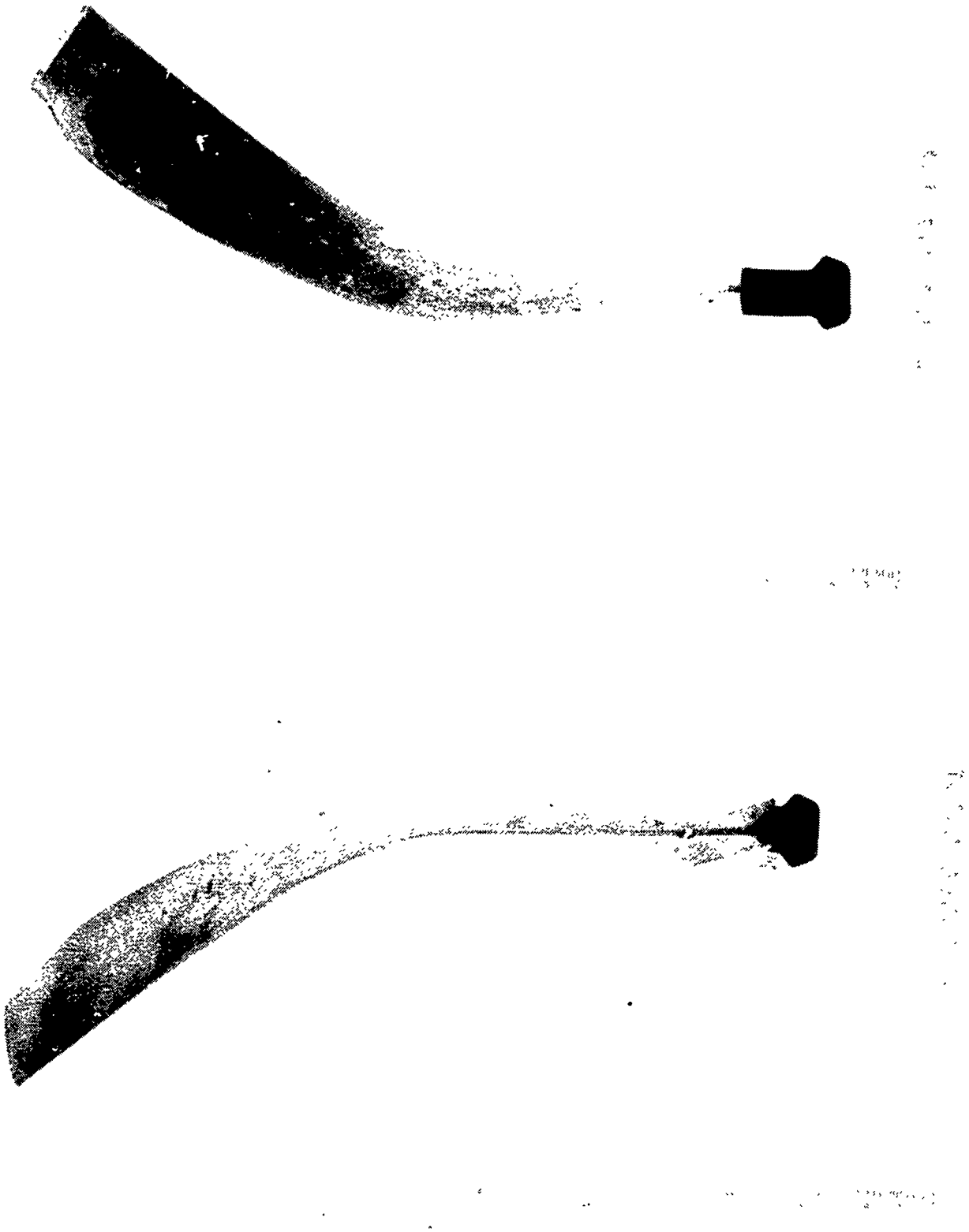

Figure 49B. Damage for Group 8B J79 Stainless Steel Blade to 680 g (1.5 pound) Artificial Bird Impact (Shot 2-0015).

Figure 50B. Damage for Group 9B J79 Stainless Steel Blade Due to 680 g (1.5 pound) Artificial Bird Impact (Shot 2-0024).

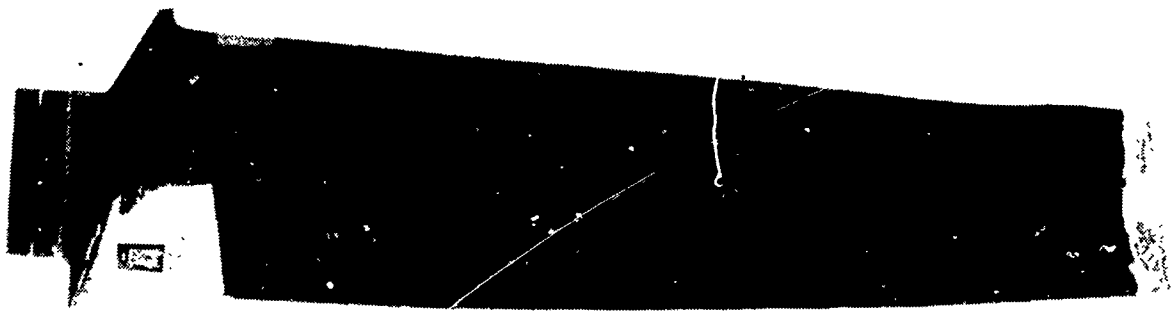

2-0222

2-0222

Figure 51B. Damage for Group 10B J79 Stainless Steel Blade Due to 5.08 cm (2.0 inch) Ice Ball Impact (Shot 2-0222).

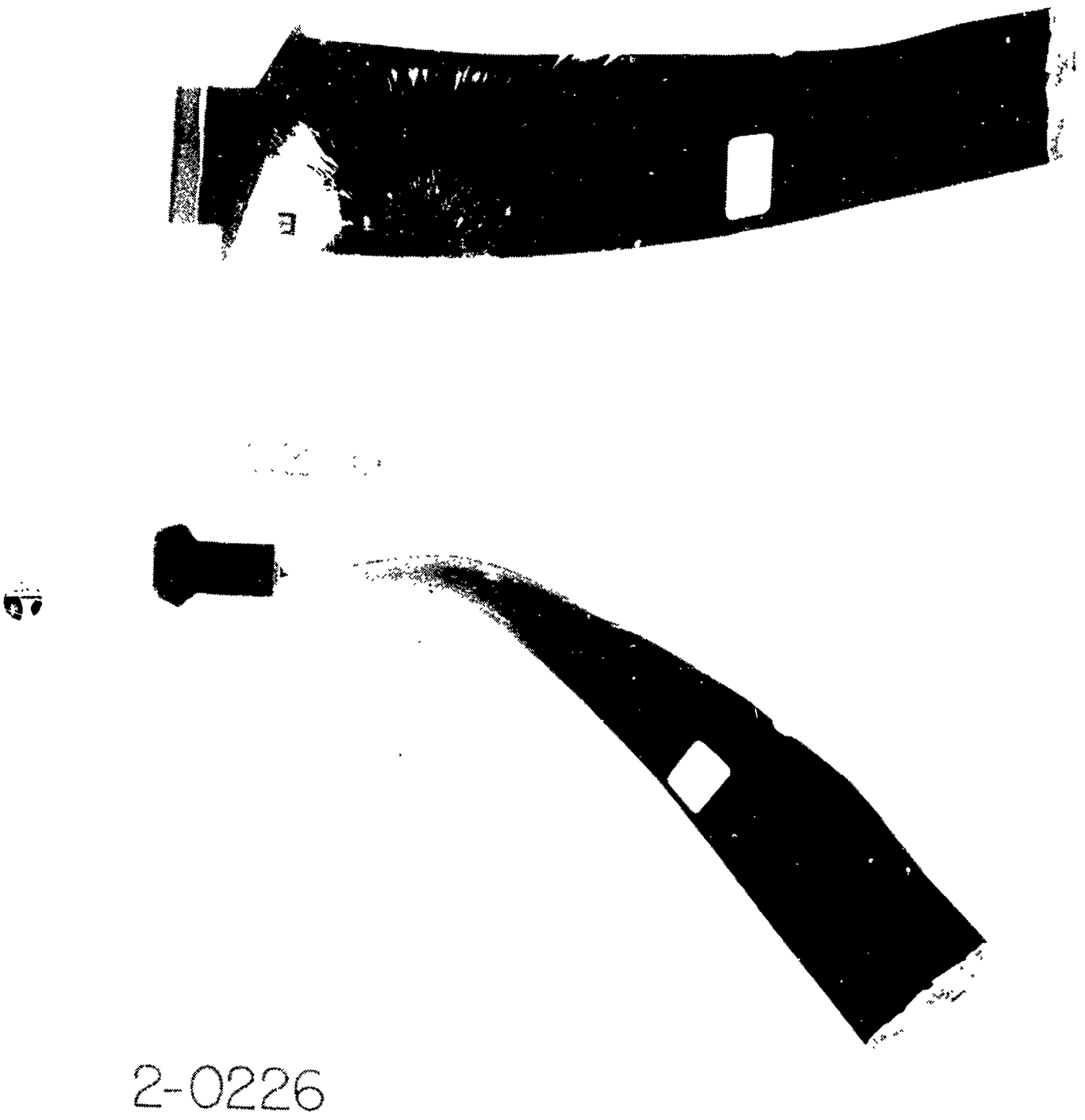

Figure 52B. Damage for Group 10B J79 Stainless Steel Blade Due to 5.08 cm (2.0 inch) Ice Ball Impact (Shot 2-0226).

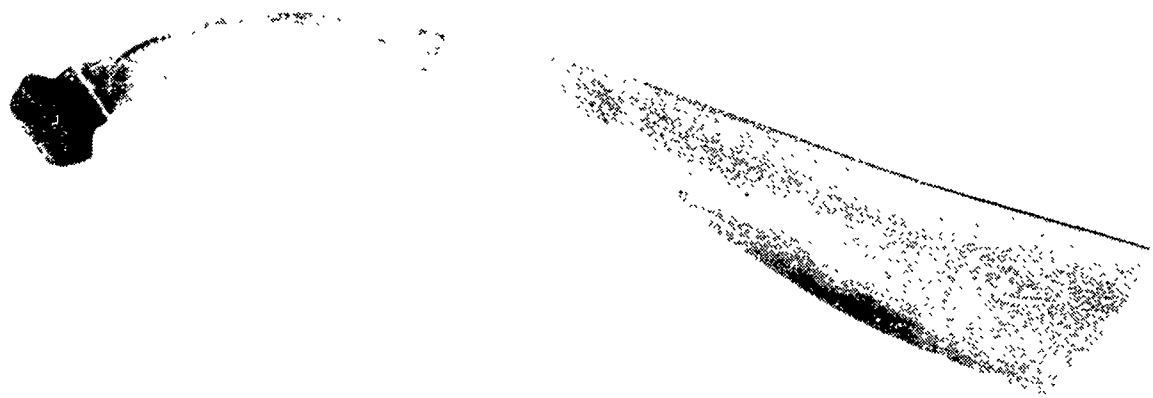

2-0235

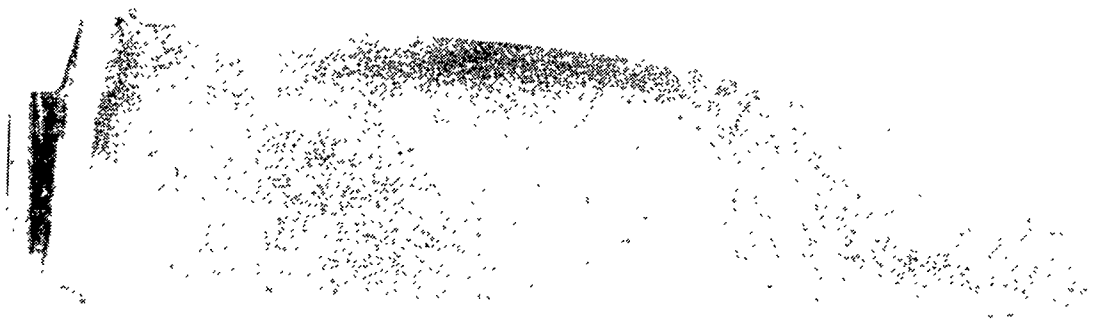

2-0235

Figure 53 B. Damage for Group 11B J79 Stainless Steel Blade Due to Ice Cylinder (Slab Ice) Impact (Shot 2-0235).

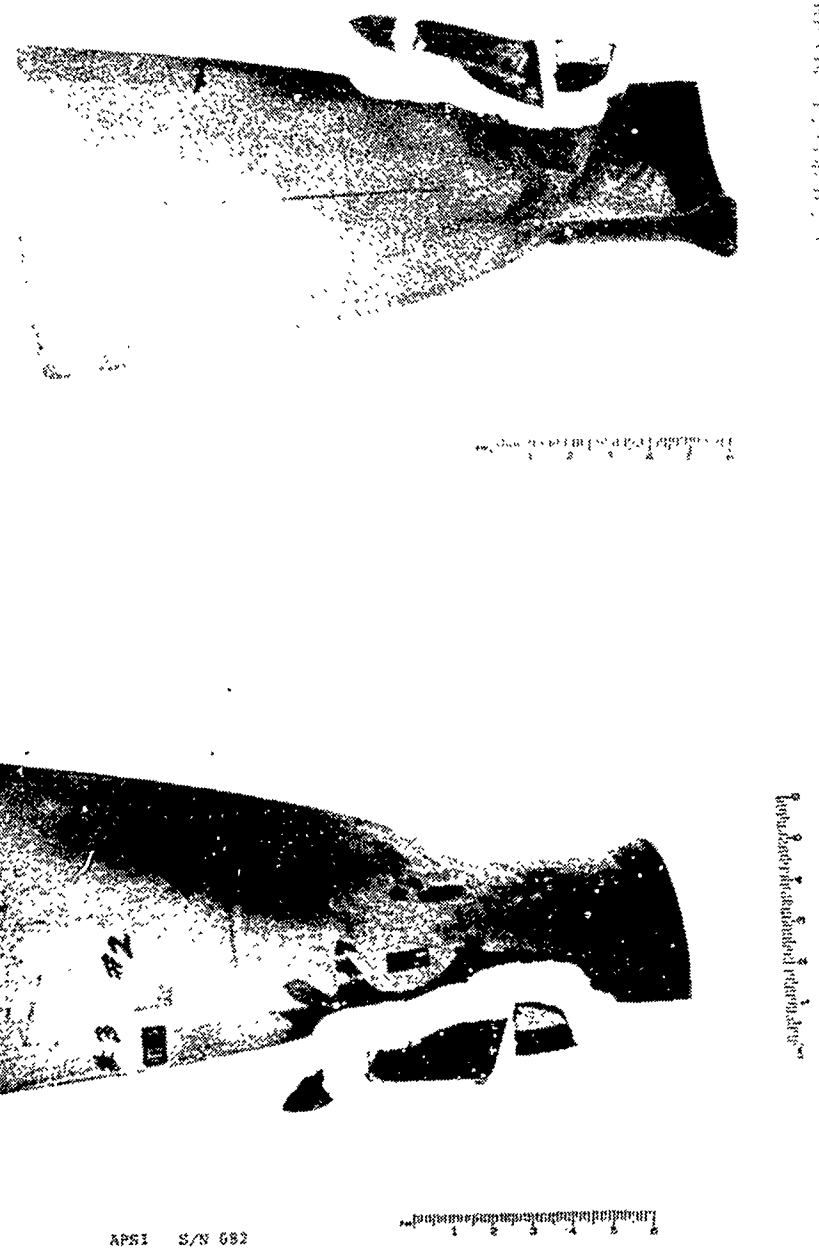

Figure 54B. Damage for Group 12B APSI Boron/Aluminum Composite Blade Due to 85 g (3 ounce) Artificial Bird Impact Shot 2-0016).

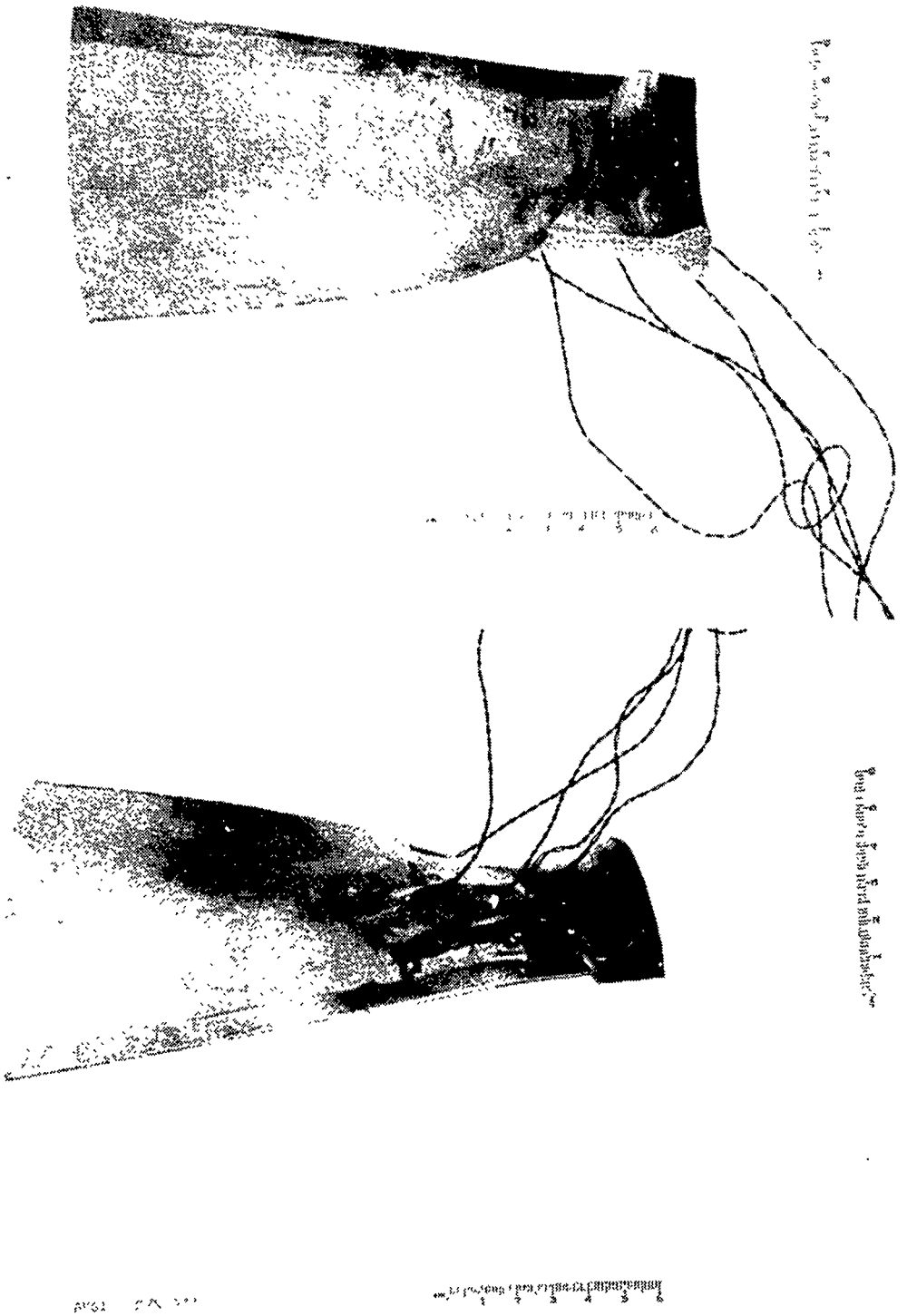

Figure 55B. Damage for Group 12B APSI Boron/Aluminum Composite Blade Due to 85 g (3 ounce) Artificial Bird Impact (Shot 2-0023).

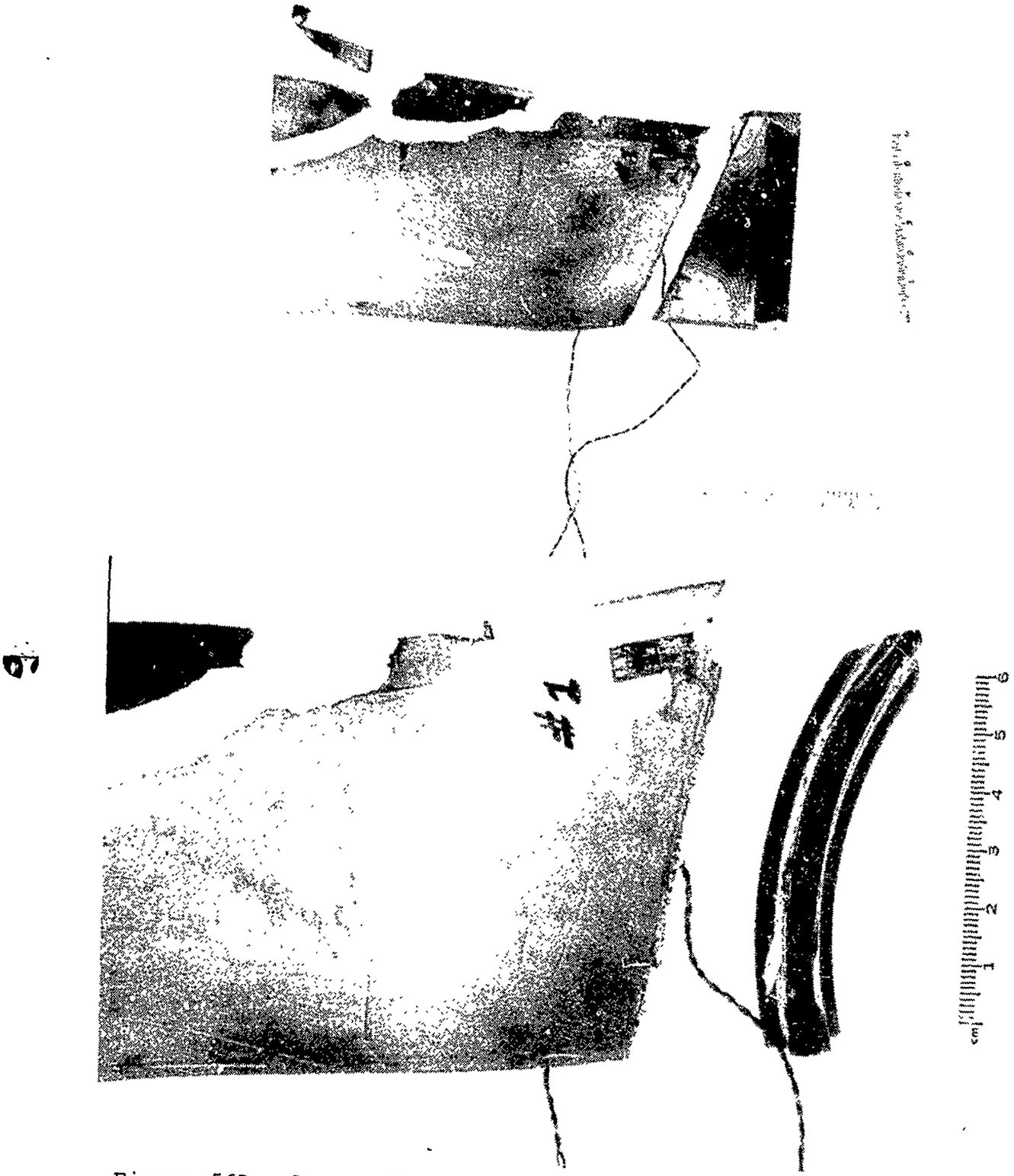

Figure 56B. Damage for Group 13B APSI Boron/Aluminum Composite Blade Due to 85 g (3 ounce) Artificial Bird Impact (Shot 2-0022).

2-0216

2-0216

Figure 57B. Damage for Group 14B APSI Boron/Aluminum Composite Blade Due to 5.08 cm (2.0 inch) Ice Ball Impact (Shot 2-0216).

2-0218

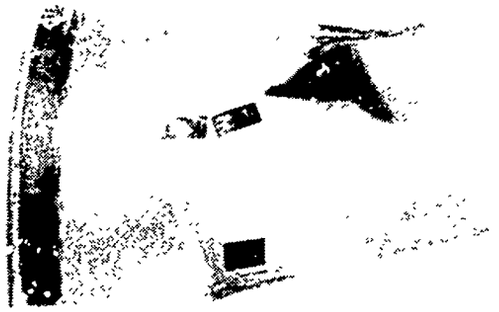

2-0218

Figure 58B. Damage for Group 14B APSI Boron/Aluminum Composite Blade Due to 5.08 cm (2.0 inch) Ice Ball Impact (Shot 2-0218).

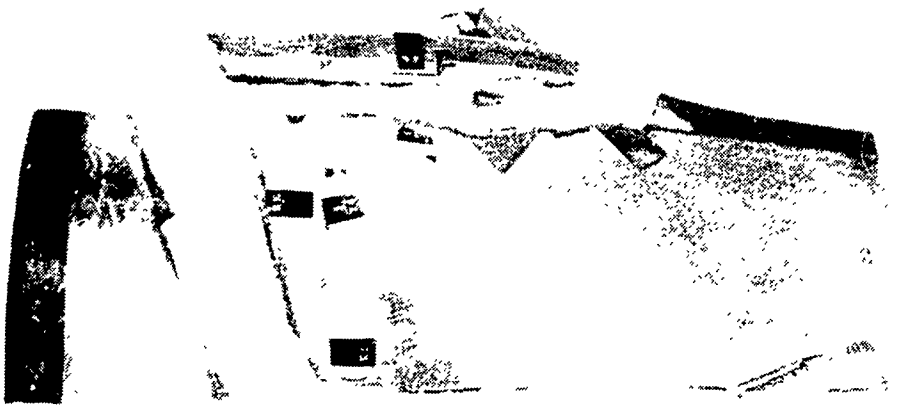

2-0233

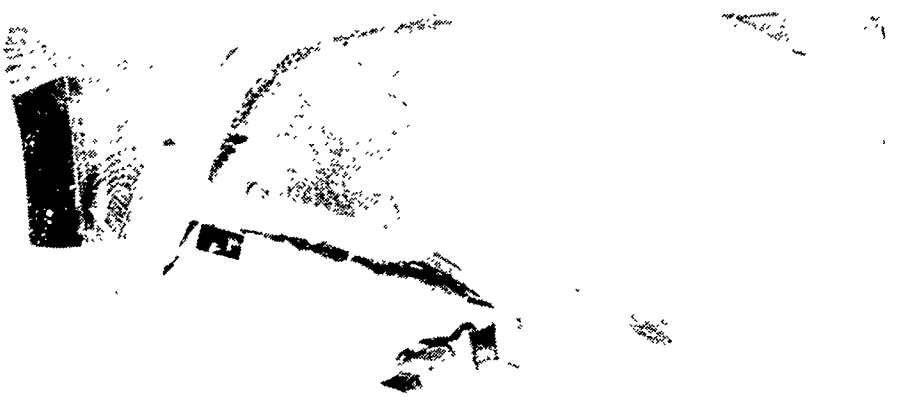

2-0233

Figure 59B. Damage for Group 15B APSI Boron/Aluminum Composite Blade Due to Ice Cylinder (Slab Ice) Impact (Shot 2-0233).